ELECTROKINETIC STABILISATION AS A SUBSIDENCE REMEDIATION TECHNIQUE

by

THOMAS CLINTON

A thesis submitted to the University of Birmingham for the degree of DOCTOR OF PHILOSOPHY.

School of Civil Engineering

College of Engineering and Physical Sciences

University of Birmingham

June 2015

Abstract

This study comprises a three part investigation into electrokinetic stabilisation (EKS): numerical modelling, laboratory trials and site trials. The numerical modelling was introduced to identify issues in the physical trials and assess proposed site trial solutions and associated configurations. The laboratory trials concentrated on electrode development and chemical stabiliser combinations in conjunction with known practical issues such as electrode polarisation and current intermittence effects. English China Clay batches combined with predetermined chemical stabiliser mixes were cured for up to 540 days and tested for standard engineering indexes and electrodes were tested for durability in liquids and under electrolysis. Optimum electrodes, determined through current transfer and durability results, along with optimum chemical combinations, determined through increase in undrained shear strength and reduction is linear shrinkage, were then combined to determine the effects on English China Clay under a mock strip footing for 30 days. It was shown that EKS has a negligible effect on the footing itself through either damage or level changes.

The methodology was developed from the laboratory trials where the optimum electrode type, chemical combination and current intermittence times were developed, and applied to a site trial near Watford, UK. Four trials were conducted consisting of: a control; a vertical electrode set-up, a vertical electrode set-up using current intermittence and a raked electrode set-up. All trials consisted of a 0.3x0.3x1.0m strip footing with treatment targeted at beneath the concrete. EKS was conducted for 56 days on a predominantly London Clay based made ground material with apparent resistivity measurements taken pre-, peri- and post-treatment where apparent resistivity measurements showed the movement of the stabilising fluids over time. Site monitoring included voltage, current, air temperature and footing underside temperatures. Post treatment testing included standard engineering index testing, chemical analysis and SEM photography to determine the effects of the treatment regime. It was determined that the vertical electrode system showed most beneficial clay improvements through the laboratory testing and apparent resistivity results and as in the laboratory trials, negligible effect on the strip footings.

Acknowledgements

I would like to begin by thanking my supervisors. Firstly, Professor Ian Jefferson who guided and encouraged me through this work, always pushing me and trying to get me to be 'glass half full'. Thank you for believing in me and helping me get this far. Thanks also to John Peterson for his financial support, industrial knowledge and providing me with work experience with Foundation Piling Ltd. Thanks also to Chris Seddon of Foundation Piling Ltd for his invaluable help with the site trials. My appreciation also goes to Dr. David Boardman and Professor Chris Rogers for their support and help.

Huge thanks and appreciation must also go to my girlfriend Laura Keil for putting up with my constant distraction and lack of paid work whilst keeping me focused and believing in myself. A massive thank you goes to my parents, Geoff and Andrea, Grandparents Peter and Diane and family for their support, both emotionally and financially, during this time which has no doubt kept me sane. Without their support and help, this would not have been possible. My brother Oliver was invaluable with his heavy lifting help on the site trials and AutoCAD knowledge. Kevin and Louise Keil also have my thanks after kindly letting me move in to their home for six months whilst conducting the site trials.

I am also grateful to the academic staff in the department for their help over the years including Dr. Alexander Royal and Dr. Gurmel Ghataora for their probing annual reviews. I would like to thank all of the Civil Engineering laboratory technicians; Mark Carter, David Coop, James Guest, Sam Melvin, Michael Vanderstam and especially Seb Ballard for their help and advice throughout this project. My thanks also go to Dr. Jackie Deans and Paul Stanley for their help using the XRF and SEM respectively.

Thanks also to Professor Nigel Cassidy who provided invaluable insight into conducting site trials whilst knee deep in freezing cold mud and providing resistivity monitoring results for use in this thesis. Thanks also to Stephen Plante, the Clay Research Group and Julian Hughes of GIP UK for their assistance during the site trials. Further thanks must also go to Aldenham School for allowing the site trials to take place on their grounds with special mention to James Fowler, Charlotte Fowler, Andrew Fraser and Hugh Bailey.

I would also like to thank everyone in F29A, F29B and F55 amongst others for help and providing distractions over the years, especially Roxy for helping in the lab, along with Dan, Aria, Sahand, Samir, Jose, Lasitha, Ramin, Sam, Alex and Giulio.

I must also thank Amey PLC and in particular Christina Jackson for her patience and support whilst I finished off this tome.

Contents

List of Figures

List of Tables

1 INTRODUCTION

This thesis is presented with the aim of exploring electrokinetic soil stabilisation (EKS) as a shallow foundation subsidence remediation technique. Presented here is a body of work that includes experimental studies in both the laboratory and on site along with complimentary numerical computer simulations in this effort.

1.1 Background

Electrokinetics and its derivatives such as electroosmosis and electrophoresis have been researched and studied since Reuss (1809) first investigated electroosmosis. Since then, electroosmosis has been used successfully starting with stabilising a U-Boat pen, (Casagrande, 1949), and then during a railway cutting exercise in Salzgitter, Germany, (Casagrande, 1952). Further on from this, modifying soil strengths has been investigated successfully, (Bjerrum, 1967), (Casagrande, 1952), (Fetzer, 1967).

Permanency of the treatments has always been subject to scrutiny with very little data to back up either view. Soderman & Milligan (1961) used electroosmosis to increase the bearing capacity of the clay around friction piles and Milligan (1995) showed no reduction in performance 36 years later.

Electrokinetic stabilisation is currently viewed as a possibly viable technique for reducing the shrink/swell capacity of a given clay in an economic manner, (Glendinning, et al., 2005), (Symes, 2012), (Jones, et al., 2014). The clays to be treated tend to be sensitive to water content changes and given that a large proportion of the south-east of England is built upon one of these clays, London Clay, the probability of a volumetrically unstable clay causing subsidence in a low rise building is very high. The water content changes tend to evolve from nearby drain leaks and/or trees and large shrubs and their seasonal water demands. Traditional methods for curtailing this are tree crowning or complete removal which are not popular with the general population due to these aesthetical landmarks improving the happiness and well-being of local residents, (White, et al., 2013). Due to this, Caroline Spelman, the Environmental Secretary to the UK government (2010 – 2012), stated in a 2010 speech at the Angela Marmont Centre for Biodiversity that in inner London, each tree was calculated to be worth £78,000. One could argue therefore that it is not just a tree that is being felled.

Current methods of stabilising hydro-sensitive clays, including over consolidation and mechanical chemical mixing, are not so practical in built up areas and quite intrusive. An alternative that is less intrusive, cost effective, safe and permanent was therefore required.

Electrokinetic stabilisation is the process whereby a chemical stabilising fluid is introduced remotely to a subsidence affected ground medium by use of a dc electrical current distributed from electrodes inserted into the medium. Where no stabiliser is introduced, improvement of the ground comes from water content reduction whereas the introduction of chemicals can alter the fabric of the clay.

1.2 Aims and Objectives

Existing research data shows that applying a dc electric current to a clay will induce electrokinetic phenomena and that ions, whether introduced inadvertently through electrode corrosion or purposefully, will be migrated into the clay. Electroosmotic consolidation is provided commercially in the UK by Electrokinetic Ltd adding weight to the effectiveness of electrokinetic phenomena and its ability to be a successful remediation solution accepted by asset owners.

This study aimed to develop electrokinetic stabilisation to establish its potential to efficiently reduce a high plasticity clay's shrink/swell capacity. Furthermore, the study will concentrate on the two core areas of EKS, electrodes and chemical stabilisers. To this end, the following objectives were set:

(1) To conduct a programme of laboratory work to assess the existing range of electrodes and to develop new prototype (renewable) electrodes to be considered for site use. Stabilisation chemical combinations are investigated to define the most effective combination to reduce shrink/swell capacity and increase shear strength in the site trials. The polarisation effect and methods of avoiding it, are explored to further enhance the ability to improve the engineering characteristics of the clay through minimising power wastage.

(2) To undertake numerical simulations using finite element analysis (FEA) of the clay under the influence of a dc electric current with the aim of supplying an indicative view of the current flow path in the clay. This included possible model electrode arrangements and refined electrode choices based on the current transfer between

the electrode and clay. Thereby reducing the number of laboratory trials required and thus saving time and cost.

(3) To integrate the numerical simulations together with the laboratory data and methodology, as part of a trial conducted on a site near Watford in the UK underlain by London Clay where a history of shrink/swell problems had been observed. The results of this site trial are evaluated for effectiveness regarding shrink/swell reductions and shear strength increases.

The overriding aim is to define a direction to develop a full scale electrokinetic stabilisation approach to deal with shrink/swell problems associated with expansive soils acting on buildings and associated infrastructure.

1.3 Contribution to Knowledge

This body of work demonstrated how the up-scaling of the laboratory based experimental procedures and methodologies can be applied to a site trial in expansive clay. It was shown that a controllable system can be implemented to target a specific treatment zone. This was underpinned through numerical modelling optimisation of electrode arrangements, chemical stabilisers and electrode insulation with geotechnical index and strength testing, and apparent resistivity measurements to confirm the efficacy of the treatment.

2 LITERATURE REVIEW

This literature review has been produced to set out the theory and ideas behind the electrokinetic processes involved in the proposed treatment solution. The treatment solution itself is not widely accepted as a standard practice technique and is not currently covered by any technical standards. This section brings together the literature available to help develop the arguments for laboratory and site testing later on. This section provides an overview of the theory behind clay-water interaction and how a clay's geotechnical characteristics can be manipulated. The effects of such manipulation are covered such as shrink and swell which leads onto the forced manipulation set out to be achieved in this research which is the electrokinetic phenomena.

2.1 Introduction

Geotechnical Engineers first recognised the link between the dry summer and building damage in 1947 with a greater impact being produced after the drought in 1976/77 where £50 million worth of insurance claims were filed for subsidence damage (£250 million adjusted for inflation in 2015). More modern estimates from 2004 put the cost of subsidence damage ranging from £185 million GBP, The Association of British Insurers (ABI) in Figure 2-1, to £400 million GBP, (Jones, 2004). Jones (2004) suggests that the ABI estimate that the claims for subsidence will reach a cost of £600 million by 2050. Jones & Jefferson (2012) state that from 2002 to 2012, the adverse effects of shrink swell behaviour of clay has cost the British economy an estimated £3 billion with Zemenu & Martine (2009) estimating the damage in France in 2002 costing more than €3.3 billion. With the expected climate change progression, (IPCC, 2009), there is an increased probability of extreme weather with longer hot/dry summers, increasing the impact of subsidence.

Traditional techniques for subsidence alleviation involve soil removal from under the foundations or underpinning typically with mass concrete, piles or a system of grout injections. These can all take a few months to complete for the average UK home, are costly and carry an environmental and social impact due to their high invasiveness.

A successful replacement treatment scheme for these traditional techniques would need to be low impact environmentally, non-invasive to the property owners and cost effective. With underpinning costing approximately £1000 per metre as of 2011, (CellarTech South West Ltd, 2011), and using approximately 1300kg of concrete per metre, the underpinning technique

cannot be sustained through periods of increasing subsidence impact and increasing environmental and economic pressures.

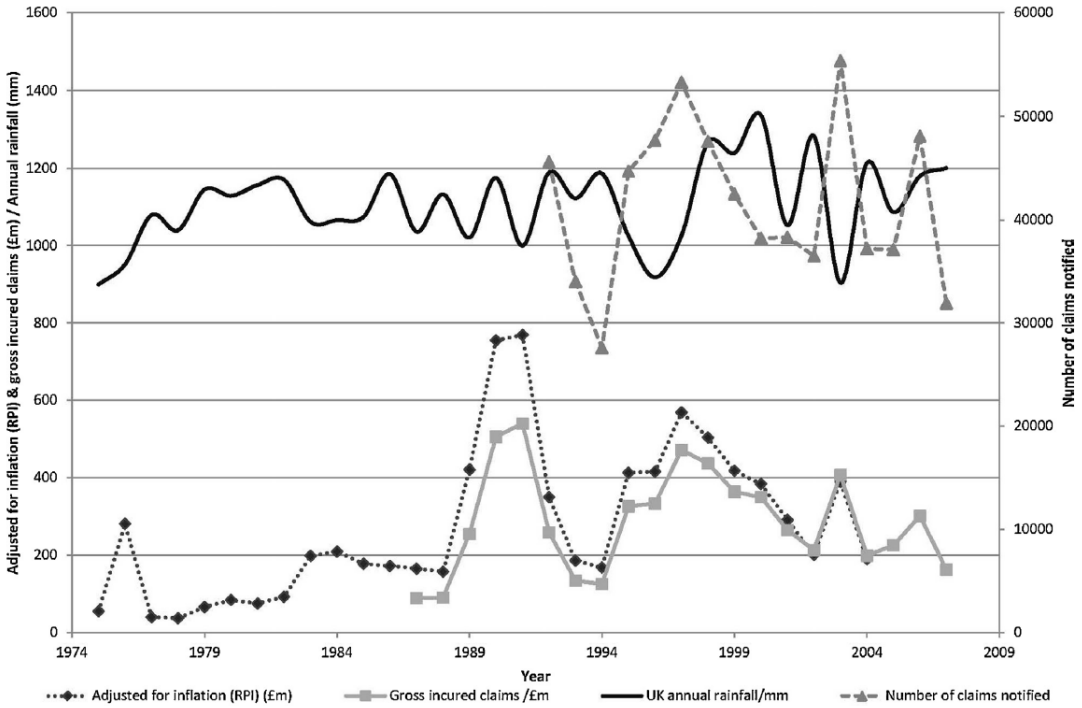

Figure 2-1: Total claims notified with value of claims and associated rainfall. Sources (ABI and Met Office). After Harrison et al. (2012).

EKS is a method by which a clay can be treated remotely, economically, safely and with very little negative environmental impact. By use of a low voltage dc electrical current, applied between electrodes inserted into the ground, stabilising chemicals can be migrated into the clay to improve its characteristics. Using EKS can reduce the cost and carbon footprint of a treatment regime whilst reducing the shrink/swell capacity and increasing the shear strength of a clay. Due to the method in which electrodes are installed and then left over a period of treatment, very little inconvenience is experienced by the property/asset owners.

To fully appreciate the mechanisms behind electrokinetic stabilisation, a comprehensive knowledge of soil and it's interactions with its contained ions is necessary. Soil has a complicated relationship with water, especially when the water is flowing. The study of the characteristics of clay-water-electrolyte systems is imperative to the understanding of the various ways in which electrokinetics can be applied in practical situations.

Presently, the process is not accepted across the industry as a method for commercial use due to the partially known effects that the stabilising chemicals have both on the clay itself and the surrounding environment. However, use of electrokinetics has progressed but currently is limited to dewatering which in itself is becoming more accepted throughout the industry, (Jones, et al., 2011).

Research into this phenomenon has been conducted since the early 20th century with mixed results. Due to the variables possessing a vast variability, previous academic research efforts do not complement each other very well, with each study using different soils, electrodes, power, sizes and electrolytes. The product of this is a process that has no standard method accepted by the international community and as such not yet widely practiced.

2.2 Clays

Clays are found globally with expansive and shrinkable clays being the root cause of subsidence problems. A clay's characteristics are defined by its mineralogy, structure, relationship with water and history.

Clay minerals are principally hydrous aluminium silicates, or lamellar aluminosilicates, (Chatterjee, et al., 1999), and are usually platelets but have been known to be needle or tubular shaped. Clay is deemed a lyophobic or hydrophobic colloid meaning it has an aversion to liquid or water with Mitchell & Soga (2005) stating that hydrophobic colloids are liquid dispersions of small particles that are two phase systems with large interfacial surface areas. Thus, they exhibit behaviours dominated by surface forces and possess the ability to flocculate in the presence of salt. This surface force domination is due to their low mass and high surface area as seen in Table 2-1.

A key characteristic of an expansive clay is its ability to absorb water. Wilun & Starzewski (1975) state that montmorillonites possess a water absorption capacity of approximately 300 – 700% greater than that of clays such as micas. When dealing with clays and in particular, expansive clays, it is vital to understand how clay and water interact. The interaction when modified can have a profound effect on the engineering behaviour of a clay and is especially important when buildings/infrastructure are nearby. It is these very interactions that are at the root cause of subsidence, (Jones & Jefferson, 2012).

When clay is exposed to water, exchangeable ions form a solution; these ions return to the soil if the water is removed. The electrical properties of a soil need to be studied with the

soil and water as a system and not separately as apart, they differ greatly from when together. When applying a force, e.g. electrical, to a clay water system, the mechanism of movement of the water molecules and how they react with their environment needs to be understood. Saarenketo (1998) states, and shows in Figure 2-2, that there are three types of water in soils;

- Adsorption water,
- Viscous water or capillary water
- Free water

Considering this, it can be concluded that the majority of the water transported through electroosmosis would be free water due to their lack of bond to the clay particles.

Table 2-1: Approximate values for specific surface of some common soil grains. After Atkinson (2007).

Soil grain	Specific surface (m^2/g)	Activity
Clay minerals		
Montmorillonite	Up to 840	>5
Illite	65-200	≈0.9
Kaolinite	10-20	≈0.4
Clean sand	2×10^{-4}	NA

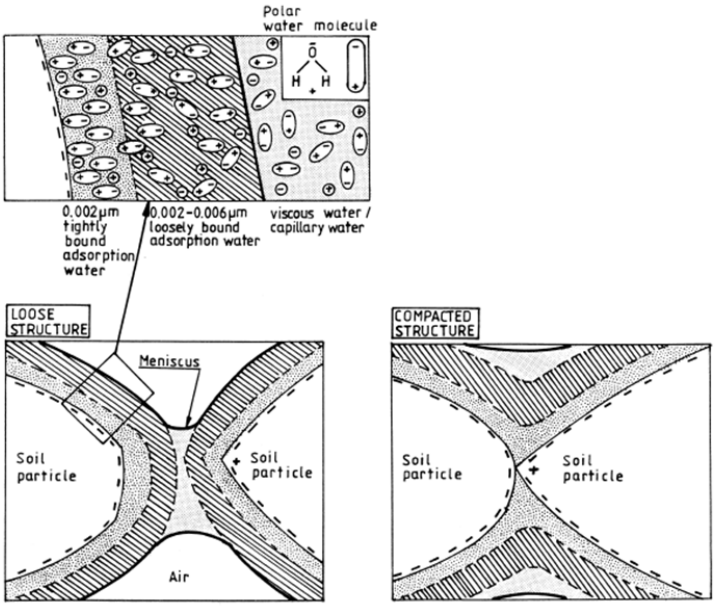

Figure 2-2: The structure of bound water in soil. After Saarenketo (1998).

2.2.1 Diffuse Double Layer

Unbalanced force fields at the clay water interface cause an interaction of the clay particles with water and dissolved ions. Dry clay possesses adsorbed cations which balance the negative electrical charge of the clay particles; excess cations are present as salt precipitates. Introducing water causes the salt to turn to a solution and the adsorbed cations try to diffuse away from the clay surface to balance the charges in such a manner that as the distance from the surface increases, the concentration of cations decreases, Figure 2-3 and Figure 2-4. This is due to the cations diffusion being restricted by the clay particle's electric field. It is stated by van Olphen (1977) that such a distribution is called an atmospheric distribution, yet this atmosphere is not entirely composed of counter-ions as previously described, but also contains co-ions which are produced by negative adsorption. Co-ions possess the same charge as the clay and thus are electrostatically repelled by the surface. The concentration of co-ions and counter-ions at any point is a function of the distance from the clay surface and can be calculated using the Poisson-Boltzmann equation where the derivation and explanation of this equation can be found in Mitchell & Soga (2005).

Audebert & de Mende (1959) state that the phase adjacent to the particle surface is actually made up of two parts due to there being a strip approximately one ion thick of ions that are too strongly bound to the particle to escape. This layer is sometimes called the Helmholtz layer and can essentially be thought of as part of the particle.

The thickness of the DDL is important as it directly affects the structural development and hydraulic conductivity among other properties of the soils, (Fukue, et al., 1999), (Fukue, 2001). The swell capacity is also determined by the DDL thickness and it is the surface area of the clay that determines most of the clays properties. Thus it is just as important to know the surface area as it is the thickness of the DDL. It is reported by van Olphen (1977) that the thickness of the DDL around a clay particle is governed by the concentration of salt and type of cations in the soil water. It is also reported that the thickness also depends on the degree of expansion of the DDL where full expansion is only achieved in an abundance of water. Dry soils cause the DDL to be very thin due to there being no expansion. This results in the clay particles being isolated from each other leading to discontinuous current flow pathways, (Nye, 1979). This effect can also be caused by introducing demineralised water into the system, (Levy & Shainberg, 1972). The increase in bulk electrical conductivity of the clay system is directly related to the expansion stage of the DDL in that the further the expansion has progressed, the

more water exists inside the DDL and the thicker the DDL becomes. At a certain point, the thickness of these DDL's causes them to come into contact with other DDLs. This produces the maximum number of continuous electric current pathways through the system, (Mojid & Cho, 2006). Waxman & Smits (1968) state that the water in a DDL has a higher electrical conductivity than the water outside of the DDL, the bulk electrical conductivity of the system will continue to increase as further DDLs come into contact. This is true until a certain point, the critical water content, where further increases in water content will cause the DDLs to become progressively more and more isolated from each other, effectively reducing the electrical conductivity of the system. For systems with non-demineralised water, separate equations from those for demineralised water take into account the presence of salt when calculating DDL thickness and critical water contents.

The thickness of this layer is controlled directly by the concentration of cations in the pore water, the magnitude of the charge density on the particle surface, the valence of the cations and the dielectric properties of the pore fluid, (Acar, et al., 1995). Barker, et al. (2004) states that the thickness of this layer is primarily controlled by the amount of cations in the pore water and the charge on the surface of the clay. This charge can be influenced by the pH. Reduction of this layer results in closer contact for the clay particles and can lead to flocculation. The higher the concentration and valence of the opposite sign ions, the more the double layer is compressed as seen in van Olphen (1977) and Table 2-2.

Table 2-2: Approximate "Thickness" of the electric double layer (DDL) as a function of electrolyte concentration at a constant surface potential. After van Olphen (1977).

Concentration of ions of opposite charge to that of the particle, mmol/dm^3	**"Thickness" of the double layer, Å** **Monovalent ions**	**"Thickness" of the double layer, Å** **Divalent ions**
0.01	1000	500
1.0	100	50
100.0	10	5

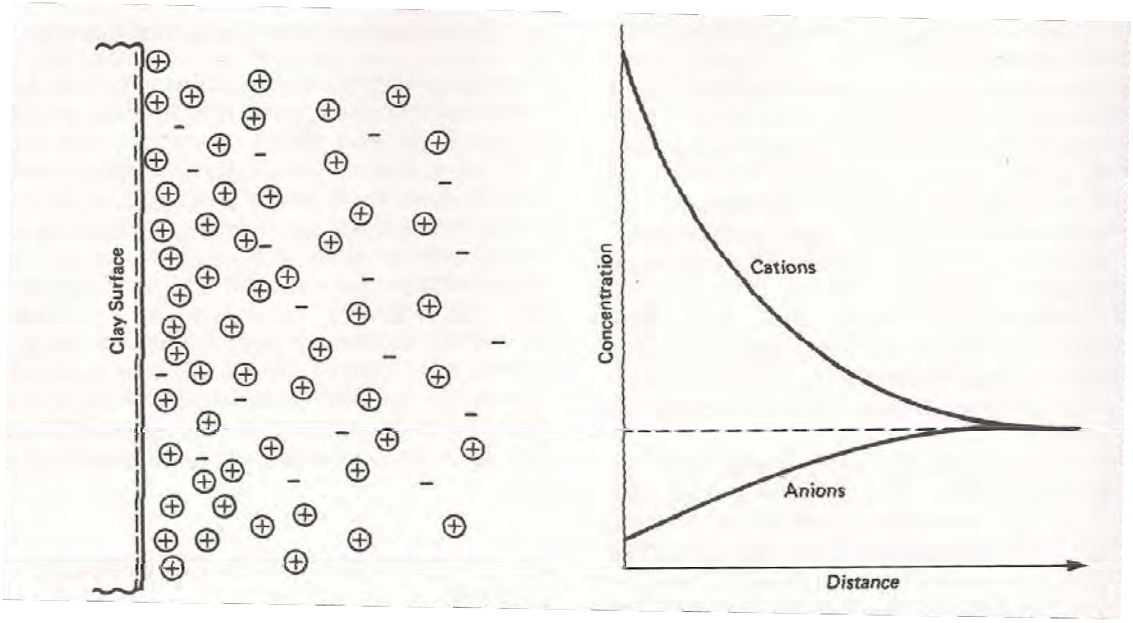

Figure 2-3: Distributions of ions adjacent to a clay surface according to the concept of the diffuse double layer. After Mitchell & Soga (2005).

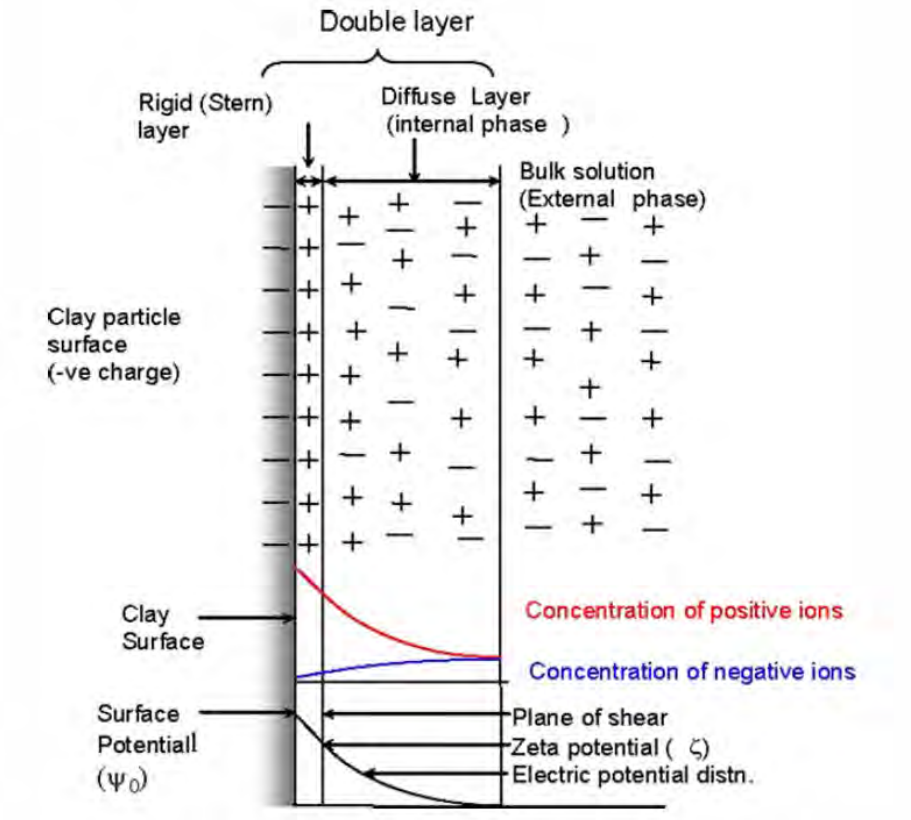

Figure 2-4: Conceptual view of double layer structure at solid/water interface. After Jones et al. (2011).

The DDL is negligibly affected by changes in temperature, (Mitchell & Soga, 2005), where an increase in temperature should lead to an increase in the thickness of the DDL, however; the increase in temperature also gives rise to a decrease in dielectric constant due to the increased energy needed to polarise fluid molecules. Table 2-3 shows how when the temperature is increased, the product DT does not vary considerably. The product DT is shown here as it is a considerable factor used to calculate DDL thickness as in Mitchell & Soga (2005).

Table 2-3: The effect of temperature on the dielectric constant of water. After Mitchell & Soga (2005).

T (^{o}C)	T (K)	D	DT
0	273	88.0	2.40×10^{4}
20	293	80.0	2.34×10^{4}
25	298	78.5	2.34×10^{4}
60	333	66.0	2.20×10^{4}

2.2.2 Zeta Potential

This zeta potential concerns the tangential movements of a charged liquid along an interface. It can be described as the electric potential in the double layer at the interface at the unknown distance between the surface of a particle and its surrounding liquid. Audebert & de Mende (1959) show that the zeta potential is not from the particle surface but instead from the Helmholtz layer, Figure 2-5, whereas Jones & Terrington (2011) show that it is from the Stern layer. It is essentially a slipping plane which can be seen in Figure 2-6.

The zeta potential will decrease with increasing electrolyte concentration due to counter ions moving from the compressed diffuse double layer to the Stern layer. It should be noted that the position of the zeta potential cannot be quantitatively determined by existing theories, (Shang & Lo, 1997). Shang (1997) also states that the electroosmotic permeability and thus the effectiveness of electroosmosis in a clay can be estimated from the zeta potential.

Equation 2-1 shows how the zeta potential is dependent on the electrical surface potential and electric double layer. These in turn are affected by the pH, relative permittivity and concentration of ions, (van Olphen, 1977).

$$\zeta = \frac{4\Pi\eta}{\mathrm{DE}}\mathrm{v_e} \qquad 2\text{-}1$$

Where ζ is the zeta potential, η is the viscosity of the liquid, D is the relative permittivity, E is the electrical surface potential and v_e is the electrically induced flow velocity.

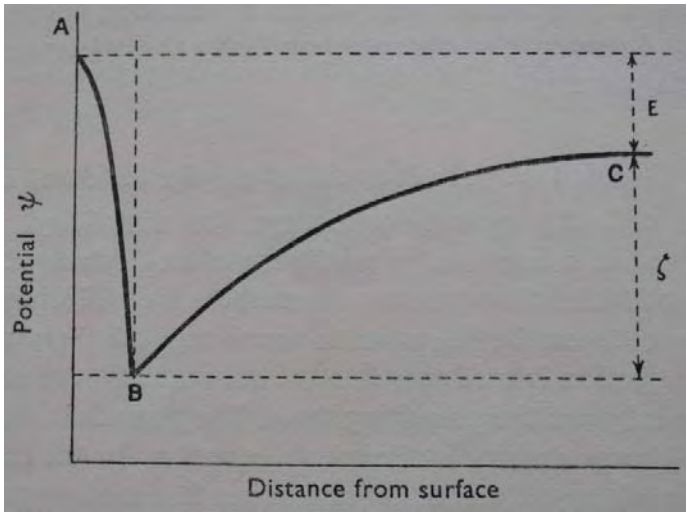

Figure 2-5: Variation of potential ψ near a charged surface. A represents the surface, B, the surface of shear, AB, the Helmholtz layer, C, a point in the liquid far from the surface. E is the thermodynamic potential and ζ is the electrokinetic potential (zeta potential). After Audbert & de Mende (1959).

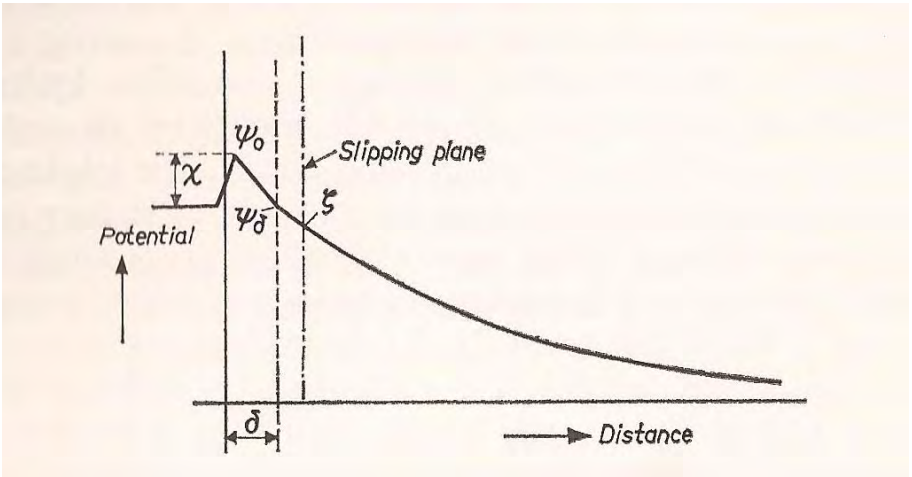

Figure 2-6: Potential distribution at the metal/solution interface. After Sparnaay (1972).

2.2.3 Cation Exchange Capacity

Cations in a clay system can be exchangeable cations owing to the fact that they can be replaced by other dissolved cations of higher replacing powers. The replacing power usually depends on the size but can also be influenced by valence and type. Lower replacement power cations can replace higher powered cations when aided by mass action, this refers to the concentration of lower power cations being high relative to the high powered ones. These exchange reactions can occur due to changing environmental effects and do not usually affect the structure but do vary the properties of the soil.

There are three sources of clay exchange capacity according to Mitchell & Soga (2005):

- Isomorphous substitution: Charge balancing cations are attracted to the surfaces and are the major source of cation exchange in clays excluding kaolin.
- Broken bonds: The importance of these increases with decreasing particle size.
- Replacement: The hydrogen of an exposed hydroxyl is replaced by another cation.

The ease of replacement of these cations is dependent on ion size, valence and concentration. If all things are equal, trivalent cations are held more tightly than divalent and divalent are held more tightly than monovalent, as can be seen here;

$$Na^+ < Li^+ < K^+ < Rb^+ < Cs^+ < Mg^{2+} < Ca^{2+} < Ba^{2+} < Cu^{2+} < Al^{3+} < Fe^{3+} < Th^{4+} \quad 2\text{-}2$$

This is the lyotropic series which states that higher valence cations will replace those of lower valence and larger cations will replace smaller cations of the same valence, (Little, 1987). So for example, Th^{4+} will replace Ba^{2+} and Ba^{2+} will replace Li^{+}. As discussed before, it is possible to replace a high powered cation with a low powered cation through mass action.

Barker, et al. (2004) states that the activity of a soil has a direct bearing upon the cation exchange capacity and therefore will affect the size of the diffuse double layer and thus the volume of water available in the pore spaces for transport.

2.2.4 Electrolysis

During the procedure of electrokinetic stabilisation electrolysis takes place. Electrolysis occurs with the application of a dc current through a water system producing reactions at the

electrodes. Oxidation occurs at the anode and reduction occurs at the cathode. The oxidation releases oxygen and hydrogen ions and the reduction releases hydrogen and hydroxide ions.

$$Anode: \quad 2H_2O - 4e^- \rightarrow O_2 \uparrow + 4H^+$$
$$Cathode: \quad 2H_2O - 2e^- \rightarrow H_2 \uparrow + 2OH^- \qquad 2\text{-}3$$

Liaki (2006) states that the reactions at the electrodes are dependent on the pore water and the electrode material.

Acid is formed by the anions in solution reacting with H^+ ions. However, some of these H^+ ions will replace exchangeable cations on the clay surface. Due to hydrogen clays being generally unstable combined with the high acidity in the soil, deterioration of the anodes causes precipitation of electrode material into the soil. This results in the soil's form altering and a gain in strength around the anode. Gases are also produced during these reactions and are known to be electrical insulators which will inhibit the EKS process, (Rittirong, et al., 2008).

The precipitated ions during EKS will cause an acid front to develop at the anode and a base front to develop at the cathode, if not removed or neutralised, with variances from 2 to 12. Hydrogen ions flow towards the cathode by electromigration, diffusion and electroosmosis. This creates a low pH area around the anode. Hydroxide ions flow towards the anode by electromigration and diffusion causing an area of high pH to develop around the cathode. The electrical gradient of the system will force these fronts to move towards each other. However, the electroosmosis induced in the system will retard the base front's movement causing the acid front to be prevalent in the soil with the exception of the area immediately surrounding the cathode. This is exacerbated by hydrogen possessing a higher ionic mobility than hydroxide ions, allowing for faster migration.

Glendinning, et al. (2005) reports that the advance of the acid and base fronts is governed by ion migration, electroosmotic flow, diffusion and the buffering capacity of the soil. During electromigration, hydrogen ions migrate faster than hydroxide ions due to their higher charge to ionic size ratio. This combined with the fact that electroosmotic flow is in the same direction as hydrogen migration and opposite to hydroxide, gives the acid front a quicker migration speed. Barker, et al. (2004) states that the higher concentration of hydrogen ions helps the acid front development too.

Barker, et al. (2004) reports that the variations in pH can change a clay particle's surface charge and thus alter the cation exchange capacity and solubility of elements within the soil. Extreme pH's can dramatically increase the solubility of aluminium oxide. He also states that to bring about traditional chemical stabilisation, the pH needs ideally raising above 10.

The development of the pH gradient can influence the solubility of electrolytes whilst also increasing the speed of deterioration of the anode causing aluminium or iron to precipitate into the soil. As a result of this precipitation, the strength of the soil in the affected area increases.

The pH variations across the soil can be controlled by buffering to avoid the aforementioned problems. This can be achieved by bubbling CO_2 into the required electrolyte. This method increases the rate and extent of electrochemical induration according to Gray (1970).

2.2.5 Electrolytes

Electrolytes are usually acids, bases or salts that are electric current conductors where the current is not transferred in an electronic manner but by ions. A current can only flow through the electrolyte when the potential difference between its two ends is greater than the electrolytes decomposition voltage. When an electric field is applied to an electrolyte, the cations move towards the negative electrode and the anions move towards the positive electrode. The electric current is then characterised as the movement of cations and anions in their respective directions due to the field.

2.2.6 Electron Mobility

An applied electric field induces a force onto the free electrons in a soil water system forcing them to accelerate in the opposite direction to the field due to their negative charge. Quantum mechanics states that there is no interaction between a moving electron and surrounding atoms in a perfect lattice, but as clays are not composed of perfect lattices, the electric current peaks almost instantly rather than infinitely increasing, (Callister, 2007). There is still a net motion in the opposite direction to the field, this is the electric current.

This leads to the conclusion that without free electrons, there can be no electric current. A soil system's free electrons are contained in its water. Thus, drying the soil and removing the

water reduces the amount of free electrons in the system leading to a reduction in the soils capacity to host an electric current.

2.2.7 Flows

Flows through soil play a major role in the characteristics of deformation, volume change and the stability of the soil and the rates at which they occur, (Mitchell & Soga, 2005). These authors also state that each flow rate, or flux, relates linearly to its driving force given that;

$$J_i = L_{ii} \cdot X_i \qquad 2\text{-}4$$

The types of flow experienced through a soil are hydraulic, chemical, electrical and thermal, with electrical being predominant in low hydraulic conductivity clays under EKS. As well as these types of flow, coupled flows exist and also play a vital role in the system. A coupled flow exists when one type of flow is induced by another type's potential gradient, (Yeung & Mitchell, 1993). Total flow is then given by;

$$\vec{J}_i = \sum_{j=1}^{n} L_{ij} \vec{X}_j \qquad 2\text{-}5$$

These flows are important in this respect as of their ability to alter the migration of ions through the medium.

Darcy's Law governs the flow through a medium caused by the introduction of a hydraulic gradient. The law states that the flow velocity or rate is directly proportional to the hydraulic gradient;

$$q_h = k_h \cdot \frac{\Delta H}{L} \cdot A \quad \text{or} \quad q_h = k_h \cdot i_h \cdot A \quad \text{where} \quad i_h = \frac{\Delta H}{L} \qquad 2\text{-}6$$

Where q_h is the hydraulic flow, k_h is the hydraulic conductivity and A is the cross sectional area normal to the direction of flow. The hydraulic conductivity is influenced by the mineralogical composition, particle size and void ratio amongst others, (Mitchell & Soga, 2005). Barker, et al. (2007) states that this flow is affected in soil by the degree of saturation, particle size, temperature and packing arrangement.

Fick's law governs chemical flow through a medium caused by the introduction of a chemical gradient. Another name for this is diffusion and it involves the transport of molecules through a medium from high concentration areas to low concentration areas;

$$J_D = D \cdot \frac{\Delta c}{L} \cdot A \quad \text{or} \quad J_D = D \cdot i_c \cdot A \quad \text{where} \quad i_c = \frac{\Delta c}{L} \qquad 2\text{-}7$$

Where J_D is the diffusion, D is the diffusion coefficient and A is the cross sectional area normal to the direction of flow. It is known that diffusion through soil acts slower than diffusion through water, especially when adsorptive clay particles are present.

Ohm's law governs the electrical flow which is produced by the introduction of an electrical gradient over the soil medium;

$$I = \sigma_e \cdot \frac{\Delta V}{L} \cdot A \quad \text{or} \quad I = \sigma_e \cdot i_e \cdot A \quad \text{where} \quad i_e = \frac{\Delta V}{L} \qquad 2\text{-}8$$

Where I is the electrical flow, σ_e is the electrical conductivity and A is the cross sectional area normal to the direction of flow. The electrical conductivity varies and is dependent on porosity, degree of saturation, composition of the pore water, mineralogy, shape, surface conductance, soil structure and temperature, (Mitchell & Soga, 2005). Barker, et al. (2007) states that this flow is affected by water content, ionic strength and soil temperature amongst other variables.

Fourier's law governs the flow of heat through a medium where the flow is induced by a temperature gradient across the medium. Heat flow through soil and rock is almost entirely by conduction, with radiation important only for surface soils and convection only important if there is a high flow rate of water or air, (Mitchell & Soga, 2005). Conductive heat flow is primarily through the solid phase of the soil.

$$Q_t = k_t \cdot \frac{\Delta T}{L} \cdot A \quad \text{or} \quad Q_t = k_t \cdot i_t \cdot A \quad \text{where} \quad i_t = \frac{\Delta T}{L} \qquad 2\text{-}9$$

Where Q_t is the thermal flow, k_t is the thermal conductivity and A is the cross sectional area normal to the direction of flow. Thermal conductivity of a soil is influenced by the density and the degree of saturation of the soil, (Mitchell & Soga, 2005).

Simultaneous flows of different types can exist in soils, even when there is only one type of driving force, (Mitchell & Soga, 2005). This is numerically represented by;

$$J_i = L_{ij} \cdot X_j \qquad 2\text{-}10$$

Where L_{ij} is the coupling coefficient.

Table 2-4: Direct and coupled flow phenomena. After Mitchell & Soga (2005).

Gradient (X) / **Flow (J)**	**Hydraulic**	**Temperature**	**Electrical**	**Chemical**
Fluid	Hydraulic conduction (Darcy's Law)	Thermoosmosis	Electroosmosis	Chemical osmosis
Heat	Isothermal heat transfer	Thermal conduction (Fourier's Law)	Peltier effect	Dufour effect
Current	Streaming current	Thermoelectricity	Electric conduction (Ohm's Law)	Diffusion and membrane potentials
Ion	Streaming current ultrafiltration	Thermal diffusion of electrolyte	Electrophoresis	Diffusion (Fick's Law)

Table 2-4, shows the different types of coupled flow and highlighted are the ones that are most relevant to this study. These phenomena and the methods of quantifying them can be investigated in more detail in Liaki (2006) and Mitchell & Soga (2005).

2.3 Clay Shrink and Swell

Clays shrink and swell due to drying and wetting as a result of the forces endured from the inter-particle attractions and repulsions. These inter-particle relationships consist of the electrostatic and osmotic forces that exist between the negative surfaces of the clay particles and the cations

in the local system, (Biddle, 1998a), (Yong & Warkentin, 1975). The susceptibility of a clay to exhibit shrinkage and swelling behaviours is linked to its cation exchange capacity (CEC) in which higher CEC's lead to greater volume change potential, (Driscoll, 1983), (Jones & Jefferson, 2012), where the CEC is a function of the structure and surface area of the clay particles. The chemical structure affects the cation exchange whilst the surface area controls the amount of water that can be adsorbed onto the clay surface. Weaver & Pollard (1973) show that a clay with a CEC value of over 10-15Me/100g will tend to show expansive tendencies. Table 2-5 shows how different British clays have different shrinkage potentials. Biddle (1998a) states that kaolinites, chlorites and illites are non-expansive whereas vermiculites and smectites are expansive in nature.

Table 2-5: Physical properties of some common British clays. After Jones (2010).

Clay Type/ Formation	**Plasticity Index (%)**	**Clay Fraction (%<2μm)**	**CEC (Me/100g)**	**Shrinkage Potential**
London	28-52	60-65	56	Medium/High
Weald	43	62	-	High
Kimmeridge	53	63-67	48	High/Very High
Boulder	32-50	37-51	-	Medium
Oxford	41	56-63	55	High
Reading	72	58	54	Very High
Gault	57-69	-	53	Very High
Lower Lias	31-60	60	50	Medium

Expansive clay is a problem met by countries the world over including the USA, Canada, France, Spain, Denmark, South Africa, Australia, Israel, Romania, China, Saudi Arabia, Zimbabwe and the UK, (Jones & Jefferson, 2012). In 1980 alone, the annual cost of damage due to expansive soil was put at US$7 billion, (Krohn & Slosson, 1980). Firm, shrinkable clays occur throughout the UK but are predominately found in the south-east usually south of a line between Exeter and Hull, (National House Building Council, 2011).

The more water absorbed into the spaces between the clay layers, the more they are pushed apart and hence the clay expands. The higher the plasticity of the clay, the more severe the volumetric instability can be, (Biddle, 1998a). It can be taken that unsaturated expansive

clay soils are the most susceptible to this instability, (Bryant, et al., 2001). Soils susceptible to shrink and swell usually do so in the upper 1.5m of soil where the seasonal variance in moisture is located unless a tree or hedge is in the close vicinity as the roots can increase this depth, (Freeman, et al., 1994), (Nelson, et al., 2001). The BRE (1993) goes on to state that whereas grass evaporation and transpiration is usually confined to the top 1.5m of soil, trees and large shrubs can extract moisture up to 6m deep. The load applied to a soil by a typical trench filled strip footing with a low rise building upon it is 20 – 60kN/m^2 but when the soil becomes desiccated, the soil can experience suction pressures of up to 1500kN/m^2, (Biddle, 1998a), which will have a greater effect on the ground movement than the dwelling itself.

Freeman, et al. (1994) states that there are multiple types of firm, shrinkable clay that occur in the UK with a wide distribution across the south-east of the country. Their water contents are close to the plastic limit, for example London Clay typically has a plastic limit of 26% and moisture content of 25 – 30%. This varies significantly near the ground surface due to rain and evaporation. Regarding London Clay, these characteristics also vary across the London basin due to its formation as discussed in section 3.2.1. Jones & Jefferson (2012) state that in humid regions such as the UK, problematic behaviour generally occurs in areas of high I_p which correlates with Table 2-5.

It is known that vegetation moisture requirements can reduce the levels of water in a soil causing shrinkage. BRE (2009) states four types of associations between the vegetation and soil movement:

- Normal seasonal movements associated with evaporation and transpiration
- Enhanced seasonal movements associated with the introduction of trees
- Long term subsidence associated with the development of a persistent water deficit
- Long term heave associated with the dissipation of a persistent water deficit.

Some trees can demand high amounts of water at some points during the seasons; Perpich, et al. (1965) reported that a tree with maximum crown can transpire 380 litres of water on a sunny day. Add this to interception losses due to the crown and evaporation and there could be a severe moisture deficit. The NHBC Standards have developed a guide for estimated water demand of trees common in the UK. It shows that high demand trees tend to have the highest mature height, (National House Building Council, 2011).

The NHBC Standards also introduce minimum foundation depths according to proximity to trees, the depths are affected by tree size and distance from foundations, (National House Building Council, 2011). Location within the UK also plays a part as it is also shown how by travelling north-west from London there can be a reduction in required foundation depth due to climate variations approximately every 50 miles. Roberts, et al. (2006) states that the majority of UK existing housing is built upon relatively shallow trench fill foundations of less than one metre depth which leads to the conclusion that shallow water content changes around houses can adversely affect much of the housing stock in the UK.

2.3.1 Shrinkage

Shrinkage is caused by an increase in the attractive bonds between the clay particles and the interstitial cations which is brought about through increased loading and/or a decrease in water content. The extent of this shrinkage is controlled by the concentration of the ions between the clay particles and their respective charges. Polyvalent cations have a high bond strength with the clay particle leading to a reduced inter layer space and thus a reduced ability to shrink.

Shrinkage cracks are not always evident on a desiccated clay's surface but can appear at depth, particularly in clays with a well-developed crumb structure, (Yong & Warkentin, 1975). Shrinkage cracking has four phases of development; zero, residual, normal and structural as seen in Figure 2-7, (Kodikara, et al., 1999). Different curves exist for different clays based upon the type of clay, structural features and stress history. Table 2-6 shows how the combination of plasticity index and clay fraction contribute together in determining the shrinkage potential.

It is known that the suction of a clay is hysteretic, in that it is variable depending on the history of drying and wetting, (Biddle, 1998a). It can also be noted that the magnitude of the suction stresses caused by vegetation are approximately 650 times smaller than those caused by desiccation.

Electro-osmosis causes a negative pore pressure to build inside the soil matrix which will lead to the shrinkage of said soil. If remediation without settlement is to be achieved by electrokinetic stabilisation then the suctions created by the process will require overcoming.

Table 2-6: Clay shrinkage potential. After BRE (1993).

Plasticity Index (%)	Clay Fraction (<0.002mm)	Shrinkage Potential
>35	>95	Very High
22 – 48	60 – 95	High
12 – 32	30 – 60	Medium
<18	<30	Low

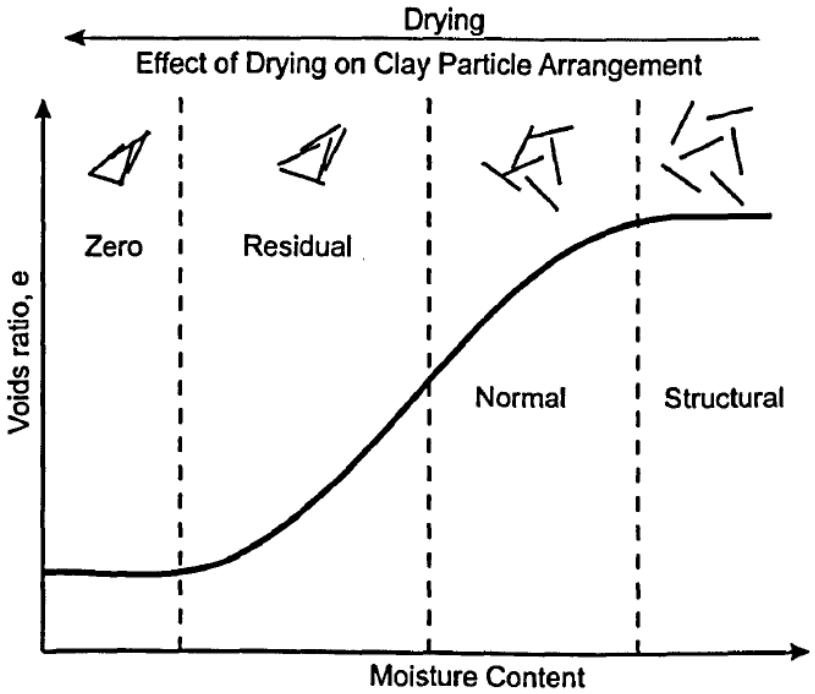

Figure 2-7: Typical clay shrinkage curve showing particle arrangement effects caused by drying. After Kodikara et al. (1999).

2.3.2 Swelling

Swelling is caused by an increase in repulsive forces brought about by clay water absorption and the penetration of ion layers, (Yong & Warkentin, 1975). Water particles are retained by clay particles due to the negative clay surface charge and the positive end of the water dipoles attracting. The negative end of the water molecule will then proceed to attract the positive ends of other water molecules and so forth through hydrogen bonding. This leads to an increase in the number of water molecules between the clay particles, forcing the clay particles apart, (Biddle, 1998a). The magnitude of this Coulomb repulsion is controlled by the concentration of

ions and their type, (Mitchell & Soga, 2005), where the presence of low ion concentrations and ions of a univalent nature will cause an increased amount of water absorption.

In reality, other influences can affect the swell behaviour of a clay. Yong & Warkentin (1975) state that confining pressures and the presence of cementing agents can affect this. As seen in Table 2-7, increasing the plasticity index (PI) of a clay leads to an increase in the degree of expansion or shrinkage.

Table 2-7: Expansive soil classification. After Holtz and Gibbs (1956).

Colloid Content (% minus .0001mm)	**Plasticity Index**	**Shrinkage Limit**	**Probable Expansion (% Volume)**	**Degree of Expansion**
>28	>35	<11	>30	Very High
20-31	25-41	7-12	20-30	High
13-23	15-28	10-16	10-20	Medium
<15	<18	>15	<10	Low

2.3.3 Subsidence

Subsidence occurs when groundwater abstraction is greater than the natural groundwater recharge of the area. This leads to lowering of the water table and consolidation of the sedimentary material as a result of increased effective stress, (Bell, et al., 1988). Freeman, et al. (1994) state that this desiccation tends to increase during the summer and decrease during the winter due to weather patterns. It is also greatest following a period of hot, dry weather and where there is no vegetation, this desiccation is limited to the top metre or so of the soil. Jones & Jefferson (2012) report that in the UK, damage is most frequent as a direct interaction with vegetation and water content variance and is usually situated around the south-east of the country. Pressure in a soil is transferred by water and soil grains so if the pore water pressure is decreased by a reduction in the groundwater level then the pressure must be transferred from the pore water to the soil grains, (Terzaghi, 1925). To adjust to the new stress conditions, the fabric of the soil structure may change; in particular the volume of the voids will most likely decrease. Subsidence of the ground surface does not occur concurrently with ground water abstraction, it occurs after the abstraction has started and is a long term effect whereas the

abstraction can be quick, (Bell, et al., 1988). The damage caused by subsidence often leads to insurance claims, (Crilly, 2001), as detailed in section 2.1.

As subsidence occurs, the stress in the soil system changes over time. Lofgren (1968) states that there are three types of stress involved in the compaction of an aquifer system. The first being gravitational stress, this is due to effective weight of overlying deposits which is transmitted downwards via grain to grain contact. The second is a hydrostatic stress due to the weight of the interstitial water which is transmitted down through the water. The third is a dynamic seepage stress imposed into the grains by the viscous drag of the downwards moving water. The first and third stresses combine to produce the 'effective stress' and changes the void ratio of the soil. The second stress has no effect on the grains and is called the 'neutral stress'.

Poland (1984) states that water level fluctuations can change the effective stresses in the soil system in two ways:

1. Increasing the level of the water table provides buoyant support for the soil grains and decreasing the level removes the support, these changes in gravitational stress are transmitted downwards to all grains below.
2. A variance in the water table level or potentiometric surface can cause vertical hydraulic gradients leading to seepage stress. If seepage stresses already are present then this change in water table level will affect the effective stress.

Atkinson, et al. (1990) states that the stress-strain response of overconsolidated clays depends on their recent stress history whilst Costa Filho (1984) observed that London Clay stiffness depended on the consolidation stress path. The influence of recent stress history however is eliminated under large strains.

2.3.4 Trees, Fauna and Induced Subsidence

The cause of tree induced subsidence (TIS) can be gathered from the interactions of three main factors; volume change of the clay, tree water usage and the local climate, (Jones, 2010). When trees and other fauna grow on a soil surface, the roots below can inflict 1000 – 2000kPa of tension in the water phase before reaching their wilting point, (Fredlund, 1987). Due to a combination of seasonal environmental changes and tree and fauna water demand, volume changes in the soil can extend to depths of over 3m, (Fredlund, 1987). However, it is also

reported that up to 90% of the tree root length occurs in the upper metre of soil with Jackson, et al. (1996) reporting that temperate broadleaves have 82% of their roots in the top 50cm whereas conifers have 70%. Roots are not often found at great depths due to the absence of mineral nutrients and also the difficulty in which the tree finds it to grow roots as roots cannot reduce their diameter to penetrate small pores. This is due to the non-capillary pore space decreasing with depth and an increasing lack of oxygen required for roots to develop. This is of interest at present considering the intention of the proposed treatment technique to add chemicals to a soil.

The distress pattern of a tree tends to follow the drip line of said tree and will extend out radially more for individual trees or clusters when compared to a linear grouping, (Bryant, et al., 2001). It is also known that the shape of a root system can be as varied as the tree's crown, (Plotnik, 2000). It can therefore be noted that when considering the action of a tree on an expansive clay, one must take into account not just the nearest tree, but the whole area.

Further details regarding trees and fauna and their effects on soil can be found in Roberts, et al. (2006).

2.4 Electrokinetics

Electrokinetic effects are what the EKS process relies upon to cause changes to occur in clay. By understanding these processes, one has a better ability to control EKS.

2.4.1 Electrokinetic Phenomena

Electrical and hydraulic flow coupling can result in electrokinetic related phenomena in fine grained soils such as clay, (Mitchell & Soga, 2005). There are four different types of electrokinetic phenomena, namely electroosmosis, streaming potential, electrophoresis and sedimentation potential, Figure 2-8. The streaming potential occurs when double layer charges are displaced in the direction of the flow when water flows under a hydraulic gradient. This generates a potential difference between the electrodes but is in the order of millivolts. Mitchell & Soga (2005) state that equation 2-11 for the volume flow rate shows that the streaming potential is taken into account, but for the most part is neglected unless using soils with very low hydraulic conductivities ($<1x10^{-10}$m/s). Electrophoresis is the movement of charged particles through a colloidal suspension under a potential difference and sedimentation potential is the

potential difference generated when charged particles move relatively to a solution. Sedimentation potential is unlikely to be a factor in this study.

$$J_v = \left[\frac{k_h}{n} + \frac{k_e^2}{\sigma_e n}\gamma_w\right] i_h + \left[\frac{k_e}{n}\right] i_e + RT\left[-\frac{\omega k_h}{\gamma_w n}\right] i_c \qquad 2\text{-}11$$

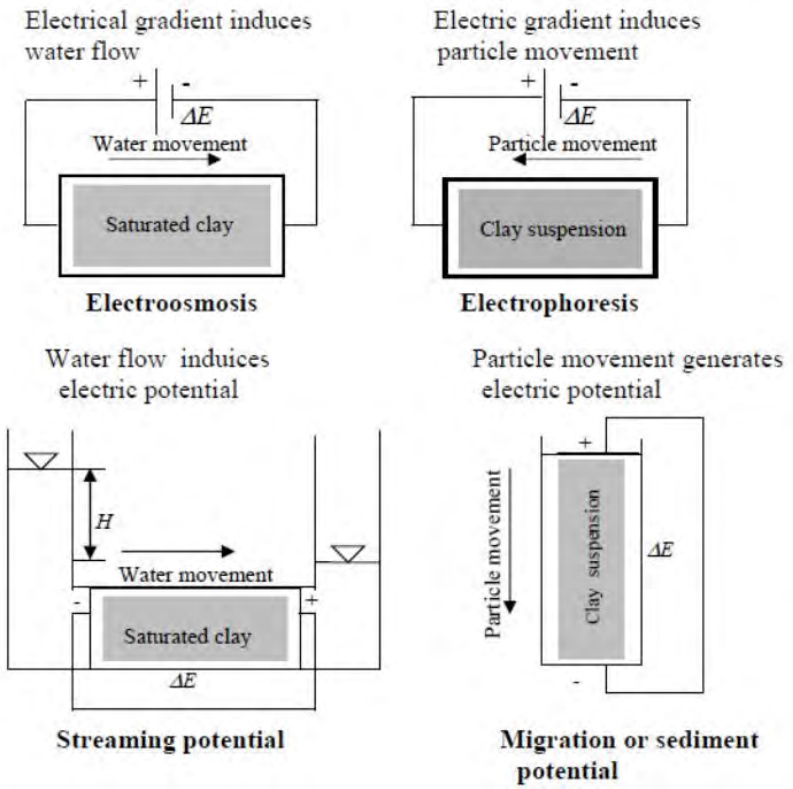

Figure 2-8: Electrokinetic phenomena (Clockwise from top left): (a) electroosmosis, (b) electrophoresis, (c) migration or sedimentation potential, and (d) streaming potential. After Karim (2014).

2.4.1.1 Electroosmosis

Electroosmosis in the present context is the transport of water molecules through a soil matrix by an electrical potential causing cations and anions to be attracted to the cathode and anode respectively. The ion migration involved sees the ions in question carry their water of hydration and exert a viscous drag on water in the region. Due to there being more mobile cations than anions in a typical negatively charged clay water system, the net movement is towards the cathode. The larger the difference in concentrations of the cations and anions, the greater the net drag on the water is. For electroosmosis to occur, Jones, et al. (2011) states that the material

in question must have an electroosmotic permeability value, K_e, high enough and an effective voltage gradient must be maintained across the material. Values of electroosmotic permeability considered high enough are those over $10^{-9}m^2/(s.V)$, (Mitchell, 1993). Electroosmosis can overcome the limitations inherent in low hydraulic permeability soils such as clays and silts when considering hydraulic grouting. Electroosmotic flow in fine grained soils can be 100 to 10,000 times greater than its equivalent hydraulic flow, (Jones, et al., 2011), however Shang (1997) states that the velocity of electroosmotic flow is comparable to a typical hydraulic flow in clay soils. Audebert & de Mende (1959) state that the electroosmotic velocity is found to be proportional to the applied field, inversely proportional to the viscosity and independent of the dimensions of the capillary so long as it is not too small. The potential of producing good electroosmotic flow is increased by the following mineralogical characteristics: high water content, low cation exchange capacity, low valencey exchange cations, high surface charge density and high surface area, low conductivity water, low salinity, a high pH and a low surface charge density per unit pore volume, (Jones & Terrington, 2011). Flow can be calculated using;

$$Q_e = \frac{K_e V}{LA} \text{ where } K_e = \frac{n\varepsilon_w \xi}{\mu} \qquad 2\text{-}12$$

Where K_e = coefficient of electroosmotic hydraulic conducvtivity, n = porosity, ε_w= water permittivity (F/m), ξ = zeta potential (V) and μ = viscosity (Ns/m^2). From this it can be seen that for a maximum flow rate, maximising the voltage gradient is required. Equation 2-12 can be rewritten using Darcy's Law of hydraulic flow as per Casagrande (1952);

$$Q = K_e i_e A \qquad 2\text{-}13$$

where K_e = electroosmotic permeability, i_e = potential gradient and A = area. Electroosmosis is at its most effective in silty clays and clayey silts with electroosmotic permeability of at least $10^{-9}m^2/(s.V)$ and hydraulic conductivity approximately 10^{-9} m/s, (Mitchell, 1993).

It can be seen from equations 2-12 and 2-13 that the electroosmotic flow rate is independent of the individual capillary size and based only upon the entire cross sectional area. The coefficient of electroosmotic hydraulic conductivity is dependent on the zeta potential which in turn is reduced by increasing salt concentrations in the pore fluid, (Mitchell & Soga,

2005). Marine clays with high salt concentrations would therefore not be suitable for treatment as the zeta potential is lowered and therefore the electroosmotic flow rate.

Several theories have been developed to explain the electroosmotic phenomena which can be found in Mitchell & Soga (2005) and is best visualised through Figure 2-9 which shows the cation velocity distribution between clay particles.

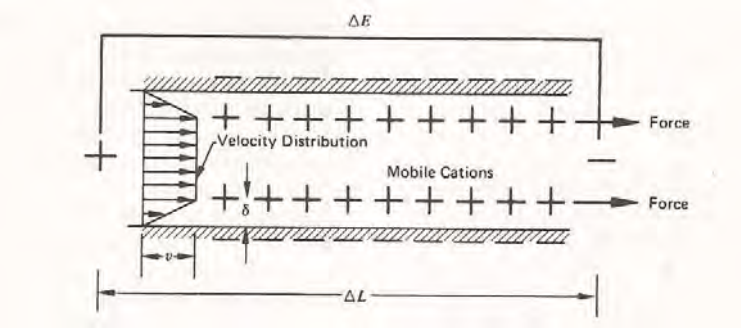

Figure 2-9: Helmholtz-Smoluchowski model for electrokinetic phenomena. After Mitchell & Soga (2005).

Electroosmosis can occur naturally through the generation of self-potentials. These occur when differing chemical conditions are adjacent to each other in a soil. The potentials created are usually up to tens of millivolts and if water accumulates at the interface between the two different chemical conditions, a slip plane can develop.

In depth analysis of electroosmosis can be found in Tikhomolova (1993).

2.4.1.2 Electrophoresis

Electrophoresis can be defined as the movement of electrically charged particles caused by the introduction of a dc electric field. Electrophoresis only occurs under dc currents as the resultant movement under ac would be zero. Hunter (1981) gives the electrophoretic force as;

$$F_e = Q_e E \; where \; Q_e = 4\pi\varepsilon_0 k_w a(1 + \kappa a)\zeta \qquad 2\text{-}14$$

Where F_e is the electrophoretic force vector, Q_e is the total electric charge on the particle, E is the electric field vector, ε_0 is the permittivity of a vacuum, k_w is the relative permittivity of water, a is the equivalent radius of clay particles, $1/\kappa$ is the thickness of the diffuse double layer

and ζ is the zeta potential. The equation is valid for $\kappa a \gg 1$. Electrophoretic direction is always towards the anode due to clay particles being negatively charged.

Although dielectrophoresis is not directly addressed during this study, it is still an important part of the area of research due to its potential for low cost ground treatment. Pohl (1978) reports that dielectrophoretic forces are imposed on clay particles via polarisation of the DDL when a non-uniform alternating current is applied to a clayey soil through electrically insulated electrodes. When an external electric field is imposed, the DDL charges are polarised. If the field is uniform, the distribution of the charges leads to the forces being applied to be equal and opposite. Ergo the resultant force applied to the polarisation charges is zero. If the electric field is non uniform then the resultant force is not zero and migration of particles can take place, (Shang & Dunlap, 1996). The relatively weak dialectrophoretic effect increases for more tightly bound cations whereas the stronger electroosmotic effect decreases, (Lockhart, 1983).

Dielectrophoresis tends to use voltages that are in the region of kilovolts but with currents that are low milliamps leading to power consumption being reported to be negligible as the current is predominantly capacitive, (Inculet & Lo, 1988). Inculet & Lo (1988) also show that by increasing the effective length of the electrodes, one can increase the average surface settlement and increase shear strengths as well as decrease water contents as expected.

2.4.2 Consolidation

Consolidation is a process by which a volumetric reduction can be achieved over time by applying a dead load to the surface of the soil, expelling water and leaving the remaining soil with a reduced volume. If electroosmosis occurs through a compressible soil with no water added to the system then volumetric reduction occurs in an equal magnitude to the water removed. With both traditional dead load consolidation and electroosmotic consolidation, the greater the saturation of the soil mass, the greater the water content reduction and hence greater volume reduction becomes possible. Water is moved by the dc current in electroosmosis from the anode to the cathode for removal causing the majority of consolidation to occur at the anode. This leads to the effective stress increasing and thus the pore water pressure must decrease to keep the total stress constant in accordance with Terzaghi's effective stress equation 2-15;

$$\sigma' = \sigma - u \qquad 2\text{-}15$$

Where σ is the total stress, σ' is the effective stress and u is the pore water pressure. Esrig (1968), Jones & Terrington (2011) and Kaniraj, et al. (2011) state that in one dimension, the pore pressure generated through electroosmosis at distance (x) from the cathode can be written as;

$$U_{eo}(x) = -\frac{k_e}{k_h}\gamma_w \cdot U(x) \qquad 2\text{-}16$$

Where k_e is the electroosmotic permeability, k_h is the hydraulic conductivity, γ_w is the unit weight of water and $U(x)$ is the electrical potential at (x) from the cathode. Rittirong, et al. (2008) report that the negative pore pressure produced by electroosmosis changes Terzaghi's equation to;

$$\sigma' = \sigma - (-u) \qquad 2\text{-}17$$

Resulting in an increase in effective stress and leading to consolidation.

The total stress, effective stress and pore water pressure do not change at the cathode due to the water draining at this point. At an indeterminate point after electroosmosis begins, a larger quantity of water develops at the cathode than the anode and so a hydraulic head can be produced, leading to hydraulic flow from cathode to anode. Electroosmotic consolidation will continue until the electroosmotic force from anode to cathode balances the hydraulic force from cathode to anode, Figure 2-10.

To reduce the sensitivity of the soil to water loss and thus shrinkage/consolidation, one must reduce the plasticity of the soil, by increasing the plastic limit and/or reducing the liquid limit. Reducing the plasticity index of a soil reduces the shrinkage limit and can be brought about by cation exchanges, (Liaki, 2006).

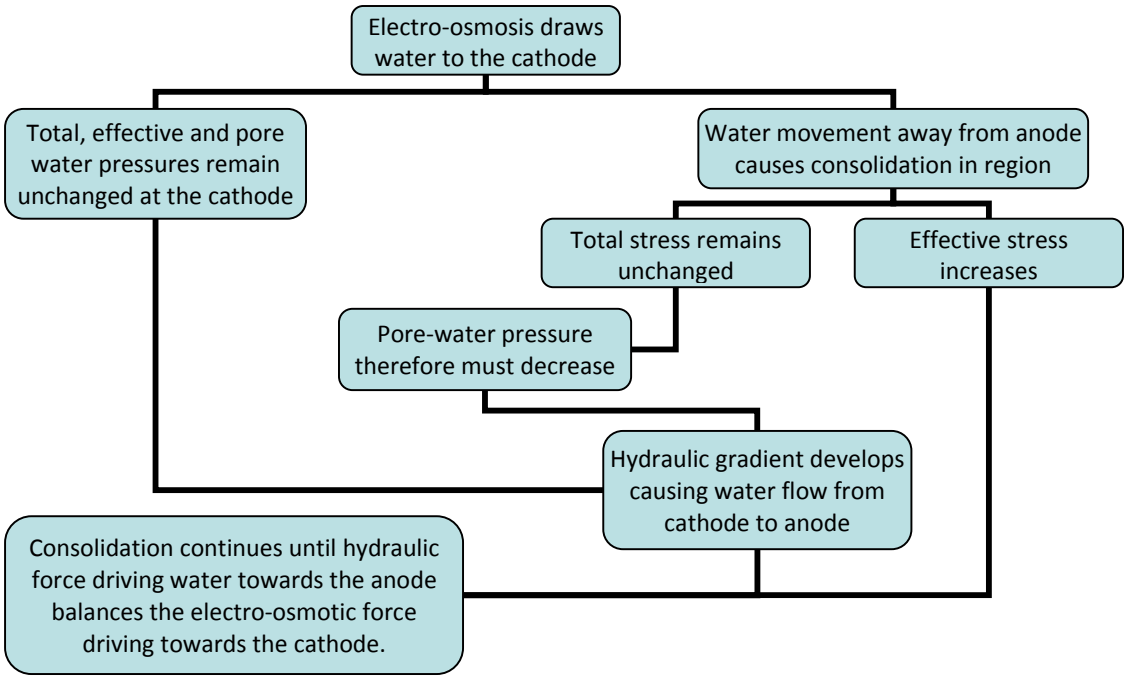

Figure 2-10: Electroosmotic consolidation process.

Consolidation settlement is assumed to continue until the hydraulic force driving the water towards the anode balances the electroosmotic force driving it towards the cathode.

Electroosmotic consolidation provides less compression in over consolidated clays than normally consolidated clays due to the former being a stiffer material. The degree of compression is a function of the effective stress and the soil compressibility where an over-consolidated clay would provide less of a change in void ratio under increasing effective stress than a normally consolidated counterpart, (Mitchell & Soga, 2005).

2.4.3 Electrokinetic Stabilisation

EKS aims to replicate traditional stabilisation techniques but in a less invasive and more economic manner. Electroosmosis and electrophoresis in soil aim to convert an unstable soil to a soil with volume stability. Gray (1970) states that the product of this conversion comes from consolidation, the development of negative pore water pressures and the modification of the flow net adjacent to cuts or excavations. The aim of electrophoresis is to introduce chemical additives to the system with the intention of producing electrochemical reactions such as induration where mineral alteration, ion exchange or introduction of new mineral phases causes a hardening of the soil. The likelihood of these electrochemical reactions taking place increases with increased current densities and pH gradients, (Gray, 1970). The electrochemical reactions

produced during this process account for strength increases that cannot be explained by water removal alone. This combined with Atterberg Limit changes points directly at electrochemical reactions being present. For Atterberg Limits to change, a change in mineralogy, particle characteristics and pore solution characteristics are needed which consolidation cannot provide, (Mitchell & Soga, 2005). Some electrochemical reactions are beneficial, such as electrochemical hardening of the soil whereas others are not, such as heating and gas production.

2.4.3.1 Chemical Stabilisers

Many chemical stabilisers have been trialled over the history of soil remediation research as discussed in section 3.6.1. The introduction of sodium silicate (Na_2SiO_3) and calcium chloride ($CaCl_2$) to clay causes reactions to take place as follows;

$$Na_2SiO_3 + 2CaCl_2 + H_2O \rightarrow 2NaCl + Ca_2SiO_4 + 2HCl$$
$$2Ca_2SiO_4 + 5H_2O \rightarrow 3CaO \cdot 2SiO_2 \cdot 4H_2O + Ca(OH)_2 + 58.6kJ$$
$$3CaO \cdot 2SiO_2 \cdot 4H_2O = Calcium\ Silicate\ Hydrate \quad \text{2-18}$$

Dicalcium silicate (Ca_2SiO_4) is the second most dominant compound in Portland cement and contributes to strength increases in cement later in curing (beyond 7 days) than tricalcium Silicate and thus instant strength gains cannot be expected through this. The dicalcium silicate hydrates to become calcium silicate hydrate (CSH) which in turn crystallises to become a strong brittle solid, (Barker, et al., 2004). The formation of CSH is deemed a pozzolanic reaction and can take 1-5 years to complete. Contamination of the CSH by CO_2 can carbonate the CSH and produce calcium carbonate ($CaCO_3$) however this should be of limited risk due to the depth at which this treatment will be carried out.

Sodium silicate and calcium chloride were not shown to be successful when used together by Heeralal, et al. (2012). Whilst a decrease was seen in the liquid limit and swell potential in the bentonite used, the strength decreased. This is most likely due to the fact that the chemicals require curing time to react and strengthen whereas testing was immediately conducted in this study.

Soil grouting usually utilises the properties of calcium through quicklime as a cementing agent. Once in the system, the calcium will react with elements such as alumina and silica to produce calcium aluminate hydrate (CAH) and calcium silicate hydrate (CSH) gels. Initially these

gels weaken the soil but over time, they crystallise into strong brittle solids, significantly increasing the strength, (Barker, et al., 2004). Depression of the pH can inhibit the dissolution of alumina and silica thus hampering the treatment. The migration of the lime into the soil also induces a reduction in water content thought to be brought about by the pozzolanic reactions consuming the water. The pozzolanic reaction products, the aforementioned gels, reduce soil permeability by crystallising in the void spaces and improve volume stability. These gels also change the mineralogy of the soil and alter the original minerals due to dissolution of compounds. Asavadorndeja & Glawe (2005) show that the simplified pozzolanic reactions are as follows and usually take 1-5 years to complete;

$$Ca^{2+} + 2(OH^{-}) + SiO_2 \rightarrow CSH$$
$$Ca^{2+} + 2(OH^{-}) + Al_2O_3 \rightarrow CAH \qquad 2\text{-}19$$

2.4.3.2 Electrode Corrosion

Dependent on electrode material, corrosion will occur at different rates. For example Eastwood (1997) states that even Electrokinetic Geosynthetic (EKG) materials precipitate matter into the soil due to their carbon polymer coating with typical degradation rates being 9.0 and 0.5 – 2.0kgA^{-1}year^{-1} for steel and carbon respectively. Precipitation of electrode material can affect the surrounding clay and also inhibit the stabilisation efforts by increasing surrounding electrical resistance and reducing the surface area of the electrode. Controlling this corrosion is vital to increasing the lifespan of the electrodes as well as increasing the economic benefits of the procedure.

Corrosion occurs when oxidation transpires at the anode produced from losing electrons whilst reduction takes place at the anode, (Daub & Seese, 1996);

$$Anode: Fe \rightarrow Fe^{2+} + 2e^{-}$$
$$Cathode: O_2 + 2H_2O + 4e^{-} \rightarrow 4OH^{-}$$
$$Thus: Fe^{2+} + 2OH^{-} \rightarrow Fe(OH)_2$$
$$Further\ oxidation: Fe^{2+} \rightarrow Fe^{3+} + e^{-} \qquad 2\text{-}20$$

Fe^{3+} ions are therefore created at the anode and then migrate, under the potential difference, across the soil towards the cathode.

The EKG electrodes are stainless steel coated in a carbon based polymer. Pugh (2002) states that the corrosion of carbon is as follows;

$$C + 2H_2O \rightarrow CO_2 + 4H^+ + 4e^-$$
$$C + H_2O \rightarrow CO + 2H^+ + 2e^- \qquad 2\text{-}21$$

As the carbon based polymer degrades, the number of carbon atoms decreases in the polymer matrix and thus the surface resistivity of the material increases. Also, it is susceptible to degradation of the inner steel if the outer carbon based polymer is damaged in any way.

2.4.3.3 Electrode Polarisation

The application of a current between two electrodes in a conductive medium leads to the movement of charges through the medium. Induced polarisation phenomena occurs due to electrical energy becoming stored in the porous media around the electrodes, (Marshall & Madden, 1959). These charges can build up around the electrodes preventing any further charge movement from occurring. If the separating charges are free, such as in water, then the process converts some of the energy to heat and is lost, (Cassidy, 2008). Figure 2-11 shows how energy is stored in the porous media between the electrodes.

Research has been conducted on the polarisation of the electrodes in resistivity measuring however this is mostly regarding electrodes under frequencies higher than dc. The usual manner of overcoming the polarisation or at least reducing it is to either cease current application or reverse the poles.

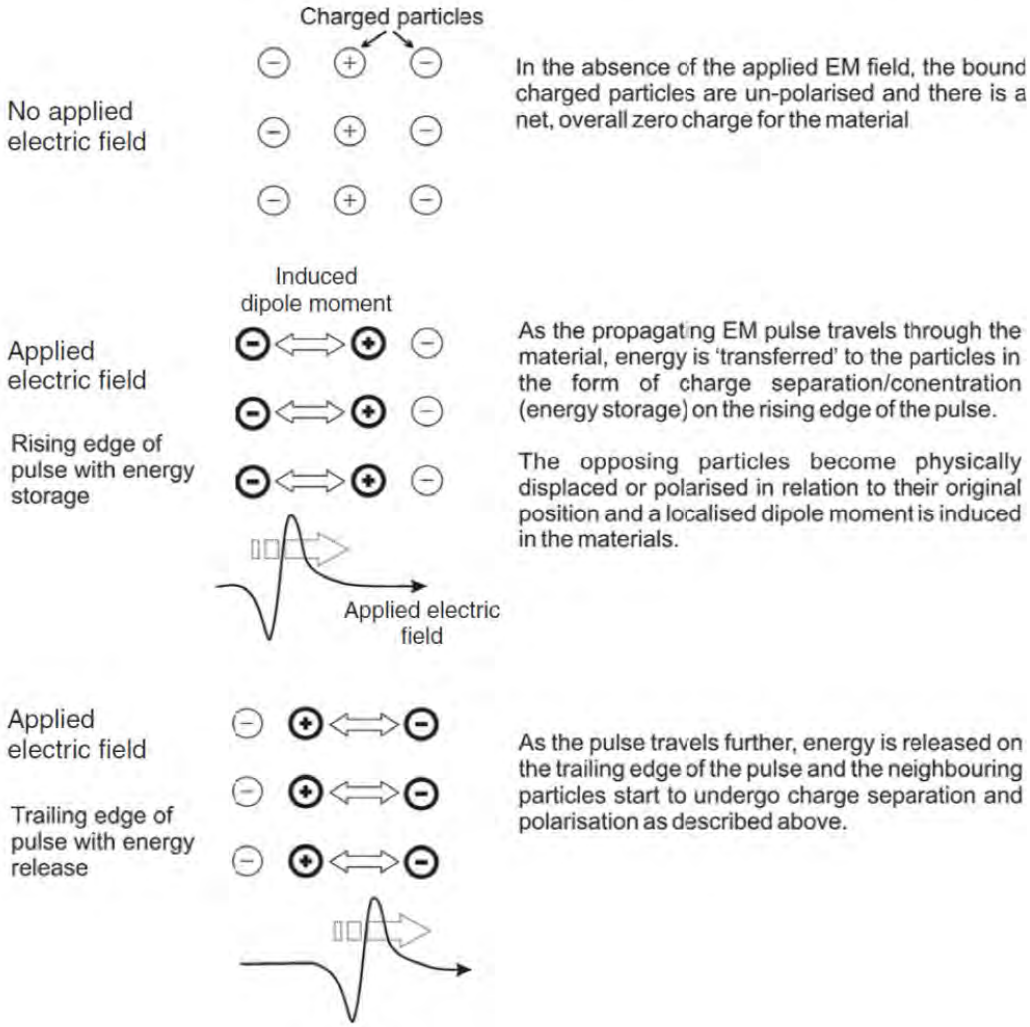

Figure 2-11: Energy storage/release, charge polarisation and the development of a dipole moment. After Cassidy (2008).

2.4.3.4 Foundations

Freeman, et al. (1994) states that multiple types of foundation have been used when constructing low rise buildings in the UK over the past few hundred years. These range from a thin layer of rubble in a ditch to modern trench fill foundations up to 4m deep.

Building regulations did not adopt the 900mm depth foundation guidance until 1965 leaving many buildings built before this time built on woefully shallow foundations. It is reported that the majority of houses in Britain are built with unreinforced concrete strip footings to a depth of between 1m and 3m, (Radevsky, 2001).

These foundations serve as a base to build cavity walls upon in which the individual leaves constructed are weaker than the older block style construction. This has therefore

required the use of stronger cement based mortars rather than the traditional lime based mortar leading to the walls being less flexible and more prone to cracking. The floors of a house traditionally were suspended and thus were not affected directly by ground movement. When the need of coal cellars declined and the use of concrete rose, these floors were replaced by concrete slabs resting on a hardcore base which were directly affected by ground movements.

As such, it can be expected that modern housing has stronger foundations but a weaker structure whereas older housing from WW2 periods possess weaker foundations but stronger structures. The application or withdrawal of fluids around these foundations would therefore result in movement which could produce cracking in the structure.

The depth of considerable influence of the pressure exerted by a foundation onto the soil beneath can be calculated using Boussinesq's pressure bulb theory. It is common practice in the UK to consider a shallow foundation's depth of influence to be equal to 2.5x the breadth of the foundation. Thus it can be deduced that when considering an average strip footing of breadth 0.6m, a depth of influence of 1.5m below the base of the foundation and 0.6m wide from the centre line of the foundation (1.2m total) is produced. With decreasing footing widths one would expect to see decreasing depths of influence also. With older buildings being built on smaller foundations, it is therefore inferred that the bulb of influence will decrease in size. From this it can be seen that the depth and width of ground affected by the building pressure under the foundation can be calculated. It is this bulb of pressure that must be treated, or at least the majority of it, to regain volumetric stability. By concentrating the treatment onto positions assessed as important by the bulb theory, one can carry out the stabilisation procedure more economically.

One may not need to treat the entire bulb to gain sufficient volume stabilisation. It may be possible to treat, for example, a portion from 20% depth to 60% and this could be sufficient. An advantage of the electrokinetic system over other treatment solutions is the ability to install the electrodes in a bespoke array pattern and length in which the treatment zone is specified from pre-treatment investigations. The electrodes being placed as close together as possible will use the least amount of electrical power in completing the treatment. However, the pressure bulb extends out further than the vertical sides of the foundation. By inserting the electrodes close to the foundation, there will be untreated areas of the pressure bulb flanking the footing. This should not be a problem due to the bulk of the bulb being treated directly under the foundation.

Soils of noticeable shrink/swell capacity could occur beneath the electrode influence zones. This is not a significant issue due to the causes of the shrink/swell behaviour being seasonal rainfall and vegetation water consumption. These predominantly affect the top metre of soil only and as such, deeper shrink/swell characteristics should not be triggered to the extent expected of the upper regions. Stiff layers in the treatment zone would cause preferential routes of flow for both electricity and fluids. It is anticipated that an increase in depth of treatment would be required to allow for diminished treatment effects in these layers.

Partial saturation of the treatment zone would inhibit the treatment due to air possessing a higher electrical resistivity than water. A water seeding pre-treatment regime whereby the soil has water introduced to increase saturation would be required. This would of course cause unwanted swell. The groundwater level will affect the zone of treatment with a high water level causing saturation of the soil and a low water level causing partial saturation and at extremes, suction. Due to the aforementioned reasons, the electrode array design would be required to be scheme specific with adaptations made for stiff layers and groundwater levels along with foundation size.

2.4.3.5 Environmental Concerns

Environmentally, little research has been conducted into the effect of electrokinetic phenomena on flora, fauna and trees. Groundwater effects can be extrapolated from the effect on effluent from published experiments. It would be expected that any groundwater in the vicinity of the electrokinetic process would be influenced by hydrogen and hydroxide ions and therefore a change in pH would be prevalent. The use of chemicals as stabilisers would add another dimension in that the groundwater would become infused with the stabiliser's ions. The levels of which, and therefore allowable levels in regard to land owners and official environmental bodies are not covered as part of this study but would require some insight before total acceptance of this process.

Due to the relatively low levels of chemicals and current used in this treatment process, the anticipated effect on the local environment would be minimal. Indeed, through the site trials conducted later in this thesis, it was noted that the local trees and grass surrounding the trials were not visibly affected by the process itself.

One further concern about using this stabilisation process commercially is applying an electrical current to the ground in proximity to humans and animals. There is potential for a

being to come into contact with the electrified ground and receive a shock, however, due to the depth of treatment and low electrical current being used, the likelihood of being electrocuted is extremely low and the likelihood of being negatively affected by said electrocution is negligible.

As seen in section 3.3.2, the usual currents required for EKS to occur effectively are below 500mA, even the use of dielectrophoresis with its inherent high voltages such as 15kV Shang & Dunlap (1996), sees an effective electrical current of approximately 2mA. Greenwald (1991) states that human contact with an electrical current of 2mA is likely to cause a slight tingling sensation and is not particularly dangerous. EKS and its applied 500mA is sufficient to kill but as stated previously, the depth at which treatment occurs and diffusion of current in the ground should lead to negligible risk.

A discussion into the reduction in carbon footprint when using the proposed electrokinetic treatment technique can be found in Appendix A and there is a low risk of unexploded ordnance being triggered by the passing of an electrical current through the ground which can be further investigated through Stone, et al. (2009).

2.4.4 Traditional Subsidence Remediation Techniques

Presently, there are multiple pre and post subsidence actions that can be taken when dealing with subsidence due to trees, including;

1. Tree crown reduction/thinning – Not a viable option due to subsidence recurrences, (O'Callaghan & Kelly, 2005).
2. Tree removal – Cost effective but socially unpopular, (Freeman, et al., 1994), (Cheney, 1988), (O'Callaghan & Kelly, 2005).
3. Root barriers – Costly and ineffective, (O'Callaghan & Kelly, 2005).
4. Artificial stabilisation (underpinning) – Costly and invasive, (BRE, 1991).
5. Lime Stabilisation – See section 2.4.4.1.
6. Soil grouting – Not usually viable due to soil types, (Alshawabkeh & Sheahan, 2003).
7. Artificial recharge of aquifers from the land surface – This involves allowing water stored at the surface to flow into the affected area in an attempt to raise the groundwater level, (Poland, 1984).
8. Paclobutrazol (PBZ) – Not viable due to safety concerns, (Roberts, et al., 2006), (Pesticide Action Network (PAN) Europe, 2007), (Grossnickle, 2000), (Watson, 2001).

9. Others include soil freezing by liquid nitrogen, hydro-fracture grouting which strengthens by introducing strengthening lenses of grout in the soil and induced consolidation by surface loading. These all have drawbacks including changes in soil volume, (Alshawabkeh & Sheahan, 2003).

As can be seen, current methods are inadequate and a cheap solution is required which does not affect the local vegetation.

2.4.4.1 Lime Stabilisation

The process envisaged in this thesis, is essentially based upon the traditional method of stabilisation through addition of lime to soil. Barker (2002) describes how when lime is added to soil, there are four processes that can take place: cation exchange, flocculation, carbonation and pozzolanic reactions. The first two are called the modification reactions and can change the workability, plasticity and swell properties of the soil. Carbonation is detrimental to stabilisation as it consumes the lime needed for pozzolanic reactions and produces weak calcium carbonates. Long term strength is gained through the pozzolanic reactions which raise the pH sufficiently to cause the dissolution of silica and alumina from the clay edges as discussed.

Through lime addition, Ca^{2+} cations are preferentially adsorbed by clay particles leading to a reduction in the diffuse water layer which promotes flocculation. The pH is also raised resulting in the edges of the clay particles suffering from broken bonds which are thought to then attach to the broken bonds of other particles.

Barker (2002) concludes that through lime stabilisation of clay, one can produce water content reduction and thus increased plastic limit, increased strength (albeit, sometimes this increase comes over time) due to pozzolanic reactions, increased or decreased permeability dependant on amount of lime addition and increased volume stability through pozzolanic reaction products and increased tensile strength.

It has been stated that lime stabilisation may not be permanent when the treated clay is open to drying and wetting cycles. Laboratory results indicate that the beneficial gains from lime stabilisation are lost after four wetting and drying cycles as the cemented aggregates began to break down, (Rao, et al., 2001).

2.5 Summary

This section has reviewed the necessary literature available regarding the background to electrokinetic processes in soil. An overview of the theory of clay-water interaction was presented followed by the tangible effects that this interaction can achieve. To this end, the shrink and swell of a clay has been detailed along with the effects of trees and foundations. A background of electrokinetic phenomena was then detailed to bring together the ideas of clay-water interaction and the manipulation of geotechnical characteristics.

While there has been much attention given to the theoretical side of the problem, it is still not completely understood and as such accepted by the wider Geotechnical community. The full efficacy of the stabilising chemicals along with simultaneous electrode polarisation and corrosion in a real world setting is a major gap in the current knowledge with electrode polarisation under a dc electric current being virtually unknown presently. Another major concern which will prevent this proposed remediation technique from being fully accepted is the lack of clarity surrounding the permanence of the chemical stabilising effects.

3 LABORATORY AND SITE TESTING

3.1 Introduction

Two main types of electrokinetic soil stabilisation experiments have been conducted; (1) bench scale studies performed in laboratories and (2) site scale studies performed on appropriate sites. While there are ample examples of bench scale studies available, they are mostly focused on dewatering and remediating soils and furthermore, by comparison, site trials are not common. The bench study type of experiment can again be broken down into two types, these being small scale and large scale with most studies making use of small. Small scale has been defined for the purpose of this thesis as an electrode spacing of <0.5m.

This section will compare the various types of experiments related to electrokinetics, be it stabilisation or remediation. Electrokinetic remediation (EKR) being the same process as EKS except EKS drives ions into the clay whereas EKR involves driving ions out. The goal of this section is to identify both the strengths in the research which can be built upon and also the gaps which require filling.

Although many tests have been reviewed, it is quite difficult to compare the results due to the plethora of variables that are present in each study. For example, electrolyte type, electrode type, voltage gradient, electric current, soil type, specimen size and test duration. However, for ease, each variable is examined separately to assess the nature of its impact as reported in the literature.

3.2 Clay

3.2.1 Clay Type

Multiple clay types have been used in electrokinetic experiments but are mainly kaolinite or montorillonite based. Natural clay samples are heterogeneous and as such will exhibit different behaviours depending on the individual chemical composition and history. This also leads to the various clay types possessing differing geotechnical characteristics such as liquid limits and plastic limits and in turn, the nature of the effect on EKS.

Characteristic values taken from previous research can be seen in Table 3-1. Relatively high liquidity indexes are seen in the majority of the cases which would not usually be found naturally or built upon. As Casagrande (1949) stated, increasing the water content of a soil increases the osmotic permeability of the soil. This high water content is preferable for

determining changes in the laboratory but in reality, for the treatment of subsiding clay that has already been built upon; these water contents are too high.

The initial water contents of the soils can vary wildly also, with Mohamedelhassan (2009) reporting 75% water content in his sample and Barker, et al. (2004) reporting 16.5 – 25.2% water content. The more realistic of these, with regards to naturally occurring soils that would be built upon, have the lower water contents. Liaki (2006) and Tajudin (2012) both used English China Clay (ECC) with water contents of approximately 50% which in a realistic subsidence context, would be too high to be built upon.

Clays such as ECC are quite homogenous in their constituents and have low activity compared to clays susceptible to shrink and swell. Although it is an inert, controllable clay that gives reproducible and repeatable results, as Liaki (2006) and Tajudin (2012) have done, it does not replicate the clay that occurs in site applications.

Table 3-1: Some clay types and their associated characteristics from the literature.

Publication	**Clay Type**	**Water Content (%)**	**Liquid Limit (%)**	**Plastic Limit (%)**	**Plasticity Index (%)**	**Liquidity Index (%)**
(Win, et al., 2001)	Singapore Marine Clay	56	71	28	43	0.65
(Ozkan, et al., 1999)	EPK Kaolin	44	56	30	26	0.54
(Shang & Lo, 1997)	Phosphate Clay	-	141	43	98	-
(Bjerrum, 1967)	Norwegian Quick Clay	31	19	14	5	3.4
(Casagrande, 1949)	Sodium Bentonite	-	600	38	562	-
(Casagrande, 1949)	London Clay	-	80	27	53	-
(Barker, et al., 2004)	Glacial Clay	16.5-25.2		15.8-16.6	-	-
(Asavadorndeja & Glawe, 2005)	Bangkok Clay	90	100	40	60	0.83
(Liaki, 2006)	English China Clay	51	55.6	34.6	21	0.78

Publication	Clay Type	Water Content (%)	Liquid Limit (%)	Plastic Limit (%)	Plasticity Index (%)	Liquidity Index (%)
(Gray, 1970)	Vicksburg Buckshot	-	50	24	26	-
(Mohamedelhassan, 2009)	Inorganic Grey Clay	75	63	22	41	1.29
(Mohamedelhassan & Shang, 2001)	Marine Sediment	100-120	59	32	27	2.89
(Abdullah & Al-Abadi, 2010)	Irbid Soil	27	74	34	40	-0.18
(Kaniraj, et al., 2011)	Clayey Silt	-	62	43	19	-
(Rittirong, et al., 2008)	Clayey Silt	60-77	90	40	50	0.47
(Chew, et al., 2004)	Singapore Marine Clay	-	80	35	45	-
(Jeyakanthan, et al., 2011)	Black Clay	86	101	35	66	0.77
(Rittirong, et al., 2008)	London Ontario Clay	38	30	16	14	1.57

3.2.1.1 London Clay

London Clay originated approximately 60 million years ago where coastal plain swamps, lakes, lagoons and beaches were situated and was laid down over much of north-west Europe in Palaeogene times, (Burnett & Fookes, 1974). London Clay varies from east to west due to its formation in that sedimentation occurred at different rates when the clay was forming due to sea currents and particle sizes. This lead to a variation in the clay's characteristics over the formation profile. The two main outcrops of London Clay in the UK are in the London Basin and the Hampshire Basin. London Clay is composed primarily of illite, smectite or kaolinite and is highly plastic, (Cripps & Taylor, 1986). London Clay formation contains pyrite dispersed about its contents, the weathering of this pyrite, according to Jones & Terrington (2011), leads to acidic groundwater. Crystals of gypsum and selenite, traces of chlorite and also zeolites are found in

the smectite bands. Diminishing abstraction of groundwater from the London area into the underlying chalk aquifer has resulted in a raised groundwater level increasing risk of shrink/swell around foundations.

Table 3-2 shows a selection of studies that utilise London Clay and their recorded natural characteristics. It can be seen that the average plastic limit is approximately 80% with liquid limit being 30%. Using the plasticity chart it can be determined that natural London Clay can be assessed as a very high plasticity clay, (Barnes, 2010). It can also be noted that the activities recorded fall within the normal activity group.

From 370 samples, Burnett & Fookes (1974) show that the mean plasticity index of London Clay is 51% with the range being 40-65%. Schmidt, et al. (2006) state that the in situ London Clay samples taken for their experiments had water contents of 30-35%.

Table 3-2: Selected studies London Clay characteristics.

Study	**Water Content (%)**	**Liquid Limit (%)**	**Plastic Limit (%)**	**Activity**
(Rouaiguia, 1988)	-	87	33	0.98
(Skempton, 1977)*	-	87	35	-
(Mesri & Cepeda-Diaz, 1986)	33	101	35	1.00
(Schmidt, et al., 2006)	30-35	-	-	-
(Barnes, 2013)	-	80	31.7	-
(Ou, 2006)	-	70-80	24-29	-
(Jones, 2010)	-	70-77	21-25	-

*Also reported in (Chandler & Skempton, 1974) and (Skempton, 1985)

By 1940, Wrigley (1940) had established that five zones or divisions existed in London Clay separated by their unique sedimentological features, Williams (1971) extended this work by introducing the notion of only three zones (Upper, Middle and Lower) but dividing each of these three zones into three sub-zones. This idea of subzones is not usually utilised in Engineering due to it being too detailed.

Burnett & Fookes (1974) state that Figure 3-1 is a fairly typical mineral size distribution diagram for sandy London Clay and it can be seen how quartz dominates the coarser fraction of the sample and the clay minerals the finer fraction. The liquid limit was shown to be fairly

irregular in that the average liquid limits saw a gradual 25-30% increase from west of London to the Essex coastline and up to 28% changes in vertical profiles where the Geological Society of London (GSoL) show that the liquid limit is approximately 80% in the east decreasing to 70% in the west. The liquid limit appears to be proportional to the total clay mineral percentage rather than the variation of the different minerals that make up the clay proportion. Regarding the plasticity index, gradual increases from west to east were observed over approximately 30% whereas Jones & Terrington (2011) report increases of approximately 45%, Figure 3-3.

London Clay has a higher activity than other soils meaning it is more sensitive to moisture level changes. The GSoL state that the average activity of London Clay is between 0.75 and 1.00. The GSoL also state that London Clay is regarded as firm to stiff, becoming hard with depth, over consolidated, fissured, inorganic, blue to grey silty clay. Parts can be laminated and can contain nodular claystones and rare sandy partings. The bulk density varies between 1.70 and 2.04Mg/m^3 dependant on weathering extent and location.

McCarter (1984) shows that as the fractional volume of water increases in a sample of London Clay, the resistivity of said clay decreases almost exponentially, Figure 3-2, where the optimum water content is shown to be >35% for a low electrical resistivity.

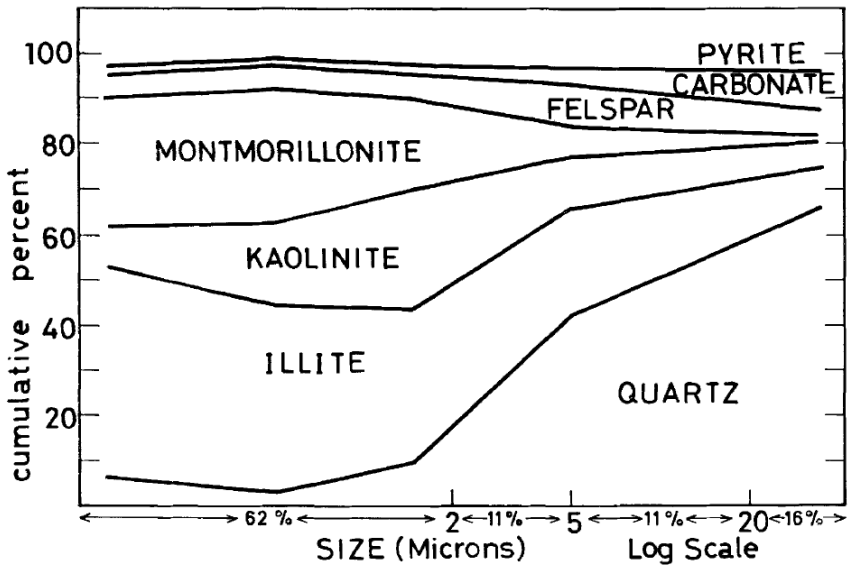

Figure 3-1: Mineral distribution size by fractions within a single London Clay sample. After Burnett & Fookes (1974).

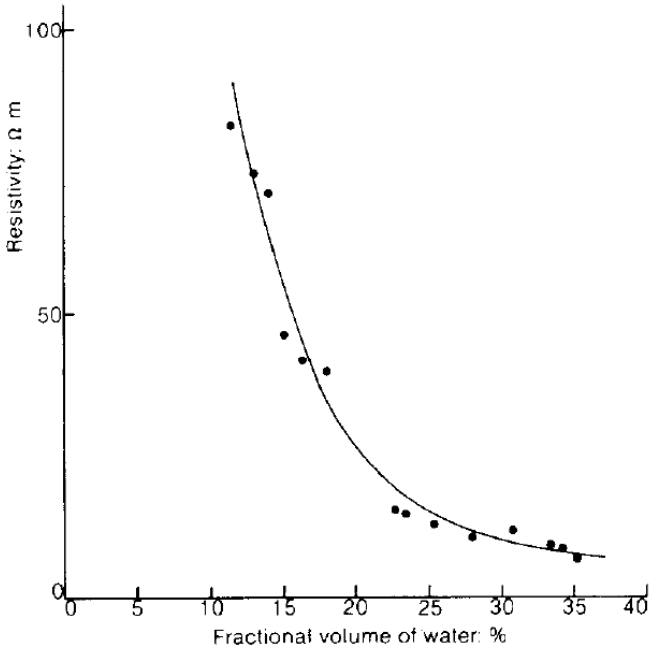

Figure 3-2: Resistivity characteristics of London Clay. After McCarter (1984).

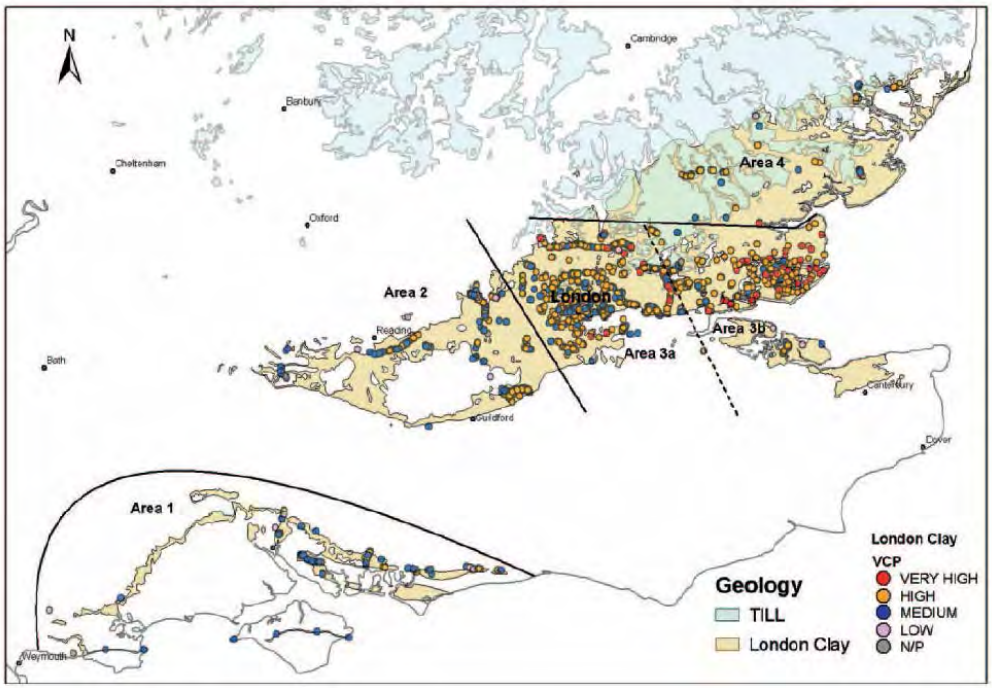

Figure 3-3: Distribution of plasticity data (Ip') across London Clay outcrop. After Jones & Terrington (2011).

3.2.2 Conductivities

There are three main types of conductivity as shown in section 2.2.7; thermal, hydraulic and electro-osmotic where the latter two being key in this research. Here, the key aim is to stabilise soil when hydraulic grouting is not an option. Table 3-3 shows that the electro-osmotic conductivities for clays are much higher than their respective hydraulic conductivities whereas for sands, the hydraulic conductivities are equal to or higher than their electro-osmotic conductivities. This is the main reason to why electro-kinesis is obsolete in sands, and thus electrokinetics should only be employed in situations where the hydraulic conductivity of the specimen is lower than the electroosmotic conductivity. If hydraulic grouting is an available option, it would normally be used as it is a cheaper option. The trend with the electroosmotic conductivities appears to show an increase with water content increase as expected.

There is also the electrical conductivity of electrode materials to consider. Table 3-4 shows the electrical conductivities of common electrode materials and as can be seen, there is a general correlation where the higher the electrical conductivity, the higher the material price. Platinum is the exception here. Utilising a high electrical conductor does mean that the process should be completed in a shorter period of time when compared to using one of lower conductivity.

Casagrande (1949) states that increasing the water content of a soil leads to an increase in the osmotic permeability of the soil and that the pore water distribution during electroosmosis varies depending on the samples access to water. Mohamedelhassan (2009) states that the electrical conductivity of a soil is a component of both its soil particles and water. Mohamedelhassan (2009) goes on to show that removing the water reduces electrical conductivity, and the remaining water's electrical conductivity increases due to reactions taking place. This increase can be larger than the water removals decrease leading to current increases hours after treatment starts.

Barker, et al. (2004) reports that the factors affecting the electrical conductivity of the soil include the solubility of the minerals present, the migration of ions into and out of the soil and the precipitation of compounds as ions mix within the pore water. Mojid & Cho (2006) state that the electrical conductivity of a clay is explained through the developmental stages of the DDL whereas water molecules are introduced to the clay they become adsorbed onto the clay surface. The clay particles become coated and continuous pathways for electron travel are created. As the water content is increased above the maximum conductivity, a decrease is then

approached due to the pathways become more distant as the water outside of the DDL's force the clay particles apart. The electrical conductivity of the water inside the DDLs is higher than that of the water molecules outside the DDLs leading to the drop in electrical conductivity.

Table 3-3: Electroosmotic and hydraulic conductivities of selected soils. After Mitchell & Soga (2005).

Material	**Water Content (%)**	**K_e in 10^{-5} (cm^2/s-V)**	**Approximate k_h (cm/s)**
London Clay	52.3	5.8	10^{-8}
Boston Blue Clay	50.8	5.1	10^{-8}
Kaolin	67.7	5.7	10^{-7}
Clayey Silt	31.7	5.0	10^{-6}
Rock Flour	27.2	4.5	10^{-7}
Na-Montmorillonite	170.0	2.0	10^{-9}
Na-Montmorillonite	2000.0	12.0	10^{-8}
Mica Powder	49.7	6.9	10^{-5}
Fine Sand	26.0	4.1	10^{-4}
Quartz Powder	23.5	4.3	10^{-4}
Norwegian Quick Clay	31.0	20.0-2.5	2×10^{-8}

Table 3-4: Room temperature electrical conductivities for nine common metals and alloys. After Callister (2007).

Metal	**Electrical Conductivity [$(\Omega\text{-m})^{-1}$]**
Copper	6.00×10^7
Aluminium	3.80×10^7
Iron	1.00×10^7
Platinum	0.94×10^7
Plain Carbon Steel	0.60×10^7
Stainless Steel	0.20×10^7

3.2.3 Resistivity

Practically, without physically investigating the soil which is about to be treated, there are few ways of determining the electrical properties in the soil within the treatment area and by proxy, the characteristics associated. Considering that electrodes and an electrical current are already in place for a treatment regime, a resistivity measurement can be taken to conclude the possibility of lenses/layers of higher electrical resistance or other obstructions in the zone of treatment. Failure to identify lenses or other obstructions would cause inefficient treatment and potentially uncompleted treatment.

A soil with a given water content, clay content and density will give a certain resistivity reading when passing an electric current through it. By comparing a reading in the field to an expected value given the ground data provided by a site investigation, one can determine whether a significant deviation from the expected value has occurred and thus conclude the existence of an obstruction.

The resistivity is expected to decrease with increasing water content in a clay and also with increasing temperature, (IAEI, 2004). This is as expected due to the ratio of free water molecules compared to fixed that comes with changing water content and temperature.

Jones, et al. (2009) and Jones (2010) discuss and use resistivity measurements of London Clay to determine underground features and clay bands with associated effects from nearby trees.

3.3 Drivers

The drivers behind EKS are of utmost importance as they, as expected, drive the migration through the clay. The driver in this instance is the electrical force applied through the current.

3.3.1 Voltage Gradients

The overwhelming majority of studies used a voltage gradient of 120 V/m or less, Figure 3-4. The reasons behind this are not always clear but are more than likely to be concerned with possible power output at experiment site and power wastage in the form of heat in the soil. It is possible that limitations of the equipment at hand was responsible. A few studies used higher gradients such as Ozkan, et al. (1999) and Asavadorndeja & Glawe (2005) with 200 V/m and Rabie, et al. (1994b) with 280V/m. It is interesting to note that all of these high gradient tests were completed using titanium electrodes.

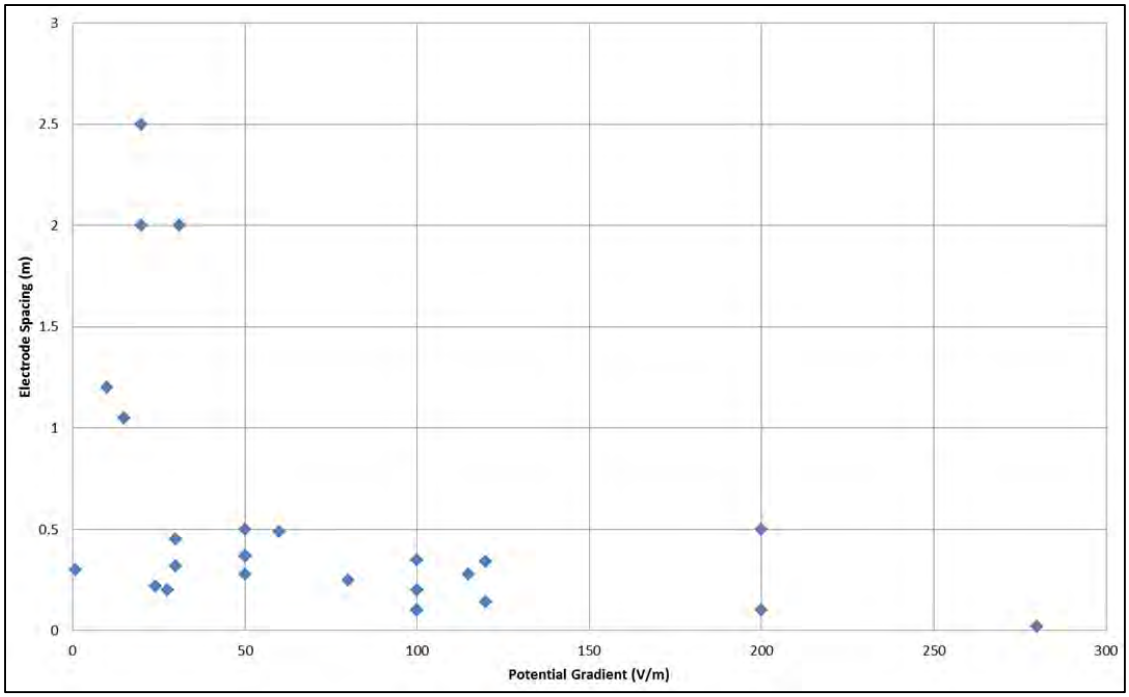

Figure 3-4: Electrode spacing against potential gradients for reviewed studies.

To avoid excessive soil heating and power wastage, an optimum voltage gradient must be reached with Kaniraj, et al. (2011) report that for peat, 120V/m is optimum whereas Casagrande (1949) states that the gradient should not exceed 50V/m to avoid desiccation. Casagrande (1949) also reports that the conductivity of London Clay is increased by 7000 times under a potential gradient of 100V/m. Gray (1970) reported observing an exponential decrease in voltage gradient over time from 100V/m due to the precipitates from the electrodes creating a zone of resistance around the electrodes. Mohamedelhassan (2009) reports that although heating through this method at some times may be beneficial, on the whole, heating and desiccation is not. His study reports that due to this the optimum voltage gradient was roughly 30 V/m in a kaolinite based clay. The build-up of oxygen and hydrogen at the anode and cathode respectively due to electrolysis, section 2.2.4, will create an increased resistance boundary between the electrode and the clay causing the temperature to rise in the area.

Figure 3-4 is a representation of the studied literature's potential gradients against electrode spacing. It shows that there is little correlation and that the majority of cases use small electrode spacing as they are laboratory based. The large electrode spacing cases tend to possess smaller voltage gradients but on the other hand do possess large currents such as 250A and 15A, Bjerrum (1967) and Milligan (1995) respectively.

As discussed in section 7, voltages of 25V at electrode spacings of 0.4m were used on the site trials, which when considering Figure 3-4, is normal for most laboratory studies in the literature. However, the site trials do use greater electrical currents. The laboratory trials presented in this body of work fall into the normal category with an average 50V/m over the trials whilst possessing an average electrode spacing of 0.35m.

3.3.2 Current

The majority of currents used in the studies reviewed have been below 500mA, Table 3-5. Site applications appear to require larger currents with Bjerrum (1967) using 250A and Sprute & Kelsh (1975) using 10-63A. This is most likely due to site applications having larger distances between electrodes than laboratory studies and thus need a higher current to maintain an effective current density. One potential reason for the lower currents in laboratory testing is the available equipment. Most bench power supplies have maximum current outputs of 3A.

Shang & Lo (1997) report that electrokinetic dewatering proves ineffective at current densities below 1A/m^2 whereas Gray (1970) states that excessive heating and power loss is recorded at current densities over 50A/m^2. It is therefore concluded that any treatment should utilise a current density between these values. The current densities recorded in this thesis were approximately 0.33A/m^2 for stainless steel electrodes in ECC and 1.5A/m^2 in the site trials in London Clay.

Over time, the current supplied to the soil in question tends to decrease. Casagrande (1949) attributes the current drop with the corrosion of the electrodes reducing the surface area of the electrodes and the soil resistivity increasing due to precipitation. He also states that anodes should be replaced when the current drops to less than 30% of its original value to keep the treatment effective.

Table 3-5: Selected studies potential differences and electrical currents.

Study	Potential Difference (V)	Current (A)
(Ozkan, et al., 1999)	50	0.09
(Stanczyk & Feld, 1964)	13-15	10.8 (A/m^2)
(Sprute & Kelsh, 1975)	300-450	10-63
(Rabie, et al., 1994)	2.75-5.5	0.03
(Bjerrum, 1967)	50	250

Study	Potential Difference (V)	Current (A)
(Rabie, et al., 1994b)	2.8 (V/cm)	0.09
(Adamson, et al., 1966)	40	1.5
(Acar, et al., 1995)	1 (V/cm)	0.005
(Alshawabkeh & Sheahan, 2003)	10	0.01
(Liaki, 2006)	0.5 (V/cm)	0.031
(Gray, 1970)	<1 (V/cm)	1-5 (mA/m^2)
(Mohamedelhassan, 2009)	10	0.08
(Mohamedelhassan & Shang, 2001)	8	0.233
(Ju, et al., 1991)	4-15	0.07-0.110
(Milligan, 1995)	115	15
(Jeyakanthan, et al., 2011)	4.5	0.005
(Rittirong, et al., 2008)	45	0.150
(Rittirong, et al., 2008) Site Trial	10	400

3.3.3 Dielectrophoresis

The vast majority of studies found in the literature have been conducted using dc current, Table 3-5. Lo, et al. (1992) studied dielectrophoresis where the electrical phenomenon of applying a low alternating current and high non uniform electric field was considered. Dielectrophoresis can be defined as the movement of uncharged particles through a medium having a dielectric constant that differs from the particle and is under the influence of a dc or ac non uniform electric field. The direction of movement depends on the dielectric constants of the particle and medium, if the particle has a larger dielectric constant, the particle will move towards increasing electric field strengths.

Shear strength increases were recorded of about 960% for Wallaceburg Clay and 150% for Gloucester Clay, (Lo, et al., 1992). However, most of these results were gained by laboratory vane testing in high water content clays so are not overly reliable. The main obstacle of using this dielectrophoresis is the high voltages needed where 18-25kV was used in this study and up to 280V used by Lockhart (1983). However, with the Gloucester clay appearing to be over consolidated after treatment, no pH change due to the effects of electrolysis and good shear strength increases, it can be concluded that this as an effective procedure.

Inculet & Lo (1988) state that due to the electrodes being electrically insulated, the current is mainly capacitive and therefore the real power used is negligible. Detailed analysis of dielectrophoresis can be found in Pohl (1978).

Regarding this body of work, dielectrophoresis will not be used due to Health and Safety regulations but will be an important step in the future of this field of study.

3.4 Electrodes

For optimum electrode performance, clay contact is required. With this contact comes the possibility for ion precipitation into the clay when electrolysis of the system water takes place. Ion precipitation can be both beneficial and a hindrance with Fe ions causing both strength gains and resistance increases, (Eastwood, 1997), (Casagrande, 1949). The shape of the electrode also affects the EKS process due to unique electric field patterns for every shape and size of electrode as discussed in section 6.3. It is therefore necessary to gather as much information regarding previous experimental electrodes as possible.

3.4.1 Electrode Material

The electrode material will affect the effectiveness of the electrode and therefore will also affect the power consumption. Mohamedelhassan & Shang (2001) reported that materials with the least electrochemical potential will have the least amount of voltage loss when in use. Their study showed that iron with an electrochemical potential of -0.44 V has a lower voltage loss at the electrode soil interface than that of copper at 0.34 V, with the advantage of iron oxide being a natural cementing agent. The only potential electrode materials with lower electrochemical potentials are aluminium and zinc at -1.662 and -0.763V respectively, (Callister, 2007). Stainless steel is partly made up of zinc and iron which would explain its success as an electrode. Mohamedelhassan & Shang (2001) provided Figure 3-5 which shows the various electrode materials against the efficiency factor β. β is the percentage of effective voltage to applied voltage of the potential drop at the electrode soil interface. The effective voltage is that which is not lost in the transference from electrode to clay. It can be seen that metallic anodes are more efficient that carbon anodes by about 20%.

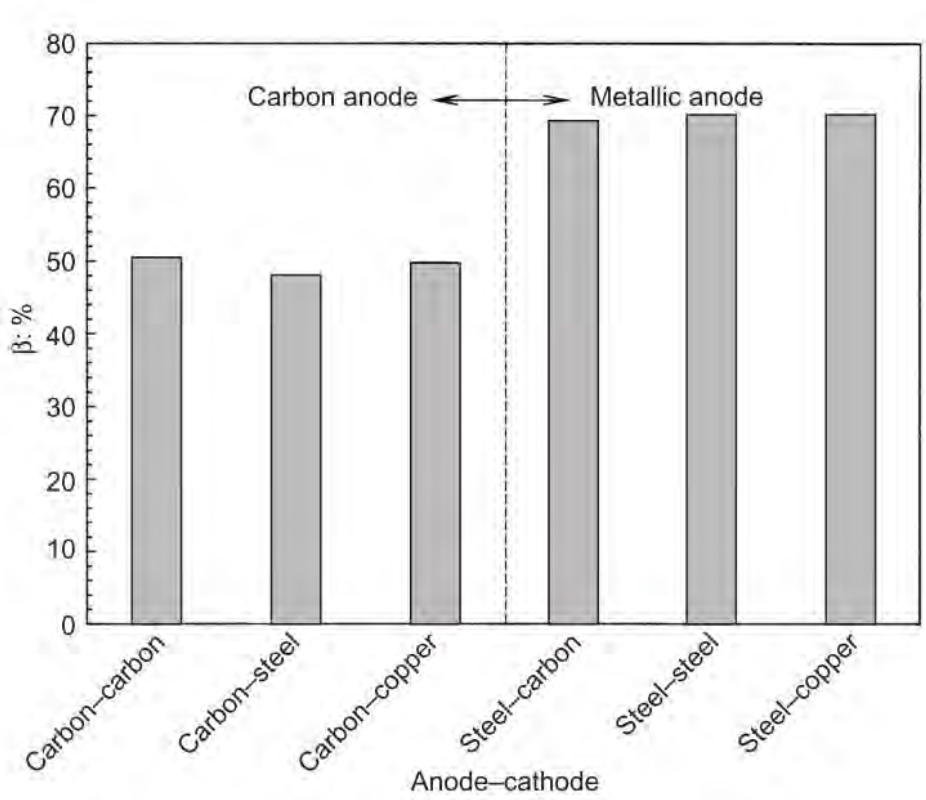

Figure 3-5: Electrode materials against the efficiency factor, β. After Mohamedelhassan & Shang (2001).

Table 3-6: Corrosion rates for common anodic materials. After Eastwood (1997).

Anode Material	**Atomic Mass**	**Degradation Reaction**	**No. Of Electrons**	**Stoichiometric predicted consumption (kg A^{-1} $year^{-1}$)**	**Typical corrosion rate (kg A^{-1} $year^{-1}$)**
Fe	55.85	$Fe \rightarrow Fe^{2+}+2e^{-}$	2	9.1	9.0
Al	26.98	$Al \rightarrow Al^{3+}+3e^{-}$	3	2.9	4.5
C (graphite)	12.01	$C+2H_2O \rightarrow CO_2+4H^{+}+4e^{-}$	4	1.0	0.5 – 2.0

Inert electrodes are sometimes used to avoid corrosion and the necessity for replacement but Eastwood (1997) states that even EKG materials precipitate matter into the soil due to their carbon coating with typical degradation rates being 9.0 and 0.5 – 2.0kg$A^{-1}$$year^{-1}$ for steel and carbon respectively, Table 3-6. EKG's are composed of a steel mesh coated in a carbon filled polymer. Szczepanik, et al. (2009) shows that at lower thicknesses, the greater the concentration of graphite in a polymer coating, the lower the surface resistance will be, Figure 3-6. Senftle, et al. (2010) shows however that due to hydrogen and oxygen adsorption by graphite electrodes, the effectiveness of graphite as an electrode material is limited. Segall &

Bruell (1992) supports this by stating that graphite electrodes produce half the fluid flow for equal power to iron electrodes.

Mendez, et al. (2012) compared stainless steel, a carbon cloth and two titanium variety electrodes in an in-depth comparison with the conclusion that the titanium was the most effective. As mentioned previously, a few studies used higher voltage gradients such as Ozkan, et al. (1999) and Asavadorndeja & Glawe (2005) with 200V/m and Rabie, et al. (1994b) with 280V/m which all used titanium electrodes. The obvious negative aspect of titanium use is its cost, with 2014 prices putting it at approximately 8x more costly than stainless steel. Almeira, et al. (2009) utilised titanium as an anode due to its ability to tolerate acidic conditions and resist oxidation with stainless steel at the cathode due to its ability to resist reduction and basic conditions. Jenny (1940) states that aluminium as an anode does not work well as it tends to develop large resistances to current. This is most likely due to corrosion and gas generation but is not specified.

Stainless steel and titanium appear to be very successful electrodes regarding electrokinetics and with stainless steel being the cheaper of the two, would also be most economical.

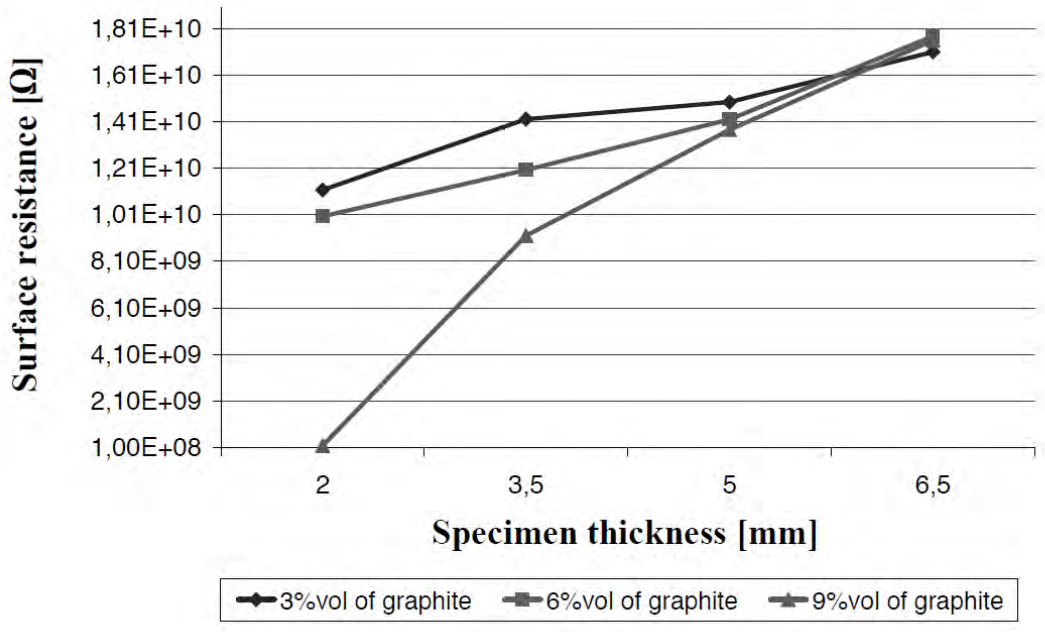

Figure 3-6: Relationship between surface resistance and specimen thickness. After Szczepanik, et al. (2009).

3.4.2 Electrode Shape

The shape of the electrode is important due to its effect on the electric field generated and the method in which the electrode will be inserted into the ground.

A small amount of test cases thus far have used flat disc electrodes in a laboratory, (Gray, 1970), (Win, et al., 2001). Whilst being successfully used, flat plate electrodes aren't practical for site use considering electrolyte insertion and effluent removal.

Flat sheet meshes have been utilised in previous studies more than flat plates. The meshes allow for a uniform electric field to be generated between the electrodes with the opportunity for fluids to pass through them for insertion and collection, (Ozkan, et al., 1999), (Shang & Lo, 1997), (Rabie, et al., 1994). Whilst again, success has been found using these meshes, laboratory experiments are a far cry from site trials. Inserting sheet mesh electrodes into the ground in a manner in which good electrode-clay contact is made is not practical.

Rods have been used successfully for dewatering clays, (Shang & Lo, 1997), (Stanczyk & Feld, 1964), (Acar, et al., 1995), (Adamson, et al., 1966). Again, rods are not practical for introducing electrolytes and extracting effluent in a site based scenario.

Hollow tube electrodes have seen success in dewatering, (Sprute & Kelsh, 1975), (Mohamedelhassan, 2009), (Adamson, et al., 1966), (Burnotte, et al., 2004), (Mohamedelhassan, et al., 2008), (Zhinkin, 1952), and for introducing chemicals into the ground, (Barker, et al., 2004). Hollow tube electrodes are ideal for site usage due to their ability to hold fluids for insertion and extraction in a similar manner to Prefabricated Vertical Drains (PVD's). PVD's have been modified to use the electrokinetic method for moving water towards the drains in a development called Electrical Vertical Drains (EVD's), (Chew, et al., 2004), (Rittirong, et al., 2008), (Nizar & Clarke, 2014).

For their simplicity, success rate in the literature and practicality of installation, hollow tubular electrodes will be pursued in this study.

3.4.3 Electrode Spacing

As seen in Figure 3-4, the electrode spacings in the literature reviewed were on average under 0.5m with a small number of case studies revealing spacings of over 1m, (Barker, et al., 2004), (Zhinkin, 1952), (Milligan, 1995), (Bjerrum, 1967). The majority of those reviewed are bench scale tests which do limit the electrode spacing to below 500mm. It can be expected that as the number of site scale tests increases, so will the average electrode spacing.

The spacing between the electrodes will affect the rate at which the EKS process takes place. As the distance between the anode and cathode increases, the duration of treatment will increase due to discontinuity of the flow of current, (Stalin, et al., 2011). A proportional increase in current with increase in spacing should negate this but would use more power.

A one anode and one cathode configuration performed better for remediating soil than a radially configured array with a central cathode according to Turer & Genc (2005). This is most likely, however, due to the electric current density profile. The one anode and cathode were plates which possess uniform fields between them whereas the radial setup consisted of poles which are not so uniform and thus wastage occurs and spots of no current density can occur as shown in section 6.3. Kaniraj, et al. (2011) showed that two anodes with one cathode is a most effective configuration whereas Almeira, et al. (2009) shows how two cathodes and one anode is most effective. These two trials were not directly compared so are not conclusive.

Direct contact with the soil to be treated has been shown to yield a higher rate of treatment. Most studies use direct contact but Mendez, et al. (2012) compares direct contact and non-direct concluding that direct produces a higher rate of hydrocarbon removal.

3.5 Economics

3.5.1 Cost

It is expected that for subsidence remediation this technique will be more economical than the traditional underpinning techniques. Related works that have been priced include Jones & Terrington (2011) in which a railway embankment was stabilised instead of using gabion baskets and slope slackening. This project resulted in a 26% cost saving. Bjerrum (1967) reports that the entire treatment of 2000m^3 cost a total of 16,000 Norwegian Krone which converted to GBP is approximately £16,000 in 2015.

Elsewhere, Burnotte, et al. (2004) report that 7% of the total cost was spent on electricity and 30% on electrode installation leading to the conclusion that the length of treatment may not majorly affect the overall cost once installation has taken place.

3.5.2 Energy Consumption

The energy expenditure over the course of this treatment varies dramatically based on specimen size and electrode types amongst other variables. Consumptions vary from 0.7kWh/m^3 for a site test to 420kWh/m^3 for a lab test, (Rittirong, et al., 2008). This large

difference is most likely due to the largely differing voltages where the lab test uses approximately 70-130V/m and the site test using approximately 7-29V/m. Asavadorndeja & Glawe (2005) report an energy expenditure of approximately 120kWh/m^3 in their studies where Adamson, et al. (1966) report a figure of 1.225kWh which based on the sizes of the specimens is about 240kWh/m^3. This could be down to the higher voltage used by Adamson, et al. (1966) or due to the fact that they were only de-saturating and not introducing chemicals. As seen in Table 3-7, power usages appear to be lower for the larger site trials. This may be due to the calculation of the kWh/m^3 values where small samples with large power supplies will have large powers compared to site trials which have a similar power supply but much larger volume of treated soil. Laboratory trials may be overpowering the electrokinetic system which leads to a higher power consumption.

These figures naturally depend on many variables but the idea is presented as to what can be reasonably expected. To minimise energy expenditure, and therefore cost, reduction of corrosion occurring at the electrodes is required. Restricting metallic ion precipitation into the soil will prevent the build-up of resistive zones around the anodes and keep the electrode surface area at a maximum, ensuring the power is not wasted through heating. Resistive zones can build up due to excess drying of the regions around the electrodes, so excessive heating through large voltage gradients should be avoided. Shang & Lo (1997) state that using an intermittent current reduces the power consumption of the set up.

Table 3-7: Selected studies and their power consumptions.

Study	**Site/Laboratory**	**Power**
(Shang & Lo, 1997)	Laboratory	16.5 (kWh/m^3)
(Stanczyk & Feld, 1964)	Laboratory	21.3 (kWh/ton of water recovered)
(Rittirong, et al., 2008)	Laboratory	430 kWh/m^3
(Segall & Bruell, 1992)	Laboratory	0.01-0.02 (kWh/L)
(Asavadorndeja & Glawe, 2005)	Laboratory	120 kWh/m^3
(Adamson, et al., 1966)	Laboratory	1.225 kWh
(Alshawabkeh & Sheahan, 2003)	Laboratory	60 kWh/m^3
(Gray, 1970)	Laboratory	30 kWh/m3
(Mohamedelhassan, 2009)	Laboratory	54 Wh
(Rittirong, et al., 2008)	Laboratory	200-430 kWh/m^3

Study	Site/Laboratory	Power
(Mohamedelhassan, et al., 2008)	Laboratory	7.5 kWh
(Zhinkin, 1952)	Site	46 kWh/m^3
(Jones, et al., 2011)	Site	11.5 kWh/m^3
(Bjerrum, 1967)	Site	30,000 kWh or 15 kWh/m^3
(Sprute & Kelsh, 1975)	Site	13 (kWh/m^3)
(Rittirong, et al., 2008)	Site	0.7 kWh/m^3
(Chew, et al., 2004)	Site	1.8 kWh/m^3

3.6 Chemistry

3.6.1 Electrolytes

Electrolytes used in previous experiments are numerous and include the following; phosphoric acid, aluminium ions, calcium ions, calcium chloride, sodium silicate, aluminium sulphate, aluminium acetate, nitric acid, sodium carbonate, aluminium chloride, sodium chloride, sodium hydroxide, potassium chloride. As can be seen, these chemicals are primarily composed of aluminium, calcium, sodium, potassium and phosphorous. Reasoning for why one particular chemical is chosen over another is not usually given although it is thought to be cost oriented. The most effective in the literature so far seems to be the phosphoric acid with large increases in undrained shear strength due to it. Gray (1970) specifies sodium chloride as suitable for use due to it being economic and its tendency not to precipitate at high pH's. Nitric acid can switch the direction of electroosmotic flow by reversing the surface charge of Boston Blue Clay in a low pH, (Alshawabkeh & Sheahan, 2004).

Xeidakis (1996) states that using magnesium and calcium together is preferable over calcium or magnesium alone due to the clay aggregate being more stable than the individual clays. It is stated that Mg-hydroxide is adsorbed by the internal clay and forms a layer of brucite which retards swelling capabilities. Adsorption of further chemicals was reduced by up to 90% by the external phase of the Mg-hydroxide on China Clay and Oxford Clay and it is reported that the introduction of these chemicals to a clay causes irreversible effects on it. This study, however, was based on the best conditions for hydroxide adsorption which included a dilute and well-dispersed clay suspension (1% clay) and a pH of 10-12, both highly unrealistic. Park, et al.

(2006) shows that the PI of kaolinite can be decreased from 18 to 7 by the addition of 100mg/L of $CaCl_2$.

3.6.2 Mixing Water

Where clay samples were produced using a powder mixed with water, consideration of the effects of the type of water used was not common. For example Abdullah & Al-Abadi (2010) mixed their clay with distilled water ensuring no alien particles could enter the mix without their knowledge of it, whereas Alshawabkeh & Sheahan (2003) mixed theirs with tap water containing unknown elements. Without a chemical break down of this tap water, it is not known what minerals were being added to the soil and thus it is not known to what extent the treatment introduces particles through precipitation and electrokinetics.

Tap water varies significantly from area to area and country to country so this effect could be large relative to each area. It is also known that tap water is more electrically conductive than distilled or reverse osmosis water (RO water), as shown in section 6.2.3, which will lead to a more effective treatment process in the time allotted.

3.6.3 pH

An acid is a solution in which the concentration of hydrogen ions exceeds the concentration of hydroxyl ions and an alkali is the opposite, (Trethewey & Chamberlain, 1995).

pH fronts move across the soil specimen due to electrolysis and can hamper ion migration. Acid and base fronts move through the soil from the anode and cathode respectively. Their migration speeds differ due to hydrogen ions migrating faster from the anode than hydroxide ions migrate from the cathode caused by water flow and a greater concentration of hydrogen than hydroxide ions, (Barker, et al., 2004). He also states that to bring about traditional chemical stabilisation, the pH needs to be raised above 10 ideally.

Electrolyte buffering is a way of controlling the pH. Gray (1970) introduced CO_2 into the catholyte to do this and reported an increased electrolytic transfer rate and an increased frontal movement. Alshawabkeh & Sheahan (2004) reported that an acid front creates higher electric conductivity near the anode. If acidification goes too far, reversal of the soils polarity can occur, causing electroosmotic flow to reverse. However, increasing electric conductivity in the soil causes the current to increase too, leading to a more efficient process.

Asavadorndeja & Glawe (2005) state that precipitation usually occurs in pH's of 7 and over while Yamaguchi & Matsuda (1975) state that for full precipitation of aluminium hydroxide, a neutral pH is needed. This suggests that chemical stabilisation should occur around the cathode region when not using the depolarisation technique, whereas, Liaki (2006) and Tajudin (2012) show most chemical stabilisation at the anode.

It has been show here that the pH of a system will affect the electrokinetic process but could also affect other objects in the environment. Rabie, et al. (1994) reports pH's of 2 to 12 over the soil sample and these extreme pH's left for long enough can do significant damage to piping and concrete foundations.

3.7 Practical Effects

3.7.1 Implementation

In practical situations, the actual implementation of the treatment system could be a problematic element of the treatment. The vast majority of case studies reviewed have been laboratory based where little concern is given to implementation due to the size of the experiments. In site applications, soil anomalies such as rocks and debris will make any attempt to insert electrodes difficult by hand. Bjerrum (1967) claims to have inserted 10m electrodes by hand into the Norwegian quick clay used in his study and Glendinning, et al. (2008) also inserted their electrodes by hand although both were dealing with a sludge like material of high water content. Burnotte, et al. (2004) inserted electrodes by drilling them into the ground using water well drills.

The hand drilling method would be economically difficult in most scenarios where a subsidence ridden clay is to be treated, leading to the following as feasible methods of electrode implementation;

- Driving poles or tubes using machinery assuming electrodes are robust enough,
- Driving mesh poles using casings again assuming robustness,
- Digging trenches and inserting mesh, this could lead to problems with electrode soil contact without an appropriate intermediate material,
- Boring hole and inserting pole/tube, again raises issues with soil electrode contact.

The above mentioned soil electrode contact issues would most likely be negligible in EKS due to the constant addition of water to the system.

3.7.2 Times

Testing times vary quite considerably dependent on the type of test and the size of the test amongst other variables. The times range from 120 minutes to 120 days where the latter was Bjerrum (1967)'s full scale site test. This full scale trial treated 2000m^3 of Norwegian Quick Clay using 0.2V/m and 190 electrodes. The 120 minute trial was conducted by Ju, et al. (1991) on a bentonite $CaCl_2$ mix in a water removal effort for a 50mm diameter cylindrical sample of 450mm length. Figure 3-7 shows a general increase in treatment time for increase in electrode spacing, this is generally true but is affected by clay type, water content, electrodes, voltage and current and electrolytes. It is known however that the improvements produced are a function of the treatment time and voltage gradient, (Nizar & Clarke, 2014).

It appears depolarisation of the electrodes can decrease the time needed to apply the treatment where Asavadorndeja & Glawe (2005) reported that the shear strength continued to increase one week after treatment ceased.

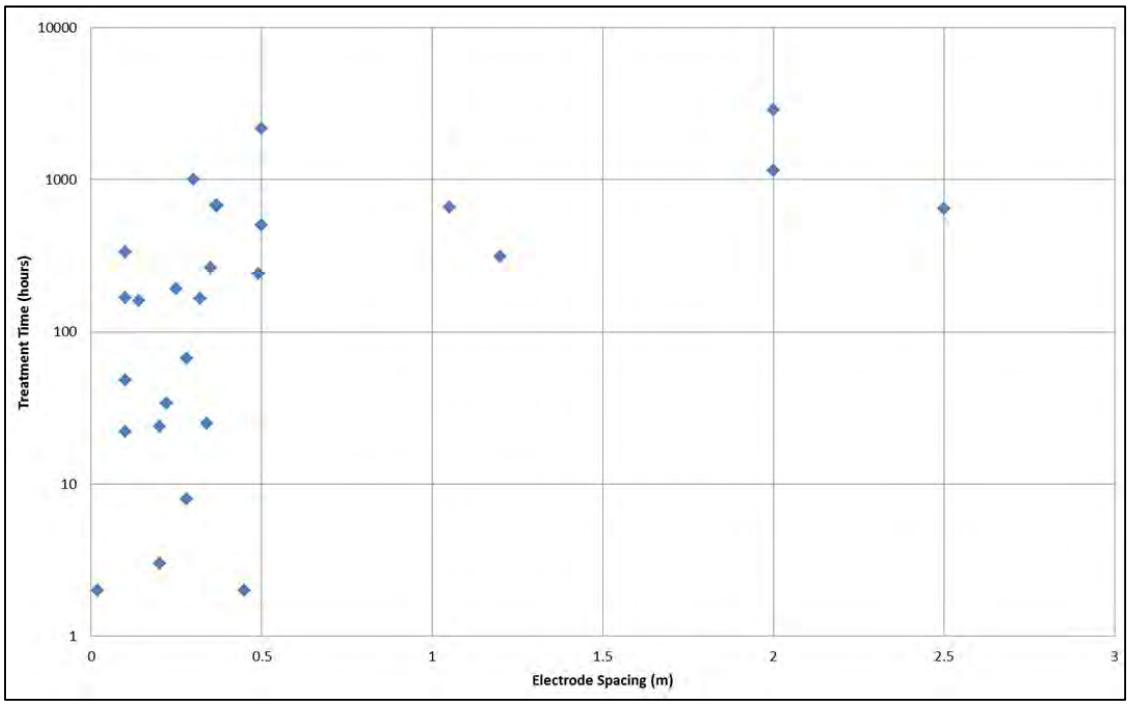

Figure 3-7: Electrode spacing against treatment times of the studies reviewed.

3.7.3 Temperature Increase

Electric current flow through any substance is likely to produce energy as heat. This is true for the soil system and the electrodes where heat is radiated from the electrodes. This heat

primarily dries the soil in the immediate vicinity of the electrodes assuming no fluid addition, reducing the efficiency of the electric current. Mohamedelhassan, et al. (2008) report that the temperature increases by 5-20°C in the treatment zone, Burnotte, et al. (2004) showed that temperatures of up to 100°C at the anode were achieved with averages of around 30-40°C across the specimen. Adamson, et al. (1966) reported that a temperature of 38°C was reached around the electrodes although from what initial temperature is unknown.

These temperatures, although laboratory based, can be compared to site temperatures at depths of 1m where yearly temperature variations can be as little as 2 or 3°C and at 2m there are no variations at all, (Roberts, et al., 2006).

3.7.4 Current Intermittence

Current intermittence is not widely used in experimental practices for this treatment. The process involves providing an electric current for a given period of time and then ceasing the current for another period of time, repeating the cycle as required.

Mohamedelhassan & Shang (2001) state that the process works by redistributing the charges via current interruption. Under a dc electric field, the clay particles and their double layers will polarise. This resulting charge orientation is against the applied field and thus reduces the effectiveness of the field to transport water. The intermittence reverses the polarisation and allows the charges to realign with the applied field, increasing efficiency. The optimal intermittence intervals are mainly dependent on the relaxation time of the system, with the relaxation time being the time taken for the double layer to realign with the applied field.

Shang & Lo (1997) report that 15 minutes on and 5 minutes off was the most effective for their cell arrangement. Their second study used a larger tank and with a longer treatment time utilised 5 minutes on and 2 minutes off and furthermore, using this process reduced power consumption. Rabie, et al. (1994)'s study was short in time and small in size and used 30 seconds on and 5-20 seconds off whereas Mohamedelhassan, et al. (2008) and Mohamedelhassan (2009) both used 2 minutes on and 2 minutes off. Mohamedelhassan & Shang (2001) used 2 minutes on and 1 minute off which lead to an increase in electroosmotic permeability of up to 100% compared to using continuous dc current, Figure 3-9.

The authors who used current intermittence all reported increased rates of stabilisation and Rabie, et al. (1994) reported that short circuiting the system when the current is off increases the rate of dewatering. Mohamedelhassan & Shang (2001) stated however that by

keeping the circuit open when the current is off, one can increase the electroosmotic permeability of the soil. The closed circuit residual current enhances the ability to realign the double layer charges but also reverses the electroosmotic flow. The open circuit residual voltage reduces the energy required to recharge the system when the current is reapplied.

Buckland, et al. (2000) reports that when using current intermittence for electrokinetic sedimentation of contaminated sediment, constant current showed better performance than intermittent current as seen in Figure 3-8. This figure shows that intermittent currents have poorer performance than constant current (power consumption coefficient of 100% is constant current). It is thought that this is due to electrokinetic sedimentation being linearly related to consumed power and thus intermittent current would not be beneficial.

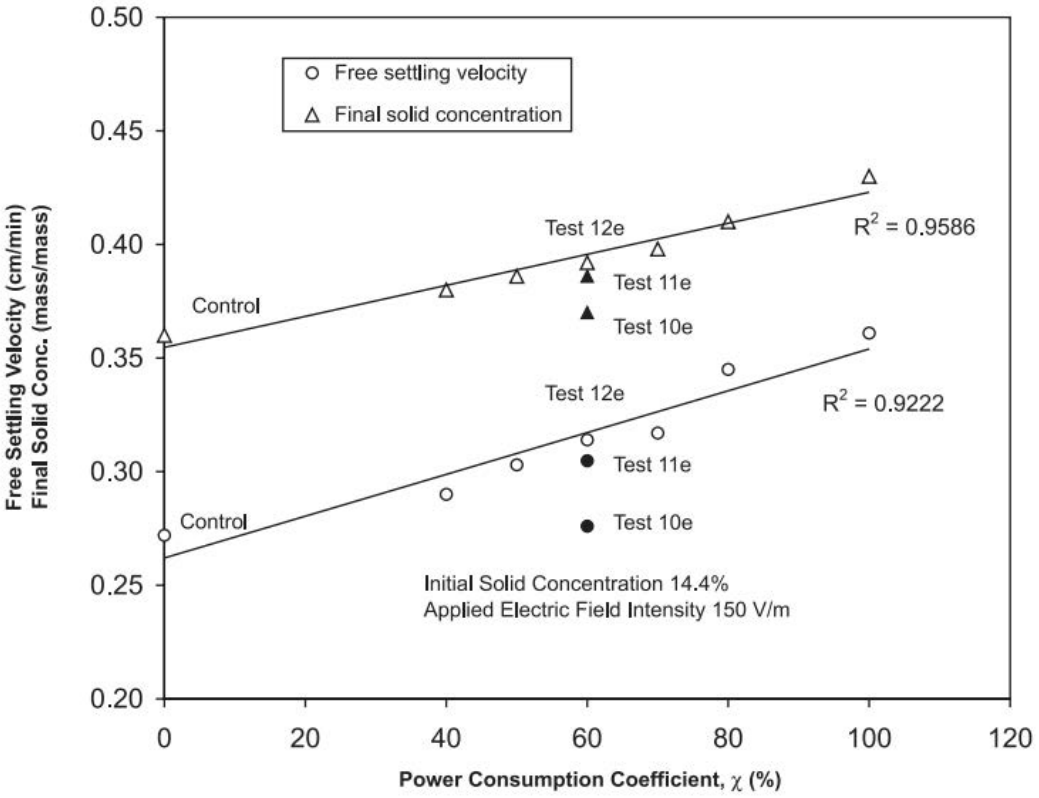

Figure 3-8: Effect of current intermittence on the free settling velocity and final concentration of contaminated Welland River sediment. After Buckland et al. (2000).

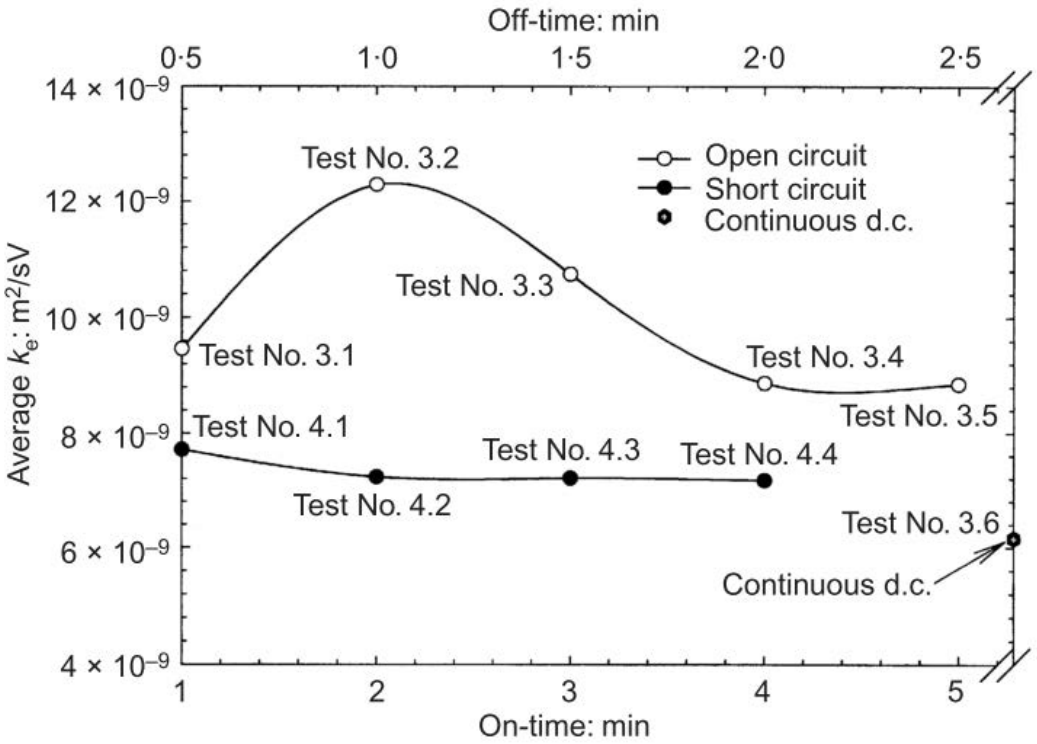

Figure 3-9: Average k_e plotted against current intermittence intervals for tests conducted with open circuit, short circuit and continuous dc. After Mohamedelhassan & Shang (2001).

3.7.5 Depolarisation Technique

Asavadorndeja & Glawe (2005) show the depolarisation technique by injecting stabilisers without the introduction of hydrogen ions. This is done by introducing hydroxide ions to the anode to equalize the hydrogen ions supplied by electrolysis. This inhibits the generation of an acid environment in the soil and also encourages the hydroxide ions to migrate from the cathode to anode. The predominantly alkaline clay is then preferential for the formation of pozzolanic reactions. This technique can reduce the time taken to perform the treatment and appears to cause the strength of the soil to increase after treatment has ceased, Figure 3-10.

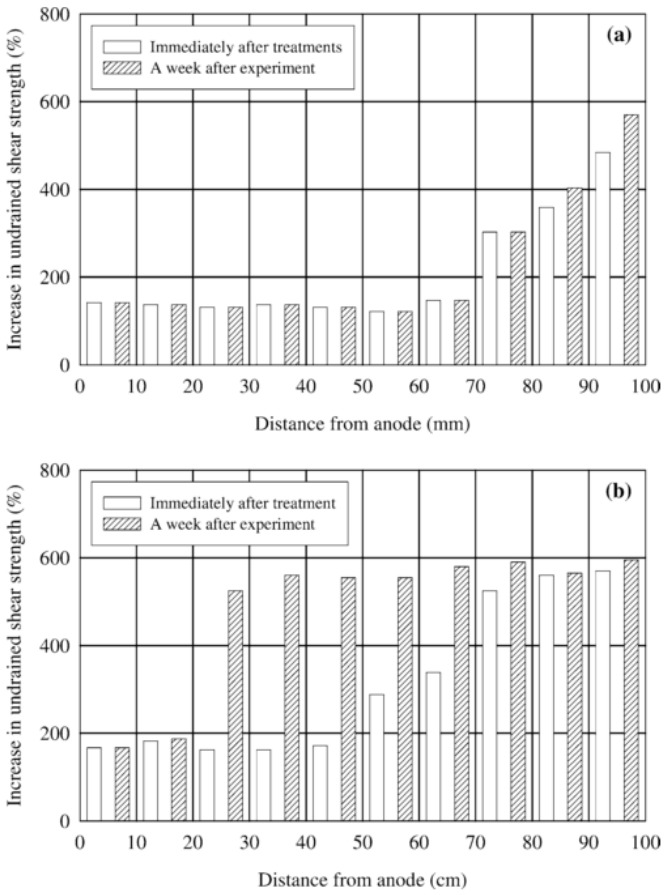

Figure 3-10: Results from treatment, (a) without depolarisation technique, and (b) with depolarisation technique. After Asavadorndeja & Glawe (2005).

3.7.6 Strength Increases

After treatments using electrokinesis, it has been shown to be possible to increase the shear strengths quite dramatically as shown in Table 3-8. Asavadorndeja & Glawe (2005) also report increases in Atterberg Limits after treatment including calcium ions.

Whilst increases in shear strength are common place when using EK treatment methods, Bjerrum (1967) reported that aside from the gain between the electrodes, reductions in shear strength were recorded below the treatment zone with no explanation as to why. These reductions may be explained by water migration following the bulb shape of the current field below the electrode tips as shown in section 6.3.

When performing electrokinetic dewatering, shear strength increases are expected due to the effective consolidation that is taking place. However, once stabilising chemicals are introduced, shear strength increases cannot be assumed. It can be noted, however, that studies

such as Ozkan, et al. (1999), Ahmad, et al. (2010), Adamson, et al. (1966), Alshawabkeh & Sheahan (2003), Liaki (2006), Gray (1970), Mohamedelhassan & Shang (2001), Abdullah & Al-Abadi (2010), Barker, et al. (2004), Rittirong, et al. (2008b), Mohamedelhassan, et al. (2008), Milligan (1995) and Zhinkin (1952) all show beneficial results from treatment including increases in shear strength and Atterberg Limit changes.

The shear strength of a clay can be modified solely through chemical introduction with sodium silicate and calcium chloride shown to initially decrease the shear strength and liquid limit of bentonite, (Heeralal, et al., 2012).

Table 3-8: Shear strengths for selected studies.

Study	Initial Shear Strength (kPa)	Post EK Shear Strength (kPa)	Shear Strength Increase (%)
(Ozkan, et al., 1999)	7	70	1000
(Ahmad, et al., 2010)	-	-	13-168
(Lo, et al., 1992)	-	-	76-172
(Bjerrum, 1967)	9.8	107	1092
(Asavadorndeja & Glawe, 2005)	-	170-600	-
(Adamson, et al., 1966)	10.7	20.3	190
(Alshawabkeh & Sheahan, 2003)	-	-	150-160
(Liaki, 2006)	8.2	9.7	118
(Mohamedelhassan, 2009)	6.3	62.5	992
(Kaniraj, et al., 2011)	0	32	>3200
(Rittirong, et al., 2008b)	3	>100	>3333
(Chew, et al., 2004)	30	42	140
(Burnotte, et al., 2004)	28	95	339
(Milligan, 1995)	260	500	192
(Rittirong, et al., 2008)	3	130	4333

3.7.7 Shrink/Swell Capacity

Altering the shrink/swell capacity of a clay susceptible to shrink and swell is advantageous, especially if the clay in question is in the vicinity of a low rise building built on shallow

foundations. Most studies do not report any shrink or swell data regarding post treatment clays. Abdullah & Al-Abadi (2010) however does report that after treatment with calcium ions, swell potential is reduced from 14.0 to 3.1% and after treatment with potassium ions is reduced to 0.4%.

Barker, et al. (2004) reports that the addition of ions such as Ca^{2+} or Al^{3+} for exchange within the clay, will lead to a reduction in the DDL. This reduction allows closer clay particle interaction and thus flocculation. The product of this is a change in workability, plasticity, permeability and swell properties.

3.8 Summary

This section has presented the historic experiments through which electrokinetic phenomena has been explored in both the laboratory and on site. Through examining the clay, flow drivers, electrodes, economics, chemistry and practical effects of the treatment solutions, a greater understanding of what is required to fill gaps in the knowledge is attained.

There are generous amounts of positive published research on the processes and effects of electrokinetic soil stabilisation, albeit not complete in its knowledge. This section should serve to prove that this treatment process is a valid research avenue with knowledge gaps in the form of the following:

- Practical installation within site applications.
- The ability to target the zone of treatment.
- The use of multiple techniques simultaneously such as intermittent current and stabilising chemical introduction.
- Current intermittence.
- Polarisation of electrodes.

The following body of work will attempt to explore these gaps and provide a suitable methodology for the application of this technique on site.

4 LABORATORY METHODOLOGY

4.1 Introduction

This section is devoted to explaining the equipment, materials and philosophies used in the laboratory testing and presents details of the laboratory setup, testing methods, and developments. The numerical simulations performed using the finite element analysis (FEA) software are also discussed here. The aim of this section is to provide data and information regarding the experiments undertaken in the attempt to address the gaps in the knowledge as discussed previously.

4.2 Numerical Simulations

Numerical simulations were completed using Quickfield Finite Element Analysis software, (Terra Analysis Ltd, 2011), a specialist FEA package used to simulate dc current densities over a conductive medium. This method of simulation was used purely indicatively to gauge electric field extents and the impact of different electrode configurations and boundary conditions. The software was used indicatively by Mohamedelhassan, et al. (2008) to examine the electric current density from a series of electrodes in a circular pattern in an effort to estimate the treatment zone.

4.2.1 Boundary Conditions

Inherent in using FEA is the need to specify boundary conditions associated with the problem in question. There are multiple boundary condition types however only one is used in this instance, Dirichlet. This boundary condition specifies the value that a boundary is to take; for example a fixed value for the voltage at the anode or at the non-conductive Perspex cell walls. Other boundary conditions are not applicable in this modelling.

4.2.2 Quickfield Calculations

Quickfield calculates the distribution of electric current by making use of Poisson's equation for scalar electric potential *U*. The equation for a planar case is;

$$\frac{\partial}{\partial x}\left(\sigma_x \frac{\partial U}{\partial x}\right) + \frac{\partial}{\partial y}\left(\sigma_y \frac{\partial U}{\partial y}\right) = 0 \qquad 4\text{-}1$$

Where components σ_x and σ_y are constant within each block. The electric current density j can be obtained from;

$$\mathrm{j} = \sigma \cdot \mathrm{grad\ U} \qquad 4\text{-}2$$

4.2.3 Simulation Procedure

The following process was followed to achieve simulations of the electrical current density in various configurations:

- Open new file for DC Conduction simulation with a standard depth (z) of 1m for site simulations and 0.22m for laboratory simulations corresponding to a nominal 1m depth in the field and the 0.22m width of the laboratory test cells.
- Required visual element of simulation is recreated on the model space.
- Each block and edge is labelled with appropriate names and given appropriate properties such as electrical conductivity and voltage.
- FEA mesh is created in each block and a field distribution produced.
- Resultant visual can be amended and edited as desired.

The same procedure was followed for each simulation with the following values unless otherwise stated. Stainless steel electrodes and ECC were used unless stated otherwise.

Table 4-1: Numerical simulation electrical conductivity values.

Material	**Electrical Conductivity (S/m)**
Stainless Steel	131,926.00
PEG	0.49925
English China Clay	0.0165
London Clay	0.05
Concrete	$1.0e^{-10}$
RO water	0.0075
Tap water and 5% chemical mix	37.00
Perpsex	$1.0e^{-15}$
Air	$1.0e^{-15}$

The values in Table 4-1 were calculated by the author with the exception of London Clay, (McCarter, 1984), RO water and ECC, (Liaki, 2006).

4.2.4 Test Cell Filter Effect

These simulations were conducted to determine the effect that the filter paper had on the overall electrokinetic process. There was concern regarding previous work that the saturated filter papers would act as flow paths for both the current and the fluid. Two scenarios were run, the first being the system with filters of electrical conductance 0.00075S/m (the same as if saturated with RO water) and the second being with the filters made of the exact same clay as in the rest of the system. The filters were not simply removed but instead recreated as clay to show the same area on the visual output. These two simulations were then repeated with the fluids changed to tap water with a 5% chemical mix as described previously, 37S/m.

4.2.5 Electrode Arrangement

Whereas a two electrode arrangement is suitable for laboratory testing, site testing requires a larger treatment area and thus more electrodes would be preferable to provide better uniformity of the current density.

Various patterns of the steel tubular electrodes were simulated to ascertain the effect of the electrode pattern and number of electrodes used.

4.2.6 Electrode Comparison

Comparisons between the stainless steel electrode and PEG electrodes were produced to assess the effectiveness of these electrodes transferring electric currents through the clay. The simulations were conducted inside the test cell with 25V power supply.

4.2.7 Clay Banding

The effect of layers of clay with different electrical conductivities was simulated to assess this effect on the current density over the whole profile. The insight provided would prove useful for both laboratory compacted samples and natural samples in the site trials whereby preferential flow path effects can be determined.

4.2.8 Electrode Electrical Conductivity

This simulation using electrodes 200mm apart was conducted to assess the effect that varying electrode electrical conductivities has on the current density levels across the clay sample between the electrodes. A point at the depth equal to the depth of the electrodes and at the midpoint between them was chosen to take readings from and compare. It was decided to compare EKG, PEG and steel in this simulation with other values of interest such as extreme low, low, lower midpoint, midpoint and extreme high. This was done to more accurately gauge the effect of changing the electrode electrical conductivity on the current density at the chosen point. The voltages chosen were 18V, 36V and 100V which convert to 90V/m, 180V/m and 500V/m respectively. A voltage of 18V was chosen as it is what is used in the laboratory tests which these simulations are based upon, 36V was chosen due to it being double 18V and 100V was chosen as an extreme value. The clay simulated had an electrical conductivity of 0.0165S/m as shown in Liaki (2006).

The electrical conductivities of the electrodes were computed using the following relationship;

$$\sigma = \frac{1}{\rho} \text{ where } \mathrm{R} = \frac{\rho \mathrm{L}}{\mathrm{A}} \qquad 4\text{-}3$$

Where σ is the electrical conductivity, ρ is the electrical resistivity, L is the length of the specimen, A is the cross sectional area of the specimen and R is the resistance of the specimen. The resistances were measured using a voltmeter and the length and area were measured using a micrometer. These values are not easily compared with published data due to the PEG not having published values available. The steel used here was Top Tubes 20mm conduit to BS4568 Class 4 which according to BS4568 has been hot dipped galvanised.

4.2.9 Site Trial Electrode Arrangement

The site trial electrode arrangement was simulated to ensure electric current leakages did not occur between the separate trials. Various arrangements were simulated within the restricted site area with the optimum plan developed for use.

4.2.10 Concrete Footing

When conducting EKS in a real world situation, one does not want to affect the concrete strip footing with the acid front. By assuming that the acid front would follow the current density profile of >1A/m^2, it can be shown that insulating the top of the electrodes to a certain depth can avoid producing these current densities near the concrete.

4.2.11 Summary

Whilst the FEA simulations can be used indicatively to gain an idea of how the electric current density will propagate through the clay, values cannot be taken as certain. The Quickfield software, whilst useful, is limited by its static 2D design ability. This means that the 3D propagation of current density (at the time of simulations) was unavailable and the ability to model a clay with changing electrical resistivity was only possible through modelling each individual iteration separately.

Nevertheless, simulations were conducted with the results shown in section 6.3.

4.3 Laboratory Setup

The laboratory setup was adapted from previous studies at the University of Birmingham, (Liaki, 2006), (Tajudin, 2012). Initial tests were conducted to repeat previous studies from which various enhancements were made. These enhancements are discussed below in section 4.3.2. Attention was then transferred to new aspects of the research.

Due to costs involved and the ability to reference back to previous research using the equipment, it was decided not to change the set up initially with the setup shown in Figure 4-1.

4.3.1 Test Cells

The test cells were constructed using 12mm thick PVC-U sheeting due to its non-conductive and chemically neutral nature. Previous research from Liaki (2006) and Tajudin (2012) developed and successfully used these cells thus it was logical to continue with them. Details of the adaptations used are given in section 4.3.2.

The test cells themselves consisted of three compartments; a central compartment for the clay and two sub compartments for fluids, Figure 4-1. The central compartment, containing the clay, had dimensions 370x220x550mm. The compartments were 550mm in height to allow

for the consolidation of slurry. Nozzles were located at the specific points for effluent flow and fluid level maintenance. See Figure 4-2.

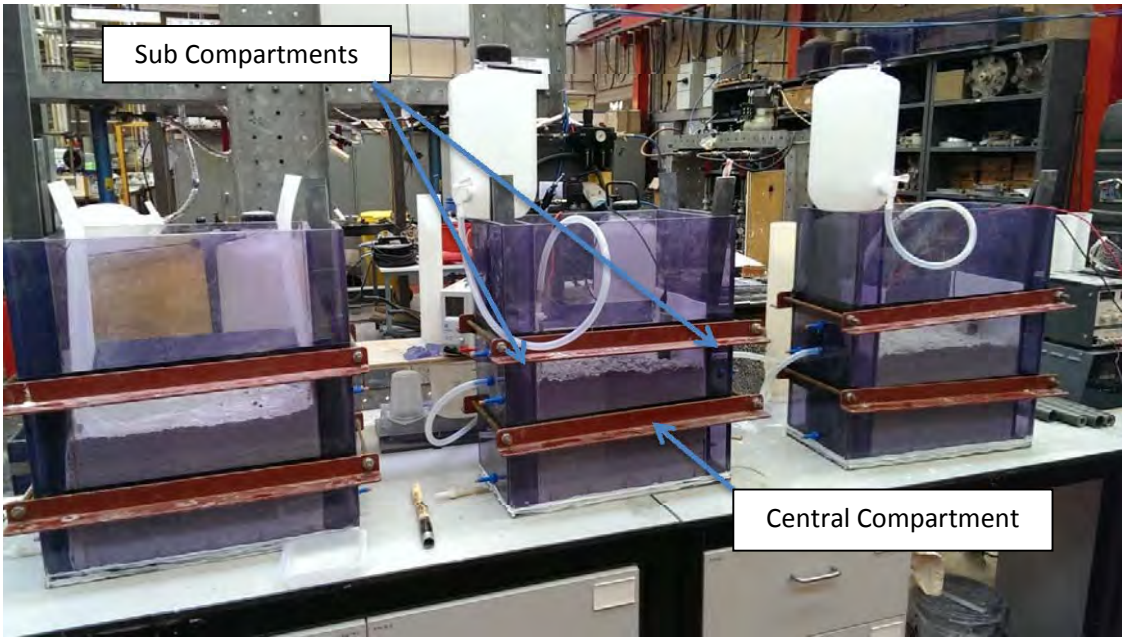

Figure 4-1: Electrokinetic cells mid setup.

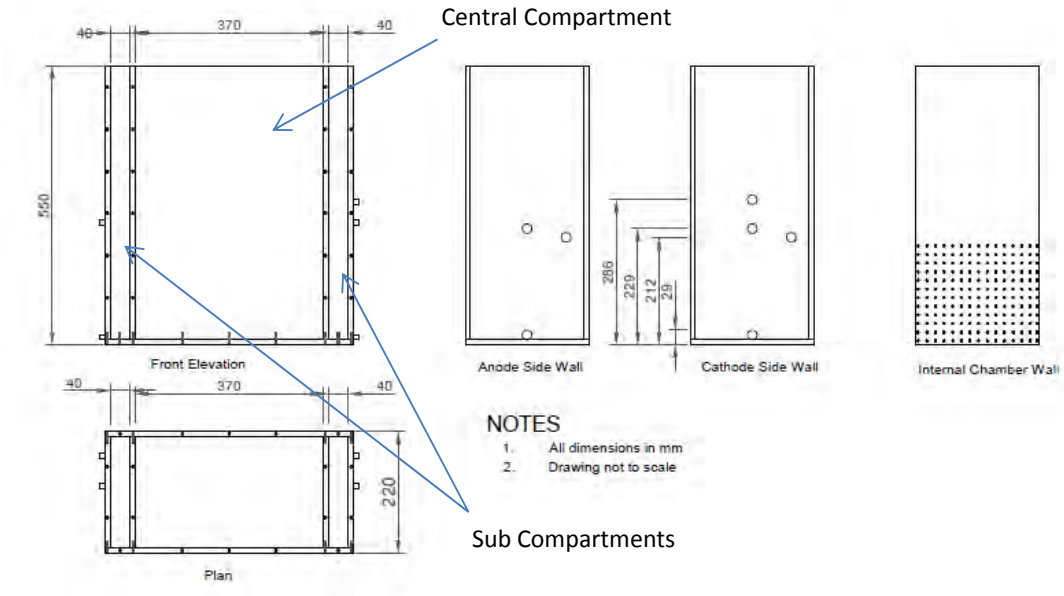

Figure 4-2: Test cell details.

The cells were developed with two detachable bases. One was perforated in the central compartment section for the allowance of drainage during consolidation and the other was solid with drainage channels to carry fluids away. Consolidation initially was from 90% water content to 51% but was changed later to a reduced 36% as a value more in line with real structure bearing clays. After consolidation, the bases were flipped upside down so the solid base was flat against the base of the clay to stop any vertical drainage. The perforations in the base were 2mm diameter and at 17mm spacings. The walls separating the central compartment from the sub compartments were also perforated with the same diameters and spacings between 25mm and 350mm from the base.

When constructing the cells, Arco Essentials silicon sealant was injected into each screw hole and between each panel to create a water tight seal. Once this silicon sealant was dried, more was spread over each joint to create a second seal. Silicon sealant was left to dry for 24 hours before any testing was conducted. Vyon-F filters were used to reduce clay particles exiting the main compartment, details of which can be found in Liaki (2006).

PVC-U sheets of 3mm thickness were cut to size to insert between the clay and the walls separating the compartments for consolidation. These sheets would be removed after consolidation and sheet like electrodes inserted in their place or kept in place if tubular electrodes were in use.

4.3.2 Test Cells Adaptations

Once the initial test evaluation were repeated, it was decided that adaptations were required to enable more realistic testing conditions such as the clay water content. The existing test cells were adapted and designs for similar cells were developed for construction.

The newly developed cells were made of the same material as the original ones with many of the same design details. The main concern from the repeat tests conducted was the leakage of the fluids from the cells. The inability to keep the fluids from leaking vertically down through the base of the cells would cause a preferential flow path for the fluids and therefore hinder the electrokinetic stabilisation testing process. It was therefore decided that a non-removable base could be built that had the ability to allow fluids to pass through as and when desired, Table 4-1. The base would consist of two layers with the top being perforated and bottom solid. The bottom would have drainage channels to allow the flow of fluids to drainage points. These channels could be blocked using various materials once consolidation is

completed. Materials such as bentonite, ice, silicon sealant and gelatine were considered as possible materials that could be injected into the base to block the water escape after consolidation but would not render the test cell irrecoverable. It was concluded that these methods would be too imprecise and difficult practically. The next step was to attempt to design a base that could have a trap door feature that could slide to open and close. The design had to extend the base of the test cell to incorporate o-ring seals around the outside and as such the strength of the cell decreased in these lip areas leading to the inability to cope with consolidation to the level required. Unused test cell adaptations can be found summarised in Table 4-2. As such, the method employed was to keep the bases separate and to plastic weld the vertical panes to reduce the likelihood of fluid leakage. The bases still required screwing to the walls to ensure they were removable.

The PVC-U sheets used to separate the fluid chamber from the clay chamber were found to be impossible to extract when using clays of lower water contents and thus it was decided to replace them with 2mm thick Teflon sheets.

Table 4-2: Unused test cell adaptations.

Test Cell Adaptation		Benefits	Dis-benefits
Fixed base with porous medium – base to contain medium which can block or allow flow as desired	Ice	Cheap and easy to manipulate, expands when freezing to ensure water tight seal.	Difficult to keep frozen, expansion may cause damage and affect testing due to temperature
	Silicon Sealant	Water tight seal when required, fairly easy to manipulate.	Difficult to clean and difficult to control until set. Expensive.
	Bentonite	Provides adequate seal when required.	Difficult to clean and difficult to ensure no contamination
	Gelatine	Easy to manipulate and cheap. Fairly water tight.	Contamination potential and preferential electrical current flow path.
Trap door base – sliding section in base which can block flow or allow flow		Easy to use	Difficult to ensure water tight seal, test cell adaptation with o-ring seals required. Current test cell deemed not capable of taking pressures after adaptations.
Block drains in base but allow base void to fill with water		Easy to use	Water could provide preferential electrical current flow path

4.3.3 Electrodes

The electrodes used all had direct clay contact to ensure power loss was kept to a minimum throughout the process. The following is a list of all the types of electrode trialled in this study:

- **Stainless steel tube** – Type 316 (1.4401 (EN Steel Number), S31600 (UNS)) was chosen as the right material for EKS due to its molybdenum content leading to an increased corrosion resistance along with being fairly cheap as discussed later.
- **Steel reinforcement bar** – High yield T10 Grade 500C.
- **Electrokinetic Geosynthetic** – The EKG used was used in previous studies and were procured by Newcastle University, (Pugh, 2002), (Pugh & Jones, 2006).
- **Hybrid** – This electrode was developed in this study as discussed in section 4.3.3.3.
- **Polyurethane, epoxy-resin and graphite (PEG)** – This electrode was also developed in this study as discussed in section 4.3.3.5.

The EKG was the only flat sheet like electrode with the test cells being originally designed to take advantage of these sheets by Liaki (2006) and thus the fluid chambers existed at either end of the clay chamber. The EKG was therefore inserted adjacent to the perforated end cell walls to ensure contact with the clay and to be able to draw the fluids through into the clay tank.

The other electrodes were of the pole/tube/rod specification and could not be used in the same way. These types were inserted into pre-augured holes in the clay and fluids were fed from the top.

4.3.3.1 Electrokinetic Geosynthetic

This electrode type has previously been used at Newcastle University by Pugh (2002) and also in previous studies at University of Birmingham, (Liaki, 2006), (Tajudin, 2012). This EKG consists of stainless steel wires coated in a high density polyethylene resin dispersed with carbon black, commercially named Cabot Cabelec 3892, Figure 4-4. It should be noted that this electrode will corrode in a corrosive environment but not as fast as steel. Eastwood (1997) reports, as mentioned previously, that EKG materials precipitate matter into the soil due to their carbon coating with typical degradation rates being 9.0 and 0.5 – 2.0kg$A^{-1}$$year^{-1}$ for steel and carbon respectively.

4.3.3.2 Stainless Steel Tube

The stainless steel tube electrodes were perforated stainless steel tubes of internal diameter 16mm and wall thickness 1mm. The tubes were perforated at regular intervals with 2mm holes.

4.3.3.3 Hybrid Electrode

The hybrid electrode was borne of the desire to produce a hollow electrode that was able to act as a drain much like a cross between the stainless steel tube and the EKG, hence the name hybrid electrode.

The hybrid electrode involved two perforated uPVC tubes at very similar diameters (23mm and 21mm) so that one would fit inside the other snugly, Figure 4-4. Between these two tubes was placed a non-perforated filter. When installed into clay, a steel reinforcement bar was inserted into the centre of the inner tube. The filter stopped clay entering the tubes and stopped some of the iron precipitates entering the clay.

The hybrid electrode performed very much like an ePVD as described in section 3.4.2.

4.3.3.4 Steel Reinforcement Bar

The steel reinforcement bars used were tempered High Yield T10 Grade 500C to BS4449: 2005. Each bar was cut to size using a rebar cutter and kept away from natural moisture whilst stored to avoid corrosion.

4.3.3.5 Polyurethane, Epoxy-Resin and Graphite Electrode (PEG)

The PEG electrode was developed over a period of time and is discussed in section 6.2.3.

4.3.3.6 Electrode Fluid Levels

To avoid preferential flow of electrical charge, flow paths of water were to be avoided. If the water level at the anode or cathode was increased to the point of overflowing over the clay top, a preferential flow path would be produced and the electrical current would not flow where required leading to power wastage.

Using the EKG sheet electrodes, providing the clay was consolidated to a depth that corresponded with the height of the drainage taps on the external wall of the test cells, the fluid could not rise above this level. However, when feeding pole electrodes inserted into the clay, this was not the case.

Feeding the pole electrodes at a pace that would not overflow the system was the aim. There were four main options of which three were attempted over the course of the project:

- Manual feeding. This was the most laborious and inaccurate method. By feeding the electrodes by hand, it could not be completely controlled and invariably, portions of the clay dried out when the fluid level dropped.
- Drip feeding. Medical drips were utilised to control the amount of flow into the electrodes in a manner as to keep the level of the fluid constant at all times. This was not completely successful with air blockages and inaccurate flow control ensuring that overflow and clay drying were commonplace.
- Float feeding. Float valves were always the best option to control the level of fluid in the electrodes. The laboratory electrodes, however, possessed inner diameters of 21mm. This small space could not accommodate any commercial float valves found and so it was decided to produce one. The smallest float valve available commercially was purchased and harvested for parts. Figure 4-3 shows the vertical float valve constructed using these parts, a plastic bottle and a glue gun. Again this method was not a complete success, partly due to inaccurate craftsmanship and partly due to the fact that to completely ensure the valve was shut when the level was sufficiently high, the float needed to be so large that the electrode was full of float. For information on the site trials float valve, see section 5.6.2.
- Dose feeding. A chemical dosing pump would have been ideal for supplying a controlled rate of fluid flow to the electrodes. This option was too expensive and from what was found, too powerful for such a small scale set of tests.

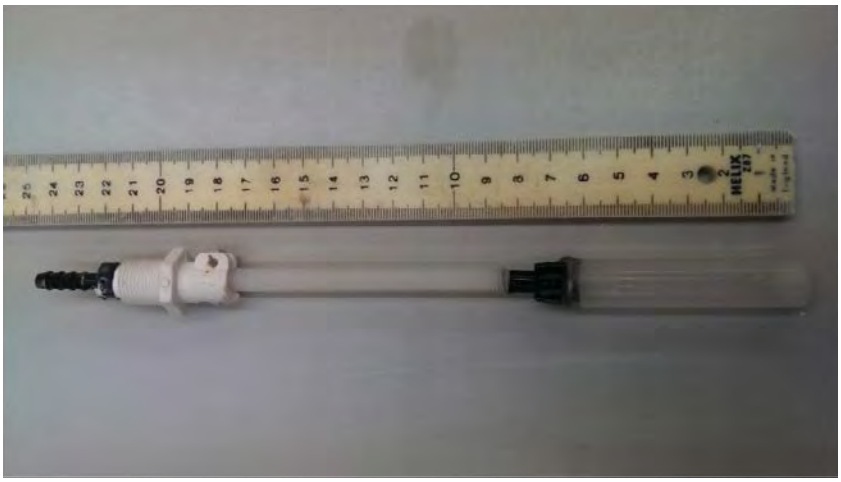

Figure 4-3: Laboratory float valve designed for tubular electrode use.

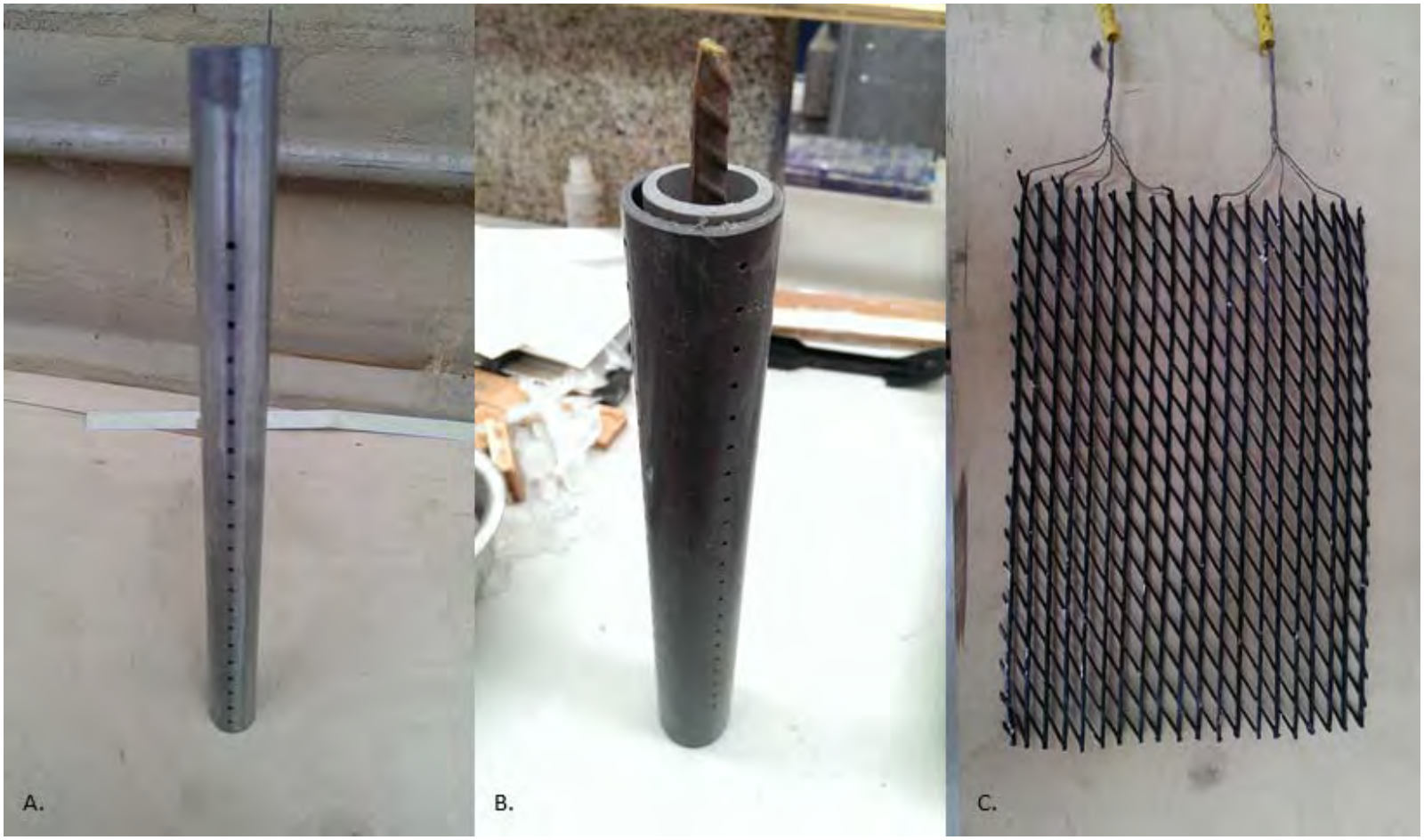

Figure 4-4: Laboratory electrode types; A. Stainless steel perforated tube, B. Hybrid electrode consisting of two plastic perforated tubes sandwiching a filter with a central rebar and C. the Electrokinetic Geosynthetic.

4.3.4 Power Supplies

The power supplies used in the laboratory were a CircuitSpecialists.eu CS15003XE, a Thandar TS3022S, a Maplin N93CX, CEE PSU 25/500's and a Farnell E30/1. These units could supply a maximum of 30V and 2A except the CS15003XE which could supply 0-50V and 3A. Another supply was used for the electrolysis testing but this was a bespoke unit built in the Civil Engineering laboratories and inherited by this study. This was capable of 0-12V. For the site trials, a bespoke power supply unit was developed.

This new unit were produced by Andrew Tanner of the University of Birmingham BioSciences Department with the intention of being able to control current flow (current reversal and current intermittence) as well as recording data regarding voltage, current and time to a memory card (Kingston Technology SDHC 8GB). The current control was able to specify time intervals between switching the current polarity and switching it on and off with the ability to have the circuit open or closed when the current is off. The maximum voltage available through these units was 55V and the maximum current was 2A. Maximum voltage was set for Health and Safety reasons and could not be exceeded.

4.3.5 Clay

4.3.5.1 English China Clay

English China Clay was utilised for most of the experiments due to its purity, availability and low activity. A good base of previous research in the related area has been performed on ECC and thus a platform has been built to extend this work from.

The ECC used here was Puraflo 50 and has elemental makeup as seen in Table 4-3 and can be seen to be fairly regular in that with the exception of silicon and aluminium, other elements in any significant quantity are scarce. This makes the clay ideal for laboratory testing as tests are repeatable without concern for the clays contents. To be sure of this, each trial was conducted using ECC from the same batch to avoid variation.

The ECC has an approximate liquid limit of 55% and plastic limit of 35%.

4.3.5.2 London Clay

The London Clay used in the laboratory testing phase was all excavated from the site trial site in Aldenham, UK. As seen in Table 4-3, the elemental breakdown of London Clay compared to ECC

is quite different with much higher amounts of certain elements such as titanium, magnesium and iron. This is purely due to the London Clay being a natural clay full of impurities and the ECC being processed for commercial usage and thus being purer.

Any elements found to be present in quantities less than 0.1% by weight for London Clay were ignored due to their small size and statistical probability of not actually being present.

Table 4-3: Chemical analysis elemental concentration for English China Clay and London Clay.

Element	ECC Concentration by Weight (%)	London Clay Concentration by Weight (%)
Si	17.68	22.44
Al	13.94	6.06
K	2.11	2.30
Fe	1.00	6.48
Rb	0.17	0.04
Mg	0.12	0.53
S	0.20	0.03
Ca	0.03	0.89
Ti	0.04	0.74
P	0.03	0.31
Na	0.07	0.16
Zr	45PPM	0.12

4.3.6 Chemical Stabilisers

The chemical stabilisers used in this study were calcium chloride ($CaCl_2$) and sodium silicate (Na_2SiO_3) supplied by Fisher Scientific. The decision to proceed with these chemicals was based upon successful previous study usage of them such as Barker (2002), Liaki (2006) and Tajudin (2012). Another factor in the choice to use these stabilisers was the fact that they are regarded as safe to use environmentally, (F.D.A., 2013), (F.D.A., 2013b), and are competitively priced.

In all trials, the calcium chloride was introduced to the anode and sodium silicate to the cathode to ensure migration across the clay samples.

4.3.7 Water

RO water was used for all testing unless otherwise stated. The intention behind this was to avoid introducing contaminants to the tests to ensure ions present are from the chemicals, electrodes or clay.

The RO water was produced by an ELGASTAT UHQ PS unit and after a service and clean possessed a conductivity of 0.06µS/cm. This water was stored in a tank after filtering and the cleanliness of said tank was suspect with algae developing inside. XRF analysis and conductivity results can be found in sections 4.4 and 6.2.3 respectively.

4.4 Elemental Analysis

Elemental analysis using the XRF was run on the control samples of water, chemicals and clay to assess the benchmark of what is in the system.

Each water molecule is composed of two hydrogen atoms and one oxygen atom. These two elements cannot be seen by the XRF and thus the majority of the water sample appears to be missing from the results. The results we do see are the contaminants present and as can be seen they are of low concentration, Table 4-4.

Table 4-4: Chemical stabiliser and water elemental breakdown.

Element	Concentration by Weight (%)			
	Sodium Silicate	Calcium Chloride	RO H_2O	Tap H_2O
Si	14.800	0.010	1.600	0.080
Al	0.041	0.010	0.000	0.103
K	0.037	0.000	0.000	0.087
Fe	0.018	0.000	0.000	0.040
Mg	0.000	0.000	0.000	0.101
S	0.298	0.480	0.000	0.012
Sr	0.000	0.010	0.000	0.000
Ca	0.009	21.300	4.200	0.003
Na	9.000	0.310	0.000	0.010
P	0.000	0.000	6.500	3.250
Cl	0.075	36.260	0.000	0.590
Zr	0.013	0.000	0.000	0.000

Both the calcium chloride and the sodium silicate contained various elements other than what they should. These could have come from either laboratory contamination or come as part of the chemicals.

The water purification system was not perfect and as such the tank the RO water was stored in was not perfectly clean which will account for the impurities present.

The result of introducing impurities into the process is the unknown component of their effect on the process in addition to the complications arising through the inability to designate any of the treatment effects purely on the intended chemical contributions.

4.5 Previous Research Repeat

A test was chosen from previous research Liaki (2006) completed and repeated to ensure the equipment and results were agreeable. The chosen test was the migration of water through ECC using EKG electrodes with the set up being identical to the one presented by Liaki (2006).

ECC was mixed to 90% RO water content in a Hobart mixer, poured into the test cells and left for 24 hours to homogenise. The clay was then consolidated to 51% water content. The uPVC sheets protecting the EKG electrodes were removed and the electrodes were connected to the power supply. The power supply was switched on and ensuring a constant head of water at the anode and cathode, the inflow and outflow was measured at regular intervals.

4.5.1 Adjustments from Previous Research

4.5.1.1 Consolidation

Initially, based on previous research and the existing laboratory setup, the clay was consolidated from its water content at mixing (approximately 91%) to its testing level of 51%, Table 4-5. After initial tests were completed, it was decided to lower the testing water content to approximately 30% to increase the shear strength to that of a more realistic clay for building a low rise building over.

The consolidation equipment consisted of a pneumatic driven hydraulic pump capable of driving three hydraulic jacks which has been used previously, (Liaki, 2006), (Tajudin, 2012). The hydraulic pump was an Enerpac Turbo II with up to 6 bar air pressure supplied to the pump which in turn supplied the jacks with up to 400kN/m^2 as determined whilst calibrating the jacks with load cells, Appendix B.

The load was then transferred to the surface of the clay by a load plate that was attached to the end of the jack. The load plates were steel with a corrosion resistant paint coating with a footprint size of 359x218mm and weight 8.55kg, Figure 4-5. The plate had drainage holes to allow vertical drainage with the design presented in Liaki (2006). Draught

excluder tape was attached to the perimeter of the loading plate to reduce the amount of slurry escaping. Steel bracing was applied to the exterior of the cells during consolidation and kept there until the end of the testing. This bracing was at 1/3 and 2/3 of the height of the tank. PVC-U strips were used as bracing for the inside of the tank.

Table 4-5: Consolidation times and pressures. After Liaki (2006).

Time (hours)	Pressure (kPa)	Average Δh (mm)
0	10.1	399
24	26.4	373
48	42.8	180
72	67.9	109
96	84.3	104

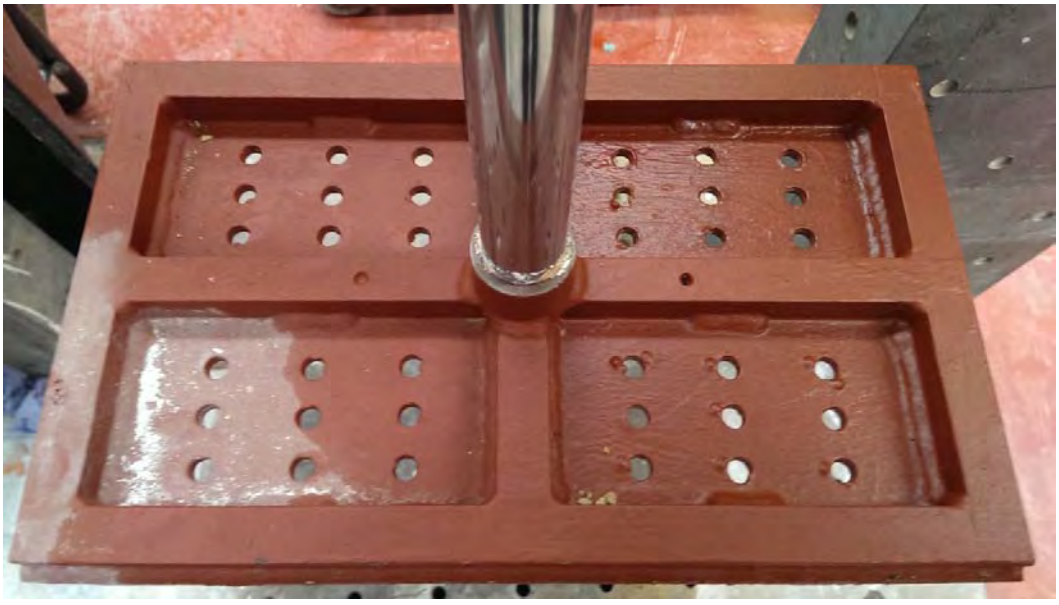

Figure 4-5: Consolidation load plate.

The clay consolidated here was done so in stages. Oedometer tests were conducted to ascertain the appropriate length of time for each load stage. On average, the height of the initial slurry was 380mm with the final height at 51% water content being 275mm and 250mm at 38% water content.

It was discovered that the hydraulic pump could narrowly achieve the pressure required to consolidate to this level however the Perspex cells could not take the pressure. At this point it was decided to move to compaction to form the clay in the cells. This in itself brings about further problems such as the fact that compaction does not reduce the void ratio of a clay. This leads to an increased level of air content. With air being an electrical insulator, its excess presence in the clay samples would reduce the electrical conductivity of the entire sample. This effect could reduce treatment efficiency by increasing time required for treatment. However, the samples compacted here were wet of optimum meaning the effect of this would be minimal.

4.5.1.2 Reduced Water Content

After a few adjustments to the consolidation rig, including replacing parts and calibrating the jacks again, another set of cells were produced to cope with consolidation to a lower water content than previously achieved. These cells were constructed to the same specifications as the existing cells but with improved joints. These improved joints consisted of more self-tapping screws and plastic welded vertical joints to minimise leaks. The water content aimed for was to be 30% with oedometer tests conducted to determine load stage details. Originally, it was envisaged that these cells would be used to conduct further testing, but this plan changed when the pressure from the jacks split the cells open. After lengthy repairs and the addition of more bracing to the boxes, it was attempted again to no avail. It was found that the lowest water content that could be reached using the current style cells was approximately 36%. Due to this not being totally representative of natural clays that would be built upon in addition to the fact that to replace all of the cells would be too expensive, it was decided that compaction would be required to reach the target water contents. Nevertheless, a low water content consolidated cell was constructed and tested for water content and shear strength to be compared with a compacted version of the same clay for comparison.

Table 4-6: Load stages for consolidation from 90% to 36% water content.

Load Stage	Pressure (kPa)	Time (hours)
Stage 1	25.00	32.75
Stage 2	50.00	39.58
Stage 3	100.00	32.75
Stage 4	200.00	14.54
Stage 5	400.00	16.19

The consolidation times and pressures were taken from Liaki (2006) for the initial consolidations. These were insufficient, however, for the lower water content consolidations. Oedometer tests were therefore conducted on ECC to determine the length of time each loading stage would need to consolidate to approximately 36%, Table 4-6.

4.5.1.3 Compaction

Due to the limitations of the consolidation sequence, it was decided that compaction should be used as an expedient version of the compression technique. With the decision to use compaction rather than consolidation, compaction tests were required. Proctor tests were carried out with different numbers of layers and blows to BS1377-4: 1990. Three, five and ten layers of clay were tested with ten, thirty, sixty and one hundred and twenty seconds of blows per layer. The Proctor tests were carried out to determine the optimal water content of the clays and then calculations were performed to determine the energy output of the jack hammer in an attempt to determine the length of compaction required to achieve the desired compaction. A hand vane was used to determine the shear strength at different points in the Proctor mould. For the electrokinetic testing phases, tests were conducted on the benchmark samples to ensure they were saturated.

Although compaction is not ideal for this application due to the resulting clay being less homogeneous than consolidated clay in addition to not expelling air from the samples, due to the inability to consolidate to the required level, compaction was the only alternative option. Proctor tests were conducted on both ECC and London Clay to ensure optimum water content for the maximum dry density under the compactive effort. The compactive effort was scaled up from the drop hammer to the electric jack hammer for larger scale testing.

$$Proctor\ Mould\ Volume = 0.00098726\ m^3$$

$$Perspex\ Cell\ Volume = 0.028512\ m^3$$

$$Proctor\ Test\ Compactive\ Effort = 60.75\ kg.m$$

$$Proctor\ Test\ Compactive\ Effort\ (J) = 595.95\ J$$

$$Work = 603.65\ \frac{kJ}{m^3}$$

$$Perspex\ Cell\ Energy = 17.21\ kJ$$

$$Tank\ Layers = 12$$

$$Energy\ Per\ Layer = 1434.27\ \frac{J}{m^3}$$

$$Electric\ Hammer\ Blow\ Energy = 16.8\ J$$

$$Electric\ Hammer\ Blows\ Per\ Minute = 900$$

$$Blows\ Needed\ for\ Energy\ Requirement = 85.37$$

$$Time\ Needed\ To\ Deliver\ Required\ Blows\ To\ Each\ Layer = 5.69\ s$$

The 5.69 seconds calculated here does not take into account that the hammer produces energy losses during its performance. From trial and error tests using the Proctor mould, Figure 4-6, it was determined that 120 seconds per layer was required for sufficient compaction with scoring of the surface of each layer surface to avoid banding in the test cell.

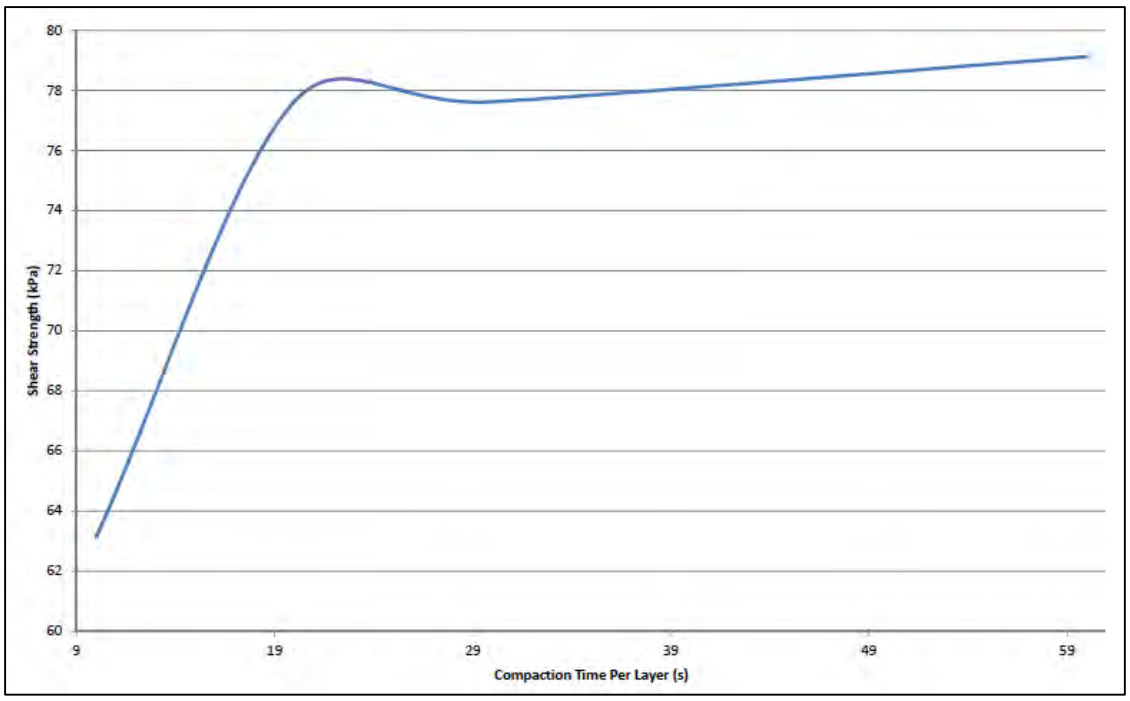

Figure 4-6: Compaction time per layer against shear strength of clay.

4.6 Chemical Combinations

To assess the effectiveness of the chemicals chosen for this study, they were mechanically mixed with English China Clay and reverse osmosis water and left to cure for various time periods. At the appropriate time intervals, samples were taken and tested for shear strength, liquid and plastic limits and pH. The chemicals, calcium chloride and sodium silicate, had molar masses as follows;

$$CaCl_2(dihydrate) = 147.014\ g.mol^{-1}$$
$$Na_2SiO_3 = 122.06\ g.mol^{-1}$$

As stated by Tajudin (2012), a concentration of 1.5mol/L gives the highest practical undrained shear strength when mixing $CaCl_2$ with ECC. Thus, this concentration was used as the standard concentration and the amount of chemical to be added to the clay was computed by multiplying the molar mass by the concentration.

The containers used for these batch tests were constructed of Perspex with dimensions 200x200x160mm. When the clay was inside the container, the lid was placed on top and sealed using silicon sealant.

The ECC placed in the containers was of 30% water content to cover the water contents between the plastic and liquid limits of ECC as stated by Liaki (2006). The specimens were mixed for 30 minutes in an Hobart mixer with their various quantities of RO water which had been mixed with the appropriate contents of the stabilising chemicals. The different chemical contents were either 5 or 10% by dry weight with constituents being either 50/50 or 66/33 where appropriate. The time periods used in these tests were 0, 7, 14, 28 days and then 545 days.

The compounds $CaCl_2$ and Na_2SiO_3 are inherently electrically neutral, and thus would flow in the direction of the hydraulic flow in the electrokinetic system. However, if the compounds are broken during the process of dissolving in the water then one would expect calcium, silicon and sodium to electrokinetically migrate towards the cathode due to their positive ionic charges.

This experiment was run with assistance from an MSc student, (Shahbuddin, 2013).

4.7 Electrode Development

The electrodes used in the laboratory testing phase can be split into two types; existing types used by studies found in the literature and types that were developed by the author. The existing types were stainless steel tubes and EKG's as discussed in section 4.3.3. The developed types were the hybrid electrode and the PEG as discussed here.

In an effort to protect the stainless steel electrode tubes from corrosion whilst still providing an electrically conductive pathway, a specialist polymer was sought that could be applied to the electrode surface. Inspiration was taken from the EKG and Cabelec 6114 was

identified as an appropriate polymer. Cabelec 6114 is an electrically nonconductive polymer with carbon black dispersed throughout its body making it conductive. Due to Cabelec 6114 being an injection moulding polymer it proved difficult to find any coating specialist companies able to apply it to a tube. Thus it was decided to produce a coating in the laboratory that could easily be applied to the tubes manually.

Mixes of epoxy resin (ER) and carbon were tested first then it was decided to try graphite with epoxy resin to try to gain a higher electrical conductivity than that of the carbon mix. Resistance was measured using a Rapid 212 DMM voltmeter which had a measurement range of 0.001 to 2MΩ. The original epoxy resin used was Emerson and Cuming Specialty Polymers Eccobond 24 and then later Easy Composites Ltd Epoxy Coating Resin was used. The carbon used was generic carbon pellets. The original graphite was Fisons Laboratory Reagent Graphite Powder and later Easy Composites Graphite Powder was used.

All electrode coatings were applied to their respective tubes using a small spatula. This gave control over the surface texture of the coating with the ability to affect surface resistivity by increasing and decreasing conductive coating elements near the surface but did not give total control over the coating thickness. Industrial application of the coatings to the tubes would better control the surface texture as well as the coating thickness and therefore increase electrical conductivity and thus effectiveness of the electrodes. Any variations in surface texture or coating thickness could potentially incur electric current densities and flow patterns that were not predicted.

4.7.1 Carbon based coating

The carbon based mix comprised of 45% carbon powder and 55% epoxy resin by weight as this was the maximum carbon content that could be practically applied to a tube. The carbon powder was first mixed with Part A of the epoxy resin before adding Part B, as prescribed by the ER manufacturers. The combination was mixed thoroughly for ten minutes before application to a tube was attempted by spreading on using a spatula.

4.7.2 Graphite based coating

The graphite based mix comprised of a range of graphite concentrations from 15% to 55% by weight. It is known that increasing the graphite content decreases the resistivity of the electrode as shown by Matzui, et al. (2013). The graphite powder was mixed into the ER thoroughly for at

least ten minutes to ensure a consistent mix. The resulting paste was applied to the tubes and smoothed over using a spatula to gain a smooth cylindrical shape. Using a nail, the tube perforations were reintroduced. Both steel and plastic tubes were tested. The plastic tube was tested to remove the potential for corrosion and also would also be much cheaper as plastic conduit is approximately £0.50 per metre length and for the same diameter; steel tubing is approximately £3.00 per metre (September 2013 prices). There would also be cost savings on the coating too with only one side of the plastic pipe needing coating whereas the steel tube would need completely coating to avoid exposing the steel to any corrosive material. Thus, one would need approximately half the coating.

4.7.3 Electrode Decay

In order to determine the effectiveness of the electrodes, it is vital for the rate of decay to be known in order to assess the life span and therefore overall cost of the EKS procedure. The following tests were conducted on both existing and the developed electrodes to gain this knowledge.

4.7.3.1 Electrode Decay Due to Liquids

There is a need to know the rate of degradation of the electrodes and the effect this degradation has on the electrodes. This need relates back to the economy and life span of the process. If the electrode degrades too soon then the economic benefits of the process start to reverse and even result in the process not completing unless the electrodes are replaced.

This test was conducted to ascertain the effect of liquids on the electrode materials alone. The electrodes were submerged in the liquids over a 285 day period, with 110mm long samples submerged in 200ml of liquid to a depth of 70mm. The liquids used in this test were RO water (pH 7) and RO water mixed with a 10% concentration of two thirds $CaCl_2$ and one third Na_2SiO_3 (pH 10.23). The 10% concentration was chosen to reflect a harsher environment than expected with the concentration chosen for the full EKS testing.

Before testing, the electrodes were weighed and the surface resistance over their full lengths was measured. The electrodes were submerged and secured vertically using duct tape as seen in Figure 4-7. After 28 days, the electrodes were extracted from their liquids and dried before being weighed to gain the percentage mass change of each electrode and their resistances were measured to gain the effect of the decay on their electrical conductivity.

Readings were taken at monthly intervals for the first three months and then after nine months. Approximately every eight days the fluids were tested to track the change in pH of the fluid as the electrodes decayed. The test specimens were kept in a sealed box to avoid fluid loss due to evaporation.

Electrode degradation was determined via the following methods:

- Visible Inspection: Using visual inspections, a preliminary determination into the effect of electrode degradation can be made.
- Mass Variation: Using this method, the electrodes were weighed using digital weighing scales before and after use. Care was taken to ensure that a minimal amount of fluid was present on the electrodes by drying using a hair dryer.
- pH: The pH of the fluids will give an indication of the level of degradation of the electrodes over time.
- Resistance Variation: A multi-meter was used to measure the linear resistance of each electrode which gives an indication as to the degradation of the electrode.

The test length was 285 days in an effort to determine how an extended period of time submerged in liquid affects the electrodes. The bulk of the readings were taken in the first 109 days as it was anticipated that the majority of the chemical changes would have taken place in the early stages of the test.

Figure 4-7: Electrode decay test setup before sealing inside box.

4.7.3.2 Electrode Decay Due to Electrolysis

Submerging the electrodes into water to assess their decay would not be a complete investigation as in reality; the electrodes are under the influence of electrolysis also. To explore this, electrodes were submerged into RO water at a distance of 100mm and a dc electric potential of 10V was applied between them.

The containers used were standard plastic Tupperware tubs of size 250x200x150mm providing a watertight and inert containment unit. The power supply unit was a bespoke unit which had 6 independent supplies of 0-12V, Figure 4-8. No voltage or current values were given by the unit and so a multi-meter was used for this purpose.

Each electrode was cut to a length of 120mm and attached to the power supply using a bulldog clip and banana plug wire. Each electrode was kept at a distance of 100mm by attaching the electrodes to a piece of wood over the top of the containers. This was deemed suitable due to its electrical insulation characteristic.

The monitoring of this test would be to measure mass, resistance and pH of the electrodes and liquids before commencement of the test and at periods of 7 days thereafter. The voltage and current would be recorded at these points too. After the test was completed and all data recordings taken, the fluid can be analysed by XRF to attain the extent of degradation of the electrodes. The total length of this test would be 28 days as it was anticipated that the metallic electrodes would be heavily decayed by this point.

Figure 4-8: Electrode electrolysis trials.

4.8 Electrode Polarisation

To get a notion of the effect of electrode polarisation a simple test was conducted to measure the current drop over time and the relaxation times associated. The aim of these tests was to show how polarisation of the electrodes could affect the EKS process and to develop methods in which this could be avoided. Also, by gaining insight into how polarisation works in a dc circuit, it would prove easier to spot in the site trials.

Conducting this test involved filling a Tupperware container of size 300x200x150mm with sand to a depth of 70mm and inserting electrodes at a spacing of 130mm. The electrodes were connected to a power supply set to 10V. A digital multi-meter was connected in series to accurately collect electrical current readings. Tap water was added to the sand at a measure of 0.5L for 5kg of sand, Figure 4-9.

The current was recorded for the first 30 minutes and then the relaxation times were recorded by breaking the circuit for increasing periods of time and recording the current upon fixing the circuit.

The electrode configurations tested were the ones to be used in the site trials. The first was a general test using two electrodes 130mm apart similar to the laboratory tests. The second used three electrodes in a straight line with the middle being a cathode betwixt two anodes,

similar to the site trial raked electrodes. The third used four electrodes as in the vertical electrode site trials.

Figure 4-9: Electrode polarisation of a four electrode array in wet sand.

4.9 Material Electrical Conductivity

To get a full picture of the extent of the EKS process in the clay, an idea of how the electrical conductivity is affected by the addition of various fluid compositions is desirable. The electrical conductivity of the clay over a variety of expected water contents was recorded as the effectiveness of the process is highly dependent on this. The greater the electrical conductivity of the clay, the quicker the process can be potentially completed. Along with this, the electrical conductivity of potential electrolytes was tested also, with RO water, tap water and tap water mixed with the 3% chemical mix determined in section 6.2.1.

To produce this set of data, powdered ECC was mixed with various amounts of RO water and tested for electrical conductivity using an electrical conductivity-meter. The same process was repeated with London Clay to attain the results for comparison and then again with London Clay and a 3% mix by weight of stabilising chemicals as specified in section 6.2.1.

4.10 Electric Field Determination

Assessing the electric pattern is necessary to determine the most effective methodology for EKS. Without economising the electrode pattern, one could be wasting energy, time and money and thus finding a method for viewing the electric field pattern was sought.

Initially it was envisioned to use probes in the clay to measure the current at certain points and build up a map of the current density over the area of treatment. However, any type of probe will inherently affect the reading that the probe gives and thus will not measure what is required.

The numerical modelling can be used to determine the current density pattern but as discussed in section 6.3, is indicative of reality and without validating cannot be relied upon. Validating is beyond the scope of this series of works but the pattern tracking here would go some way to validating the numerical modelling but is not conclusive.

The following methods were trialled to assess the structure of the electric field.

4.10.1 Dye Precipitation

The dye precipitation test was designed to allow a unique view of the flow of the electric field through the clay. A standard setup was achieved using the Perspex cells and ECC. The voltage applied across the specimen was 55V/m with a supply of RO water mixed with green food dye connected to the anode. The aim was to allow the food dye to precipitate through the clay under the influence of the electric current.

After treatment, the clay was removed from the Perspex cell and sliced using a cheese wire. It was predicted that a pattern similar to that of the electric field would be observed as the green dye had migrated through the clay along the field lines and deposited at the highest density points.

4.10.2 Dipole Scattering

The lettuce seed test was inspired by a well-known school project in which students attempt to make electric field patterns appear between two electrodes under a potential difference.

A non-conductive basin is filled with 0.5cm of vegetable oil and the electrodes inserted and connected to a power supply. Lettuce seeds are scattered over the surface of the oil and a 50V potential was applied. The lettuce seeds act as electrical dipoles and align with the electric

field in a conductive fluid. Each electrode type and arrangement was to be tested in this manner and the pattern photographed and compared to the numerical model equivalent.

4.11 Electrokinetic Tests

Full laboratory tests were performed to further the knowledge and understanding of the processes at work in electrokinetic soil stabilisation at a larger scale than most tests found in the literature. This testing would also be used to validate the methodology that would be used in the site trial. A summary of the electrokinetic tests and their variables can be found in Table 6-1.

The chemical stabilisers utilised in the full EKS tests were calcium chloride ($CaCl_2$) and sodium silicate (Na_2SiO_3). Details of these and their effect can be found in section 6.2.1.

4.11.1 Previous Research Repeat

A typical test was chosen from Liaki (2006) to repeat in the laboratory. The experiment was repeated as closely as possible to the original to check that the results agree and that the equipment worked sufficiently. This was also an opportunity to improve and adapt any of the process or equipment.

EKG electrodes were used to forcibly migrate water through ECC consolidated to 51% water content in the standard test cells. A power supply induced 50V/m through the electrodes for 28 days. RO water was supplied to the electrolyte tanks keeping a constant level.

Monitoring included recording voltage and current along with Atterberg Limits, pH, water contents and shear strengths post completion.

4.11.2 Electrode Type Choice 1

To choose which electrode type to continue with for the EKS tests and site trials, it was necessary to determine which would be suitable for both effectiveness and economy. From the literature it was decided that stainless steel tubing and EKG were the most suitable for the nature of this testing. Another electrode was developed to compliment these two electrodes called the hybrid electrode as discussed in section 4.3.3.3.

This experiment involved passing a dc electric current across consolidated clay at 45% water content between the various electrode types. The voltage used was a constant 55V/m to give a varying current over the profile and RO water was supplied to the clay height at each

electrode. The EKG test had RO water being supplied to the electrode tanks whilst the tubular electrodes had water applied directly into the tubes.

Effluent flow, current and voltage values were recorded at regular intervals and undrained shear strength was determined after the testing along with electrode degradation by measuring mass loss. These characteristics were used as a determination of the success of this test as the primary role of the electrodes is to apply a current to the clay to force migration of ions in it. Atterberg Limits and elemental analysis would have shown nothing worthwhile due to the fact that stabilisers were not introduced into the system.

During installation of these electrodes into the clay, centre point distances between anode and cathode were kept at a constant 350mm across the electrode types with the exception of the EKG which due to its sheet like nature was placed next to the cell end walls at a spacing of 370mm. The tubular electrodes were inserted into pre hand augured holes and were inserted to a depth of 230mm to avoid touching the base of the cell.

4.11.3 Electrode Type Choice 2

It was decided to conduct a second stage of electrode choice experiments after the notion of using a plastic electrode with a conductive polymer was developed in section 6.2.3, called the PEG electrode. In order to compare this new electrode type with the previous electrode type experiment, it was necessary to compare them directly with both stainless steel tubing and the EKG.

The test was run using the standard test cells with RO water used as the fluid for migration. A voltage gradient of 55V/m was used on ECC compacted at 32% water content. The test was run for 28 days with readings of current, voltage and effluent flow taken every 24 hours. After test completion, the electrodes were weighed and shear strengths were taken.

During installation of these electrodes into the clay, centre point distances between anode and cathode was kept at a constant 350mm across the electrode types with the exception of the EKG which due to its sheet like nature was placed next to the cell end walls at a spacing of 370mm. The tubular electrodes were inserted into pre hand augured holes and were inserted to a depth of 230mm to avoid touching the base of the cell.

Due to leakage issues, this experiment became the Long Term PEG Trial as discussed in section 4.11.4.

4.11.4 Long Term PEG Trial

A 540 day trial was conducted on compacted ECC to assess the effect of using PEG electrodes to drive water through the clay. ECC was compacted at 32% water content into a test cell and then the electrode holes were hand augured. RO water was supplied to the installed PEG electrodes using medical drips. The electrodes were 300mm apart and inserted to a depth of 225mm. A voltage of 30V was applied to the electrodes with water being topped up when required.

After completion, shear strengths and water contents were taken to assess the water migration extent through the clay.

4.11.5 PEG Cathode Trial

Leading on from the results gained from the Electrode Type Choice results for the PEG electrode, it was decided to ascertain whether the PEG electrode could be used in any capacity in EKS in an effort to reduce costs but still have an effective system. To this end, tests were conducted with a stainless steel anode and a PEG cathode in combination after evidence to this combination's success was reported, Figure 3-5.

For this test, three test cells were used with each containing 32% water content compacted ECC to a depth of 250mm. The electrodes were inserted into pre hand augured holes at 350mm spacings to a depth of 230mm. A dc power supply produced an initial voltage of 20V which was increased to 50V after two weeks to ensure stabilisers were being migrated after concerns over the PEG's higher electrical surface resistivity leading to a higher electrical current requirement. RO water was used with appropriate stabilising chemicals at each electrode. The level in each electrode was kept constant using medical drip devices.

The voltage and current were recorded every 24 hours and then shear strength, XRF analysis, water contents and Atterberg Limits were recorded after the test.

4.11.6 Current Intermittence

Through the literature review, it was discovered that utilising current intermittence on the power supply to the electrodes can reduce the power consumption of the system. The studies that had used current intermittence did not specify why certain time intervals were chosen and thus it was necessary for this testing to determine appropriate times.

The times chosen reflected those in the literature with 15 minutes on 15 minutes off, 30 minutes on 15 minutes off and 45 minutes on 15 minutes off. A constant current test was also

produced to ascertain the effect of current intermittence compared to it. A final test was produced using the 30 minutes on 15 minutes off timing but instead of using stainless steel electrodes like the other tests, PEG electrodes were used, Table 4-7.

Each test was conducted in a Perspex cell of 200x200x160mm dimensions filled with ECC compacted at 30% water content and the electrodes were all fed fluids through medical drips.

The current intermittence was run for 14 days with the voltage and current recorded along with fluid inflow and outflow to the electrodes and their pH, Figure 4-10. After testing, the undrained shear strength and water contents were recorded across the sample locations, Figure 4-11.

This experiment was run with the assistance of an MSc student, Spear (2014).

Table 4-7: Current intermittence test details.

Cell	**On/Off Interval (Minutes)**	**Power On Ratio (%)**	**Electrode Type**
A	Constant	100	Steel
B	15/15	50	Steel
C	30/15	67	Steel
D	45/15	75	Steel
E	30/15	67	Graphite

Figure 4-10: Current intermittence trial setup. A: Fluid containers, B: Power supplies, C: Flow regulators and D: Electrokinetic test cells.

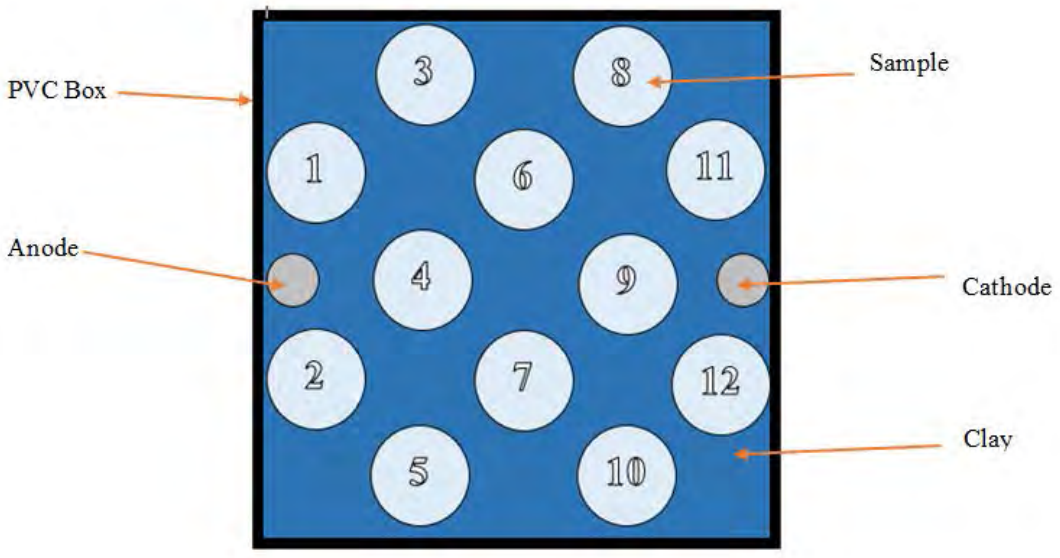

Figure 4-11: Current intermittence sample locations plan view. After Spear (2014).

4.11.7 Mock Foundation

To assess the EKS effect on a mock foundation, a breeze block was cut to size to fit in the test cell. The breeze block was cut smaller than the width of the test cell to ensure rotation was possible. Four dial gauges per mock foundation were positioned as to measure the movement of each corner with the dial gauges fixed to the inner sides of the test cells.

The test was performed on ECC compacted at a water content of 15% to ensure water seeding would be necessary before EKS could take place efficiently. This would allow the water seeding effect to be gauged on the mock footing.

The power supplies were set to a constant voltage of 20V which powered the stainless steel electrodes placed in pre drilled holes in the clay. For the first seven days of treatment, water was added to both anodic and cathodic chambers to avoid hydraulic head where possible. After the seven days of seeding, the stabilising chemicals were added at their respective electrodes.

Voltage, current and dial gauge measurements were recorded throughout the test with shear strength, water content, Atterberg Limits and shrinkage limits taken post completion. Visual inspections and weighing the breeze block mock foundations were also performed to assess and degradation that may have been caused by the EKS process.

4.12 Experimental Characteristic Analysis

4.12.1 Shear Strength

Shear strengths were gained by the use of a Pilcon Engineering hand shear vane for in-situ testing and a TRITECH 50kN compression test machine for unconfined triaxial testing on cored samples. All testing was performed to BS1377-7: 1990.

4.12.2 pH Levels

The pH measures the level of hydrogen activity in the clay which is sensitive to the ambient temperature. The apparatus used for this measurement was a Hanna HI 98127 pHep®4 pH/Temperature Tester which is calibrated to both alkaline and acidic solutions and temperature calibrated.

The clay specimens were dried and crushed to allow the creation of a suspension with RO water which was then pH tested as per BS1377-1: 1990.

It is known that the introduction of salts into a clay affects the electrical conductivity of the clay and in turn can alter the pH data to give false readings, (Kissel, et al., 2009).

4.12.3 Electrical Conductivity

The conductivity of the clay was measured to assess how it is affected by the electrolysis and presence of stabilising chemicals. The measurements act as an estimation into the amount of dissolved salts in the system and thus the ability and extent of its ability to conduct electricity. All tests complied with BS7755-3.4: 1995.

A Hanna HI 8733 conductivity-meter was the chosen piece of apparatus to determine the conductivities and was measured in micro Siemens per centimetre (µS/cm). The device is able to operate within 0.0 – 199.9mS/cm and 0 – 50˚C.

During testing the samples were kept at a normal room temperature (approximately 22˚C) and samples were tested directly after extraction.

Saarenketo (1998) shows a kaolinitic clay's electrical conductivity against volumetric moisture content as seen in Figure 4-12. If it is considered that the majority of flow through electroosmosis is in the form of free water, then it can be assumed that EKS will work most effectively in kaolinitic clays of water content >30%.

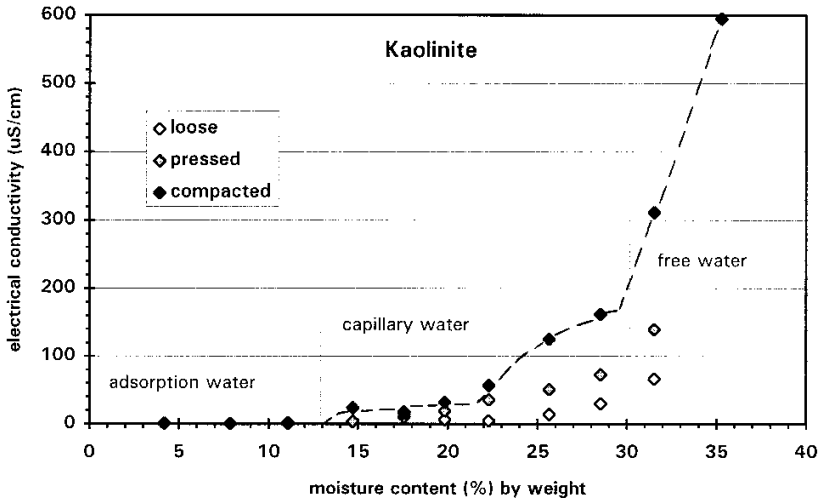

Figure 4-12: Electrical conductivity against gravimetric moisture content in kaolinitic clay. After Saarenketo (1998).

4.12.4 Soil Resistance

The soil resistance was determined using Ohm's Law where;

$$V = I \cdot R \tag{4-4}$$

Where V is the voltage over the specimen, I is the current induced over the specimen and R is the resistance of the specimen.

The obvious limitation of this method of determining soil resistance is the fact that the area between the electrodes is treated as one resistivity whereas in reality there is most likely a gradient. The other practical option would be to insert probes at required points across the sample and read off the resistances when needed. This however would interfere with the electric field itself and inevitably the results of the experiments.

4.12.5 Water Content

Water content testing from each experiment complied with BS1377-2: 1990.

4.12.6 Atterberg Limits

Each sample taken from a test cell was tested for liquid limit (LL) and plastic limit (PL) and shrinkage limit (SL) according to BS1377-2: 1990.

The plasticity index (PI) is a percentage used for defining the shrinkage potential of a given soil;

$$I_P = W_L - W_P \tag{4-5}$$

Where W_L is the LL and W_P is the PL.

The values given are approximations as structure and hysteretic effects are ignored. Section 4.12.7 shows how the linear shrinkage testing was performed.

4.12.7 Linear Shrinkage

Linear shrinkage testing was carried out to BS1377-2: 1990 using the linear shrinkage mould. Natural clay was rifled to remove course particles and then mixed with RO water to the calculated liquid limit.

4.12.8 Elemental Analysis

Elemental analysis was conducted using a Bruker X-Ray Flourescence S8 Tiger machine. The S8 Tiger can determine concentration by weight percentages of elements between and including sodium and uranium on the periodic table. Rubidium will show up on any results due to the device using the element to scan the samples therefore rubidium can be ignored. Due to the sensitivity of this device, contaminants from the laboratory or human handling can be found in the results therefore it is important to ensure any object coming in contact with the samples is cleaned with RO water.

Both solids and liquids can be assessed using the S8 Tiger. Liquids are analysed as they are and solids are prepared dependant on their nature. In the present case, solids are oven dried at 106°C and then ground using a SIEBTECHNIK Tema Mill Laboratory Disc Mill. The container for the mill was cleaned with RO water between each sample grind to avoid cross contamination. Metals are flattened and processed without any changes.

4.12.9 Electrode Resistance

The surface resistivity of a material is the material's ability to leak away localised charges. Electrode surface resistances were measured using a Maester M450 voltmeter which has a reading range of 0 – 2MΩ. Measurements were taken whilst the electrode was resting on a nonconductive surface with no other interference at a distance of 300mm between the probes where possible. Five readings for each electrode were taken and the average value reported.

Resistivity values were calculated using equation 4-6;

$$R = \frac{\rho L}{A} \qquad 4\text{-}6$$

Where R denotes the resistance of the material, ρ is the resistivity of the material, L is the length of the material and A is the area of the material. The sizes of each electrode were taken as the sizes used in the laboratory experiments.

4.12.10 SEM Microstructure

The Scanning Electron Microscope (SEM) used was a Philips XL30 FEG ESEM from the University of Birmingham's Materials and Metallurgy department with assistance from Paul Stanley. The unused steel samples were deemed electrically conductive enough to use without coating

whereas the other samples such as PEG and concrete were not. These samples were sputter coated with gold and platinum (separately) to a thickness of 5nm to ensure electrical conductivity.

Photographs were taken of various points on the samples surface at a range of magnifications. Multiple points were used to get a better overall view of the sample, albeit a very small part of a small sample of a large object. Thus the limits of this endeavour are understood. The ranges of magnifications used were 75x to 50,000x in order to observe the general structure and the microstructure. Once magnified, the visuals were captured and used for comparisons.

4.12.11 Sample Extraction

Liquid samples were taken using syringes and stored in screw cap plastic bottles in a fridge at 4.0 ± 0.5°C.

Clay samples taken after test completion were conducted using steel core tubes. Once hand vane readings had been taken, the cores were inserted and clay removed. A core extractor was used to remove the clay from the core and the clay samples were wrapped in cling film, placed in a numbered sealable plastic bag and kept in the fridge at 4.0 ± 0.5°C for testing later.

Unless otherwise stated, samples were taken as shown in Figure 4-13 and the Top and Bottom depths were at 1/3 and 2/3's of the total sample depth. For clarity, the results taken laterally across the samples were averaged.

1	3	5	7
2	4	6	8

Figure 4-13: Sample locations. Anodes were inserted between 1 and 2 with Cathodes between 7 and 8.

4.13 Summary

Through this section, details of the laboratory testing regime have been presented. It is shown how the laboratory setup was achieved and further developed from the inherited equipment in

the University of Birmingham laboratory. Details of the tests conducted are presented with the methodologies followed for geotechnical characteristic analyses.

Through this laboratory testing regime, an idea as to how the chemicals and electrodes will behave during the EKS process was intended on being gained with the intention of taking the lessons learnt forward to the site trials. A development of the methodology was also to be produced with the goal of site application in mind at all times.

It was anticipated that repeats of each experiment should be conducted to ensure reliability of results however due to time constraints and problems outlined later in this thesis, this was not always possible. As such, repeats of a select few experiments were completed. The equipment and procedures used for the experiments and testing throughout this work have been designed to generally accepted guidelines as specified by British Standards. The nature of laboratory and site testing however, presents the probability that errors are made and contaminations occur. The production of control tests should reasonably negate any contamination errors along with any other errors.

5 SITE TRIAL METHODOLOGY

5.1 Introduction

This section presents the site trial details covering the location, geology, methodology, equipment and testing. The objective of performing site trials was to observe the process of EKS in a real world setting which is largely out of the author's control, characterised through ground conditions likely to be little understood and heterogeneous. Laboratory scale trials are useful for understanding the process in a controlled environment but not a realistic one. To understand if the process has any real world applications, it is required that it is run in a true to life setting at near to or exactly full scale. As such, a site trial was devised to further develop the methodologies studied in the literature review and laboratory trials.

5.2 Site Details

The site chosen was the Headmaster's garden at Aldenham School in Hertfordshire WD6 3AJ, UK (515656E, 197327N), Figure 5-1, Figure 5-2, Figure 5-3 and Figure 5-4. The site in question consisted of a grass area with multiple tree and fauna overlying an outcrop of volumetrically unstable London Clay. This site was chosen over the others considered due to its fulfilment of the following criteria:

- Known History: A history of regular monitoring of site characteristics such as levels, ground resistance and weather by The Clay Research Group (CRG) and Jones (2010).
- Sub-strata of high shrink swell capacity: An outcrop of London Clay to near surface.
- Easy access: Easy access yet secure due to being private land.
- Ease of use: Relatively flat for easy use, Figure 5-1.

Other sites considered were a quarry in Kent, a field and a back garden in Essex. All options featured London Clay but the Aldenham site proved fruitful in negotiating the project details.

The ground conditions of the Aldenham site have been monitored by the Clay Research Group since 2006 and under the PhD of Glenda Jones, (Jones, et al., 2009), two resistivity arrays and two precise levelling point lines were inserted into the ground from a willow tree in the Headmaster's garden. Over the 8 year period since the equipment was installed, monthly

resistivity measurements were taken until 2011 and monthly levels have been taken by both Glenda Jones and then the CRG.

Figure 5-1: Site trial area with nearby subsidence affected house.

The Aldenham site existed as the garden of a 1960's built detached domicile undergoing shrink/swell related subsidence. The Willow (Salix Spp.), Table 5-1, is situated approximately 30m away from the domicile and approximately 40m downslope of a similar willow. Hedges, young trees and shrubs form the perimeter of the garden. The site is 95-93m above sea level sloping from east to west (high to low).

Table 5-1: Willow tree characteristics.

Characteristic	**Value**
Tree Name	Willow (Salix Spp.)
Height (m)	~14
Trunk Diameter DBH*(m)	0.57
Age	~40
Canopy Diameter (m)	10

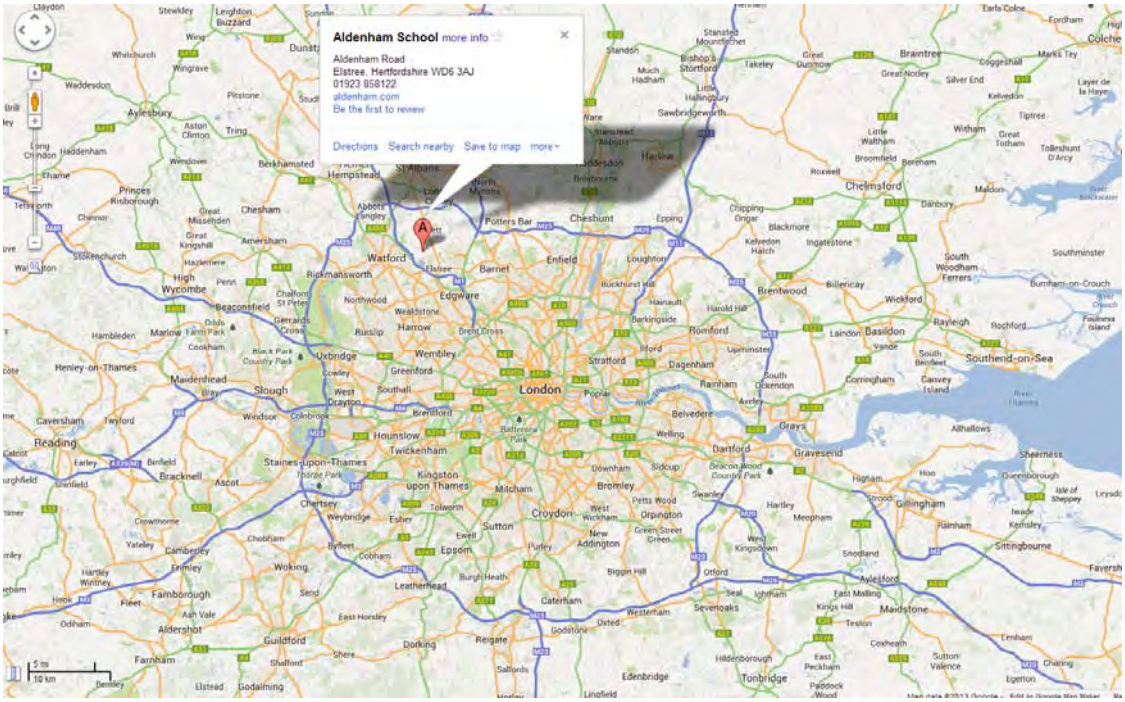

Figure 5-2: Aldenham School location from Google Maps.

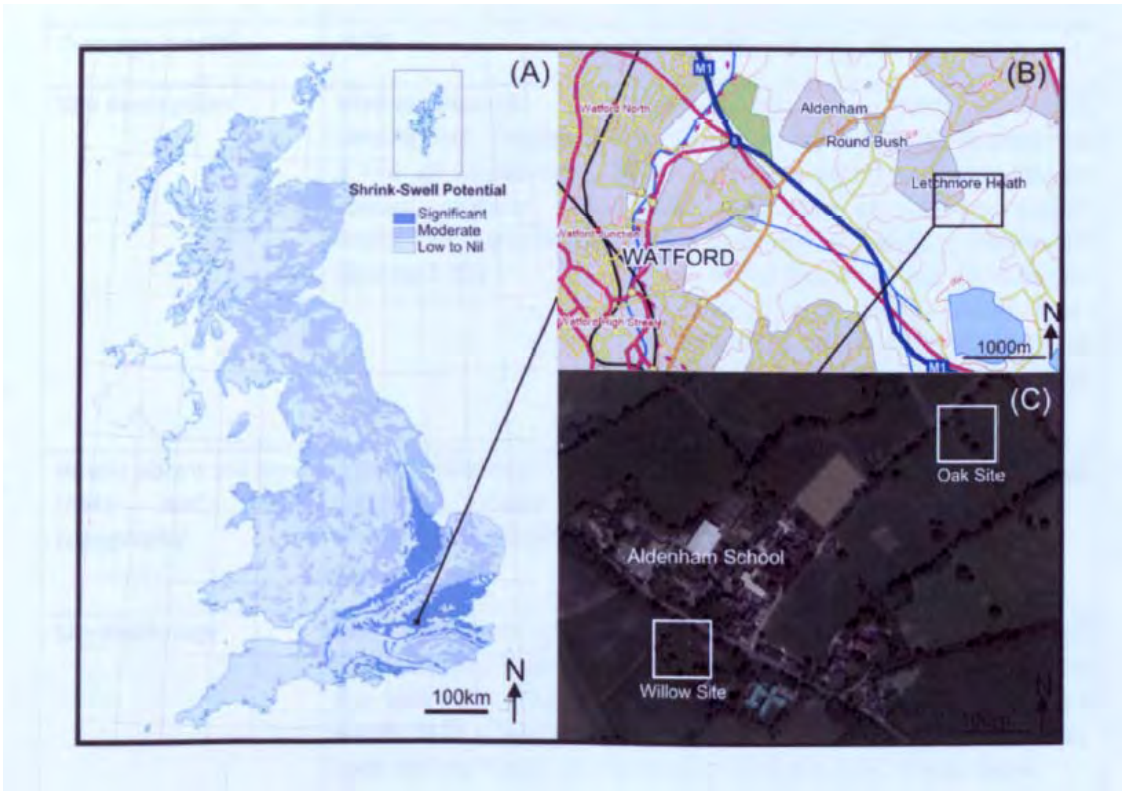

Figure 5-3: Site trial map with shrink swell potentials. After Jones (2010).

Figure 5-4: Site trial map from Google Maps.

5.3 Site Geology

The site stratigraphy was determined in 2006 by Mat Lab Ltd under instruction from Glenda Jones, (Jones, 2010). The results of the borehole investigation in Figure 5-5 show that gravel is expected from the surface down to approximately 400mm and then clay is found to 6m. This is taken at 9m from the Willow tree as this is the approximate area the site trial will be situated.

The LL is expected to be 70-77%, PL is 21-25% and PI 45-54% as shown in Figure 5-5. This leads us to conclude that the clay is highly expansive which corroborates the history of subsidence at the property.

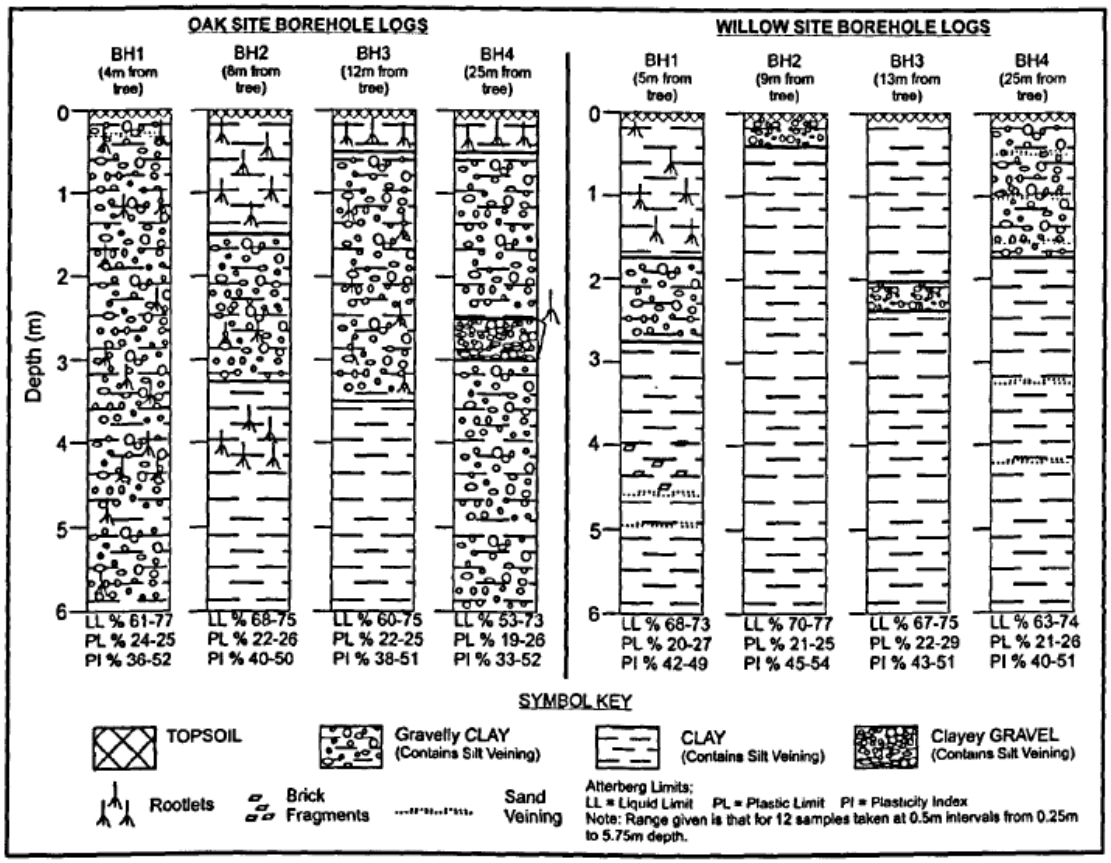

Figure 5-5: Site trial borehole logs. After Jones (2010).

5.4 Site Plan

Numerous variations of the plan for the Aldenham site were contemplated and either dismissed or adapted depending on budget, objectives and allowances from Aldenham School. The original plan was to construct eight full size (600x1000x2000mm) concrete strip footings between the existing resistivity arrays to test using different permutations of the EKS process. Each footing would be loaded to 40kN/m using hydraulic jacks attached to a loading frame that would use friction piles to transfer load to the ground to simulate a low rise building foundation load. Kentledge blocks were then considered as a loading medium but discarded due to safety concerns over the large weights required.

After the initial site visit it was agreed that this would be too large a construction for the area and so was reduced to four footings. Site dimensions were agreed with the owners to be 5x7m and FEA simulations were initiated to ensure that the current paths did not interfere between tests. Using the FEA simulations it was clear that interference would occur and thus the

decision was made to reduce the size of the footings to 0.3x0.3x1.0m, ensuring no current leakage between tests. Quickfield was used to determine the distance needed between each footing to prevent current being leaked from one test to another where it was found that 2m was required between each footing to bring the leakage down to less than 1% of what is needed for effective fluid migration, (Gray, 1970).This reduction in size also lead to easier removal from site after the trials and also a higher possible voltage gradient across the footings.

Subsequent meetings alluded to the fact that loading the footings via friction piles could serve to dampen any movement that could be seen in the footings and so would be unhelpful in concluding on the effect of the treatment on existing structures. It was therefore decided not to load the footings and therefore allow any movement caused by the treatment technique to manifest fully for measurement.

Figure 5-6: Site trial pile installation.

The reference frame was adapted to be anchored using six 6m x 0.25m diameter piles and scaffolding poles as seen in Figure 5-6, Figure 5-7 and Figure 5-8. The piles were reinforced with a scaffolding pole inserted into the centre of the pile which protruded 0.3m above ground

level to affix the reference frame to. The top level of each pile was constructed to 0.3m below ground level to ensure ease of burial after completion.

The four mock reinforced concrete strip footings were set out as follows:

- Footing 1: Footing 1 was the raked electrode test. The electrodes were inserted from the one side of the footing to replicate the idea of treating a house footing from the exterior only. Three electrodes were inserted from the one side of the footing at points shown in Figure 5-7 at an angle of 45 degrees under the footing.
- Footing 2: Footing 2 was the standard stainless steel electrode test. This involved four stainless steel electrodes 40mm BSP being inserted vertically at points seen in Figure 5-7. Each side of the footing had both an anode and a cathode to enhance and localise the spread of the current density. This is explained in more detail in the numerical simulation section 6.3.
- Footing 3: Footing 3 was the control test. The reinforced concrete footing was cast in the ground but not treated using EKS, instead it was left for the test period to act as a benchmark for how the ground would react normally. Thermocouples were still used on this footing to ascertain any natural changes on temperature under the footing. The same post treatment tests were conducted on this trial as all the other trials.
- Footing 4: Footing 4 was the current intermittence test. This involved the exact same test setup as footing 2 but with intermittent current being applied. From the laboratory tests, an on off ratio of 30 minutes on to 30 minutes off was devised and applied to the test constantly for the entire test period. The idea of this was to increase the level of treatment whilst decreasing the power and thus cost of the treatment.

The concrete footings were designed and constructed using C20 grade concrete to mirror what would be used in reality. By doing this it was possible to monitor any adverse effects that the EKS process may have had on the concrete in a commercial situation.

As part of the agreement to allow this testing to go ahead, a few stipulations were made by Aldenham School. Firstly, a 1m tall picket fence was to be erected around the site to block off the view of the test whilst being aesthetically pleasing, Figure 5-9. The second was to place a sign on the fence explaining details about the trials and why they were taking place, Appendix C. The third was that the author explained the present research to the School's A-Level students and gave them a guided tour of the site.

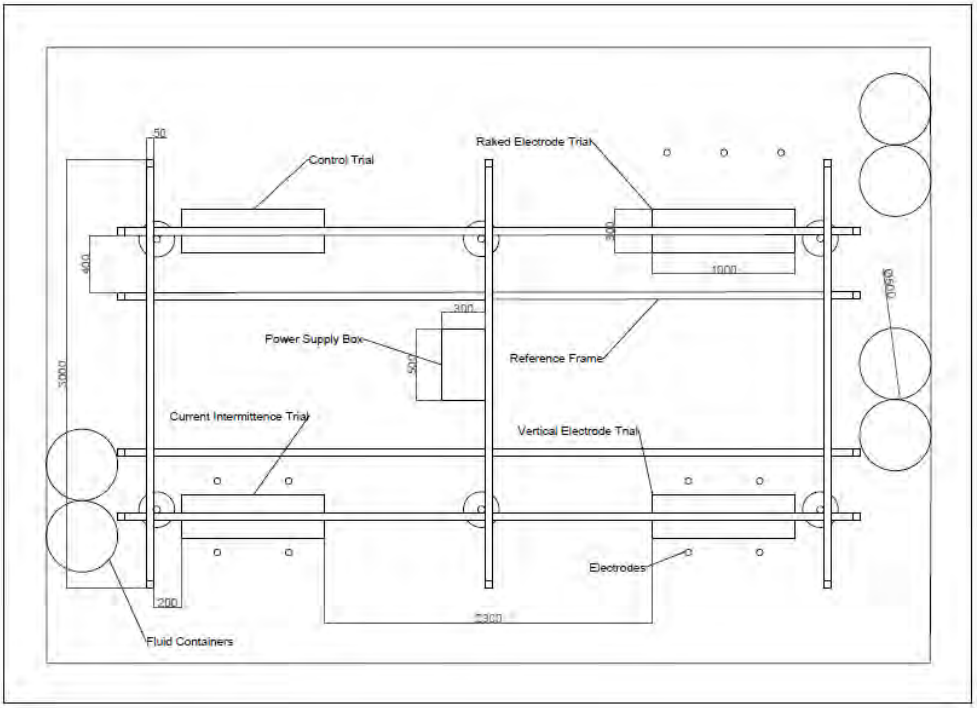

Figure 5-7: Site trial aerial plan.

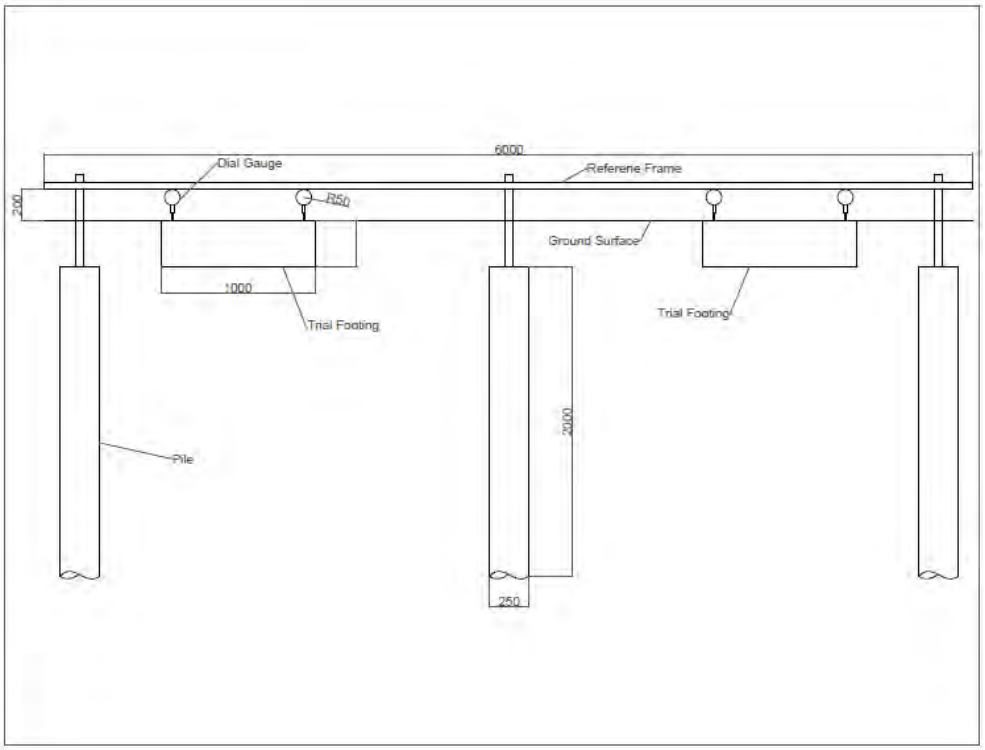

Figure 5-8: Site trial side plan.

Figure 5-9: Site trial site setup.

5.5 Monitoring

Each footing was monitored at regular intervals over the two month trial period. The thermocouples and dial gauges were read twice a week to keep track of the changing temperatures and footing levels. The voltage and current was to be tracked by the bespoke power supply unit and saved to a memory card. The initial plan of using telemetric data loggers to record this data turned out to be too expensive for the site design and level monitoring by total stations and reflection prisms was considered but again proved too costly. The manual dial gauges were decided upon due to their simplicity and low cost.

Although the final monitoring setup was not ideal due to a constricted budget, adaptations were made for manual readings to be taken regularly enough to prove useful, albeit not as accurately as the automated systems. It was considered that this simpler method however, was more durable than the electronic system would have been.

5.5.1 Voltage and Current Monitoring

The voltage and current were to be monitored by the power supply which had a memory card to record all data at regular intervals. Although this proved to work well in the laboratory, the system proved less durable on site and as such manual readings were taken to ensure data was preserved.

5.5.2 Level Monitoring

The manual dial gauges were supplied by Arbil with the mounts that attached the gauges securely to the reference frame fabricated by Foundation Piling Ltd, Figure 5-10. The gauges had maximum extensions of 50mm and an accuracy of 0.01mm. Due to the possibility of witnessing more movement than the 50mm dial gauges can measure, the gauge mounts were produced with the ability to move the gauge vertically as needed. Due to the mount being built of mild steel, each part was coated with red oxide paint to avoid rusting and the chance of being unable to move the gauge. Each gauge was secured inside a Tupperware box with the bottom end removed for measurement access.

The dial gauges were calibrated for temperature by assessing their level readings at various temperatures. The laboratory, a fridge and a freezer were used for this. Table 5-2 shows the temperatures and level readings gained from this which shows that over the expected 10mm movement, temperature error may account for up to 0.16%. In the context of footing movement, it is something that can be ignored. In the site trials, the scaffolding poles that the gauges were affixed to would expand and contract with varying temperatures however it is thought that they would expand and contract equally simultaneously leading to relative level changes being recorded which were sought anyway.

Table 5-2: Temperature effect on dial gauges.

Dial Gauge	Temperature (°C)	Level Reading (mm)
DG 065	-5.000	-0.015
DG 065	4.000	-0.012
DG 065	20.000	0.000
DG 066	-5.000	-0.016
DG 066	4.000	-0.008
DG 066	20.000	0.000
DG 068	-5.000	-0.009
DG 068	4.000	-0.006
DG 068	20.000	0.000

Figure 5-10: Dial gauge with fabricated scaffold mount.

5.5.3 Resistivity Monitoring

Ground resistivity measurements were recorded by Professor Nigel Cassidy of Keele University in an attempt to build resistivity profiles under the footings over the treatment period. The two existing resistivity arrays were not used due to their distance from the trials and so a new grid was established around footings 1 and 2 (raked and vertical electrode trials). The grid was composed of 64 nodes with each node being 0.5m apart.

The measurements were taken using Time Domain Reflectometry (TDR) whereby an electrical current is sent between specific nodes inserted into the ground to gather resistivity measurements. By measuring in three directions and between nodes at various distances, a profile of resistivity can be compiled for the ground underneath the trials.

The TDR measurements were taken before the trials were initiated but after the site was built, the second set of measurements were taken after water had started migrating through they clay, the third set were taken during the chemical introduction and the last set taken after the trials had finished.

The TDR cables can be seen in Figure 5-9 as the yellow cables.

5.5.4 Weather Monitoring

The weather station on the site became inoperative weeks before the start of the site trials and a new one wasn't available until after the site trial took place. It was thus decided to track temperature and rainfall via online services. Temperatures were compared to the air temperatures taken on site for an indication of site accuracy.

The weather station utilised was approximately 10 miles away in Northolt (51-33N, 000-25W) at 38m above sea level.

5.5.5 Temperature Monitoring

In the site trial, the temperature was monitored through the use of K-Type thermocouples that have error percentages of ±2.2%. The thermocouples are a rugged method of measuring the temperature of a region that is not practical to be reached manually. In this case, the thermocouples were buried at specific points under the concrete footings, as seen in Figure 5-11, with one left at 100mm above ground level to ascertain the air temperature. The pattern in which the thermocouples were placed in was to ensure data can be collected;

1. On the thermal gradient between a positive and negative electrode (top of the T shape)
2. At the centre point between all electrodes
3. At the centre point between the other two electrodes.

The plug connection ends of the thermocouples were wrapped in plastic bags and sealed inside a Tupperware box for protection. The measurement end of the thermocouple was protected by folding duct tape over it and then sealing in a plastic bag on recommendations from Professor Nigel Cassidy, Figure 5-12. Before concrete was poured into the footing excavations, each thermocouple was buried slightly under the clay and the wire was pushed into a channel that was cut along the base and up the side of the excavations, Figure 5-13.

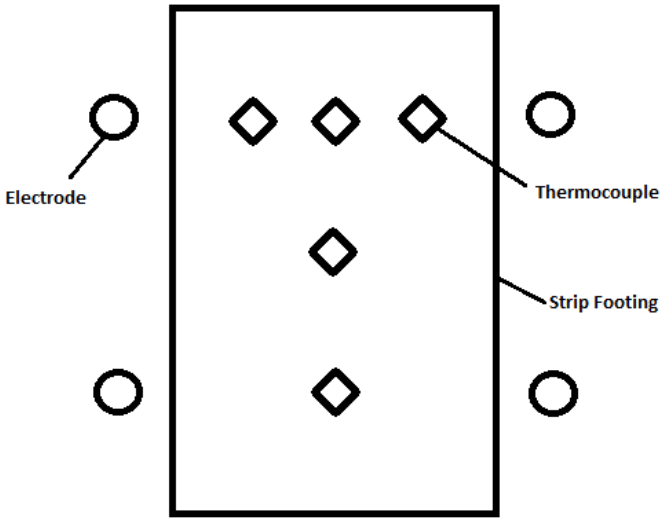

Figure 5-11: Thermocouple layout under strip footings.

Figure 5-12: K-Type thermocouple in protective bag ready for insertion.

Figure 5-13: Thermocouples buried under clay with wiring hidden in channels in the side and base of footing excavations.

5.5.6 Electrolyte Monitoring

The electrolyte levels were monitored manually. Visual inspections were made and top ups administered if required to keep a constant hydraulic head.

5.6 Equipment

The following equipment and materials were used for the site trials either by being developed by the author or being sought externally.

5.6.1 Electrodes

The electrodes used in the site trials were 40mm BSP stainless steel tubing from Valgram Ltd. Each electrode was cut to its 1m length before transporting to site. The electrode cap was milled from solid polyurethane and was inserted into the bottom end of each electrode to stop electrolyte leaking vertically out the end and also to protect the electrode whilst insertion took place, Figure 5-16. The electrode topper comprised a plastic Tupperware box with the electrode connected to the base and a mini float valve in the side, Figure 5-15. The fluid was to travel from the water butts and through the float valve into the electrode topper. The flow would stop once

the float valve closed. The float valve's placement was such that the level of the fluid inside the topper was lower than the level of the ground surface to avoid a hydraulic head developing by fluid flowing over the surface and causing a preferential current flow path and a waste of chemicals.

Each electrode had 4mm diameter holes drilled through them. These perforations were only in the direction of required flow, so in the direction of the oppositely charged electrode. The upper part and back side of the electrodes were insulated using Hammerite Red Oxide rust paint as it had proven to possess a sufficient electrical resistance in the laboratory in an effort to gain directed flow. Duct tape and shrink wrap were considered but paint was deemed to most likely to stay intact on electrode insertion. The numerical modelling suggested that the insulation of the electrodes should be to twice the depth of the footing which in this case was 600mm out of the 1000mm length electrodes to avoid chemical flow towards the foundation. It was decided to insulate to 400mm to ensure that maximum effects on the clay could be found after the trials. This was the priority and drilling deeper with longer electrodes would have taken too much time.

The electrical power wiring was connected to the electrode originally by bulldog clips but after arriving on site this was changed for a lug and bolt system to avoid corrosion of the joint. The whole connection was covered in silicon sealant and duct tape in an effort to avoid corrosion. Figure 5-14 shows the connection detail.

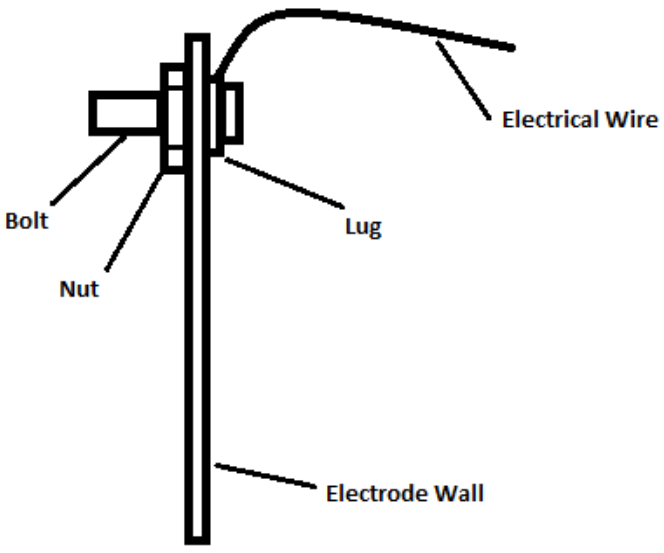

Figure 5-14: Electrode to power supply cable connection detail.

Figure 5-15: Modified float valve from within the electrode topper.


Figure 5-16: Site trial electrodes with end caps and red oxide paint cover.

5.6.2 Fluid Containment

The fluids, sodium silicate and calcium chloride mixed with H_2O, were placed in their respective 210L water butts separately. A problem foreseen with the storing of the chemicals in the water butts was the possibility of the chemicals settling out of suspension and either blocking the tubes or not flowing into the electrode. Industrial mixers and electric hand drills were considered as tools to keep the mixture moving and in suspension but were eventually disregarded due to expense and impracticalities respectively. The option chosen was to attach a mains powered disco ball motor to the water butt lid, which revolved at approximately 1.5 turns per minute, with a plasterers paddle fixed to its connector, Figure 5-17. The disco ball motor was a Eurolite MD-1015 and the paddle was supplied by Homebase. This development allowed a steady mixing of the fluids over the course of the experiment.

The water butts were connected at their side base to the electrode topper by a tap and hose piping which was all sealed before use using jubilee clamps and silicon sealant. To allow smooth flow, the water butts were not airtight.

Figure 5-17: Water butt stirring mechanism attached to the base of the water butt lid.

5.6.3 Power Supply

The electrodes were connected to the power supply by cables and banana plugs. The power supply itself was a bespoke model designed and constructed by Andrew Tanner of the

BioSciences Department at the University of Birmingham. The power supply was developed and built before it was planned to use more than one of each electrode. This lead to the power supplied being shared by each of the pairs of electrodes. As such, 25V was supplied to each footing, but due to the sharing, each pair of electrodes actually received half of this. Therefore, the maximum voltage gradient available was 41.6V/m. It was anticipated that this would not cause a problem but would produce results lower than those expected with the full voltage gradient as originally planned.

The power supply unit had the ability to record the voltage, current and time of each set of outputs to a Kingston SDHC memory card. The unit was able to record any power cuts onto the memory card and had the options of reversing the poles and current intermittence at desired time periods.

Other options to power the trials were considered such as batteries and photovoltaic panels. For the predicted power usage over the trial period, it was not deemed necessary to buy large batteries or photovoltaic panels. These should be considered for larger projects or commercial ventures which would see the power supply being reused and therefore cost per project fall.

5.6.4 Chemicals

The chemicals used were the same as those used in the laboratory experiments detailed in section 4.6. Calcium chloride was applied to the anodes and sodium silicate was applied to the cathodes. To achieve the required 2:1 ratio mix required to produce the desired reactions, twice the amount of calcium chloride was introduced over sodium silicate. Due to ion migration speeds and the acid front development, more calcium chloride will penetrate the treatment zone than sodium silicate. This can lead to the centre of treatment not being at the target zone centre.

5.6.5 Mock Strip Footings

The mock strip footings used to replicate actual low rise building strip footings were designed as beams to allow easy removal from site. Therefore the beams were reinforced, reinforcement design can be found in Appendix D.

The footing reinforcement cages were constructed off site by Foundation Piling Ltd and delivered to site. These were placed in the excavations with concrete spacers attached to

provide 25mm cover for the reinforcement, Figure 5-18. Formwork was used along the vertical lengths as shown in Figure 5-18. Formwork was used in an attempt to gain a clearer visual depiction through the resistivity measurements and furthermore, the depth at which treatment would be taking place would be below this level making any surface gaps unimportant. The time between foundation construction and treatment was approximately two months; any gaps present at the time of construction would have closed up in this time.

The concrete itself was mixed by hand from a sand/coarse aggregate mix, Portland cement and tap water. As mentioned previously, C20 grade concrete was desired to replicate what would be used in reality for this type of foundation. Sample cubes were taken of this concrete for laboratory testing to ensure it was C20 standard. A concrete compression testing machine was utilised to test the concrete to failure to determine the compressive strength where it was found that all footing concrete was within 15% of C20 standard strength.

Test cubes were taken whilst mixing the concrete were tested at 28 days for compressive strength and the results can be seen in Table 5-3. Specimens 3 and 3A were taken from the same mix and therefore an accurate average of this can be taken which gives 20.71N/mm^2 which is a 3.55% error from theoretical C20 concrete.

Table 5-3: Concrete cube strength values with error compared to theoretic C20 strength.

Sample	**Compressive Strength (N/mm^2)**	**Error Compared to C20 (%)**
3	19.22	3.9
3A	22.20	11.0
4	22.80	14.0

Figure 5-18: Site trial footing reinforcement and shuttering before concrete pouring.

5.7 Post Completion Testing

Samples were taken from beneath each footing for testing in the laboratory. The locations of these samples can be seen in Figure 5-19 and Figure 5-20. The sample locations shown were chosen as adequate examples of the various sections of treatment zone. Each location is directly under a thermocouple to combine the temperature data with the samples taken. These samples were originally intended to be extracted using U100 cores for ease and accuracy but due to budget and logistical limitations, this was not possible. GIP UK offered assistance in men to help dig the samples by hand and test a handful of the samples. Notably, the centre location for each trial was at a depth of 0.5 – 0.7m. The constrained budget for post-treatment testing was overcome through the author conducting extensive testing in the University of Birmingham laboratory using the hand extracted samples. Effective sample management such as double bagging and storing the samples in a fridge as soon as possible reduced the effect of the constrained budget on the project. A more comprehensive testing suite would have been accomplished had the full set of laboratory tests been completed by GIP, what was completed however, did provide a good indication of the treatment process effects.

Samples taken from under each footing were sealed in bags and clingfilm where necessary and transported to the University of Birmingham laboratory as soon as possible on the day of extraction. The samples were then stored in airtight conditions in a temperature controlled room at 4.0 ± 0.5°C. The samples brought back to the University of Birmingham were tested for water content, Atterberg Limits, linear shrinkage, chemical composition, pH and conductivity. All testing was done to British Standards as detailed in section 4.12.

Once extracted, the concrete footings were delivered to the University of Birmingham. Here they were visually inspected for any changes to the concrete relative to the control footing. Samples were to be taken from the centre of the bottom face of each footing to view under SEM and XRF to determine any microscopic changes.

The electrodes, once removed, were weighed and measured for electrical resistance. Samples were also taken of these for SEM and XRF evaluation with clay being washed off with RO water beforehand.

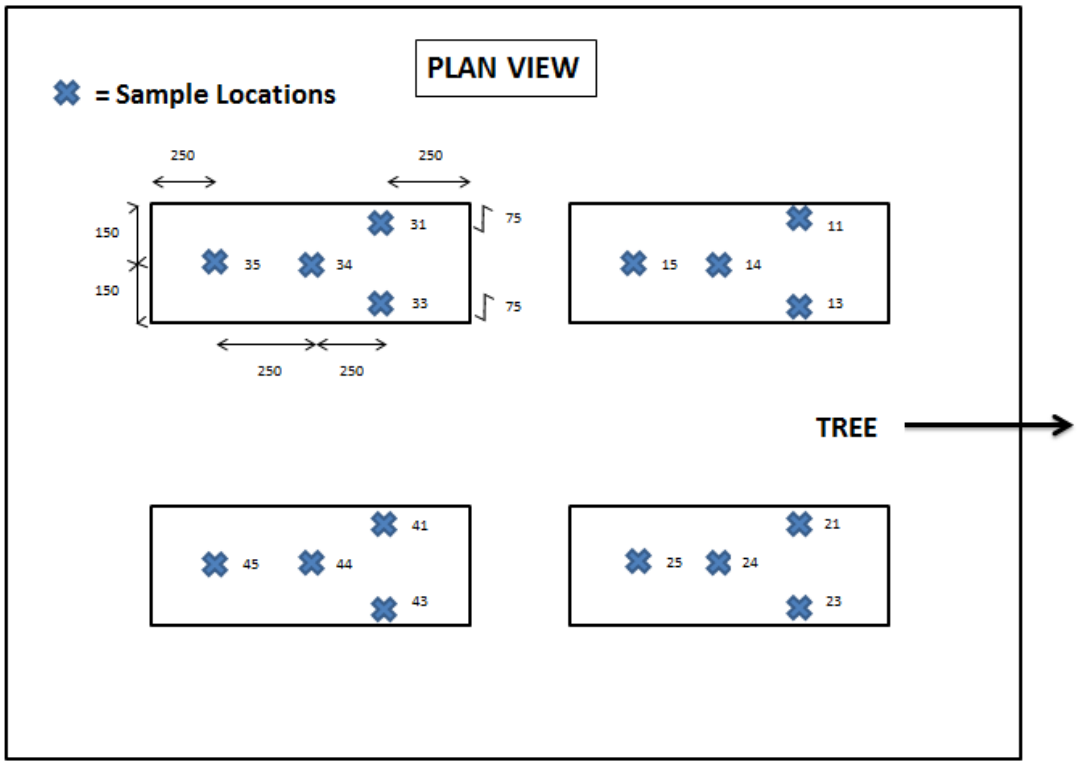

Figure 5-19: Site trial sample locations aerial view.

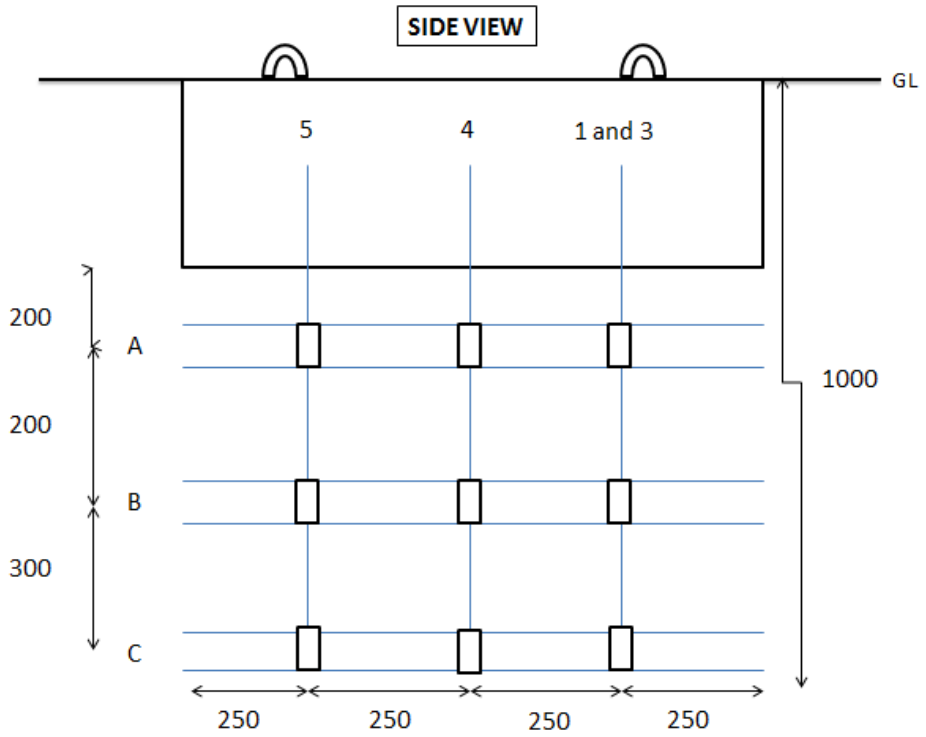

Figure 5-20: Site trial sample locations side view.

5.8 Treatment Time

The optimal treatment time is the time taken to introduce the ideal amount of the stabilising chemicals into the ground to cause the desired effect. More time taken will result in wasted chemicals and power and less time will risk not completing treatment.

As a basic estimate, one can calculate the time taken to introduce the chemicals into the ground by using Darcy's Law as an estimate for the electroosmotic flow rate and the total chemical mass needed in the soil.

Using a voltage of 55V across a span of 310mm and a 3% target total chemical concentration broken into 1/3:2/3 parts ($(Na_2SiO_3)/(CaCl_2)$), one can deduce that the total chemical concentration will be achieved in the soil in less than 48 days. This is assuming ideal conditions however and does not take into account the changing electroosmotic permeability of the soil.

It is noted that by increasing the voltage over the soil, the treatment duration decreases whereas the volume of soil treated does not have an effect. The total amount of chemicals required depends on treatment volume.

Based on this calculation it was decided to run the experiment for two months. Due to the reduced voltage gradient applied, treatment is anticipated to not have fully completed in the allotted time.

5.9 Effects on Concrete

The effects of the EKS process on the concrete strip footing are of great importance to the future acceptance of this technique as a stabilising solution. If the concrete is negatively affected in any way, the technique will not be accepted. It is therefore important to demonstrate that whilst the chemicals and pH fronts are manoeuvring through the clay, the concrete is at a distance away from the zone of influence so no damage takes place.

Whereas weighing and calculating mass loss of concrete in the lab is practical and precise, on site it is not. The footings were cast in-situ so weighing the concrete that was hand mixed on site was impractical considering the accuracy required. It was therefore concluded that chemical analysis and SEM photography would be used. The chemical analysis would be XRF scanning to gain an idea of the effect any chemicals nearby would have on the concrete's chemical structure and the SEM photography would show up any microscopic damage caused.

5.10 Temperature Effects

The effect of temperature on the electrokinetic process is as of yet unknown. The possibilities of the effects include modifying the state of the stabilising fluids and water in the soil to affecting the rate of reaction in the soil. To enable the most efficient method of the process will inevitably require a sufficient understanding of the role that temperature has to play. It is important to remember that the thermal effect on EKS may be negligible due to the depth at which the process will be taking place under the ground surface. Seasonal temperature variations are limited to the top 0.5m usually, (Kalogirou & Florides, 2014), and the targeted treatment zone in the site trials is 0.4 – 1.0m below ground level.

Considering only the viable temperatures over the site trial period in Watford, UK, one can build an average temperature range that would realistically be encountered. Table 5-4 shows that the average minimum daily temperature ranges from 1.8˚C to 4.4˚C between November and February but there are temperatures of -7˚C on record. These are rare occurrences however and fall outside of what is deemed necessary to plan for.

Table 5-4: Watford temperatures.

Month	Average (˚C)	Average minimum daily temperature (˚C)	Coldest night on record (˚C)
November	7.6	4.4	-1.0
December	5.8	3.0	-5.0
January	4.9	2.0	-2.0
February	5.0	1.8	-7.0

5.10.1 Effects on Clay

When the air temperature decreases to a point where the soil becomes frozen, one can mistakenly assume that the water in the soil is frozen too. This is incorrect as it has been accepted that unfrozen water in a frozen soil system exists, Figure 5-21, and strongly influences the heat and mass transport processes, Kozlowski (2007). This unfrozen water may potentially be able to migrate through the frozen soil system with the migration mass being dependent on the amount of unfrozen water in the system and the capillaries available for travelling through. This can be calculated using Figure 5-22.

Using the Kozlowski (2007) equation $W_{nf} = 0.042S + 3$, for a London Clay of specific surface area $62 m^2 g^{-1}$, (Tan, et al., 2003), an unfreezable water content of London Clay of 5.6% is produced. As seen in Figure 5-21 however, there are different phases of frozen water and ground temperatures in the UK rarely reach -11˚C so the unfreezable limit should not be reached.

Kozlowski (2007) does show however, that even at a temperature of -2˚C, one can expect approximately 45% of a clays water to be unfrozen. With approximately half of a clay's water frozen at -2˚C, the clay's ability to host flowing water is reduced, thus the hydraulic conductivity must be reduced.

It must be stressed again however that at the depth of treatment on site, the air temperature should not affect the process noticeably.

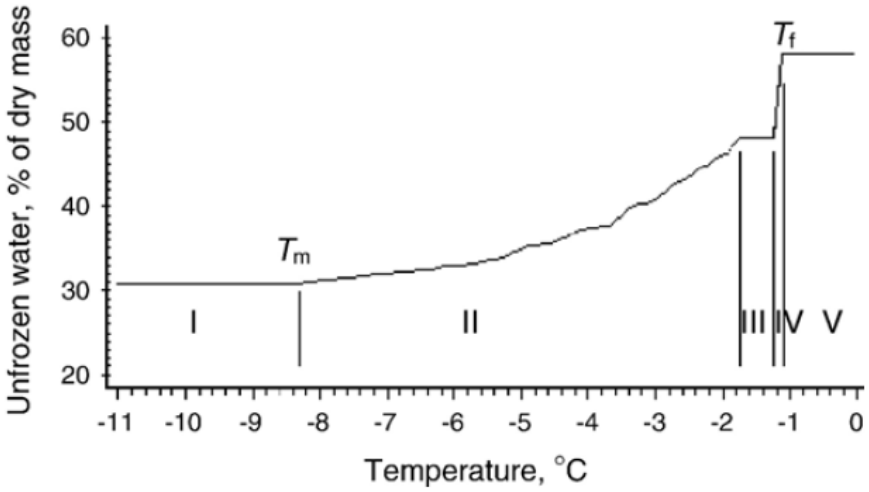

Figure 5-21: Experimentally determined plot of unfrozen water content with the characteristic zones of the phase composition change process, after Kozlowski (2007).

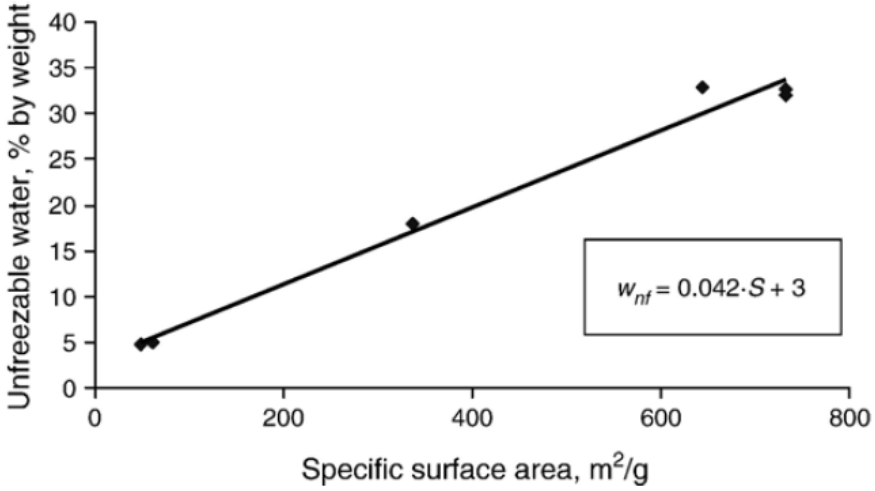

Figure 5-22: The average unfreezable water content vs. specific surface area for six model soils, after Kozlowski (2007).

5.10.2 Effects on Stabilising Fluids

The effects of temperature on the stabilising fluids are limited to the change in state of the fluids. From the literature it can be seen that sodium silicate has a freezing point of -2˚C, (Hoffman, 1965), whereas PQ-Corporation (2003) states that if silicate cools to its freezing point, the water component begins to crystallise leaving the remainder of the water over saturated with SiO_2. This results in the silica polymerising into a gel and is not easily reversible. Calcium chloride has a freezing temperature of -3˚C due to freezing point depression, (ASA, 2002).

If these temperatures are accurate, then it is plausible to assume that a 3% by weight mix of these chemicals in water will depress the freezing point although perhaps only slightly leading to the potential for the chemical mix to freeze before EKS can take place.

5.10.3 Effects on Chemical Reaction

It is well known that the rate of a reaction, with only a few exceptions, depends on the temperature at which the said reaction is taking place with an increased temperature leading to an increased rate of reaction. By using the Arrhenius equation, equation 5-1, it can be seen that by only changing the temperature of the reactants from 0 to 20˚C, one can increase the rate of reaction by 450%;

$$k = Ae^{-\frac{E_A}{RT}} \qquad 5\text{-}1$$

Figure 5-23 shows how the rate of reaction varies with the variation in temperature for an arbitrary reaction.

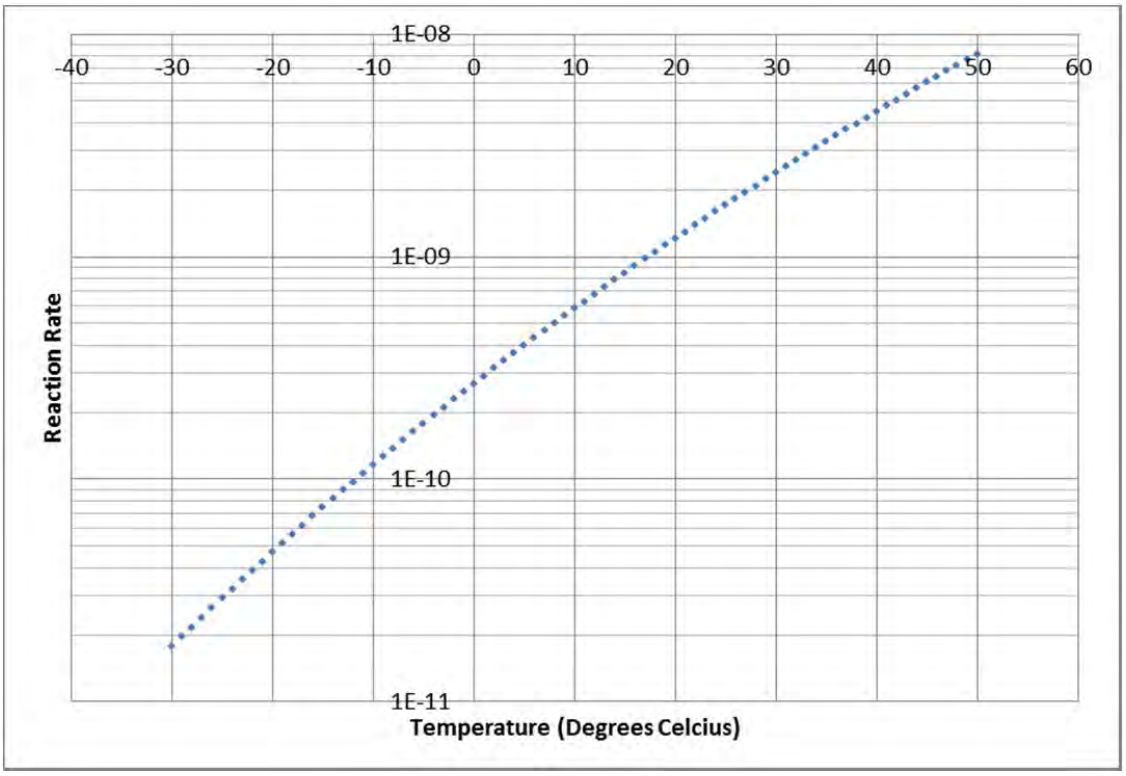

Figure 5-23: Reaction rate variance with temperature for an arbitrary reaction.

5.10.4 Methods of Keeping Reactions at Higher Than Ambient Temperature

Keeping the reaction at a higher than ambient temperature is not simple with thermal leakage at all parts of the process hampering efforts made. Bubble wrap was used to insulate the water butts and pipe lagging for the hose pipes to retard thermal leakage. Bubble wrap was chosen over more advanced lagging materials due to its low cost and adaptability. A generous amount was wrapped around and duct taped in place.

To keep the fluid's temperature higher than the ambient temperatures, fish tank heaters were considered for the water butts. To calculate the heater power required, heat loss calculations were computed which produced a heater of 99.7W power, assuming a 15˚C variance in temperature. With a 20% addition for error, a 150W fish tank heater was deemed powerful enough to heat the fluids and with a current draw of 0.65A each, would not put the overall site at risk of overloading.

Clay is known to have a low thermal conductivity, (Mitchell & Soga, 2005), and thus should not be affected by the extreme cold spells during the colder months of the year. It was thought that due to this, and the fact that the treatment zone was over 0.4m below the ground surface, that no thermal driver would be required.

5.11 Decommissioning

At the conclusion of the site trials, the following was undertaken;

- The system was turned off and power was cut to the site,
- All erroneous equipment was removed from the site,
- The electrodes were disconnected from the power supply and the power supply was removed,
- Each dial gauge was removed along with their respective mounts,
- The picket fence was taken down and removed,
- The scaffolding pole frame was dismantled and removed from site,
- A mini digger was brought onto site to lift the strip footings out of the ground and load onto the back of a flatbed truck,
- The mini digger dug around the top of each pile to allow an angle grinder in to cut the scaffolding poles in the piles off at pile cap level,
- These holes were refilled,

- The mini digger was used to remove some of the electrodes from the ground that were too difficult to remove by hand,
- Shear vane testing and sample taking were conducted using hand augers and a hand shear vane,
- A landscaping contractor was approached to make good the garden.

This would conclude the site trails and just leave laboratory testing to complete.

5.12 Summary

The information presented in this section covers the site location, geology, methodology and testing regime. The goal of this section was to take the methodologies and lessons learnt that were developed in the laboratory trials and use them in a real world scenario. Successful implementation here would give an indication that further study into this treatment solution is warranted in the future.

Although ideal implementation was not achieved here due to the nature of site trials, the methodologies used were successful in their design and completion.

6 LABORATORY RESULTS AND DISCUSSIONS

6.1 Introduction

This section concerns the laboratory and numerical modelling results and has been split into these two sections respectively. A previous research test was repeated to identify issues with equipment and the methodology that this thesis is based upon. Chemical stabilising combinations and electrode types were then investigated along with electrode power issues. This lead onto the testing of a new polymer based electrode with a final test using the proposed technique under a mock footing. Complimentary numerical modelling was produced to identify issues in the laboratory and site trial phases whilst providing assessments on the efficacy of electrode layouts in both the laboratory and on site.

A separate section is dedicated to the accuracy and repeatability of the rests rather than repeat statements in each test section, section 6.2.14.

6.2 Laboratory Tests

The following section contains the results gained from the laboratory and the numerical simulations. Table 6-1 shows a summary of all of the laboratory tests and their variables.

Table 6-1: Laboratory Test Variables Summary

Electrokinetic Test	Constants	Variables
Previous Research Repeat	• EKG electrodes • English China Clay • 0 – 28 days • RO water • Water content (51%) • Voltage (50V/m)	• N/A
Chemical Combinations	• English China Clay • 30% water content • RO water • 200x200x160mm • 0 – 545 days	• $CaCl_2$ and Na_2SiO_3 combinations
Clay Electrical Conductivity	• 200x200x160mm	• Clay type (ECC and LC) • Stabilising chemical content (0 – 3%) • Temperature • Water type (RO, tap, chemical mix) • Water content
Electric Field Determination – Dye Precipitation	• English China Clay • Voltage (55V/m)	• Green dye

Electrokinetic Test	Constants	Variables
	• RO water • Stainless steel electrodes • 0 – 28 days	
Electrode Polarisation	• Sand • 300x200x70mm • 10% water by weight • Voltage (10V) • Rebar electrodes • 30 minutes on time	• Electrode arrangement • Relaxation period
Current Intermittence	• English China Clay • 200x200x160mm • Water content (30%) • 0 – 14 days	• Current intermittence times • Stainless steel and PEG electrodes
Electrode Type Choice 1	• English China Clay • Voltage (55V/m) • RO water • 370x220x550mm • Water content (45%)	• Electrode type
Electrode Coating	• Electrode lengths	• Electrode type

Electrokinetic Test	Constants	Variables
	• Electrode coating application method	• Electrode coatings
Electrode Decay through Fluid Interaction	• Electrode lengths (110mm) • RO water (200ml) • Chemical combinations with RO water (200ml) • 0 – 285 days	• Electrode type
Electrode Decay through Electrolysis	• Electrode length (120mm) • Electrode spacing (100mm) • Voltage (10V) • RO water • 0 – 28 days	• Electrode type
Long Term PEG Trial	• English China Clay • Water content (32%) • PEG electrodes • Voltage (100V/m) • 370x220x550mm • RO water • 0 – 540 days	• N/A

Electrokinetic Test	Constants	Variables
PEG Cathode Trial	• English China Clay • Compaction • Water content (32%) • RO water and stabilising chemicals • Electrodes • 0 – 28 days	• Voltage (20V – 50V)
Mock Foundation	• English China Clay • Water content (15%) • Water seeded • Voltage (20V) • Mock foundation • 370x220x550mm	• Water seeding stopped after 7 days

6.2.1 Previous Research Repeat

After repeating the pilot tests conducted by Liaki (2006), the following results were gained for comparison with the original study. At set up and consolidation, there were three cells in use. The control cell was produced along with one of the electrokinetic cells. The other electrokinetic cell experienced uncontrollable leakage through the base and was discarded after attempts to seal the leaks failed.

6.2.1.1 Electric Current

The electric current measured over the 7 day trial is shown in Figure 6-1. It can be seen that there was an immediate reduction in current followed by a slower rate and then a slight increase at the 5 day mark. This increase could be due to surface flooding although no such thing was witnessed by the author. The current then continues to decrease. The decrease in current is most likely due in part to degradation of the EKG electrode but also due to the creation of gases around the electrodes which act to insulate them. When compared to the electrical current reported by Liaki (2006) over 7 days, it can be seen that the reduction seen in the repeat test is greater than that seen in Liaki's research, Figure 6-1. It is anticipated that this is due to degradation of the EKG electrodes due to age. Unfortunately, Liaki did not report electrode surface resistance readings for comparison with the electrodes used in this test.

6.2.1.2 Liquid Limit

The liquid limits recorded across the treated specimen are shown in Figure 6-2. It is noted that the liquid limit sees the largest increase at the anode which then decreases towards the cathode with a slight increase at the cathode over the 210mm point. It can also be seen that the liquid limit increases over the entire specimen compared to the control, most likely due to the structural changes taking place due to electrokinesis. This is equally similar to the trend seen in Liaki (2006) over 7 days, Figure 6-2.

6.2.1.3 Plastic Limit

The plastic limits recorded over the distance between the electrodes are shown in Figure 6-3 where it is noticed that the plastic limit is increased all over the test specimen with the exception of 140mm from the anode which decreased over the 7 days. This change indicates a

change in the consistency of the clay as with the liquid limit. This trend is similar to that shown by Liaki (2006) for 7 days between the ranges of 70-280mm from the anode.

6.2.1.4 Water Content

The change in water content between the electrodes over 7 days is shown in Figure 6-4. It is seen as expected, and presented in Liaki (2006), that the water content increases at the anode due to input of water at this point with a slight increase in the centre of the specimen and then the greatest increase at the cathode where the electroosmotic force is directing the water in the system. This test shows a greater increase in water content at the anode and cathode than Liaki, Figure 6-4.

6.2.1.5 Linear Shrinkage

The linear shrinkage recorded here is reported in Figure 6-5 and has a similar trend to the corresponding data in Liaki (2006) with a decreasing linear shrinkage with distance from the anode. The linear shrinkages recorded here are also higher than the control indicating a negative impact on the susceptibility to volume change by electroosmosis alone.

6.2.1.6 pH

Figure 6-6 presents the pH variance over the specimen after 7 days of treatment. The general trend is similar to Liaki (2006) but with slightly higher pH's and a migration of the acid front which is greater in Liaki's. This could be due to variances in the EKG used where the present author made us of older EKG electrodes.

As expected the pH is reduced at the anode and increased at the cathode with the acid front appearing to have migrated further than the base front. This is as expected due to reasons discussed previously.

6.2.1.7 Undrained Shear Strength

Figure 6-7 shows that the present study's repeat experiment follows a similar trend to Liaki (2006) with a distinctive increase towards the cathode and then decrease at the cathode. From Liaki (2006) it can be seen that the general increase in undrained shear strength at the anode is brought about at around 28 days. Figure 6-8 also shows that the repeat experiment sees a decrease in undrained shear strength with increasing water content as expected. Liaki's original experiment however shows more of an increase in undrained shear strength with water

content. This could be explained through the inaccuracy of hand shear vane testing in low strength materials.

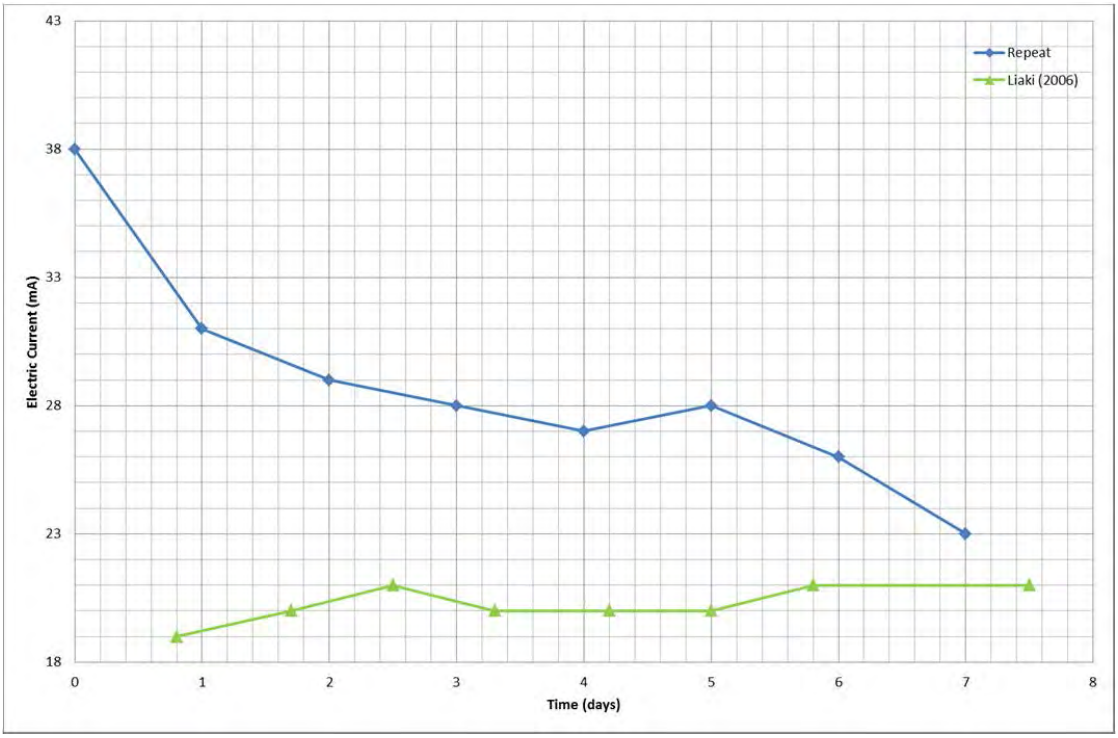

Figure 6-1: Previous research repeat electric current. Liaki (2006) data estimated from Liaki (2006).

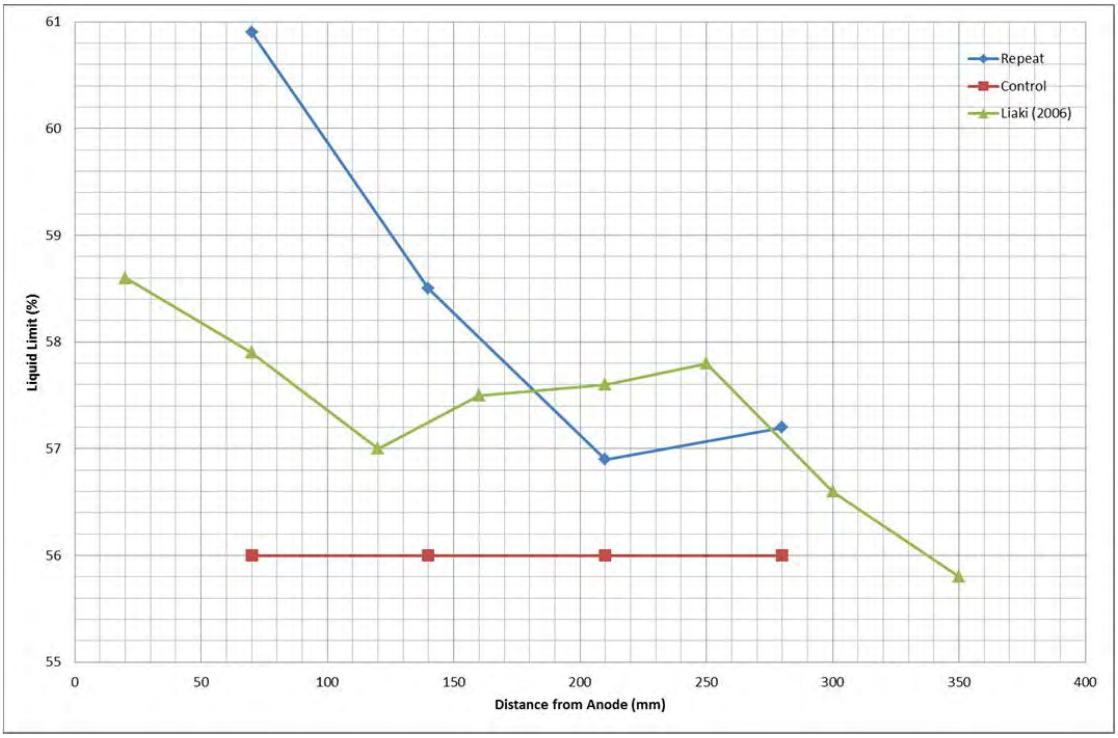

Figure 6-2: Previous research repeat liquid limits. Liaki (2006) data estimated from Liaki (2006).

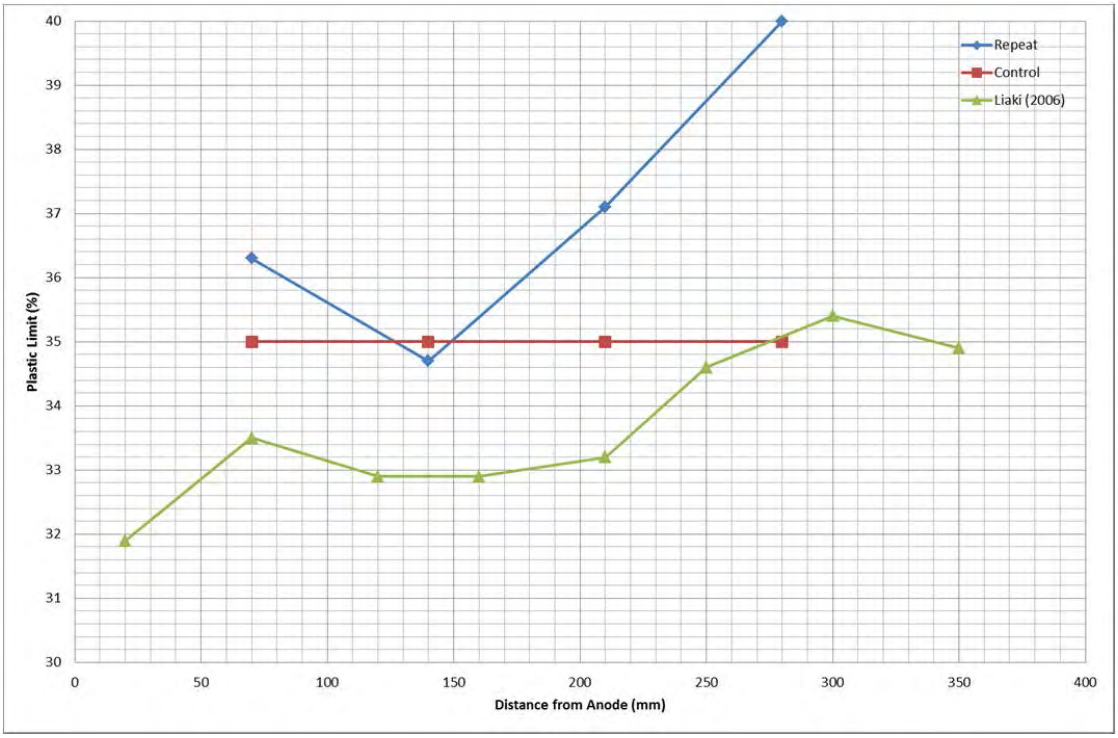

Figure 6-3: Previous research repeat plastic limits. Liaki (2006) data estimated from Liaki (2006).

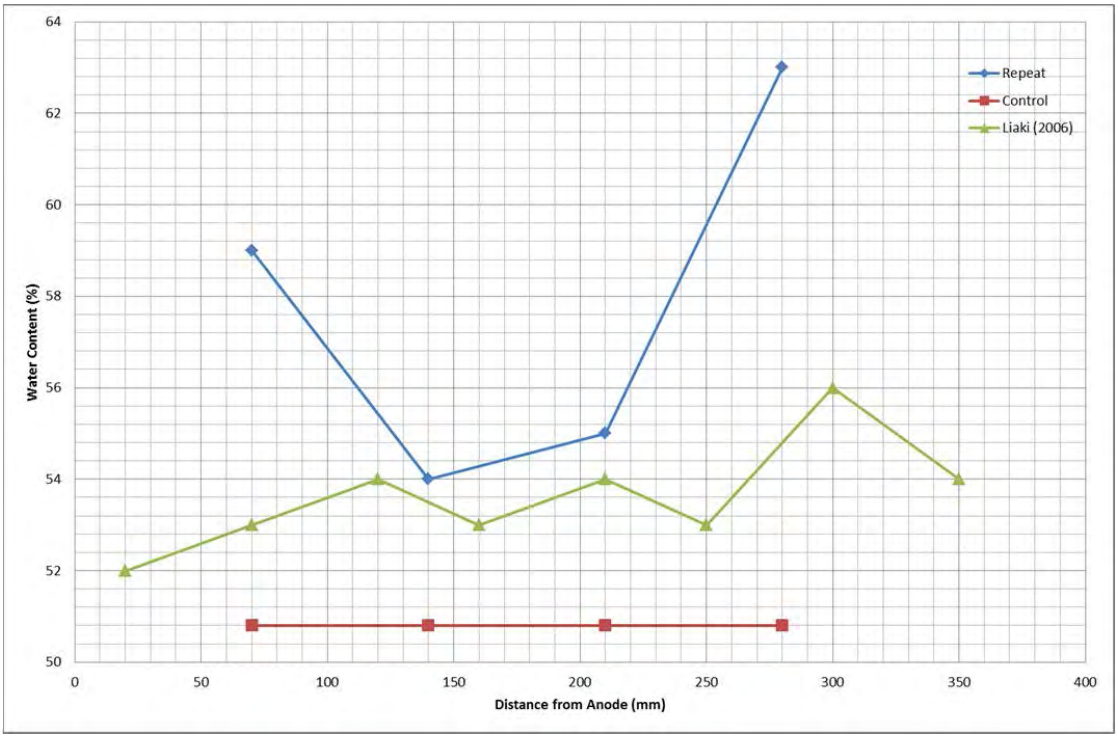

Figure 6-4: Previous research repeat water contents. Liaki (2006) data estimated from Liaki (2006).

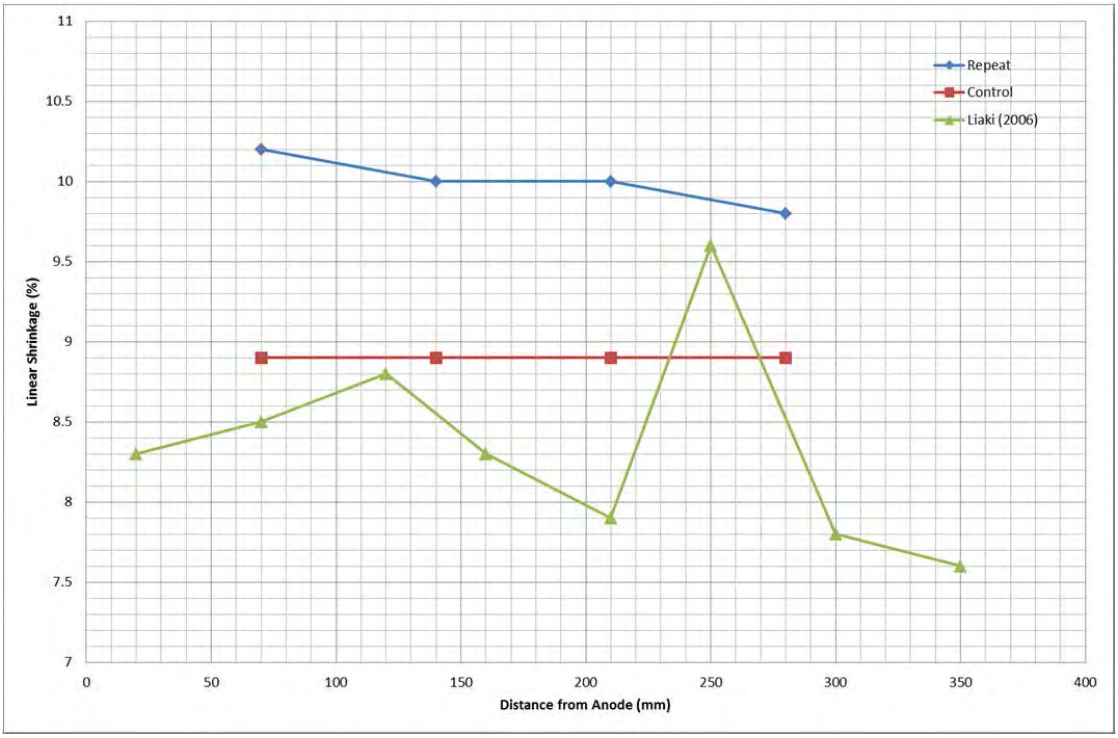

Figure 6-5: Previous research repeat linear shrinkage. Liaki (2006) data estimated from Liaki (2006).

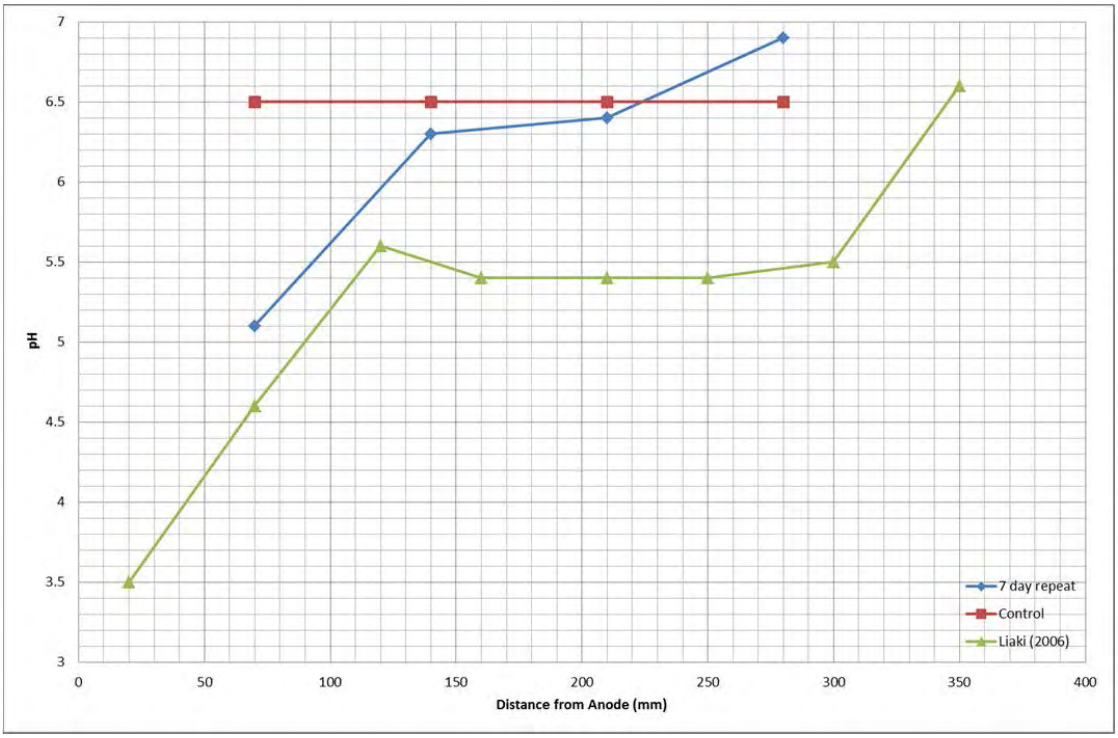

Figure 6-6: Previous research repeat pH. Liaki (2006) data estimated from Liaki (2006).

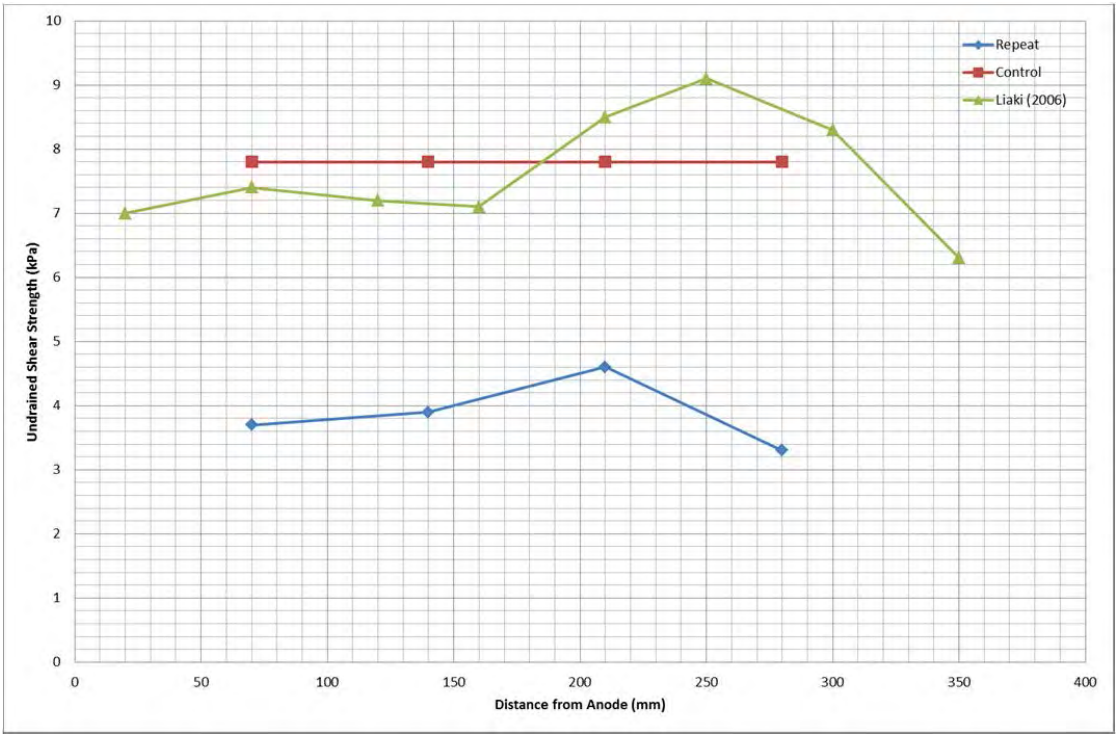

Figure 6-7: Previous research repeat undrained shear strength. Liaki (2006) data estimated from Liaki (2006).

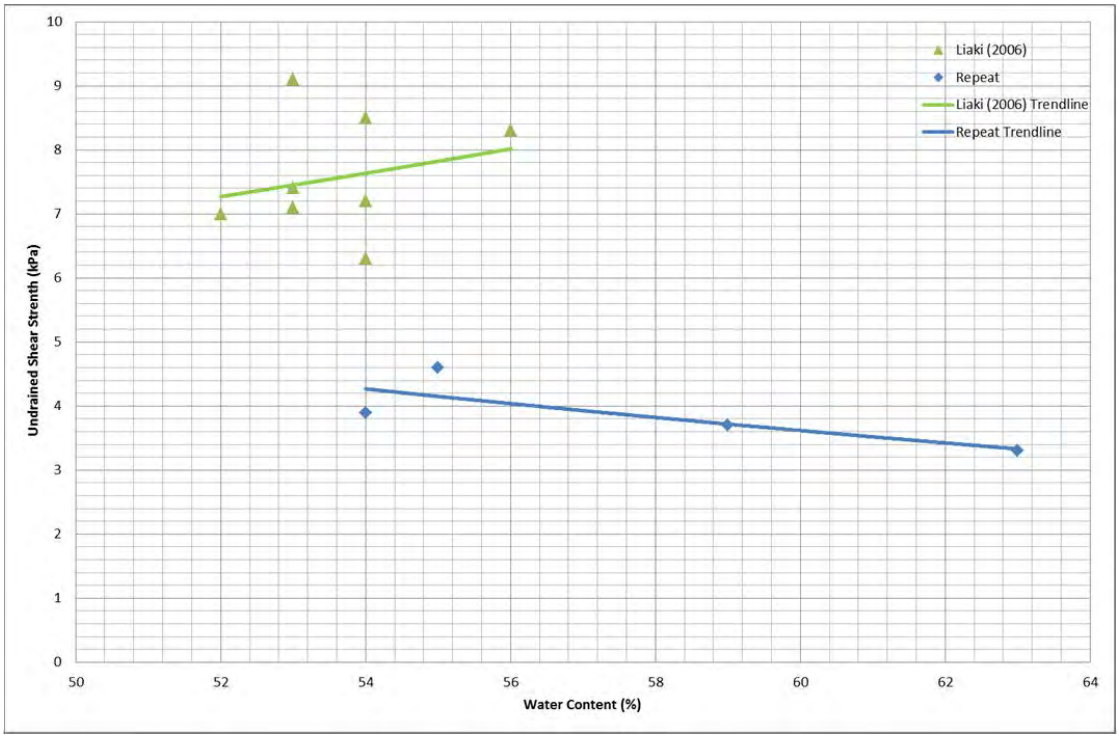

Figure 6-8: Previous research repeat undrained shear strength against water content. Liaki (2006) data estimated from Liaki (2006).

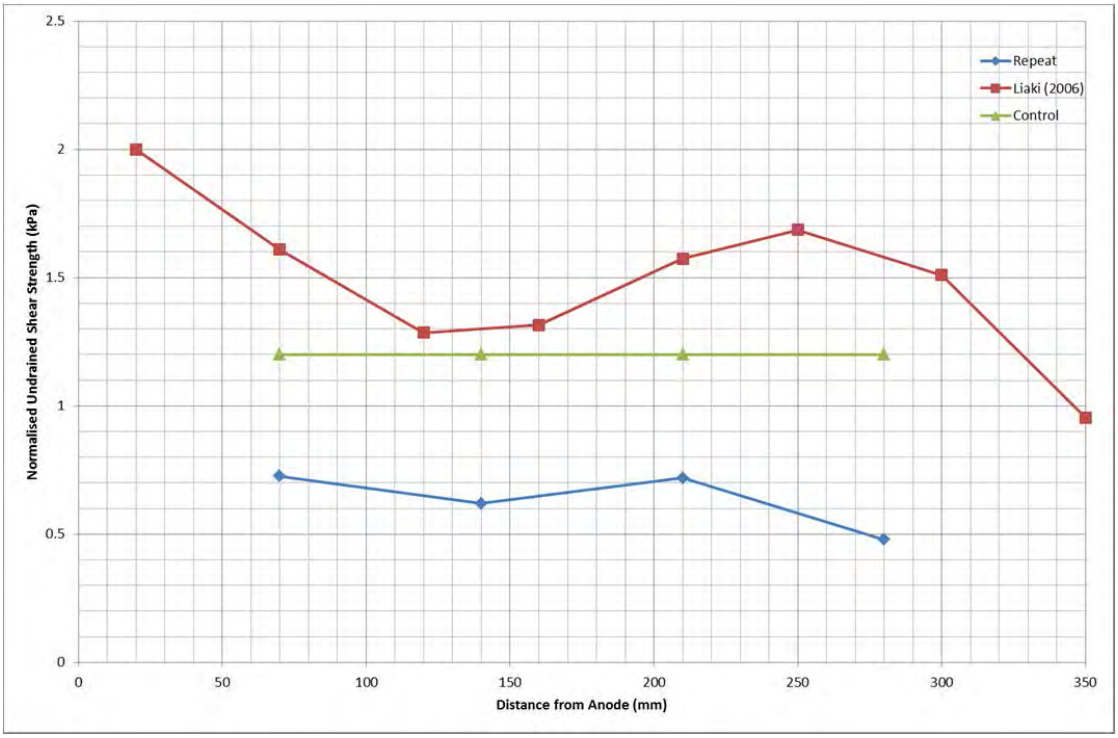

Figure 6-9: Previous research repeat test undrained shear strength normalised to pH.

6.2.1.8 Summary

The data recorded for this comparison and improvement test correlates very well with the corresponding data in Liaki (2006) considering the age difference in the electrodes and the use of differing batches of English clay. It is anticipated that these differences lead to the reduction in electrical current which in turn lead to the reduced pH changes and water content at the cathode. Figure 6-9 shows how when normalising the undrained shear strength to the pH, it can be seen that both the original Liaki (2006) test and the repeat test follow a very similar trend with a generally decreasing undrained shear strength from anode to cathode.

Due to this comparison showing similar trends with Liaki's original test, it was possible to progress using the equipment knowing that it functioned adequately and that the data used as a basis for this thesis can be relied upon.

Part of the reason for conducting this experiment was to define any areas that could be improved or enhanced. It was decided after this experiment to make a number of changes as detailed below:

- Construct a new set of Perspex boxes using plastic welding to avoid the inevitable leaks that come with a screwed unit. It was later found that the plastic welding was not as strong as the screwed units and as such broke under the pressure of compaction. Additional bracing was constructed to alleviate this problem.
- Due to the hydraulic head of the fluid tanks decreasing over time, it was decided that another method that didn't require constant attention would be suitable. The details of this can be found in section 4.5.1.
- Previously a thin piece of Perspex has been used to block the end walls during consolidation and then when removed, the EKG could be inserted in its place. This was replaced by a piece of Teflon to ease removal for lower water content trials.
- The location of the test rig was directly under a heater which cannot be turned off. It was noticed that the top of the clay was becoming desiccated and so the heater was turned to face away from the test area.
- Grooves were milled into the base and side edges of the cells to form a channel to better hold the silicon sealant in an effort to reduce leakage from the base of the cells.
- The initial consolidation stage was to be performed using small laboratory weights due to the lowest hydraulic jack pressure causing leakage of the clay slurry around the loading plate, this was either not a problem or was ignored in Liaki (2006).

- Whereas Liaki (2006) achieved 8 test locations from anode to cathode, it became obvious during the repeat tests that this was not possible with such a low strength material without severely contaminating samples through massive disturbance. It was therefore determined as seen in this section, that four test locations from anode to cathode would provide a less disturbed and therefore better reflection of trends.

6.2.2 Chemical Combinations

The results from the chemical combination tests are shown in Table 6-2 for days 0 to 540. No results were taken between day 28 and 540 due to limited sample availability and the desire to test after a minimum of 12 months. As such, the full planned testing regime was conducted with one long term test undertaken after 540 days.

6.2.2.1 Shear Strength

Figure 6-10 shows the change in shear strength over time for the various chemical combination mixes with ECC. All data here was collected using the hand shear vane with the exception of the 540 day results, which after attempts with the hand shear vane were unsuccessful, undrained triaxial testing was performed. It is accepted that triaxial testing and hand vane testing do not completely agree in that triaxial testing tends to produce a higher shear strength than hand vane testing would on the same sample, (Black, et al., 2009). Conversely, it was concluded by Ahmad (1975) that in situ hand vane testing will yield greater shear strengths than triaxial testing majorly due to sample disturbance when removing the sample from the bulk and at low strengths, the hand vane tends to be less accurate. In the present case it is sufficient to provide an indication of trends.

Figure 6-10 shows that the largest increase in shear strength was after 540 days in the 10% mix of (2/3 $CaCl_2$: 1/3 Na_2SiO_3) with an increase from 95 to 328kPa. The 10% $CaCl_2$ mix performed worst where it produced a 540 day result lower than the control test along with the 10% Na_2SiO_3 and the 5% $CaCl_2$: 5% Na_2SiO_3 mix. These results are surprising due to previous studies using Na_2SiO_3 mixed with kaolinite and left to cure show increasing unconfined compressive strengths with increasing Na_2SiO_3 content, (Moayedi, et al., 2011). As expected, the 2/3 to 1/3 mix type performed best with 10% ending with the highest shear strength followed by 5% and then 3%.

Table 6-2: Chemical combinations trials results.

Concentration $CaCl_2$:Na_2SiO_3	Time (days)	Water Content (%)	Liquid Limit (%)	Plastic Limit (%)	Plasticity Index (%)	Cu' (Kpa)	pH	Conductivity (mS/cm)
5% $CaCl_2$: 5% Na_2SiO_3	0	30.00	61.5	27.4	34.1	66.4	9.96	10.57
	7	31.00	60.2	24.5	35.7	94.8	10.01	11.25
	14	31.00	60.6	27.0	33.6	92.6	10.03	11.31
	28	31.00	60.7	28.3	32.4	94.8	10.02	10.99
	540	29.88	61.3	26.0	34.9	124.1	7.12	11.21
10% Na_2SiO_3	0	30.00	67.9	26.9	40.9	73.2	12.04	8.81
	7	29.00	54.1	19.4	34.7	103.2	11.56	9.10
	14	29.00	52.4	21.5	31.0	102.8	11.51	9.60
	28	28.00	52.3	23.1	29.2	134.4	11.56	9.40
	540	26.88	60.0	16.4	43.5	143.1	10.44	9.55
10% $CaCl_2$	0	29.00	50.2	24.2	26.0	45.0	6.15	15.23
	7	29.00	46.6	19.9	26.8	51.8	4.82	16.20
	14	28.00	45.4	16.7	28.7	51.0	4.92	18.10
	28	28.00	43.4	18.5	24.9	53.2	5.53	18.40
	540	27.27	51.7	25.3	25.6	116.6	4.36	18.90
10% (2/3 $CaCl_2$: 1/3 Na_2SiO_3)	0	29.00	57.7	23.9	33.8	95.3	10.01	14.03
	7	28.00	55.6	24.7	30.9	134.6	9.96	13.85
	14	28.00	57.5	26.6	31.0	138.6	9.98	14.60
	28	28.00	58.0	25.5	32.5	138.8	9.99	14.50
	540	28.17	84.1	38.3	45.6	328.0	7.46	13.94
5% (2/3 $CaCl_2$: 1/3 Na_2SiO_3)	0	30.00	60.4	24.7	35.7	82.8	9.66	8.66
	7	30.00	61.7	26.8	34.9	96.3	9.69	8.88
	14	29.00	62.1	26.4	35.7	135.2	9.65	8.35

Concentration $CaCl_2$:Na_2SiO_3	Time (days)	Water Content (%)	Liquid Limit (%)	Plastic Limit (%)	Plasticity Index (%)	Cu' (Kpa)	pH	Conductivity (mS/cm)
	28	30.00	62.7	28.2	34.5	135.4	9.62	8.30
	540	28.66	79.2	38.6	40.3	231.4	7.56	8.10
3% (2/3 $CaCl_2$: 1/3 Na_2SiO_3)	0	30.00	61.9	26.6	35.2	96.8	9.43	6.62
	7	30.00	63.7	28.6	35.1	134.6	9.54	6.47
	14	30.00	63.9	28.6	35.2	136.4	9.47	6.17
	28	30.00	63.5	28.4	35.1	138.2	9.40	6.10
	540	28.73	64.0	19.9	44.0	200.4	7.29	5.67
Control	0	30.00	56.7	24.4	32.3	81.8	5.55	0.07
	7	29.00	56.7	24.4	32.3	81.8	5.55	0.07
	14	29.00	56.7	24.4	32.3	-	5.55	0.07
	28	29.00	56.7	24.4	32.3	81.8	5.55	0.07
	540	28.06	73.0	25.2	47.7	199.3	5.49	0.05

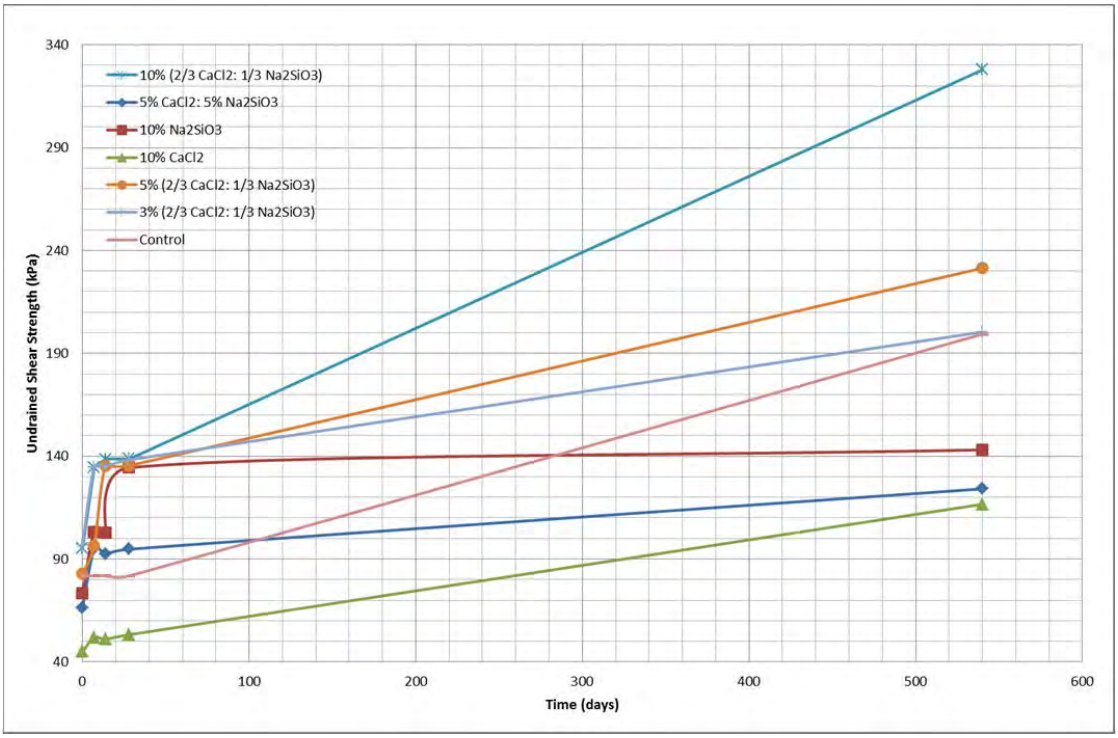

Figure 6-10: Chemical combination shear strength over time.

6.2.2.2 Water Contents

Figure 6-11 shows the water content changes over time for the different chemical combination mixes. Ideally one would find a fairly constant water content initially with a drop over the long term time period due to the water being used in the pozzolanic reactions. The decreases seen in the different mixes are quite consistent with the exception of the 10% Na_2SiO_3 and the 10% mix of (2/3 $CaCl_2$: 1/3 Na_2SiO_3) where both, after an initial loss, do not decrease in the long term. The values recorded here are very narrow in range though and so variation over each sample could have caused this.

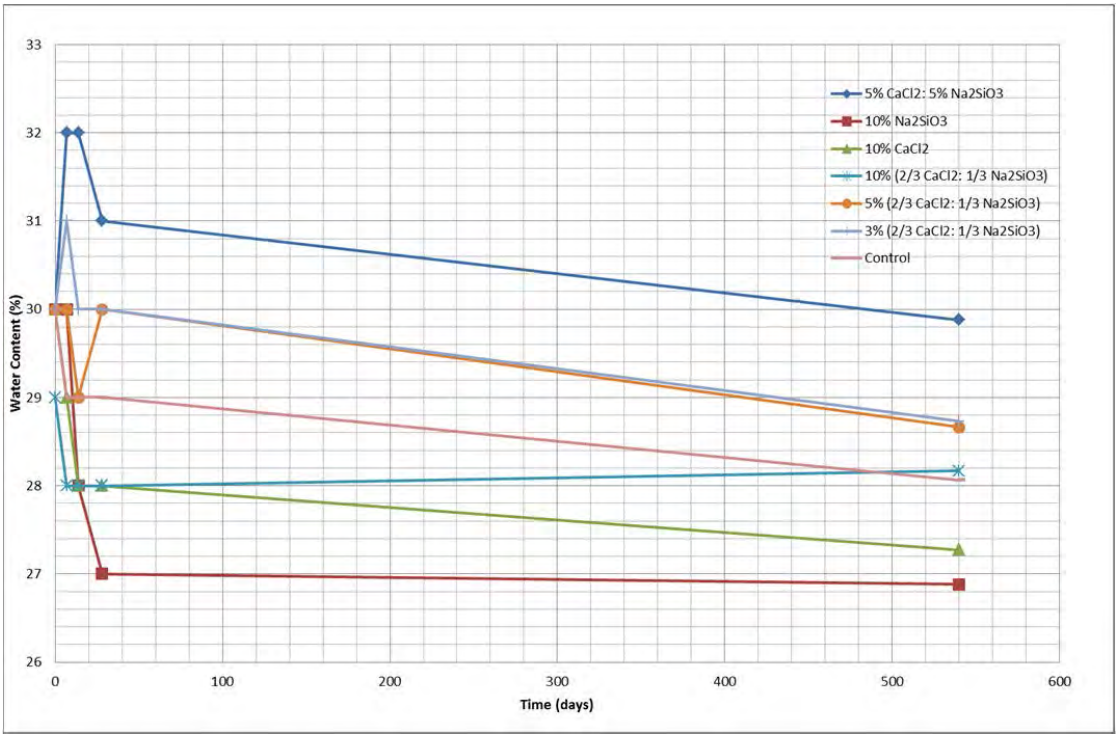

Figure 6-11: Chemical combinations water content over time.

6.2.2.3 Plastic Limit

The plastic limits of the samples taken over the trial period are shown in Figure 6-12. It is seen here that the three 2/3: 1/3 mixes all increase by approximately 12 percentage points over the 540 day trial whereas the control and the 10% $CaCl_2$ increase by approximately 1 percentage point. The 5% $CaCl_2$: 5% Na_2SiO_3 mix decreases by 1 percentage point over the total time period and the 10% Na_2SiO_3 decreases by over 10 percentage points. Both mixes that experience decreases in the plastic limit over the full trial length have at least 5% Na_2SiO_3 in their contents.

Due to the benefits of increasing the plastic limit, including reducing the amount of shrinkage likely to be experienced at varying water contents, the three 2/3: 1/3 mixes have the best results. The other effects of increasing the plastic limit include the reduction in plasticity index which in turn leads to a reduction in shrink/swell capacity which is advantageous regarding the aim of this thesis.

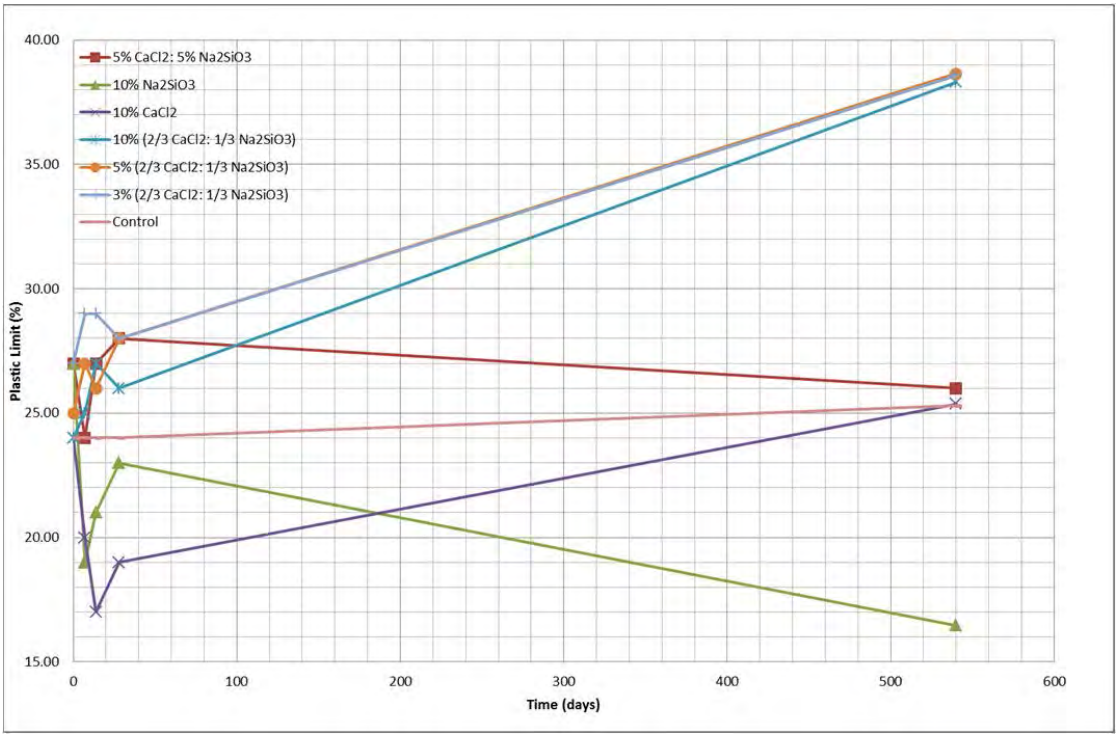

Figure 6-12: Chemical combinations plastic limit over time.

6.2.2.4 Liquid Limit

Increasing the liquid limit results in the clay being able to hold a larger content of water without changing consistency. It is seen from Figure 6-13 that all of the mixes increase in liquid limit over the trial length with only the 10% Na_2SiO_3 experiencing a decrease. The addition of sodium carbonate by Bain (1971) to kaolinite showed a similar decrease in liquid limit. The largest increase in liquid limit was seen in the 10% mix of (2/3 $CaCl_2$: 1/3 Na_2SiO_3) as expected due to the beneficial combination of both chemical stabilisers in a relatively high concentration compared to the other trials.

Decreasing the liquid limit would be advantageous in regard to the aims of this thesis as this would lead to a reduction in the shrink/swell capacity of the clay through a reduction in the plasticity index.

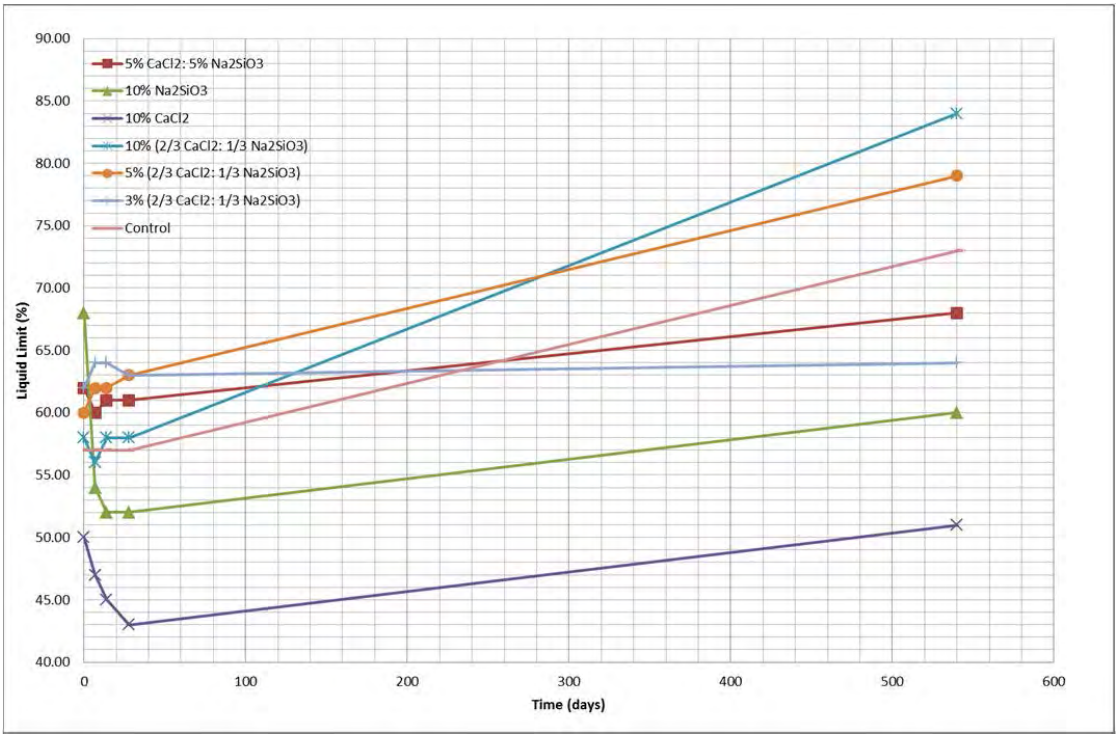

Figure 6-13: Chemical combinations liquid limit over time.

6.2.2.5 Plasticity Index

The plasticity indexes for the chemical combinations tests can be found in Figure 6-14 where it is noticed that all of the indexes increase over the 540 days with the exception of the 3% (2/3 $CaCl_2$: 1/3 Na_2SiO_3) mix which decreases by approximately 10% and the 10% $CaCl_2$ which decreases by approximately 0.5%.

If one considers the plasticity chart in BS5930: 2015 then one can determine the plasticity of each of these clays before and after treatment. These results are shown in Table 6-3. It can be seen that on Day 0, all of the mixes are equally High in plasticity whereas after the 540 day duration, the 10% (2/3 $CaCl_2$: 1/3 Na_2SiO_3), 5% (2/3 $CaCl_2$: 1/3 Na_2SiO_3) and control mixes have all increased to Very High plasticity. It is unknown why the control test has an increased plasticity unless contaminants were introduced into the clay at some point in the periodic testing or at the initial mixing stage.

Reducing the plasticity index in turn reduces the capacity of the clay for shrink/swell behaviours. As can be seen in Figure 6-14, the 3% (2/3 $CaCl_2$: 1/3 Na_2SiO_3) is the only mix to achieve this reduction. Reducing the plastic limit also has the advantage of reducing the range of water contents at which the soil will behave in a plastic manner. This, combined with an

increase in plastic limit, produces a soil which for the low water contents expected around strip footings, would behave more like a solid than plastic or liquid.

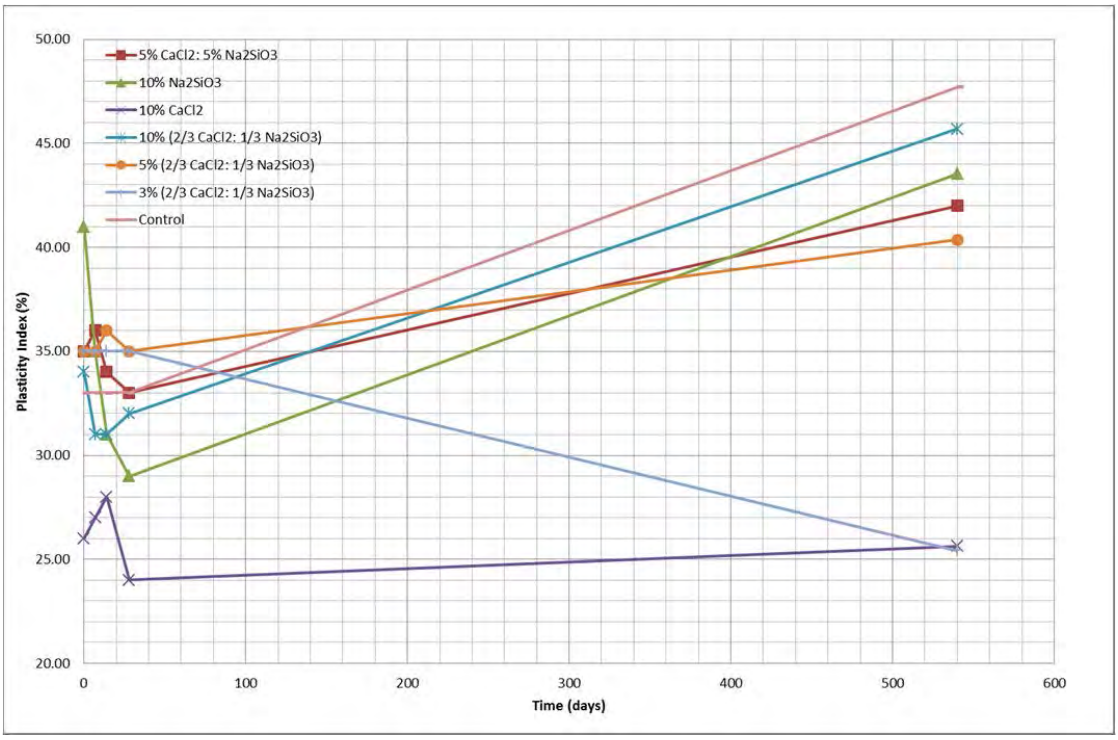

Figure 6-14: Chemical combinations plasticity index over time.

Table 6-3: Chemical combinations plasticity comparison over time.

Clay Mix	Day 0 Plasticity	Day 540 Plasticity
5% $CaCl_2$: 5% Na_2SiO_3	High	High
10% Na_2SiO_3	High	High
10% $CaCl_2$	High	High
10% (2/3 $CaCl_2$: 1/3 Na_2SiO_3)	High	Very High
5% (2/3 $CaCl_2$: 1/3 Na_2SiO_3)	High	Very High
3% (2/3 $CaCl_2$: 1/3 Na_2SiO_3)	High	High
Control	High	Very High

6.2.2.6 pH

Figure 6-15 shows the pH variance over time for each of the chemical combinations. It is noticed that all of the pH's, control being the exception, decrease by between 1 – 3% approximately.

It can be seen that the naturally high pH Na_2SiO_3 mix drops from 12 to approximately 10.5 over the 540 days. The $CaCl_2$ mix is seen to start at approximately 6.2 and decrease over the 540 days to 4.4. The rest of the mix types all have initial pH's of between 9.5 and 10 which reduce over the 540 days to between 7 and 7.6. The control mix is seen to have very little variance in time of the pH and so it can be assumed that the chemicals within the other trials are the cause of the pH changes in that the chemical reactions taking place enhance the amount of hydrogen ions consumed.

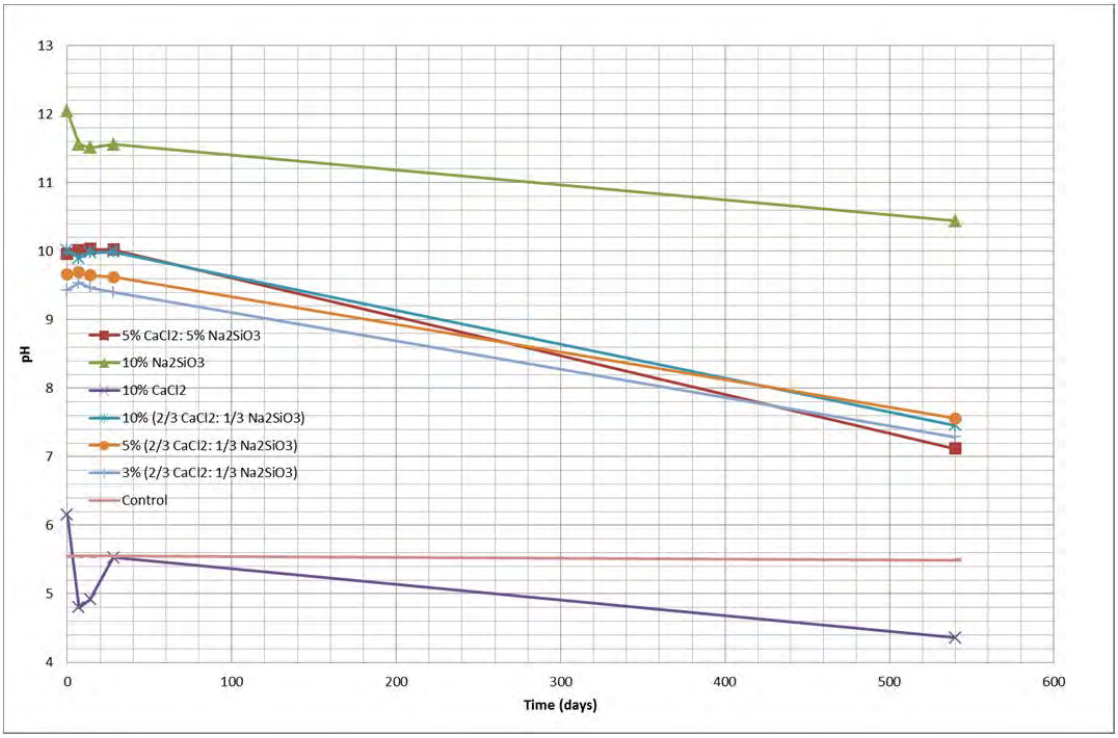

Figure 6-15: Chemical combinations pH over time.

6.2.2.7 Conductivity

Figure 6-16 shows the conductivity of the chemical combinations mixes and their variance over time. As expected, the mixes with the greatest amount of $CaCl_2$ have the highest conductivity with the control having near zero. The 10% Na_2SiO_3 mix possesses a higher conductivity than

other mixes containing $CaCl_2$ through the mass of ions in the system where the lower mixes have 3.33% and 2% $CaCl_2$.

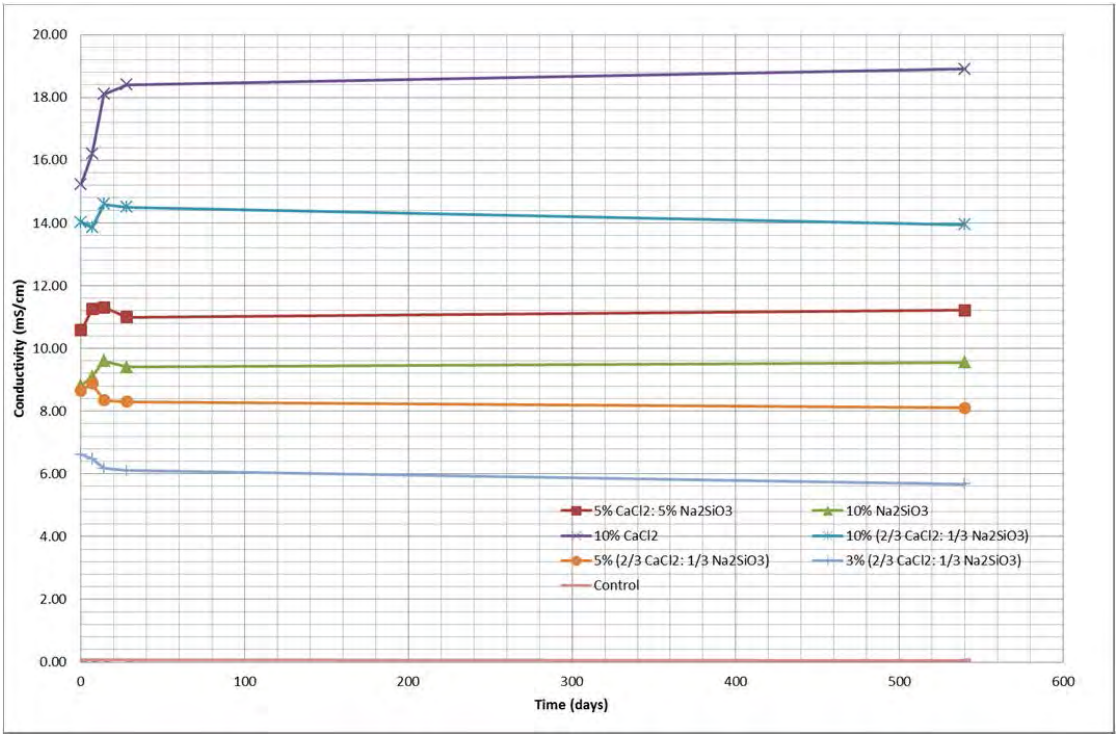

Figure 6-16: Chemical combinations electrical conductivity over time.

6.2.2.8 Summary

As seen in Figure 6-17, the characteristic shear strength for a given water content curve for each mix can help determine a mix's successfulness. By taking the control curve as the benchmark it is noted that 10% $CaCl_2$ has a curve below that of the control meaning that for a given water content, the clay has a lower shear strength than that of untreated clay. The 10% Na_2SiO_3 mix is quite similar with the exception of the higher water contents where the curve crosses the control curve. The 10% (2/3 $CaCl_2$: 1/3 Na_2SiO_3) mix is very similar to the control curve whereas the 5% $CaCl_2$: 5% Na_2SiO_3 curve is more horizontal indicating that the water content has not affected the shear strength of the clay. The 5% (2/3 $CaCl_2$: 1/3 Na_2SiO_3) and 3% (2/3 $CaCl_2$: 1/3 Na_2SiO_3) mixes have clearly improved over the control with the 3% mix being most improved due to its highest shear strength for a given water content.

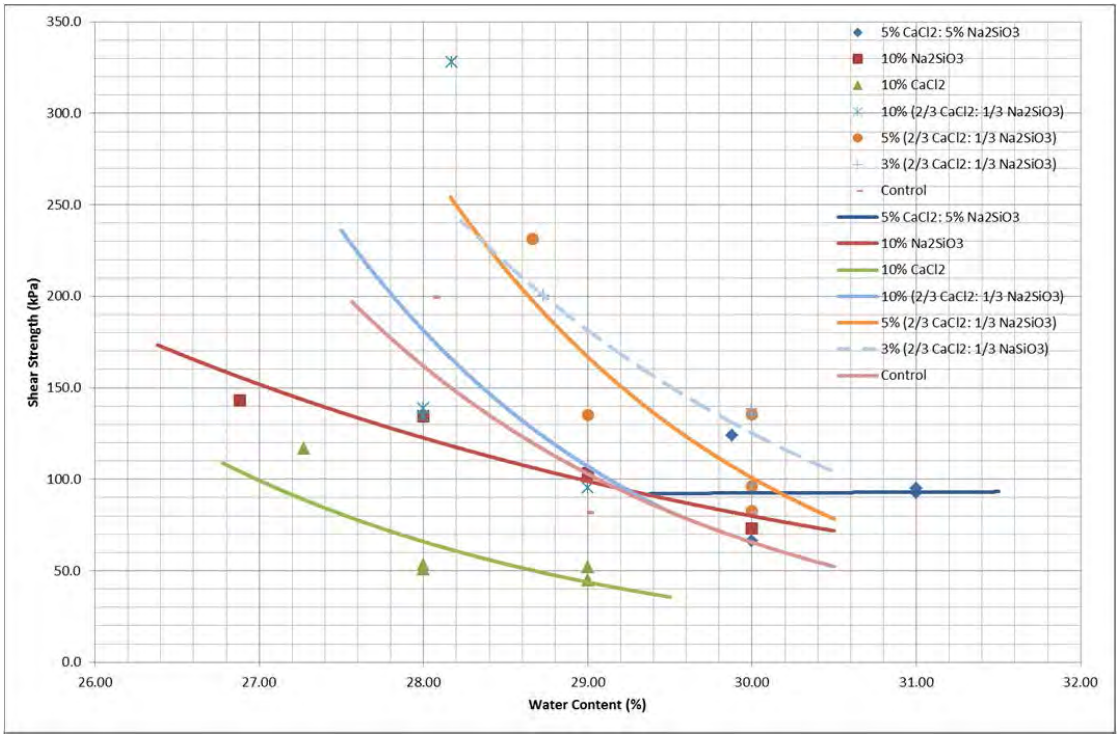

Figure 6-17: Chemical combinations water content against shear strength.

Figure 6-18 shows the change in plasticity index with cost of treatment for the chemical combinations tests. It is seen that there is a definite trend for a larger plasticity index change as the treatment cost is decreased. It would therefore appear that the 3% (2/3 $CaCl_2$: 1/3 Na_2SiO_3) not only possesses the best strength increase over the control test but is also the best value for money treatment option.

Figure 6-19 shows the undrained shear strength normalised to pH over the test duration. It can be seen that when removing the pH effect from the data, the undrained shear strength is quite consistent until approximately the 30 day mark upon which an increase is seen up to 540 days. This is as expected when taking into consideration the accuracy of the hand shear vane at low strengths along with the time dependency of pozzolanic reactions.

The chemical combination ratio was developed in the laboratory based upon the chemicals used in previous studies, (Barker, 2002), (Liaki, 2006) and (Tajudin, 2012). Over the range of concentrations mechanically mixed with ECC, the 3% concentration by weight was shown to be most successful. This concentration had the most improved characteristics such as shear strength for given water content. Whereas the electrical conductivity and pH were not the highest, the cost implication of using a 3% mix was enough to warrant its confirmation as the

optimal mix. The strength increases seen across the $CaCl_2$ and Na_2SiO_3 mixes are thought to be pozzolanic reaction products leading to a continuous increase in strength over 1-5 years.

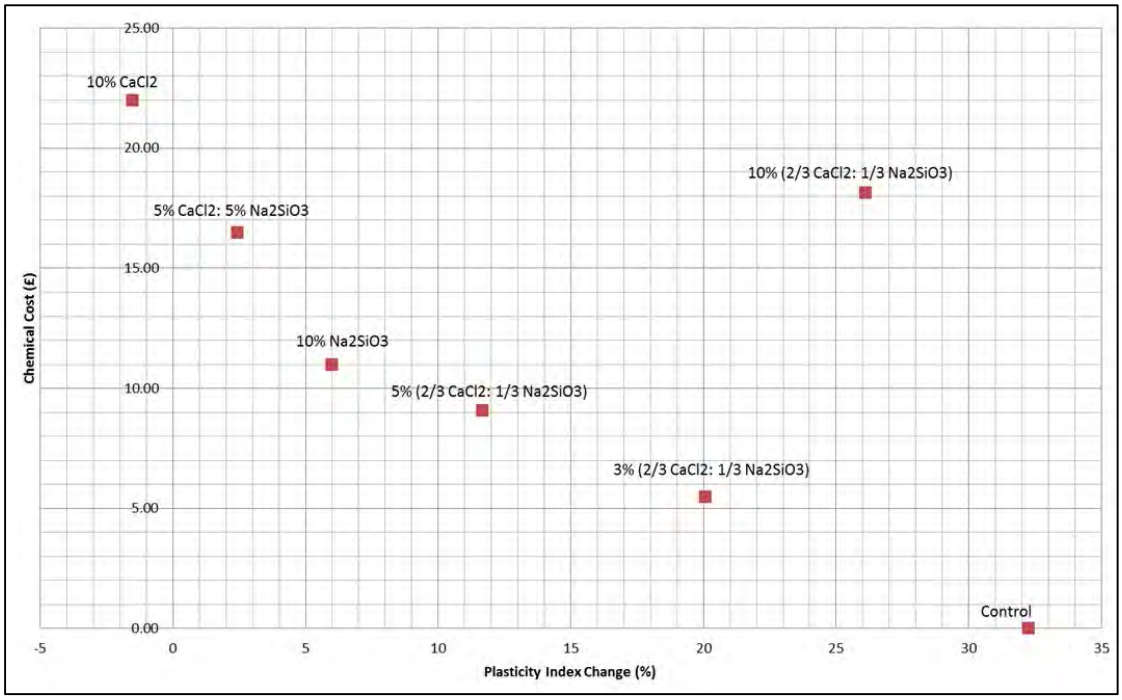

Figure 6-18: Chemical combinations chemical cost against resulting change in plasticity index.

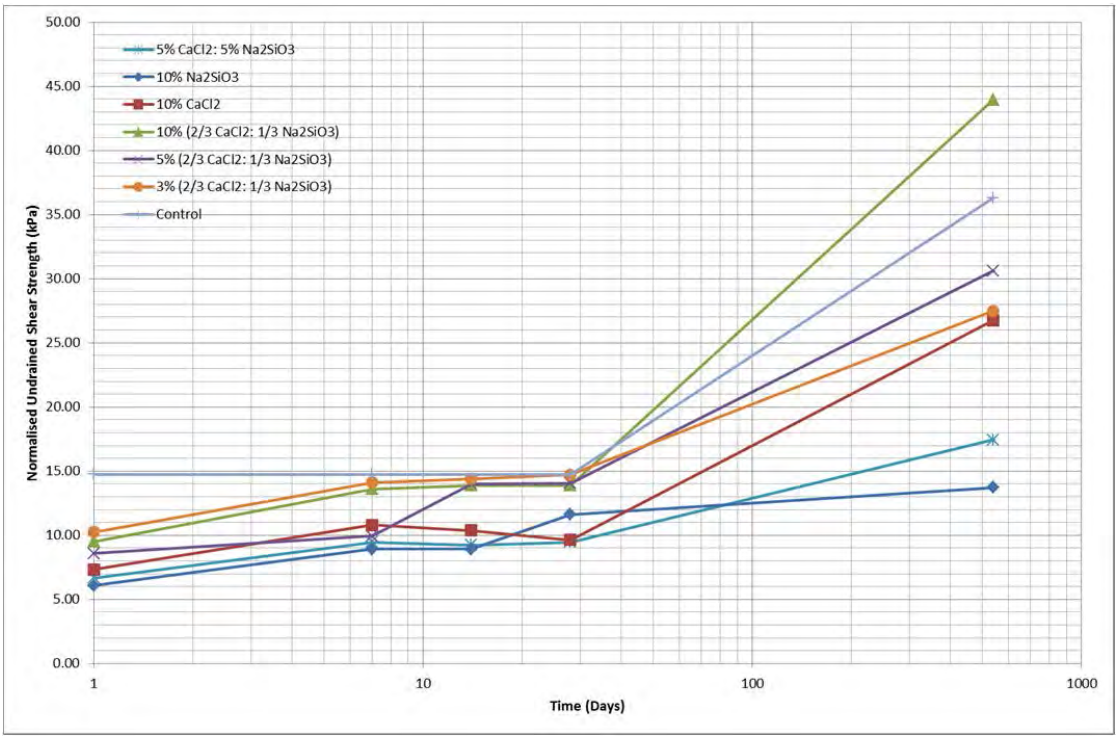

Figure 6-19: Chemical combinations undrained shear strength normalised to pH.

6.2.3 Clay Electrical Conductivity

Electrical conductivities of both the fluids associated with the proposed treatment technique along with the clays were measured over varying water contents and temperatures to assess the effects of uncontrollable environmental effects that may be encountered on site.

6.2.3.1 Water Content

The results gained from these tests show the expected increase in electrical conductivity with increase in water content. It is seen that between 32% and 40% water content for ECC, there is a fivefold increase in electrical conductivity as seen in Figure 6-20. Above and below these values it appears that the electrical conductivity plateaus. It is interesting to note that the plastic limit of ECC is approximately 35%. The majority of electrical charge is carried by the free water and thus the electrical conductivity increases rapidly as free water increases. Figure 6-21 shows that in London Clay, the free water stage is seen at approximately 24% water content whereas in ECC it is closer to 34%.

Figure 6-21 shows the change in electrical conductivity with increasing water content and stabilising chemical mix of London Clay. It can be seen that the London Clay mixed with the stabilising chemicals possesses a higher electrical conductivity as expected and increases over fluid content increase until the plateau at approximately 40%. It can be noted that both London Clay mixes begin a dramatic increase of electrical conductivity at approximately the plastic limit for this London Clay, 25%, with the chemical stabiliser mix curve increasing at lower fluid contents than the RO water mix due to the chemicals being more electrically conductive than the RO water alone. At the peak of likely water contents to be encountered, the London Clay mixed with the stabilising chemicals has a peak of 50,200µS at 35% water content with the London Clay mixes with RO water being 16,330µS at 40% water content. This is a 3x increase from the addition of the stabilising chemicals which in reality could result in a decreased required EKS treatment time.

The variation of the electrical conductivity of a clay with varying water content can be explained by the different stages of the DDL around the clay particles as explained by Mojid & Cho (2006).

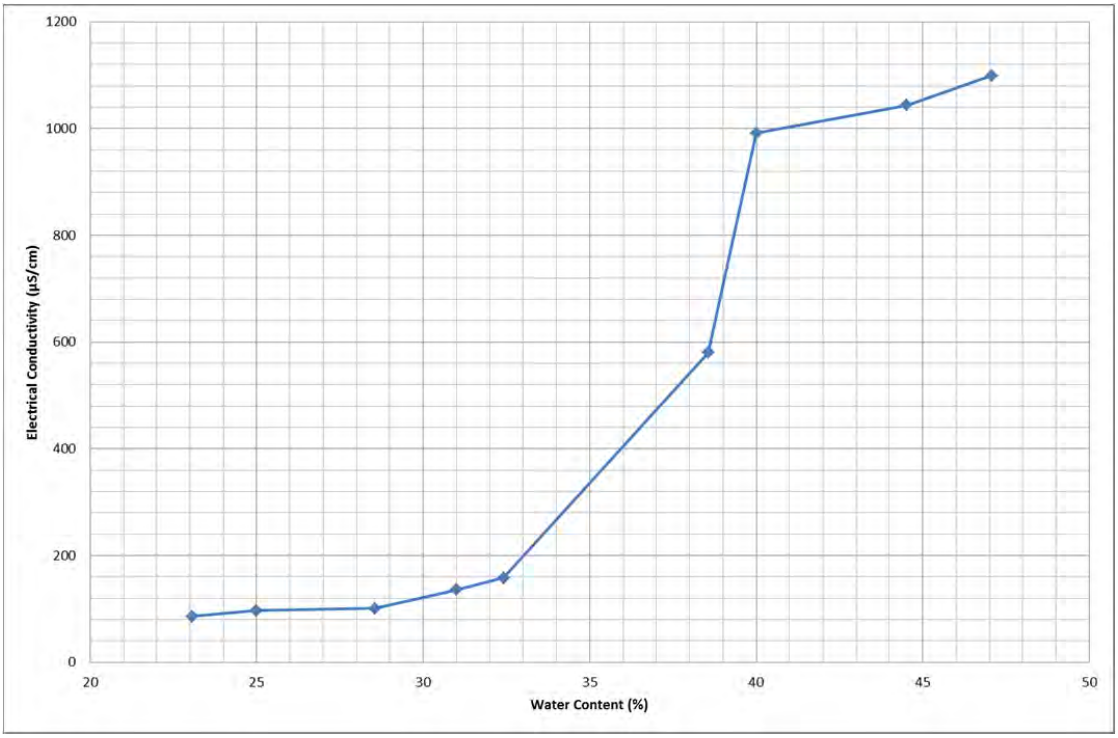

Figure 6-20: Electrical conductivity of ECC with increasing water content.

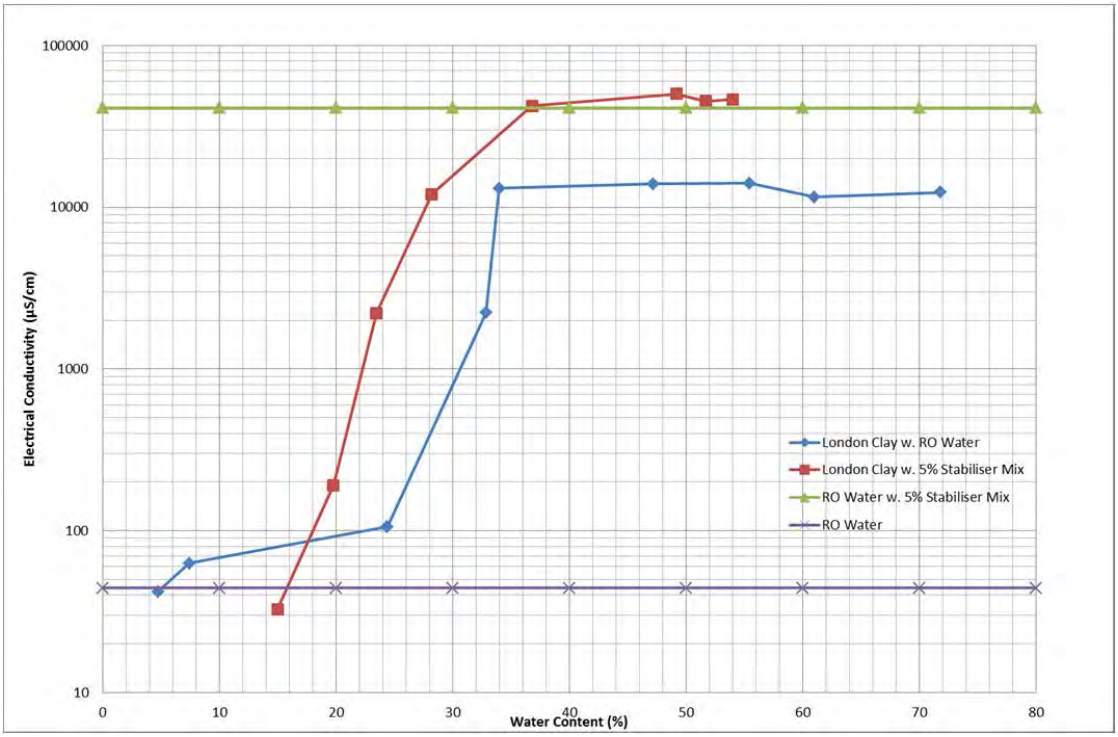

Figure 6-21: Electrical conductivity variance of London Clay mixed with RO water and stabilising chemicals at 20°C.

6.2.3.2 Temperature

Figure 6-22 shows how the temperature of the fluids can affect their electrical conductivity. As expected, the tap water mixed with a 5% concentration of the chemical stabilisers in a 2/3:1/3 combination possesses the highest electrical conductivity followed by the tap water and then the RO water. This is expected purely due to the conductive ions present in the fluids.

The RO water experiences an approximate 300% increase in electrical conductivity over the temperature increase of 20°C whereas the tap water sees an increase of 8%. The tap water and 5% chemical mix sees a decrease of 20%. The increases in electrical conductivity with increasing temperature are logical in that the additional energy given to the atoms in the fluid cause agitation and thus the passing of electrons becomes easier. The reduction seen in the tap water and chemical mix is a surprise. One possible explanation is that the two chemical stabilisers added to the tap water began to react with each other and thus became less able to pass electrons through after bonding together. This warrants more research as it could affect where it is that would be ideal for the chemicals to meet in the clay.

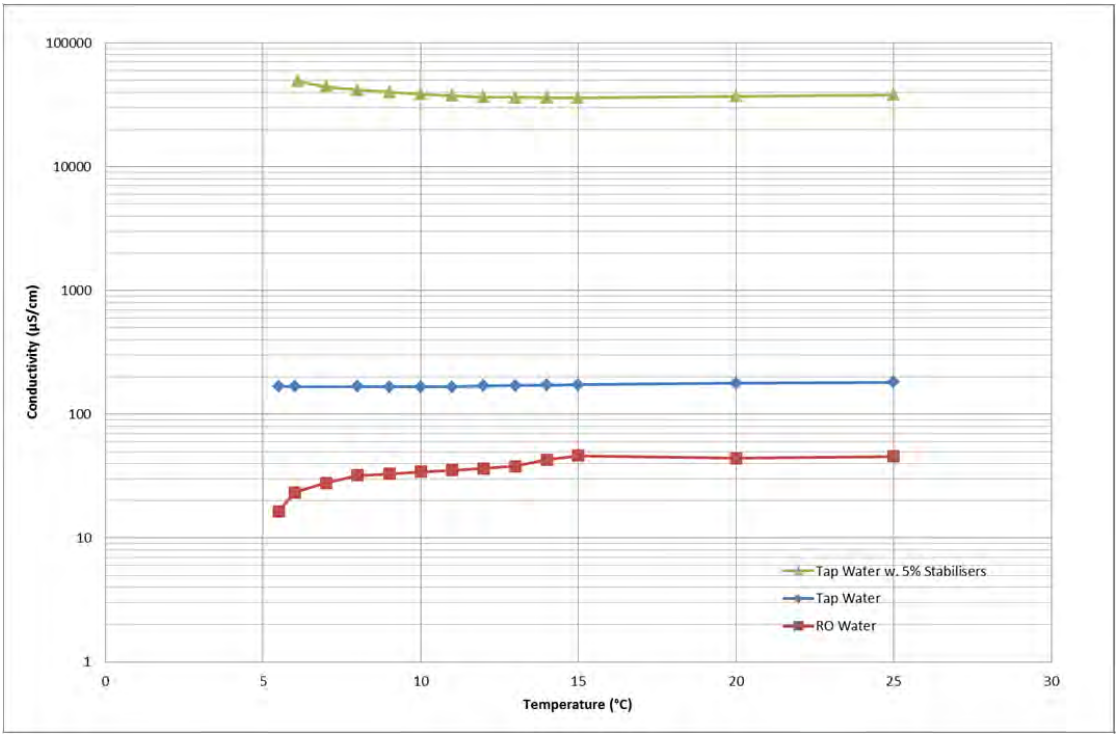

Figure 6-22: Electrical conductivity of fluids at varying temperatures.

6.2.3.3 pH

The change in pH of the fluids was measured over varying temperatures and is displayed in Figure 6-23. The tap water sees virtually no change in pH over the 20°C increase in temperature with the tap water and 5% chemical mix seeing less than a 1 pH reduction. The RO water decreases by nearly 2 pH over the temperature increase. The author speculates that this could be due to the method in which the water is stored. The container and RO unit had regular algae build up (sterilised periodically) and an increase in temperature will cause these algae to grow. Algae can lower the pH of a system through respiration and the release of CO_2, (Muha, 2007).

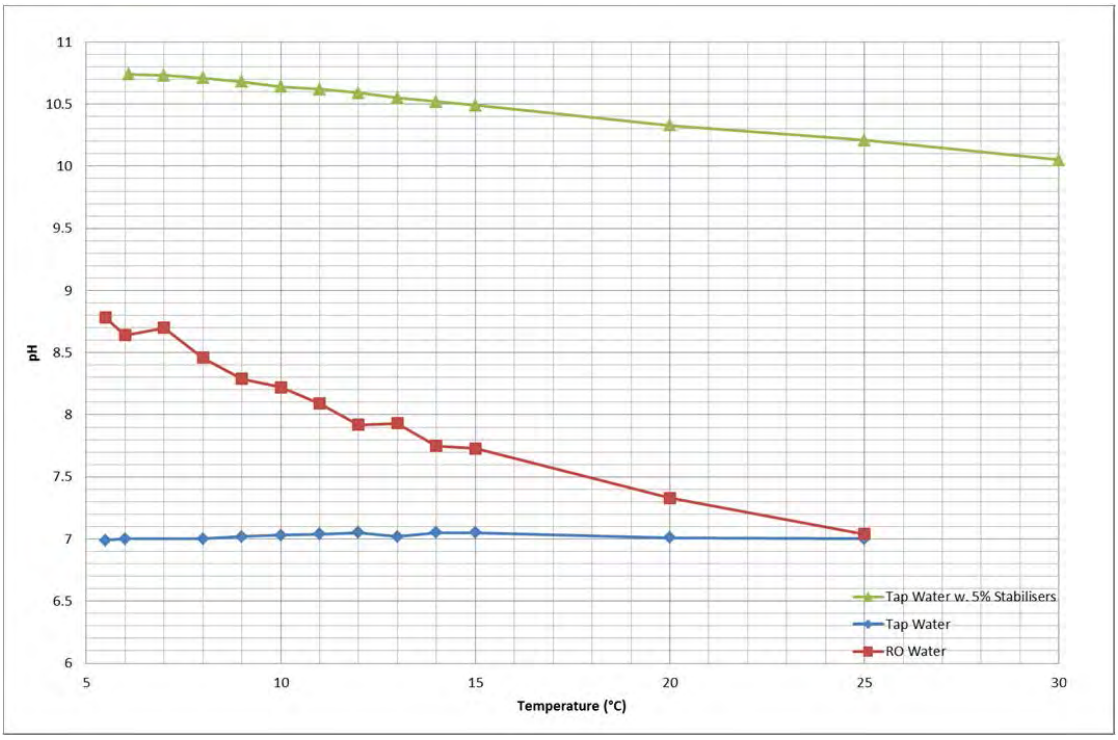

Figure 6-23: pH of fluids at varying temperatures.

6.2.3.4 Summary

It is anticipated from the results of the clay electrical conductivity experiments, that with increasing temperature, one should expect both a reduction in conductivity and pH of the stabilising fluids. Considering that heat is a by-product of introducing an electrical current into clay, this will be impossible to avoid. It is known however, from section 5.10.3 that an increase in temperature will increase the rate at which the chemical reactions take place. It is suggested that there is a 'Goldilocks' temperature range for the use of this treatment technique which would need identifying in future research.

It is also suggested that in the site trials, a minimum clay water content of 34% would be required for optimum electrical conductivity of the material. Achieving this, through water seeding for example, would ensure a more efficient treatment regime.

6.2.4 Electric Field Determination

Both the dye precipitation and dipole scattering did not gain results. The dye did not precipitate into the clay. The RO water was migrating through the clay and was being collected at the cathode; however the dye had not been able to penetrate the clay. It is thought perhaps a higher current density is required for this. The dipole scattering was equally ineffective in the fact that at low voltages, no movement is produced. A high voltage power supply (4kV) is required which was not available for use.

6.2.5 Electrode Polarisation

The electrode polarisation results can be seen in Figure 6-24. It can be seen that to achieve a given percentage electric current loss, 20% for example, the two electrode system took the least amount of time followed by the three and then four electrode systems. This means that in reality, if the same trends exist on mediums other than sand, a four electrode system would be able to sufficiently conduct a current across a clay for a longer period of time without needing to be relaxed.

Figure 6-25 shows the electrode relaxation times for the two, three and four electrode systems. The two electrode and three electrode systems are very similar in their relaxation times in that both take approximately 1,200 seconds to regain 15% of their lost current due to polarisation. The four electrode system takes approximately 35,000 seconds for relaxation to increase the current by 15%.

If one was to pick 10% as an arbitrary percentage loss and gain through polarisation and relaxation, the total ‘on’ current time could be calculated over a 24 hour period. In this instance, the two, three and four electrode would have total ‘on’ percentages of 40, 72 and 94%. This means that the four electrode system would be most efficient as an electrode option when combating electrode polarisation as the electrode can be running as usual for 94% of the time meaning the EKS process could be completed in a shorter time that that of a lesser amount of electrodes.

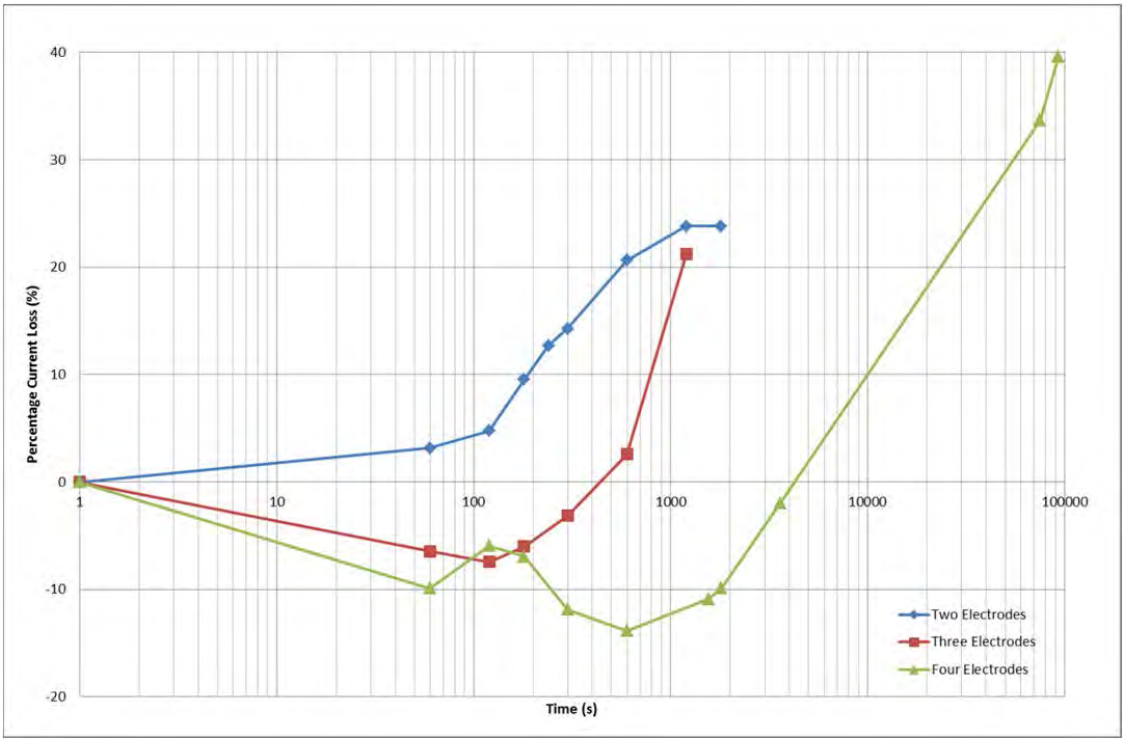

Figure 6-24: Electrode polarisation.

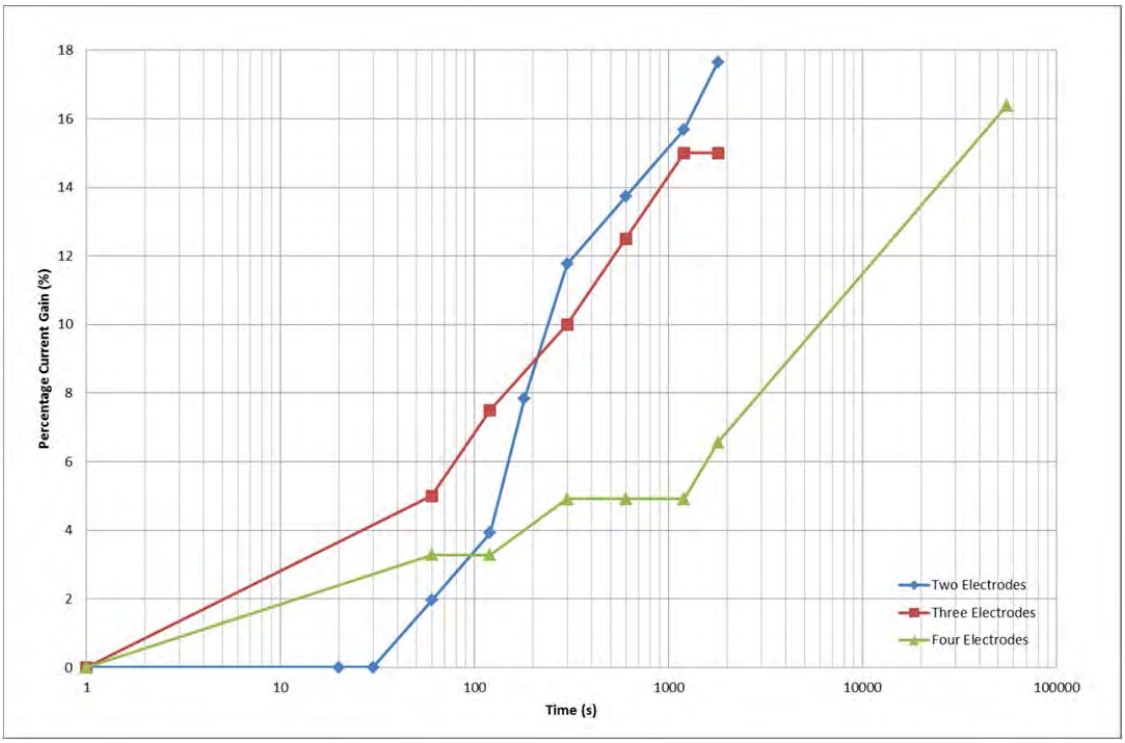

Figure 6-25: Electrode relaxation.

6.2.6 Current Intermittence

The current intermittence tests were conducted with a few issues. These issues included leaking from the medical drips which evidently are not designed to be used continuously for extended periods of time. Another issue was a faulty multi-meter where the current function was in error for the first nine days of the testing. It was fixed for the last five days and successful readings of the current were taken. Other than the aforementioned, the testing was conducted successfully with viable data available for discussion.

Table 6-4 presents the data taken from monitoring and post treatment testing. It must be noted that the power values are the sum of the last five days testing and not the entire length of the trial.

All of the data has been presented graphically against the power ratio used. So the control trial had a power ratio of 0 as there was no current applied and the constant trial was 1 as the current was on constantly. The ratios can be found in Table 6-4.

Table 6-4: Current intermittence results.

Power Interval (minutes)	Power Ratio	Power* (W)	Average Shear Strength (kPa)	Average Water Content (%)	LL (%)	PL (%)	PI (%)	LS (%)
Control	0.00	0.0	61.7	33.0	56.0	27.9	28.1	7.5
15 on, 15 off	0.50	4.3	49.8	34.7	55.0	29.5	25.5	7.0
30 on, 15 off	0.67	4.6	53.2	34.0	57.5	29.5	28.0	6.1
45 on, 15 off	0.75	5.0	44.7	35.0	65.0	31.1	33.9	6.2
Constant	1.00	3.3	54.5	33.5	55.0	28.0	27.0	6.7
30 on, 15 off (PEG)	0.67	2.9	46.3	35.4	58.0	31.5	26.5	7.2

*Power data is calculated from the last 5 days of treatment due to technical issues.

6.2.6.1 Water Content

Figure 6-26 shows the average water content over the specimens after the 14 day treatment process in relation to the power ratio used. As expected, the water content of the samples increases with power ratio until the 0.75 ratio whereby a small decrease is seen thereafter as the power ratio reaches 1.00. This indicates that the higher the power ratio, the more electric current is passed through the clay leading to a greater flow rate. This is until constant power is

reached meaning that the electrodes must have become polarised to some degree and the break in current was relaxing the system leading to an increased flow rate.

The PEG trial showed a lower water content than its stainless steel equivalent likely due to the lower electrical current flowing through and driving the flowrate.

6.2.6.2 Shear Strength

The average shear strengths over the different power ratios can be found in Figure 6-27. It can be seen that the trend is almost the inverse of Figure 6-26 in that the control trial has the highest shear strength with a decrease to the minimum before increasing slightly at the constant trial. The minimum shear strength is however not at the 0.67 power ratio but at the 0.75. This indicates that a change other than water content has affected the clay.

The PEG trial possessed higher shear strength than the stainless steel equivalent but this was most likely due to the water content.

6.2.6.3 Plastic Limit

Figure 6-28 shows the plastic limits for the various power ratios. The constant current increased by 0.1 over the 14 day trial with the maximum increase seen at the 0.67 power ratio. The PEG trial is seen to possess the same plastic limit as the 0.5 power ratio meaning it has used more power to attain the same plastic limit increase.

6.2.6.4 Liquid Limit

Figure 6-29 shows the liquid limits over the 14 day trial for each power ratio tested. It can be seen that the maximum liquid limit is at the 0.75 power ratio with 0.5 and constant current both decreasing below the control. Both 0.67 trials are approximately equal with an approximate 2% increase over the control.

6.2.6.5 Plasticity Index

The plasticity index data can be seen in Figure 6-30. It is shown that all of the trials possess decreased plasticity indexes compared to the control trial with the exception of the 0.75 power ratio trial which increases by approximately 6%.

6.2.6.6 *Linear Shrinkage*

The linear shrinkage of the samples over the power ratios are shown in Figure 6-31. It is seen that there is a reduction in shrinkage for all of the trials, including the PEG trial. The greatest reduction was seen with the 0.67 power ratio with a reduction of 1.4%. The PEG trial saw a 0.3% reduction in linear shrinkage over the control which was the smallest decrease of all the trials over the control.

6.2.6.7 *Power*

The power consumption over the last 5 days of each trial is shown in Figure 6-32. As expected, the power consumption increases as the power ratio increases. This is with the exception of the PEG trial due to the low transference of current and the constant power trial. The constant power trial has a lower power consumption than the intermittent trials most likely due to the polarisation of the electrodes resulting in lower current being transferred through the clay.

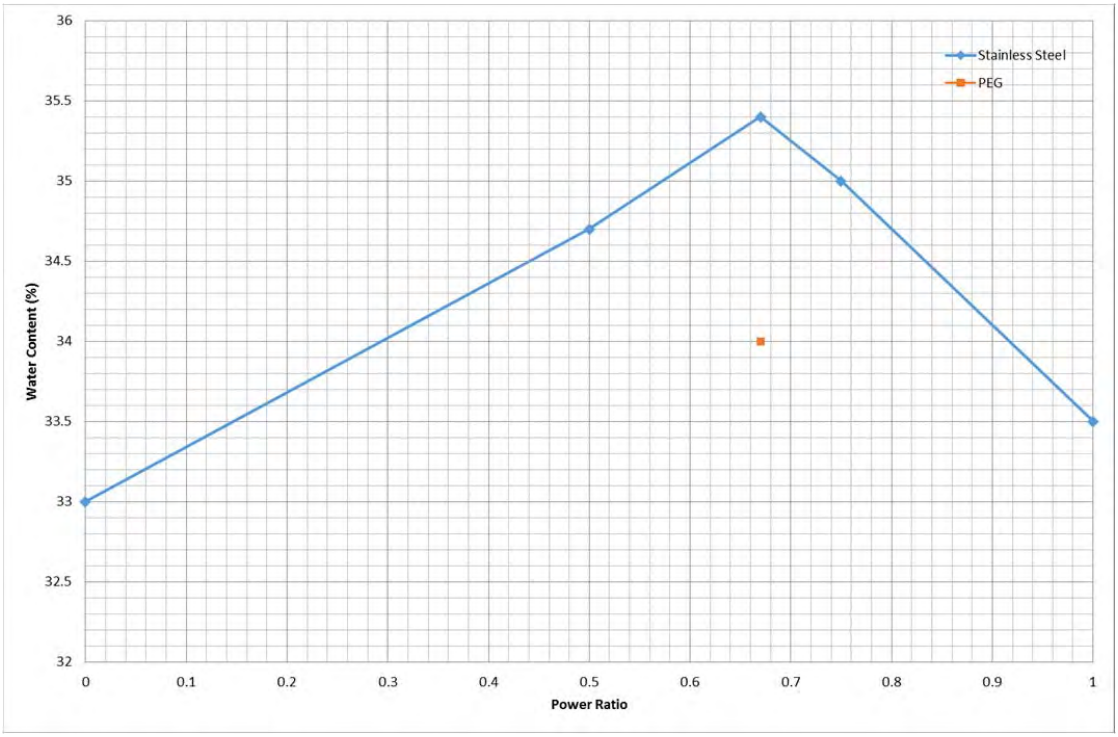

Figure 6-26: Current intermittence water contents.

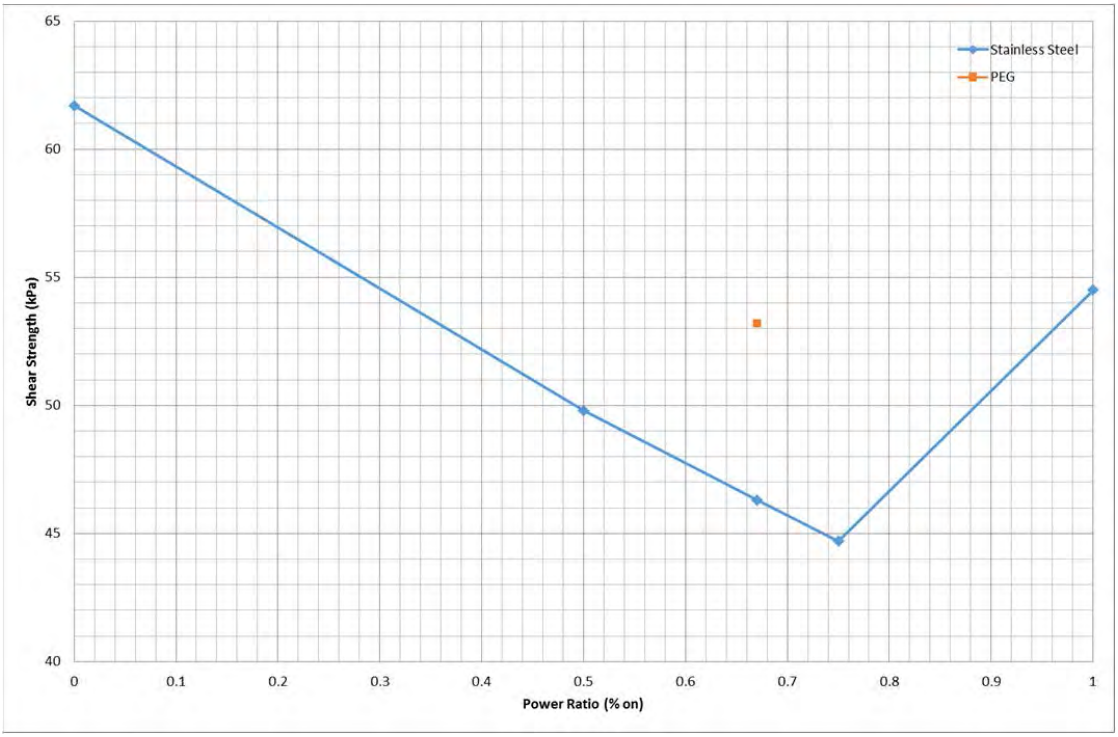

Figure 6-27: Current intermittence shear strengths.

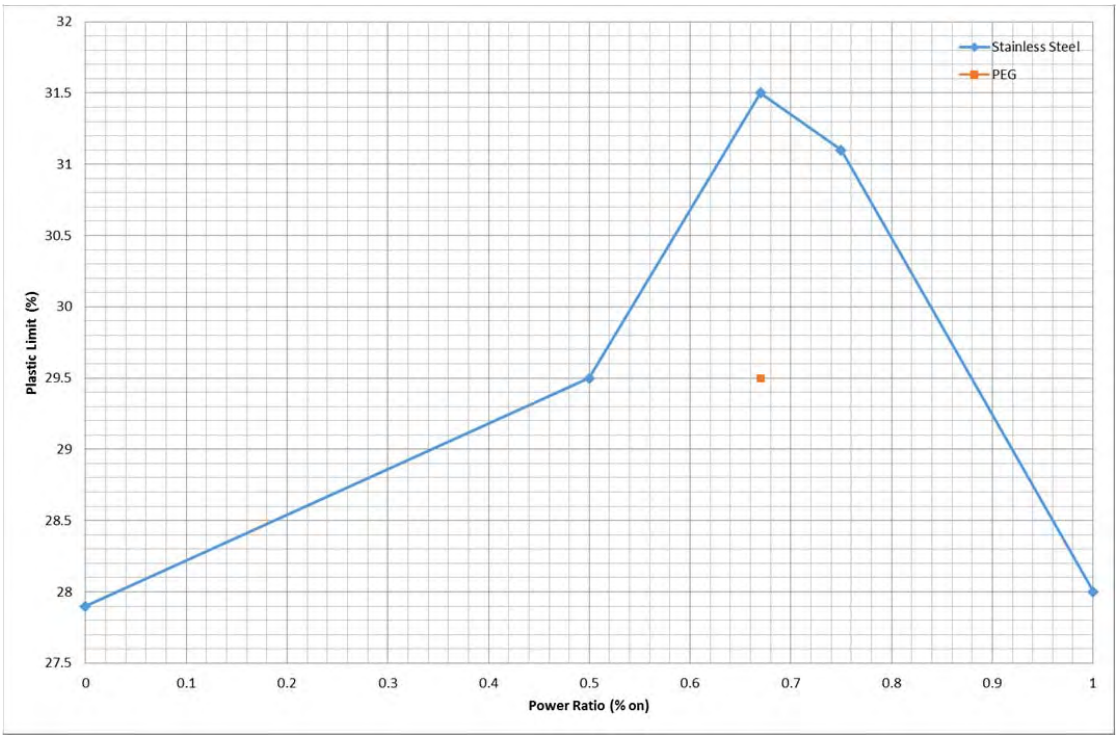

Figure 6-28: Current intermittence plastic limits.

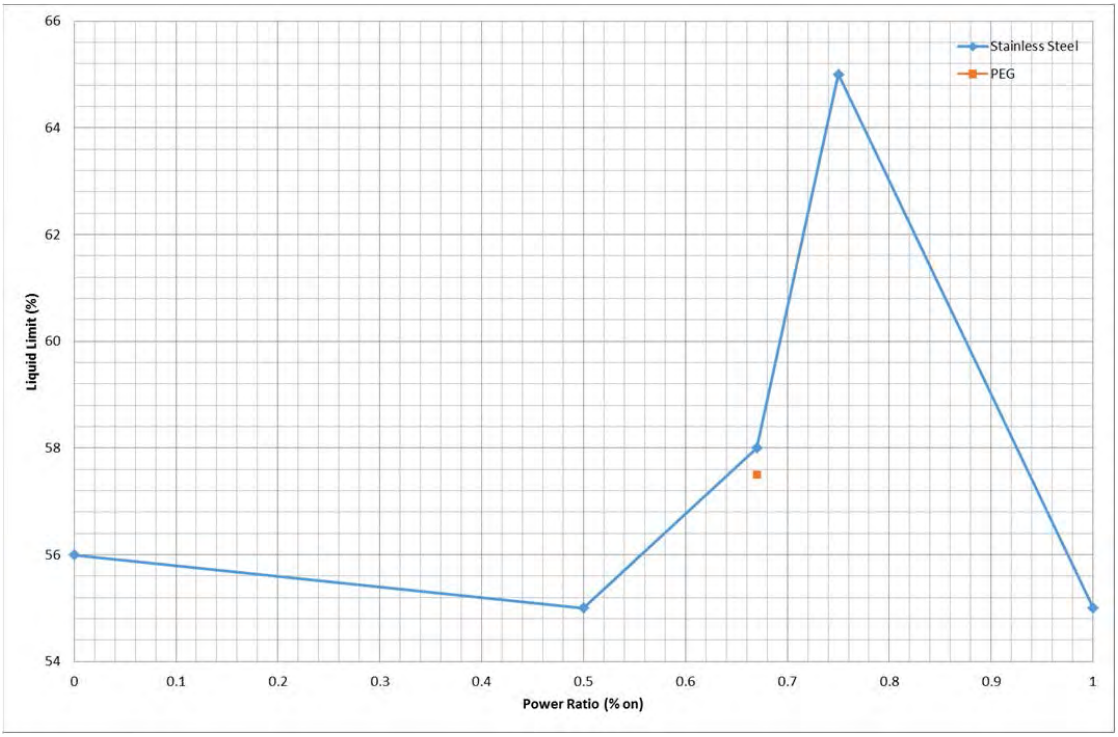

Figure 6-29: Current intermittence liquid limits.

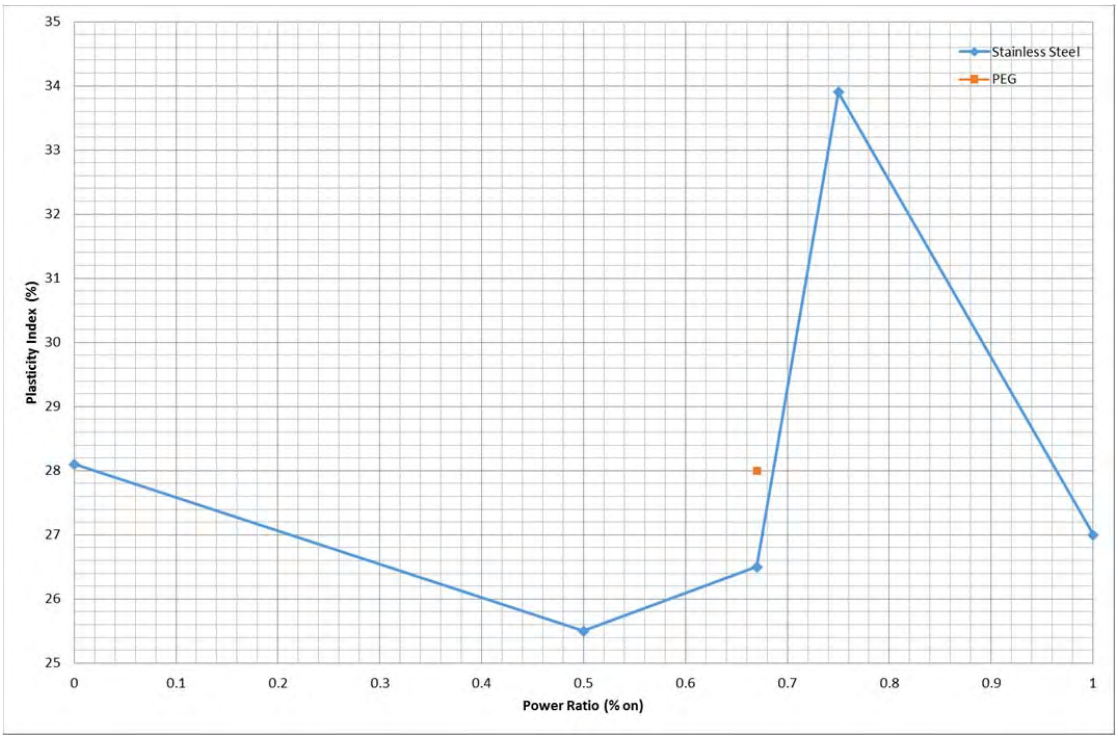

Figure 6-30: Current intermittence plasticity index.

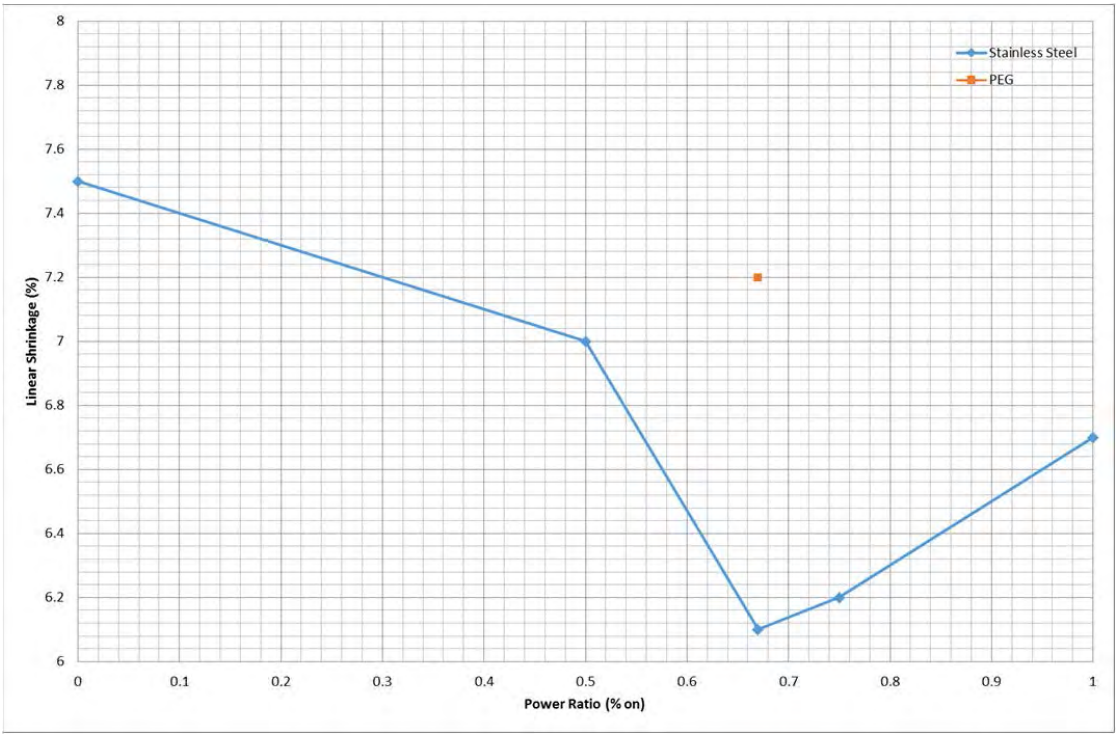

Figure 6-31: Current intermittence linear shrinkage.

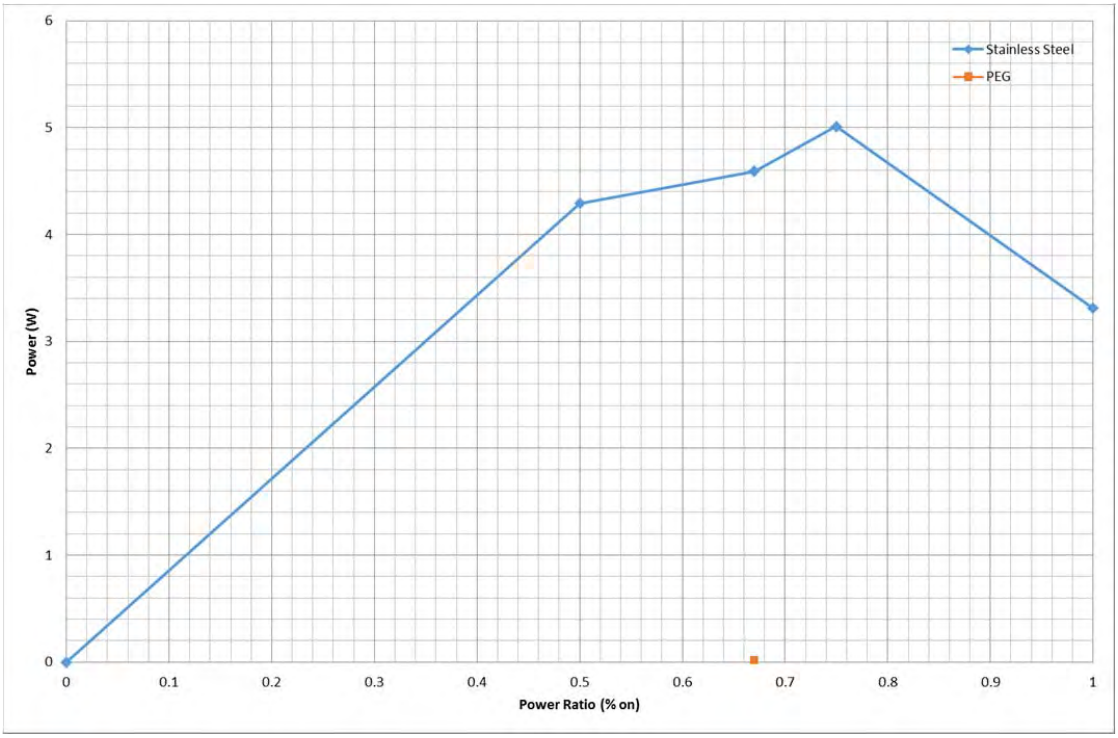

Figure 6-32: Current intermittence power consumption over the last 5 days of trial.

6.2.6.8 Summary

This section has seen varying current intermittence time periods applied to the ECC over 14 days. It was found that the varying times produced varying outcomes with the most successful in clay characteristic alterations being between 0.67 and 0.75. Generally, the higher the power ratio, the greater the improvements to the clay. This is anticipated to be due purely to the amount of current being supplied and hence amount of stabilising fluids being migrated into the clay. It could also indicate that for these electrodes in this clay, only a short electrode relaxation time is required to depolarise.

Figure 6-33 shows the shear strengths for each trial over the varying water contents found across the specimens. This indicates that the 0.67 power ratio has had a beneficial impact on the clay whereas the other current intermittence timings have not. It may also be evident that the PEG and constant trials would prove to be beneficial at higher water contents, the evidence is purely indicative though.

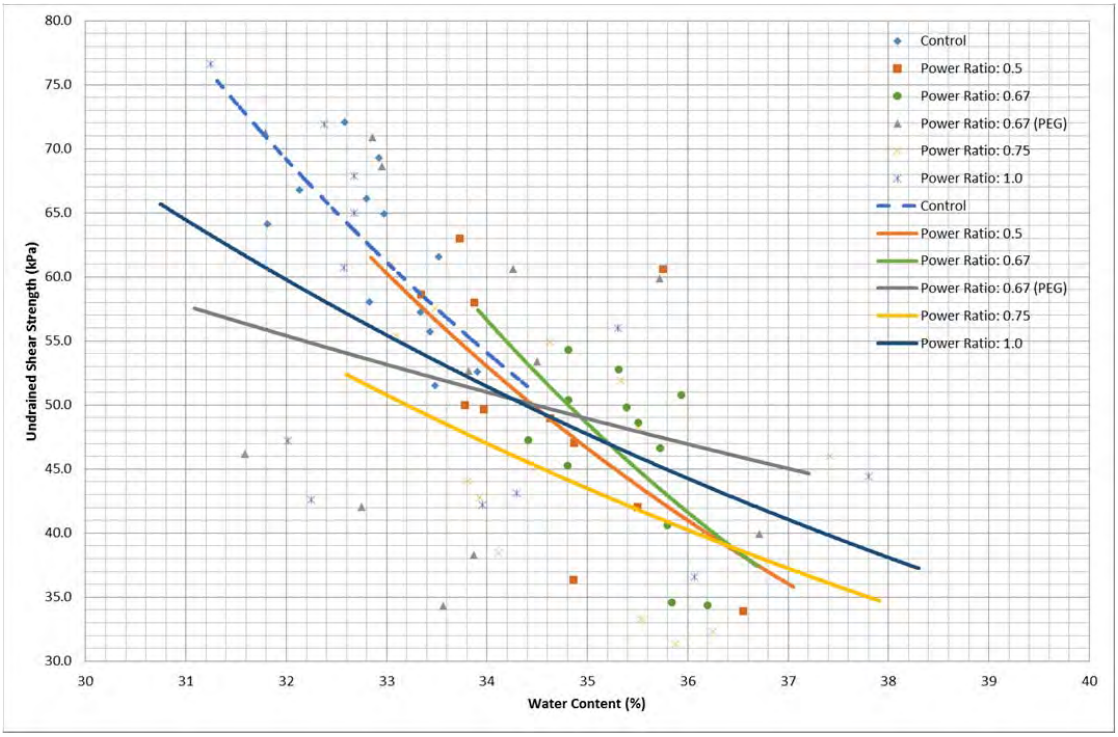

Figure 6-33: Current intermittence shear strength change with water contents detailed.

6.2.7 Electrode Type Choice 1

The three electrode types that were compared here were steel tube, EKG and the hybrid electrode.

6.2.7.1 Power

As seen in Figure 6-34 and Table 6-5, over the life span of the test, each electrode has an approximately equal average voltage. However, the stainless steel has a larger average current and average power by approximately an order of magnitude, Figure 6-35. This leads to the total power consumed by the stainless steel being much larger than the other electrodes. The voltage readings shown in Figure 6-34 show an erratic EKG where the reasoning for this was the use of an analogue power supply for this test leading to human error in reading the gauge rather than a digital display in the other tests.

Due to each test having the same clay makeup such as equal water contents, there is no reason for the clay in the stainless steel test to have a lower electrical resistance. The reason for this higher average current and thus power must be down to the electrodes themselves. It is thought that the stainless steel electrodes have a better electrode clay interface as the steel is touching the clay whereas for the other electrodes there is a plastic barrier leading to losses in the effort of passing the plastics. As seen in Figure 6-35 the current of the stainless steel test does decrease over time with the reason being that as the electrode decays, the electrical conductivity decreases.

6.2.7.2 Effluent Flow

Regarding the flow of water through the systems, the two pole electrodes (hybrid and stainless steel) have a different electrical pattern through the soil than the sheet electrode (EKG); this is shown in section 6.3. This will lead to different flow patterns and thus differing the amount of energy used to push equivalent amounts of fluid. The cumulative effluent from the EKG and hybrid are within 15% of each other and the power is 30% different. Table 6.5 also shows the power per litre of fluid moved across the clay with the EKG being the most economical at 6.66 Watts per litre and the stainless steel being least at 31.48W/L. Of course in reality, time taken for equipment to be on site would be taken into account, so the savings made on power may be dwarfed by the cost of keeping equipment on site for the extra time needed to pass all the fluid through.

The EKG flow between the hours of 300 to 700 hours is unexplained. Power was being supplied and fluid was available however none was drawn through the clay. After 700 hours the flow restarted again. Unfortunately there was not time to rerun this test to ascertain if this was an anomaly or not. A possibility is that the electrodes became polarised and as such ineffective. A brief power disruption would have relaxed and restored the electrodes to their initial state as discussed in section 6.2.5.

6.2.7.3 Undrained Shear Strength

Hand shear vane recordings were taken but with an average of 4kPa in each trial cell, ignored due to the inaccuracy of a hand vane at such low strengths. These strengths did however show a decrease at the cathode which was most pronounced in the stainless steel test, most likely due to its large effluent flow. Undrained shear strengths can be found in Appendix E.

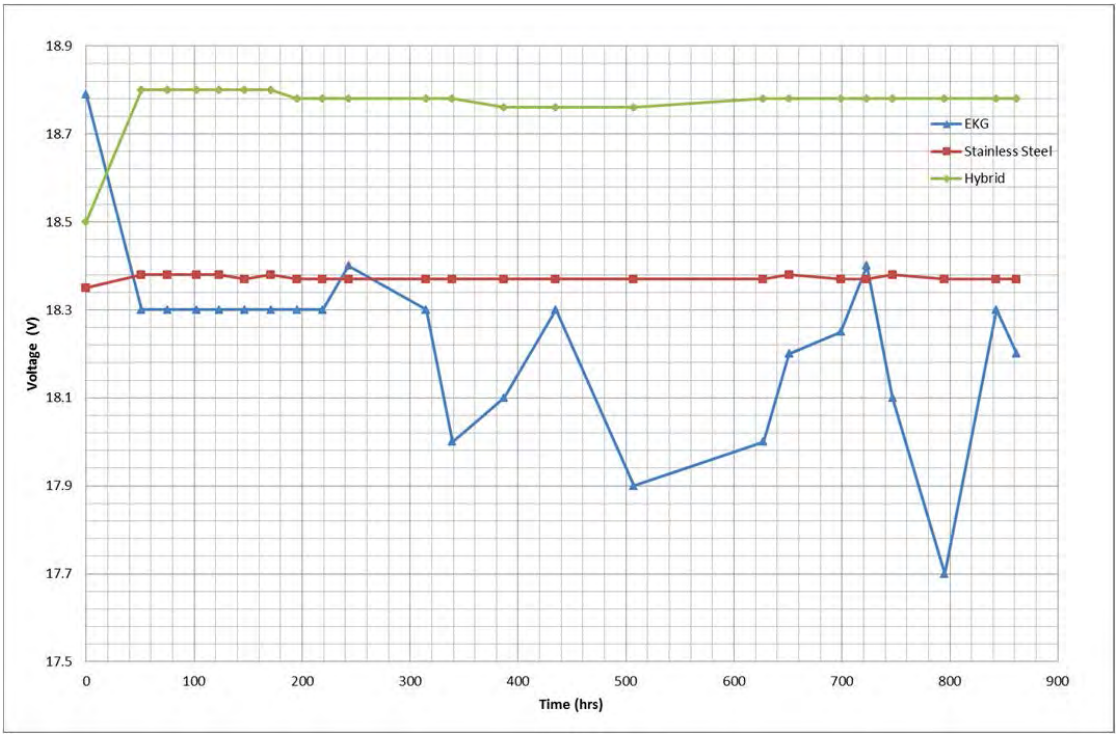

Figure 6-34: Electrode Type Choice 1 voltages.

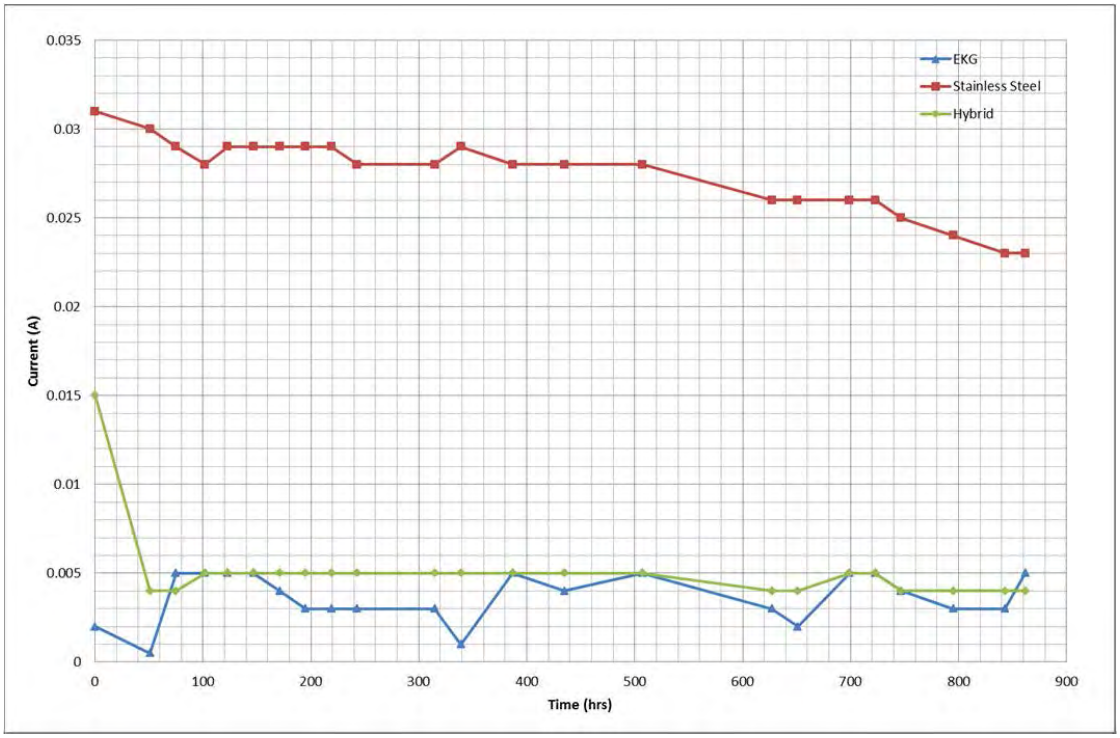

Figure 6-35: Electrode Type Choice 1 electric current.

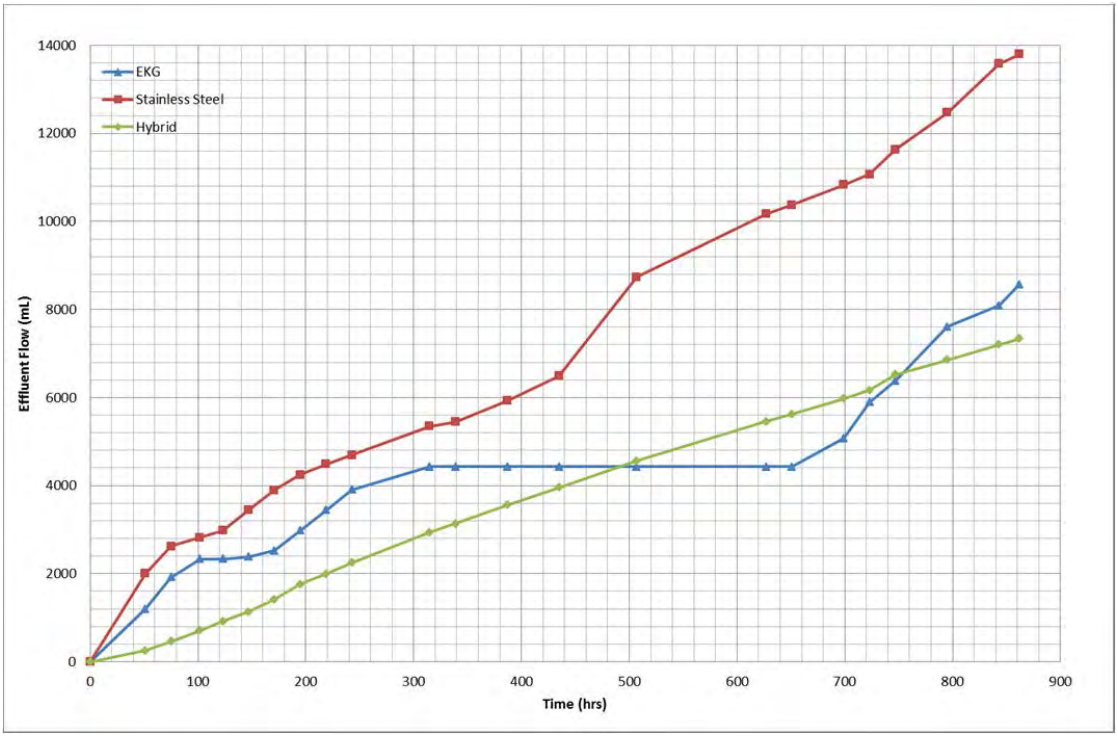

Figure 6-36: Electrode Type Choice 1 effluent flow.

Table 6-5: Electrode Type Choice 1 power consumptions.

Test	Average Voltage (V)	Average Current (mA)	Average Power (W)	Total Power (Wh)	Power per L (W/L)
EKG	18.2	3.6	0.0662	57.1	6.6
Stainless Steel	18.3	27.4	0.5040	434.5	31.5
Hybrid	18.7	5.0	0.0954	82.3	11.2

6.2.7.4 Summary

The fact that the clay used for the Electrode Type Choice 1 testing was low strength was not an issue as the intention of this test was to ascertain the most effective electrode type regarding electric current transference and fluid migration. The most effective was determined to be the stainless steel as expected due to electrical current transferred and fluid migrated. It is interesting to note however, from Figure 6-37, that the most efficient electrode for fluid migration is the EKG with stainless steel performing worst. This is another indicator that the polymer based electrodes would be appropriate for long term installations but the stainless steel electrodes are still most effective in the short term.

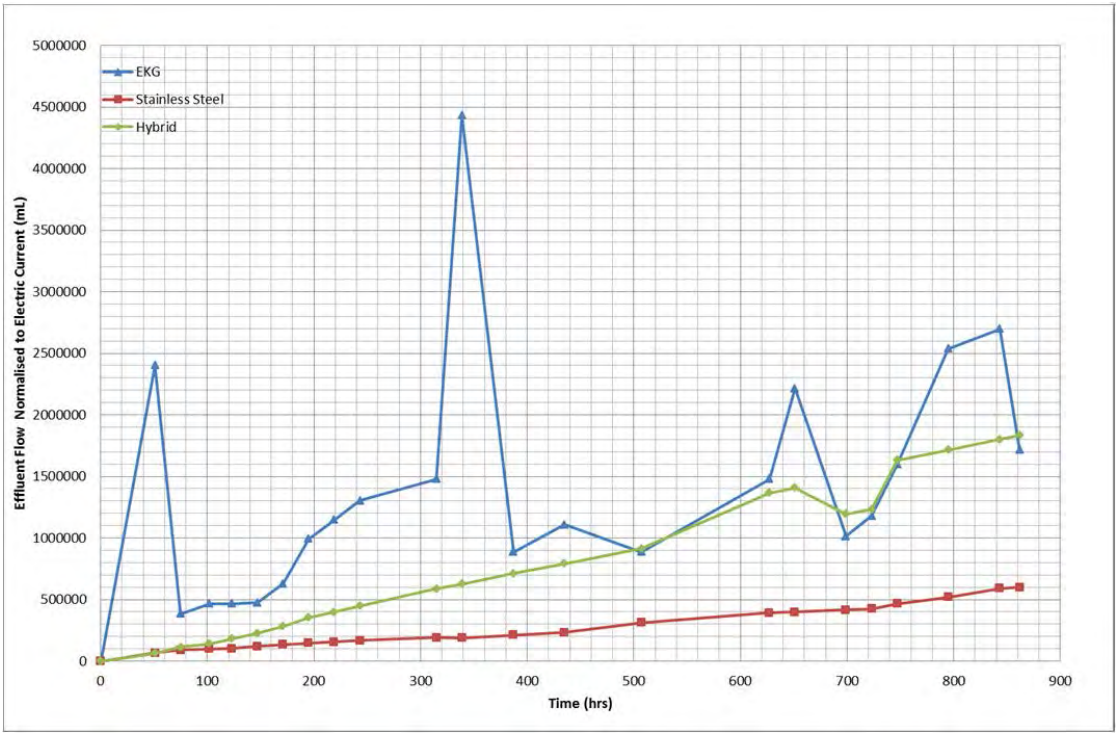

Figure 6-37: Electrode Type Choice 1 effluent flow normalised to electric current.

6.2.8 Electrode Coating

The resistances of the new electrode coating mixes can be seen in Table 6-6 with traditional electrode types for comparison and are displayed graphically in Figure 6-38.

Table 6-6: Electrode materials and their corresponding electrical resistances.

Electrode Material (Concentration)	Surface Resistance (Ohms)
Stainless steel	0.1
Plastic tube with Eccobond ER and graphite coating (PEG Prototype) (55%)	500
Steel with Eccobond ER and graphite coating (SEG) (55%)	5,000
EKG (New)	10,000 – 40,000
EKG (Used)	100,000 – 150,000
Plastic tube with Eccobond ER and carbon mix	135,000
Plastic tube with new ER and graphite coating (15%)	>3,300,000
Plastic tube with new ER and graphite coating (25%)	1,800,000
Plastic tube with new ER and graphite coating (30%)	250,000
Plastic tube with new ER and graphite coating (35%)	17,000
Plastic tube with new ER and graphite coating (45%)	730
Plastic tube with new ER and graphite coating (50%)	120

6.2.8.1 Carbon Mix

It was found that due to the larger particle size of the carbon available, the resulting paste was not very workable when applying to a tube. It was, however, managed and readings were successfully taken. With a surface resistance of 135,000 Ohms, it is approximately equivalent to a used EKG electrode, Figure 6-38.

This means that the use of a carbon mix in this form has no future as a coating for an electrode in EKS, the EKG is made of carbon black dispersed in a polymer however. A suggested content by weight of 20 – 30% is required for a suitably conductive coating, (Jones, et al., 1996). Pugh (2002) goes on to show that there are three stages of varying carbon content's electrical conductivity, Figure 6-39, which is similar to that seen for the graphite content, Figure 6-40.

6.2.8.2 Graphite Mix

As seen in Figure 6-40, the greater the concentration of graphite contained in the epoxy resin mix, the lower the surface electrical resistance of the coating. Due to the requirement for an electrically conductive electrode, the lower resistance is desired.

The greatest effect that the concentration of graphite has on the electrical resistance of the electrode is between 30% and 35% with a decrease of approximately 30 times. Up until approximately 25%, the resistance shows no sign of decreasing dramatically as the majority of the mix is the electrically resistant epoxy resin. 50% was the maximum concentration used in this test due to the difficulties of mixing the blend at higher concentrations. In fact, the 50% sample was not applied to a tube due to its low workability.

It was found that when applying the graphite mix to the tubes, albeit with a lower graphite content, over smoothing the surface resulted in a layer of ER being brought to the surface leading to no electrical conductivity. This was less of a problem using 45% graphite powder as the mixture was too grainy to produce a smooth surface of likes seen when no conductivity was produced.

At concentrations of 35% and over, PEG electrodes become more viable as their electrical resistance drops below that of a new EKG electrode, however at 40% graphite content and above, the paste mixed became too unworkable to be used practically.

The PEG prototype with a concentration of 55% graphite was very successful. With a surface resistance of 500 Ohms, it was much more electrically conductive than the other types with only stainless steel and the PEG (50%) possessing lower resistances. This success came at a price though with the type of epoxy resin and graphite used being approximately 5 times the price of the regular PEG trials.

6.2.8.3 Others

The EKG electrodes displayed various resistance behaviours depending on the direction of measurement. Measuring down a vertical strand gave a lower resistance than across multiple strands. It is assumed that this is due to the fact that the steel wires inside the polymeric coating are not present in all strands of the electrode. The resistance measurements of both used and new EKG were quite erratic. As expected though, the used EKG possessed an electrical resistivity 5x larger than that of the new version due to the degradation of the electrode over usage, (Pugh, 2002).

As expected, the stainless steel electrode possessed the lowest electrical resistance at 0.1 Ohms. The steel electrode coated in epoxy resin and graphite at 55% concentration yielded a surprising result. It was expected that due to stainless steel making up the core of this electrode, it would have a lower surface resistance than the plastic tube version (steel with epoxy-resin graphite (SEG), Figure 6-38). This was not the case though and the SEG possessed an electrical resistance 10x higher than that of the plastic tube PEG prototype. This was the catalyst to experiment with plastic tube electrode coatings. The reasoning behind this has not yet been discovered but may be concerned with the electric current pathway through the electrode. In the PEG type electrodes, the current will stay in the coating completely as the plastic tube is completely insulating whereas the steel core SEG will most likely share the electrical current to a degree with the majority travelling through the steel and not the coating due to the steel's lower electrical resistivity.

6.2.8.4 Electrode Resistivity

The electrode resistivity values calculated can be seen in Figure 6-41 where it is shown that, as expected, the stainless steel has the lowest resistivity followed by the reinforcement bar and then the PEG and EKG.

The PEG's surface resistance may be lower than the EKG but the shape of the electrode also plays a major part in determining its effectiveness in transferring current through the clay. From laboratory testing, it was found that the PEG electrodes do not perform well but EKG electrodes do. This is contrary to what is expected due to the resistivity of the EKG being higher than that of the PEG. Therefore this must be explained by the footprint size of the EKG, as the resistivity calculations use the surface area of the electrode and the EKG has many holes in between the mesh. This mesh may act like a honeycomb structure and increase the effective size of the electrode thus the increasing the resistivity.

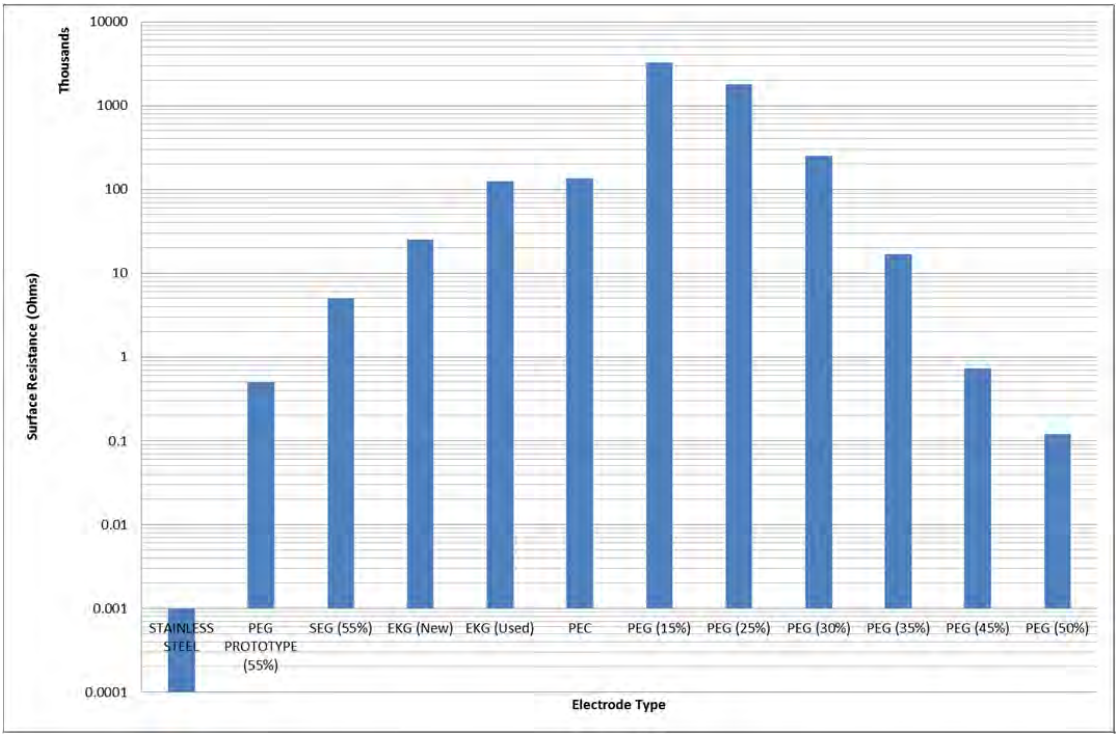

Figure 6-38: Various electrode type's electrical resistances.

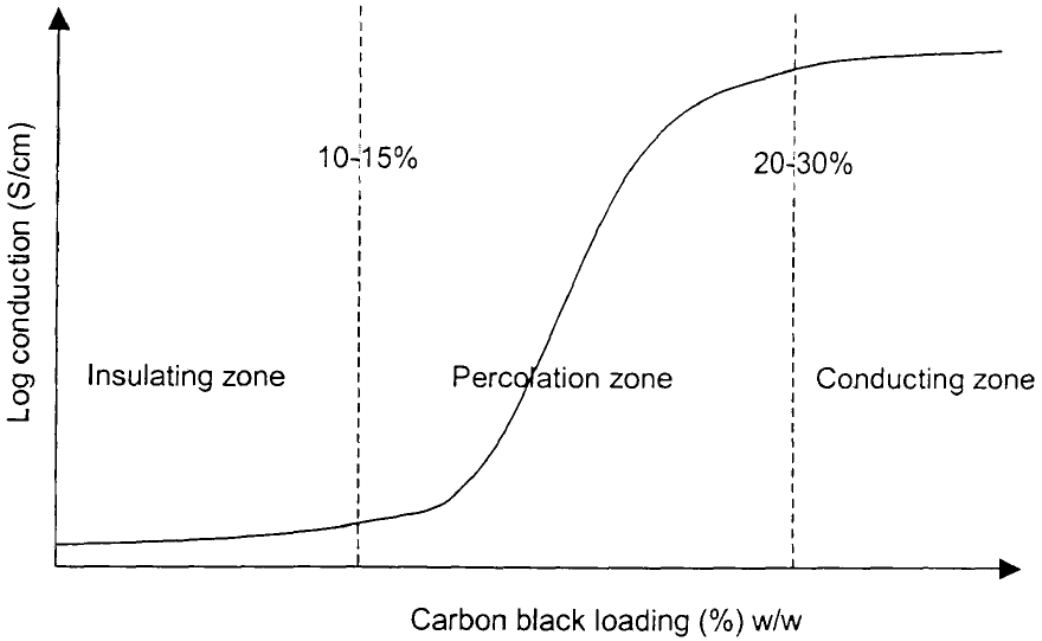

Figure 6-39: Carbon black content against electrical conductivity. After Pugh (2002).

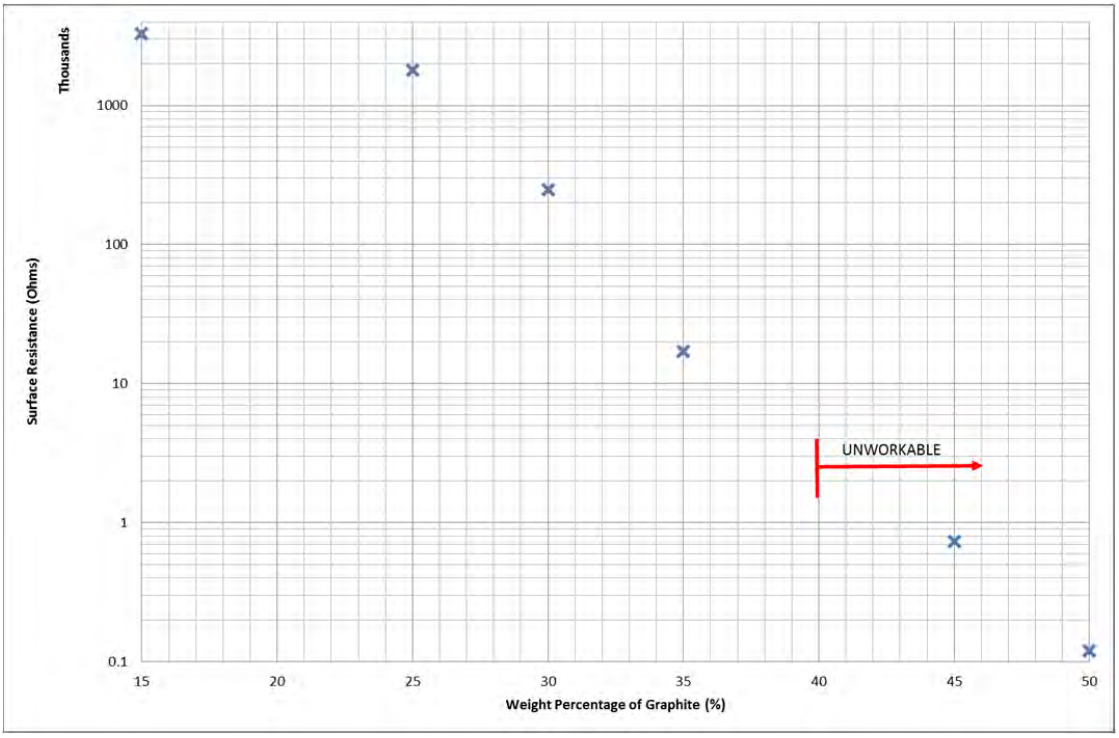

Figure 6-40: Graphite concentration of epoxy-resin against surface electrical resistance.

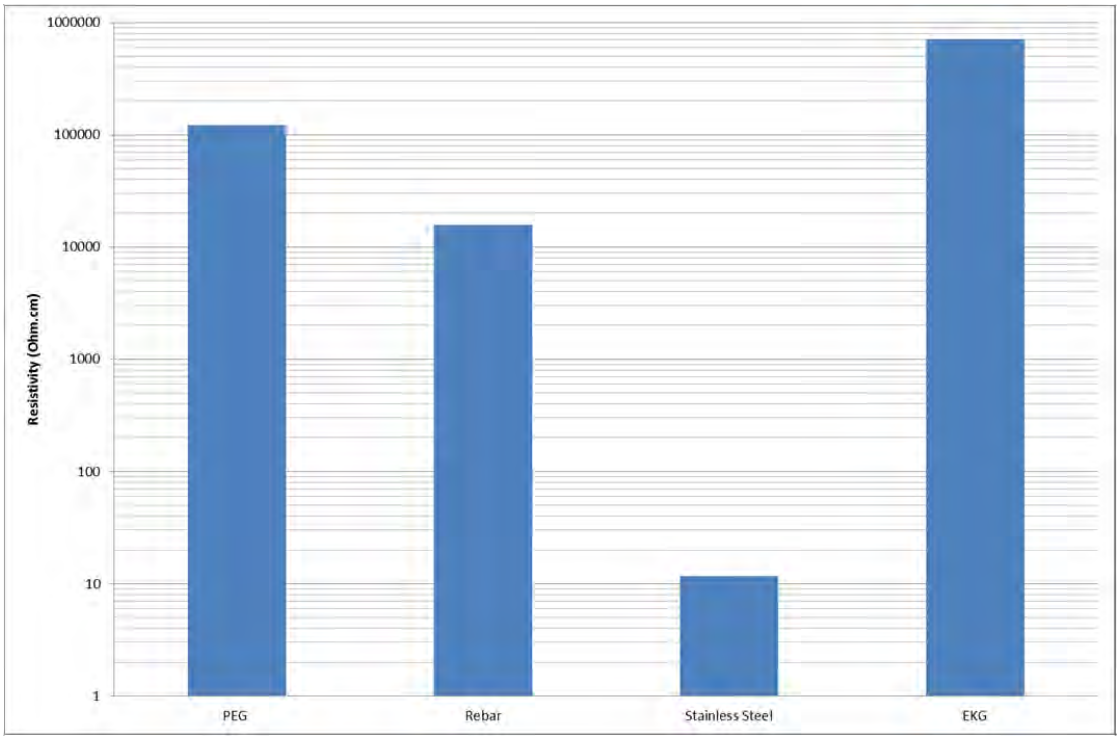

Figure 6-41: Electrode material resistivity.

6.2.8.5 Summary

This electrode coating section set out to determine if a new electrode type, similar in nature to the EKG, could be created that would provide the low electrical resistance required to power EKS and also be formed in a manner in which insertion into clay would be simple and cheap.

It has been shown here that the PEG type electrode is the most suited for EKS when compared with the EKG and SEG type electrodes due to its lower electrical resistance at 35% concentration and its pole form which would lead to an easier installation process that the EKG. Obviously, the stainless steel tube still outweighs the PEG type electrodes in both of these cases but does have the negative attribute of relatively quick corrosion and degradation compared to PEG which is not conducive to electrode re-use over multiple treatment schemes.

6.2.9 Electrode Decay through Fluid Interaction

Stainless steel, PEG and steel reinforcement bars were used to determine the effect of the EKS process on the electrodes.

6.2.9.1 pH

As seen in Figure 6-42, the time period up to 109 days shows all pH's decreasing and then up to the 285 day period there is an increase for the electrode materials in the chemicals. The water based electrode materials are seen to initially increase over the first few days to then steadily decrease and then increase in the same manner as the chemical tests. It is also seen that the pH's appear to be grouped. Group 1 contains the materials in the chemical mix, this is expected as the initial pH of the liquid is high. Group 2 consists of the two PEG electrodes in water and the two steel electrodes in water. Group 3 consists of the two rebar electrodes in the water. This was expected due to the corrosion undergone by the rebar.

6.2.9.2 Mass

Figure 6-43 shows the mass variation over time of the electrode materials in the liquids. The largest percentage change in mass of the electrodes is for PEG which was in the chemical mix. This could be down to deposition of the chemicals onto the electrode surface leading to an increase in weight. The rebar mass variation is very small even though material had flaked away from the electrodes and settled on the bottom of the beaker. This is most likely due to the fact that rust has a higher mass compared to the equivalent amount of steel. The mass lost due to

flaking must be approximately equal to the mass gain from the steel oxidising to rust. The gain in mass seen on the water based stainless steel electrode is most likely due to the rust having a higher mass than the steel. The PEG electrodes in water have a relatively large increase in mass. The only explanation for this would be that a chemical reaction is taking place whereby mass is being added to the electrode.

6.2.9.3 Surface Resistance

Figure 6-44 shows the resistance variation over the electrodes over the time they were left in their respective liquids. A personal communication with Professor Nigel Cassidy suggested that any resistance over 1MΩ would be too high to measure using a normal multi-meter and would be a sufficiently ineffective electrode too. Although the PEG electrodes do have the highest initial resistance, after 56 days they appear to have increased less than the others. After 56 days they are the most conductive electrodes. They are however, at this point, quite ineffective electrodes as their resistances are too high. As seen in Figure 6-44, the variation of the PEG electrode resistance is much less overall than the metal electrodes. The metal electrodes are much more conductive initially but over a short period of time become ineffectual.

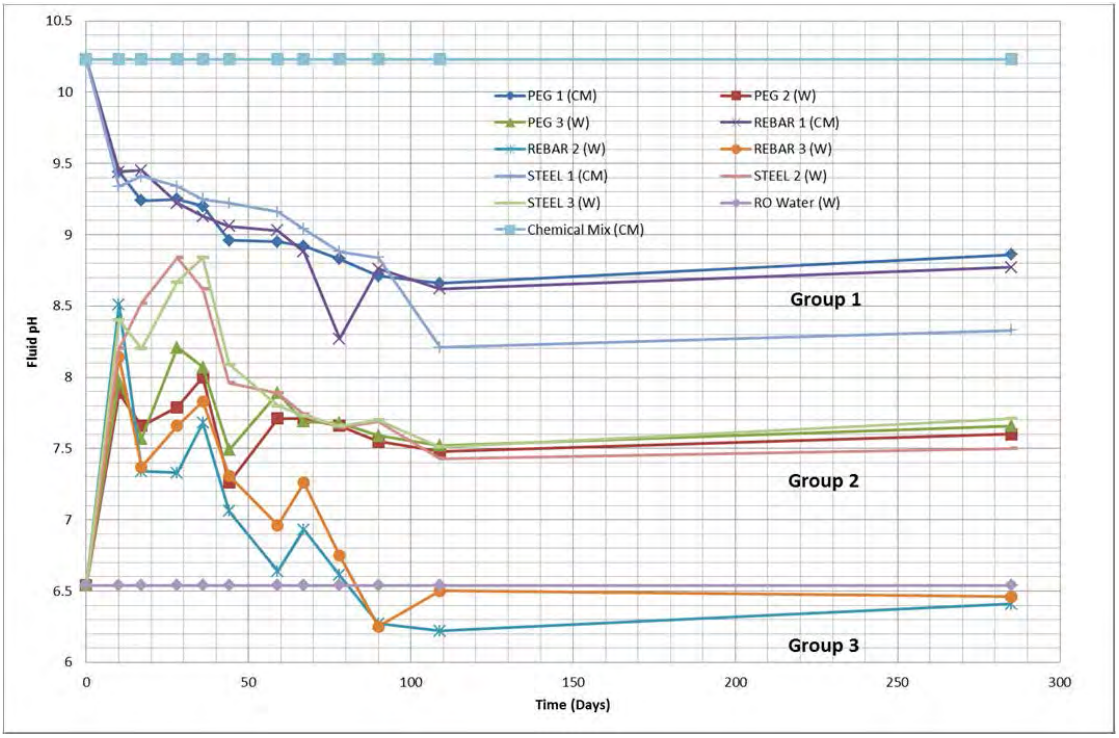

Figure 6-42: Fluid pH change over time.

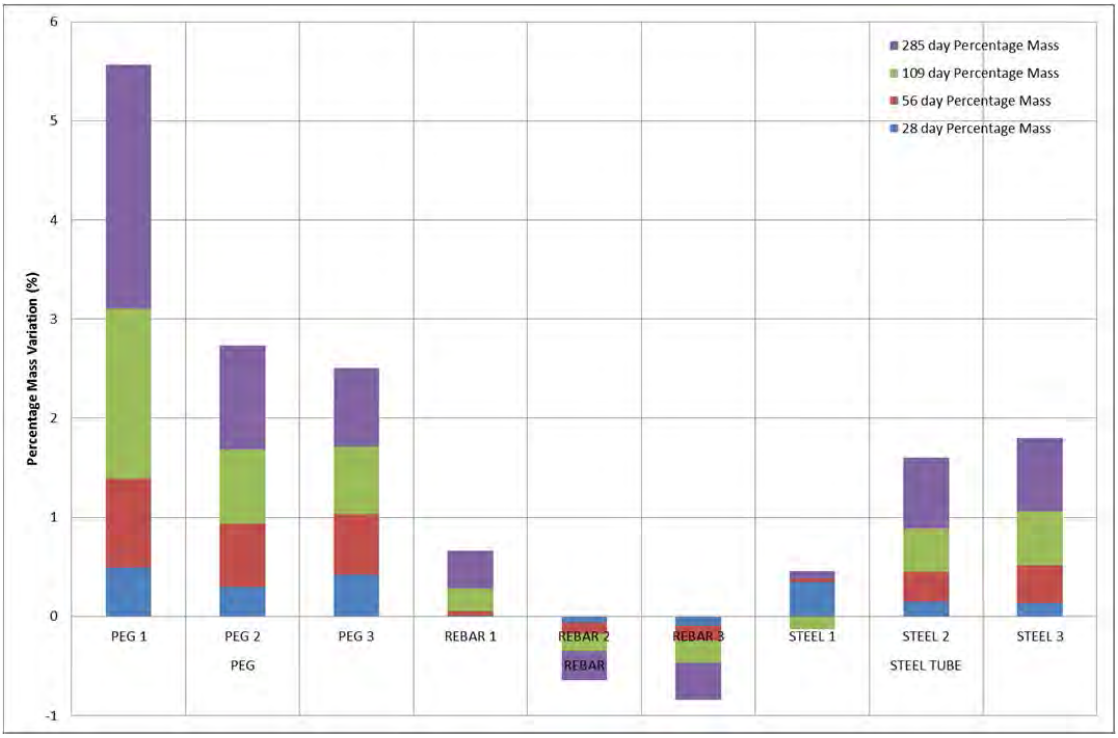

Figure 6-43: Electrode mass variation over time.

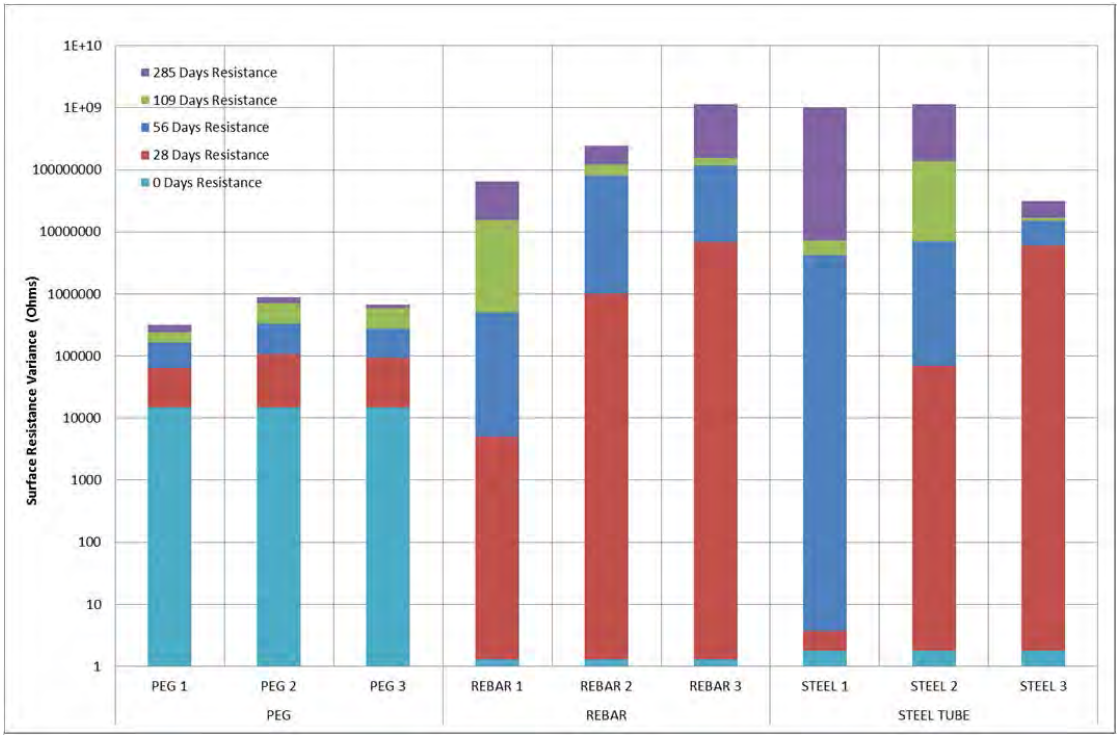

Figure 6-44: Electrode electrical surface resistance variance over time.

6.2.9.4 Summary

In a RO water environment, the PEG and stainless steel electrodes show most pH gain which has previously been cited as beneficial toward electrokinetic treatment. In the chemical mixture environment, as would be present in actual electrokinetic chemical stabilisation, the stainless steel electrodes show the smallest pH decrease over 90 days followed by a significant decrease. With an estimated treatment time of 40 – 60 days, this would prove insignificant. Furthermore, although the stainless steel electrodes do experience a dramatic increase in surface resistance over time, due to the anticipated treatment length being less than 90 days it can be concluded that stainless steel electrodes would be most beneficial of all the electrode types for this study's single use site trial.

6.2.10 Electrode Decay through Electrolysis

The electrodes were submerged into RO water and an electric potential of 12V was applied over a period of 40 days to determine the effect of electrolysis on the electrodes.

6.2.10.1 Power

Figure 6-45 shows the voltages for each trial where it is seen that all of the trials appear to follow the same trend. It's thought that the power supply inconsistency is only evident in the voltage readings. The current readings, as shown in Figure 6-46, are more pertinent as they show the reduction in current transference between electrodes. It is anticipated that the fluctuations in voltage could be associated to a fluctuation in the mains power in the laboratory as all of the tests show the same trend.

The electric current can be seen in Figure 6-46 whereby it is shown that initially the stainless steel electrodes hold the greatest current followed by the rebar and then EKG and PEG as expected. There is a rapid drop off of current over the first 14 days for the stainless steel and rebar electrodes due to corrosion of the metal which increases the resistivity of the electrode. After the first 14 days, all four electrode types possess a similar current value and by day 24, the EKG possesses the greatest electrical current, albeit a very small one. It is anticipated that the decrease in current transference is due partly to corrosion and surface area loss and partly to polarisation as discussed in section 6.2.5.

6.2.10.2 pH

The variation of pH over the test duration is shown in Figure 6-47. It can be seen that there is an initial increase in all four electrode type's fluid pH in the first 7 days and then a steady decrease towards their approximate initial pH's. The stainless steel electrode shows the highest pH over the first 25 days which is beneficial to electrokinetic treatment, after which all electrodes become generally equal. It is anticipated that the pH of the fluid may be linked directly to the current in that the current controls migration of hydrogen ions which control pH levels. The corrosion and thus electrical current decrease therefore producing a reduction in pH after the initial boost.

6.2.10.3 Mass

Table 6-7 shows the mass changes of the electrode over the test duration. It can be noted that for all electrode types, the anode loses mass and the cathode gains mass as one would expect from this type of electrochemical reaction. The rebar anode is the electrode which sees the greatest mass change followed by the stainless steel. Their metallic nature makes this an expected result with the polymer protected electrodes losing the least mass.

Table 6-7: Electrolysis electrode mass change over time.

Electrode Type		**0 Days**	**7 Days**	**40 Days**
		Weight (g)	**Weight (g)**	**Weight (g)**
Rebar	Rebar Anode	109.14	108.97	108.44
	Rebar Cathode	110.39	110.39	110.41
PEG	PEG Anode	31.02	31.16	31.04
	PEG Cathode	29.82	29.94	29.95
SS	Stainless Steel Anode	79.93	79.75	79.28
	Stainless Steel Cathode	79.14	79.25	79.42
EKG	EKG Anode	5.20	5.20	5.15
	EKG Cathode	4.83	4.84	4.85

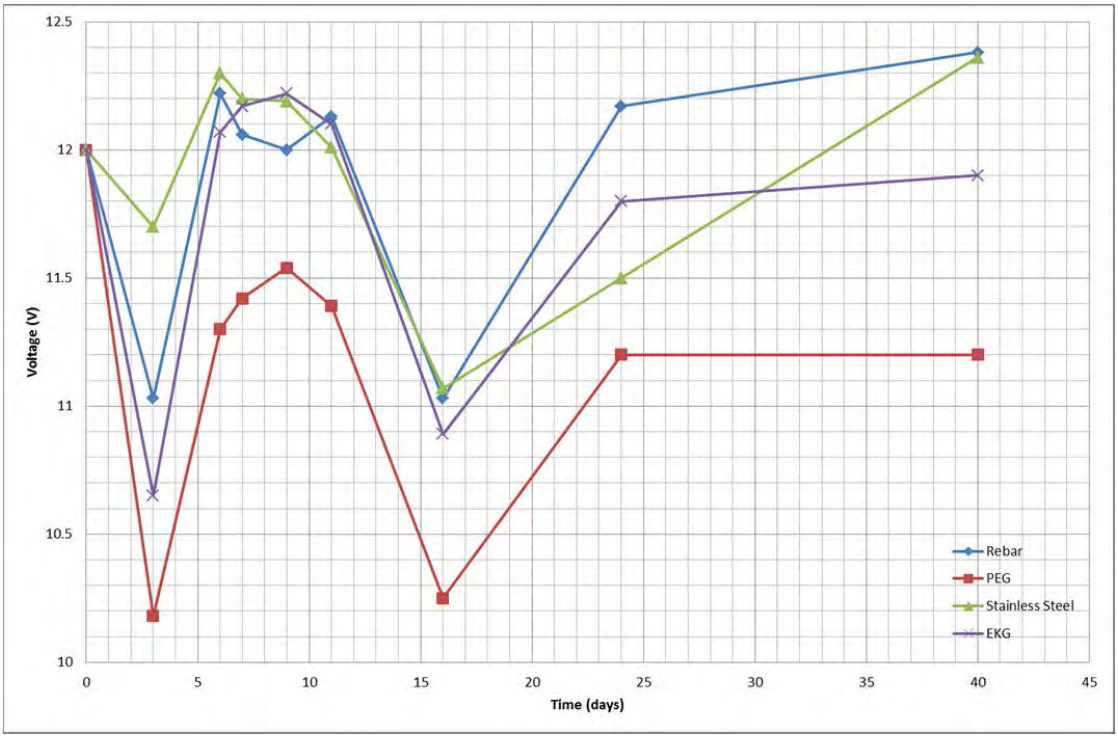

Figure 6-45: Electrolysis voltages over time.

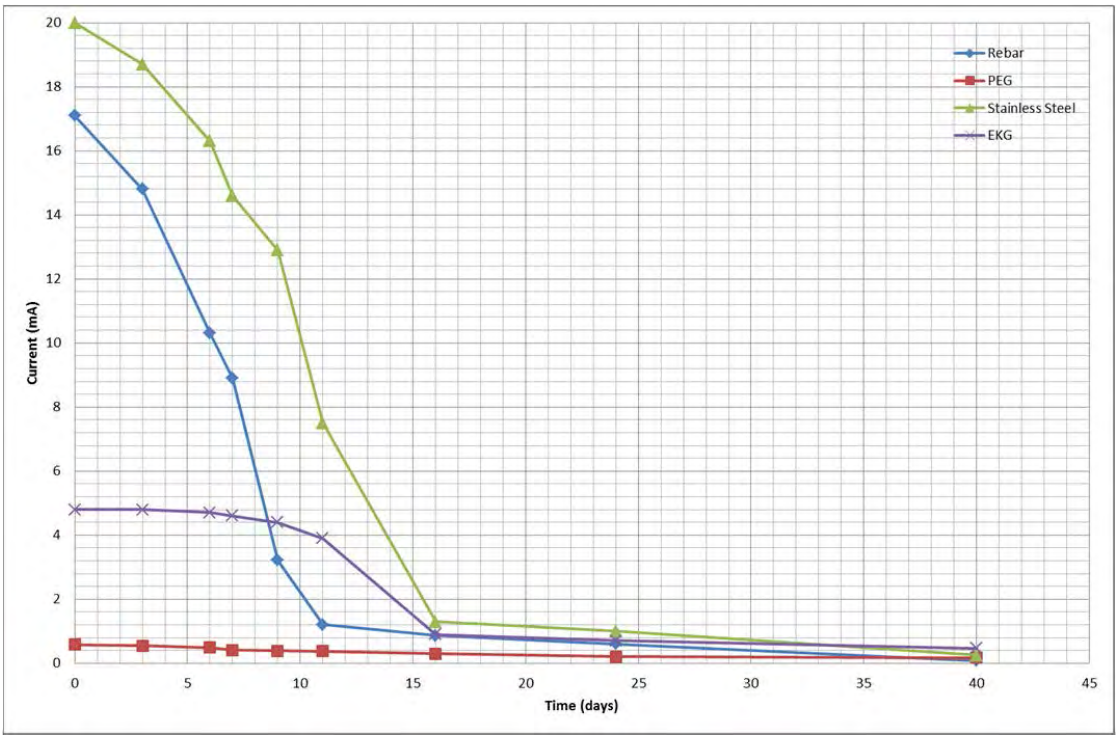

Figure 6-46: Electrolysis electric current over time.

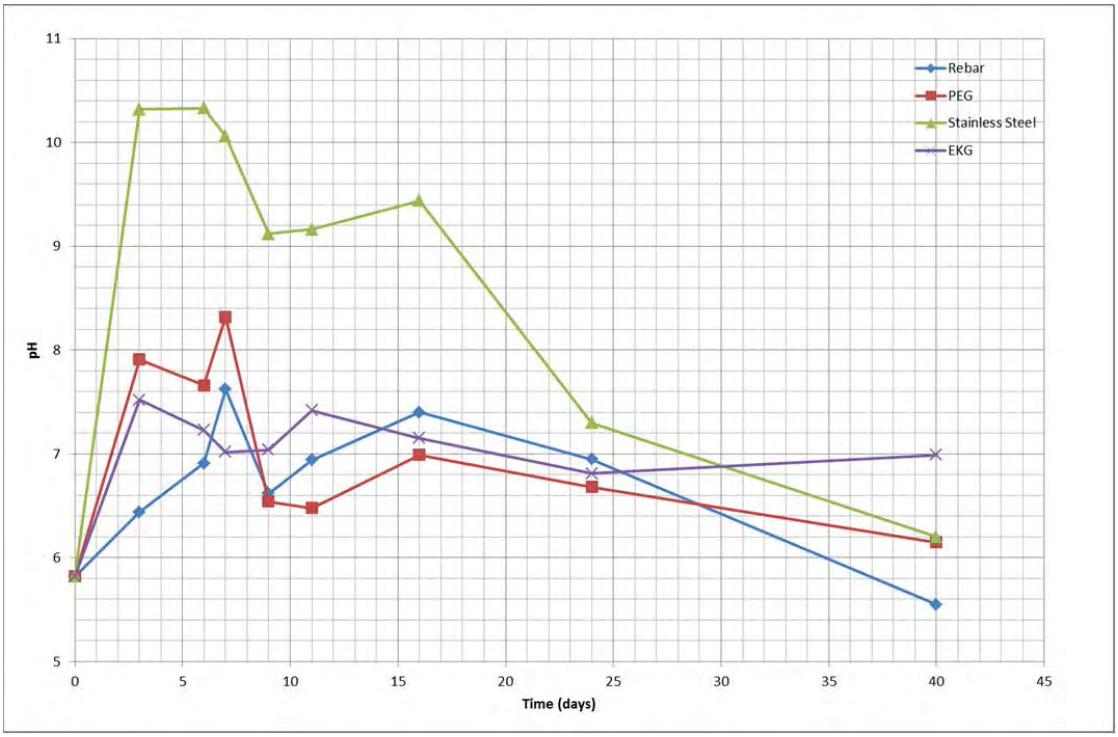

Figure 6-47: Electrolysis fluid pH over time.

6.2.10.4 Summary

With stainless steel possessing the higher electrical current and pH attributes, it can be concluded that stainless steel would be the most beneficial electrode for use in electrokinetic treatment over a period of up to 30 days. Beyond this time it is clear that the stainless steel electrodes would become as effective as the polymer based electrodes, the difference being that for the first 30 days, the stainless steel electrode produced a greatly superior electrode. For longer lengths of treatment, the polymer based electrodes become more preferable considering the reduced mass loss.

6.2.11 Long Term PEG Trial

The 504 day PEG trial was concluded and tested for water content and shear strength to ascertain the success of using PEG electrodes for both anode and cathode.

6.2.11.1 Voltage and Current

The voltage and current recorded for the long term PEG trial can be seen in Figure 6-48. As seen the voltage does not change over the trial period but the current does decrease rapidly at first but then less so over time. The drop in current was likely to be caused by a build-up of gas

around the electrodes from electrolysis as the degradation of PEG electrodes is quite negligible as seen in section 6.2.10. Polarisation of the electrodes cannot be ruled out also.

6.2.11.2 Water Contents

As shown in Figure 6-49, the water content of the clay is seen to increase to its maximum at the anode and then decrease to below the control towards the centre at the bottom of the sample. It is seen to increase again at the cathode.

The top of the sample has increased water content over the whole profile compared to the control test leading to the affirmation that water has been migrated by electroosmosis. The larger increases at the anode and cathode are likely to be due to these sections having water being supplied to them leading to hydraulic permeation. The fact that the water content is higher around the anode than around the cathode leads to the conclusion that water was being slowly migrated from the anode into the clay. The bottom section of the clay is seen to have lower water contents than the top with a lower than control value at 200mm from the anode.

6.2.11.3 Shear Strength

Figure 6-50 shows how the shear strength of the bottom section increases over the control and especially so in the centre of the profile. This is likely to be due to the water content being lowest in the centre. The top section is seen to decrease below the control but again be at its maximum at the centre of the profile. This again is likely to be caused by the water content profile.

The bottom section has increased above the control over the whole profile whereas the top section has decreased below the control over the whole profile. The decrease in the top section could be explained by the increase in water content however only a small portion of the bottom section has a lower than control water content. This would indicate a change in structure of the clay which is confirmed by Figure 6-51 where the control curve is composed of data from the control test in section 6.2.1 as it was very similar clay with varying water contents and strengths. This figure shows how indicatively that for a given water content, the bottom section possesses a greater shear strength. If the curves were extrapolated it is likely that this figure would show that the bottom section would have a greater shear strength for a given water content than the control test. The top section would be very similar to the control.

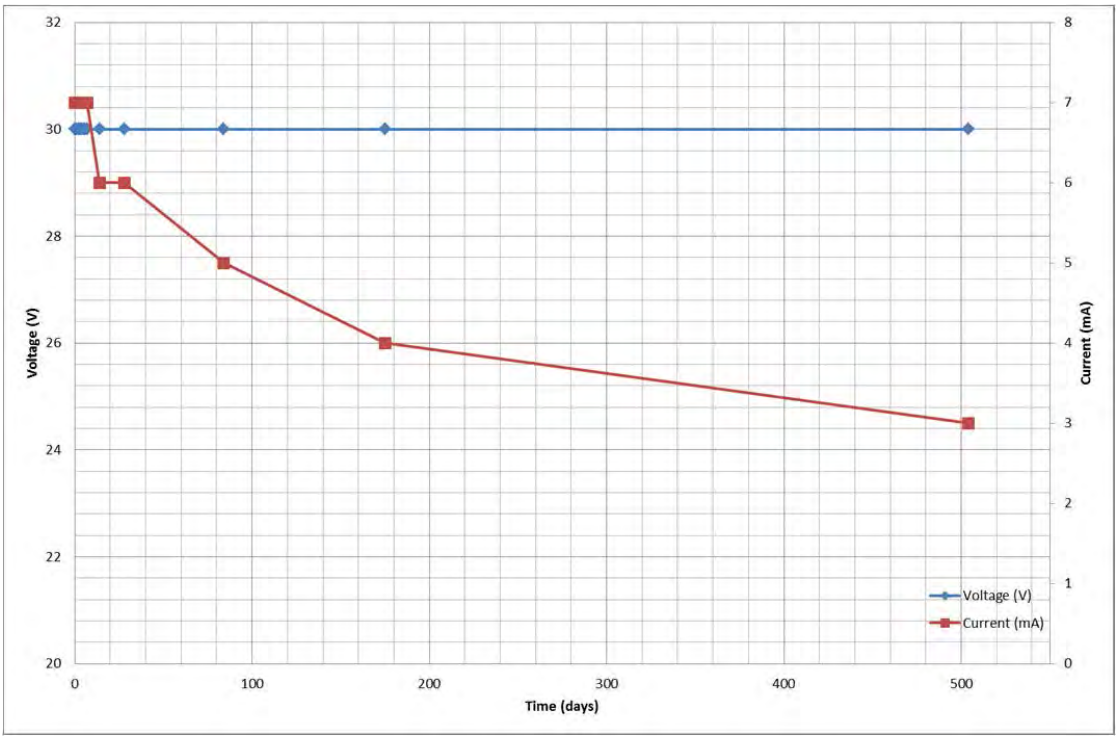

Figure 6-48: Long Term PEG trial voltage and current.

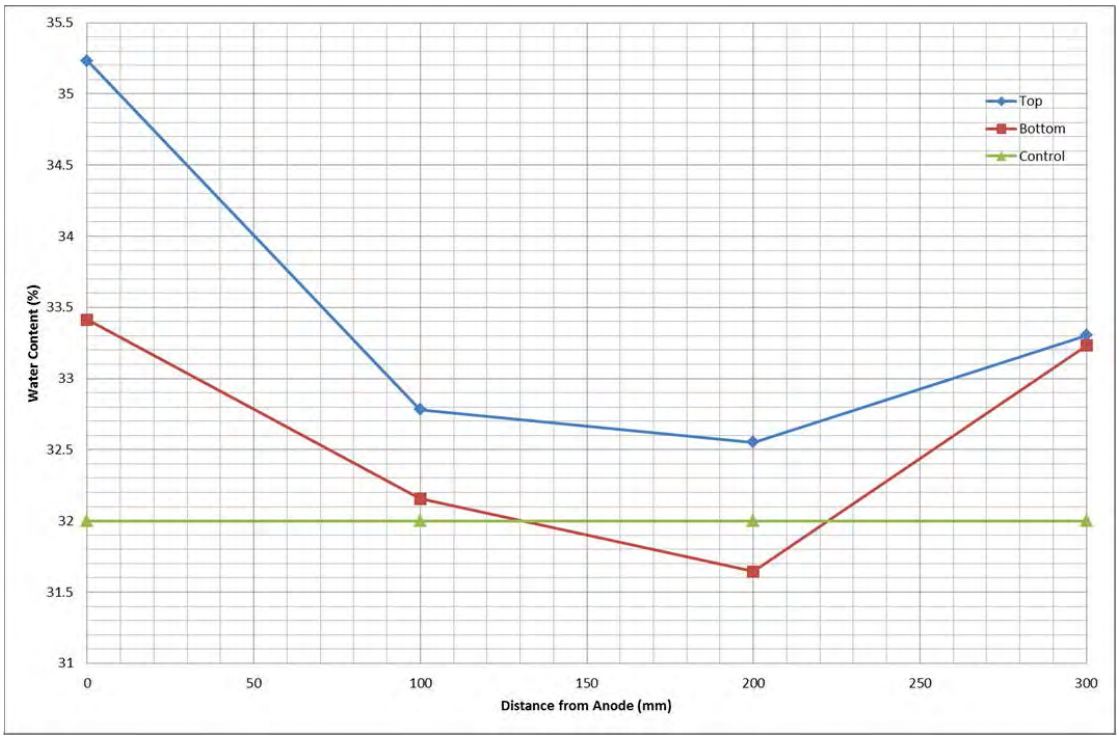

Figure 6-49: Long term PEG trial water contents.

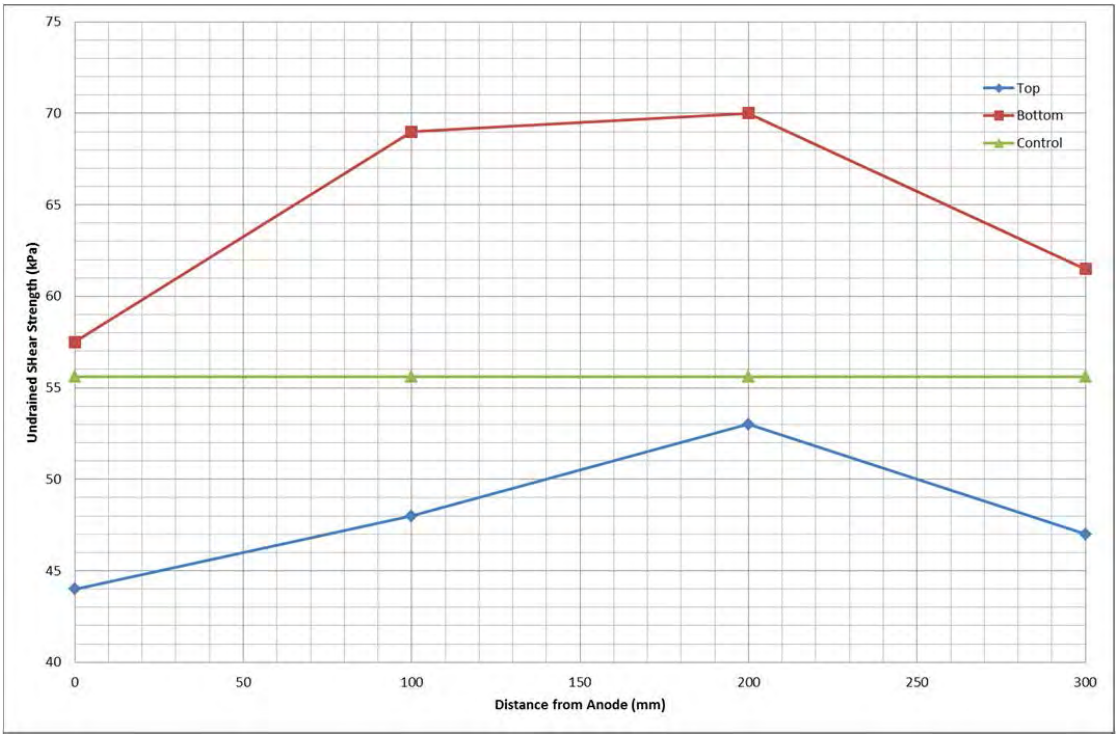

Figure 6-50: Long term PEG trial shear strengths.

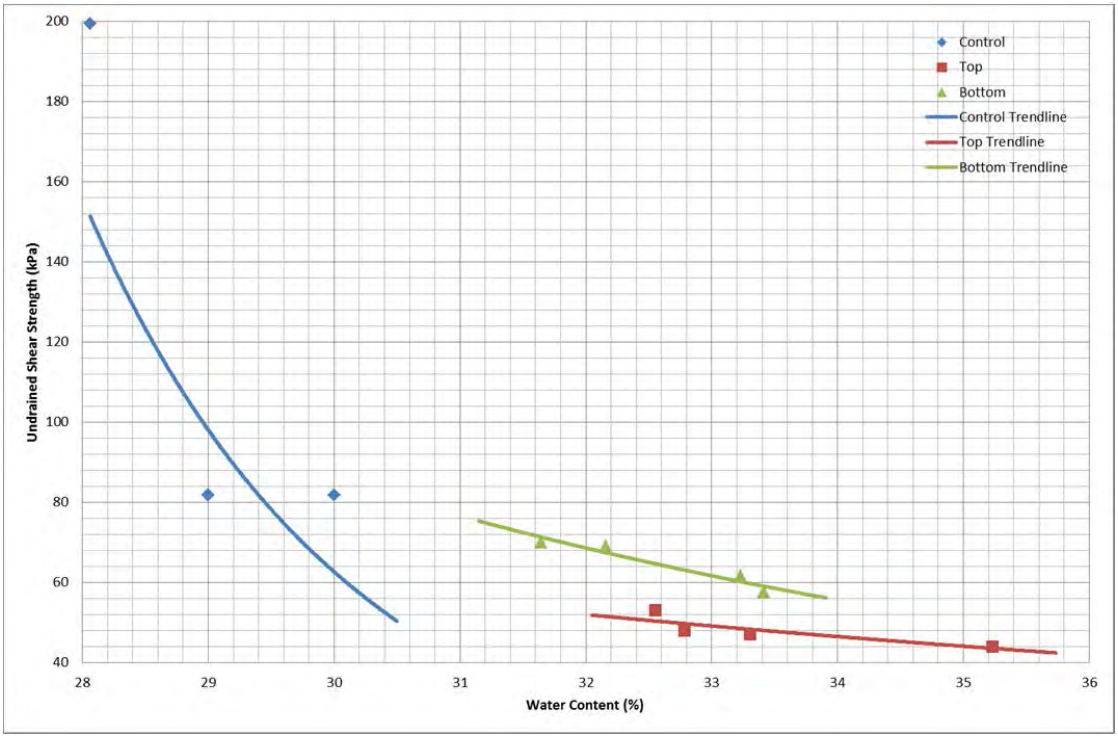

Figure 6-51: Long term PEG trial undrained shear strength change with water content.

6.2.11.4 Summary

In summary, this long term test of passing water through ECC by way of electroosmosis using PEG electrodes for both the anode and cathode has shown that the PEG electrode can be used successfully. The slow rate at which the electroosmosis takes place with PEG electrodes however is likely to inhibit any practical use in reality.

6.2.12 PEG Cathode Trials

The trials using stainless steel as anodes and PEG's as cathodes is presented herein. The trials were run for a period of 28 days in an effort to migrate water across the ECC specimens. The first four days used 20V but it was decided to increase this on the fifth day to the power supply's maximum 50V to ensure the highest possible current through the clay.

6.2.12.1 Voltage

Figure 6-52 shows the recorded voltages for both trial A and B and it is seen, as expected due to a fixed voltage, that they remain as set on the power supplies.

6.2.12.2 Current

The recorded electric currents for both A and B are presented in Figure 6-53 where it should be noted that on Day 5 the voltage was increased from 20 to 50V leading to an increase in the current accordingly. Both trials reach their maximum current at Day 10, it has likely taken until this time for the water content of the clay to increase enough to allow a higher current flow. Both trial's currents then decrease over the remainder of the time due to a combination of gas build up at the electrodes causing an insulating barrier to form and the corrosion of the electrodes themselves due to electrolysis. The stainless steel electrodes decreased in mass whilst the PEG electrodes both increased, Table 6-8, and it is known that a corroded stainless steel anode precipitates Fe ions into the clay which increase the clays electrical resistance and also decreases the electrodes electrical conductivity.

6.2.12.3 Shear Strength

Both trials have experienced a reduction in shear strength over the profile of the clay samples, Figure 6-54 and Figure 6-55. This is expected due to the increase in water content of the clay. It is also shown that the shear strength decreases with distance from the anode for the bottom

section of both trials and the top section saw a decrease at the anode which then increased in the centre to then decrease at the cathode. Figure 6-62 and Figure 6-63 however, show that the water content is not overly increased at the anode in the top section compared to the bottom indicating that the strength gain of the bottom over the top is not due to a reduction in water content.

For both trials, the middle results show a tendency for the shear strength to increase towards the centre of the sample. This section is the 'target zone' as mentioned throughout this study. Unfortunately due to the sampling method, water contents for these locations were not achieved for further discussion.

6.2.12.4 Plastic Limit

The plastic limits across the trials are shown in Figure 6-56 and Figure 6-57. It is shown that there is a slight increase at the anode followed by a reduction towards the centre and then increase towards the control at the cathode for trial A at the bottom section. Trial B at the bottom follows the same trend but at a higher plastic limit leading to an increased plastic limit over the control at both the anode and cathode.

The top section of trial A saw a fairly steady plastic limit from 0–200mm and then an increase of approximately 1% at the cathode whilst constantly being lower than the control. Trial B however saw again a steady plastic limit from 0–200mm but then the increase at the cathode is less than 1% but is above the control. The differences here between trial A and B will be purely due to the nature of plastic limit testing as the differences are small.

The trend shown here for the plastic limits mirrors that shown in the previous research repeat in 6.2.1 and in Liaki (2006).

6.2.12.5 Liquid Limit

Figure 6-58 and Figure 6-59 show the liquid limits over the trials. It is shown that for both trials and at both depths, the liquid limit is decreased with increasing distance from the anode. Only trial A decreases to below the control at the cathode leaving a majority increase in liquid limit over the trials. It should be noted here that the top section of these trials both have higher liquid limits than the bottom section. The increases in liquid limits around the anodes are likely to be due to the clay flocculating with the voids between able to hold a greater volume of water.

6.2.12.6 Plasticity Index

The plasticity index for the trial, Figure 6-60 and Figure 6-61, show an overall increase over the samples with the maximum increase at the anode then decreasing to the cathode. Whilst experiencing an overall increased liquid limit and plasticity index over both trials, using the plasticity chart, one can determine that the degree of plasticity of the clay increased over the control clay. The cathode zone in trial A did see a decrease in plasticity; however, this was the only location. The flocculation of the clay particles by the application of the electric current is the driver for this change as chemical introductions were not produced.

6.2.12.7 Water Content

The water contents of both trials increased at all locations over the control, Figure 6-62 and Figure 6-63. This was expected due to the constant availability of water to the electrodes. The greatest water contents were seen at the electrode locations with the cathodic region possessing the greatest due to the direction of travel for the water. The water contents are seen to be consistent for both top and bottom sections in both trials. The difference between both trials is approximately 5% which could be accounted for in the testing or storage stages of the trials.

6.2.12.8 Linear Shrinkage

The linear shrinkage results shown in Figure 6-64 and Figure 6-65 show a decrease over both depths. Both trials show an approximate 2% decrease in linear shrinkage over the control. A difference of up to 1% is seen at the anode compared to the cathode, thought to be due to the precipitation of Fe^{3+} ions from the stainless steel anode. The Fe^{3+} ions are known coagulants and thusly increase shrinkage. It is known from (Di Maio, et al., 2002) that a kaolinitic clay with an increased flocculation and increased liquid limit should possess a reduced shrinkage over a clay with lower liquid limit and less flocculation. This is likely to be the cause of the overall reduction in linear shrinkage.

6.2.12.9 pH

As is expected, a reduction in pH is witnessed at the anode and across the majority of the clay samples, Figure 6-66 and Figure 6-67. This is due to the acid front that is developed through electrolysis possessing a greater ionic mobility and is moving in the direction of flow leading to it

moving further through the clay. The concentration of the base front is therefore limited to the cathodic region as seen by the increases there to pH8-pH11.

6.2.12.10 Electrical Conductivity

The electrical conductivities shown in Figure 6-68 and Figure 6-69 both follow the same trend as the water contents in section 6.2.12.7. This is most likely due to the electrical conductivity of a clay being directly affected by the water content as discussed in section 6.2.3.

It is noticed that the electrical conductivity has increased over the control for both trials and that the increase is greatest at the electrode regions. Again this is likely to be due to the water contents.

Both trials show that the bottom section of the clay at the cathode possesses a lower electrical conductivity than the top section whereas at the anode it is greater. A possible explanation for this could be that ions in the clay were being attracted to the cathode and adsorbed to its surface both increasing the mass of the cathode and decreasing the electrical conductivity of the clay in the area.

6.2.12.11 Electrode SEM

SEM microscopy of the steel and PEG electrodes was conducted to ascertain the damage produced through the EKS process on the electrodes themselves. Figure 6-70 shows how stainless steel is altered through EKS with the surface unrecognisable at 10,000x magnification. The stainless steel anode in this figure shows the build-up of what is thought to be CSH gel crystals on the surface of the steel and the surface of the steel is degraded compared to the new stainless steel. The new stainless steel shows the original steel delivered from the manufacturer and stored in the University of Birmingham laboratory. There does appear to be some corrosion pitting here. The PEG Cathode shows the PEG cathode after use, it can be seen that even after washing, clay platelets still cover the surface. Closer inspection does however reveal that there appears to be no damage to the actual electrode surface when compared to the new PEG. This is as expected as it is known from previous research that a polymer based conductive electrode will degrade slower than a steel electrode, (Pugh, 2002).

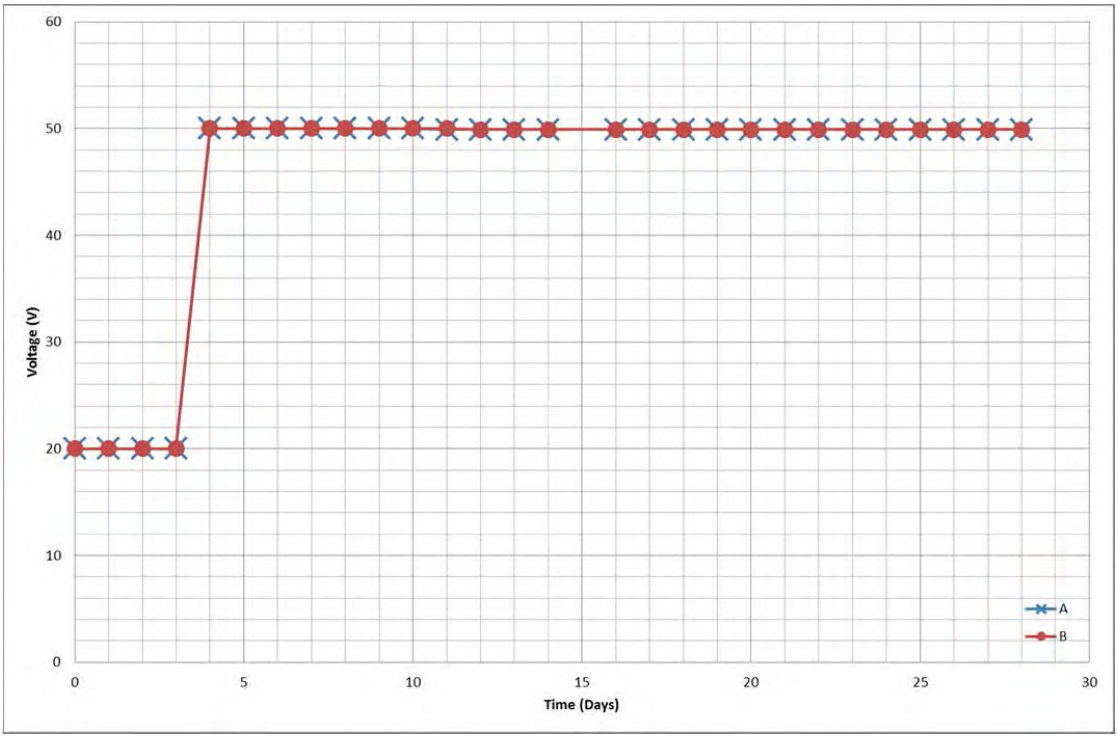

Figure 6-52: PEG Cathode voltage.

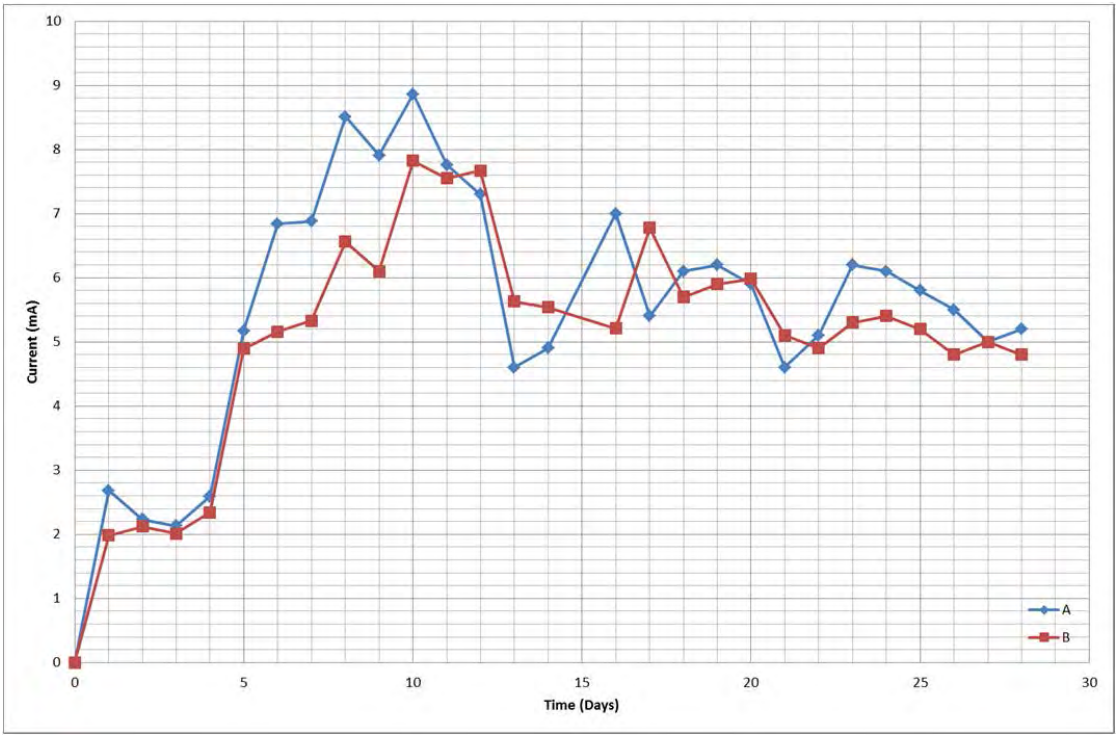

Figure 6-53: PEG cathode electric current.

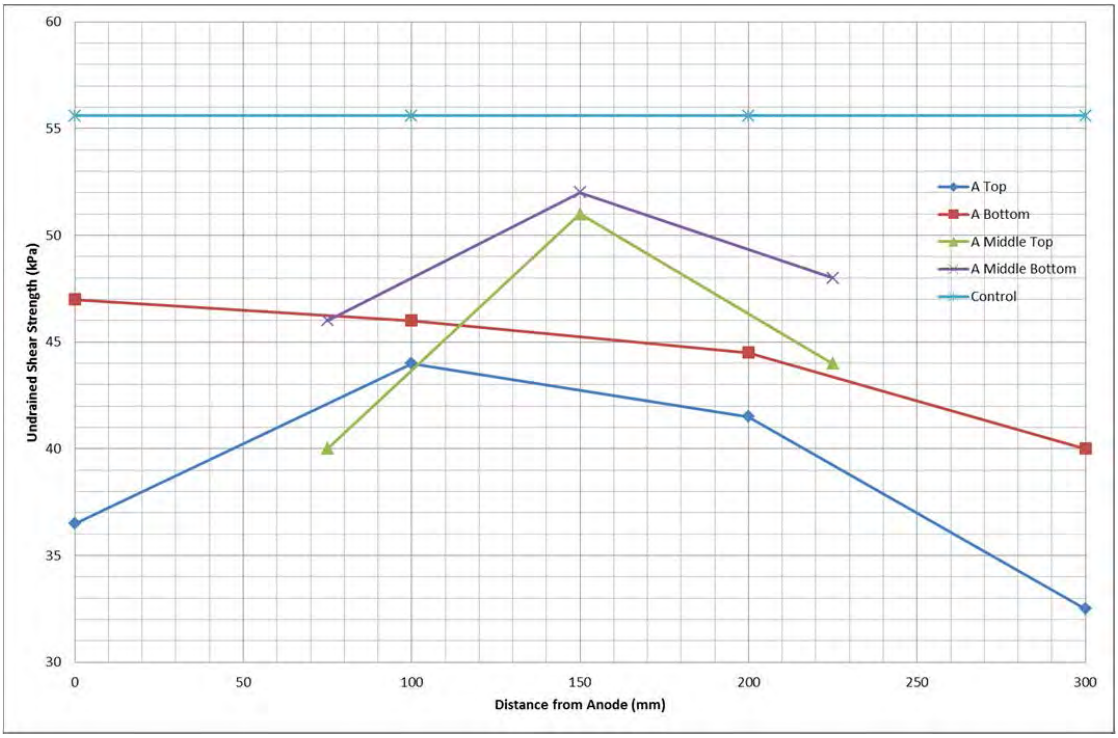

Figure 6-54: PEG cathode A shear strength.

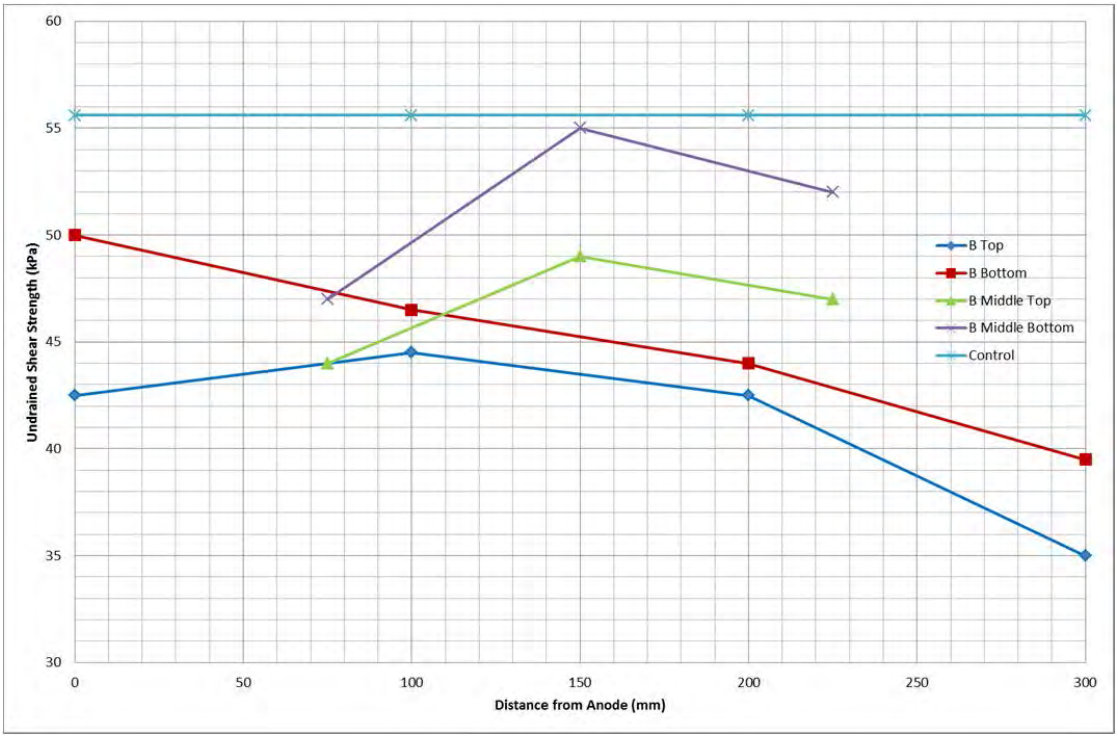

Figure 6-55: PEG cathode B shear strength.

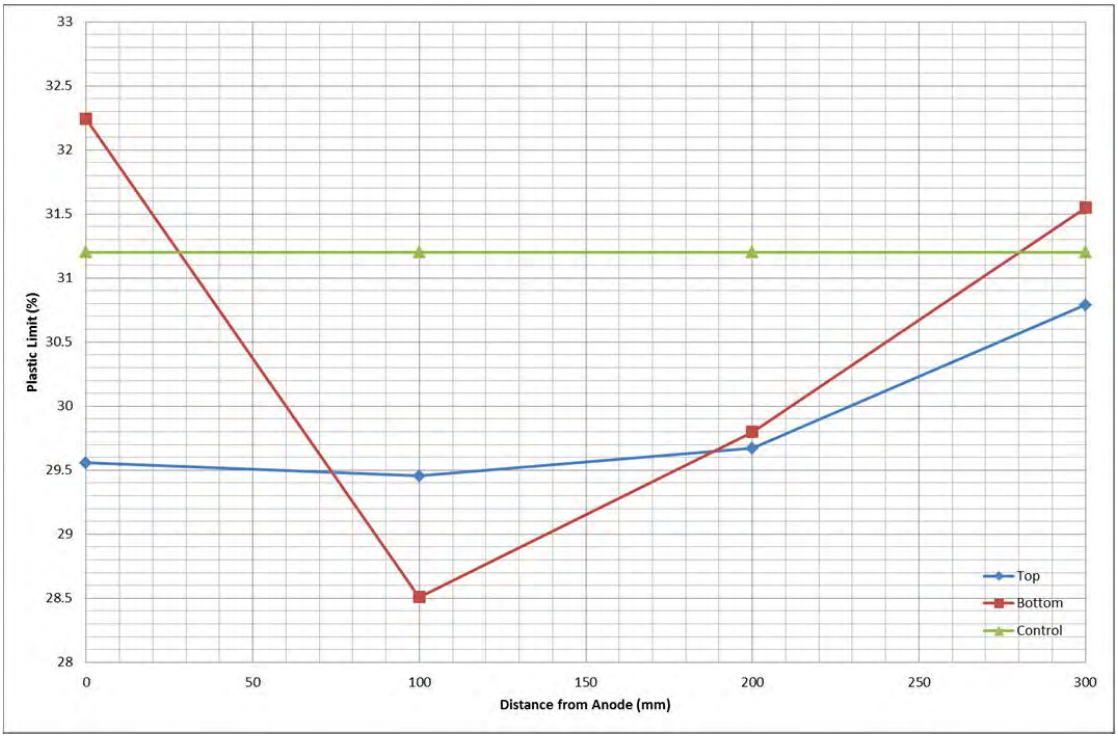

Figure 6-56: PEG cathode A plastic limit.

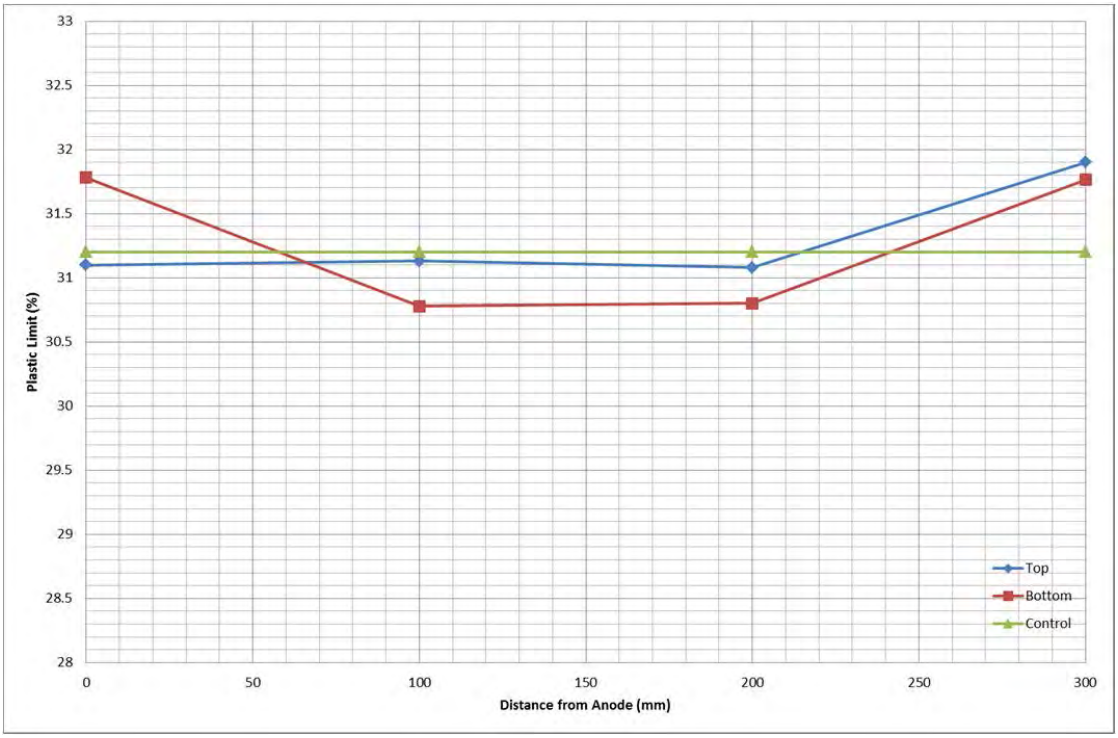

Figure 6-57: PEG cathode B plastic limit.

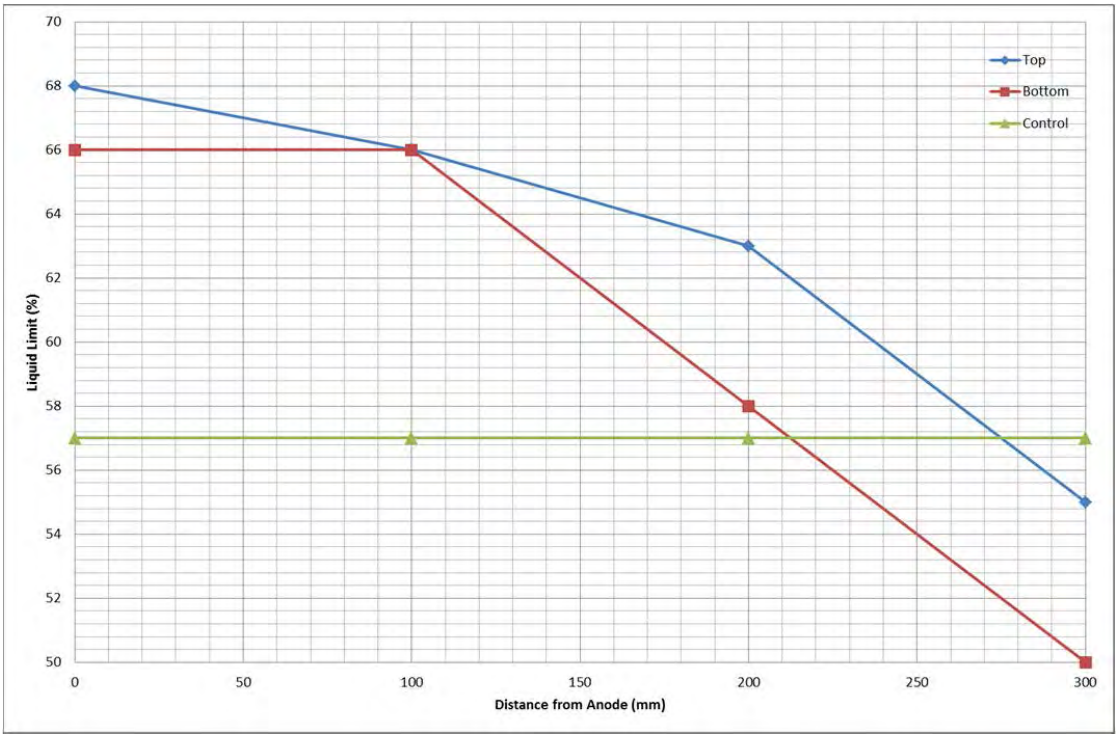

Figure 6-58: PEG cathode A liquid limit.

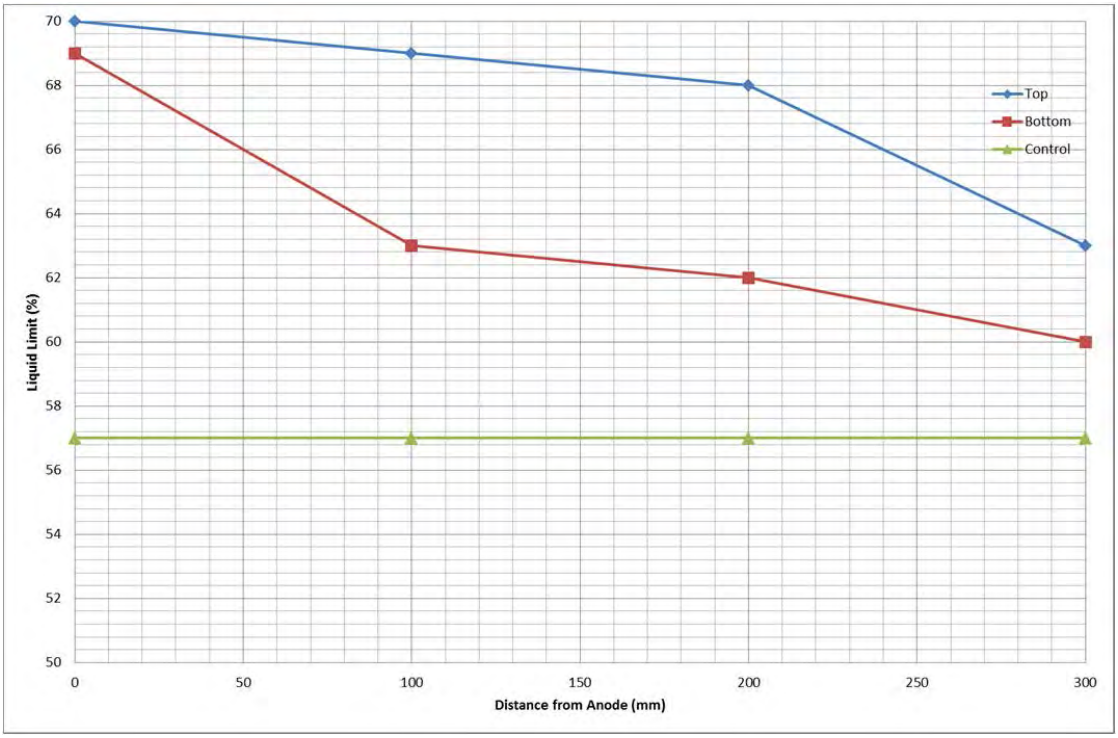

Figure 6-59: PEG cathode B liquid limit.

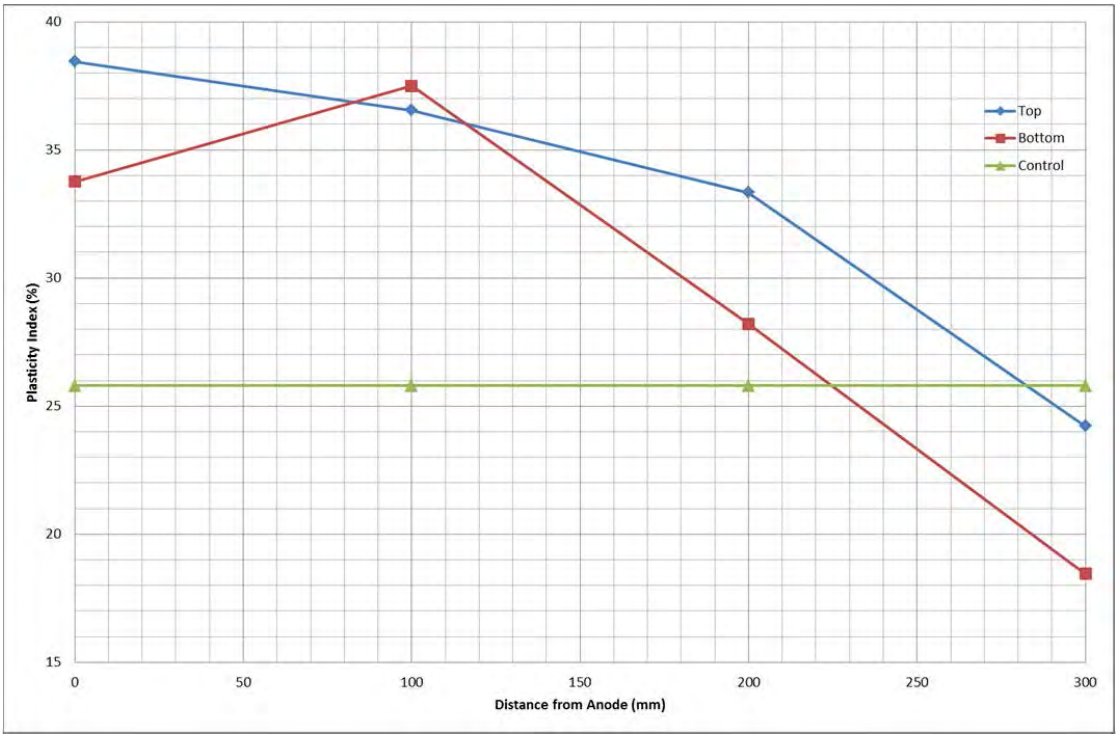

Figure 6-60: PEG cathode A plasticity index.

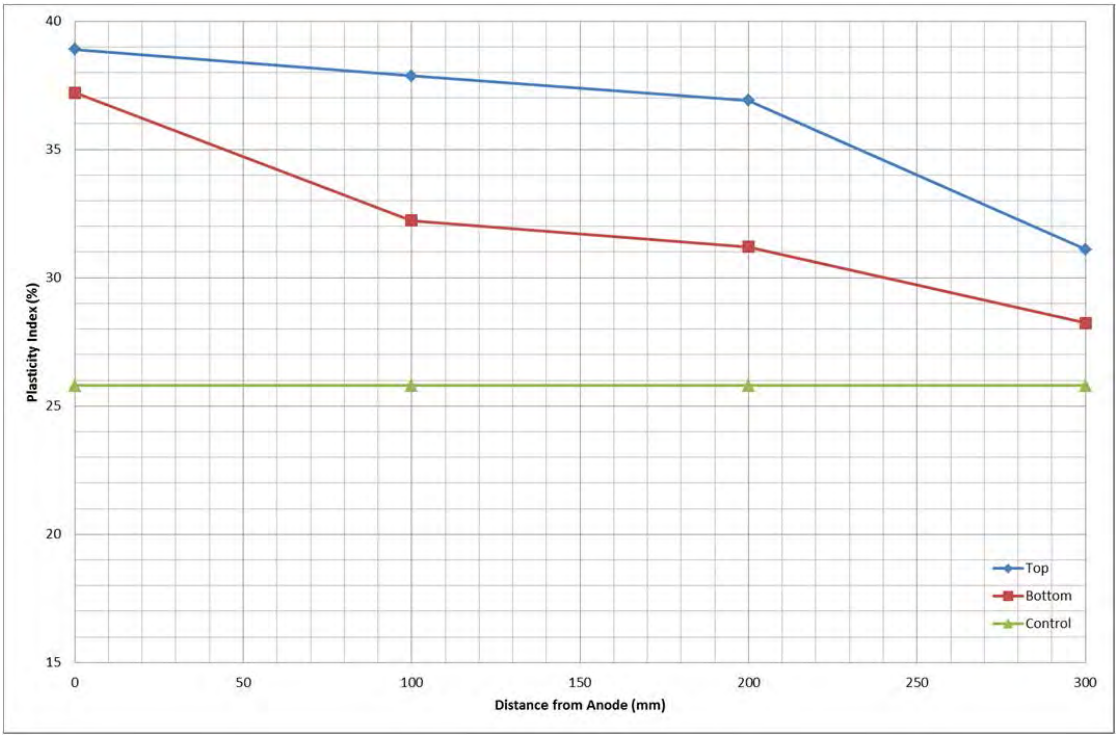

Figure 6-61: PEG cathode B plasticity index.

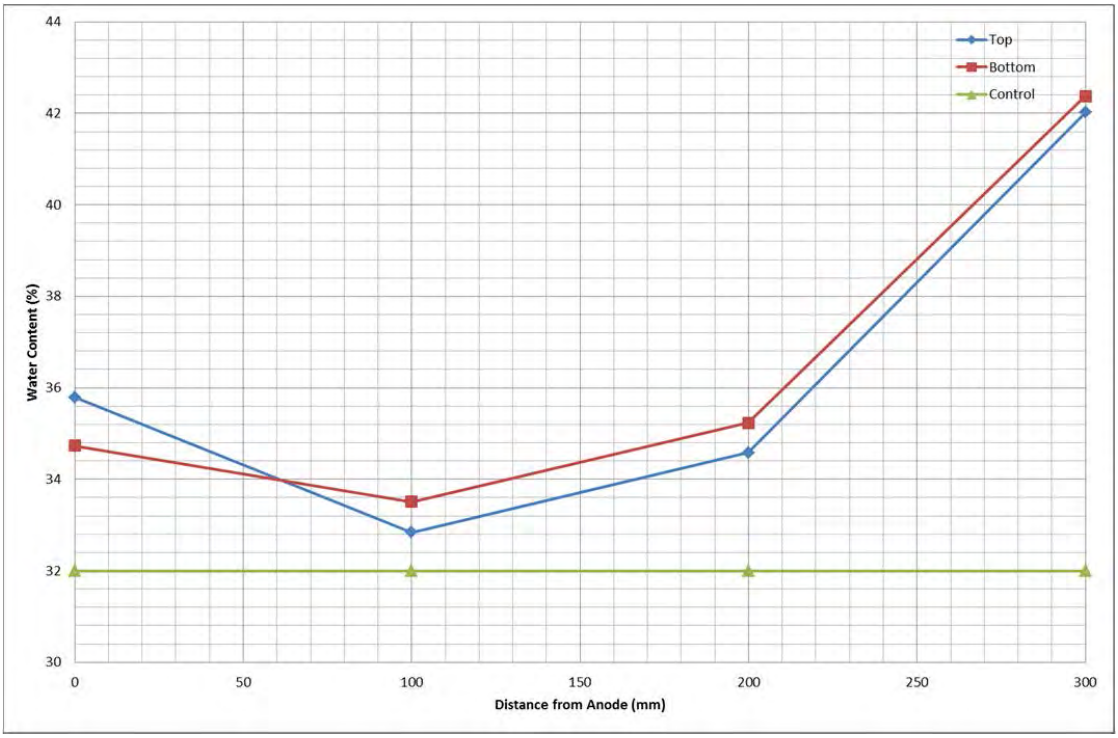

Figure 6-62: PEG cathode A water content.

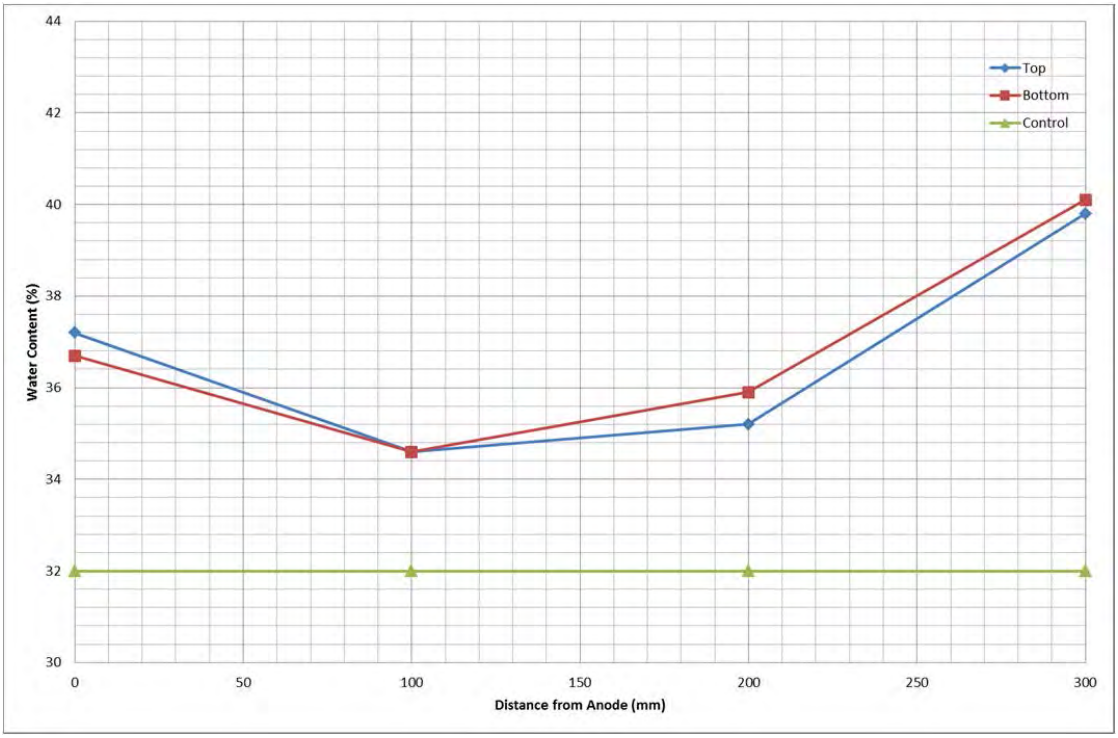

Figure 6-63: PEG cathode B water content.

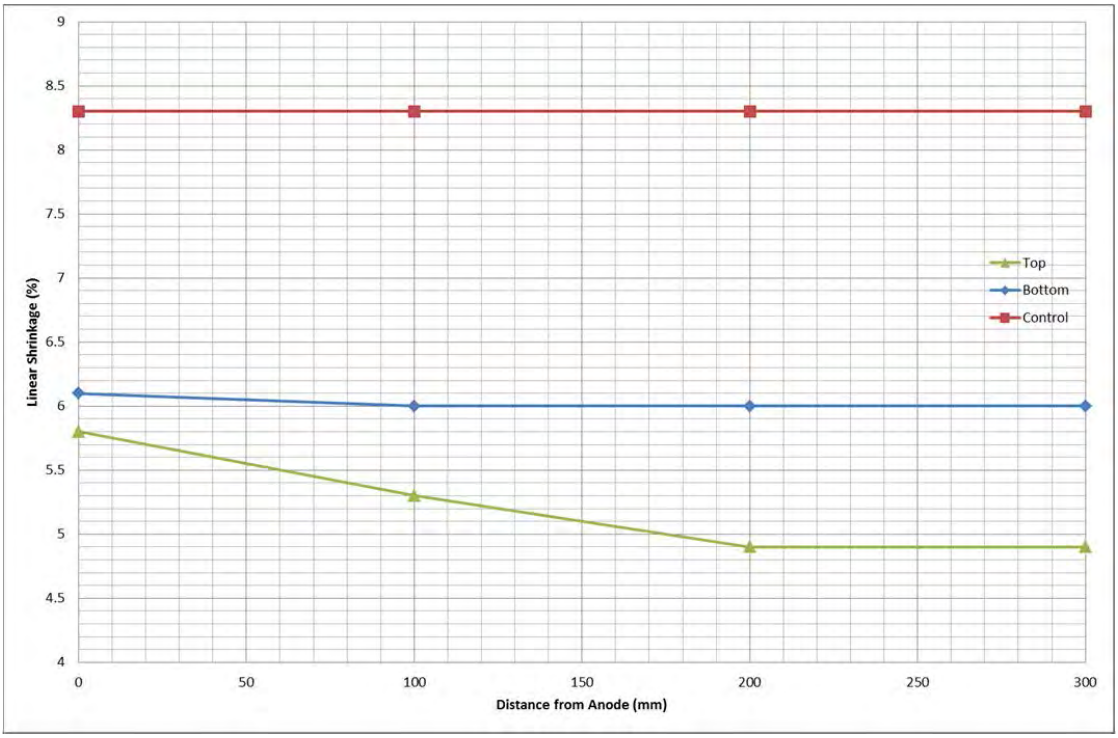

Figure 6-64: PEG cathode A linear shrinkage.

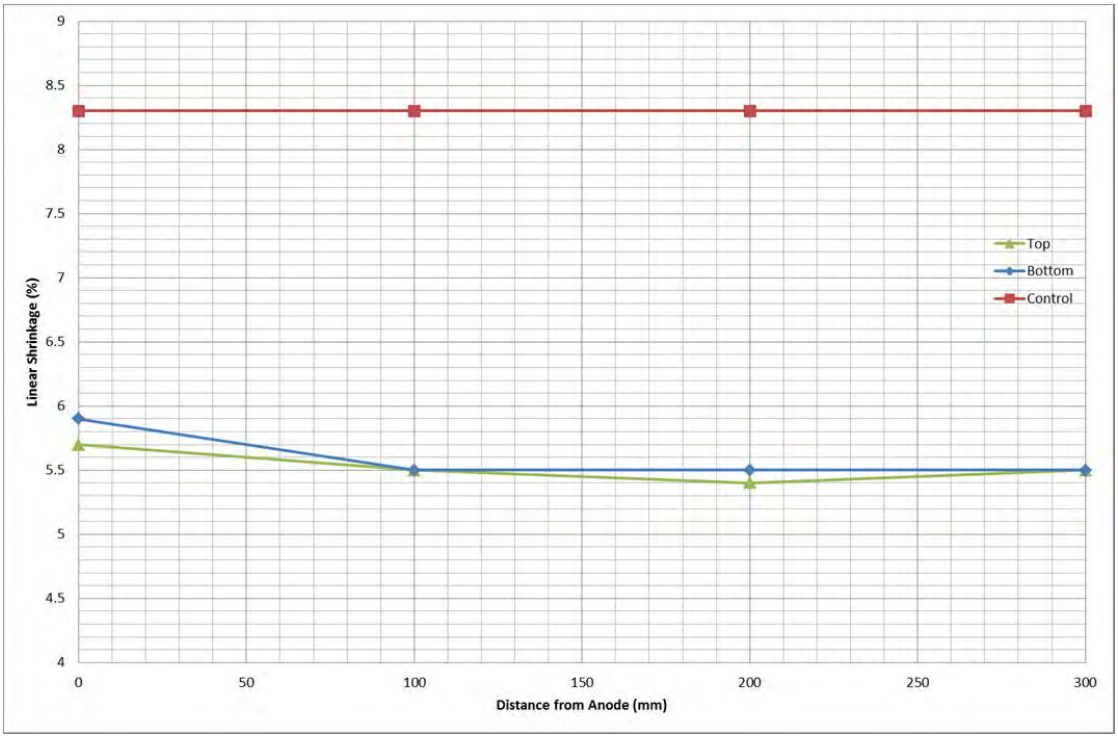

Figure 6-65: PEG cathode B linear shrinkage.

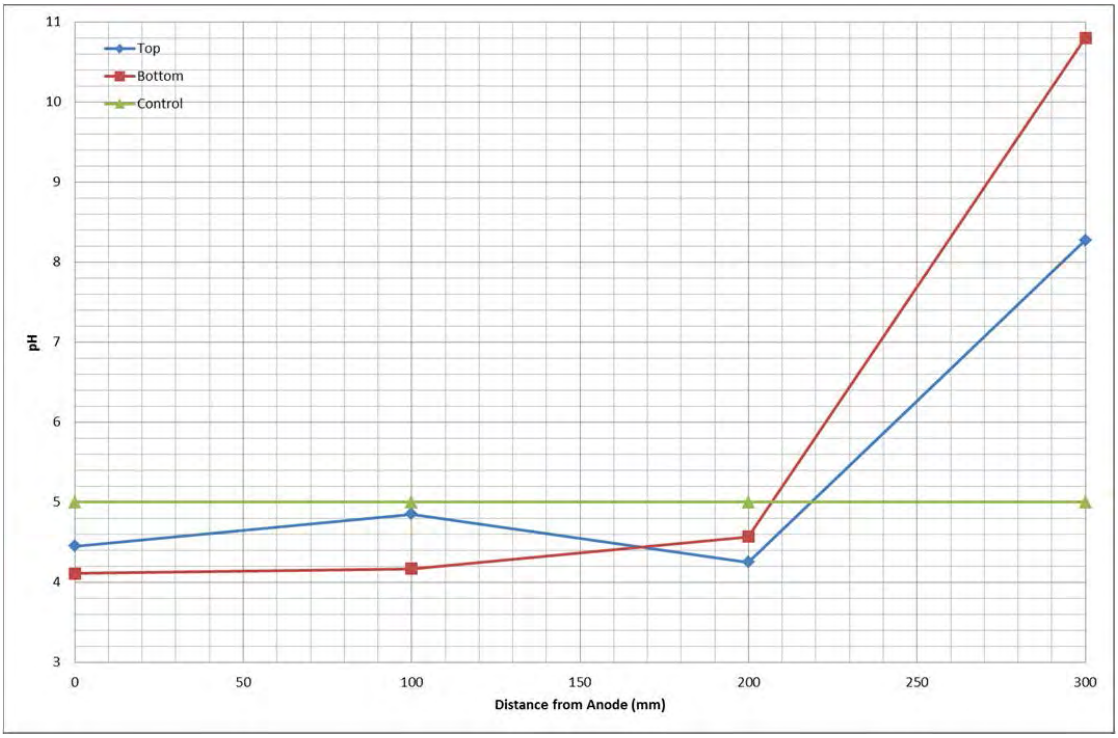

Figure 6-66: PEG cathode A pH.

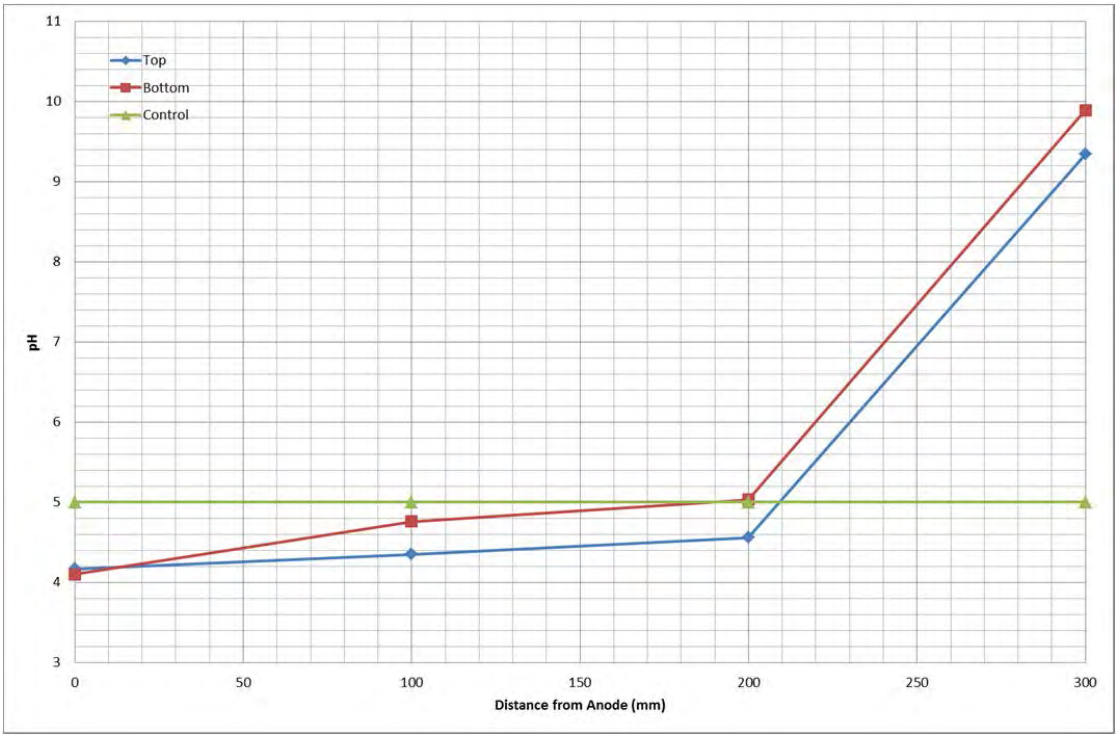

Figure 6-67: PEG cathode B pH.

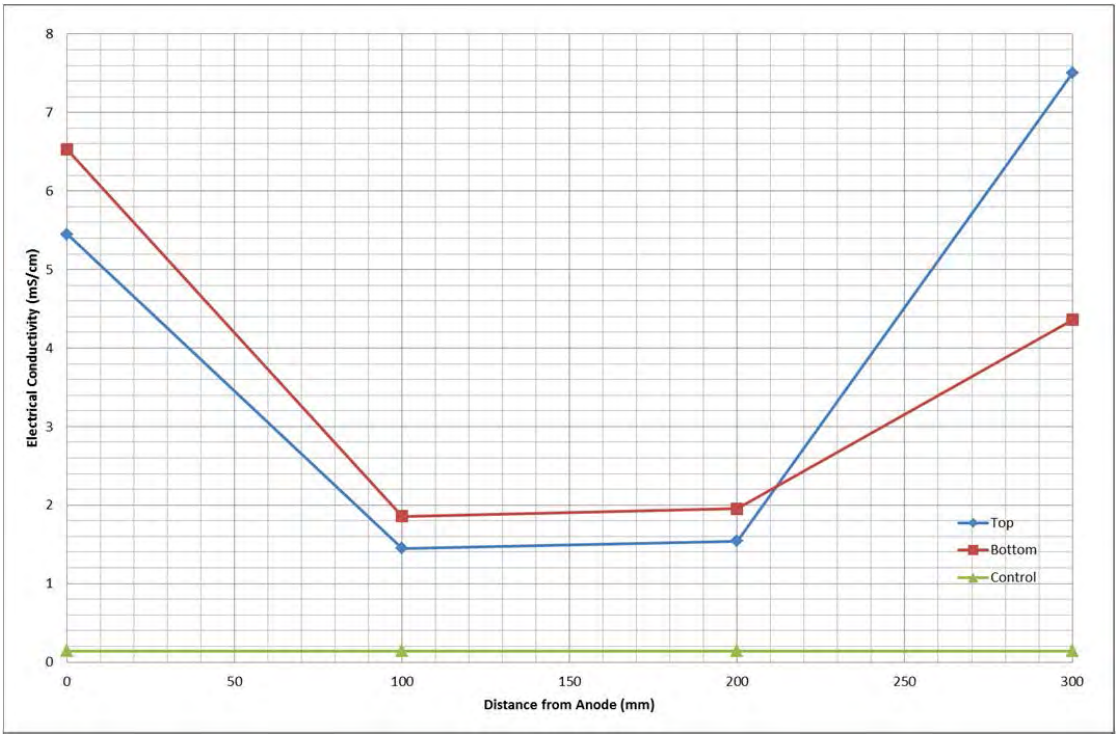

Figure 6-68: PEG cathode A electrical conductivity.

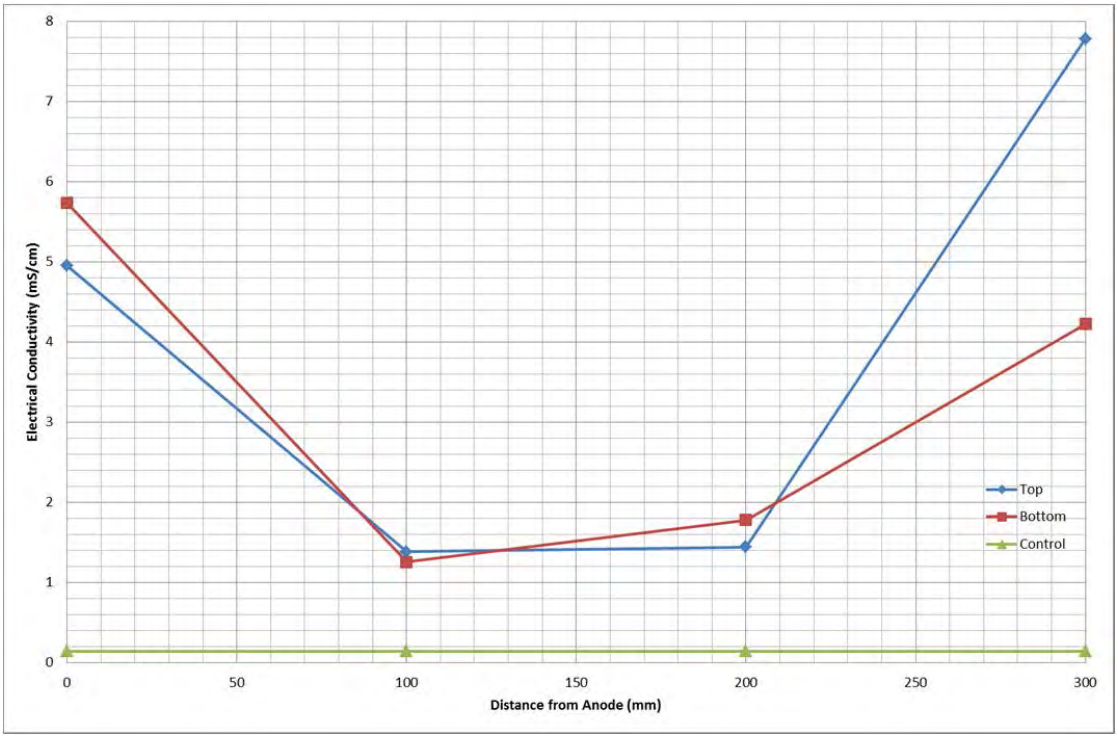

Figure 6-69: PEG cathode B electrical conductivity.

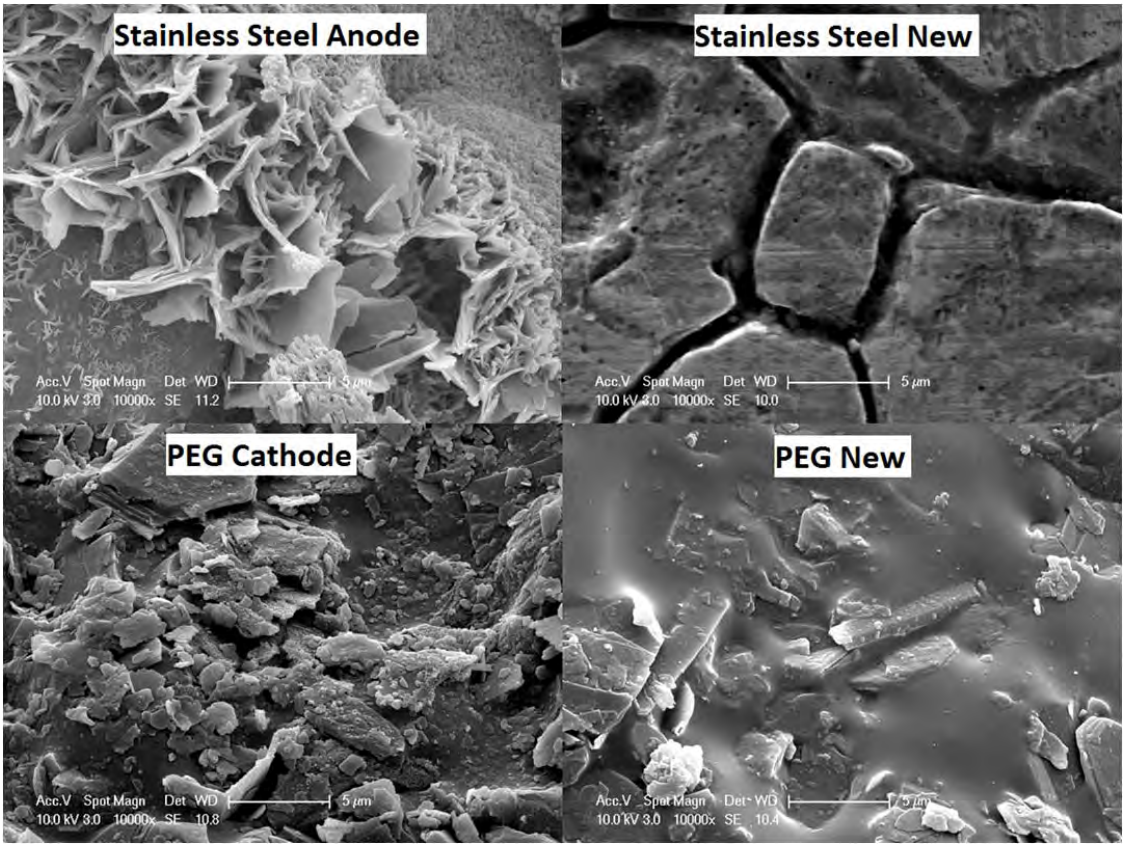

Figure 6-70: SEM microscopy of stainless steel and PEG electrodes before and after use.

Table 6-8: PEG cathode electrode mass variance.

Electrode	Mass Before (g)	Mass After (g)
A – Stainless Steel	177.5	175.32
A – PEG	63.36	63.54
B – Stainless Steel	174.6	173.29
B – PEG	67.33	67.87

6.2.12.12 Summary

The potential of using a stainless steel anode and PEG cathode combination in a site trial is limited due to the high electrical resistivity of the PEG compared to the stainless steel. This stainless steel/PEG combination is not efficient purely due to the high surface resistivity of the PEG electrode. PEG electrodes may be cheaper to produce and last longer due to reduced degradation but with such small currents flowing through the soil, treatment time would be increased and thus cost more. Furthermore, Figure 6-71 shows the shear strength against varying water contents for this trial where it can be seen that for both A and B, a definitive trend

can be seen. The control curve is shown to be below that of the treated samples leading to the conclusion that the treatment technique has improved the soil samples. This is most unexpected when considering the minimal fluid movement throughout the experiment and is worthy of further study. Figure 6-72 also shows that after normalising the shear strength data to pH, one can see a very definitive trend across the treated samples. Precipitation at the anode and increased water content at the cathode can explain this trend.

It has been shown here that the process of electroosmosis is taking place in the clay as flocculation has resulted in linear shrinkage reduction and liquid limit increases. It would be helpful in the future to compare this test directly with a comparable test with both electrodes made of stainless steel to determine its success fully.

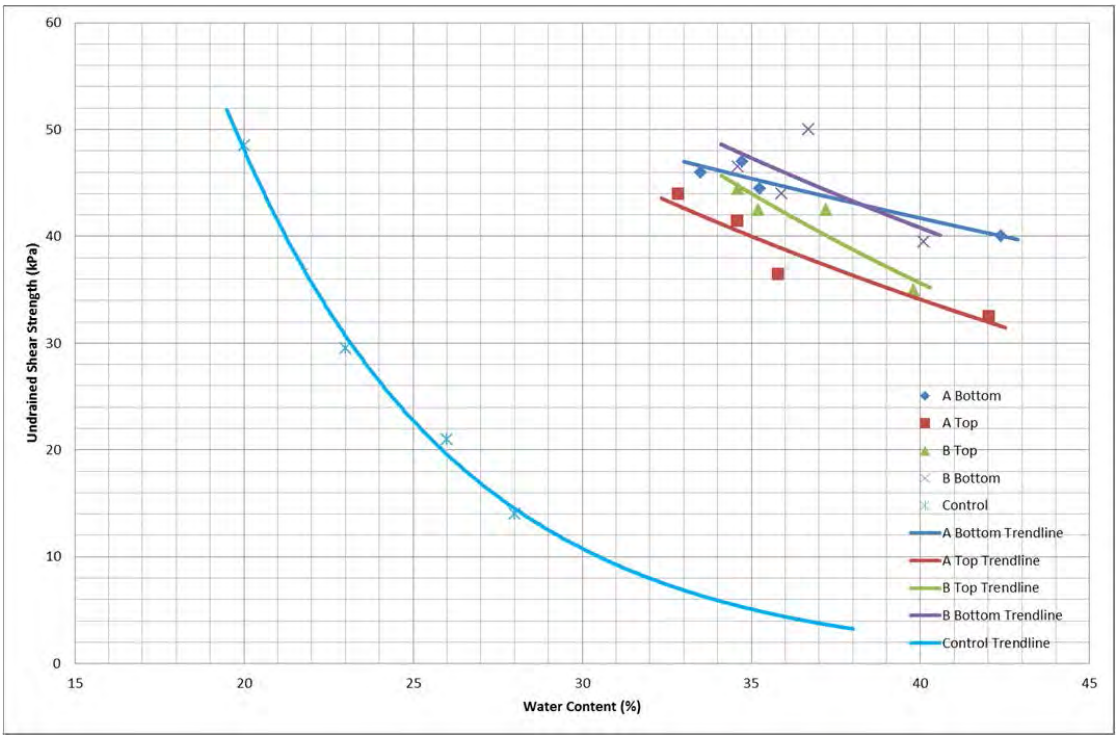

Figure 6-71: PEG cathode shear strength against water content.

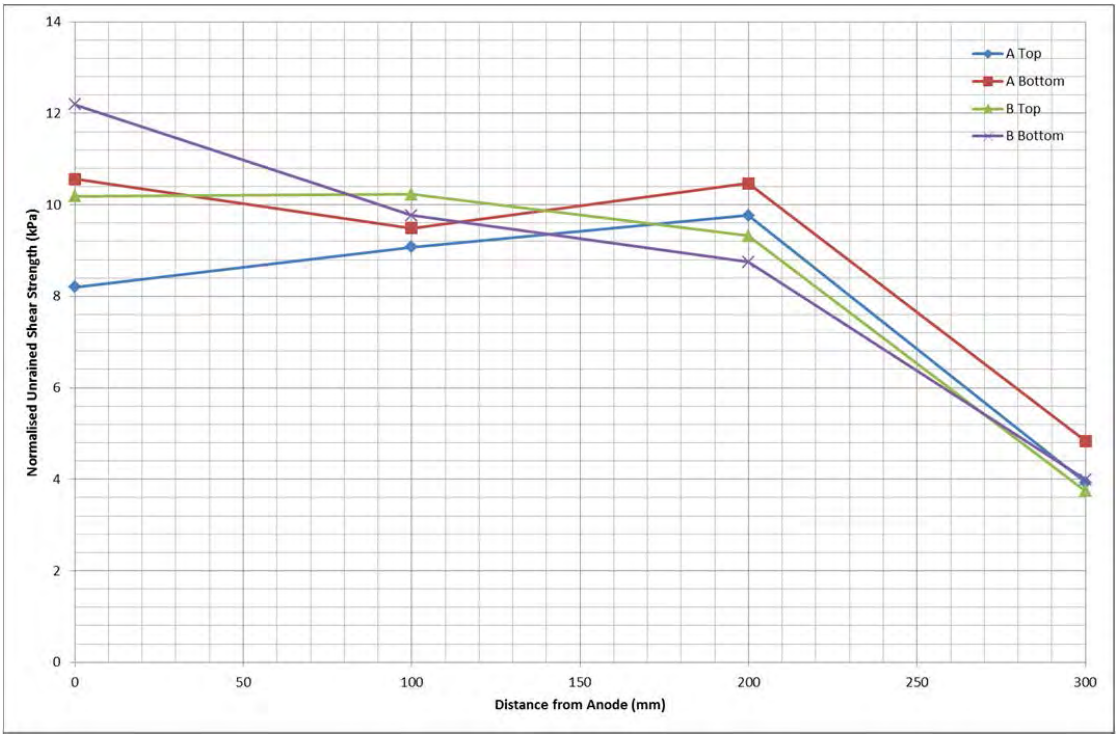

Figure 6-72: PEG cathode shear strength normalised to pH.

6.2.13 Mock Foundation

The mock foundation testing was completed over a thirty day period with the first 7 days dedicated solely to water seeding the clay sample whilst monitoring the footing level variance. After this 7 days period, the stabilising chemicals were introduced at their respective electrodes.

6.2.13.1 Levels

As seen in Figure 6-73, the levels both of the mock footings increased with the introduction of fluids to the system as expected. The chemicals were introduced on day 7 and as seen, there is no visible effect on the level of the footings over the introduction of water. As expected, the control test had no variance in level whatsoever.

One might expect the levels nearest the cathode to increase to a greater extent than those nearest the anode. But as Figure 6-73 shows, this is not true here. Z1, Z2, A1 and A2 were all nearest the cathode on each trial respectively and yet these do not have the greatest level change.

The large increase in the level seen between zero and one days is expected as a clay with low water content is introduced to water, the steady plateau of the level is then thought to

be due to the clay reaching a point where enough water had been adsorbed by the clay particles and so any more introduced was migrated through.

Although the water content of this clay is effectively doubled over the treatment time, the effect on the mock footing level is negligible with the largest movement being less than 0.4mm.

6.2.13.2 Voltage, Current and Power

The voltage and current were recorded over the test and then the power calculated from these. The voltage was set to a constant 20V and did not waiver. Figure 6-74 shows the current plotted graphically where it can be seen that the electrical current in both Z and A become quite stable between days 2 and 5. After the addition of the chemical stabilisers on day 6, it is then apparent that the electrical current increases dramatically. This is due to the addition of minerals into the system water that increase the electrical conductivity of the system. It is interesting to note that at day 5, the electrical current with only RO water in the system had plateaued along with the dramatic reduction in level variance as seen in Figure 6-73. The addition of the chemical stabilisers doesn't appear to affect the levels of the mock footing but does increase the electrical current flowing through the system.

Power follows the current trend exactly due to the voltage not varying from 20V and so it has not been included graphically here. Trial Z ended with a cumulative power of 12W with A possessing a cumulative power usage of 8W.

6.2.13.3 Water Contents

Figure 6-75 and Figure 6-76 show the water content profiles recorded across the test specimens. As expected, both tests show an increase in water content over the entire profile due to the water seeding and then continual supply of water throughout the test. They also show that the water contents in the cathodic zones are up to 20% higher than that of the anodic zone. The anodic water contents of both test cells A and Z both show water contents of approximately 25-27% water contents leading to cathodic zones of 37-47%.

6.2.13.4 Shear Strengths

Figure 6-77 and Figure 6-78 show the shear strength profiles for test cells Z and A. It is seen that the strength of the clay specimens is highest in the anodic zone as expected due to the lower

water contents than the cathodic region and the addition of the stabilising chemicals. The control test had an average strength of 55.6kPa across its profile.

6.2.13.5 pH's

Figure 6-79 and Figure 6-80 show the increase in pH across the clay profiles from 4 at the anode to 10-12 at the cathode. This is as expected due to the migration of hydrogen and hydroxide across the clay. It is interesting to note that the acid front migration has spread further at the bottom of the sample than top which ties in with the increased engineering characteristic changes at the bottom over the top.

6.2.13.6 Chemical Analysis

Chemical analysis was performed on the clay samples at predetermined points across the profile. The results of this analysis can be seen in Figure 6-81 – Figure 6-84.

From Figure 6-81 and Figure 6-83 it can be seen that the migration of Fe_2O_3 across the specimen occurs from anode to cathode. The concentration of the Fe_2O_3 can be seen to decrease as the distance from the anode is increased. The spike in Fe_2O_3 seen in Figure 6-81 at 200mm from the anode is thought to be due to the fluid leakage over the surface of the clay and found under the mock footing, remnants of which can be seen to have stained the footing.

The CaO concentration can be seen to increase over the profiles at both the top and bottom.

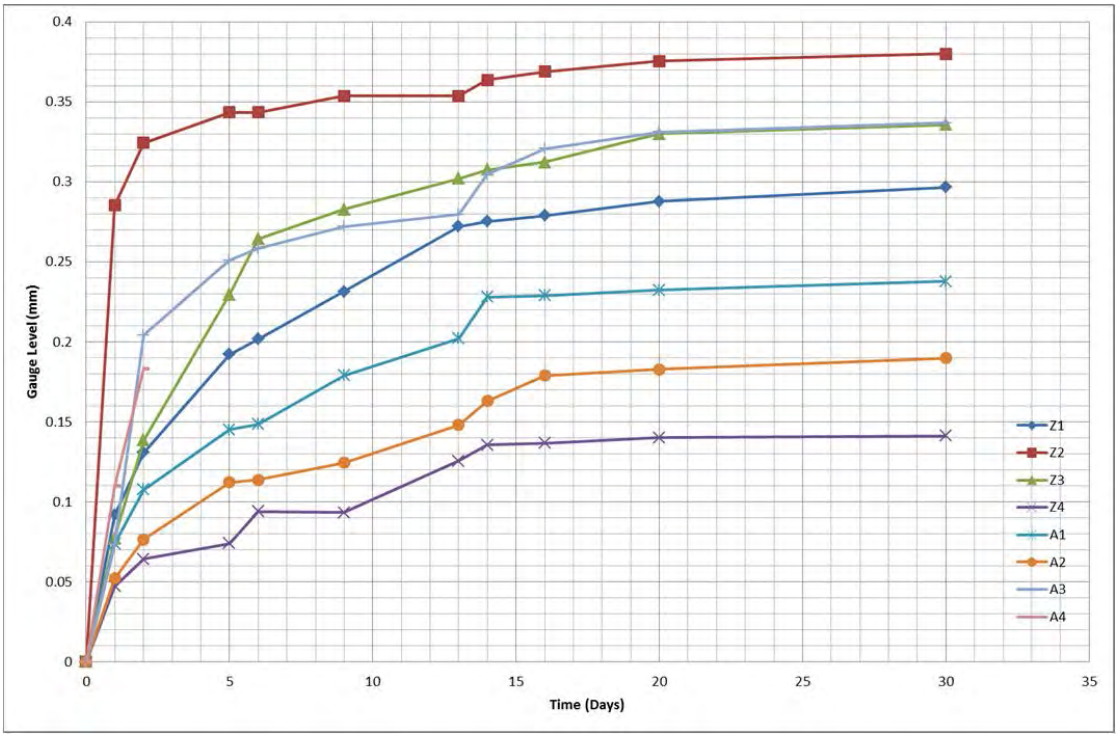

Figure 6-73: Mock foundation footing levels.

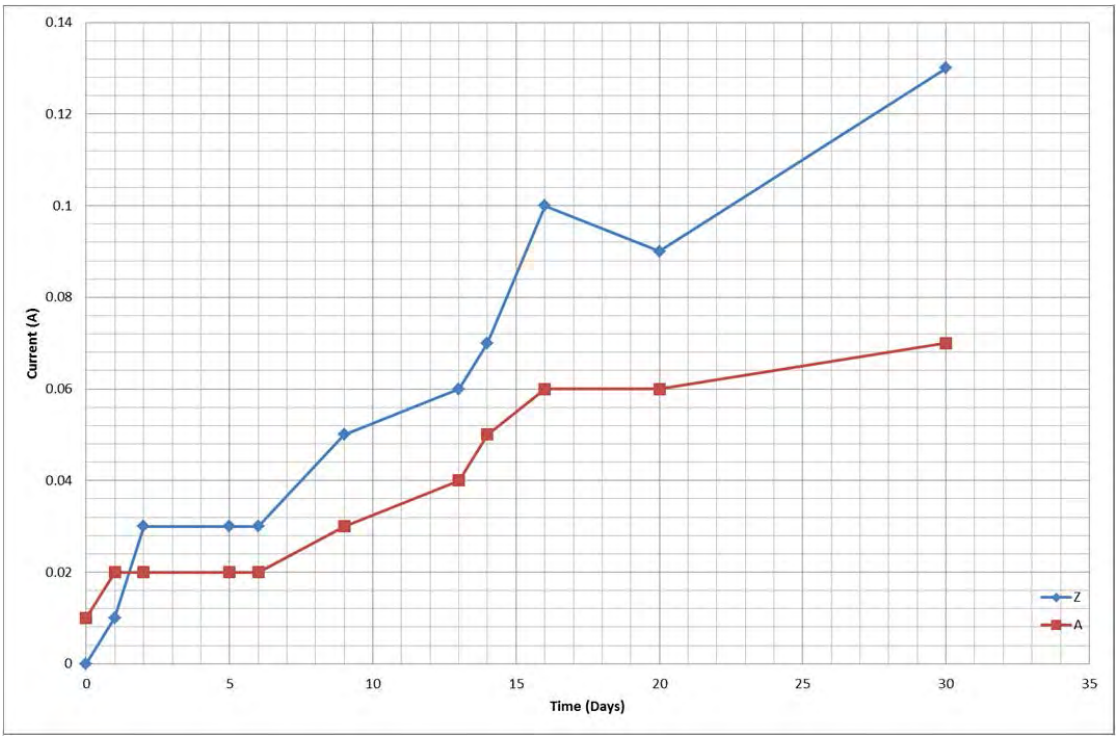

Figure 6-74: Mock foundation electric current.

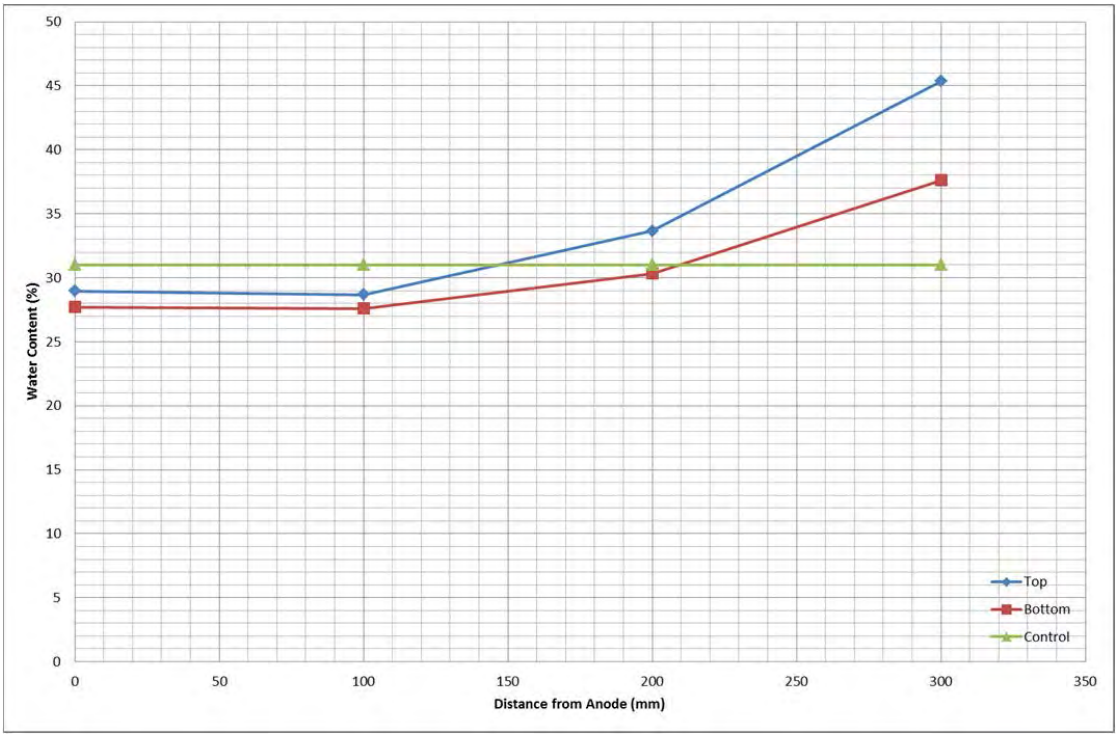

Figure 6-75: Test cell Z water contents.

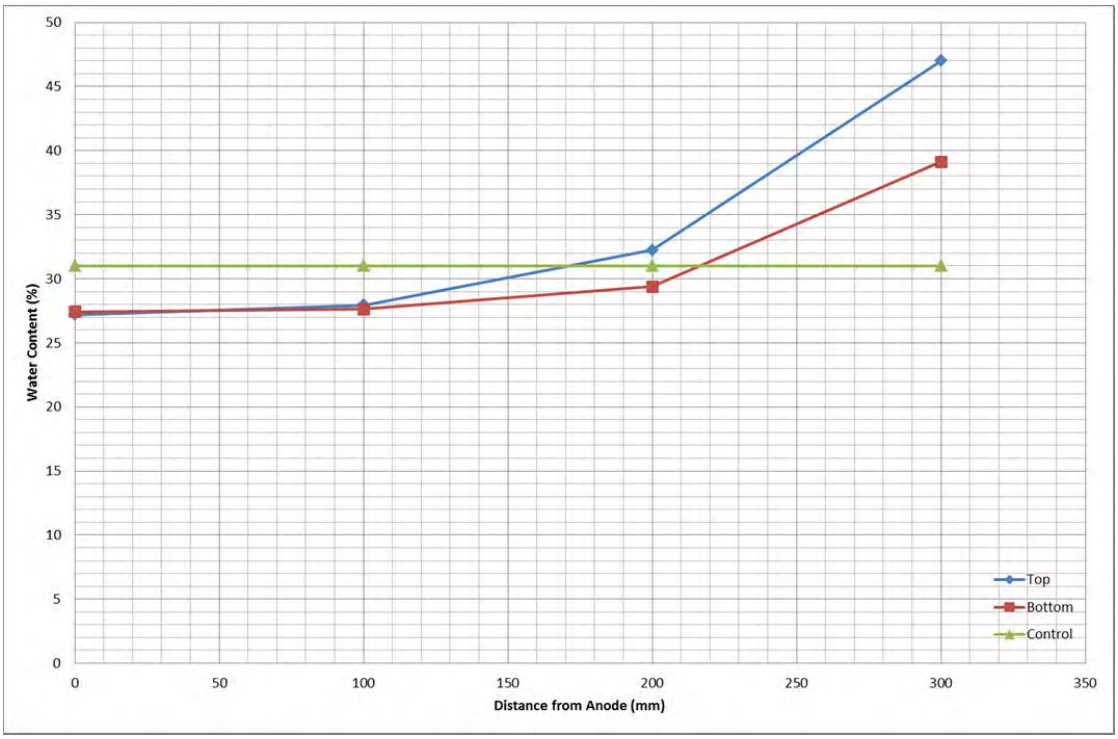

Figure 6-76: Test cell A water contents.

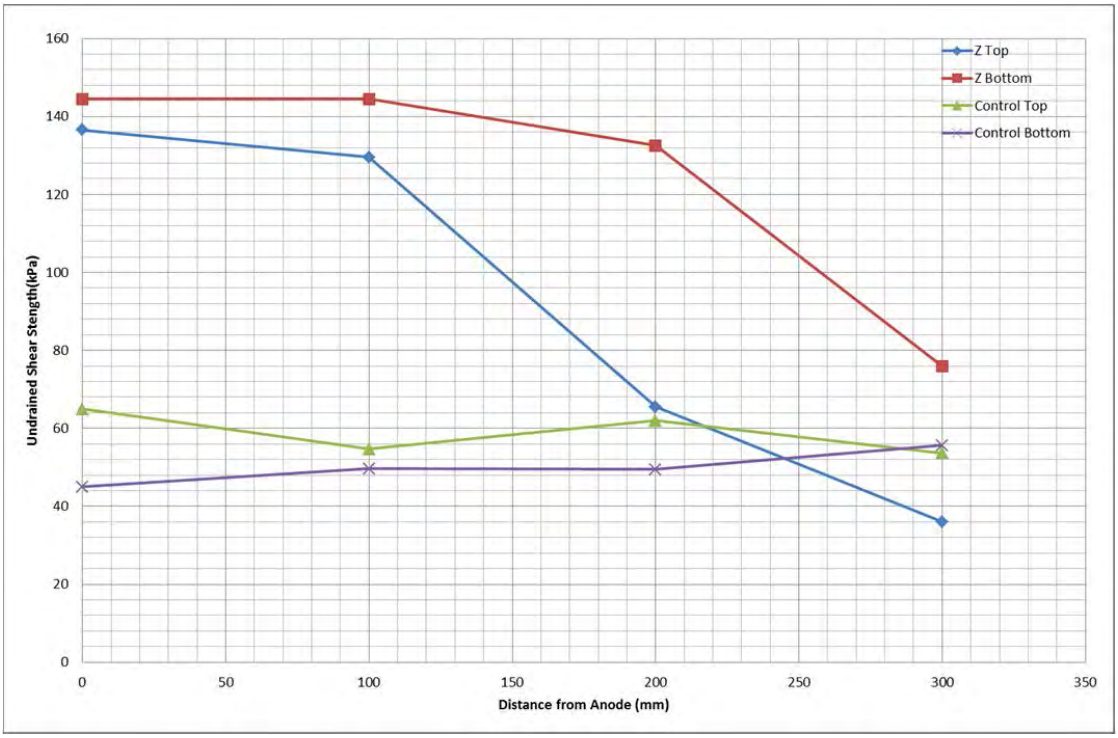

Figure 6-77: Test cell Z shear strength profiles.

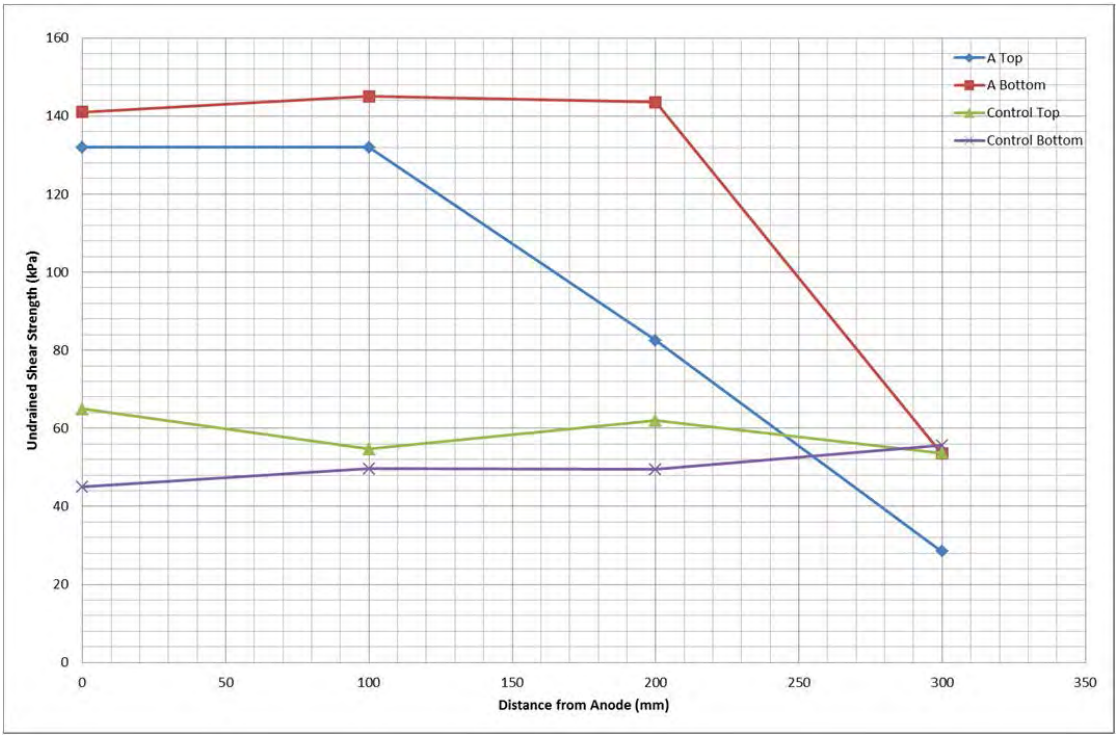

Figure 6-78: Test cell A shear strength profiles.

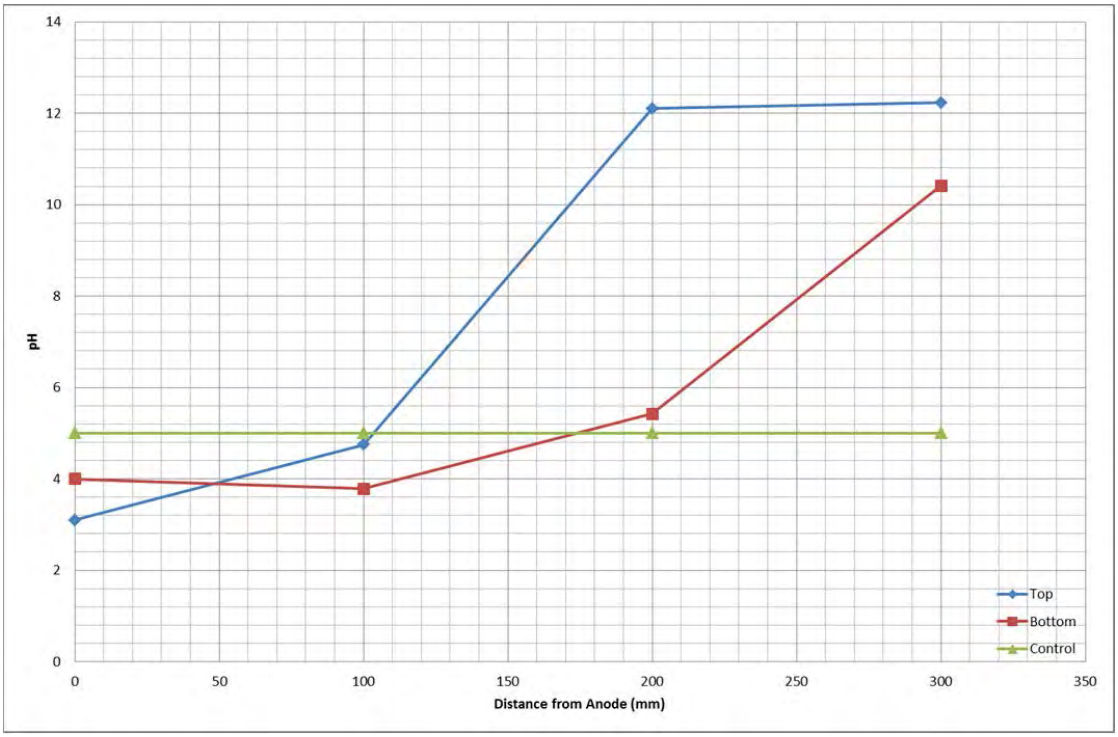

Figure 6-79: Test cell Z pH profile.

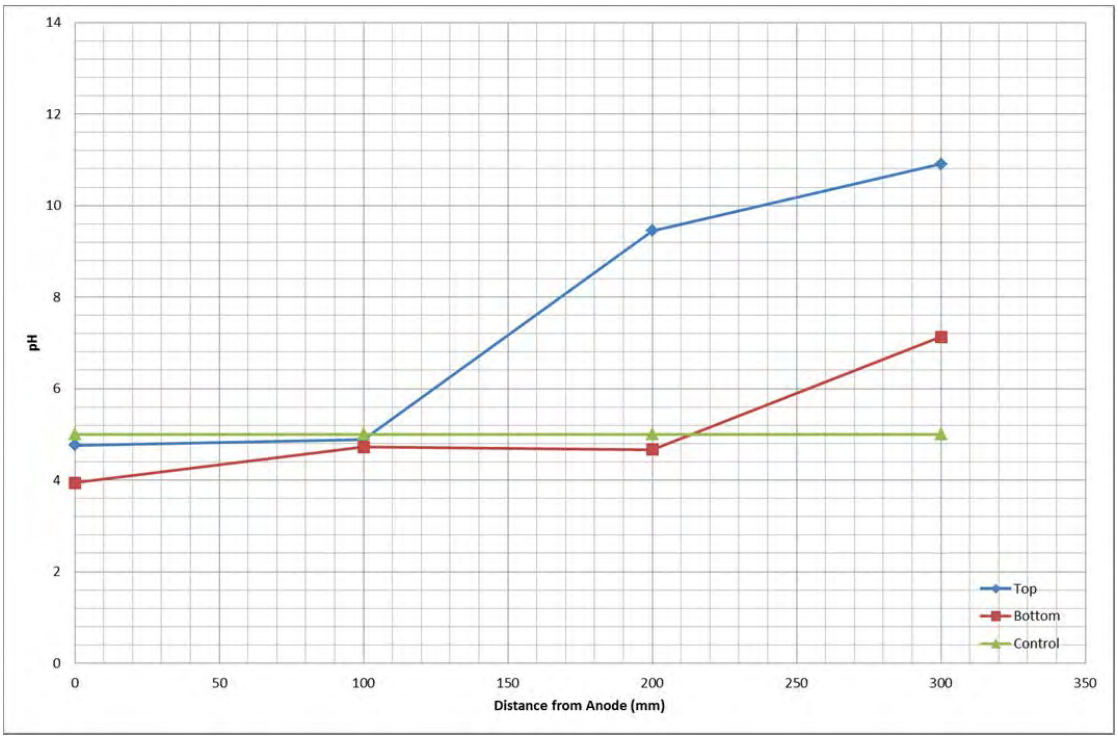

Figure 6-80: Test cell A pH profile.

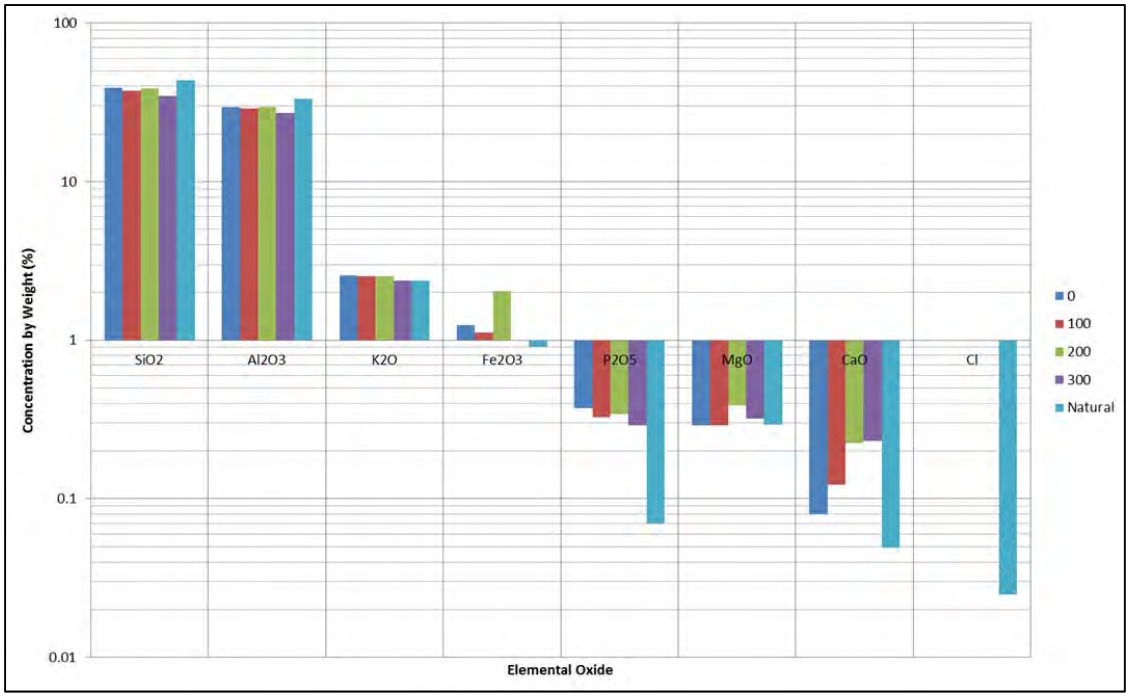

Figure 6-81: Test cell A top chemical analysis from 0 to 300mm from anode.

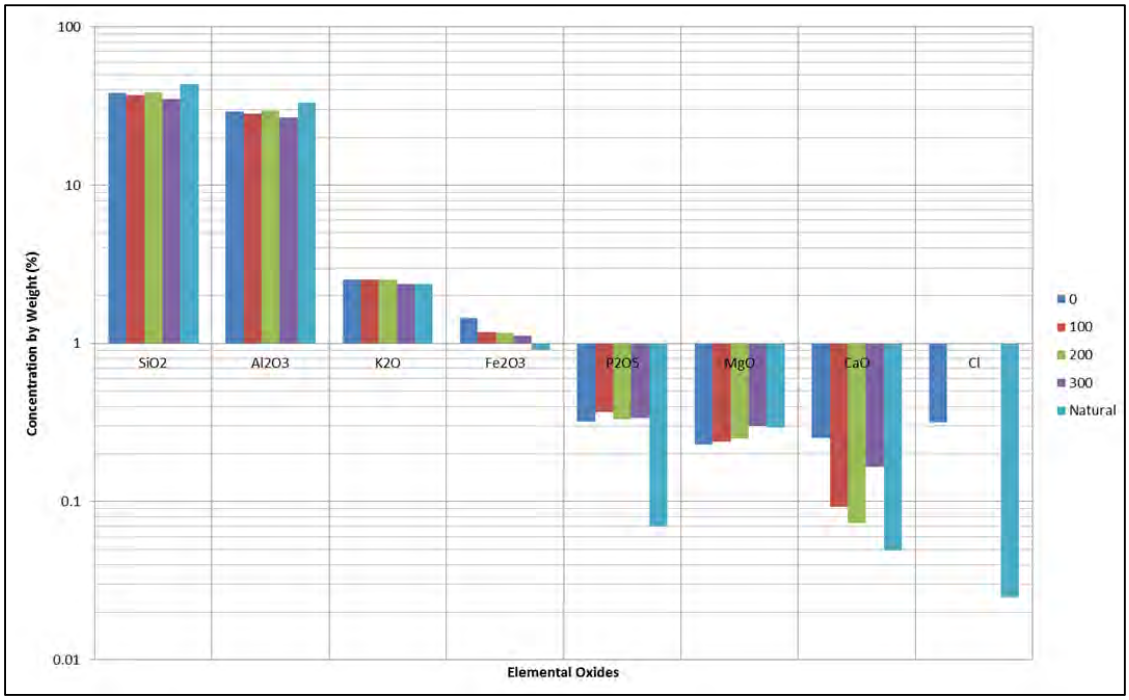

Figure 6-82: Test cell A bottom chemical analysis from 0 to 300mm from anode.

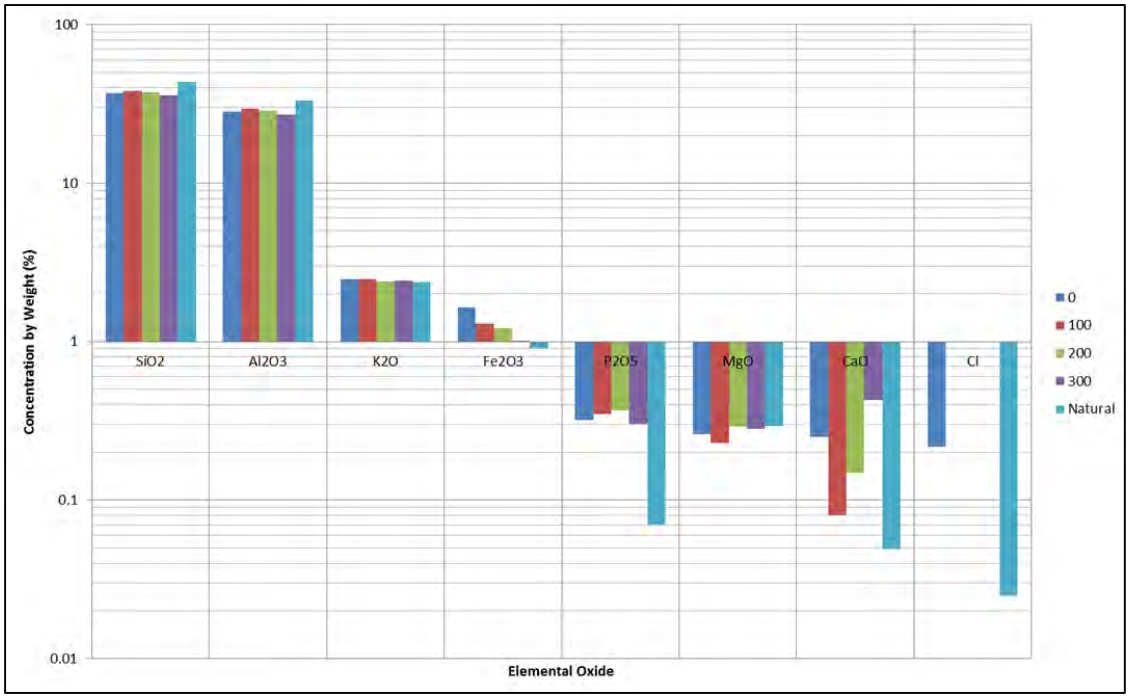

Figure 6-83: Test cell Z top chemical analysis from 0 to 300mm from anode.

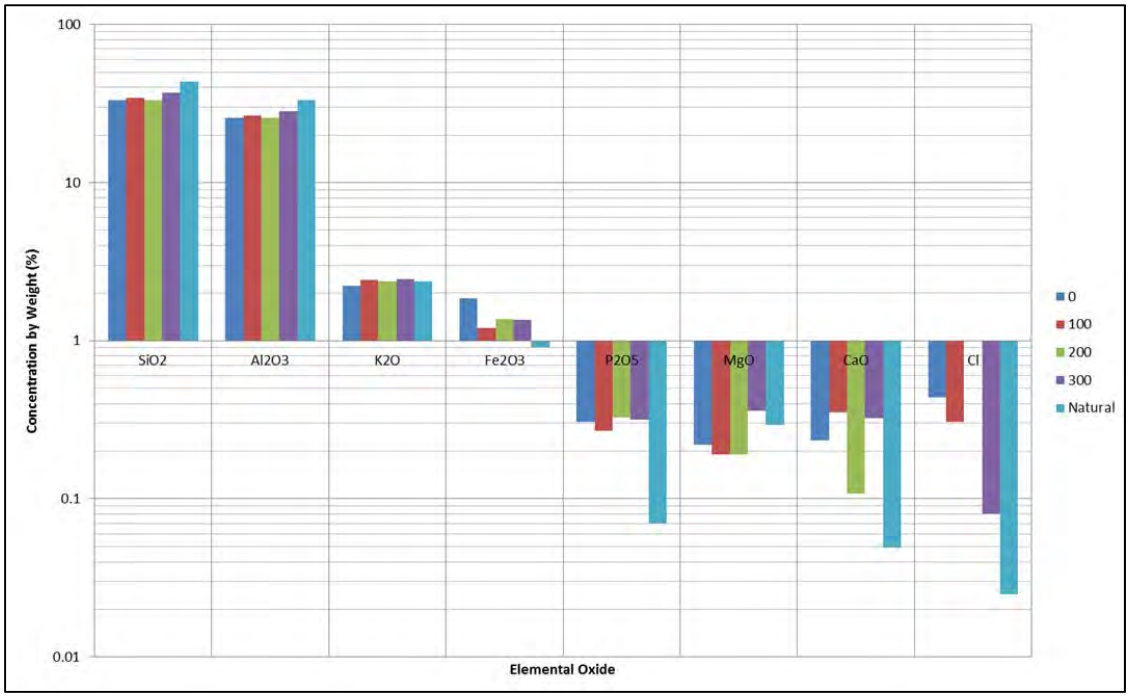

Figure 6-84: Test cell Z bottom chemical analysis from 0 to 300mm from anode.

6.2.13.7 Summary

In summary, the effect on the foundation of the introduction of the chemical mixture over that of water is negligible. The process of electrokinetic migration of the chemical compounds is shown here to be taking place through the chemical testing results along with the changes in shear strength, water content and pH's. The level results show that the introduction of water produces heave in the samples but the further introduction of the chemical stabilisers provides no extra movement.

Figure 6-85 shows the shear strength over the samples between anode and cathode normalised to pH. As can be seen, the normalised shear strength at the anode in test 'Z' is much greater than its 'A' test counterpart. Furthermore, the water content at this point is higher in test 'Z' than test 'A'. It is anticipated that cementation has occurred at this point due to electrode precipitation which is supported by the chemical analysis. It can be noted that the relationship between pH and undrained shear strength is shown quite clearly in Figure 6-86 in that an increasing pH shows a reduction in undrained shear strength. This opposes Barker (2002) and is anticipated to be due either to the relative short period of time between treatment and testing, or an example of clay flocculation due to the increased Fe ions in the anodic regions combined with low pH. It is envisaged that if cured for longer, the higher pH would have caused dissolution in the clay and hence the beginnings of pozzolanic reactions leading to strength increases.

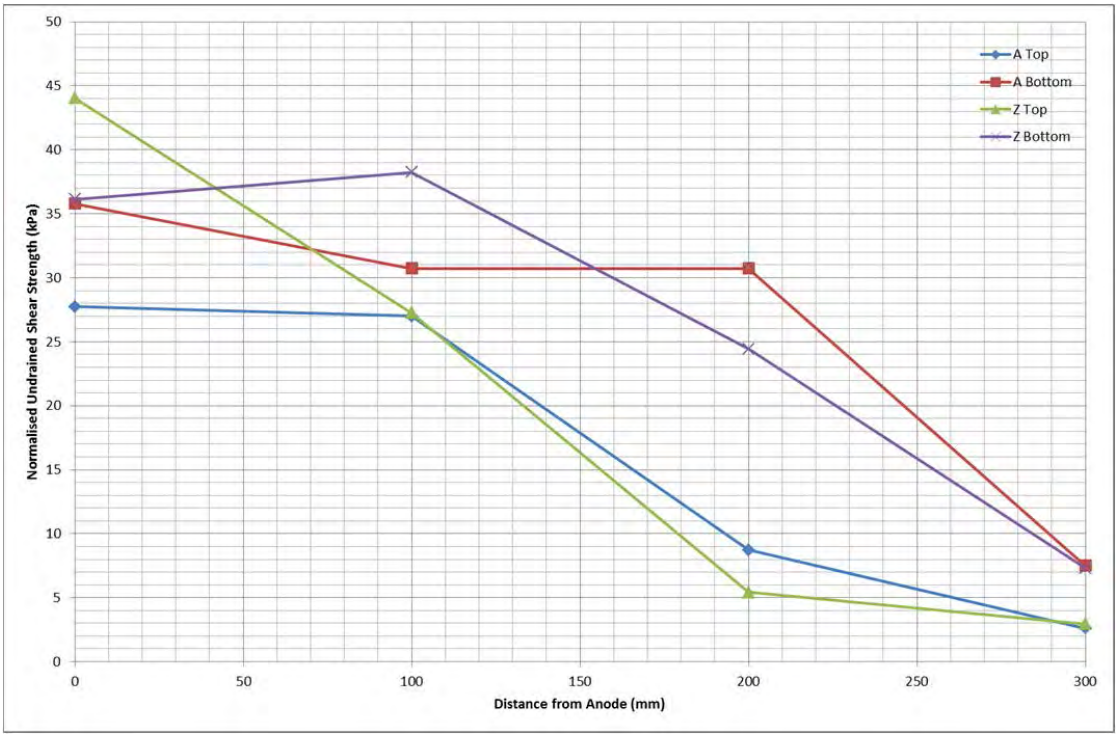

Figure 6-85: Undrained shear strengths across mock foundation experiments normalised to pH.

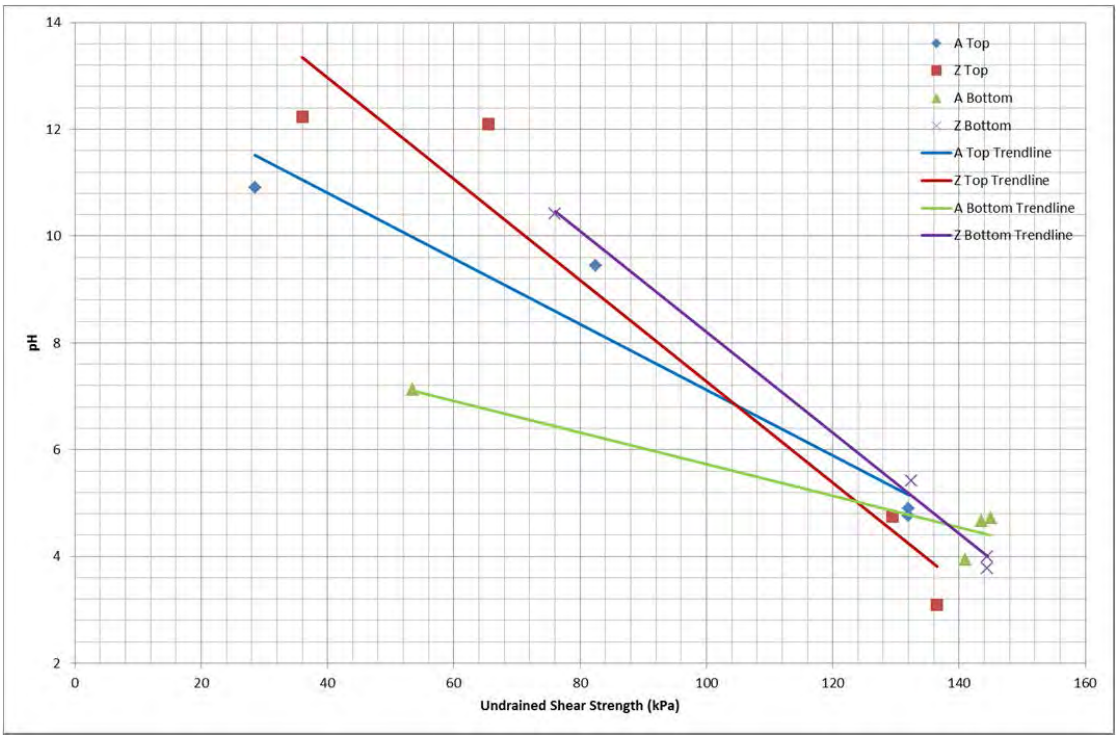

Figure 6-86: Mock foundation undrained shear strengths against pH.

6.2.14 Accuracy and Repeatability

6.2.14.1 Water Contents

Where water content samples were to be taken across the four locations between anode and cathode as previously discussed, two sets of each sample were taken, one each side of the central electrode line. The water contents used in this section have been the averages of these values along the longitudinal axis of the test setup. Each individual sample location was subject to a minimum of two water content samples being processed and the average being used.

6.2.14.2 Undrained Shear Strength

Undrained shear strength locations were the same as the water content and Atterberg Limit testing locations. The hand vane testing was conducted first and then sampling tubes used to extract the location for subsampling. As such there were two hand-vane tests conducted at each longitudinal location with the values used herein the average of the two.

6.2.14.3 Atterberg Limits

Atterberg Limit testing was conducted to BS1377-2: 1990. For liquid limit testing, the standard specifies two tests for each sample where variations exist up to 0.5mm, in this study three tests were conducted to maximise accuracy. For the plastic limits, the water content allowance difference was increased from 0.5% to 1.0% as recommended by Liaki (2006). The plastic limit testing regime is a fairly inaccurate and highly dependent on the operator and as such instead of using two samples, three were used.

6.2.14.4 Linear Shrinkage

Linear shrinkage testing was conducted to BS1377-2: 1990, on samples straight out of the liquid limit testing process. Water content was also calculated on these samples to ensure a negligible variation, this was confirmed as no greater than 3.5% difference between linear shrinkage samples and the equivalent liquid limit samples.

6.2.14.5 pH and Conductivity

The pH and conductivity testing was conducted twice on each sample to improve accuracy. The pH meter was re-calibrated after every five samples to ensure readings were accurate. All probes were thoroughly rinsed with RO water after every reading.

6.2.14.6 Chemical Analysis

Two oven dried samples from each sampling location were used for chemical analysis with the average reported here. Equipment was cleaned using RO water and gloves were worn whilst handling samples and associated equipment to avoid contamination.

6.2.14.7 SEM Photography

Whilst one cannot take averages of SEM photography, one could take numerous photographs to get an overall picture of what is happening and where. Due to the time taken to prepare SEM samples and actually use the SEM, the cost implications were too great to repeat samples or locations.

6.2.15 Laboratory Tests Summary

The chemical combination ratio was developed in the laboratory based upon the chemicals used in previous studies, (Barker, 2002), (Liaki, 2006), (Tajudin, 2012). Over the range of concentrations mechanically mixed with ECC, the 3% concentration by weight was shown to be most successful. This concentration had the most improved characteristics such as shear strength for given water content. The electrical conductivity was not the greatest and pH not the highest but the cost implication of using a 3% mix was enough to warrant its confirmation as the optimal mix. The strength increases seen across the $CaCl_2$ and Na_2SiO_3 mixes are thought to be pozzolanic reaction products leading to a continuous increase in strength over 1-5 years.

Once the most efficient chemical stabiliser mix had been determined, attention was transferred to the electrodes. The initial testing using the hybrid electrode showed that the development of electrodes can yield positive results and so the PEG was developed, inspired by the EKG electrode, (Pugh, 2002), (Pugh & Jones, 2006), (Glendinning, et al., 2005), (Glendinning, et al., 2008). From the literature it was evident that the majority of studies, being laboratory based, did not consider electrode shape and thus meshes were commonly used. Installing a mesh in a real world situation around a strip footing would be impractical whereas installing a tube is straightforward with machinery existing to do that very job. A 35% graphite to epoxy resin mix was established as the optimal ratio due to its workability, electrical conductivity and similar concentration electrical conductivity trends seen in the literature. A plastic tube was used as the core of the electrode due to the performance being greater than that of a steel core and costing approximately 20% of the price of steel (2015 prices). The effectiveness of the PEG is

not certain at this point in the research, section 6.2.11 and section 6.2.12 both show the PEG being used as a treatment electrode and both show that the PEG does work but in a limited fashion. The numerical simulations, section 6.3, of the PEG against the stainless steel electrodes show that this limited effectiveness is due to the inherent higher electrical surface resistance of the PEG over the stainless steel. In reality, a longer treatment time would be required to reach the same level of treatment as when using stainless steel electrodes. This is despite the success of EKG's in the literature and section 6.2.7 even though the EKG possesses a higher surface resistance and electrical resistivity than the PEG. Due to this uncertainty, these electrodes were not used in the site trials.

Polarisation phenomena can affect electrode negatively in the fact that the build-up of charges at the electrodes can effectively insulate them and reduce the amount of current able to pass between them. Section 6.2.5 shows how an attempt to understand this process in a dc electric field was conducted. It was shown that by increasing the number of electrodes in the system, the time taken to polarise the electrodes also increases along with quicker relaxation rates. The current intermittence trials in section 6.2.6 show evidence of polarisation as the constant current trial performed worse than the intermittent trials where relaxation overcomes polarisation. The site trial's current intermittence trial did not show improvements over the vertical electrode trials as suggested in the literature, (Mohamedelhassan & Shang, 2001). This could have been however, due to the ground resistance being very high in this part of the site as demonstrated by the power supply being unable to supply a constant voltage and thus supplied a constant current.

When applying the EKS process to a clay, the electrical conductivity of the clay water system will affect the time taken for treatment to be completed. As expected, an increase in electrical conductivity is seen for the fluids with conductive ions present such as tap water and the tap water with chemical mix. The tap water and chemical mix produced a 300% decrease in electrical conductivity when increased in temperature from 5 to 25°C. Whereas it was thought that the winter should be avoided when conducting EKS to reduce frozen fluids and slow chemical reactions, it may however be more prudent to avoid summer to ensure the fluid electrical conductivity is at its maximum. Overall, a mild Spring or Autumn day would likely be optimum.

6.3 Numerical Simulations

The numerical simulations can be split into categories depending on their simulation type. All simulations were conducted as discussed in section 4.2.

6.3.1 Test Cell Filter Effect

As can be seen in Figure 6-87 and Figure 6-88, there is very little difference between the two RO water scenarios. This is likely to be due to the RO water possessing an electrical conductivity less than that of the clay. The simulations involving the tap water and 5% chemical mix do show a difference however, Figure 6-89 and Figure 6-90. Due to the higher electrical conductivity of the fluids than the clay, a preferential flow path is created through the filter. In this instance though the current density through the clay is sufficient for electroosmosis to occur.

When applying conductive fluids to the system, the filter paper does create a flow path for the electric current and potentially the fluids themselves. With this system setup however, there is no alternative method.

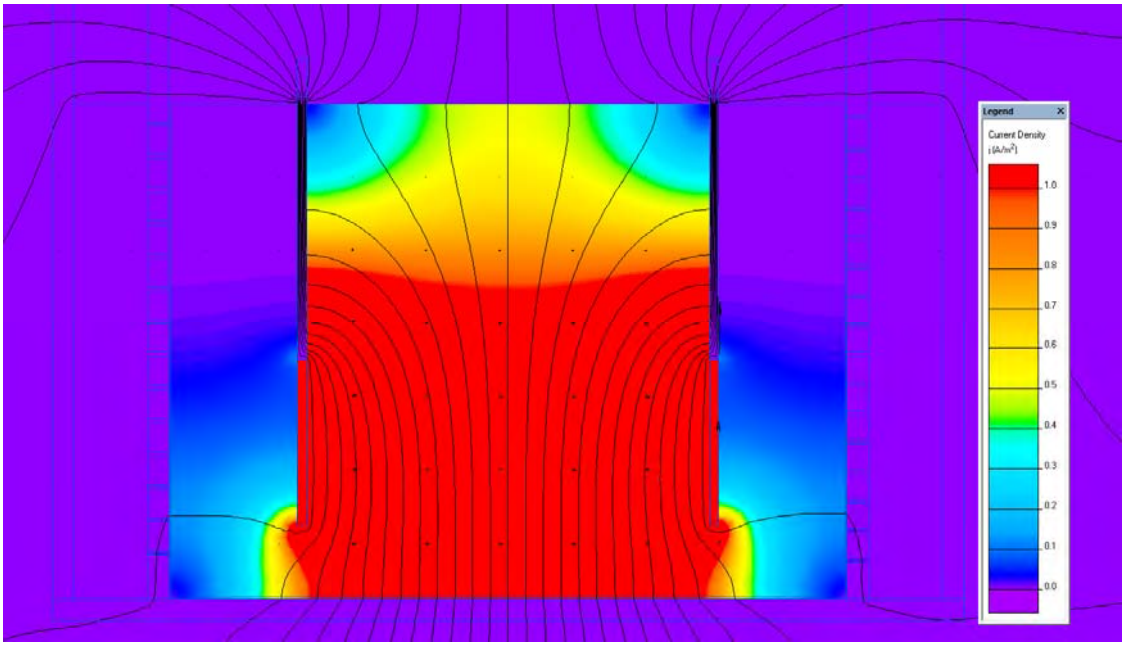

Figure 6-87: Test cell filter paper simulation - no filter with RO water.

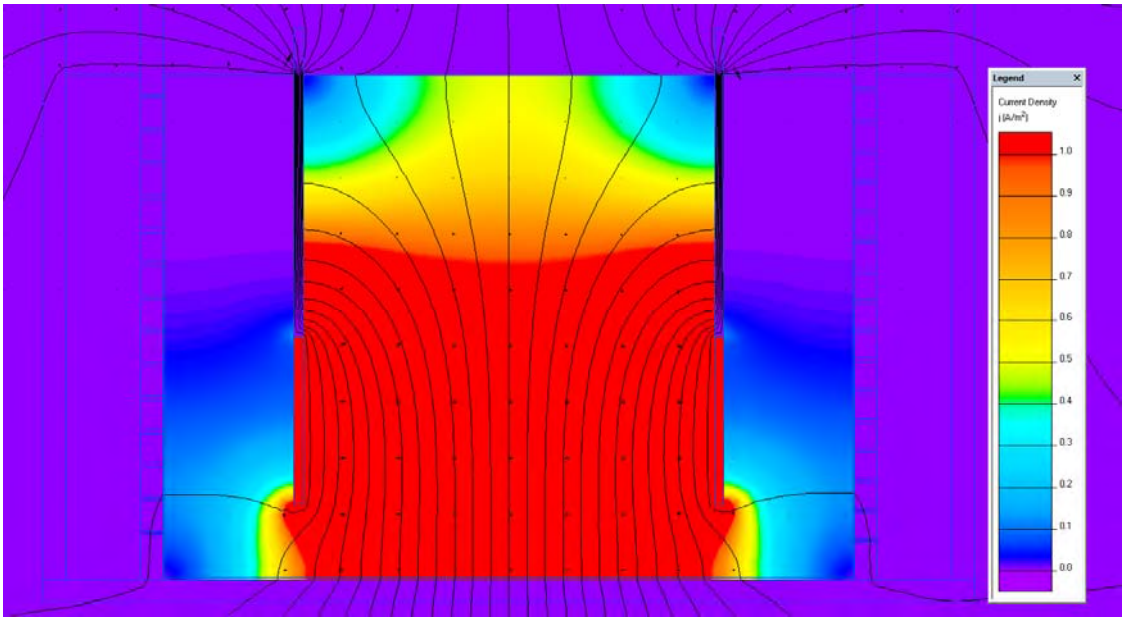

Figure 6-88: Test cell filter paper simulation - filter paper with RO water.

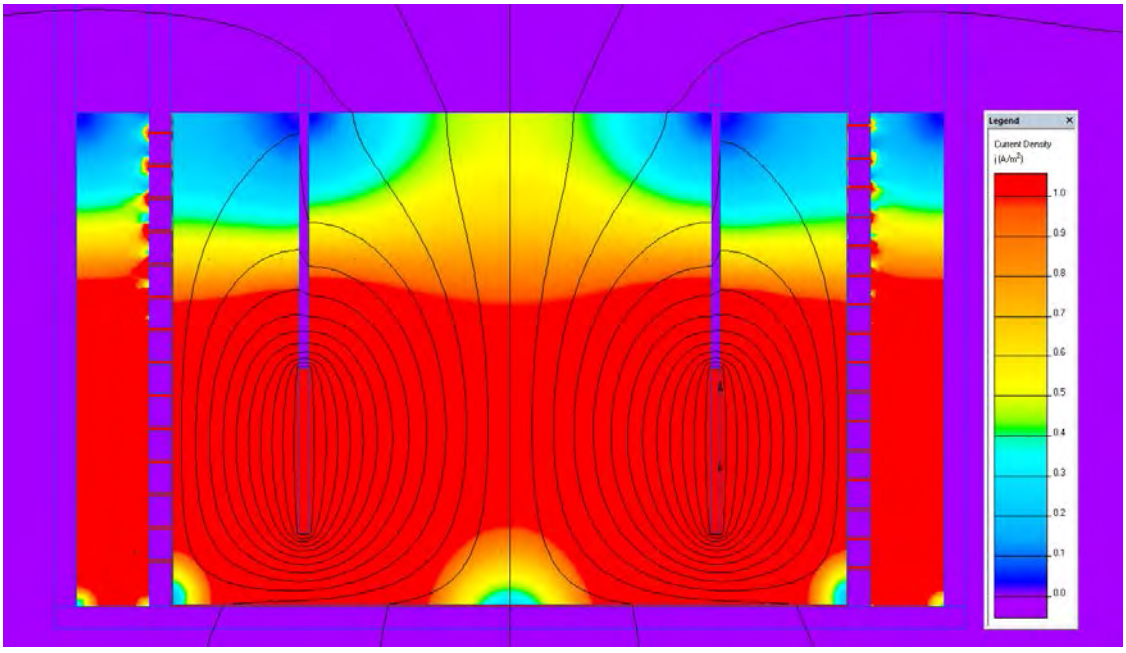

Figure 6-89: Test cell filter paper simulation - filter paper with tap water and 5% chemical mix.

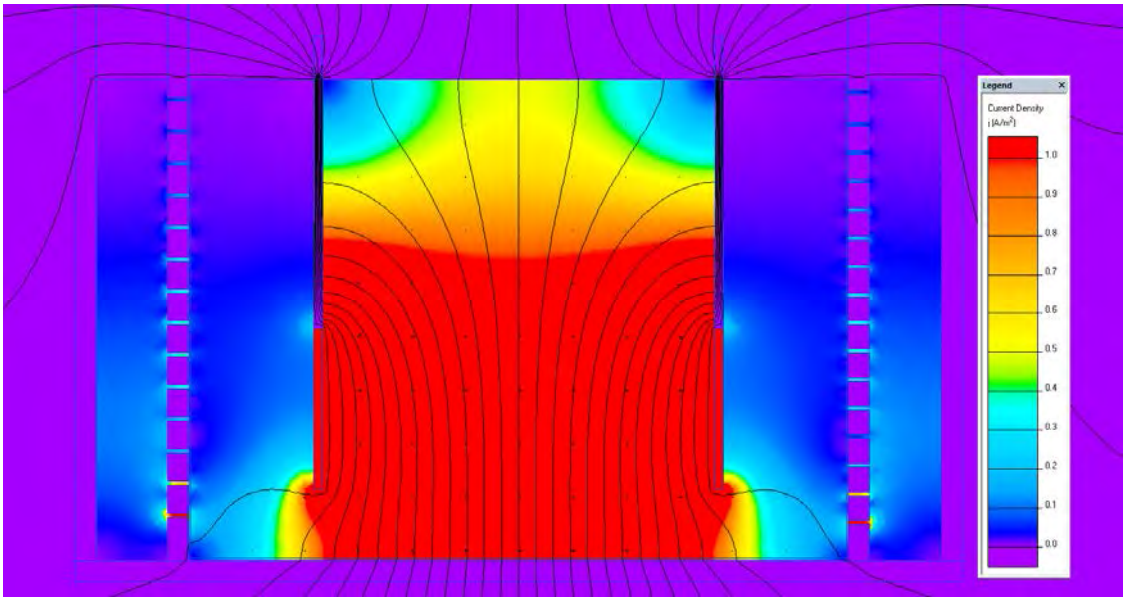

Figure 6-90: Test cell filter paper simulation - no filter paper with tap water and 5% chemical mix.

6.3.2 Electrode Arrangement

It can be seen from Figure 6-91 to Figure 6-98 that whilst increasing the number of electrodes is beneficial in that the area treated can be increased; current density voids appear as seen in Figure 6-94 to Figure 6-97. Figure 6-98 shows an offset rectangular arrangement that is not affected by a current density void and could be used practically with a strip footing running horizontally through its centre. The voids exist due to current flow between positive and negative electrodes and there is only peripheral flow diagonally. Figure 6-93 and Figure 6-98 both show that by offsetting the electrodes, the voids can be avoided leading to a more uniform treatment zone.

It should be noted that these simulations are purely indicative and not validated.

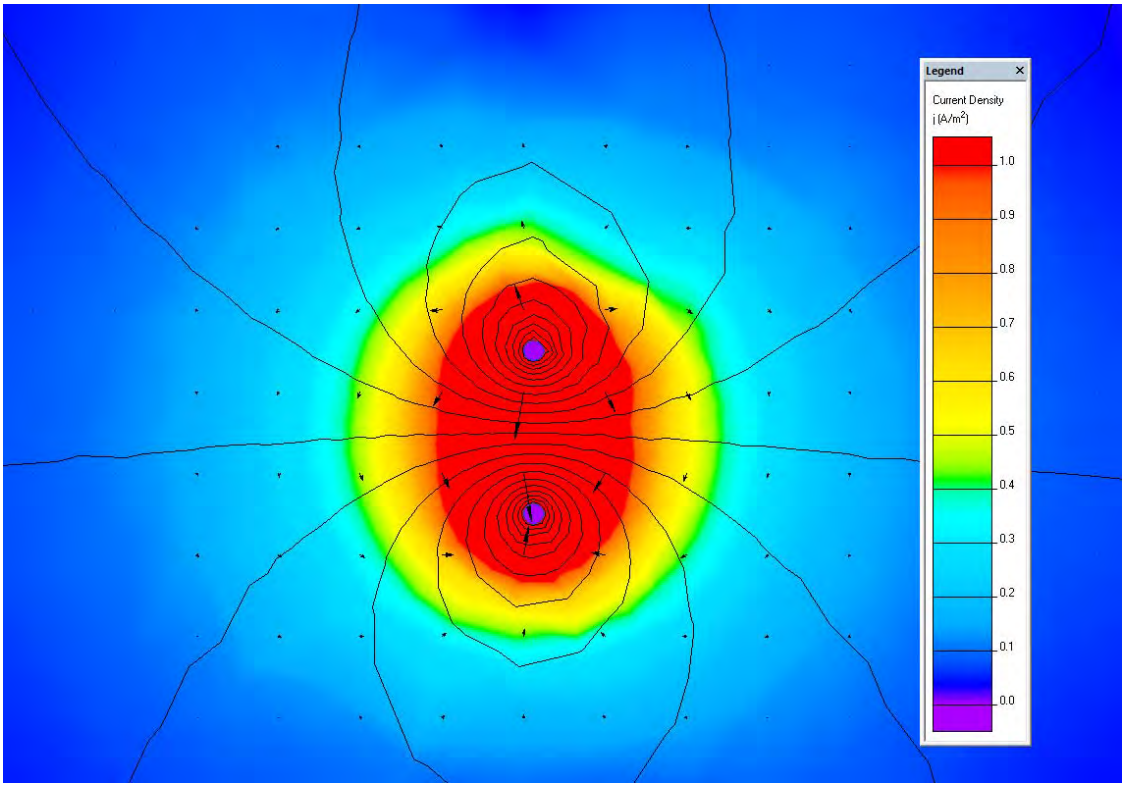

Figure 6-91: Electrode arrangement - two electrodes.

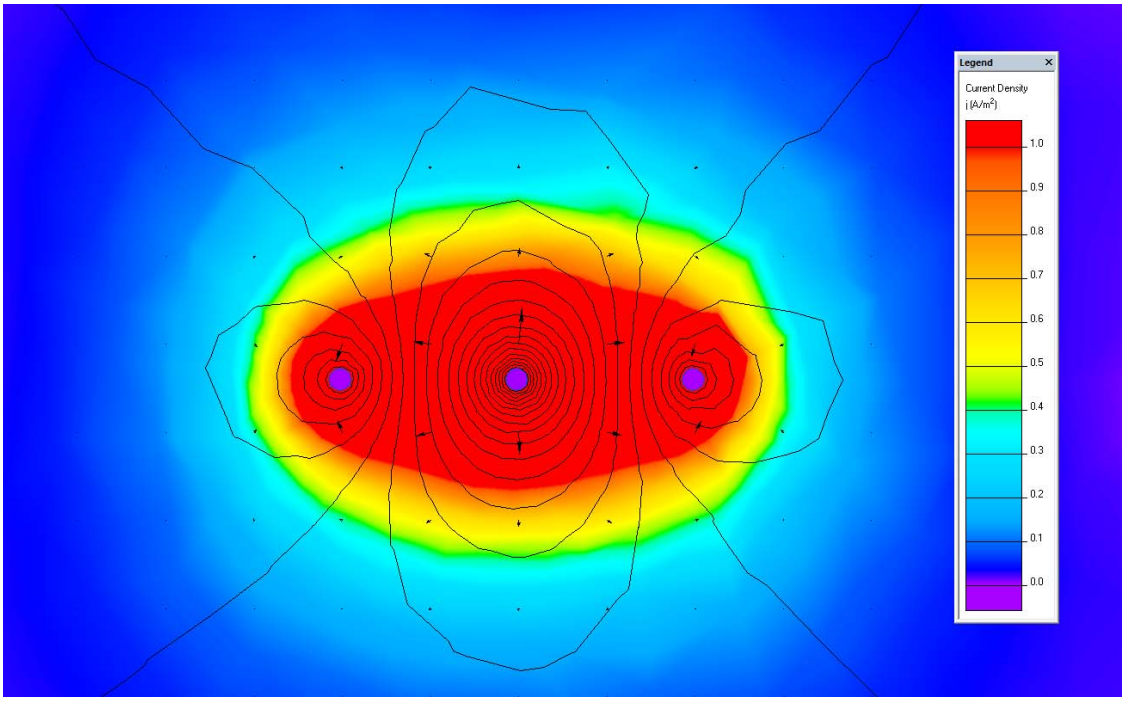

Figure 6-92: Electrode arrangement - three electrode straight.

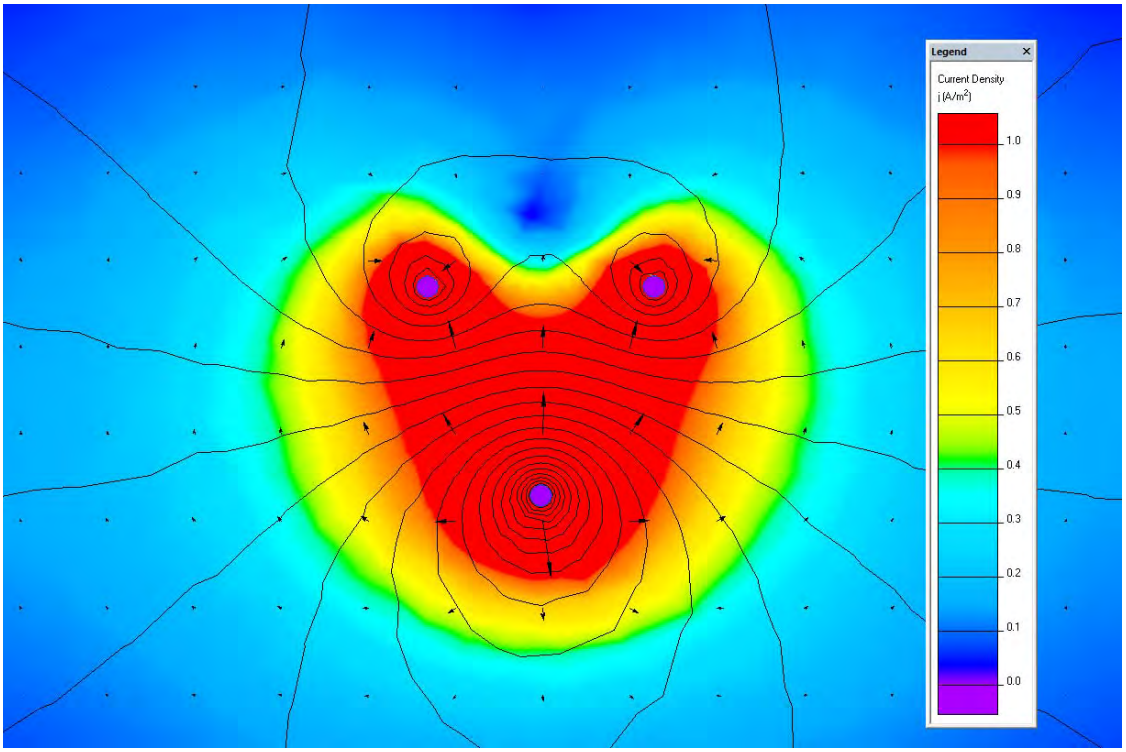

Figure 6-93: Electrode arrangement - three electrodes triangular.

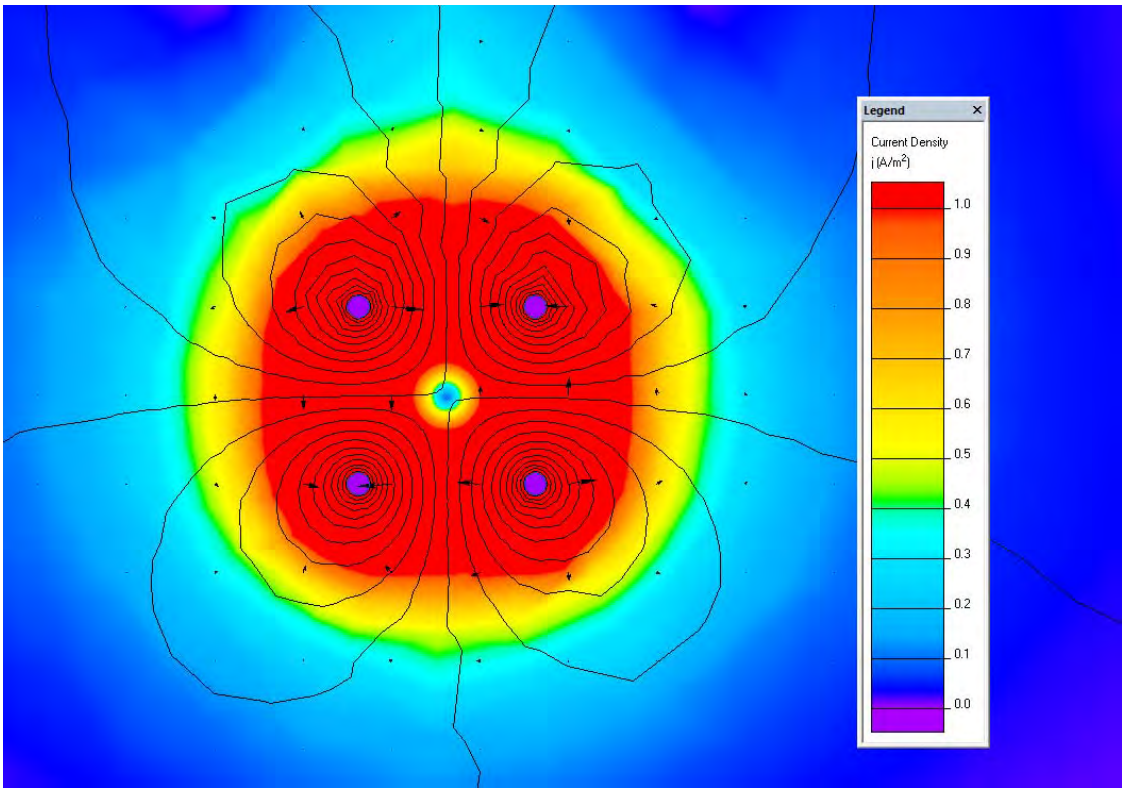

Figure 6-94: Electrode arrangement - four electrodes square.

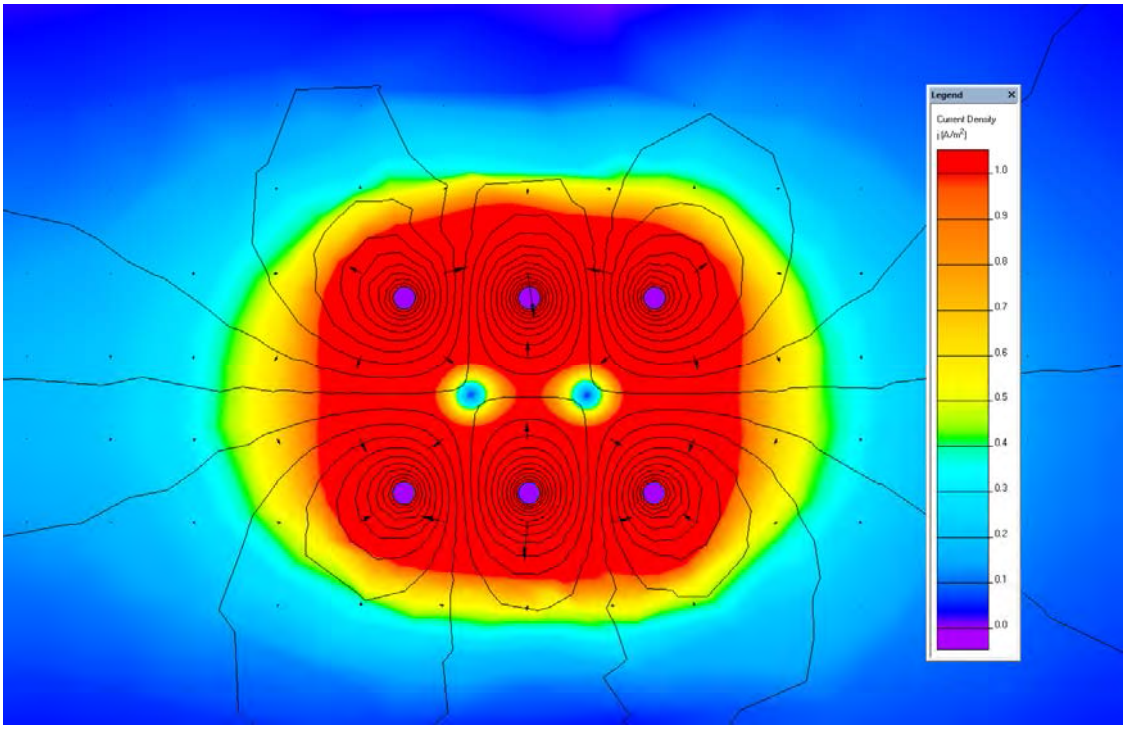

Figure 6-95: Electrode arrangement - six electrodes rectangular.

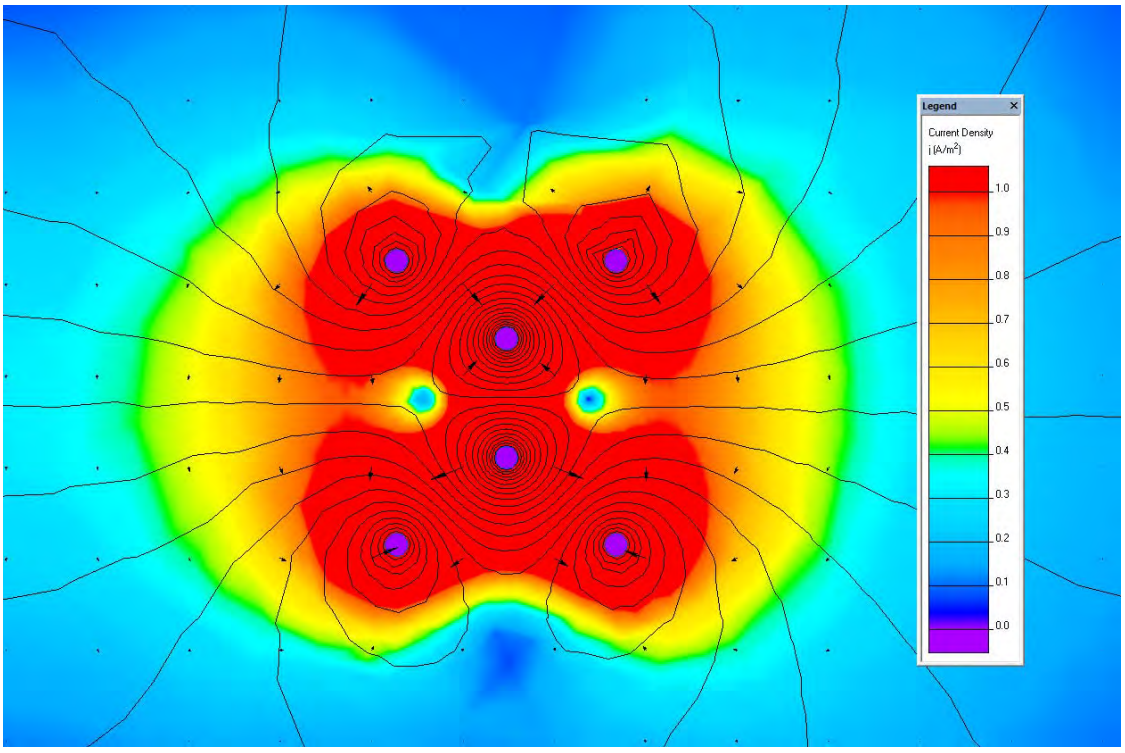

Figure 6-96: Electrode arrangement - six electrodes alternative.

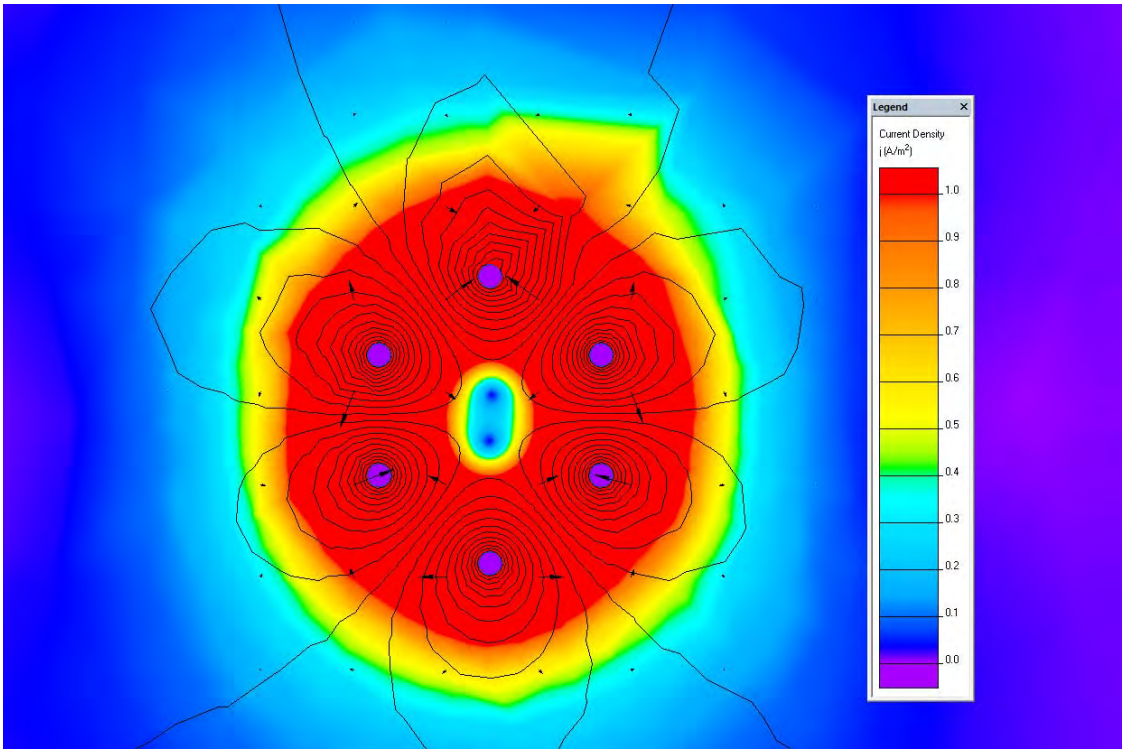

Figure 6-97: Electrode arrangement - six electrodes star.

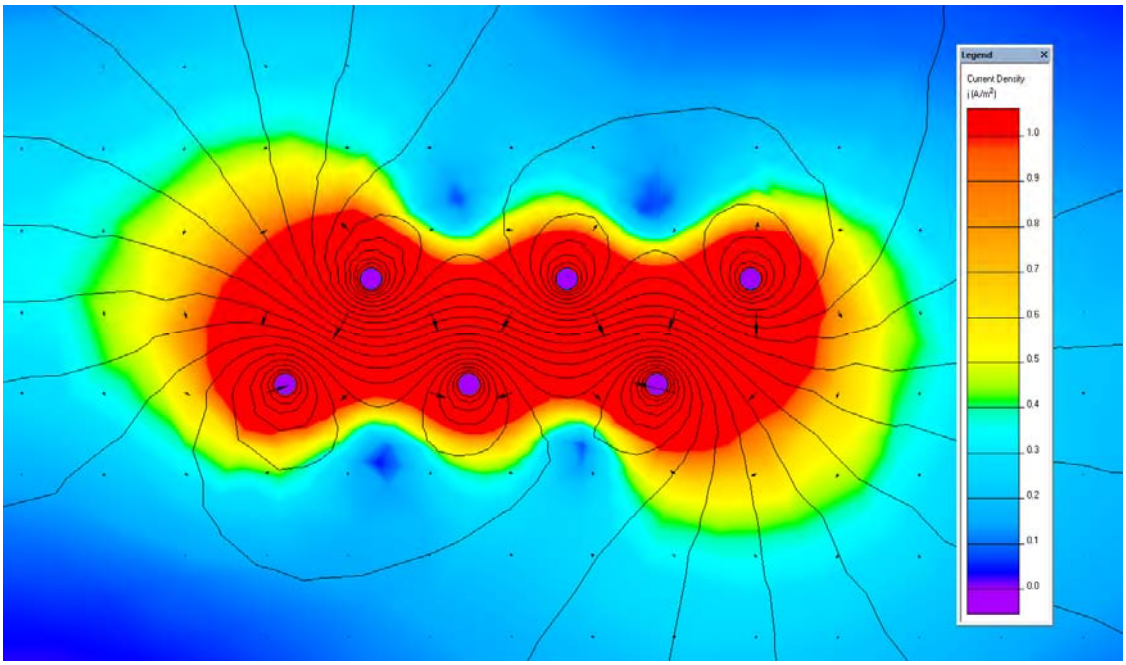

Figure 6-98: Electrode arrangement - six electrode rectangular offset.

6.3.3 Electrode Comparison

The comparison between PEG electrodes and stainless steel electrodes can be seen in Figure 6-99 and Figure 6-100 where the pattern of current density varies between the two. The stainless steel electrodes transfer the current very well throughout the entire sample whereas the PEG electrodes appear to transfer the current more efficiently near the top of the electrode than the bottom. This is likely due to the electrical resistance offered by the PEG electrode compared to the stainless steel as corroborated throughout the experimental work.

Figure 6-101 and Figure 6-102 show the same configuration as Figure 6-99 and Figure 6-100 but without the current density range capped. It can be seen that the current density is at its maximum in the filter paper. It should be noted that at the centre point at the ends of the electrodes, the current density is 1.26A/m^2 and 0.35A/m^2 for the stainless steel electrodes and PEG electrodes respectively.

Figure 6-103 shows how the three different electrode types require different voltage gradients to achieve the previously stated ideal 1A/m^2 value of current density under the same conditions. By requiring a lower voltage gradient, the stainless steel proved to be a more efficient electrode.

The fact that stainless steel appears to conduct electrical current more efficiently into the clay is expected and indicated that the stainless steel electrodes would be the most suitable choice for further development. This conclusion is echoed by the electrode type choice experiments as shown in section 6.2.7 where stainless steel is shown to be the most effective electrode for transferring electrical current into the soil and thus producing electroosmotic flow.

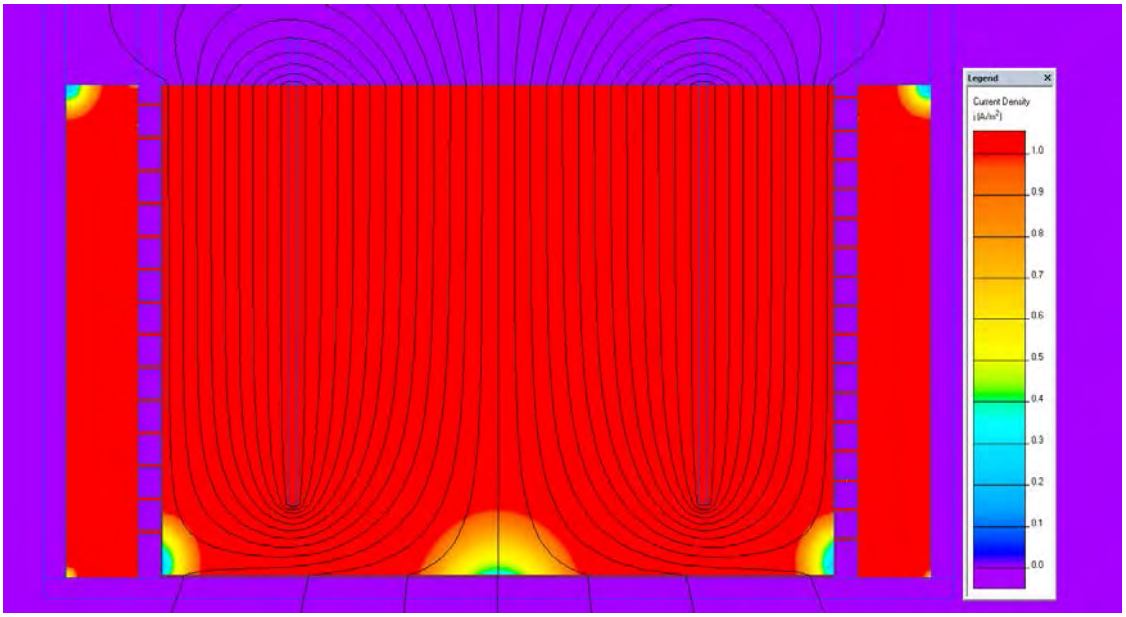

Figure 6-99: Electrode comparison - stainless steel with filter.

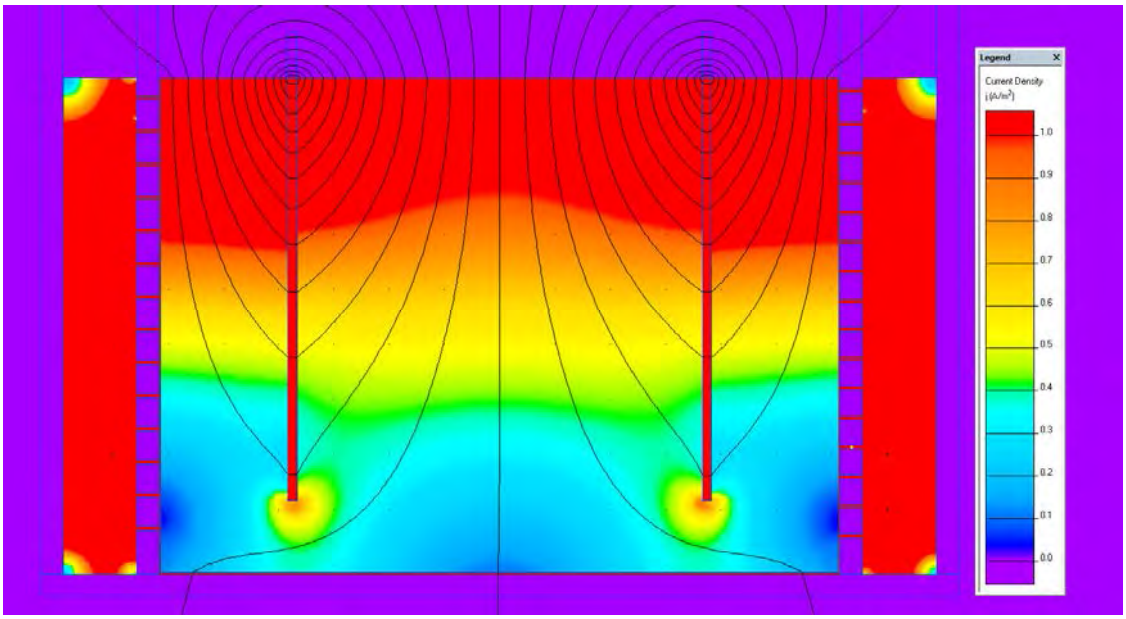

Figure 6-100: Electrode comparison - PEG with filter.

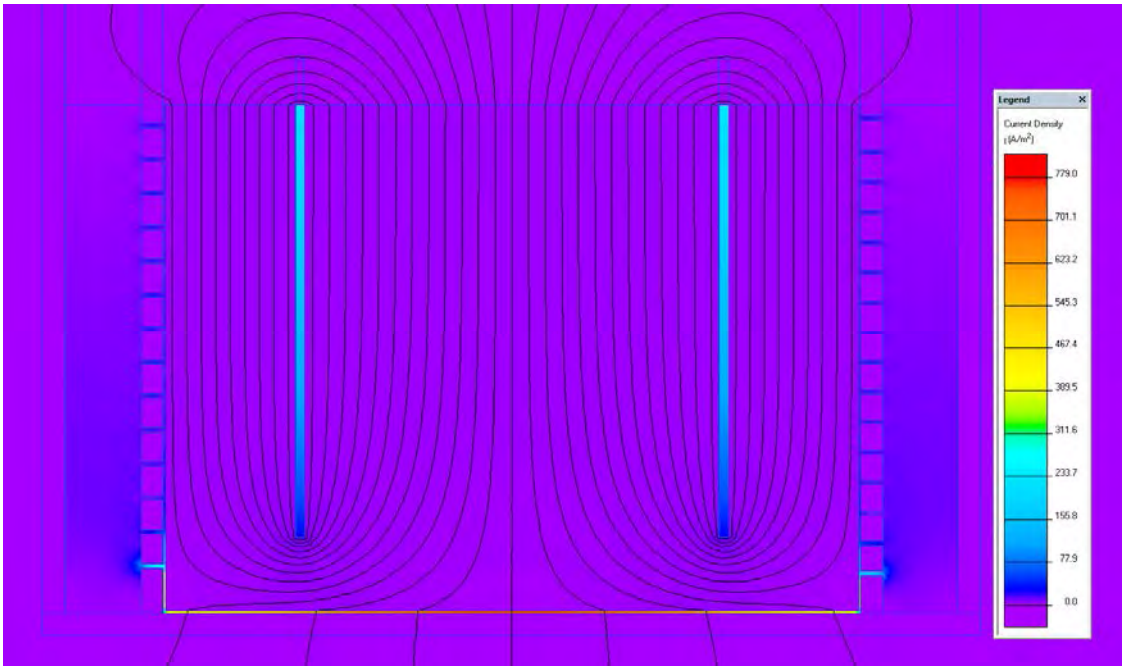

Figure 6-101: Electrode comparison - stainless steel electrodes with filter.

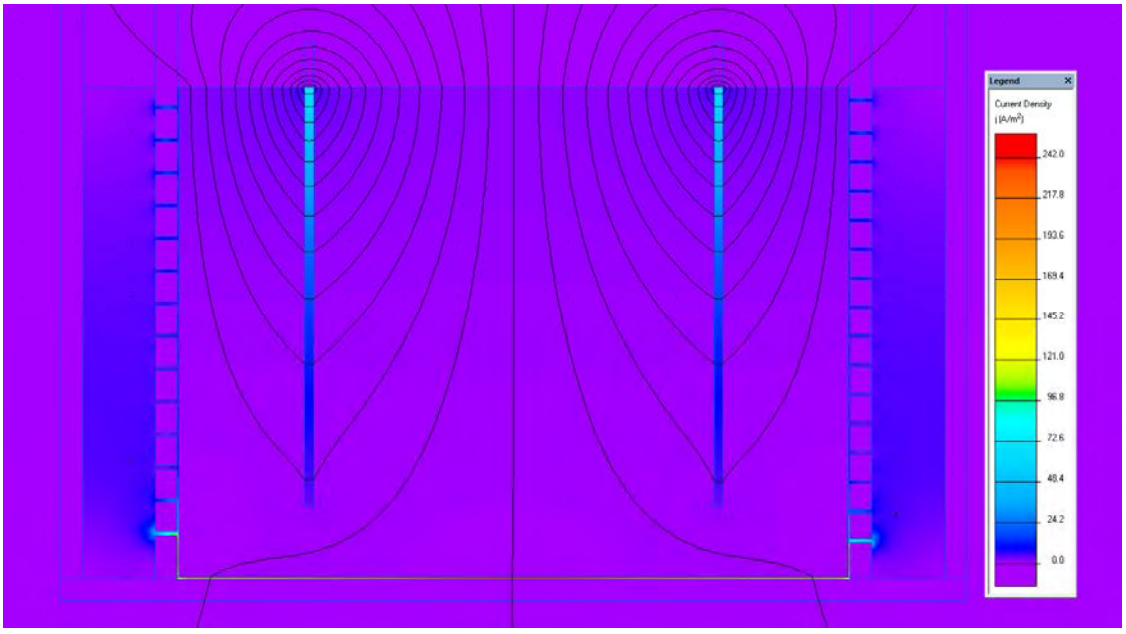

Figure 6-102: Electrode comparison - PEG electrodes with filter.

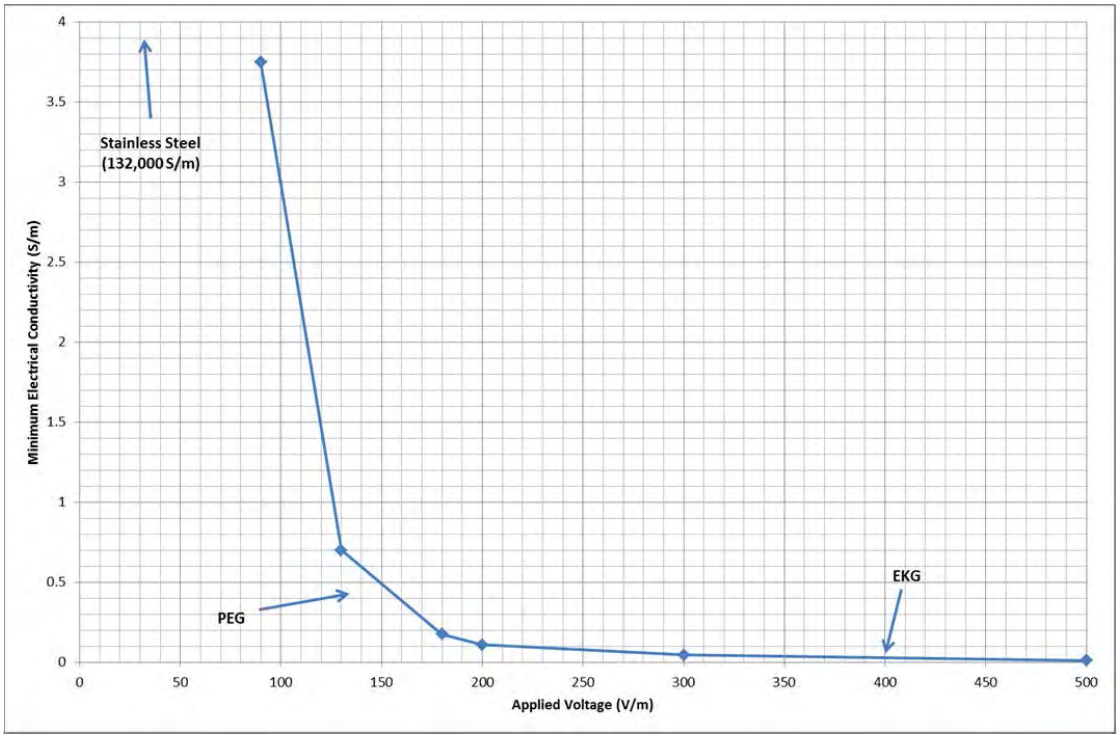

Figure 6-103: Electrode comparison - minimum electrical conductivity required to achieve current density of 1A/m^2.

6.3.4 Clay Banding

As seen in Figure 6-104 and Figure 6-105, changing the electrical conductivities of the clay bands will cause preferential flow. Figure 6-105 shows a clay of 0.001S/m clay bisected with a band of 0.0165S/m clay where it is seen that the majority of the electrical current density is then found inside this band. Figure 6-104 shows a clay of 0.008S/m bisected by a band of 0.0165S/m clay. As seen, the bands electrical conductivities are much closer in this figure and as such the share of electrical current density is much more spread out over the sample.

With the method of compacting the clay in the lab, if a layer possesses a higher electrical conductivity, this preferential flow could occur. Also, the very act of compacting leaves boundaries between the layers, albeit minimised by scoring the surfaces. These boundaries, if saturated by a conductive fluid, will also act as a preferential flow path.

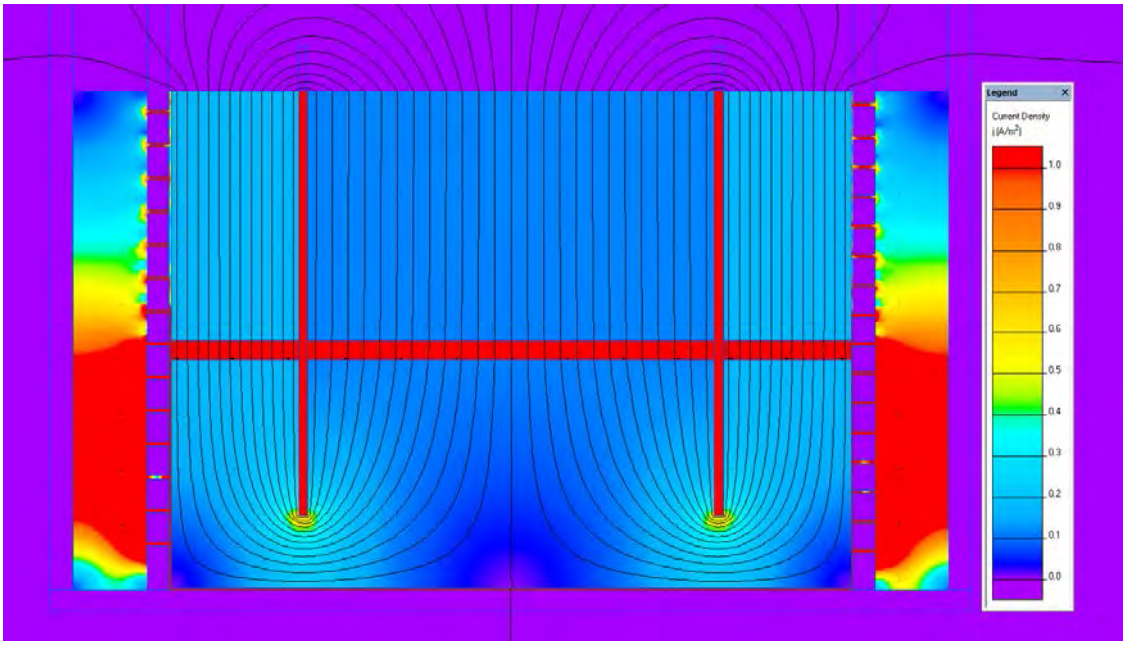

Figure 6-104: Numerical simulations clay banding.

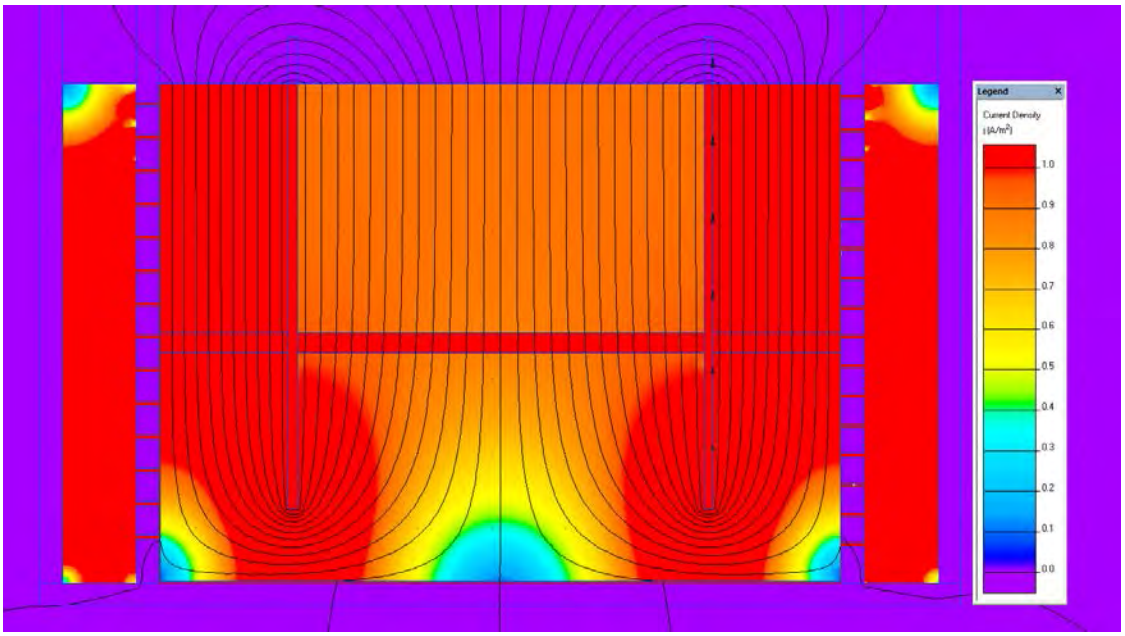

Figure 6-105: Numerical simulation clay banding 2.

6.3.5 Electrode Electrical Conductivities Variation Effects

As seen in Table 6-9, the general trend is that the lower the electrical conductivity of the electrode, the lower the current density is at the chosen point. This is true up until lower midpoint, midpoint, steel and extreme high. These four electrical conductivities all give extremely similar values of current density. This figure also shows that as the applied voltage is

increased, there is an increase in current density induced. This effect is stronger between 90 and 180V/m and less so after.

Table 6-9 shows how the current density varies at the chosen point as the electrical conductivity is varied but with constant applied voltages. Each potential gradient shows the same trend but with different values. It can be seen that electrical conductivities of over 10S/m give no extra current density at the chosen point (but are usually materials that are more expensive (silver, platinum)). It is also seen that a plateau begins to form under 0.001S/m. Gray (1970) stated that current densities under 1A/m^2 prove ineffective for dewatering. Thus, it can be said that for this bench scale test at 90V/m, an electrode with a minimum electrical conductivity of 3.75S/m would be required. For voltages of 180V/m and 500V/m, electrical conductivities of 0.175S/m and 0.012S/m are required respectively. As seen in Table 6-9, EKG electrodes have an electrical conductivity of approximately 0.027S/m, well below the 3.75S/m required and yet they perform dewatering perfectly well at 90V/m. Regarding specific electrode types, to attain a current density of 1A/m^2 from the PEG electrode, an applied voltage of approximately 138V/m is needed whilst stainless steel needs less than 90V/m.

Table 6-9: Current densities produced from various electrodes under different voltage gradients.

Electrode Type	**Electrical Conductivity (S/m)**	**90 V/m Current Density (A/m^2)**	**180 V/m Current Density (A/m^2)**	**500 V/m Current Density (A/m^2)**
EXTREME LOW	0.00001	0.000435	8.70E-04	0.0024
VERY LOW	0.001	0.036	7.21E-02	0.1998
LOW	0.01	0.1736	0.34728	0.964
EKG	0.027277	0.257	0.517	1.4314
PEG	0.49925	0.654	1.3092	3.636
LOWER MIDPOINT	10	1.113	2.2261	6.1835
MIDPOINT	500	1.1722	2.3443	6.512
STEEL	131926.1	1.1862	2.346	6.59
EXTREME HIGH	1000000	1.1733	2.3465	6.518

Figure 6-103 shows the minimum electrical conductivity of the electrodes needed to achieve a current density of 1A/m^2. It is seen, as expected, that the higher the voltage applied to the electrode is, the lower the electrical conductivity required is. This is due to higher electrical conductivity electrodes being more efficient at passing along their electrical current whereas lower electrical conductivity electrodes will not be as efficient and thus a higher voltage is needed to achieve an equal current density.

6.3.6 Site Trial Electrode Arrangement

Figure 6-106 and Figure 6-107 show the final design for the site trials. Figure 6-106 shows the current density field around the raked electrode trials as an aerial view of a selected slice of the clay. When the individual trials are put together in Figure 6-107, it is shown that current leakage between trials is not sufficient to cause effective electroosmosis as it is below 1A/m^2. This is acceptable for the site trials and the space restrictions involved.

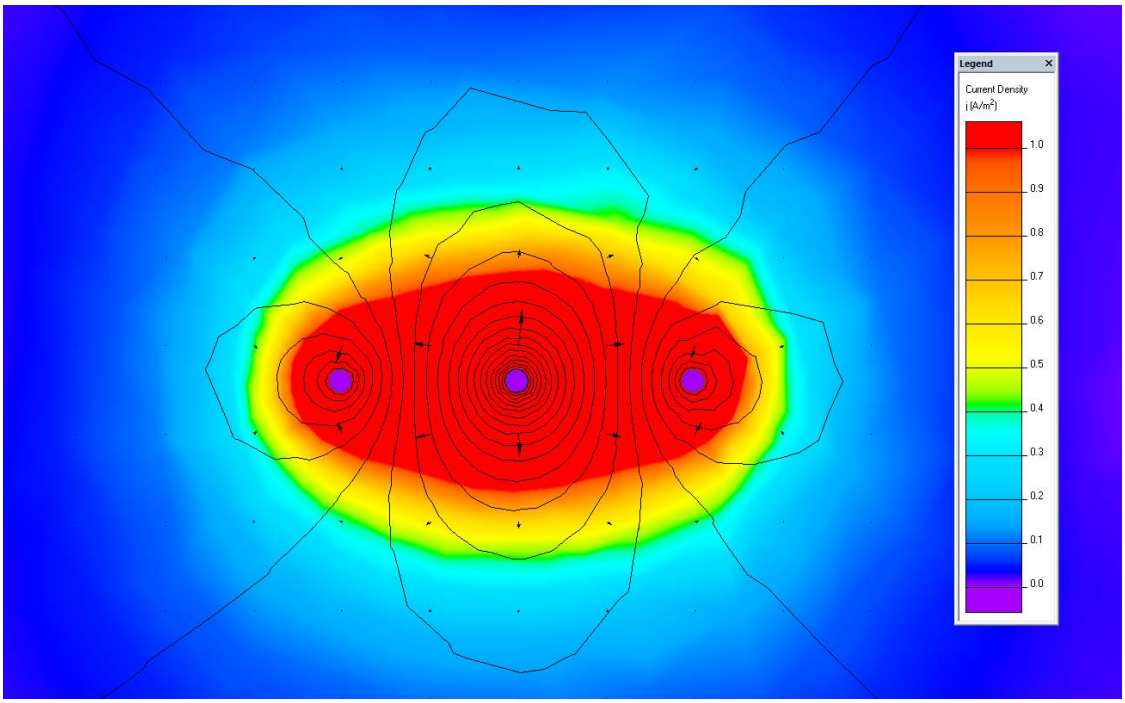

Figure 6-106: Raked electrode simulation aerial view.

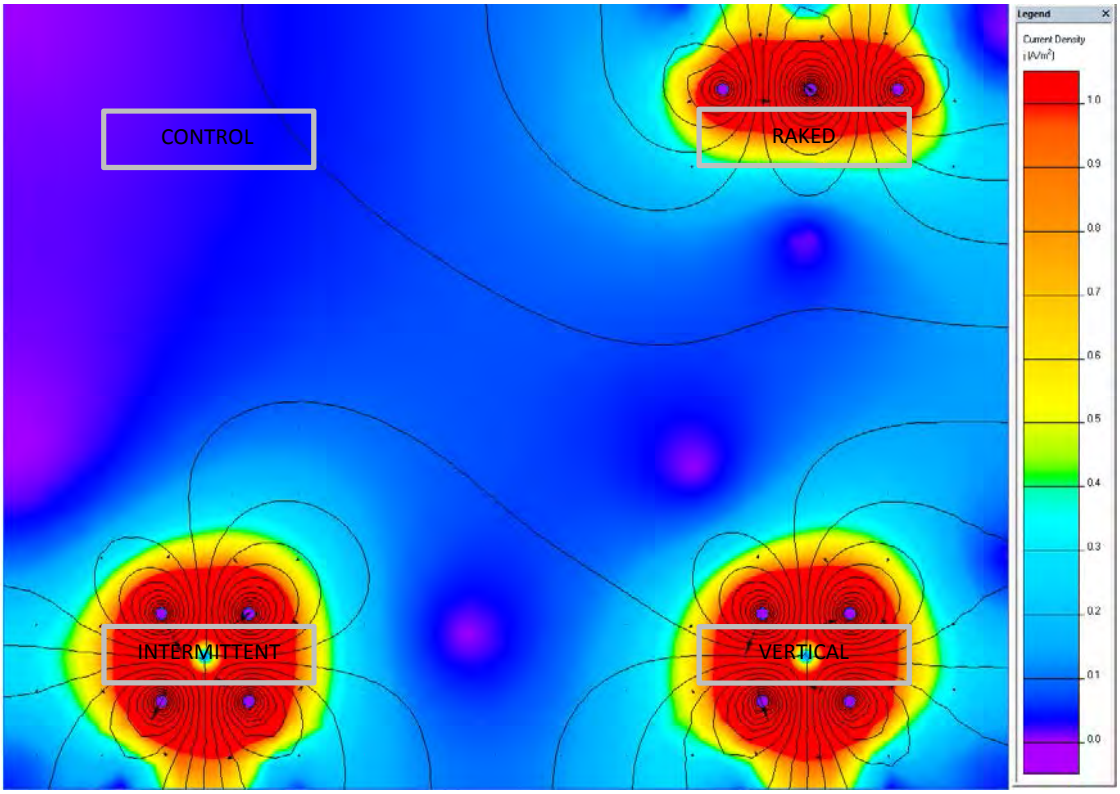

Figure 6-107: Site trial set out optimal layout.

6.3.7 Concrete Footing

Through various combinations of electrode insulation depth, it was established that under a voltage gradient of 18V between electrodes 22cm apart, insulating the electrodes to double the depth of the foundation is sufficient to avoid the current density pushing the acid front to the foundation location, Figure 6-108.

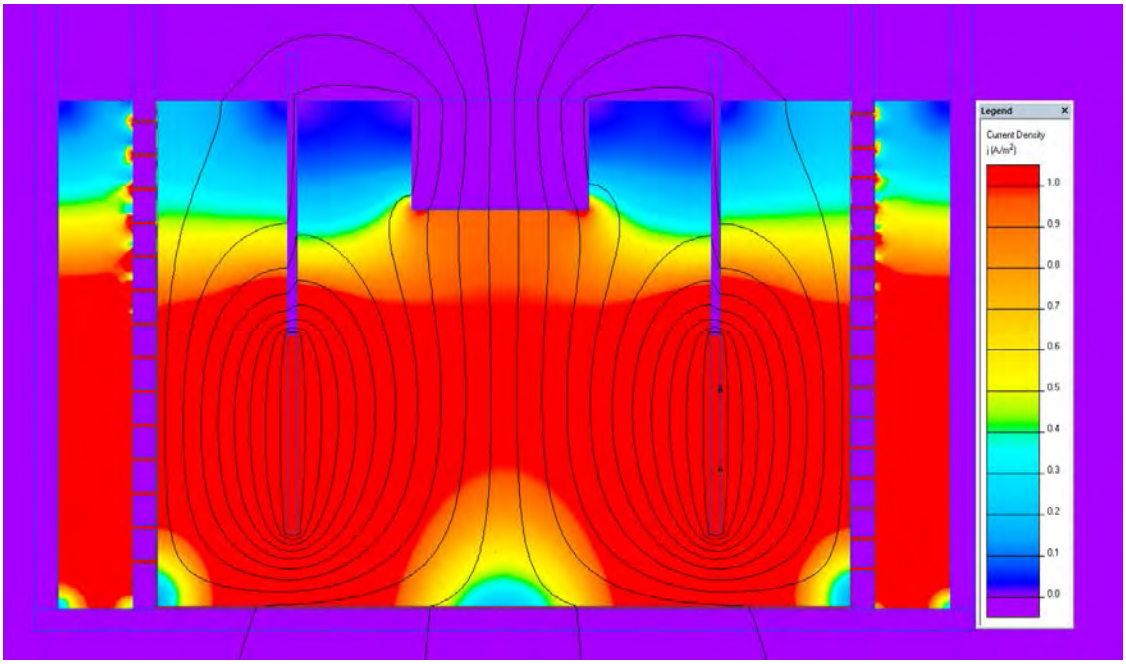

Figure 6-108: Numerical simulation concrete footing.

6.3.8 Numerical Simulations Summary

This section has shown some of the possibilities when simulating dc current densities in a clay medium where the current density can be used as an indicator for electrically induced fluid flow. Although no validation of the software has taken place, the results can be used indicatively.

The test cell filter effect has found that an impact is produced by the filter paper only when a fluid of greater electrical conductivity than the clay is being used. With the need for filter papers to avoid blocked drainage holes, this cannot be avoided. As Figure 6-21 shows however, once the clay reaches a certain water content, it will have an approximately equal electrical conductivity as the fluid in the filters and such should not affect the system. The problems will occur when using clay which is dry of this water content.

With the electrode arrangement simulations it was found that offsetting the electrodes eliminated the current density voids. Unfortunately, due to an update of the software, this void was not discovered until after the physical testing of the site trials samples had taken place whereby the centre of the four electrode systems was a chosen testing location. It's interesting to note that the current density blackspot in the centre of the four electrode system is removed when offsetting the electrodes as in Figure 6-98.

When comparing the stainless steel electrodes and the PEG electrodes using this simulation software, it was found that the stainless steel provides an increased uniformity of

current density to the clay than the PEG as expected. It also shows that the PEG current density will decrease with depth from the electrode power connection due to the PEG's electrical resistance. This would prove problematic when considering electrodes of a potential 2m length as could be expected on some commercial schemes.

The site trials were simulated to ensure current leakage between trials was not produced. A design for the size of each footing and distance between footings was devised using the data calculated here with final simulations taking into consideration the depth of electrode insulation required to avoid current density levels around the concrete footing becoming large enough to allow the acid front to migrate to the location. It was found that the insulation depth required was twice the depth of the footing from the ground surface.

6.4 Laboratory Results Summary

This section has taken ideas gained from the literature base and built upon them in a laboratory setting to increase the understanding behind their methodologies and mechanisms and take them a step forward.

A previous research study experiment was repeated to assess both the existing methodologies and equipment available in the laboratory. It was determined that the methodology was sound but some equipment required modification for improved performance.

Chemical combinations were evaluated for their effectiveness in increasing shear strength and decreasing shrink/swell behaviour in English China Clay. The 3% mix by weight of 2/3 $CaCl_2$ and 1/3 Na_2SiO_3 proved most effective for improving the clay when mechanically mixed. Its increase in shear strength and low cost make it a viable option for stabilising clays.

The electrical conductivity of the system will inevitably affect the effectiveness and therefore speed of treatment. As expected, the introduction of charged ions into the system increased the electrical conductivity of the system. It is interesting to note that RO water saw a 300% increase in electrical conductivity over the 20°C temperature increase whereas the tap water and chemical mix saw a 20% decrease over the same temperature range. From this it could be taken forward that for site trials, a cooler ambient temperature may be more beneficial for electrokinetic effectiveness.

Polarisation of the electrodes looks to be a retarding factor on site which could render them ineffective very early into a treatment regime. It was found by testing various electrode arrangements that the four electrode system was most effective at delaying the onset of

polarisation and was also most effective in its relaxation process. It would suggest that due to the available charge in the system being spread between multiple electrodes, the build-up of charge is therefore diminished by increasing the number of electrodes.

The current intermittence trials proved that polarisation of the electrodes does occur in a clay system and that by interrupting the power supply, the system is allowed to relax leading to a recharge in power supplied to the clay. It was found that a power supply ratio of between 0.67 and 0.75 is ideal for ECC at approximately 33% water content and when using stainless steel electrodes. It is unfortunate that London Clay was not tested using intermittent current as it is anticipated that the optimum power supply ratio would be different for each clay.

The majority of this section has been dedicated to the development of the electrodes in their ability to be practical yet electrically effective as from the literature it was found that studies in this area tend to use various materials, shapes and types which leads to a fragmented knowledge base. The electrodes used in the literature all tend to be impractical too, meshes cannot be inserted easily around a strip footing and materials like platinum and copper being expensive and a likely target for thieves. Therefore, an electrode type was developed called the PEG, based on the EKG which had successfully been used in the literature. The 35% graphite mix for the PEG electrode was shown to be most effective for workability and electrical attributes. Theoretically, this PEG is a more effective electrode than the EKG and it is thought may prove to be so if professionally moulded like the EKG. It's electrical surface resistance was lower than the EKG along with its electrical resistivity. It was proven to successfully perform, albeit slowly, in the PEG trial which saw the PEG electrodes used as both anode and cathode. The low transference of current to the clay lead to the development of the PEG cathode trial in an effort to reduce costs of EKS treatment by using a longer lasting cathode. Figure 6-109 shows the comparison between the previous research repeat using the EKG, the PEG cathode trial and the long term PEG trial. Taken only indicatively, it can be seen that the PEG cathode tends to be improved over the other trials at higher water contents with the long term PEG trial being more successful at lower water contents. The PEG cathode possessed a higher electric current than the long term PEG trial and is more successful at higher water contents. The long term PEG trial was run for a longer period of time than the PEG cathode and was more successful at lower water contents. This is logical and can be shown using equation 2-15 and equation 2-16, where a high water content would lead to a low viscosity and ultimately a high flow rate whereas a low water content would lead to a low flow rate. This would result in a longer treatment time

requirement to produce an equal flow, where flow is a proxy for clay fabric alteration. This is useful in that when treating a clay, one can economise by deciding on a long treatment time or higher electrical current by water content of the clay.

The degradation of the PEG electrode in fluids and then under electrolysis was promising in that the electrodes do not lose mass and over longer periods of time such as 56 – 109 days, possess lower surface resistances than stainless steel. The main negative is the current transference from the PEG to the medium between the electrodes is very low compared to the other electrodes. The reasoning behind this has yet to be found as the resistivity and surface resistance are lower than that of the EKG but is anticipated to be related to electrode shape. It is suggested that the re-usable electrode could be more suitable for long term treatments or permanent installations due to its long term effectiveness.

The mock footing trial was produced to assess the effect of the chemical migration under electrokinesis on the level of a strip footing and the integrity of it. It was shown here that the levels were not noticeably affected and no impact on the strip footing was observed.

The numerical simulations show indicatively how the filter paper can affect the EKS process when using highly conductive fluids, offset electrode arrangements are optimal for avoiding current voids and stainless steel electrodes are more effective than the developed PEG electrodes. It was also shown that a band of clay or boundary filled with fluid that is more electrically conductive than the surrounding clay will form a preferential flow path for the current and likely the fluids too. It was then shown that the electrodes should be insulated to twice the depth of the footing to avoid interference between the electrical current and the foundation.

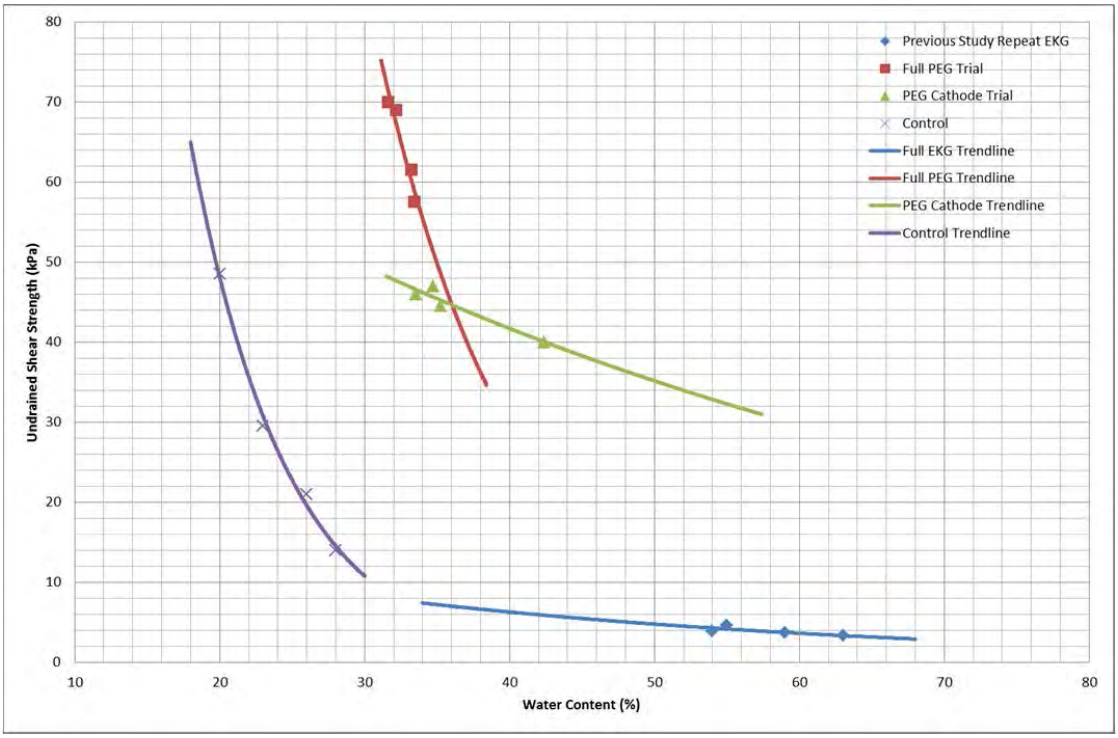

Figure 6-109: Comparison of EKG and PEG arrangements in ECC.

7 SITE TRIAL RESULTS AND DISCUSSIONS

7.1 Introduction

This section concerns the results gained from the electrokinetic soil stabilisation site trials and the discussion of this data. Knowledge and data from previous sections will be drawn upon to clarify and highlight certain points within the data that are of particular use. Particular focus will be shown to the following:

- Are the stabilising chemicals shown to migrate to the treatment zone and successfully manipulate the geotechnical characteristics of the location?
- Does the EKS process affect the surrounding environment?
- Is the process economical compared to traditional methods?
- Is the methodology used herein, practical?

Further photographs can be found in Appendix G.

7.2 Methodology

Here, the methodology used will be discussed and weaknesses highlighted for further development. During installation of the electrodes and foundations, it was found that the sub surface was not as the historical ground investigation borehole indicated. The treatment programme was designed to operate in London Clay however the sub surface was found to consist of made ground. This in itself introduced considerable delays in electrode hand installation and would go on to affect the treatment process through the provision of a severely heterogeneous stratum. It should be noted however that the made ground was comprised of London Clay with London Clay content increasing with depth as seen through visual inspections of the electrode drilling tailings. Due to the variability of the material it would be too difficult to estimate London Clay content. It is considered that this lack of homogeneity is actually of benefit as any positive results garnered from this experiment can be deemed promising for future work due to the 'worst case' characteristics of this treatment soil matrix. As such is it suggested that the arguments presented herein have validity.

7.2.1 Electrode Implementation Practicalities

The method upon which the electrodes were inserted into the ground was an extension of the method used in the laboratory. Whereas the laboratory clay was homogenous, site clay is not.

The gravel, brick fragments and stones proved to be difficult to drill through. Hand auguring the ground to a 1m depth is not practical considering the time it took to get the eleven holes completed. The author spent fifteen days drilling the electrode holes and had to build a 6ft spike to hammer through bricks, stones and gravel along the way.

Furthermore, due to the holes being hand augured and then the electrodes being inserted afterwards, the holes were not a perfect fit for the electrodes. This led to insulation coating being scraped off by stones and gaps between the electrode and the clay. The missing insulation coating would have led to current leakage, albeit minimal, and the gaps led to excess fluid being forced up and onto the ground surface instead of into the electrode container.

7.2.2 Stabilising Fluid Implementation Practicalities

The system devised to apply the stabilising fluids in a controlled manner into the electrode containers did not function as expected. The system as described in section 5.6.2 proved to leak and intermittently stop allowing fluid flow. Resealing was attempted but it is thought that the Tupperware used for the electrode toppers was coated with a non-stick material. Evo-Stick PVC Weld adhesive and hot glue were used to try and keep the electrode topper attached to the electrode topper base but nothing resulted in success.

Once the flaw was discovered, it was decided to replace this system with hand filling the electrode containers with the stabilising fluids. This was more time consuming and less remote than planned but did appear successful.

7.2.3 Sample Extraction

Although U100 extraction was planned for these site trials, it proved impossible to follow through with. The only remaining option was manual extraction. This proved difficult in the quagmire like conditions where due to the footings being extracted, the sides of the excavations began to collapse and the trenches filled with water. A water pump was required to dewater each trench before sample taking could begin. The immediate areas around each electrode were destroyed by digging, the mini digger and removal of the electrodes so only one out of eleven was intact enough to take samples.

Due to the external contractor, GIP UK, taking some samples for testing, no remainder of that clay was received leading to gaps in the testing for shrinkage and pH due to not having enough of that locations clay for testing.

7.2.4 Monitoring

After the telemetric data logger ideas were scrapped, the dial gauges were to be read manually. The dial gauges were difficult to read due to their proximity to the ground, cabling from the resistivity measuring equipment, condensation on the Tupperware boxes and deterioration of the ground from traversing the site. It was also noticed that the gauges would jump if the scaffolding poles were knocked, which at near ground level they were frequently. After the test completion, the poles were deliberately knocked to determine the effect. It was seen that the gauges would jump but return back to their original readings so no permanent damage was done. The intermittent current footing produced level data for the first few days but then after a rainstorm, the footing dropped significantly vertically downwards. The drop was so significant that the dial gauges could not be moved far enough down to meet the top of the footing without moving all of the reference frame. It was decided therefore to carry on without this data. The reason for the drop was unknown but could be due to an unforeseen cavity under the footing or possibly due to the mice living around the footings.

The power supply had a memory card to record all data which was tested in the laboratory successfully but once on site was intermittent as to if it would actually record anything. Thus it was necessary to take readings manually when on site in case of the event of failure to record.

Monitoring the temperature thermocouples was straightforward but as proved with the intermittent test, the thermocouples are fragile. Two of the thermocouples stopped transmitting data on day 46, possibly due to rodent activity.

7.3 Monitoring Results

The trials to which the following data belongs to consisted of two weeks of water seeding followed by six weeks of chemical introduction.

7.3.1 Voltages

The voltages measured in the site trials are shown in Figure 7-1. As seen, the raked and vertical electrode trial footings have regular voltages of approximately 25V whereas the intermittent current trial has a dynamic voltage. The reason for this was not ascertained on site as connection and wiring checks revealed no problems and the power supply was thoroughly checked in the lab before and after the site trials and anticipated performance was recorded.

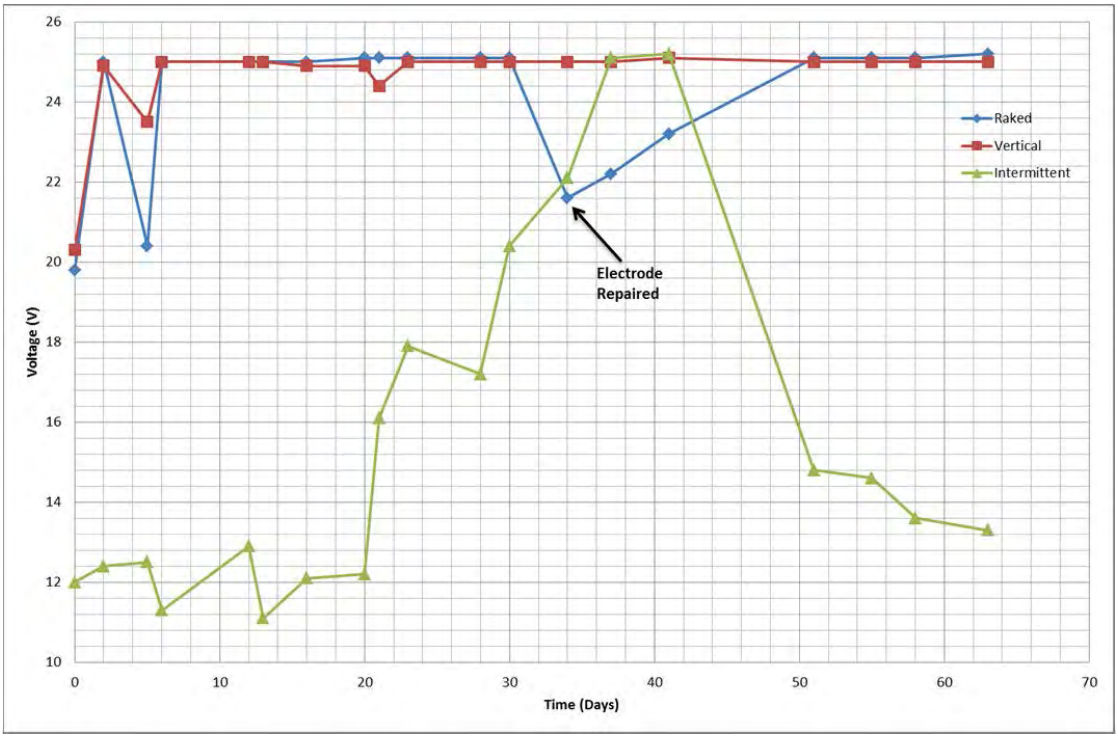

Figure 7-1: Site trials voltages.

7.3.2 Current

The electric currents measured on site are shown in Figure 7-2. As seen here, the electrode performance for conducting the electric current is variable. Obviously once the electrodes were installed, removal for inspection was impossible so the only method of ascertaining their effectiveness was the level of electrical current passed between the electrodes. Figure 7-2 also shows where connections were replaced and heavy rain and surface flooding occurred. It is observed that the power interruption from a tripped socket on day 6 saw the current drop for the raked and vertical electrode trials and continued to drop until a short rise was seen on day 21 when the site surface had flooded from heavy rain. The current intermittence seemed unaffected. The raked electrode trial continued to drop to 0A for a few days when advice was sought from Professor Nigel Cassidy regarding the possibility of electrode polarisation being the culprit. Further investigation into the wiring revealed a corroded wire not visible from previous inspections. At this point the wiring was repaired and an instant return to the initial current was observed leading to the assumption that the electrode was sufficiently undamaged by corrosion to continue.

Days 34 to 37 saw the ground frozen with negative air temperatures recorded. There is a dip in the electrical current seen at this point in Figure 7-2 most likely due to the electrical

conductivity of the clay and electrolyte being reduced by freezing. It is most likely to be just the electrolyte being affected by the temperature decrease here as the clay is at a depth at which ambient temperatures have little effect. Day 55 saw the electrode connections and wiring being repaired for the vertical electrode trial. This saw an immediate boost to the electrical current as expected. The electrical current did not return to original levels thus leading to the assumption that the electrode itself was degraded at this point. The decrease in electrical current in the raked electrode trial from day 34 onwards was found to be due to electrode corrosion after electrode extraction as no damage was revealed through usual inspections during the testing. Although the intermittent current trial electrodes were corroded after extraction, it can be seen from Figure 7-2 that the corrosion had little effect on the electric current supplied. It should be noted that the current intermittence trial showed the most consistent current transfer.

Figure 7-3 shows the change in temperature recorded under the footings with change in electrical current supplied to the clay. As one would expect, the vertical electrode trial saw an increase in temperature with increase in electrical current. The raked electrode trial saw no increase in temperature with increase in current and the current intermittence trial saw a rapid increase in temperature over increase in electrical current. One could speculate that the vertical electrode trial and current intermittence trial should not experience a change in temperature with electrical current as if this does happen, then the influence of the EKS is in the zone of the footing. From the numerical simulations in section 6.3 it can be seen that the electric current will reach the footing but not at a high enough concentration to cause effective electroosmosis. It could however be enough for clay temperature change.

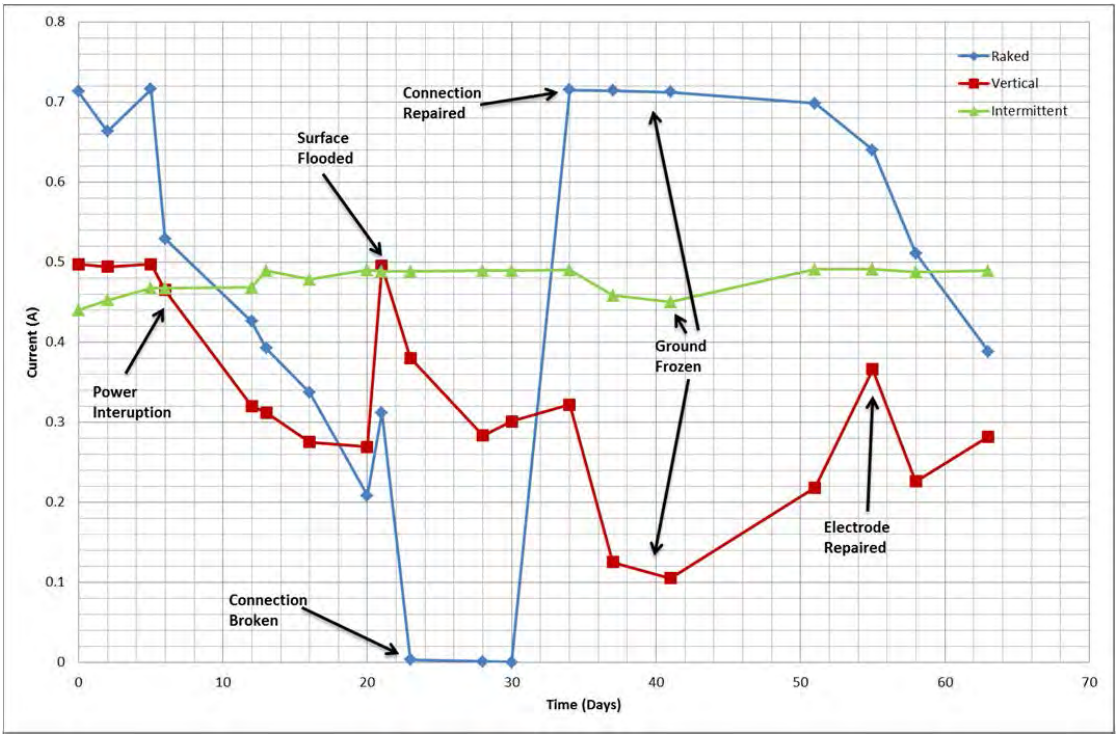

Figure 7-2: Site trial electrical currents annotated to show site conditions.

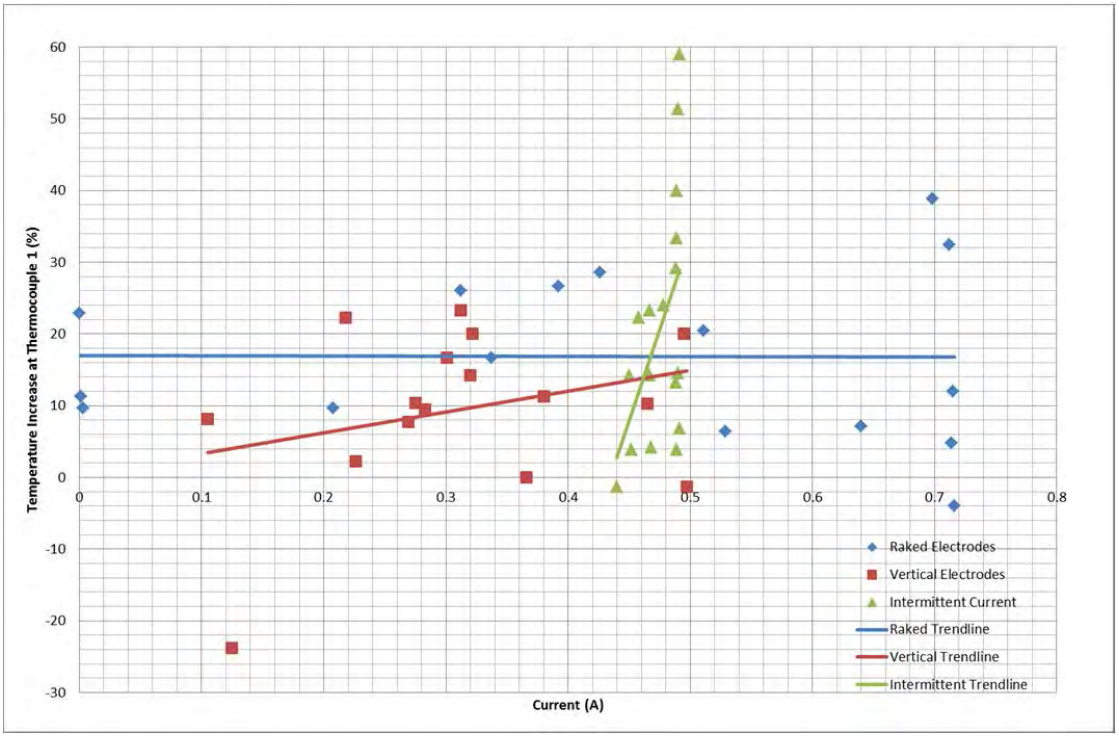

Figure 7-3: Site trial current against temperatures underneath the mock footings.

7.3.3 Power and Cost

The power calculated can be seen cumulatively in Table 7-1 and Figure 7-5. It can be seen that the general increase gradients can be matched to the current trends in Figure 7-2. The raked electrode trial can be seen to increase dramatically in current between day 30 and 40 whilst it is also seen that a 50W increase in power exists. This is due solely to the fact that power is the product of the voltage and current; an increase in current will see an increase in power.

Table 7-1 and Figure 7-4 show the power usages over each trial's lifespan. It is interesting to note that the raked electrode trial uses the most power followed by the vertical electrode trial and then the current intermittence trial. The vertical electrode trial and current intermittence trial are similar in power with only approximately 11W difference whereas the raked electrode trial is nearly 50W greater than the vertical electrode trial. This could be due to the electrode arrangement. The current intermittence trial using the least amount of power correlates with previous studies as seen in section 3.7.4.

Table 7-1: Site trial total power usages and total power costs.

Trial	Total Power Usage (W)	Total Power Cost (£)
Raked Electrode	204.55	1.94
Vertical Electrode	152.33	1.22
Current Intermittence	141.43	1.30

The cost of each trial was calculated and the cumulative results are shown in Figure 7-5. Due to the cost of the trials being linked directly with the electrical power consumption, the trends in this figure match the trends in Figure 7-4. It can be seen that there is a sharp rise in cumulative cost in the raked electrode trial once the electrode connections are replaced on day 34.

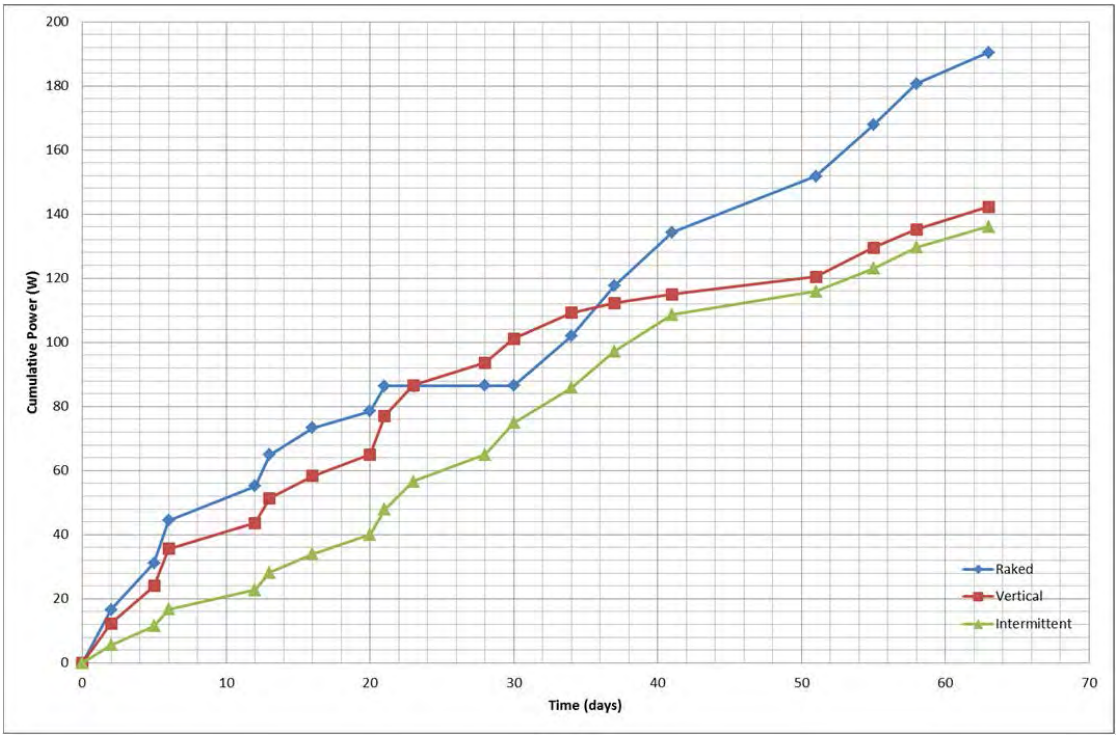

Figure 7-4: Site trial cumulative electrical power usage.

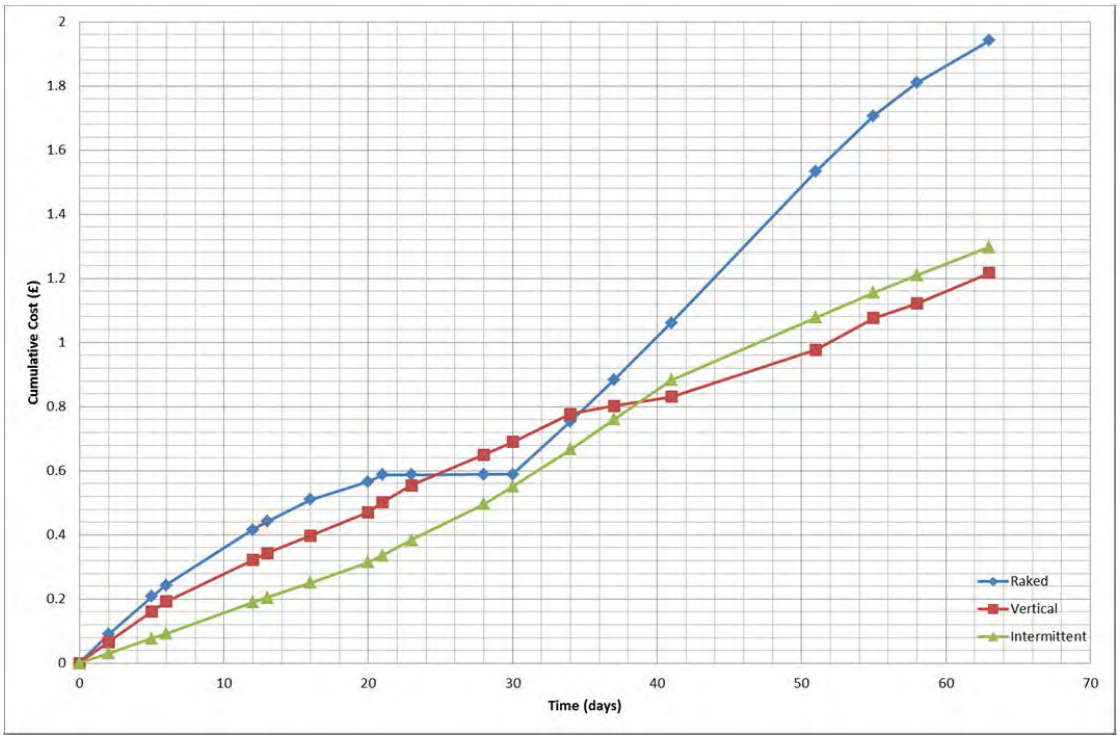

Figure 7-5: Site trial cumulative electricity costs.

7.3.4 Ground Resistivity

The resistivity measurements taken by Professor Nigel Cassidy are presented graphically in Figure 7-7 – Figure 7-10. Figure 7-7 shows the readings taken before the EKS process was initiated but with the electrodes in place in the ground. Figure 7-8 shows the readings taken on day 6 of the EKS whilst just water was being migrated through the soil. Figure 7-9 shows the readings taken on day 34 when water and the stabilising chemicals were being migrated. Finally, Figure 7-10 shows the readings taken after the trial had completed.

It should be noted that the top rectangle on each layer in each figure represents the footing belonging to the raked electrode trial and the bottom rectangle represents the vertical electrode trial footing with the orientation being that the Willow tree is to the right of each figure.

Figure 7-7 shows how before the treatment process had begun, the apparent resistivity appears to be fairly consistent with depth below ground level with peaks and dips as expected in natural clay. The low apparent resistivity of the section in the top left of Layer 1 in this figure could be due to the trench dug to allow installation of the raked electrodes. Figure 7-8 then shows that after 6 days of EKS, the apparent resistivity over the whole area at all depths drops. This could be seasonal due to the rain. It is interesting to note that over the three depths at this date, the lowest apparent resistivity exists under the footings indicating a higher water content in the treatment zone area.

Day 34 shown in Figure 7-9 shows that low apparent resistivity readings exist under or around the trial footings but not as precisely as the targeted treatment zones were planned. This may be due to the drop in electrical currents for both trials at the time. The final readings were taken after the culmination of the trials and can be seen in Figure 7-10. Here can be seen that after the electrode connections were repaired, the apparent resistivity decreases again under the trial footings, especially at the 0.8m depth.

Table 7-2 and Figure 7-6 shows how the average apparent resistivity drops after EKS is initialised for both trials with a steady increase over the rest of the experiment. This may be due to surface flooding leading to preferential current flow and frozen ground and the initial drop due to seasonal water contents. Another feature noticed is that apparent resistivity appears to decrease with depth at all stages of the trials.

Table 7-2: Site trials apparent resistivity readings estimated from graphical figures.

Day	Layer (m)	Trial 1 Apparent Resistivity (Ohm.m)	Trial 2 Apparent Resistivity (Ohm.m)
Before	0.8	40-60	40-60
	1.3	35-60	22.5-45
	1.8	30-90	10-70
6	0.8	31-36	30-34
	1.3	18-34	27-30
	1.8	16-27	18-23
34	0.8	36-40	34-43
	1.3	23-36	28-30
	1.8	19-29	22-23
After	0.8	32-37	32-39
	1.3	23-34	28-31
	1.8	16-29	22-25

Aside from the EKS treatment beginning, tree root die off can't be discounted for the transition between before EKS and 6 days, as when the ground becomes wetter due to seasonal rain, extended tree roots tend to die off. This lack of water suction along with seasonal water content increases could be the reason that apparent resistivity appears to decrease. This would be surprising at 1.8m depth however.

Day 34 sees the apparent resistivity at 0.8m depth increase, this is the day when ambient air temperatures dropped to -6.5°C and caused the ground to freeze near the surface and the electrode connections at the vertical electrode trial were also repaired.

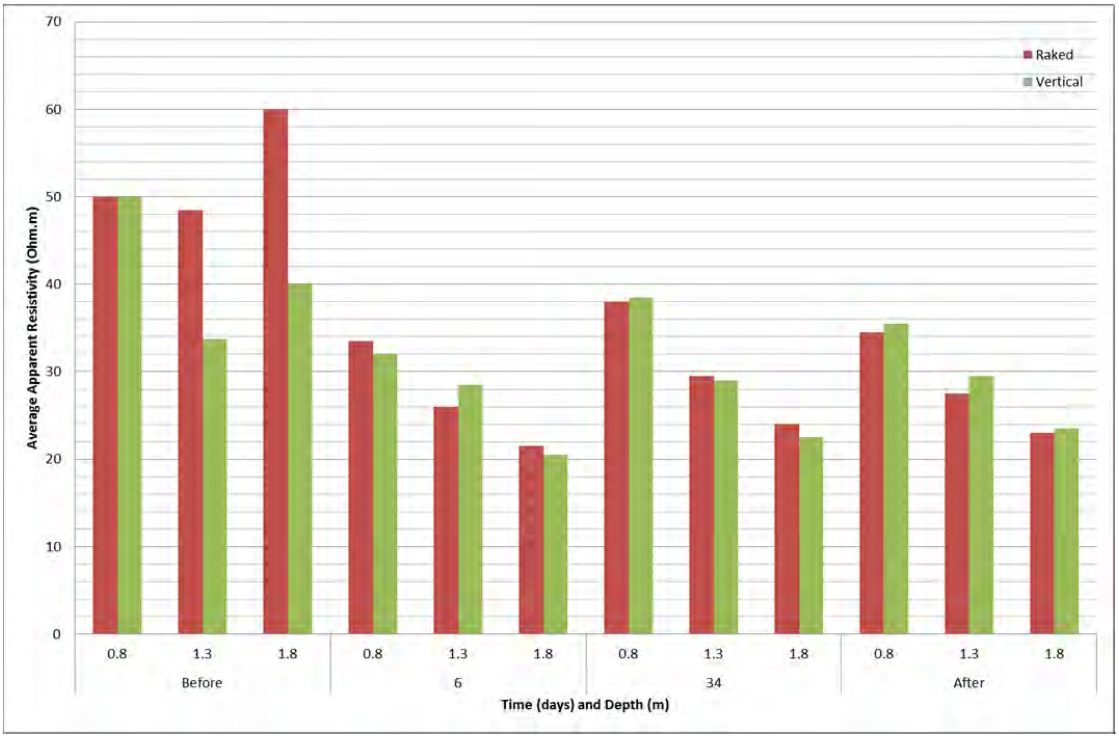

Figure 7-6: Site trial average apparent resistivity under strip footings.

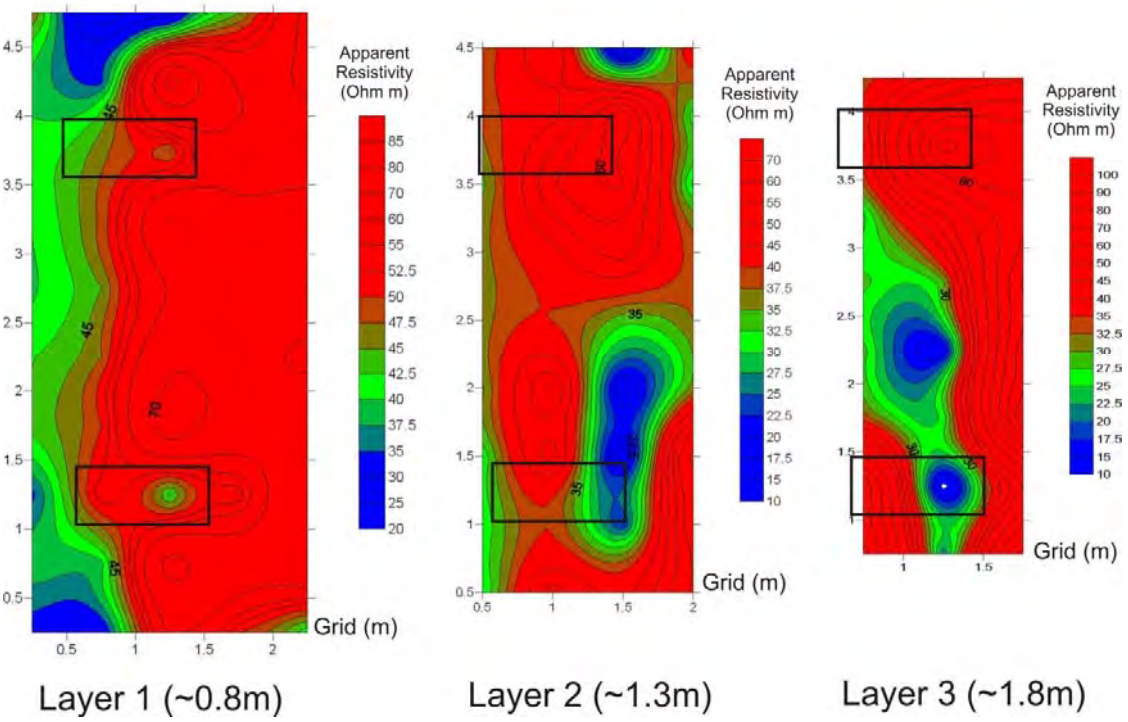

Figure 7-7: Site trial ground resistivity before treatment.

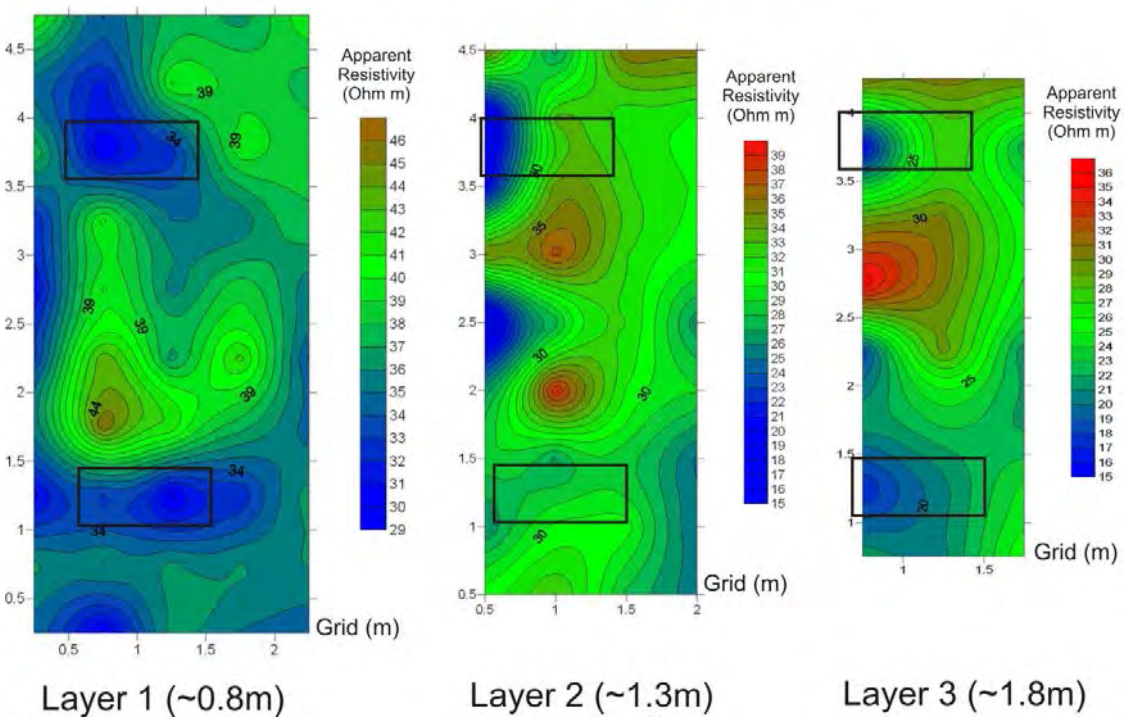

Figure 7-8: Site trial ground resistivity Day 6.

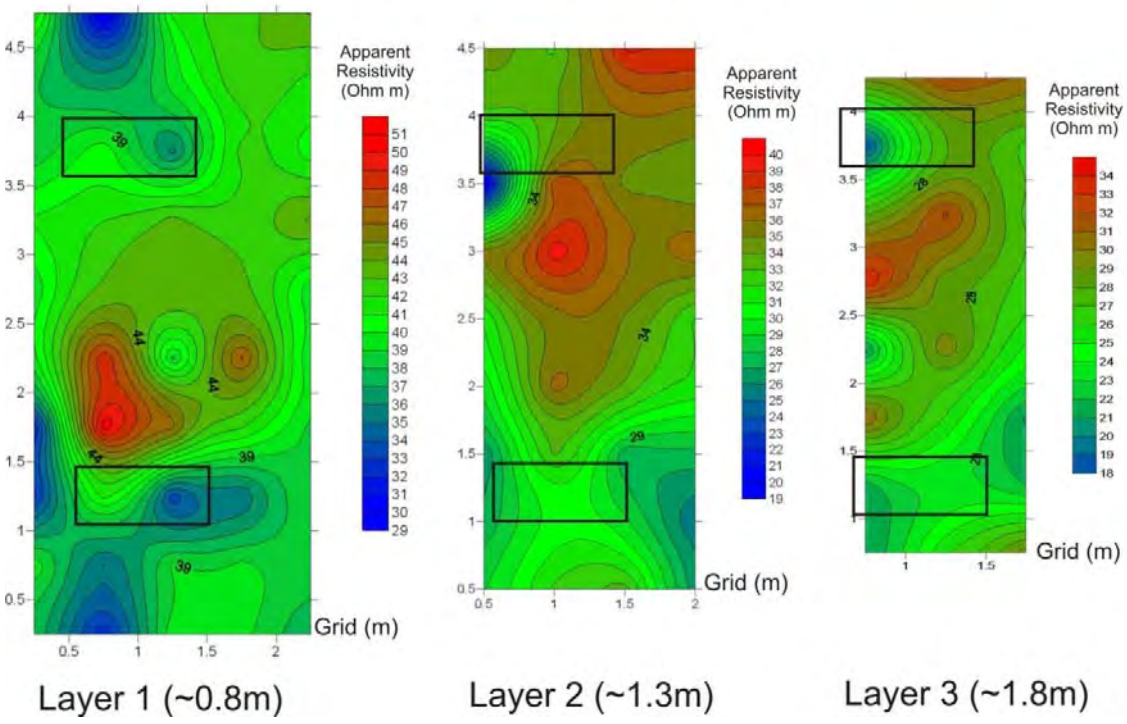

Figure 7-9: Site trial ground resistivity Day 34.

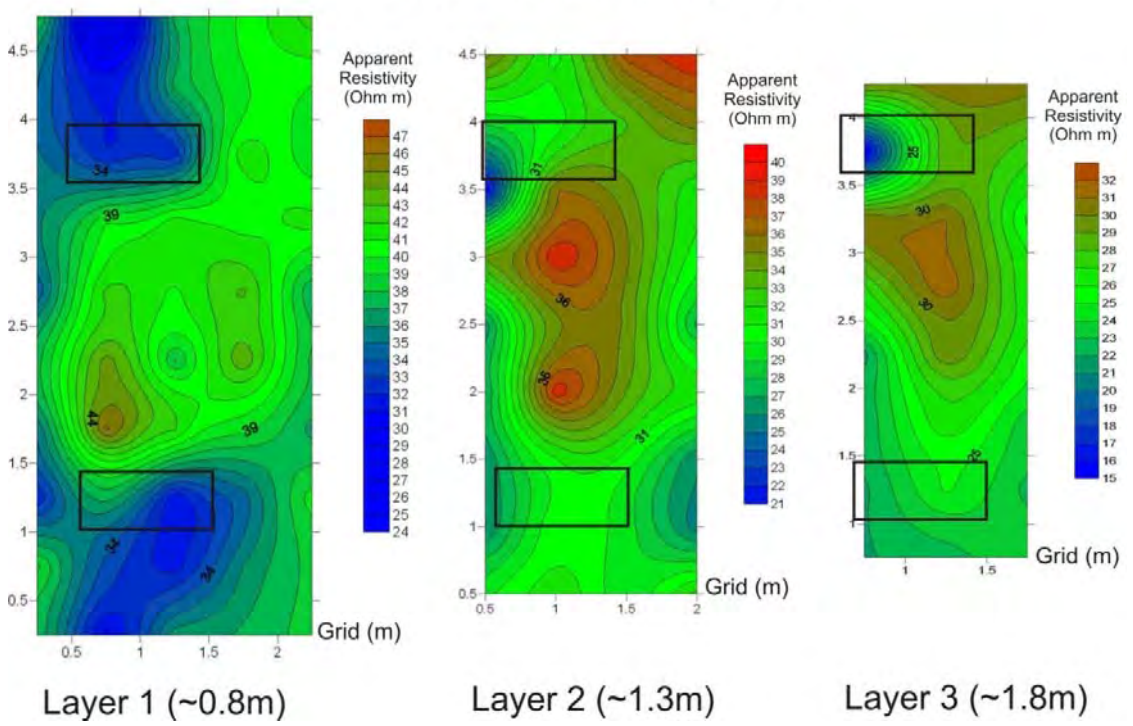

Figure 7-10: Site trial ground resistivity after treatment.

7.3.5 Temperatures

The temperatures measured under each footing are shown in Figure 7-11 to Figure 7-14. Each figure shows the ambient air temperature measured at the time of taking the readings.

It is seen that the temperatures under the footings generally follow the trend of the ambient air temperatures. This is as expected as the thermocouples were placed 300mm below ground level. It is known that an electric current travelling through a medium possessing resistance will create heat, it is therefore expected that heating of the clay around the treated trials will be present. Indeed this is seen from Figure 7-15 where the percentage increase in temperature over the control test for each trial is presented. It is seen that each treated trial has an average higher temperature in the clay beneath it than the control trial. When comparing the percentage temperature increase under each footing to the ambient air temperature, there is not an immediate correlation. It does however look as though when the ambient air temperature rises, the percentage temperature increase decreases. This is probably due to the EKS process keeping the clay at a fairly stable temperature, so when the air temperature warms the control clay slightly, the differential affect is reduced. It should also be noted that there is a

drop in percentage temperature increase on day 32 when a dramatic drop in air temperature is observed. This may be due to the excessive drop in air temperature affecting all four trials.

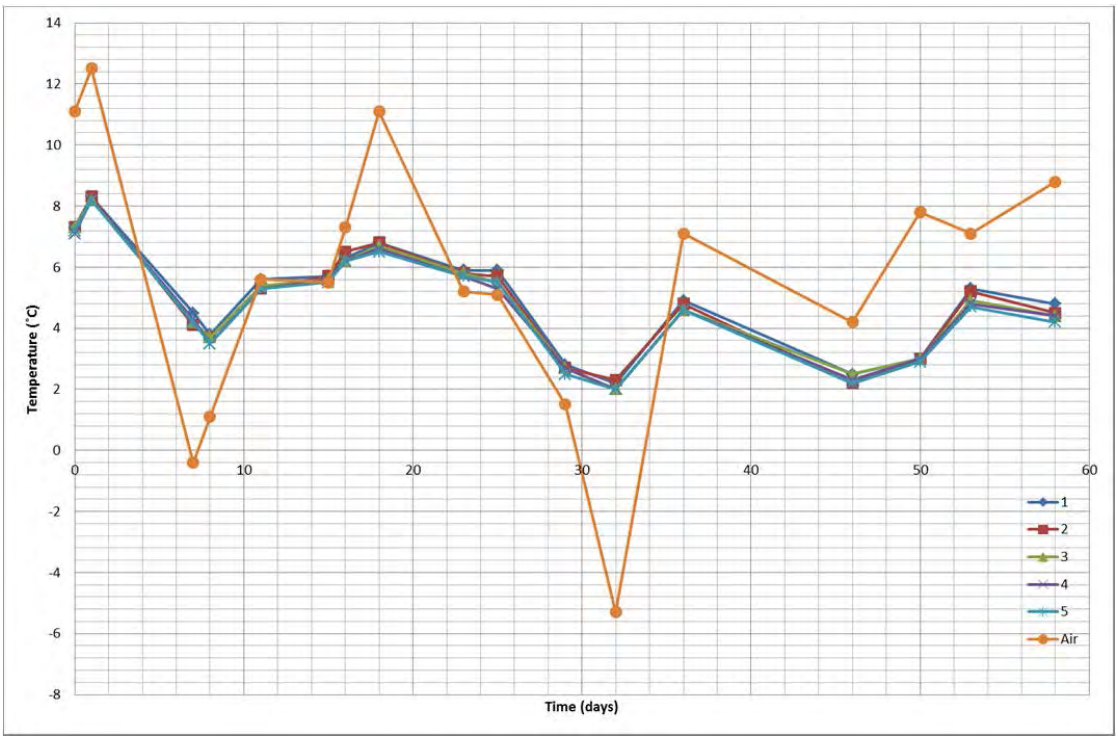

Figure 7-11: Site trial temperatures under raked electrode trial footing.

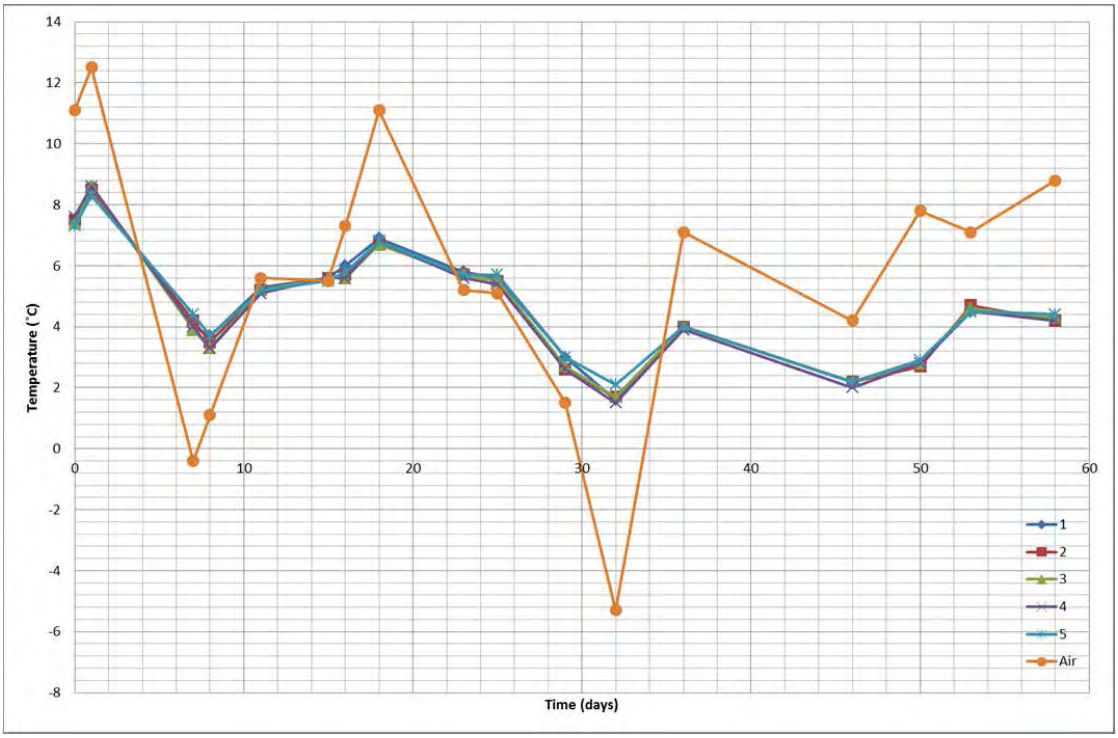

Figure 7-12: Site trial temperatures under the vertical electrode trial.

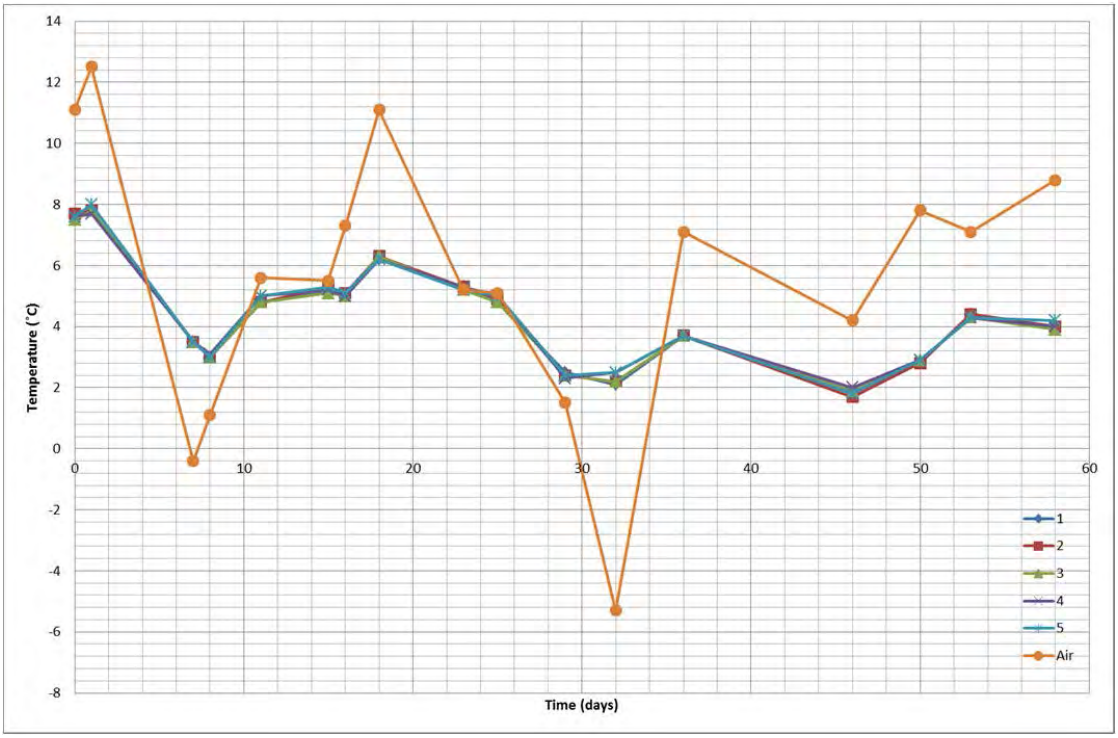

Figure 7-13: Site trial temperatures under control trial footing.

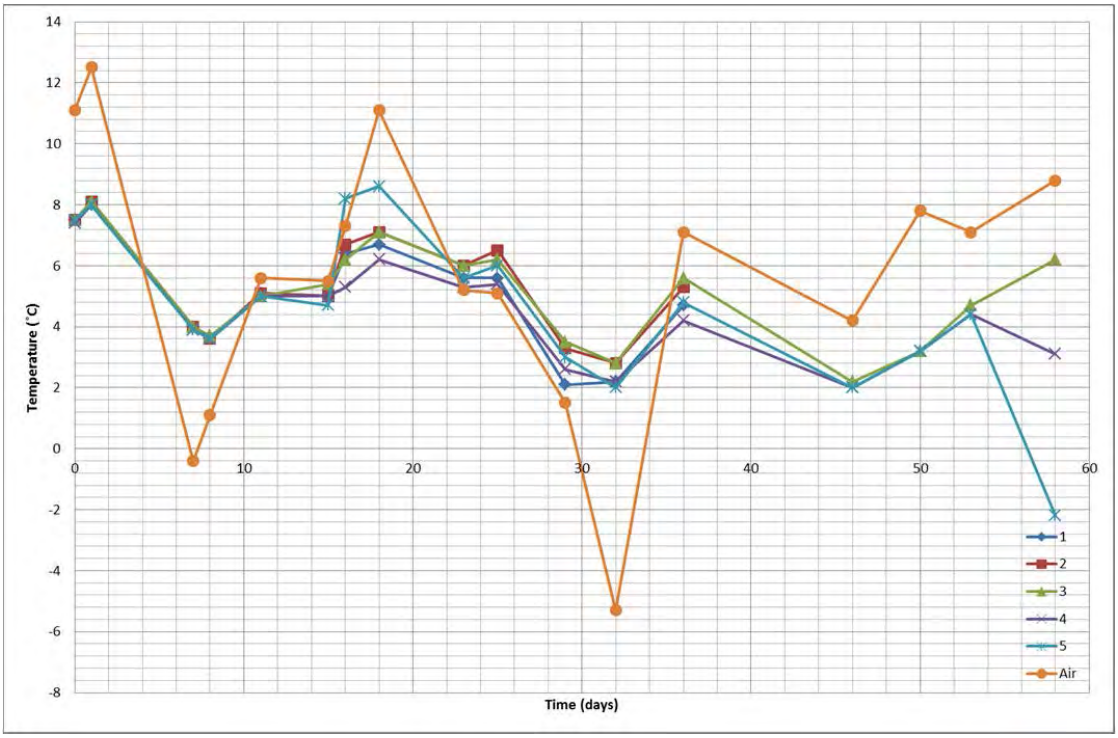

Figure 7-14: Site trial temperatures under intermittent current trial footing.

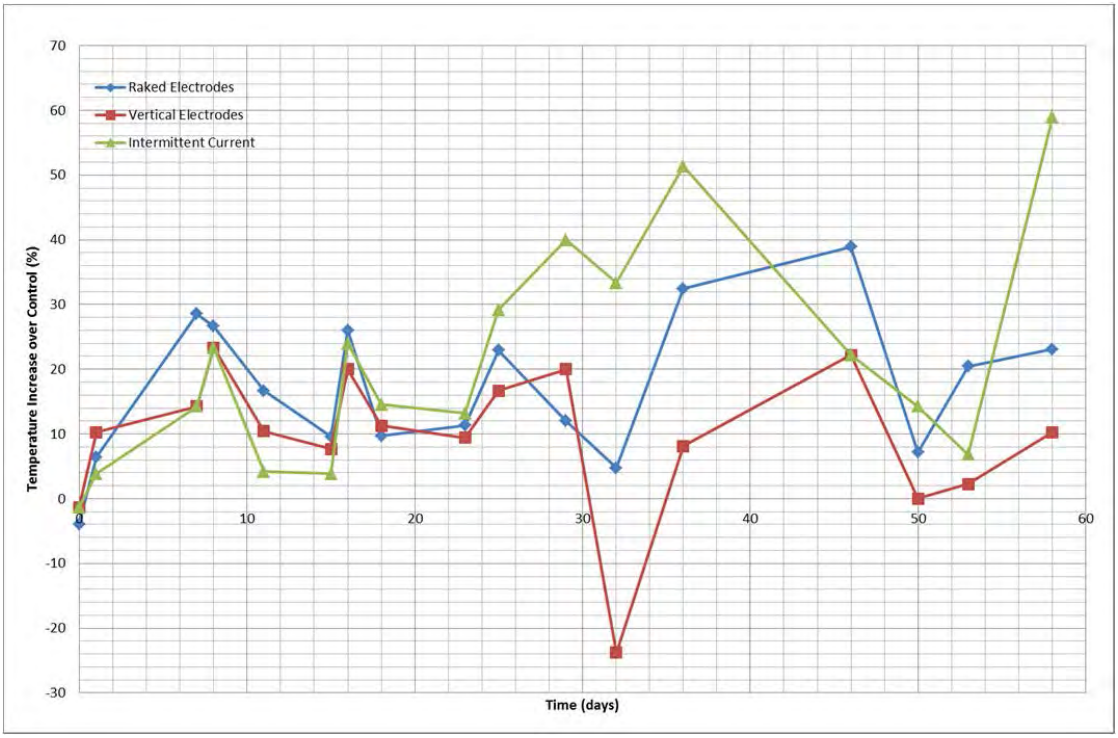

Figure 7-15: Site trial temperature increase for each footing over control footing.

7.3.6 Levels

The level data collected at regular intervals from the dial gauges can be found in Figure 7-16 to Figure 7-18. As seen from these figures, the levels between the raked electrode trial, vertical electrode trial and control trial vary very little over the treatment period. It can therefore be assumed that the process that has taken place under these footings has not negatively impacted the level of the footings.

Dial gauge 3 in the raked electrode trial does not follow the trend quite as the others do, this could be due to walking near the footing or a faulty gauge.

The current intermittence trial failed to collect worthy data due to the trials footing sinking after a significant surface flood leading to the gauges unable to reach the footing.

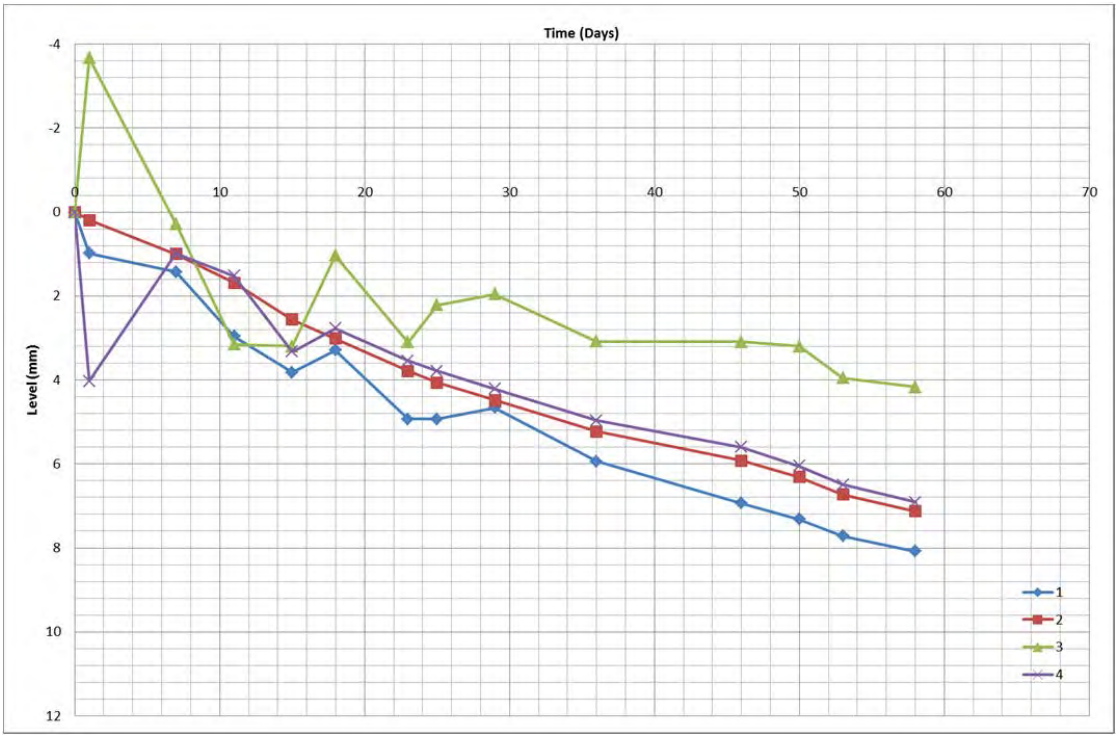

Figure 7-16: Site trial raked electrode trial footing levels.

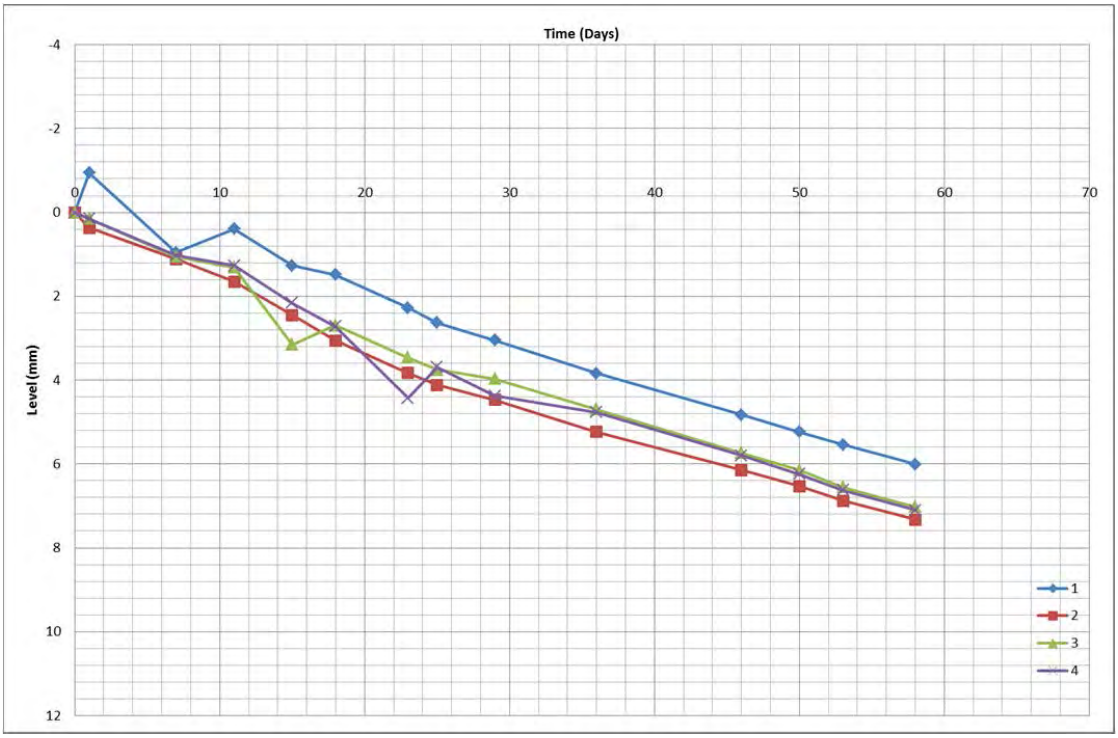

Figure 7-17: Site trial vertical electrode trial footing levels.

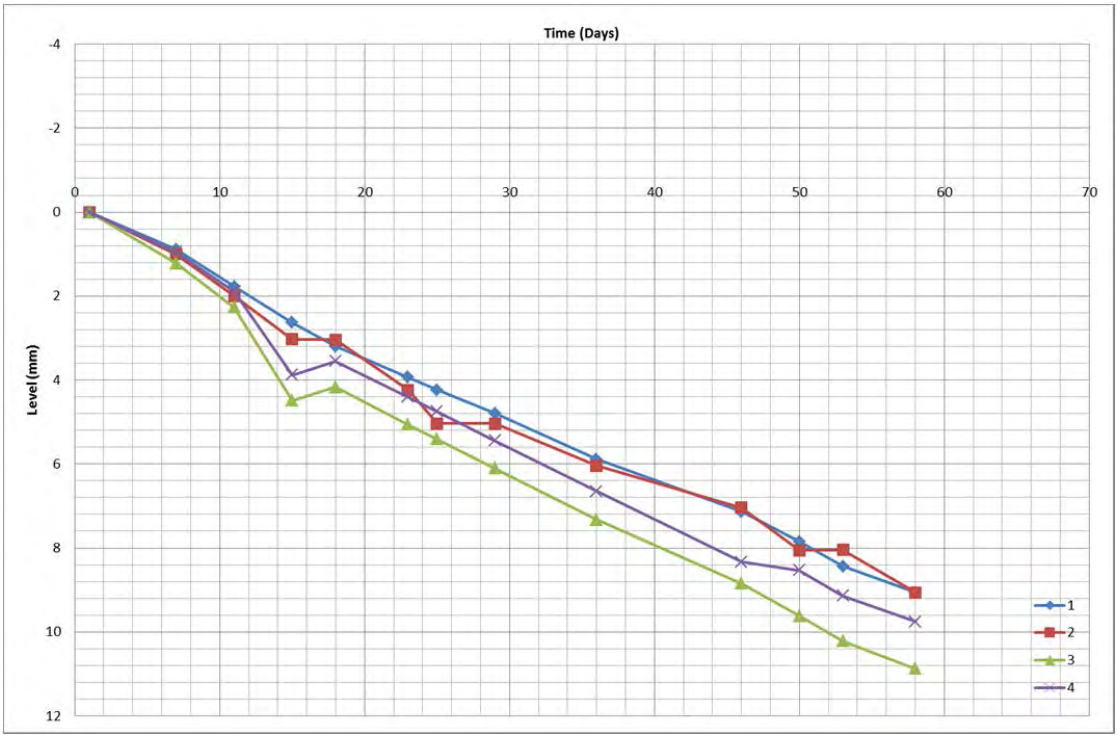

Figure 7-18: Site trial control footing levels.

7.3.7 Environmental Effects

Due to timing commitments and scheduling, the tree analysis by Duramen Consulting was not performed after the first reading. The tree did not appear to be damaged at all by the EKS process from a visual inspection by the author though. This is as expected due to the small size of the treatment zones compared to the size of the tree root system. Furthermore, the grass around the experimental zones did not visually appear to be harmed through and after the experiment.

A family of mice lived near the experimental set up with evidence of residence under the foundations. This would appear to indicate that the currents and chemicals did not harm the mice and as such would not be in danger of the proposed treatment technique.

7.4 Post Completion Results

The following section is a compilation of the site trial data gathered from testing the clay under the footings for each trial. Table 7-3 shows this data which will then be discussed. Testing marked with * denote tests carried out by GIP UK and tests marked with an x denote tests not carried out due to clay samples either not being possible to extract or clay samples being used up by previous testing.

As with any site testing, accuracy over that gained in laboratory settings is diminished due to site variability. Every effort was made to ensure accuracy and reliability of the data gathered at this stage and clear evidence of trends was produced which when considered in conjunction with the geophysical data produced, shows definite improvements in the clay geotechnical characteristics.

In these results, the centre of a trial is the very centre point under the footing and the end point is directly underneath thermocouple 5.

Table 7-3: Site trial clay data.

Sample Location	Level (m)	Average Level (m)	Water Content (%)	Liquid Limit (%)	Plastic Limit (%)	Plasticity Index (%)	Liquidity Index (%)	Linear Shrinkage (%)
Raked Electrode Trial - Centre	0.3-0.5	0.400	25.861	59.000	25.483	33.517	0.011	15.468
	0.5-0.7	0.600	28.578	70.000	25.840	44.160	0.062	17.857
	0.7-1.0	0.850	37.550	92.000	33.207	58.793	0.074	17.391
Raked Electrode Trial - End	0.3-0.5	0.400	10.416	70.000	27.600	42.400	-0.405	15.217
	0.5-0.7	0.600	28.681	72.000	26.594	45.406	0.046	17.143
	0.7-1.0	0.850	28.744	84.000	29.951	54.049	-0.022	20.000
Vertical Electrode Trial - Centre	0.3-0.5	0.400	19.112	72.000	30.779	41.221	-0.283	17.266
	0.5-0.7*	0.600	22.000	73.000	23.000	50.000	-0.020	x
	0.7-1.0	0.850	14.024	x	x	x	x	x
Vertical Electrode Trial- End	0.3-0.5	0.400	20.865	66.000	31.188	34.812	-0.297	17.143
	0.5-0.7	0.600	27.118	71.000	32.367	38.633	-0.136	18.571
	0.7-1.0	0.850	26.122	69.000	29.311	39.689	-0.080	18.929
Control Trial- Centre	0.3-0.5	0.400	21.492	85.000	25.876	59.124	-0.074	18.571
	0.5-0.7*	0.600	29.000	80.000	25.000	55.000	0.073	24.000
	0.7-1.0	0.850	25.057	61.000	24.322	36.678	0.020	17.143
Control Trial - End	0.3-0.5	0.400	22.813	66.000	25.677	40.323	-0.071	17.266
	0.5-0.7	0.600	20.747	68.000	26.075	41.925	-0.127	17.266
	0.7-1.0	0.850	21.569	72.000	27.986	44.014	-0.146	19.286
Intermittent Current Trial - Centre	0.3-0.5	0.400	14.111	86.000	28.100	57.900	-0.242	18.705
	0.5-0.7*	0.600	31.000	81.000	23.000	58.000	0.138	18.000
	0.7-1.0	0.850	23.660	68.000	24.853	43.147	-0.028	15.827
Intermittent Current Trial - End	0.3-0.5	0.400	31.763	87.000	37.944	49.056	-0.126	20.714
	0.5-0.7	0.600	18.726	77.000	34.290	42.710	-0.364	19.424
	0.7-1.0	0.850	17.053	73.000	32.922	40.078	-0.396	17.143

7.4.1 Strength

The dynamic cone penetrometer (DCP) yielded the results seen in Figure 7-19 for around the test site. It can be seen that the general trend is that the strength increases with depth below ground level. It is evident that the ground at the site area is very inconsistent as seen by the difference in strengths, where at depths of over 0.5m, a range of 4000kN/m^2 can be produced. The spikes seen, for example 6m from the tree at 0.5m depth can be assumed to be bricks or something equally hard. After excavations had taken place, bricks, breeze block, large boulders, stones, wiring and glass were all found in the trenches and electrode holes. Due to these erroneous materials that were throughout the site, the strength readings should not be taken at face value.

The site strength variance is shown in Figure 7-20, where it can be seen that the strength is fairly variable, especially at depth. Features exist that increase the strength readings such as stones and bricks as mentioned previously.

Figure 7-20 shows that the strength under the treated footings is not negatively affected by the treatment, compared to the control test. This could be due to the fact that, as seen in section 6.2.1, the strength of the combined chemicals in clay increases over a longer period of time than here. It should be noted that although the centre of site strength appears to be much higher than the trial strengths, the trial pits, were left unfilled for two days before testing could commence. These pits had filled up with surface water and could have seeped into the clay and reduced its shear strength. This is corroborated by the centre of site surface strengths being similar to that of the trial surface strengths. This is also corroborated somewhat by the water contents below the trials, as discussed in section 7.4.2 where the water contents do decrease with depth which would naturally cause the shear strength to increase with depth.

It would be expected that the shear strength would be at its maximum around the anodes. Figure 7-22 shows the shear strengths over the six point plan (Figure 7-21) for the raked electrode trial where points 1, 2, 5 and 6 are nearest to the anodes. Indeed they do possess higher average strengths than 3 and 4 which are nearest the cathode. This could be explained by the water content being higher near the cathode and not necessarily that chemical stabilisation has been achieved, this is corroborated by the water content under the footing, it is found that the average water content nearest the cathode is approximately 8% higher than at the anode.

The results gained in Figure 7-22 only exist from 0.5m and below due to the requirement to dig a sump in the trench to extract the surface water using a bilge pump.

Figure 7-23 shows the shear strengths taken over the six point plan for the vertical electrodes trial. Again it can be assumed that the highest strength should be near the anodes which in this instance are nearest points 2 and 5 whereas the cathodes are nearest 1 and 6. As seen from Figure 7-23, the results are not as expected which is most likely due to the number of obstructions encountered whilst taking the readings leading to erroneous results.

Figure 7-24 shows the shear strengths taken over the six point plan for the control trial. This figure shows how variable the ground under the footings could be. With no interference whatsoever, the top 1m of the subsurface ranges in shear strength form approximately 40 to 120kPa.

Figure 7-25 shows the shear strengths taken over the six point plan for the current intermittence trial. It can be seen that an increase in shear strength is produced at 0.7m depth for all locations. This depth has a reduced water content which could go some way to explaining this. Depth 0.5m has an average water content of 38% whereas 0.7 and 1.0m have water contents of 30%. This would explain the increase in shear strength at 0.7m but not the decrease again at 1.0m. It is interesting to note that although the 0.7m depth has an average water content of 30%, the water content of the area nearest to the anode at point one on Figure 7-25 has a water content of 39%. This would explain the lower value of shear strength at this point.

Figure 7-26 shows the average shear strengths for each trial with their respective error bars consisting of the range of values recorded over each footing. Curved trend lines here are for illustration. Again we see large errors due to the irregular makeup of the ground. It is evident that the average shear strength under the raked electrode footing did not increase with depth, however the range in water content over these depths was approximately 4% which is equal to that of the control trial. The control trial shows increased shear strength at 0.7m, as mentioned earlier, whereas the raked electrode trial shows nothing. This cannot be completely as a result of the water content of the clay.

Figure 7-27 shows the average water content at each depth under each trial plotted against the average shear strength measured under each trial in an effort to gain perspective on the effect of the water content change on the shear strength. It is noticed that each depth on each trial has a tendency to exist on a curve. The control curve is how the London Clay would be

expected to behave with decreasing shear strength for increasing water content. By taking this curve as a benchmark, one can determine the effect of the EKS on the other trials.

For the vertical electrode trial, it is noticed that the curve has been shifted vertically in Figure 7-27. This means that for a given water content, effectively the same clay has a higher shear strength, approximately 35kPa higher. The raked electrode trial curve exists below the control curve leading to the idea that the EKS process has negatively impacted on this clay in that reducing the water content of this clay does not increase the shear strength. The intermittent current trial curve lies between the control and the vertical electrodes trial meaning that the trial was somewhat successful in positively altering the clay but not as successful as the vertical electrode trial. The curve does cross the control curve at the lower water contents meaning that the effect seen on the intermittent current trial clay is more prevalent at higher water contents than lower.

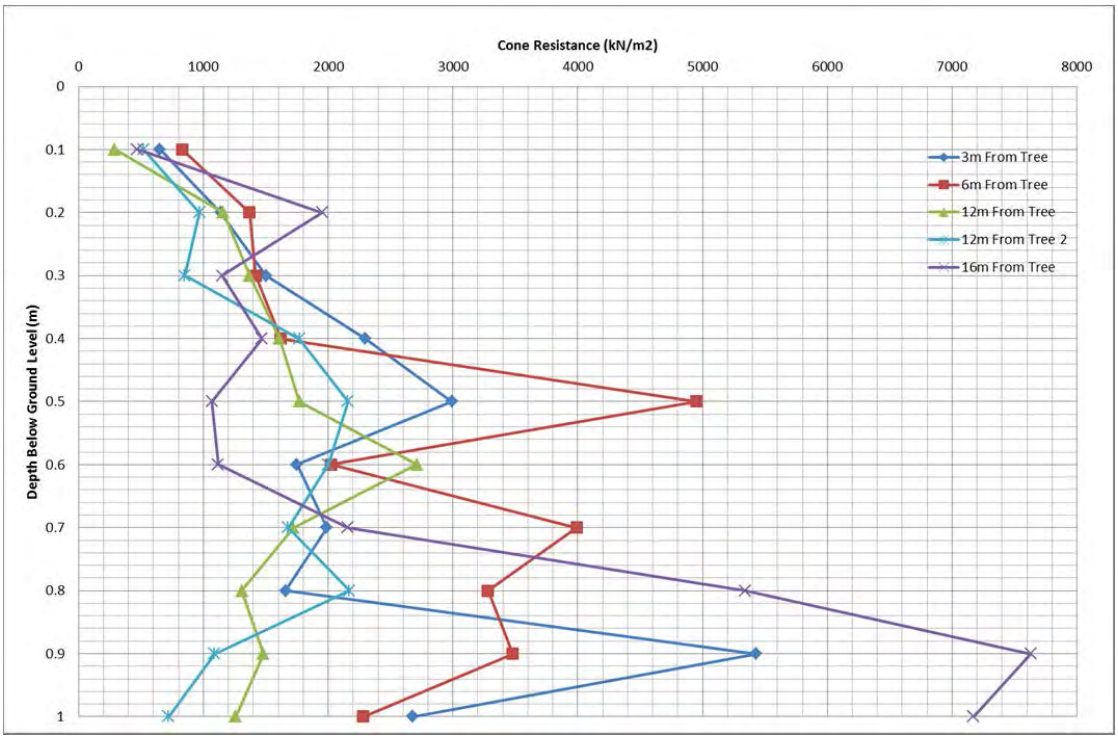

Figure 7-19: Site trial Dynamic Cone Penetrometer results for outside site area.

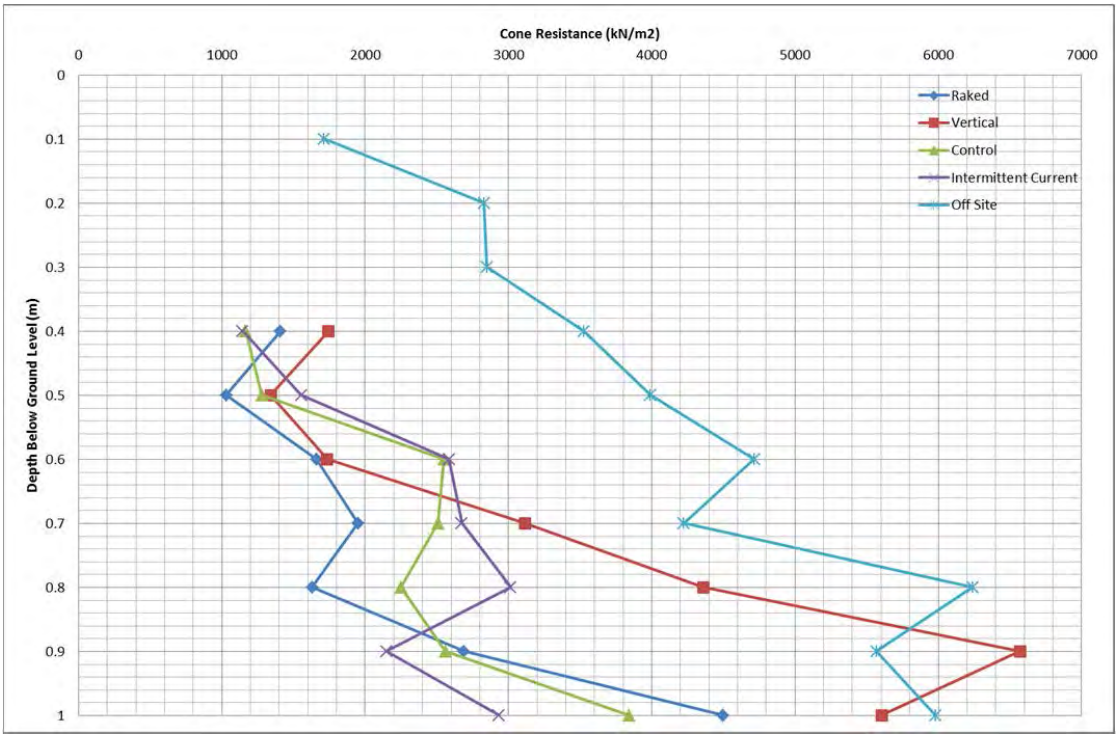

Figure 7-20: Site trial Dynamic Cone Penetrometer averages over each trial.

5	3	1
6	4	2

Figure 7-21: Shear strength record locations under each foundation.

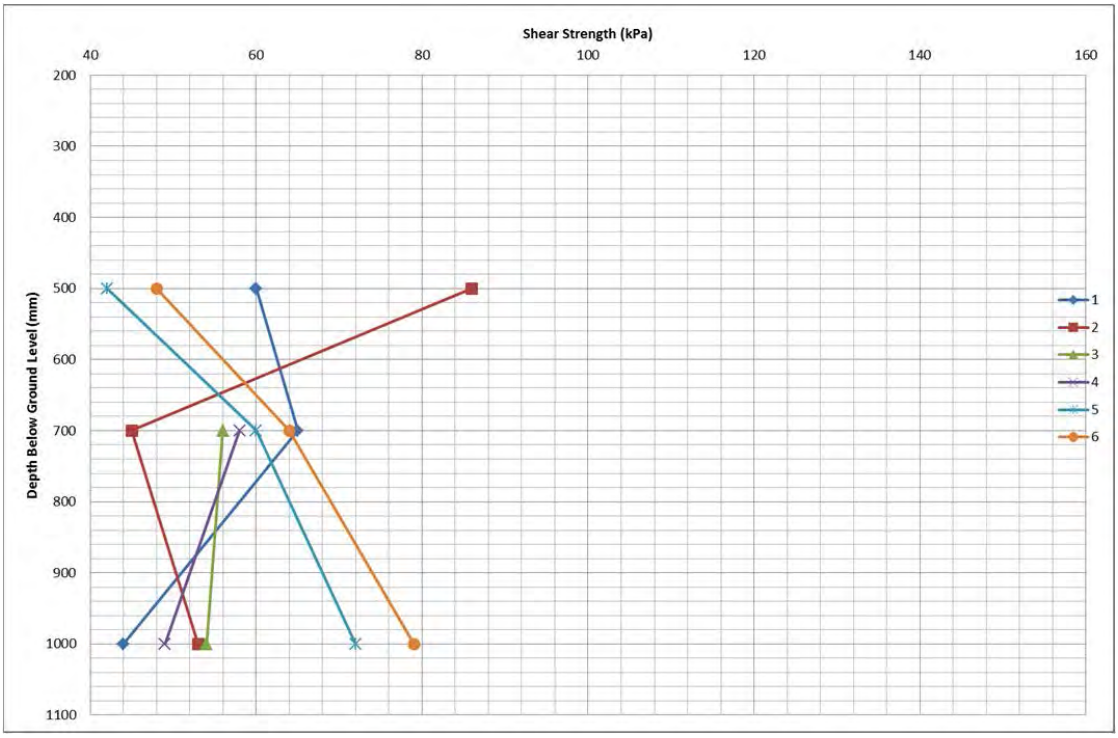

Figure 7-22: Site trial hand vane shear strengths under raked electrode footing.

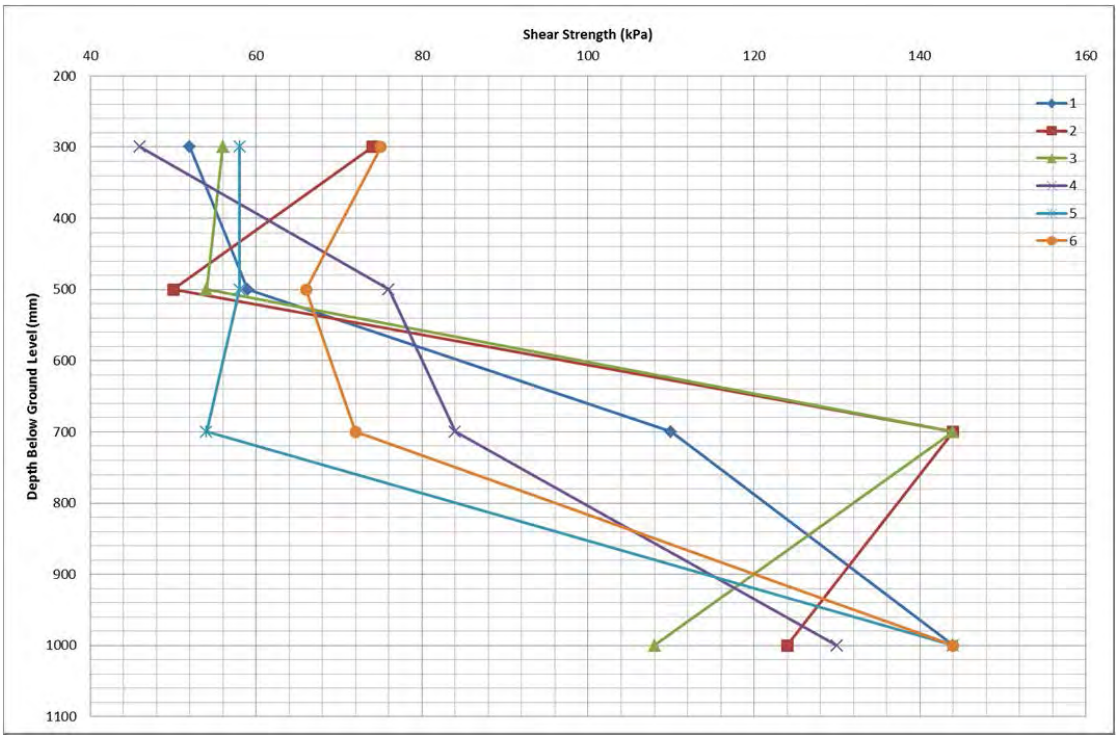

Figure 7-23: Site trial hand vane shear strengths under vertical electrode footing.

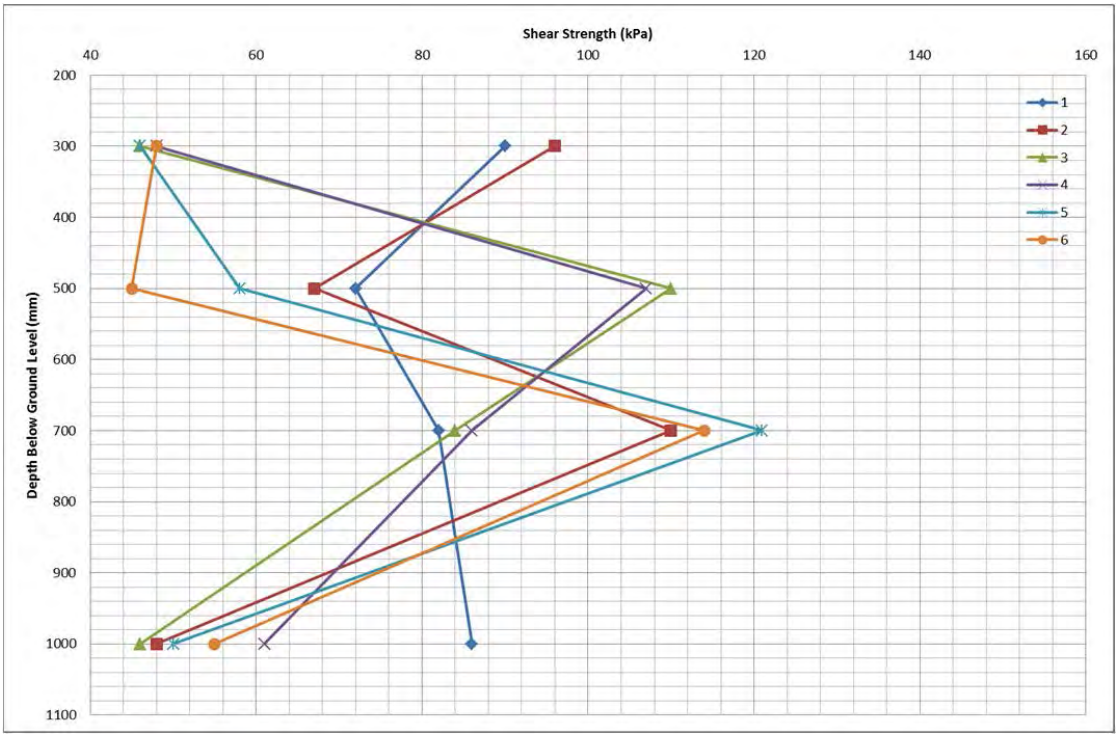

Figure 7-24: Site trial hand vane shear strengths under control footing.

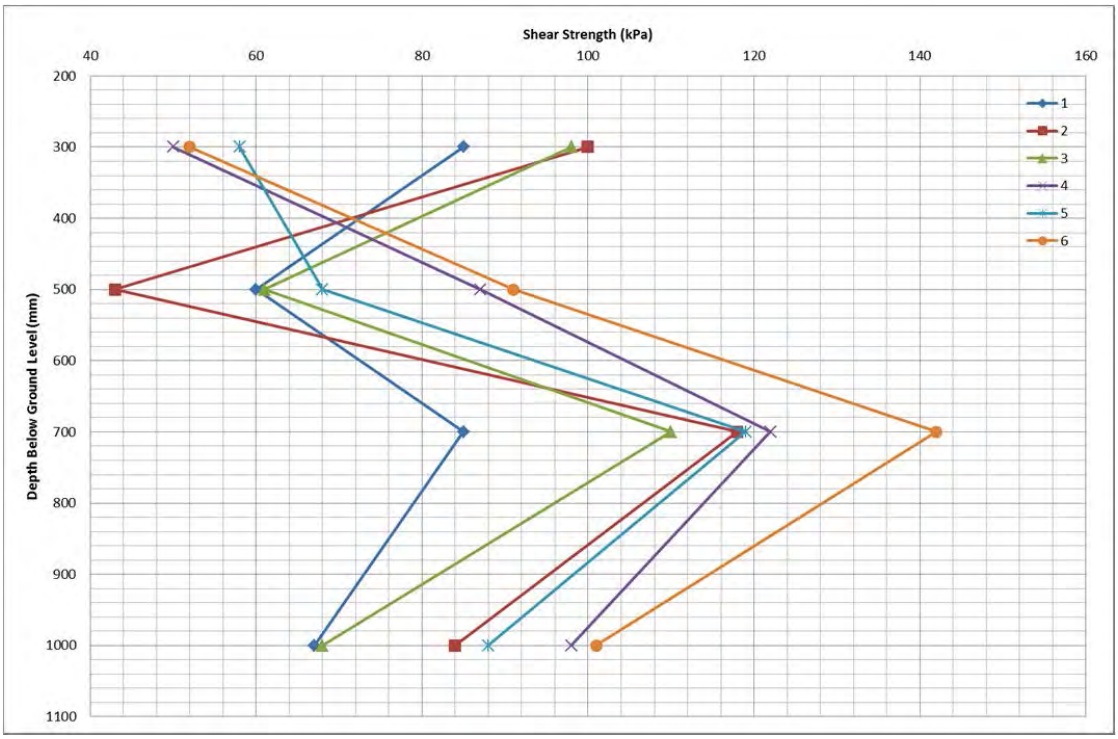

Figure 7-25: Site trial hand vane shear strengths under intermittent current footing.

Figure 7-26: Site trial average hand vane shear strengths under each trial footing with ranges.

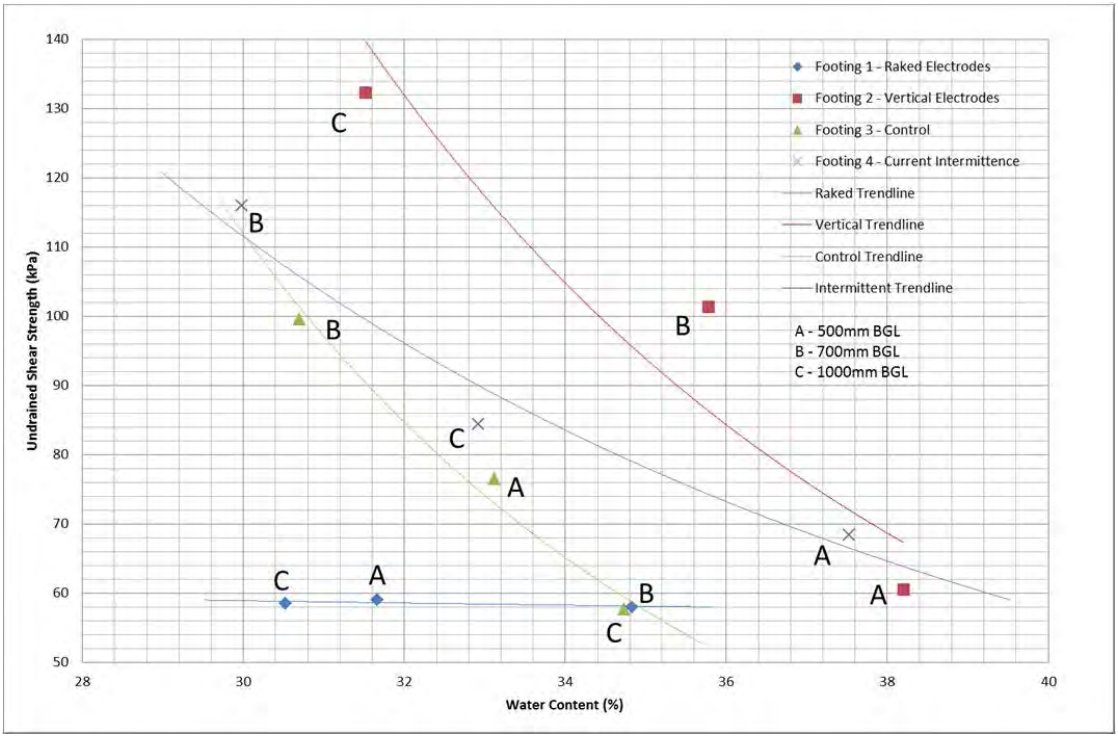

Figure 7-27: Site trial hand vane shear strengths against average water contents under each trial footing.

7.4.2 Water Contents

The average water contents for each trial at depths 0.5m, 0.7m and 1.0m can be found in Figure 7-28. As is expected, the water content tends to decrease with depth with the exception of the control trial. The current intermittence and the vertical electrode trials both have high water contents at 0.5m depths. This may be due to the fact that the site was sloping slightly and both of these trials were on the low side of the slope so surface water would have travelled in their direction.

Figure 7-29 shows the raked electrode water contents where it can be seen that the contents vary wildly from 12.5% to 46%. It would be expected that the water content would be highest around the cathode and in this instance the nearest sample location was number 4. Number 4 however does not appear to possess the highest water content. This may be caused by the orientation of the electrodes and the resultant flow path.

The vertical electrode trial water contents are shown in Figure 7-30. The expected higher cathode water content area is not found here, in fact, quite the opposite. The sample location nearest the anode is found to have an increased water content compared to the cathode.

The control trial water contents are shown in Figure 7-31 where it can be seen that the water contents over the three depths at all sample locations are fairly consistent compared to the other trials. The contents at 0.5 and 0.7m depths have a maximum range of 7% with the 1.0m depth have a range of approximately 12%.

The current intermittence trial water contents are presented in Figure 7-32. It is shown that locations 3, 4 and 5 have similar trends in their water contents at all depths whereas location 1 has an increase over this trend at depth 0.7m. Location 1 is nearest location to a cathode which could explain this increase in water content. Location 3 is nearest to an anode and this sees a depression in water content at 0.7m depth although locations 4 and 5 do too which would make this non conclusive.

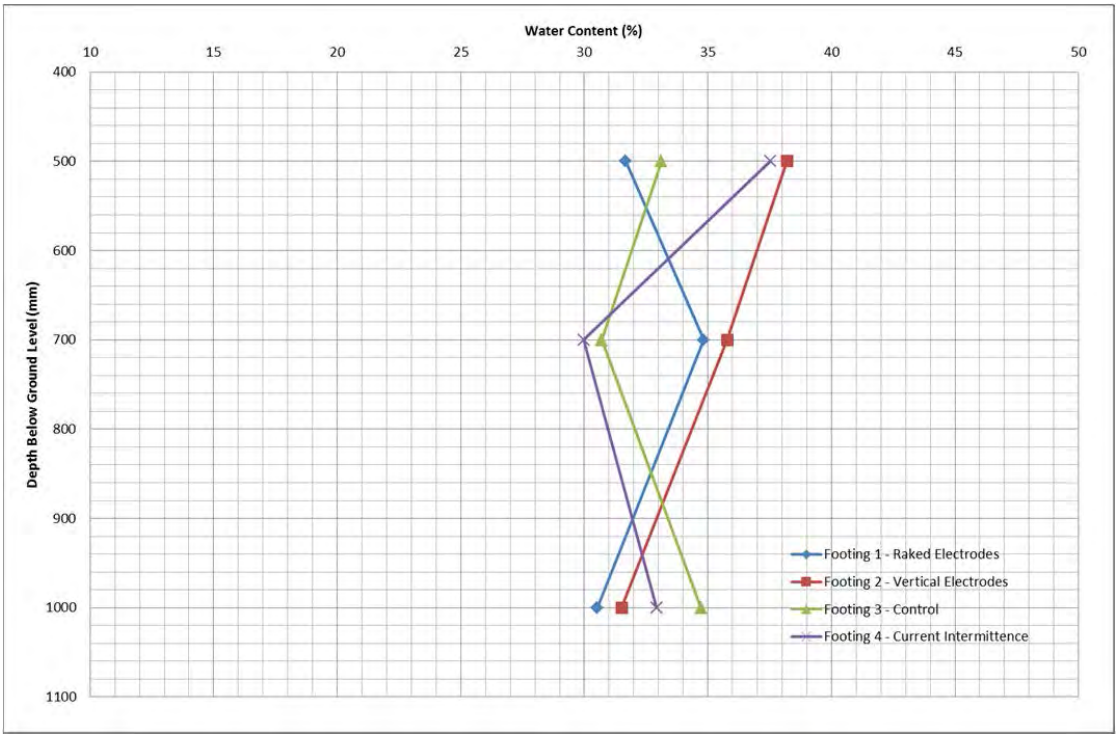

Figure 7-28: Site trial average water contents over depth under each trial footing.

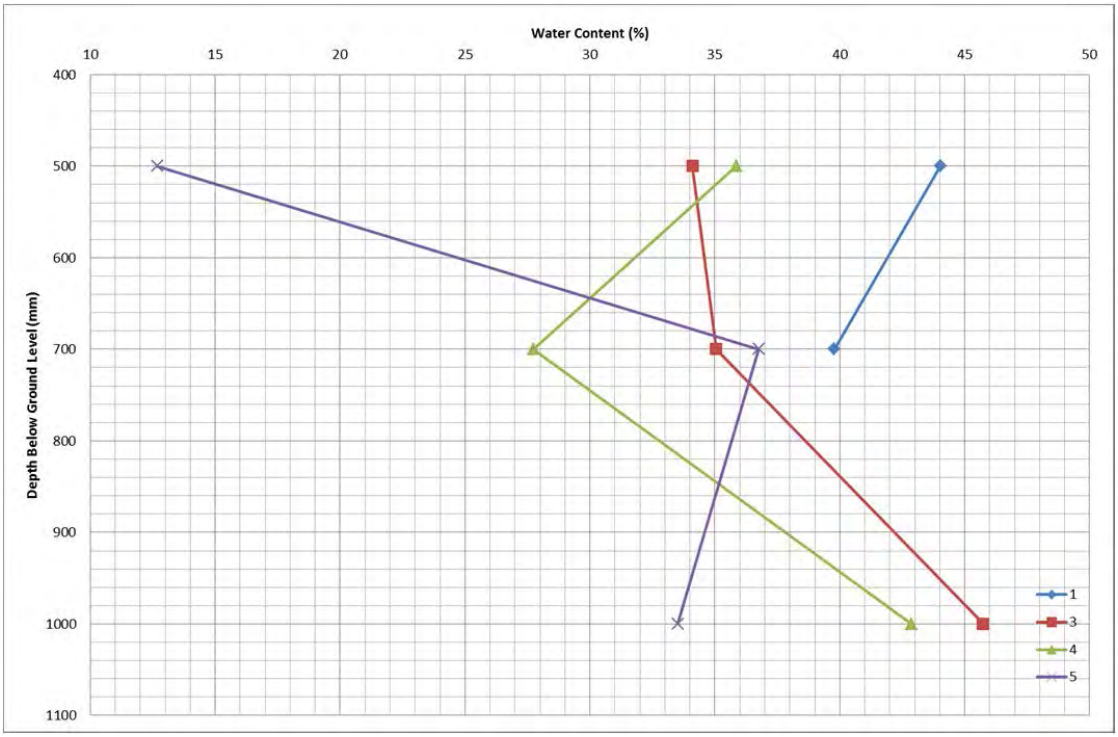

Figure 7-29: Site trial raked electrode trial water contents.

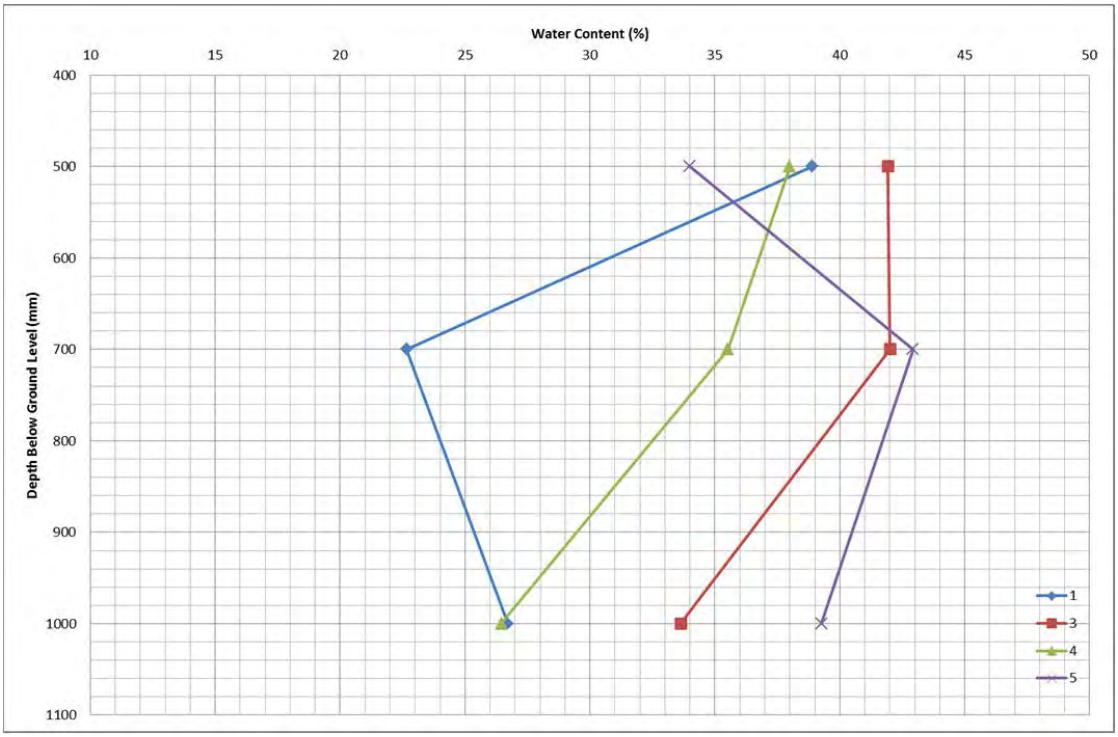

Figure 7-30: Site trial vertical electrode trial water contents.

Figure 7-31: Site trial control water contents.

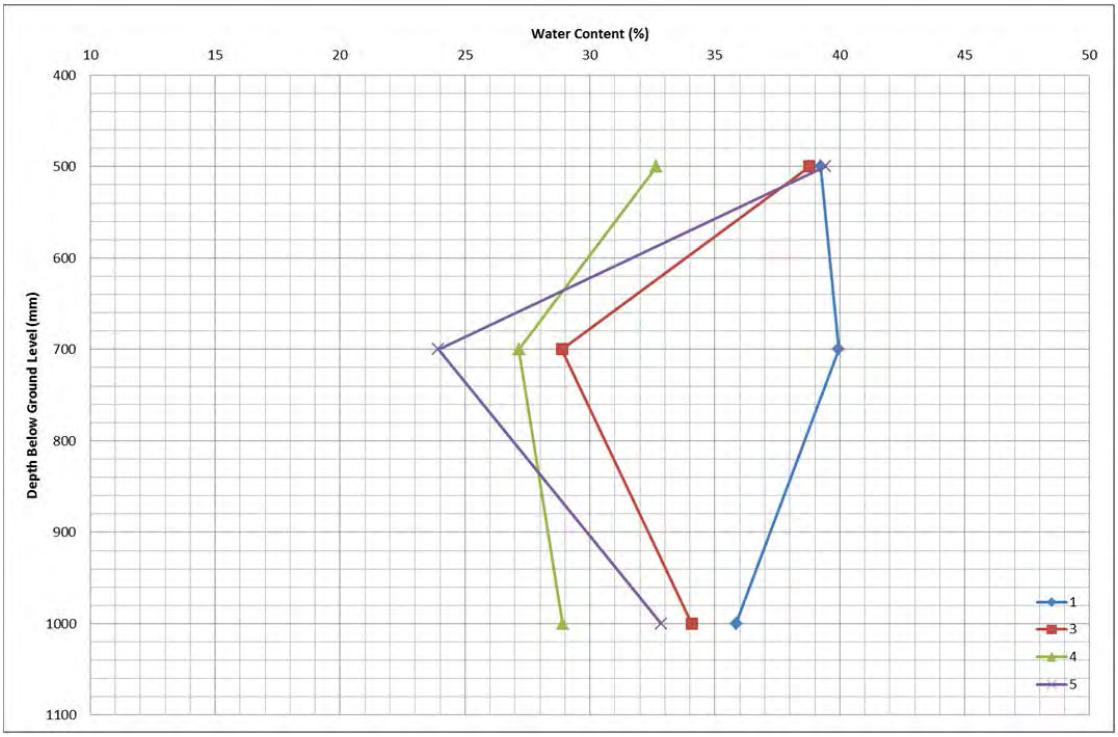

Figure 7-32: Site trial current intermittence trial water contents.

7.4.3 Plastic Limits

Without the pre-trial plastic limits in the immediate vicinity of each trial, it is difficult to determine any change over the EKS trials. It can be noted however, from Figure 7-33, that the control trial decreases with depth by approximately 1.5% and the end location sees a 1.0% increase. The raked electrode trial was witness to an increase at both locations and the intermittent current trial saw a decrease at both electrodes. The vertical electrode trial saw a decrease at both locations with the largest decrease seen at the centre at 0.7m depth. This location was tested by GIP UK however so this may be a variance in result due to the tester.

It is interesting to note that the raked electrode's plastic limits appear to increase over the control at depth and that the locations with the greatest increase in plastic limits are the ends of the vertical and current intermittence tests, both of which used vertical electrodes.

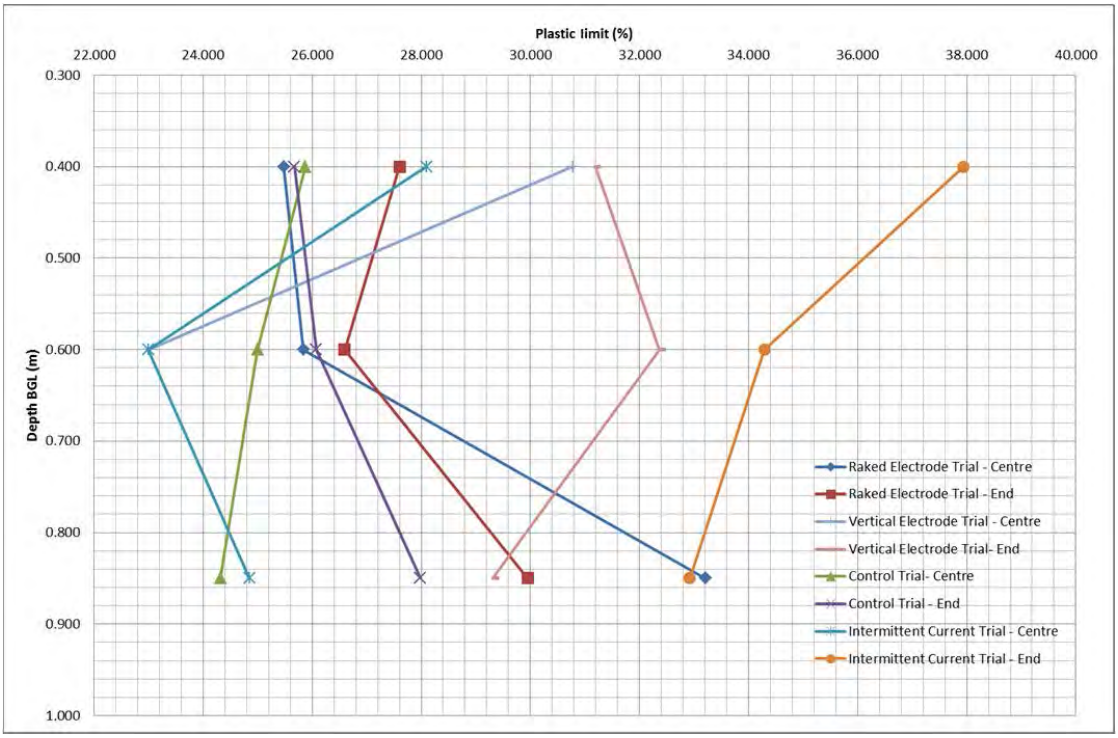

Figure 7-33: Site trial plastic limits.

7.4.4 Liquid Limits

Figure 7-34 shows the liquid limits produced from testing the clay underneath each trial footing. Again, due to not having pre-trial data for the immediate area, it is difficult to determine the effect that EKS has had on the clay.

It is noted however that the control trial, raked electrode trial and intermittent current trial all possess the same trend for liquid limit as plastic limit in that the control decreases over depth at the centre and increases at the end, the current intermittence trial decreases at both locations and the raked electrode trial increases at both locations. The vertical electrode trial however, increases over depth at both locations for liquid limit whereas it decreases at both for the plastic limit.

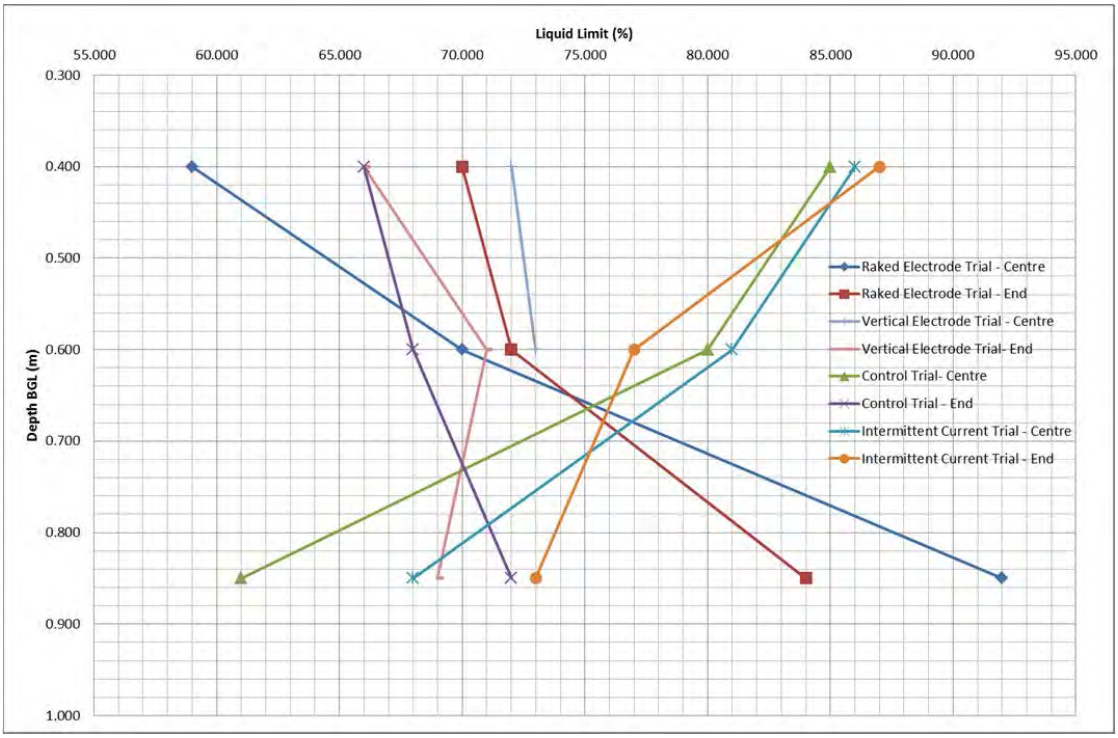

Figure 7-34: Site trial liquid limits.

7.4.5 Plasticity Index

The plasticity index is shown in Figure 7-35. It can be seen that both the raked electrode trial and the vertical electrode trial both experience increases in plasticity index over depth whereas the current intermittence trial sees a decrease over depth. The control trial sees a decrease at the centre and an increase at the end location.

When using the plasticity chart from BS5930: 2015, one can determine the plasticity of the clay from the plasticity index and liquid limit. When examining the 1.0m depth centre locations, it is found that according to the plasticity chart, the control trial clay is high plasticity clay, the raked electrode trial is extremely high plasticity clay, the vertical electrode trial at 0.5 – 0.7m depth is very high plasticity clay and the current intermittence trial is high plasticity clay. Without knowing the initial Atterberg Limits it is impossible to confirm any changes but it is interesting to note that the vertical and raked electrode trials possess the highest plasticity and are also the two trials nearest to the tree.

Due to the erratic nature of the liquid limit results and thus plasticity index results, no discernible trend can be identified.

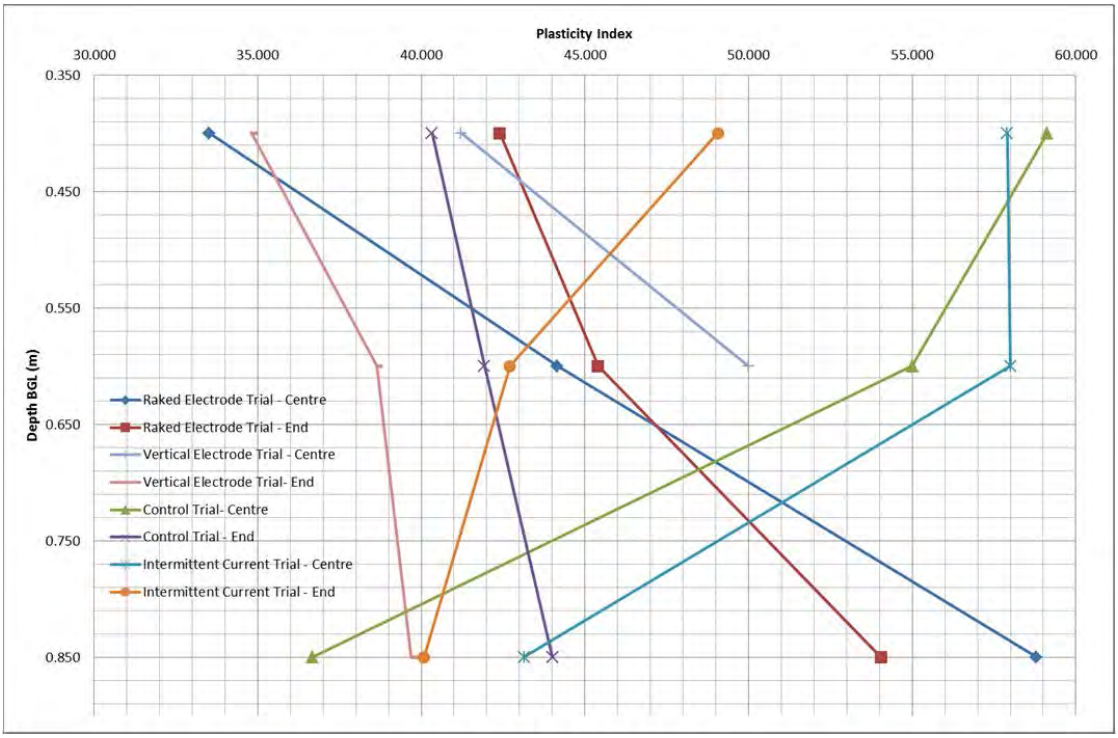

Figure 7-35: Site trial plasticity index with depth.

7.4.6 Linear Shrinkage

As seen in Figure 7-36, the linear shrinkages range from approximately 15 to 24%. The 24% value appears to be an outlying data point which incidentally was produced by GIP UK and unfortunately there was not enough clay remaining from this sample to conduct the test again.

It is difficult to determine any changes in these values from before EKS to after due to the nature of the irregular subsurface conditions. It can be noted, however, that the intermittent current trial clay has a decreasing linear shrinkage with depth where the raked electrode trial has a general trend for increasing linear shrinkage. The vertical electrode trial saw an increase in linear shrinkage at the end of the footing but a decrease in the centre where the target zone exists. Without pre-trial data this data could be the natural state of the clay.

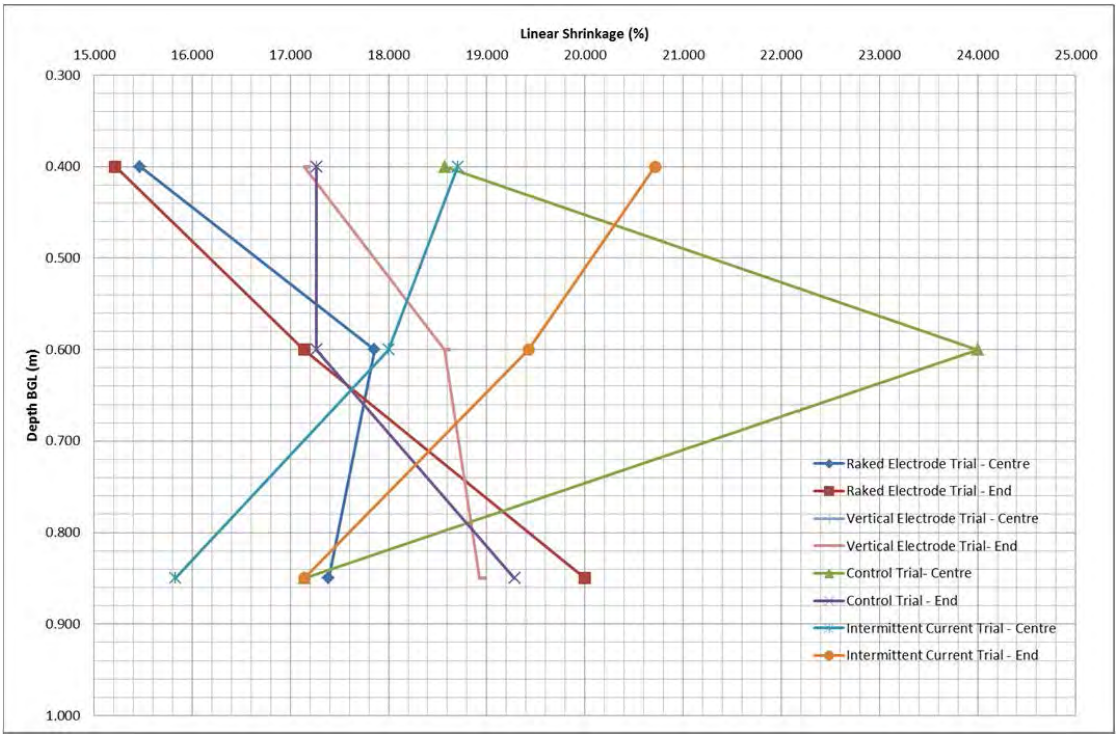

Figure 7-36: Site trial linear shrinkage over each trial.

7.4.7 pH

Figure 7-37 shows the pH variance with depth under each trial footing. It can be seen that there is very little change in pH with depth at these locations which would indicate that the acid front developed through EKS has not migrated there. It was expected that the acid front would be strongest in the target zone and thus leave the shallower locations with a higher pH than the deeper ones. This is not seen here where the vertical electrode trial appears to increase in pH with depth. The control trial, however, increases at the centre and decreases at the end and the intermittent current trial saw a small decrease with depth along with the raked electrode trial.

These results are not conclusive evidence of chemical migration or electroosmosis through these locations. It is anticipated however that one should only consider the end results as the centre results may be showing an area of untreated clay when considering the numerical modelling showing a dead zone at the centre of a four electrode system. If this is the case, then it can be seen that the raked electrode system increases in pH whilst the current intermittence and vertical electrode systems decrease over the control. This would lead to the conclusion that the acid front has migrated further in the current intermittence and vertical electrode systems than raked.

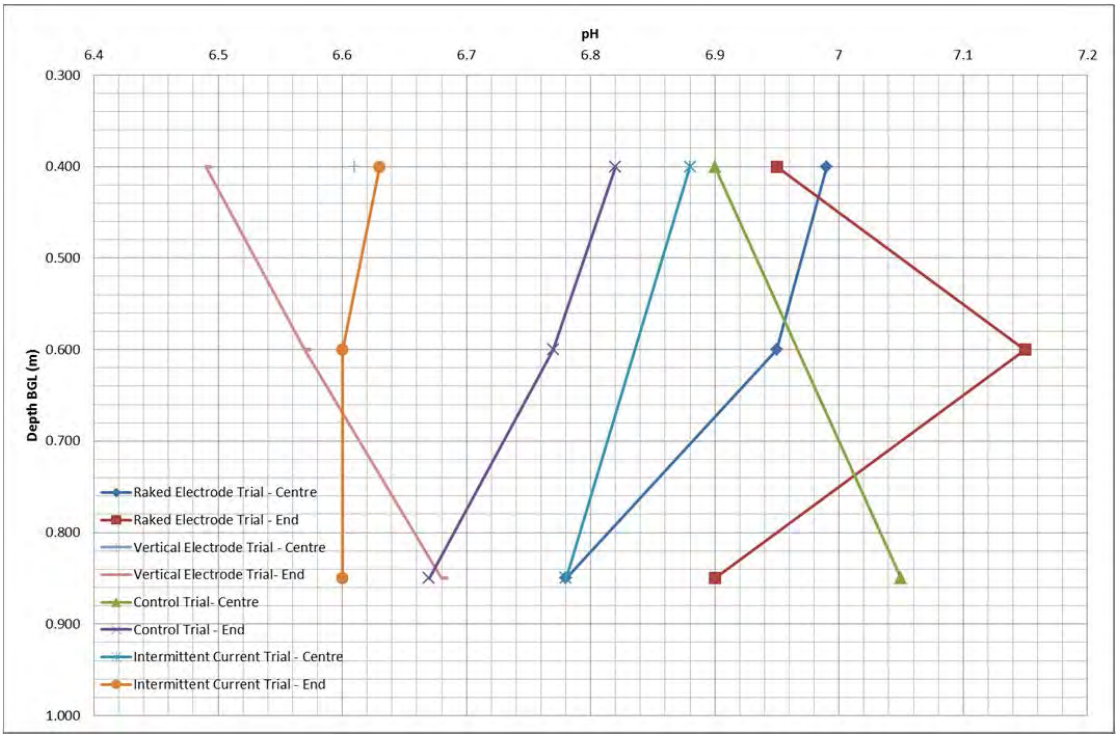

Figure 7-37: Site trial pH variance with depth for each trial.

7.4.8 Electrodes

Indicative of cementation, some of the electrodes discussed in this section required removal using an excavator.

7.4.8.1 Mass

Once removed from the ground, the electrodes were weighed, Table 7-4, and displayed for viewing in Figure 7-38 to Figure 7-40. It is expected that the anodes will lose mass due to precipitation of iron into the clay and the cathode will usually gain weight. It is seen here that the anodes tend to lose weight whilst the cathodes gain weight. Electrode 1A1 is an exception as this electrode broke on extraction with approximately 60% of the electrode being recovered.

From Figure 7-41 it can be seen that 1A2 (anode) has corroded extensively with a section of the steel missing in the direction of flow whilst 1C (cathode) has no corrosion visible to the naked eye. It can be safely assumed that the missing part of 1A2 has corroded and precipitated into the nearby clay. Similar degradation occurred on the other anodes used in the trials. Cathode 43 from the intermittent current trials was extracted with a hardened coating of what is most likely to be sodium silicate. This is an indication that not all of the sodium did migrate through the clay at this point and has been shown to occur before, (Mohamedelhassan,

et al., 2008). Anode 41 shows, like 1A2, that extensive corrosion has taken place with sections missing completely over the length of the exposed steel surface.

Figure 7-38: Raked electrodes after use. Anode – Cathode – Anode (1A1 – 1C – 1A2).

Figure 7-39: Vertical electrodes after use. Anode - Cathode - Cathode – Anode (21, 22, 23, 24).

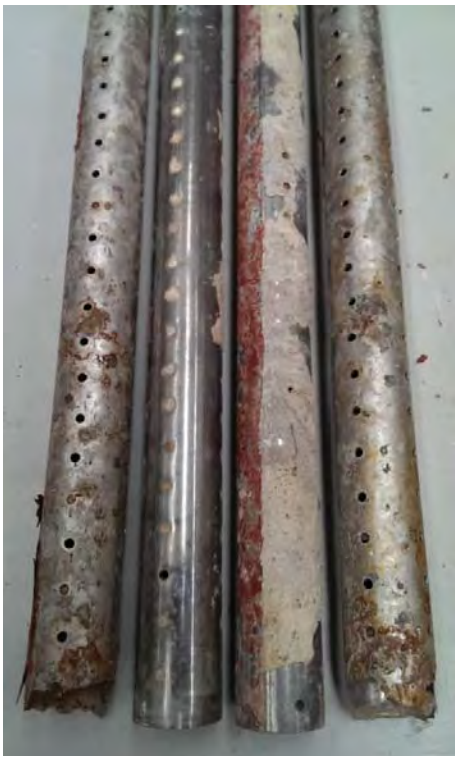

Figure 7-40: Current intermittence electrodes after use. Anode - Cathode - Cathode – Anode (41, 42, 43, 44).

Table 7-4: Site trial electrode mass before and after treatment.

Trial	Electrode Type	Electrode	Mass Before (g)	Mass After (g)	Mass Change (g)	Mass Change (%)
Raked	Anode	1A1	1117.88	581.19	-536.69	-48.01
	Cathode	1C	1104.9	1107.33	2.43	0.22
	Anode	1A2	1106.11	1093.69	-12.42	-1.12
Vertical	Cathode	21	899.77	930.81	31.04	3.45
	Anode	22	917.5	994.09	76.59	8.35
	Anode	23	846.57	915.62	69.05	8.16
	Cathode	24	908.88	847.68	-61.2	-6.73
Intermittent	Anode	41	1120.41	966.8	-153.61	-13.71
	Cathode	42	1124.8	1068.83	-55.97	-4.98
	Cathode	43	945.44	989.37	43.93	4.65
	Anode	44	1126.56	966.74	-159.82	-14.19

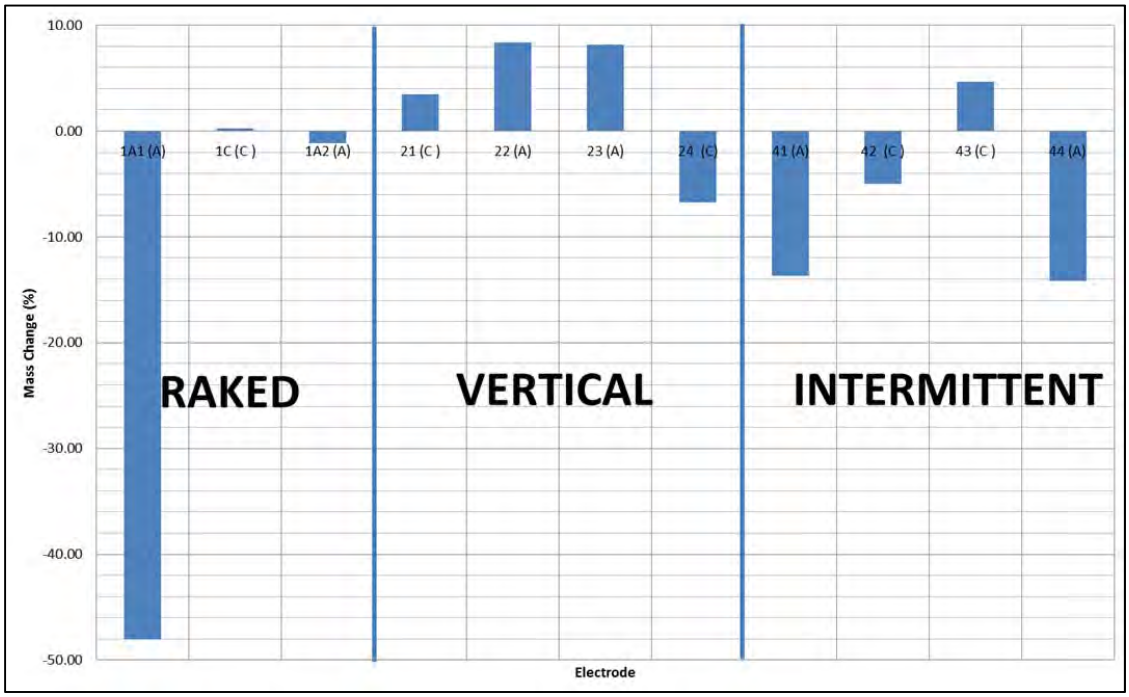

Figure 7-41: Site trial electrode mass variance. (A) = Anode, (C) = Cathode

7.4.8.2 SEM Photography

Two electrodes were chosen for SEM microscopy to assess the damage done over the EKS process. These electrodes were 22 and 24 which were vertical electrode trial anodes and cathodes respectively. Figure 7-42 shows how unused steel, stored in the University of Birmingham Civil Engineering laboratory, albeit mildly corroded, is a far cry from the site used

electrodes. The site trialled electrodes can be seen to be corroded and pitted through electrolysis and rusting leading to a drop in electrical conductivity and thusly effectiveness. This surface degradation is confirmation of the fact that Fe ions are precipitated into the clay.

Further SEM photography can be found in Appendix F.

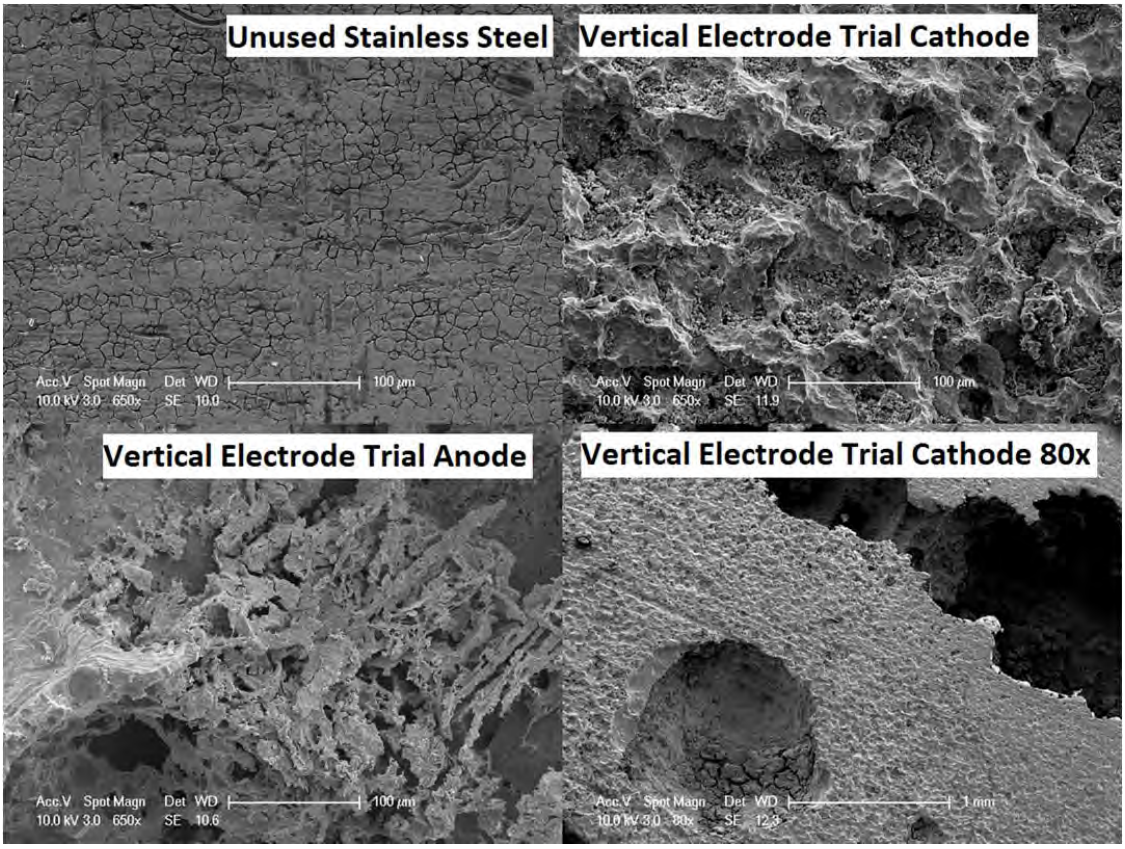

Figure 7-42: SEM microscopy of site trial electrodes - vertical.

7.4.9 Concrete Footings

Inspecting the underside of the concrete strip footings with the naked eye, it was seen that there was no discoloration or visible erosion of the concrete.

SEM photography was used to outline any microscopic damage done to the concrete that is not visible to the naked eye; Appendix F. Figure 7-43 shows the microstructure of the concrete on the underside of the concrete strip footings. It can be seen that due to the samples not being sliced, the pictures are different to concrete SEM photographs found in the literature, (Winter, 2015). These pictures show mostly the cement hydrate product which exists as the matrix that binds the aggregates together. As seen in Figure 7-44 also, there appears to be no

major variance between all four concrete samples and as such it can be inferred that no damage has taken place. This is as expected due to the target zone being far enough below the footing that a 100mm buffer zone existed between the predicted effective electric current flow path and the footing.

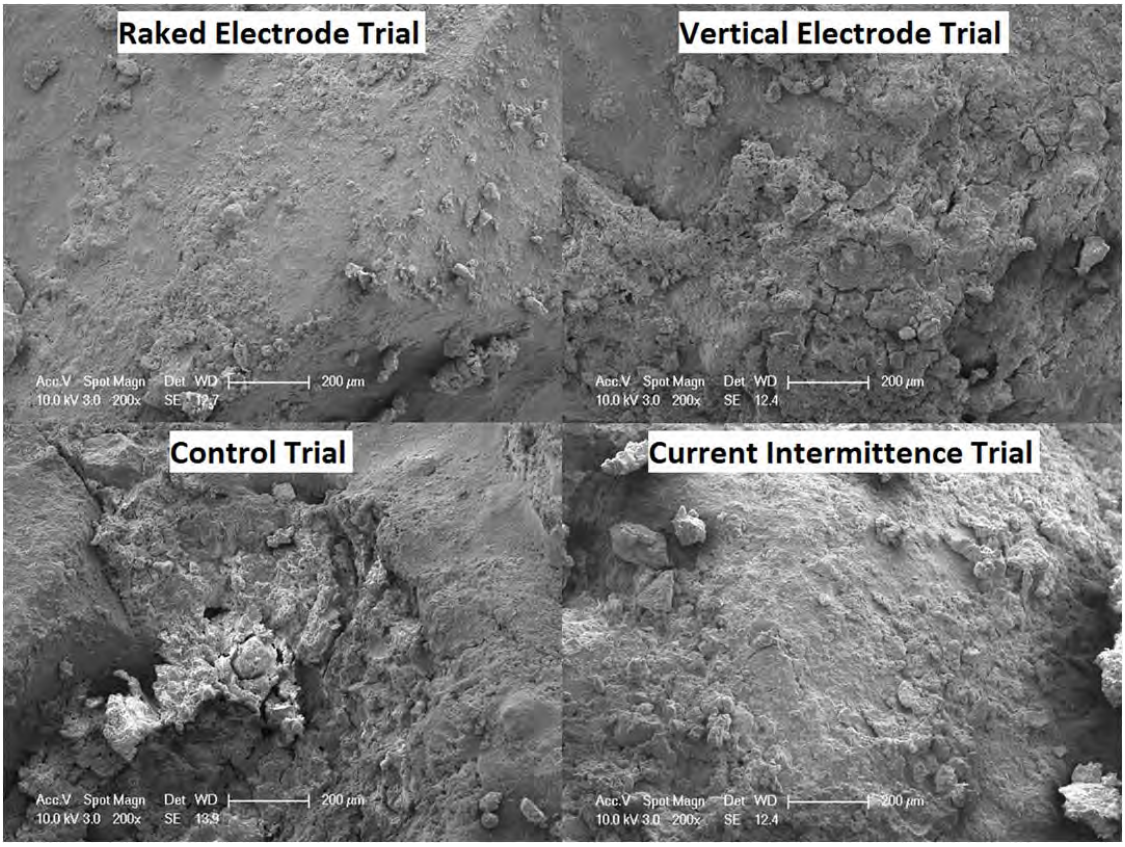

Figure 7-43: SEM microscopy of undersides of concrete strip footings at 200x magnification.

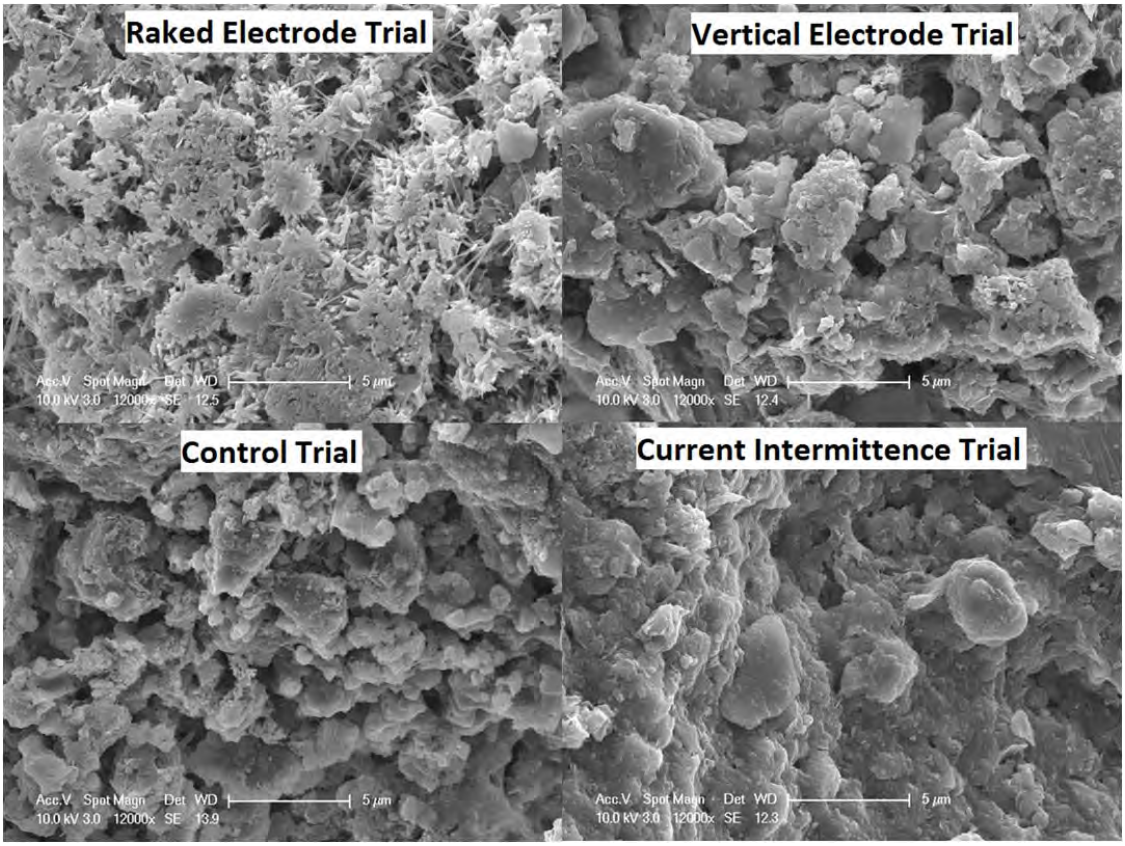

Figure 7-44: SEM microscopy of underside of concrete strip footings at 12,000x magnification.

7.4.10 Elemental Analysis

The elemental analysis results are displayed in Figure 7-45 to Figure 7-49 and have been separated into each element for clarity. For comparison, the control trial's initial and post EKS elemental contents are shown where they are the same. This was due to there being no excavations around the control trial before the EKS began to gather samples. As there was no EKS around the control trial, it can be assumed that the elemental analysis would be constant over the 58 days of testing.

Whereas fluids could not be measured with any accuracy due to leaking and ground surface water, the addition of chemicals was. Each footing treated received approximately 1kg of stabilising chemicals split as described in section 6.2.1.

Figure 7-45 shows the silicon content over the four trials and it's variance with depth both before and after the EKS treatment has taken place. It can be seen that the post EKS silicon content is fairly consistent with the pre EKS contents. The vertical electrode trial shows most difference with its 0.7m depth content increasing by approximately 1% after the trails and its 0.5m depth content decreasing by almost 0.9%. It is possible that the process in this area has

pushed the silicon deeper below ground surface which is a trait that can be seen beginning in the intermittent current trial and the raked electrode trial but to a lesser extent.

Figure 7-46 shows the iron content over the four trials and its variance with depth both before and after the EKS treatment has taken place. It can be seen that the raked electrode trial has post EKS iron contents all within 0.5% of their initial contents. The vertical electrode trial shows a reduction in iron content over the EKS process for 0.5m and 1.0m depths but a 1.1% increase at 0.7m depth. The same trend is seen for the intermittent current trial where 0.5m and 1.0m experience reductions in the content of iron but 0.7m depth sees an increase of over 1%. This increase around 0.7m deep is most likely due to the migration of Fe ions through the clay from the degradation due to electrolysis of the electrodes. Any natural Fe ions in the clay appear to have been forcibly migrated from the 0.5m and 1.0m depths but have not been replaced with electrode Fe ions which would explain the drop in content for these depths. This may be due to the 0.7m depth being towards the centre of the target zone resulting in a higher electric field presence and therefore higher rate of migration. It should also be noted that section 7.4.8.2 shows how the stainless steel has degraded to the point where a large quantity of Fe ions would have been precipitated into the clay which would account for the increased Fe content.

Figure 7-47 shows the aluminium content over the four trials and it's variance with depth both before and after the EKS treatment has taken place. It can be seen that the initial contents are fairly consistent with the exception of the vertical electrode and raked electrode trials side of the site which sees a 1.25 – 2.0% increase at a depth of 1.0m. The raked, vertical and intermittent current trials all saw decreases in the aluminium content at the 1.0m depths with the vertical electrode trial seeing the largest at 1.7%. The 0.5 and 0.7m depths of this trial saw increases of over 0.5% however. The decreases seen at 1.0m depths may be caused by the migration of Al ions through that clay which are not being replaced by the stabilisers, water or electrode material.

Figure 7-48 shows the calcium content over the four trials and it's variance with depth both before and after the EKS treatment has taken place. It can be seen that for the raked electrode trial, there is an increase for the 0.5m and 1.0m depths and a decrease for the 0.7m depth. The vertical electrode trial saw an increase in all depths with 1.0m depth producing the largest at approximately 0.15%. The increases for the vertical electrode trial appear to increase with depth as expected. The current intermittence trial experienced a decrease at 0.7m as in the

raked electrode trial. The 0.5m depth saw no change and a 0.08% increase was found at 1.0m depth. The fact that the raked and intermittent current trials saw a decrease in Ca ions at 0.7m depth indicates a problem with the supply of Ca ions at the electrodes. The chemical stabilisers were applied to the electrodes as discussed in section 7.2.2 and did appear to be flowing through the electrode leading to the possibility that the Ca ions have migrated into the clay, but not to the centre of the target zone. The electric current has been strong enough though to migrate the Ca ions that were there onwards.

Figure 7-49 shows the sodium content over the four trials and it's variance with depth both before and after the EKS treatment has taken place. It is seen that the initial contents across the trials is consistent with a 0.12% range. The raked electrode trial shows some increase, albeit 0.7 and 0.3% at 0.5 and 0.7m depths respectively. No increase is witnessed at the 1.0m depth though. This could be due to the orientation of the electrodes and their possible flow pattern caused by this. The vertical electrode trial sees an increase in sodium content at every depth at approximately 0.6 – 0.8%. The intermittent current trial produced no increase at 1.0m depth, a 0.5% increase at 0.5m depth and a 3.6% increase at 0.7m. This could either be a feature of the exact piece of clay tested or the intermittent currents ability to minimise electrode polarisation has enabled sodium ions to migrate further through the clay than the other trials. To eliminate the possibility of XRF error, this sample was tested twice and the results were confirmed.

Chlorine is produced by the electrolysis that takes place in the system and so it was expected to be found in the clay. No chlorine was found except for a 0.07% concentration at the vertical electrode at 1.0m depth. It is anticipated that during the electrolysis, gases are formed and released at the electrodes. One such gas could be Cl_2 leaving little to no chlorine in the clay system itself.

Oxides were not used in the analysis in this instance due to the inherent error associated. The XRF technique involves guessing the most likely oxide for each element which may not always be the oxide present.

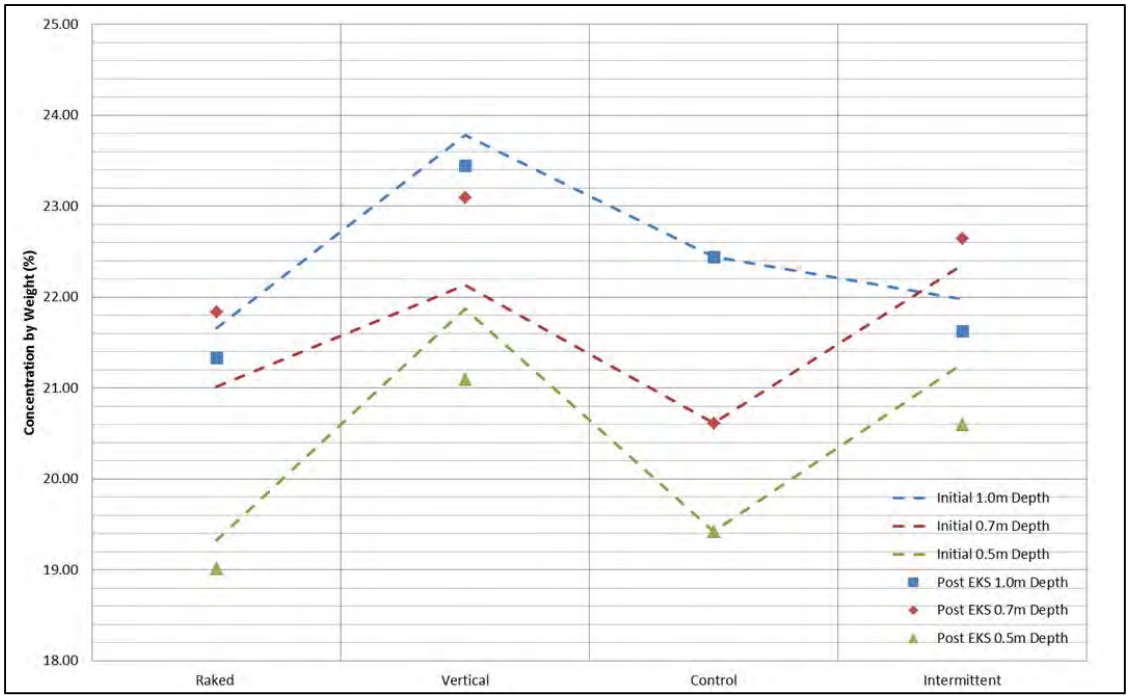

Figure 7-45: Site trials silicon content.

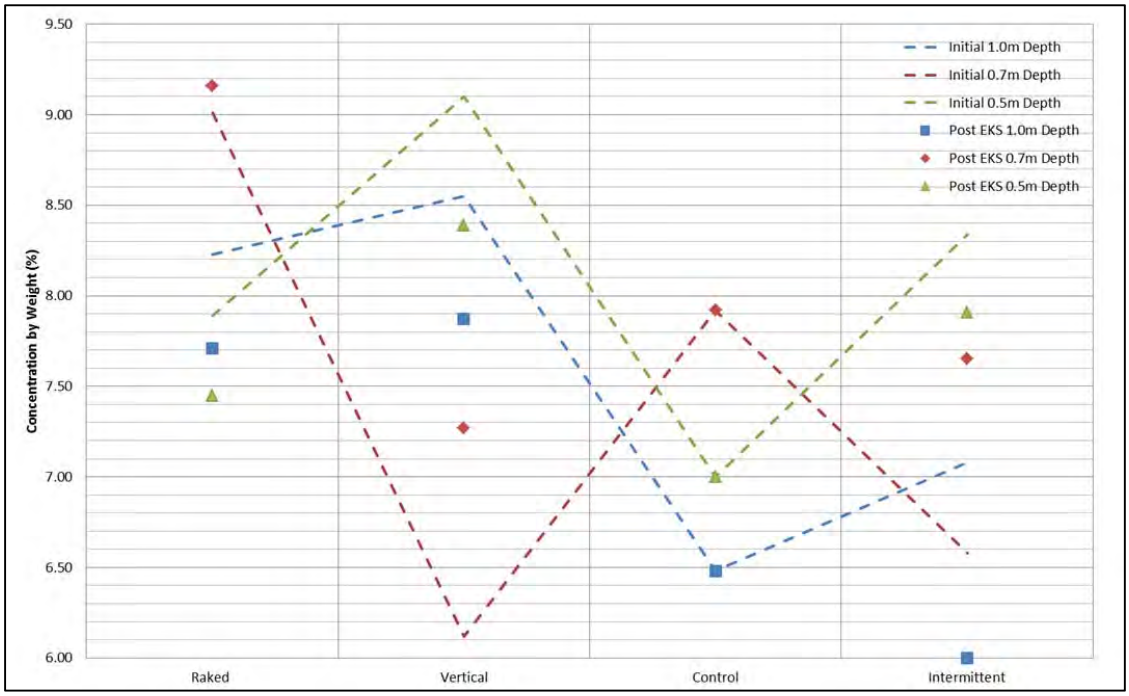

Figure 7-46: Site trials iron content.

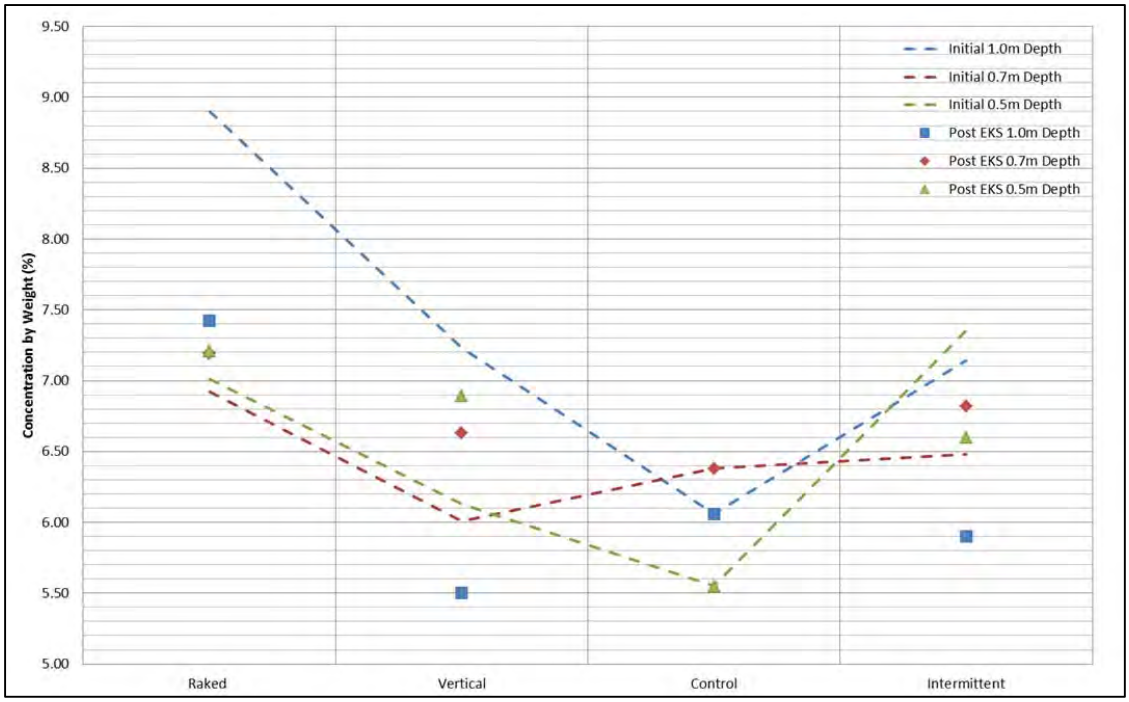

Figure 7-47: Site trials aluminium content.

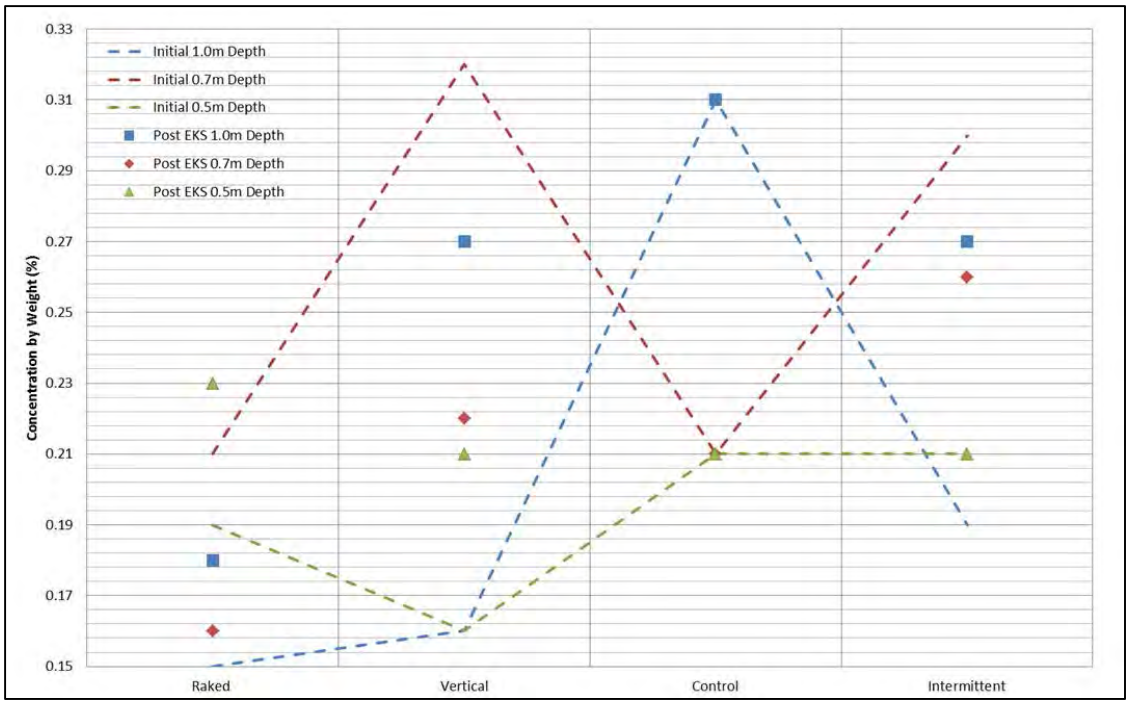

Figure 7-48: Site trials calcium content.

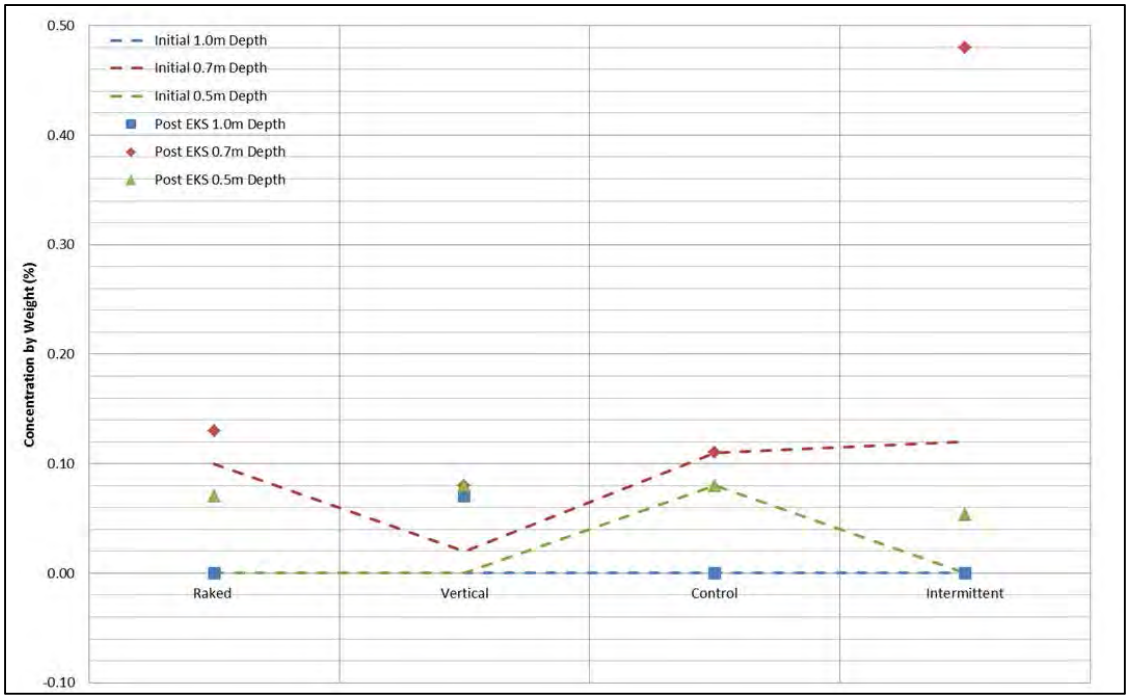

Figure 7-49: Site trials sodium content.

7.5 Summary

Overall, it can be said that this site trial was a success in that much was learnt about the installation process in a natural environment and whilst the results don't clearly show chemical migration into the target zone, flow was established and changes have taken place. A summary of these changes can be found in Table 7-5 for clarity.

Table 7-5: Site trials post trial testing summary.

Attribute	Raked	Vertical	Control	Intermittent
Undrained Shear Strength	Generally follows control, for given water content is improved over control	Follows control to 0.6mBGL at which point a dramatic increase is seen, for given water content is improved over control	Increases with depth, strength increases with water content decrease	Generally follows control, strength appears unaffected by water content and below control for given water content
Water Content	Reduces with depth	Reduces with depth	Increases with depth	Reduces with depth
Plastic Limit	Increases with depth with shallower section similar to control	Raised but decreases with depth (still above control)	Generally consistent with depth	Decreases with depth but end is significantly above control
Liquid Limit	Increases with depth	Slight increase with depth,	No discernible trend	General decrease with depth

Attribute	Raked	Vertical	Control	Intermittent
Plasticity Index	Increase with depth	Slight increase with depth,	No discernible trend	General decrease with depth
Linear Shrinkage	Increase with depth, reduced at shallow depths	Slight increase with depth, around control	General consistency with depth if anomalous result omitted	General decrease with depth
pH	General decrease with depth, slightly above control	General increase with depth, lower than control	General consistency with depth	Slight decrease with depth, slightly lower than control
Electrodes	Anodes lose mass with cathode gains	Anodes gain most mass – possibly chemicals	N/A	Anodes lose mass
Chemical Analysis	Fe loss at 0.5m and 1.0m Al loss at 1.0m Ca loss at 0.7m and gain at 0.5 and 1.0m Na gain at 0.5m and 0.7m	Si gain at 0.7m Fe gain at 0.7m Al gain at 0.5m and 0.7m Ca gain at 0.5m and 1.0m Na gain at all depths	Benchmark	Fe loss at 0.5m and 1.0m and gain at 0.7m Al loss 0.5m and 1.0m and gain at 0.7m Ca gain at 1.0m and loss at 0.7m Na gain at 0.7m

From the chemical analysis it is seen that the vertical electrode trial has been the most successful at moving sodium into the target zone and calcium at the 1.0m depth. The vertical electrode trial also has an increased strength at a given water content over the control and other trials. This can only happen if chemical or structural changes have taken place within the clay. It should be noted that these tests were carried out at the centre point of the footings where from section 6.3 it can be seen that there exists a current void in this position. The initial numerical simulations conducted did not show these voids and therefore the centre point was chosen. The simulations were run again after the site trials took place to check the images and there was a change, likely due to a software update. Furthermore, with the acid front likely to be migrating quicker than the base front, the actual centre of treatment may be closer to the cathode than the centre.

The intermittent current appeared to have a detrimental effect on the clay with shear strength reduction quite evident without a water content increase. The current transference of this current intermittence system did suggest that perhaps polarisation was avoided producing a consistent current. The raked electrode trial appeared to have little effect on the clay despite chemical stabilisers being introduced. It is thought that an artefact such as a lens under the footing is likely to have negatively affected the results of this trial. Due to there being not

enough clay samples taken before treatment, the lack of initial index testing has proven to lead the plastic limit, liquid limit and shrinkage limit data inconclusive but indicative of trends. It should also be noted that the changes shown here, albeit small, were conducted without any degradation to the concrete footings and also no level change over that of the control trial.

The 25V supplied to the site trial electrodes was the maximum that could be due to Health and Safety regulations; however, this 62.5V/m is below the previously used 100 – 140V/m which has proved successful in the laboratory trials and the literature review. Whilst the site trial has successfully shown that improvements have been induced through the chemical analysis and resistivity measurements, a combination of poor subsurface clay, unfortunate test locations and restricted power supply has somewhat masked the EKS effect.

The focus of this section as explained in section 7 can be concluded as follows. The lack of damage to the foundations and resistivity results show that the effects of the treatment technique don't appear to spread much further than the intended treatment zone. This treatment technique is relatively cheap compared to the importation of concrete or steel for other solutions. When considering other factors such as time on site, the economic benefits possible here are significant. The methodology used during this section has proven to be effective and it is anticipated that if used commercially, improved equipment and installation techniques would prove advantageous.

8 CONCLUSIONS

This thesis has reviewed the appropriate literature regarding the use of electrokinetics in clays to determine the knowledge gaps. These gaps were then explored in laboratory trials and numerical simulations. The laboratory trials concentrated mainly on the electrode efficacy and the effect of the EKS chemical combinations on the clay water system whilst numerical modelling was used to explore undesirable effects in the laboratory equipment and electrode arrangements on site. The culmination of this work was the development of a site trial which consisted of three permutations of the EKS treatment solution and one control test.

It has been shown through this thesis, that the original objectives were met and achieved through the stages of laboratory studies, numerical modelling and then scaled up site trials;

(1) It has been presented here that the historic predominantly laboratory based EKS technique can be scaled up to site trial level effectively. Re-usable electrodes were shown to have advantages over their iron based peers especially when considering durability and life span but saw diminished effectiveness compared to stainless steel regarding electric current transfer to the clay. The re-usable prototype PEG was shown to be most suitable when constructed using a graphite to epoxy-resin mix of 35% graphite by weight. For the site trials it was determined that short term effectiveness was paramount and as such stainless steel was opted for. It was shown that a 3% mix by weight of 2/3 $CaCl_2$ and 1/3 Na_2SiO_3 proved most effective in increasing shear strength and reducing the shrink/swell capacity of English China Clay. Furthermore, current intermittence showed the potential to reduce power consumption and increase treatment rates whilst also reducing the effect of electrode polarisation.

(2) Numerical Modelling was used for optimising electrode arrangements and treatment depths to maximise treatment efficacy whilst avoiding foundation contact. This culminated in the conclusion that offset electrodes should be utilised to avoid current density blackspots and electrodes should be electrically insulated to twice the depth of the foundation to avoid interference with the foundation. This will allow for a more uniform targeted treatment zone.

(3) The use of EKS in the site trial was shown to be effective even under difficult conditions. Vertical stainless steel electrodes were shown to provide the greatest

response to an electric current input with clear improvement of the expansive clay shown through geotechnical characteristic testing. This evidence is enhanced when coupled with the apparent resistivity modelling which provided a near real time progress of the treatment by determining fluid migration. Furthermore, through targeting a treatment zone beneath the foundation, no adverse effects were shown in relation to the strip footings including movements and chemical/acid damage. The current intermittence set-up also showed improvement over the control test but not to the extent of the vertical. The raked electrode set-up showed deterioration in the ground beneath the strip footing possibly due to a high permeability lens. This shows the need for a detailed ground investigation at any proposed scheme location but an effective treatment can be possible even if the treatment zone sits within made ground. If there is sufficient clay content in the made ground, improvements can be made.

It is suggested that to improve the EKS system for commercial viability, further up-scaled work is required in which mix valves are utilised for fluid control, commercial electrical connections are installed for durability and the electrodes are commercially installed through pre-augured holes.

9 FURTHER RESEARCH

The research presented here serves to prove that there are future applications available to EKS whether it be in the current form or not. The following are suggestions for future research into the subject area based upon ideas and realisations from throughout the thesis progression.

- Validating FEA simulation software like Quickfield would be beneficial in the modelling of the current flow through the clay. If a dynamic modelling software becomes available then the change in ground conditions and consequent change in treatment process can be modelled.
- Research into dielectrophoresis would be a possible future avenue to explore due to its claimed negligible power usage and ability to migrate ions through clay.
- Further investigating the PEG electrode would be helpful as it has potential as a cheap, re-usable electrode. If commercially produced, it may be successful.
- A detailed study into the use of current intermittence in a site setting would be advantageous for a more economic and environmentally friendly treatment solution. Its ability to depolarise an electrode system is very beneficial for longer term treatments.
- A study into the rate at which the stabilising chemicals can be delivered to the treatment zone would improve efficiencies of the system.
- To improve industrial acceptance of this treatment solution, solid data regarding the effects of EKS on the local biology would be beneficial.

References

Abdullah, W. & Al-Abadi, A., 2010. Cationic-electrokinetic improvement of an expansive soil. *Applied Clay Science,* Volume 47, pp. 343-350.

Acar, Y. et al., 1995. Electrokinetic remediation: Basics and technology status. *Journal of Hazardous Materials,* Volume 40, pp. 117-137.

Adamson, L., Chilingar, G., C., B. & R., A., 1966. Electrokinetic dewatering, consolidation and stabilization of soils. *Engineering Geology,* 1(4), pp. 291-304.

Ahmad, K., Taha, M. & Kassim, K., 2010. Electrokinetic treatment on a tropical residual soil. *Procedings of the ICE - Ground Improvement ,* 164(GI1), pp. 3-13.

Ahmad, N., 1975. *Evaluation of in-situ testing methods in soils.* PhD Thesis ed. s.l.:Luisiana State University.

Almeira, J., Peng, C. & Wang, Z., 2009. Effect of different electrode configurations on the migration of copper ions during the electrokinetic remediation process. *Asia-Pacific Journal of Chemical Engineering,* Volume 4, pp. 581-585.

Alshawabkeh, A. & Sheahan, T., 2003. Soft soil stabilisation by ionic injection under electric fields. *Ground Improvement,* 7(4), pp. 177-185.

Alshawabkeh, A. & Sheahan, T., 2004. Coupling of electrochemical and mechanical processes in soils under DC fields. *Mechanics of Materials,* 36(5-6), pp. 452-465.

ASA, 2002. *Binary Phase diagram: The Calcium Chloride - water system.* [Online]
Available at: http://www.phasediagram.dk/binary/calcium_chloride.htm
[Accessed 10 10 2014].

Asavadorndeja, P. & Glawe, U., 2005. Electrokinetic strengthening of soft clay using. *Bulletin of Engineering Geology and the Environment,* Volume 64, pp. 237-245.

Atkinson, J., 2007. *The Mechanics of Soils and Foundations.* 2nd ed. s.l.:Spon Text.

Atkinson, J., Richardson, D. & Stallebrass, S. E., 1990. Effect of recent stress history on the stiffness of overconsolidated soil. *Geotechnique,* 40(4), pp. 531-540.

Audebert, R. & de Mende, S., 1959. *The Principles of Electrophoresis.* London: Hutchinson Scientific & Technical.

Bain, J., 1971. A plasticity chart as an aid to the identification and assessment of industrial clays. *Clay Minerals,* 9(1), pp. 64-78.

Barker, J. E., 2002. *Ion migration associated with lime piles. Unpublished doctoral thesis..* Birmingham: University of Birmingham.

Barker, J., Rogers, C. & Boardman, D., 2007. *Ion migration associated with lime piles: a review.* s.l., s.n., pp. 87-98.

Barker, J., Rogers, C., Boardman, D. & Peterson, J., 2004. Electrokinetic stabilisation: an overview and case study. *Ground Improvement,* 8(2), pp. 47-58.

Barnes, G., 2010. *Soil Mechanics - Principles and Practice.* 3 ed. London: Palgrave Macmillan.

Barnes, G., 2013. *The plastic limit and workability of soils - Unpublished Thesis.* s.l.:The University of Manchester.

Bell, F. G., Culshaw, M. G., Cripps, J. C. & Lovell, M. A. (., 1988. Engineering Geology of Underground Movements. *Geological Society Engineering Special Publication No. 5,* pp. 363-376.

Biddle, P., 1998a. *Tree root damage to buildings. Volume 1 - Causes, Diagnosis and Remedy..* s.l.:s.n.

Biddle, P., 1998b. *Tree roots and foundations. Arboricultural research and information note 142.* Farnham: Arboricultural Advisory and Information Service.

Bjerrum, L., 1967. Progressive Failure in Slopes of Overconsolidated Plastic Clay and Clay Shales. *Journal of the Soil Mechanics and Foundations Division, ASCE,* 93(SM5), pp. 1-49.

Black, J., Stanier, S. & Clarke, S., 2009. Shear wave velocity measurement of kaolin during undrained unconsolidated triaxial compression. *Proceedings of the 62nd Canadian Geotechnical Conference.*

Bohn, H., McNeal, B. & O'Connor, G., 1985. *Soil chemistry, Second Edition.* New York: John Wiley & Sons.

BRE, 1991. *BRE Digest 184 - Foundation movement and remedial underpinning in low-rise buildings,* s.l.: BRE.

BRE, 1993. *BRE Digest 240: Low rise buildings on shrinkable clay soils: Part 1,* UK: British Research Establishment.

BRE, 2009. *BRE Digest 298: Low rise building foundations: the influence of trees in clay soils,* UK: British Research Establishment.

Bryant, J. et al., 2001. Tree root influence on soil-structure interaction in expansive clay soils. In: *Expansive Clay Soils and Vegetative Influence on SHallow Foundations.* s.l.:ASCE, pp. 110-131.

Buckland, D., Shang, J. & Mohamedelhassan, E., 2000. Electrokinetic sedimentation of contaminated Welland River sediment. *Canadian Geotechnical Journal,* Volume 37, pp. 735-747.

Burnett, A. & Fookes, P., 1974. A regional engineering geological study of the London Clay in the London and Hampshire basins. *Quarterly Journal of Engineering Geology,* Volume 7, pp. 257-295.

Burnotte, F., Lefebvre, G. & Grondin, G., 2004. A case record of electroosmotic consolidation of soft clay with improved soil-electrode contact. *Canadian Geotechnical Journal,* Volume 41, pp. 1038-1053.

Calabresi, G. & Scarpelli, G., 1985. *Effects of swelling caused by unloading in overconsolidated clays.* s.l., s.n., pp. 411-414.

Callister, W., 2007. *Materials Science and Engineering an Introduction, Seventh Edition.* s.l.:John Wiley and Sons.

Casagrande, L., 1949. Electro-osmosis in soils. *Geotechnique,* 1(3), pp. 159-177.

Casagrande, L., 1952. Electroosmotic stabilization of soils. *Journal of Boston Society of Civil Engineers,* 39(1), pp. 51-83.

Cassidy, N., 2008. Chapter 2 - Electrical and magnetic properties of rocks, soils and fluids. In: H. Jol, ed. *Ground Penetrating Radar Theory and Applications.* Eau Claire: Elsevier, pp. 41-72.

CellarTech South West Ltd, 2011. *CellarTech South West Ltd.* [Online]
Available at: http://www.cellarconversionsouthwest.co.uk/index.php
[Accessed 13 08 2016].

Chandler, R. J. & Skempton, A. W., 1974. The design of permanent cutting slopes in stiff fissured clays. *Geotechnique,* 24(4), pp. 457-466.

Chatterjee, A., Iwasaki, T., Ebina, T. & Miyamoto, A., 1999. A DFT study on clay-cation-water interaction in montmorillonite and beidellite. *Computational Materials Science,* Volume 14, pp. 119-124.

Cheney, J., 1988. 25 years' heave of a building constructed on clay, after tree removal. *Ground Engineering,* 21(5), pp. 13-27.

Chew, S. et al., 2004. A field trial for soft clay consolidation using electric vertical drains. *Geotextiles and Geomembranes,* Volume 22, pp. 17-35.

Clarke, D. & Smethurst, J., 2010. Effects of climate change on cycles of wetting and drying in engineered clay slopes in England. *Quarterly Journal of Engineering Geology and Hydrogeology,* Volume 43, pp. 473-486.

Costa Filho, L., 1984. Technical note: A note on the influence of fissures on the deformation characteristics of London Clay. *Géotechnique,* 34(2), pp. 268-272.

Crilly, M., 2001. Analysis of a database of subsidence damage. *Structural Survey,* 19(1), pp. 7-15.

Cripps, J. & Taylor, R., 1986. Engineering characteristics of British over-consolidated clays and mudrocks I: Tertiary deposits. *Engineering Geology,* Volume 22, pp. 349-376.

Cutler, D. F. & Richardson, I. B. K., 1989. Tree Roots and Buildings. In: 2nd ed. s.l.:Longman Scientific and Technical, p. 71.

Daub, G. & Seese, W., 1996. *Basic Chemistry.* 7th ed. New Jersey: Prentice Hall Incorporation.

Day, R., 1994. Swell-shrink behaviour of compacted clay.. *Journal of Geotechnical Engineering,* 120(3), pp. 618-623.

Di Maio, C., Hueckel, T. & Loret, B., 2002. *Chemo-Mechanical Coupling in Clays.* Lisse, The Netherlands: Swets & Zeitlinger.

Dif, A. & Bluemel, W., 1991. Expansive soils under cyclic drying and wetting. *Geotech Test J,* 14(1), pp. 96-102.

Driscoll, R., 1983. The influence of vegetation on the swelling and shrinking of clay soils in Britain. *Geotechnique,* Volume 33, pp. 93-105.

Eastwood, B. J., 1997. A Fundamental Study of the Electrochemical Failure Mechanisms of a Novel Impressed Current Cathodic Protection System, Unpublished Doctoral Thesis. In: s.l.:University of Newcastle Upon Tyne, p. 182.

Eisenberg, D. & Kauzmann, W., 1969. *The structure and properties of water.* London: Oxford University Press.

Environment Agency, 2013. *Environment Agency Carbon Calculator.* [Online]
Available at: http://www.environment-agency.gov.uk/business/sectors/136252.aspx
[Accessed 27 March 2013].

Esrig, M., 1968. Pore pressure, consolidation, and electrokinetics. *Journal of the soil mechanics and foundations division,* 94(SM 4), pp. 899-921.

F.D.A., -. U. F. a. D. A., 2013b. *Select Committee on GRAS Substances (SCOGS) Opinion: Calcium chloride.* [Online]
Available at:
http://www.fda.gov/Food/IngredientsPackagingLabeling/GRAS/SCOGS/ucm260880.htm
[Accessed 4 1 2015].

F.D.A., -. U. F. a. D. A., 2013. *Select Committee on GRAS Substances (SCOGS) Opinion: Sodium silicate.* [Online]
Available at:

http://www.fda.gov/Food/IngredientsPackagingLabeling/GRAS/SCOGS/ucm260997.htm [Accessed 4 Januray 2015].

Fetzer, C., 1967. Electro-osmotic Stabilization of West Branch Dam. *Journal of Soil Mechanics and Foundations Div,* Volume 93, pp. 85-106.

Fredlund, D., 1987. The prediction and performance of structures on expansive soils. *Proceedings, predictions and performance in geotechnical engineering,* pp. 51-60.

Freeman, T. J., Littlejohn, G. & Driscoll, R., 1994. *Has Your House Got Cracks – A guide to subsidence and heave of buildings on clay.* London: Thomas Telford Services Ltd..

Fukue, M., Minato, T., Horibe, H. & Taya, N., 1999. The micro-structures of clay given by resistivity measurements. *Engineering Geology,* Volume 54, pp. 43-53.

Fukue, M. M. T. M. M. H. H. a. T. N., 2001. Use of a resistivity cone for detecting contaminated soil layers. *Engineering Geology,* Volume 60, pp. 361-369.

Gasson, P. & Cutler, D., 1990. Tree root plate morphology. *Arboricultural Journal,* Volume 14, pp. 193-264.

Glendinning, S., Jones, C. & Lamont-Black, J., 2005. Chapter 35 The Use of Electrokinetic Geosynthetics (EKG) to Improve Soft Soils. In: s.l.:Elsevier Geo-Engineering Book Series, pp. 997-1043.

Glendinning, S., Jones, C., Lamont-Black, J. & Hall, J., 2008. Treatment of lagooned sewage sludge in situ using electrokinetic geosynthetics. *Geosynthetics International,* 15(3), pp. 192-204.

Gray, D., 1970. Electrochemical hardening of clay soils. *Geotechnique,* 20(1), pp. 81-93.

Greenwald, E., 1991. *Electrical Hazards and Accidents - Their Cause and Prevention.* New York: Van Nostrand Reinhold.

Gregory, P., 1988. Growth and functioning and plant roots. In: *Russell's Soil Conditions and Plant Growth.* London: Longmans, pp. 113-167.

Grossnickle, S., 2000. Ecophysiology of northern spruce species: performance of planted seedlings. In: Ottawa: National Research Council of Canada, p. 407.

Guven, N., 1992. Molecular aspects of clay-water interactions, In: Clay-water interface and its rheological implications, CMS workshop lectures. *Clay Minerals Society,* pp. 6-10.

Harrison, A. et al., 2012. The relationship between shrink-swell occurence and climate in south-east England. *Proceedings of the Geologists' Association,* Volume 123, pp. 556-575.

Harrison, J. et al., 2012. The relationship between shrink-swell occurance and climate in south-east England. *Proceedings of the Geologists' Association,* 123(4), pp. 556-575.

Heeralal, M., Ramana Murty, V., Praveen, G. & Shankar, S., 2012. *Influence of calcium chloride and sodium silicate on index and engineering properties of bentonite.* Pattaya (Thailand), ICEEBS.

Hillel, D., 1998. Environmental Soil Physics. In: San Diego: Academic Press, p. 771.

Hoffman, H., 1965. *Contrails.* [Online]
Available at: http://contrails.iit.edu/DigitalCollection/1965/AFAPLTR65-108article14.pdf
[Accessed 10 10 2014].

Holtz, W. & Gibbs, H., 1956. Engineering properties of expansive clays. *Trans. of ASCE.*

Hunter, R., 1981. *Zeta Potential in Colloid Science.* New York: Academic Press.

Hunt, R., Dyer, R. & Driscoll, R., 1991. *BRE Report 184 Foundation movement and remedial underpinning in low-rise buildings,* s.l.: British Research Establisment.

IAEI, 2004. *Soares Book on Grounding and Bonding.* 9th ed. USA: IAEI.

Inculet, I. & Lo, K., 1988. *Dielectrophoretic consolidation of clays..* Pittsburgh, Pennsylvania, Industry Applications Conference, The 23rd Annual Meeting.

IPCC, 2009. *UN Summit on Climate Change Statement,* s.l.: IPCC.

Jackson, R. et al., 1996. A global analysis of root distributions for terrestrial biomes. *Oecologia,* Volume 108, pp. 389-411.

Jenny, A., 1940. *The anodic oxidation of aluminium and its alloys.* London: Griffin.

Jeyakanthan, V., Gnanendran, C. & Lo, S., 2011. Laboratory assessment of electro-osmotic stabilization of soft clay. *Canadian Geotechnical Journal,* Volume 48, pp. 1788-1802.

Jones, C., Fahker, A., Hamir, R. & Nettleton, I., 1996. Geosynthetic materials with improved reinforcement capabilities. *Proceedings of the International Symposium on Earth Reinforcement,* Volume 2, pp. 865-883.

Jones, C., Lamont-Black, J. & Glendinning, S., 2011. Electrokinetic geosynthetics in hydraulic applications. *Geotextiles and Geomembranes,* Volume 29, pp. 381-390.

Jones, C. et al., 2014. The environmental sustainability of electrokinetic geosynthetic strengthened slopes. *Proceedings of the ICE - Engineering Sustainability ,* 167(3), pp. 95-107.

Jones, G., 2010. *Imaging and monitoring tree induced subsidence in expansive clays using electrical resistivity imaging.* Unpublished Thesis ed. s.l.:Keele University.

Jones, G. et al., 2009. Imaging and monitoring tree-induced subsidence using electrical resistivity imaging. *Near Surface Geophysics,* pp. 191-206.

Jones, L., 2004. *Cracking Open,* s.l.: Planet Earth Autumn 2004 (www.nerc.ac.uk).

Jones, L. D. & Terrington, R., 2011. Modelling volume change potential in the London clay. *Quarterly Journal of Engineering Geology and Hydrogeology,* Volume 44, pp. 109-122.

Jones, L. & Jefferson, I., 2012. Chapter C5 - Expansive Soils. In: *Institution of Civil Engineers Manuals Series.* s.l.:ICE Manuals.

Ju, S., Weber, M. & Mujumdar, A., 1991. Electroosmotic dewatering of bentonite suspensions. *Seperations Technology,* Volume 1, pp. 214-221.

Kalkan, E., 2011. Impact of wetting-drying cycles on swelling behaviour of clayey soils modified by silica fume. *Applied Clay Science,* Volume 52, pp. 345-352.

Kalogirou, S. & Florides, G., 2014. *Measurements of ground temperatures at various depths.* Nottingham, UK, 3rd International Conference on Sustainable Energy Technologies.

Kaniraj, S., Huong, H. & Yee, J., 2011. Electro-osmotic consolidation studies on peat and clayey silt using electric vertical drain. *Geotechnical and Geological Engineering,* pp. 1-19.

Karim, M., 2014. Electrokinetics and soil decontamination: concepts and overview. Journal of Electrochemical Science and Engineering, 4(4), pp. 297-313.

Kissel, D., Sonon, L., Vendrell, P. & Isaac, R., 2009. Salt concentration and measurement of soil pH. *Communications in Soil Science and Plant Analysis,* Volume 40, pp. 179-187.

Kodikara, J., Barbour, S. & Fredlund, D., 1999. Changes in clay structure and behaviour due to wetting and drying. *Proceedings of the 8th Australian - New Zealand Conference on Geomechanics,* pp. 179-186.

Kozlowski, T., 2007. A semi-empirical model for phase composition of water in clay-water systems. *Cold Regions Science and Technology,* 49(3), pp. 226-236.

Krohn, J. & Slosson, J., 1980. Assessment of expansive soils in the United States. *Proceedings, 4th International Conference on expansive soils ,* Volume 1, pp. 596-608.

Lambe, T., 1979. *Soil Mechanics, SI Version.* USA: John Wiley & Sons.

Lessard, G., 1978. Traitement Chimique des Argiles Sensibles d'Outardes-2, Memorie de M.Sc.A.. In: s.l.:Ecole Polytechnique de Montreal, p. 187.

Levy, R. & Shainberg, I., 1972. Calcium-magnesium exchange in montmorillonite and vermiculite. *Clays and clay minerals,* Volume 20, pp. 37-46.

Liaki, C., 2006. *Physiochemical study of electrokinetically treated clay using carbon and steel electrodes, Unpublished Doctoral Thesis.* s.l.:University of Birmingham.

Little, D., 1987. *Fundamentals of the stabilisation of soil with lime, Bulletin No. 332,* USA: National Lime Association.

Lockhart, N., 1983. Dielectrophoresis in clay suspensions. *Powder Technology,* Volume 35, pp. 17-22.

Lofgren, B., 1968. Analysis of stress causing land subsidence. *United States Geological Survey,* Volume 600-B, pp. 219-225.

Lo, K., Ho, K. & Inculet, I., 1992. A novel technique of electrical strengthening of soft sensitive clays by dieletrophoresis. *Canadian Geotechnical Journal,* Volume 29, pp. 599-608.

Marshall, D. & Madden, T., 1959. Induced polarization, a study of its causes. *Geophysics,* Volume 24, pp. 790-816.

Matzui, L., Vovchenko, L., Perets, Y. & Lazarenko, O., 2013. Electrical conductivity of epoxy resin filled with grpahite nanoplatelets and boron nitride. *Mat.-wiss. u. Werkstofftech.,* Volume 44, pp. 2-3.

McCarter, J., 1984. The electrical resistivity characteristics of compacted clays. *Geotechnique,* 34(2), pp. 263-267.

Mendez, E. et al., 2012. Effects of electrode material on the efficiency of hydrocarbon removal by an eletrokinetic remediation process. *Electrochemica Acta,* Volume 86, pp. 148-156.

Mesri, G. & Cepeda-Diaz, A., 1986. Residual shear- strength of clays and shales.. *Geotechnique,* 36(2), pp. 269-274.

Milligan, V., 1995. First application of electro-osmosis to improve the friction pile capacity - three decades later. *Proceedings of the ICE - Geotechnical Engineering,* 113(2), pp. 112-116.

Mitchell, J., 1993. *Fundamentals of Soil Behaviour.* 2nd ed. New York: John Wiley & Sons.

Mitchell, J. & Soga, K., 2005. *Fundamentals of soil behaviour.* 3rd ed. s.l.:John Wiley & Sons.

Moayedi, H. et al., 2011. Effect of Sodium Silicate on Unconfined Compressive Strength of Soft Clay. *EJGE,* pp. 289-295.

Mohamedelhassan, E., 2009. Electrokinetic strengthening of soft clay. *Ground Improvement,* 162(G14), pp. 157-166.

Mohamedelhassan, E. & Shang, J., 2001. Effects of electrode materials and current intermittence in electro-osmosis. *Ground Improvement,* 5(1), pp. 3-11.

Mohamedelhassan, E., Shang, J., Ismail, M. & Randolph, M., 2008. Electrochemical stablilisation for offshore model caissons. *Proceedings of the ICE – Ground Improvement,* 161(3), pp. 131-141.

Mojid, M. & Cho, H., 2006. Estimating the fully developed diffuse double layer thickness from the bulk electrical conductivity in clay. *Applied Clay Science,* 33(3-4), pp. 278-286.

Muha, L., 2007. The Skeptical Fishkeeper - The Algae Detective. *Tropical Fish Hobbyist Magazine*, July.

National House Building Council, 2011. *NHBC Standards.* UK: s.n.

Nelson, J. & Miller, D., 1992. *Expansive Soils: Problems and Practice in Foundation and Pavement Engineering.* New York: John Wiley & Sons.

Nelson, J., Overton, D. & Durkee, D., 2001. Depth of wetting and the active zone. In: *Expansive Clay Soils and Vegetative Influence on Shallow Foundations.* s.l.:ASCE, pp. 95-109.

Nizar, K. & Clarke, B., 2014. Electro-osmotic piles. *Ground Improvement,* 167(GI2), pp. 135-144.

Nye, P., 1979. Diffusion of ions and uncharged solutes in soils and soil clays. *Advances in Agronomy,* Volume 31, pp. 225-272.

O'Callaghan, D. & Kelly, O., 2005. Tree-related subsidence: Pruning is not the answer. *Journal of Building Appraisal,* 1(2), pp. 113-129.

Ou, C.-Y., 2006. *Deep Excavation - Theory and Practice.* London: Taylor & Francis Group.

Ozkan, S., Gale, R. & Seals, R., 1999. Electrokinetic stabilization of kaolinite by injection of Al and PO43- ions. *Ground Improvement,* Volume 3, pp. 135-144.

Page, R., 1998. Reducing the cost of subsidence damage despite global warming. *Structural Survey,* 16(2), pp. 67-75.

Park, J., Vipulanandan, C., Kim, J. & Oh, M., 2006. Effects of surfactants and electrolyte solutions on the properties of soil. *Environmental Geology,* Volume 49, pp. 977-989.

Pauling, L., 1960. *The nature of the chemical bond and the structure of molecules and crystals: An introduction to modern structural chemistry.* New York: Cornell University Press.

Perpich, W., Lukas, R. & Baker, C., 1965. Desiccation of soil by trees related to foundation settlement. *Canadian Geotechnical Journal,* Volume 2, pp. 23-29.

Pesticide Action Network (PAN) Europe, 2007. *State of the art Integrated Crop Management and organic systems in Europe, with particular reference to pest management,* s.l.: s.n.

Plotnik, A., 2000. *The Urban Tree Book; An Uncommon Field Guide for City and Town.* New York: Three Rivers Press.

Pohl, H., 1978. *Dielectrophoresis.* s.l.:Cambridge University Press.

Poland, J., 1984. *Guidebook to studies of land subsidence due to groundwater withdrawal.* Paris: Unesco.

PQ-Corporation, 2003. *PQ liquid sodium and potassium silicates - storage and handling.* [Online] Available at: http://www.pqcorp.com/Portals/1/lit/bulletin_17-70.pdf
[Accessed 10 10 2014].

Pugh, R., 2002. *The application of electrokinetic geosynthetic materials to uses in the construction industry, Unpublished Doctoral Thesis.* s.l.:University of Newcastle upon Tyne.

Pugh, R. & Jones, C., 2006. *Electrokinetic Geosynthetic Structure.* US, Patent No. US 7,150,583 B2.

Rabie, H., Mujumdar, A. & Weber, M., 1994b. Electroosmotic dewatering of bentonite in thin beds. *Seperation Technology,* Volume 4, pp. 180-182.

Rabie, H., Mujumdar, A. & Weber, M., 1994. Interrupted electroosmotic dewatering of clay suspensions. *Separation Technology,* Volume 4, pp. 38-46.

Radevsky, R., 2001. Expansive clay problems - How are they dealt with outside the US?. In: *Expansive Clay Soils and Vegetative Influence on Shallow Foundations.* s.l.:ASCE, pp. 172-191.

Rao, S., Reddy, B. & Muttharam, M., 2001. The impact of cyclic wetting and drying on the swelling behaviour of stabilized expansive soils. *Engineering Geology,* Volume 60, pp. 223-233.

Reeves, G., Sims, I. & Cripps, J., 2006. CLay materials used in construction. *Geological Society, London, Engineering Geology Special Publication,* Volume 21, pp. 1-526.

Rendig, V. & Taylor, H., 1989. *Principles of soil-plant interrelationships.* New York: McGraw-Hill.

Reuss, F. F., 1809. Memoires de la Societe Imperiale des Naturalistes de Moscou. Volume 2, p. 327.

Rittirong, A., Douglas, R., Shang, J. & Lee, E., 2008. Electrokinetic improvement of soft clay using electrical vertical drains. *Geosynthetics International,* 6(G13), pp. 131-141.

Rittirong, A. & Shang, J., 2005. Electro-osmotic Stabilisation. *Ground Improvement Case Histories,* 3(34), pp. 967-996.

Rittirong, A. et al., 2008b. Effects of electrode configuration on electrochemical stabilization for Caisson anchors in calcareous sand. *ASCE Journal of Geotechnical and Geoenvironmental Engineering,* 134(3), pp. 352-369.

Roberts, J., Jackson, N. & Smith, M., 2006. *Tree roots in the built environment.* UK: The Stationary Office.

Rouaiguia, A., 1988. Residual shear strength of clay-structure interfaces. *International Journal of Civil and Environmental Engineering IJCEE-IJENS,* 10(3).

Saarenketo, T., 1998. Electrical properties of water in clay and silty soils. *Journal of Applied Geophysics,* Volume 40, pp. 73-88.

Schmidt, A., Chapman, D. & Rogers, C., 2006. Physiochemical changes in London clay adjacent to cast iron pipes. *IAEG2006,* p. 313.

Segall, B. & Bruell, C., 1992. Electroosmotic contaminant removal processes. *Journal of Environmantal Engineering - ASCE,* 118(1), pp. 84-100.

Senftle, F., Grant, J. & Senftle, F., 2010. Low voltage DC/AC electrolysis of water using porous graphite electrodes. *Electrochimica Acta,* Volume 55, pp. 5148-5153.

Shahbuddin, A., 2013. *The Efficiency of electrolytes, water and other mediums at transferring DC current from an electrode to soil, Unpublished M.Sc. Dissertation.* s.l.:University of Birmingham.

Shang, J., 1997. Zeta potential and electroosmotic permeability of clay soils. *Canadian Geotechnical Journal,* Volume 34, pp. 627-631.

Shang, J. & Dunlap, W., 1996. Improvement of soft clays by high voltage electrokinetics. *Journal of Geotechnical Engineering,* Volume 122, pp. 274-280.

Shang, J. & Lo, K., 1997. Electrokinetic dewatering of a phosphate clay. *Journal of hazardous materials,* Volume 55, pp. 117-133.

Skempton, A. W., 1977. Slope stability of cuttings on brown London clay. Proc., 9th Int. Conf. Soil Mech. and Found. Eng.. *Japanese Society of Soil Mechanics and Foundation Engineering,* Volume 3, pp. 261-270.

Skempton, A. W., 1985. Residual stengths of clays in landslides, folded strata and the laboratory. *Geotechnique,* 35(1), pp. 3-18.

Soderman, L. & Milligan, V., 1961. *Capacity of friction piles in varved clay increased by electro-osmosis.* Paris, Proceedings of the 5th International Conference on Soil Mechanics and Foundation Engineering.

Sparnaay, M., 1972. *The Electrical Double Layer, The International Encyclopdeia of Physical Chemistry and Chemical Physics.* UK: Pergamon Press.

Spear, N., 2014. *Electrokinetic Grouting of English China Clay using Intermittent Currents, Unpublished M.Sc. Dissertation.* s.l.:University of Birmingham.

Sposito, G., 1984. *The surface chemistry of soils.* New York: Oxford University Press.

Sposito, G., 1989. *The chemistry of soils.* New York: Oxford University Press.

Sprute, R. & Kelsh, D., 1975. Laboratory experiments in electrokinetic densification of mill tailings. *U.S. Bureau of Mines Report of Investigations,* Volume 8034, p. 47.

Stalin, V., Shantha Devi, A. & Arun Murugan, R., 2011. Influence of IMC, spacing and voltage on the effectiveness of electro-kinetic phenomena of soil stabilization. *Geo-Frontiers,* pp. 957-966.

Stanczyk, M. & Feld, I., 1964. *Electro-dewatering tests of Florida phosphate rock slime.* Michigan: U.S. Department of the Interior Bureau of Mines.

Stone, K. et al., 2009. *Unexploded ordenance (UXO). A guide for the construction industry.,* London: CIRIA.

Symes, C., 2012. A Little Nail Treatment. *Ground Engineering*, February, pp. 18-20.

Szczepanik, M., Stabik, J., Lazarczyk, M. & Dybowska, A., 2009. Influence of graphite on electrical properties of polymeric composites. *Archives of Materials Science and Engineering,* 37(1), pp. 37-44.

Tajudin, S., 2012. *Electrokinetic stabilization of soft clay, Unpublished Doctoral Thesis.* UK: University of Birmingham.

Takahashi, Y. et al., 2004. Arsenic behavior in paddy fields during the cycle of flooded and non-flooded periods. *Environmental Science and Technology,* 38(4), pp. 1038-1044.

Tan, T., Phoon, K., Hight, D. & Leroueil, S., 2003. *Characterisation and Engineering Properties of Natural Soils - Volume 2.* Lisse, Netherlands: Swets and Zeitlinger.

Taylor, H. & Gardner, H., 1963. Penetration of cotton seedling taproots as influenced by bulk density, moisture content and strength of soil. *Soil Science,* Volume 96, pp. 153-156.

Terra Analysis Ltd, 2011. *QuickfieldTM.* Svendborg, Denmark: s.n.

Terzaghi, K., 1925. “Structure and volume of voids of soils” in Erdbaumechanik auf Bodenphysikalisher Grundlage. Pp. 10-13. Translated by A. Casagrande in From Theory to Practise in Soil Mechanics (1960). In: New York: John Wiley and Sons, pp. 146-148.

Tikhomolova, K. P., 1993. *Electro-osmosis.* London: Ellis Horwood Limited,.

Trethewey, K. & Chamberlain, J., 1995. *Corrosion for Science and Engineering.* 2nd ed. UK: Longman Group Limited.

Turer, D. & Genc, A., 2005. Assessing effect of electrode configuration on the efficiency of electrokinetic remediation by sequential extraction analysis. *Journal of Hazardous Materials,* Volume B119, pp. 167-174.

van Olphen, H., 1977. *An Introduction to Clay Colloid Chemistry.* 2nd ed. USA: John Wiley and Sons.

Watson, G., 2001. Tree size affects root regeneration and top growth after transplanting. *Journal of Environmental Horticulture,* Volume 19, pp. 119-122.

Waxman, M. & Smits, L., 1968. Electrical conduction in oil-bearing sands. *Society of Petroleum Engineers Journal,* Volume 8, pp. 107-122.

Weaver, C. & Pollard, L., 1973. *The chemistry of clay minerals.* 15 ed. s.l.:Developments in Sedimentology.

White, M., Alcock, I., Wheeler, B. & Depledge, M., 2013. Would you be happier living in a greener urban area? A fixed-effects analysis of panel data.. *Pschological Science,* 24(6), pp. 920-928.

Williams, G.M., 1971. *On the stratigraphy and palaeontology of the London Clay*. Unpublished PhD Thesis, Univ. London

Wilun, Z. & Starzewski, K., 1975. *Soil Mechanics in Foundation Engineering.* London: Surrey University Press.

Win, B., Choa, V. & Zeng, X., 2001. Laboratory investigation on electro-osmosis properties of singapore marine clay. *Soils ans Foundations,* 41(5).

Winter, N., 2015. *SEM imaging of cement and cementitious materials.* [Online]
Available at: http://semcementtraining.com/sem-cement-imaging/
[Accessed 14 3 2015].

Wrigley, A. G., 1940. *Faunal Succession in the London Clay, illustrated in some new exposures near London*. Proceedings of the Geologists' Association, Vol.51, 230-245.

Xeidakis, G., 1996. Stabilisation of swelling clays by Mg(OH)2. Changes in clay properties after addition of Mg-hydroxide. *Engineering Geology,* 44(1-4), pp. 107-120.

Yamaguchi, T. & Matsuda, S., 1975. Stabilization of sand feasible to liquefaction by means of a kind of grouting applying electroosmosis. pp. 411-421.

Yazdandoust, F. & Yasrobi, S., 2010. Effect of cyclic wetting and drying on swelling behaviour of polymer-stabilized expansive clays. *Applied Clay Science,* Volume 50, pp. 461-468.

Yeung, A. T. & Mitchell, J. K., 1993. Coupled fluid, electrical and chemical flows in soils. *Geotechnique,* 43(1), pp. 121-134.

Yong, R. & Warkentin, B., 1975. *Soil Properties and Behaviour.* s.l.:Elselvier Scientific Publishing Company.

Young, H. D. & Freedman, R. A., 1996. *University Physics, with Modern Physics*. Volume 2. 9th Edition. Pearson.

Zemenu, G. & Martine, A., 2009. Analysis of the behaviour of a natural expansive soil under cyclic drying and wetting. *Bulletin of Engineering Geology and the Environment,* Volume 68, pp. 421-436.

Zhinkin, G., 1952. Experience in using electrochemical soil reinforement for stabilising roadbeds. *Leningr. Inst. Inzhenerov Zheleznodorozhnogo Transporta, Sbornik,* Volume 144, pp. 64-79.

Zhuang, Y. & Wang, Z., 2007. Interface electric resistance of electroosmotic consolidation. *Journal of Geotechnical and Geoenvironmental Engineering,* Volume 1617.

APPENDIX A – Carbon Footprint

Using the Environment Agency's Carbon Footprint Calculator, (Environment Agency, 2013), it can be established that concrete XC4 is most likely to be used for house foundations with exposure to fresh water cyclic wet and dry. This shows that the embodied CO_2 per tonne of concrete used is 0.114 tonnes. On a house with ground floor total wall length of 40m, for example, this gives a total footprint of 6.679 tonnes, assuming 0.6 x 1.0 m footing with unknown cement type, 10% recycled aggregate and travelling 15 miles by road to the site.

The National House Building Council states that when building around trees that can cause clays to shrink and heave, one must found at certain depths and distances from the trees, (National House Building Council, 2011). This is not always viable, especially in cases where tree protection orders exist, but also this does not stop the plantation of trees and large bushes post-construction. Thus, following the NHBC guidelines for size of footings under a home, one can still be caught short with post construction planting. This is a reason to have the built in electrodes in the foundations during construction in-case they are ever needed. Along with the fact that by incorporating these built in electrodes into the foundation, one can effectively reduce the size of the foundation as the extra depth is not needed to combat shrink and swell. This in turn reduces the amount of concrete and therefore the carbon footprint of the scheme. By reducing the depth of the foundation by just 100mm, it is possible to bring the carbon footprint down to 6.006 tonnes saving over 650 kg of CO_2 from being released per house. The (National House Building Council, 2011) state that when founding near trees in soil with shrink/heave potential, a high potential requires a minimum of 1.0m depth foundation, Table A-1. If by pre-installing this system, one can reduce this to a medium potential, foundation depths can be reduced also.

With over 100,000 new homes built in 2010 (this number being down from a recent peak of over 150,000 in 2007), this 650kg would add up to at least 65,000 tonnes of CO_2 saved every year. The Woodland Trust suggests donating £25.00 per tonne of CO_2 produced to offset a carbon footprint, due to the fact that it costs this much to plant enough trees to absorb 1 tonne of CO_2 from the atmosphere. Following these guidelines, to put the environmental benefit into fiscal terms, the CO_2 saved by reducing the foundation depth by 100mm would cost £1,625,000 per year.

(Jones & Terrington, 2011) reports that using electrokinetic treatment for stabilising a railway embankment instead of gabion baskets and slope slackening produced a CO_2 reduction of 47%.

Using this method of electrode installation during building construction would allow buildings to be built closer to trees whilst reducing the amount that need removing before construction begins, helping in the reduction of CO_2 being released. The other benefit is there would be a large reduction in disturbance for the home owners by not needing to spend time and money installing electrodes into the ground around the foundations at the time of incident, the electrodes just need to be powered. If the angled electrode was to be used, drilling through the foundation is needed at specific points; this could be avoided if pre-installed electrodes were in use.

The author would argue that pre-installing this system would not be an admission of poor design or unsuitable ground by the home developer, but a system designed to economically and imperceptibly treat unstable ground considering the future is uncertain with the plantation of trees, bushes and climate change.

Table A-1: Minimum foundation depths. After (NHBC, 2011).

Volume Change Potential	Minimum Depth (m)
High	1.0
Medium	0.9
Low	0.75

APPENDIX B – Consolidation Equipment

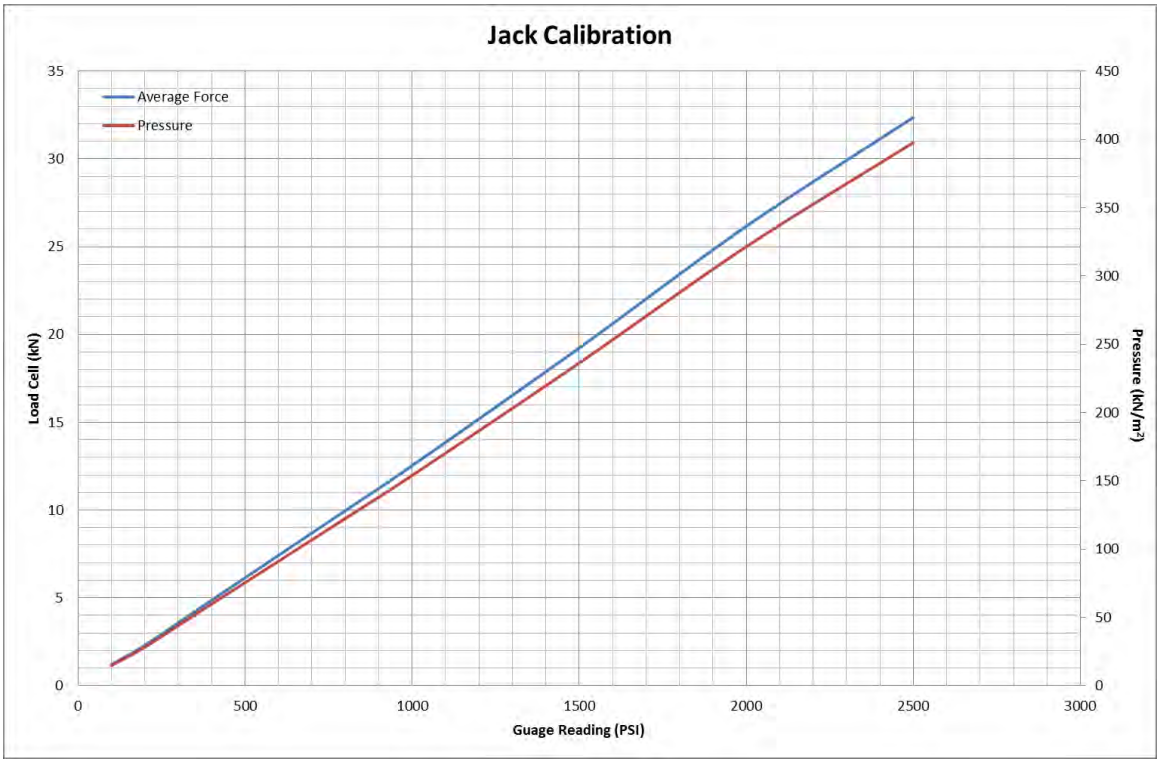

Figure B-1: Calibration of hydraulic jacks for consolidation

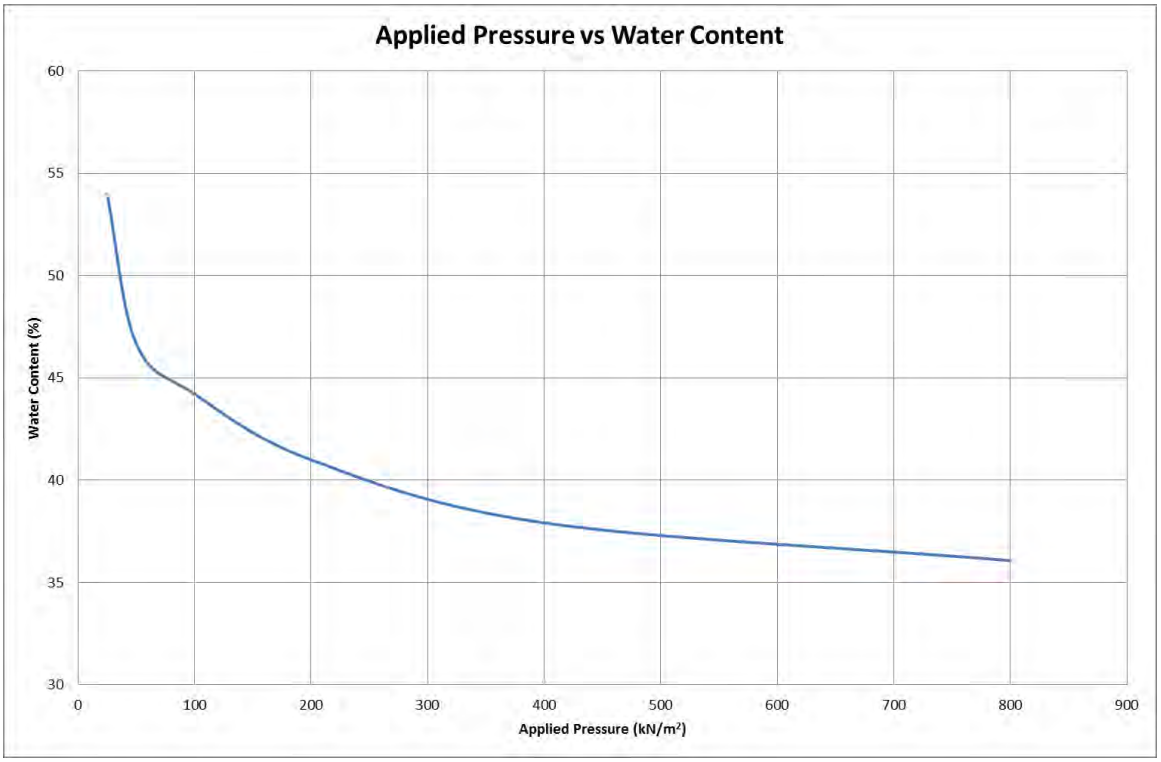

Figure B-2: Applied hydraulic jack pressure against resultant water content of sample

APPENDIX C – Site Trials Sign

ELECTROKINETIC SOIL STABILISATION
ALDENHAM SCHOOL FIELD TRIAL

UNIVERSITY OF BIRMINGHAM

Foundation Piling Ltd

Clay Research Group

Current research at the School Of Civil Engineering, University of Birmingham is developing a methodology for remotely stabilising clay susceptible to subsidence and settlements problems. Subsidence typically costs up to £500 million p.a. in insurance claims and remedial works. This site trial, the culmination of detailed laboratory and computer modelling, is being used to develop a new novel treatment approach that is both relatively cheap to use and non-invasive to the householder.

The field trial consists of four concrete mock strip footings simulating house foundations. The clay under these footings is then treated using the Electrokinetic Stabilisation, a process to strengthen and reduce the risk of volumetric change whilst deterring trees from rooting in the vicinity.

The poles marked black hold gauges that allow both vertical and horizontal movements of the footings to be monitored. This will allow the full potential impact of the treatment approach to be assessed. The steel poles with plastic boxes on top are the electrodes, which supply a low (and safe) electrical current into the ground so that the stabilising fluids (supplied via the water butts), can be injected precisely where it is needed. The added advantage of this approach is that normal safe stabilising fluids can be used so avoiding any negative environmental effects in the ground or to the surrounding flora and fauna.

Name: Professor Ian Jefferson
Tel: 0121 4147972
Email: i.jefferson@bham.ac.uk

APPENDIX D – Site Trials Beam Design

Tom Girton's Groundbeams

Groundbeams will be designed for lifting out only, as they will not be loaded in-situ

Dimensions

1000mm len
300mm deep
300mm wide
30mm cover

Anticipated Reinforcement

4 No H12 bars - Bottom
2 No H12 bars - Top
R6 links.

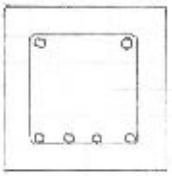

Loading - lifting out only

Concrete - $300^{t} \times 24 = 2.16\ kN/m \times \frac{2}{(FOS)} = 4.32\ kN/m$ say $4.5\ kN/m$

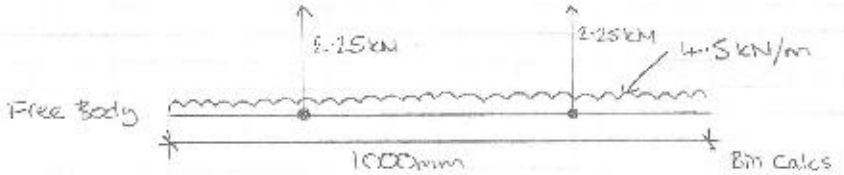

Bm Calcs
Cantilever @ root:

$wl^2/2 = \frac{4.5 \times 0.5^2}{2}$

$= 0.14\ kNm$

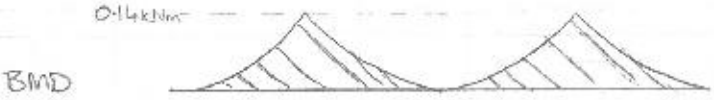

Simply Supported

$\frac{wl^2}{8} = \frac{4.5 \times 0.5^2}{8}$

$= 0.14\ kNm$

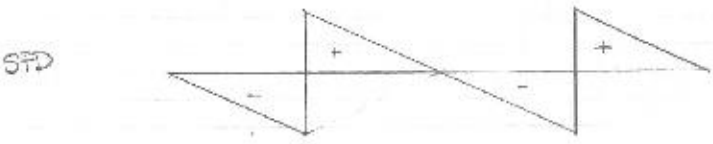

MAX SF = 1.13 kN

Find As Required

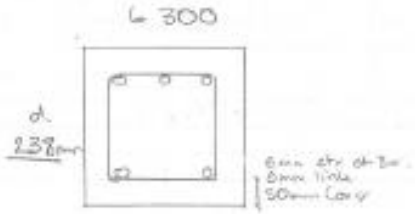

1. Find K factor

$K = M/f_{ck}bd^2$

$= \frac{0.114 \times 10^6}{25 \times 300 \times 238^2}$

$= \frac{0.114 \times 10^6}{42483000}$

$= 3.30 \times 10^{-2}$

2. Find $z/d = 0.950$

3. Find $z = d(z/d) = 238 \times 0.950 = 226.1$

4. Find $A_s = M/(0.87 f_{yk} z)$

$= \frac{0.114 \times 10^6}{0.87 \times 226.1 \times 500}$

$= 1.16.23 \text{ mm}^2$

For maximum spacing use 3 No H12 top + 3 No H12 Bottom

Find Shear links Required

1. $V_{Ed} = 1.13 \text{ kN}$

2. $v_{Ed} = \frac{V_{Ed}}{0.9 \times b_w \times d}$

$= \frac{1.13 \times 10^3}{0.9 \times 300 \times 238}$

$= 0.018 \text{ N/mm}^2$

3. Strut Cap $= 3.10 \text{ N/mm}^2$ (4) $V_{Rd} > v_{Ed}$? OK

5. $\theta = 22°$

6. Find V_{Ed2} (Shear force at distance d from face of support).

1·13kN in @ 250mm $\quad \frac{1.13}{250} \times 62 = 0.28\text{kN} = 280\text{N}$

7. $v_{Ed2} = \frac{V_{Ed2}}{0.9 \times 300 \times 238} = \frac{280}{0.9 \times 300 \times 238} = 0.004\text{ N/mm}^2$

8. Calc A_{sw} Req'y $= A_{sw}/s = 0.00092_{req'd\ for\ 6w}$

$= 0.00092 \times 0.004 \times 300$

$= 1.104 \times 10^{-3}\text{ mm}$

9. Minimum $= 0.000_{8\,6w} = 0.0002 \times 300 = 0.24 \leftarrow A_{s\ req'd}$

10. Minimum spacing 75mm

Maximum spacing $0.75d = 0.75 \times 238 = 178.5\text{mm}$ say 150mm

11. R6 @ 150 spacings

Lifting eye - Steel size required

- $2.25\text{kN} \times 2 = 5\text{kN}$ 5000N
- $\frac{5000\text{N}}{500\text{N/mm}^2} = 10\text{mm}^2$ ← Not a lot then!

Ground Beam Details - Erdington School

Bending List

BM	Type	Size	No Mem	No Bars	Total No	Length Bar	Shape Code	A	B	C	D
1	H	12	4	6	24	900	00	900	–	–	–
2	H	10	4	7	28	800	22	200	320	60	300
3	R	6	4	2	8	960	51	200	200	–	–

Sketches

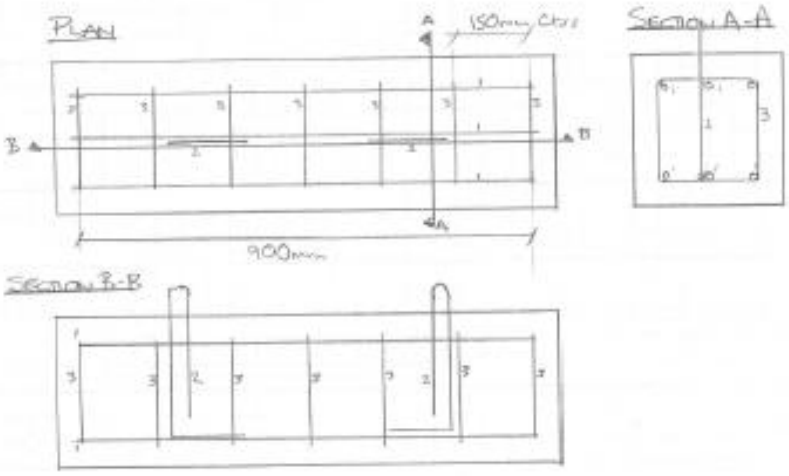

APPENDIX E – Electrode Type Choice 1 Undrained Shear Strengths

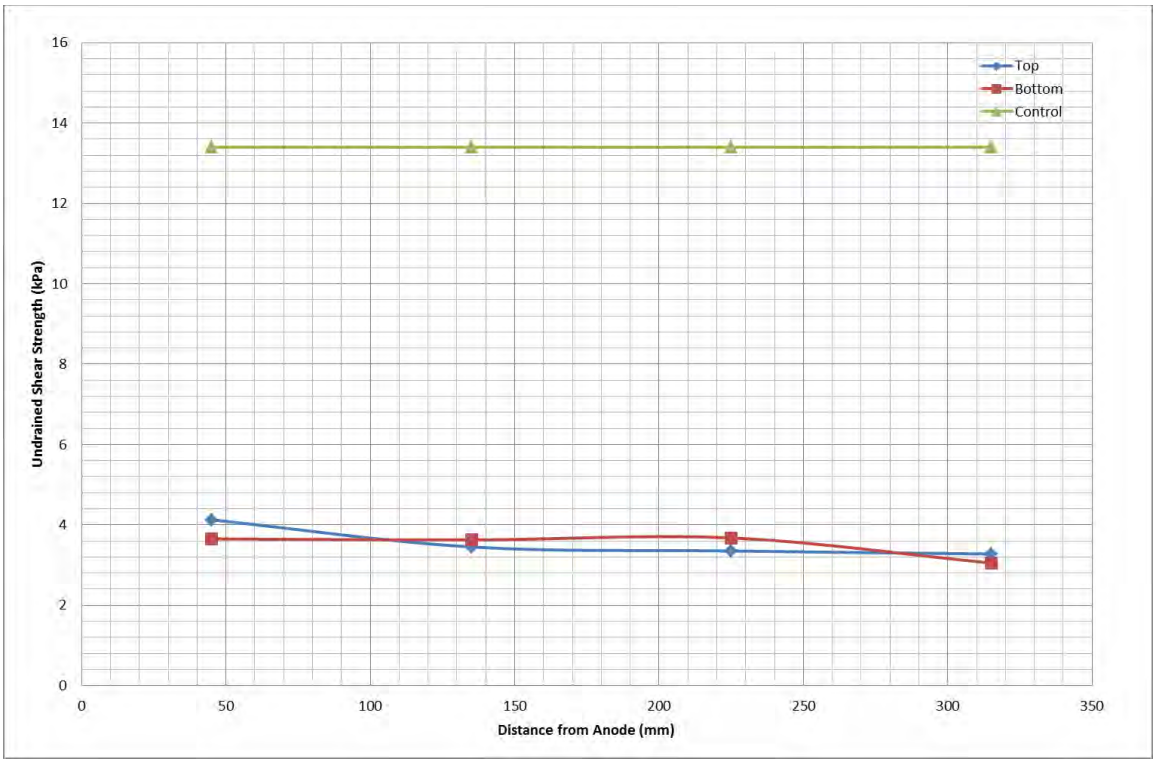

Figure E1: Electrode Type Choice 1 EKG Undrained Shear Strengths

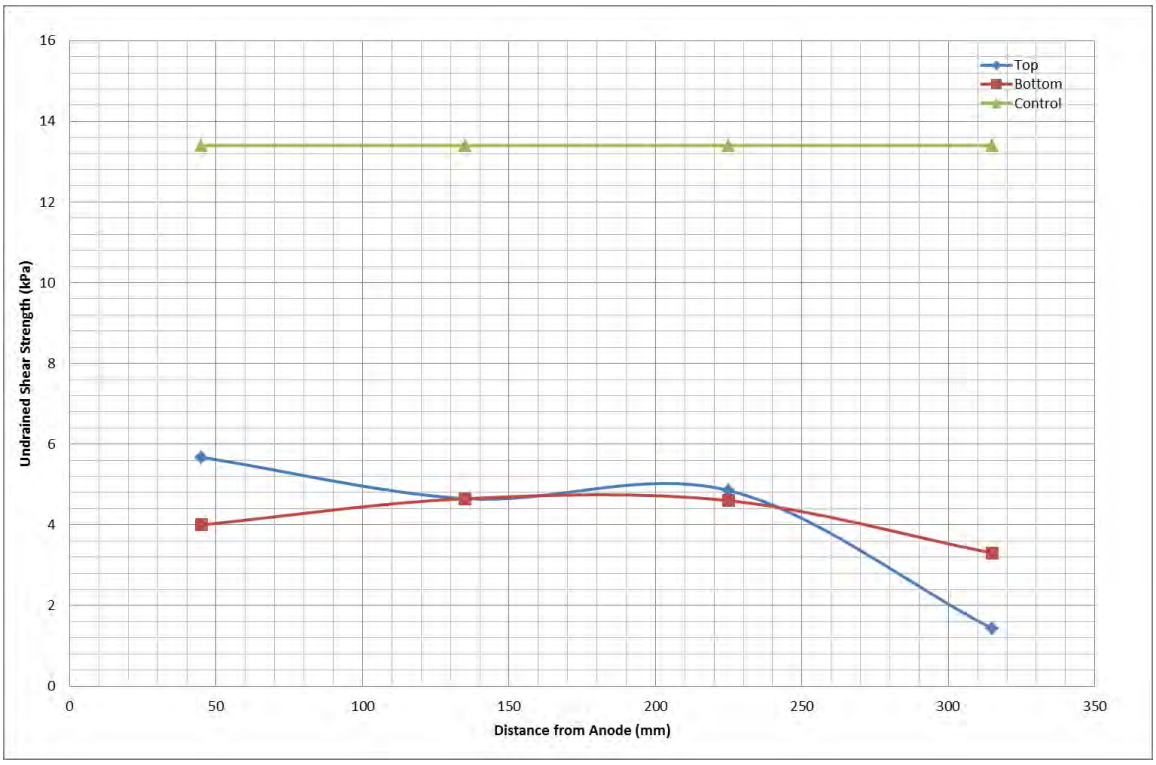

Figure E2: Electrode Type Choice 1 Stainless Steel Undrained Shear Strengths

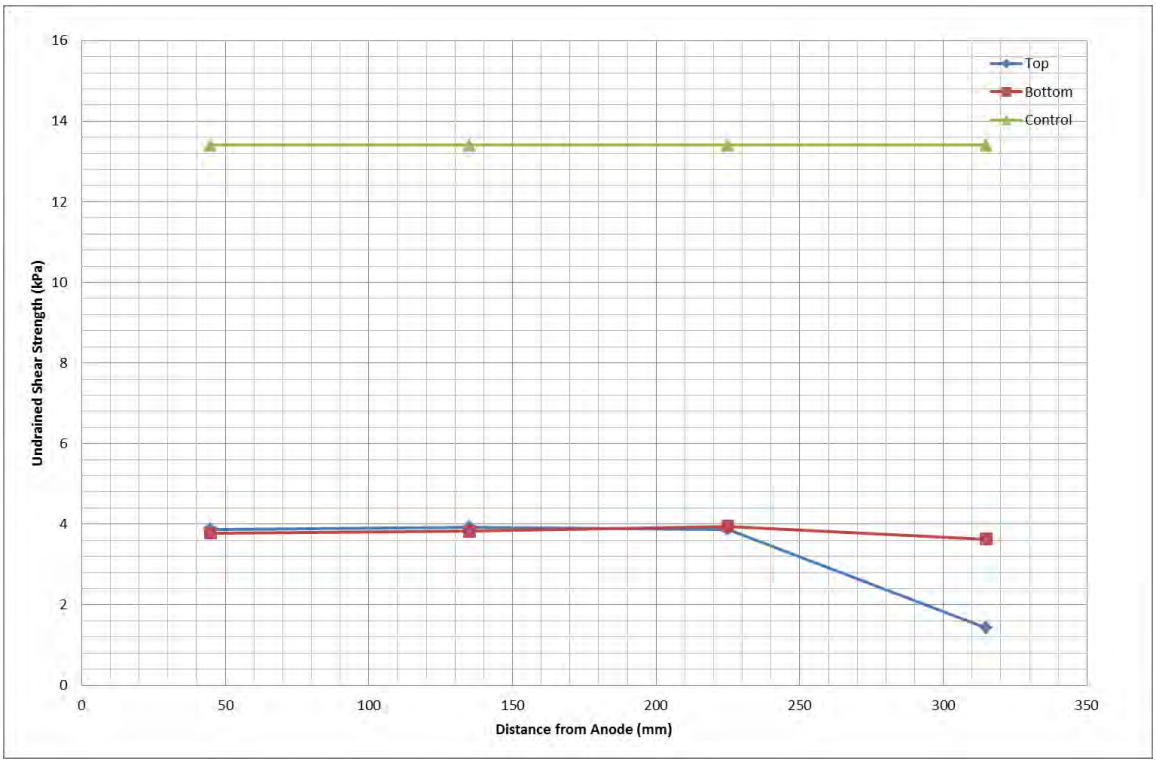

Figure E3: Electrode Type Choice 1 Hybrid Electrode Undrained Shear Strengths

APPENDIX F – SEM Photography

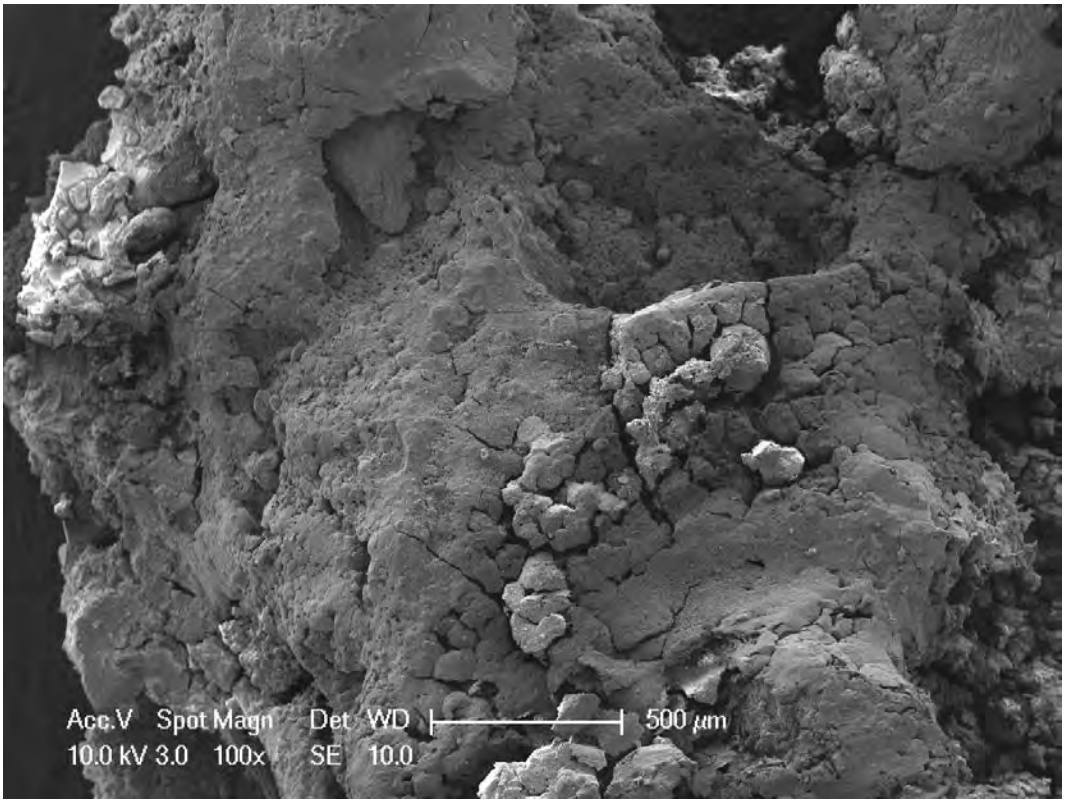

Figure F-1: A hardened hydrated Calcium Chloride 100x

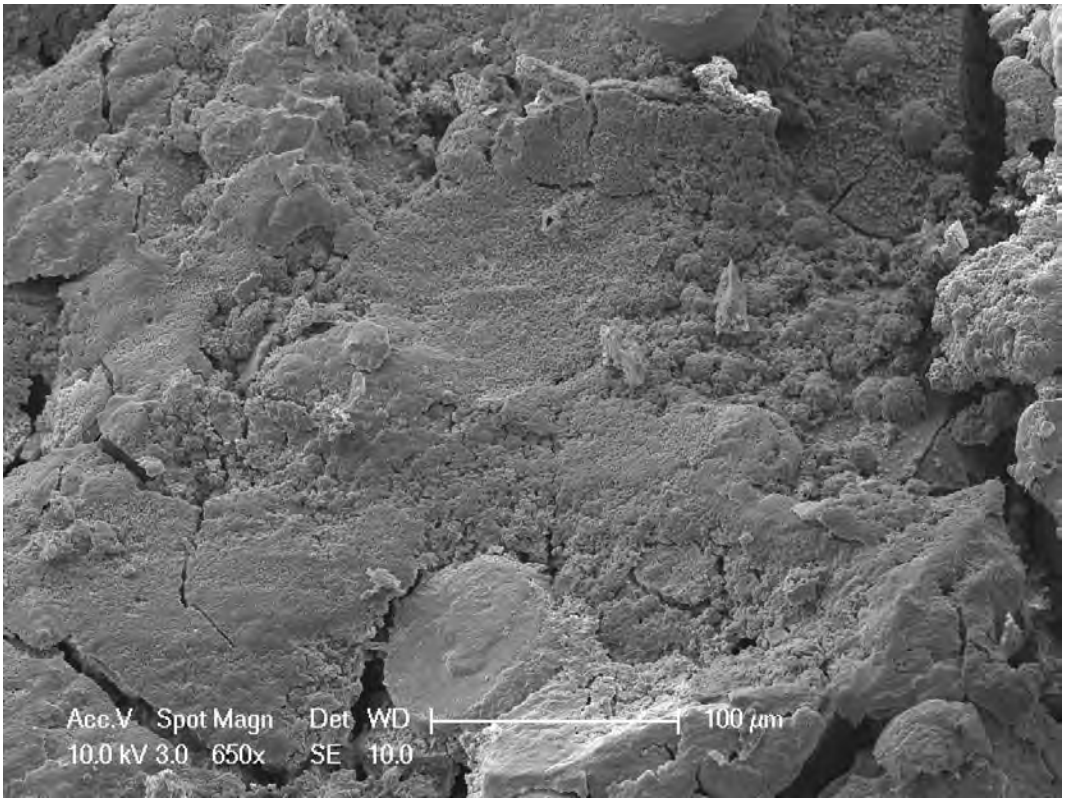

Figure F-2: A hardened hydrated Calcium Chloride 650x

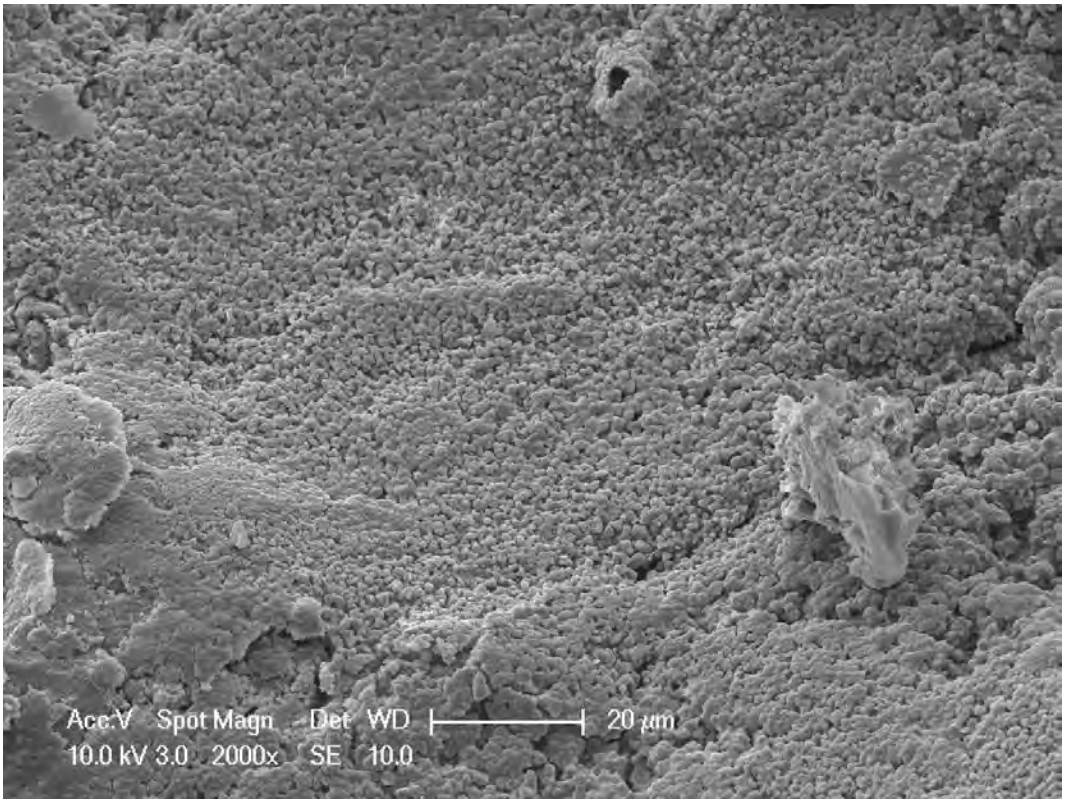

Figure F-3: A hardened hydrated Calcium Chloride 2000x

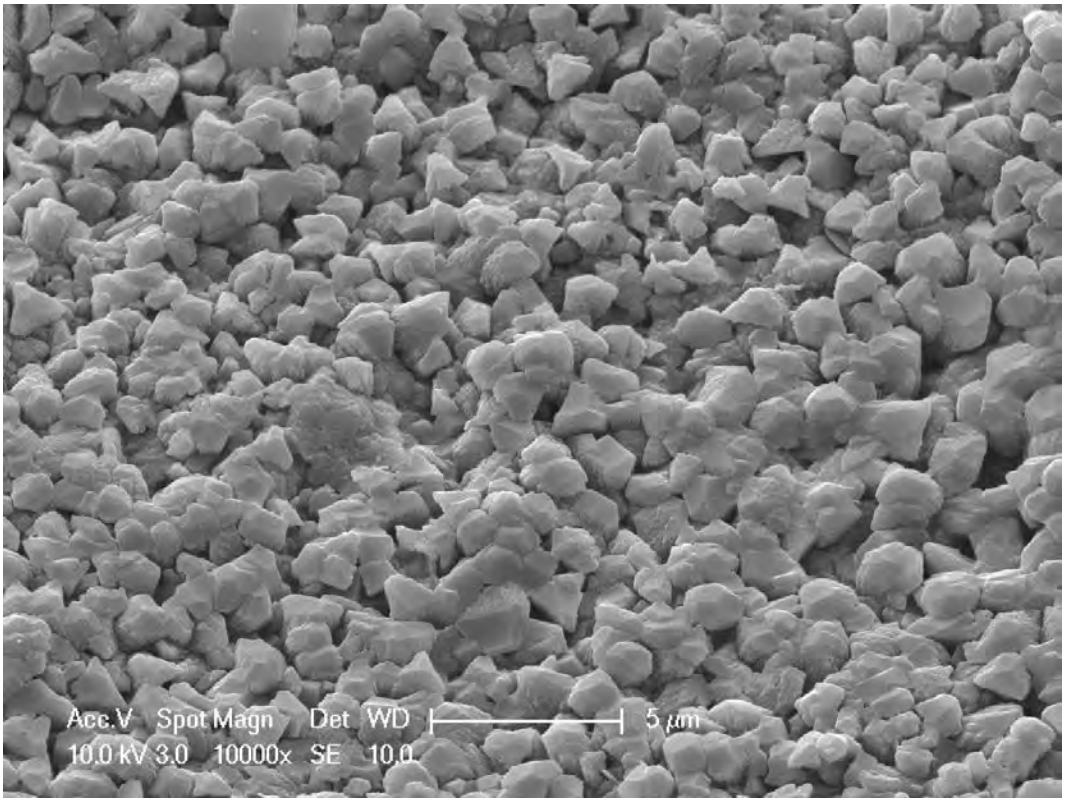

Figure F-4: A hardened hydrated Calcium Chloride 10,000x

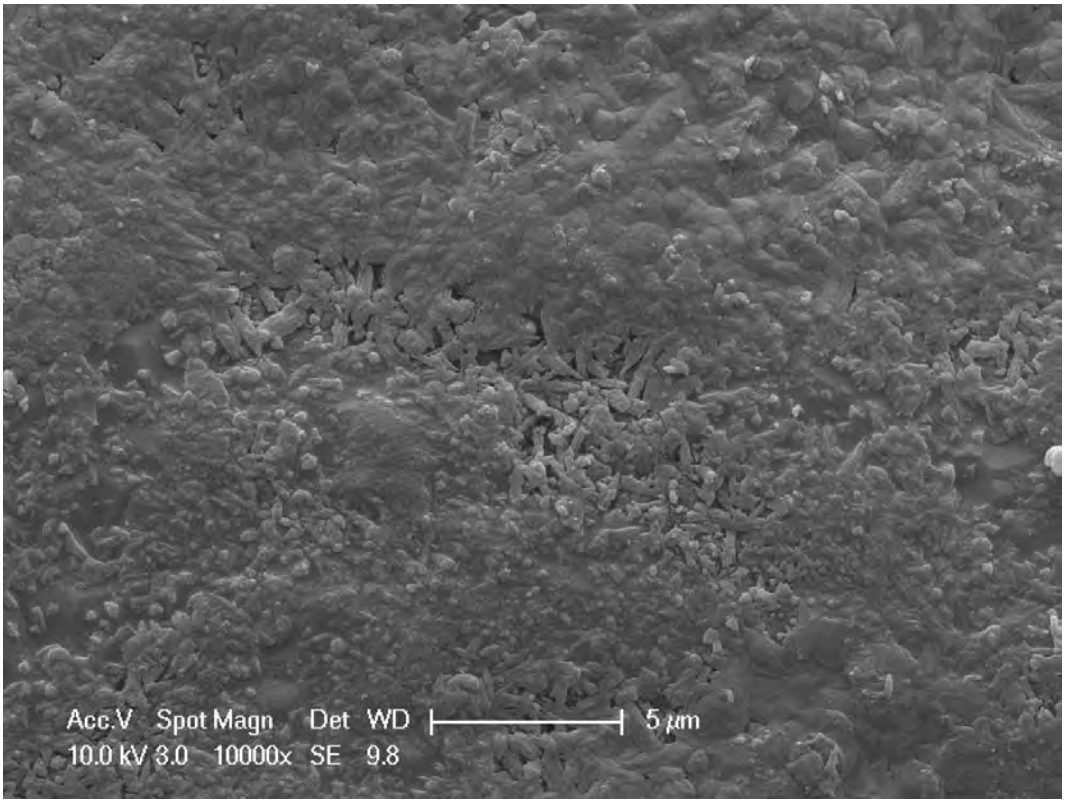

Figure F-5: A hardened hydrated Calcium Chloride 10,000x

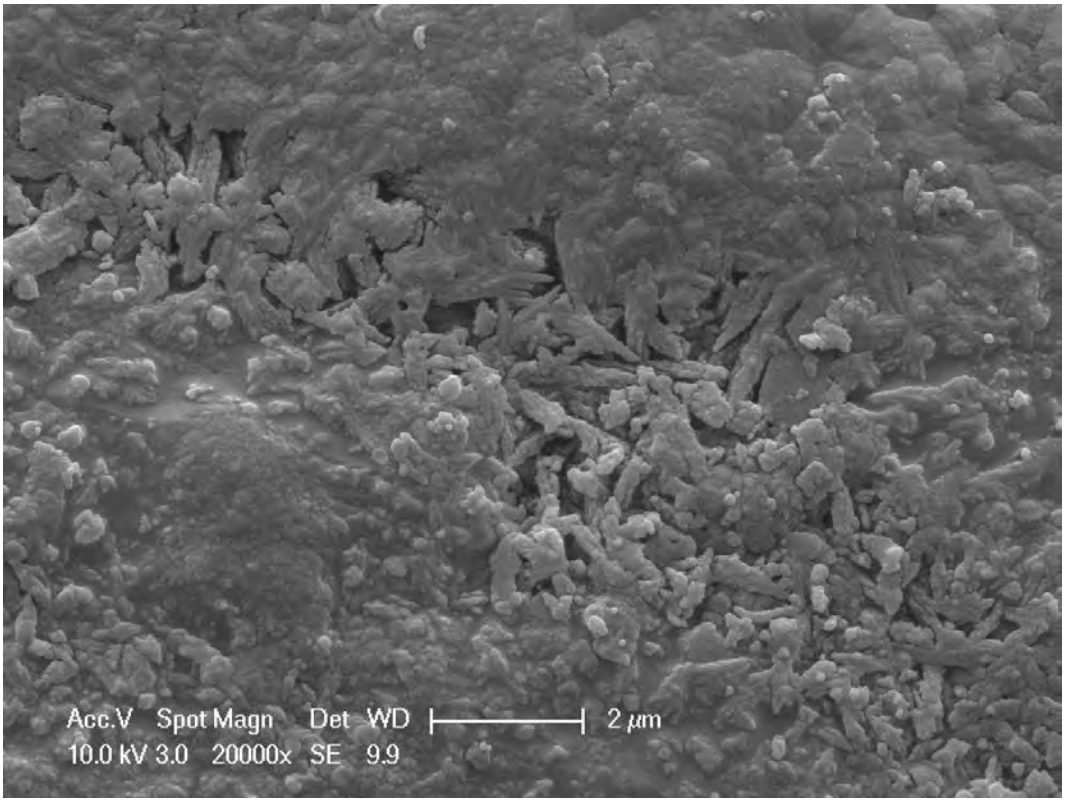

Figure F-6: A hardened hydrated Calcium Chloride 20,000x

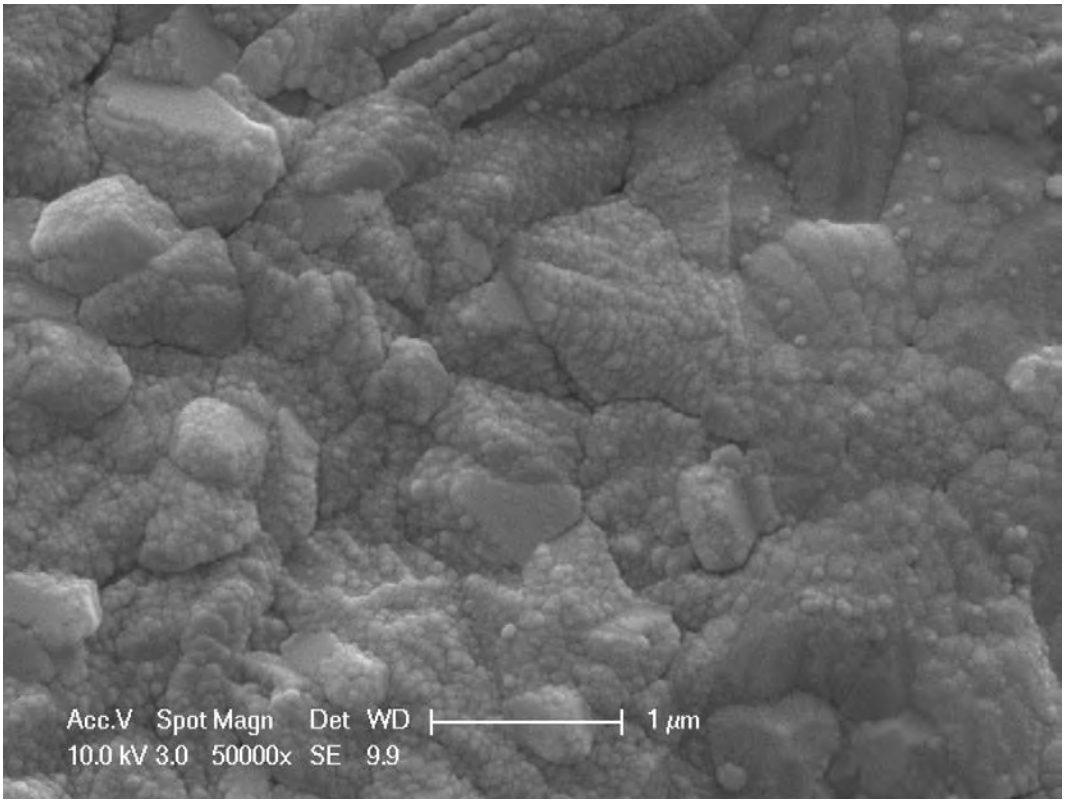

Figure F-7: A hardened hydrated Calcium Chloride 50,000x

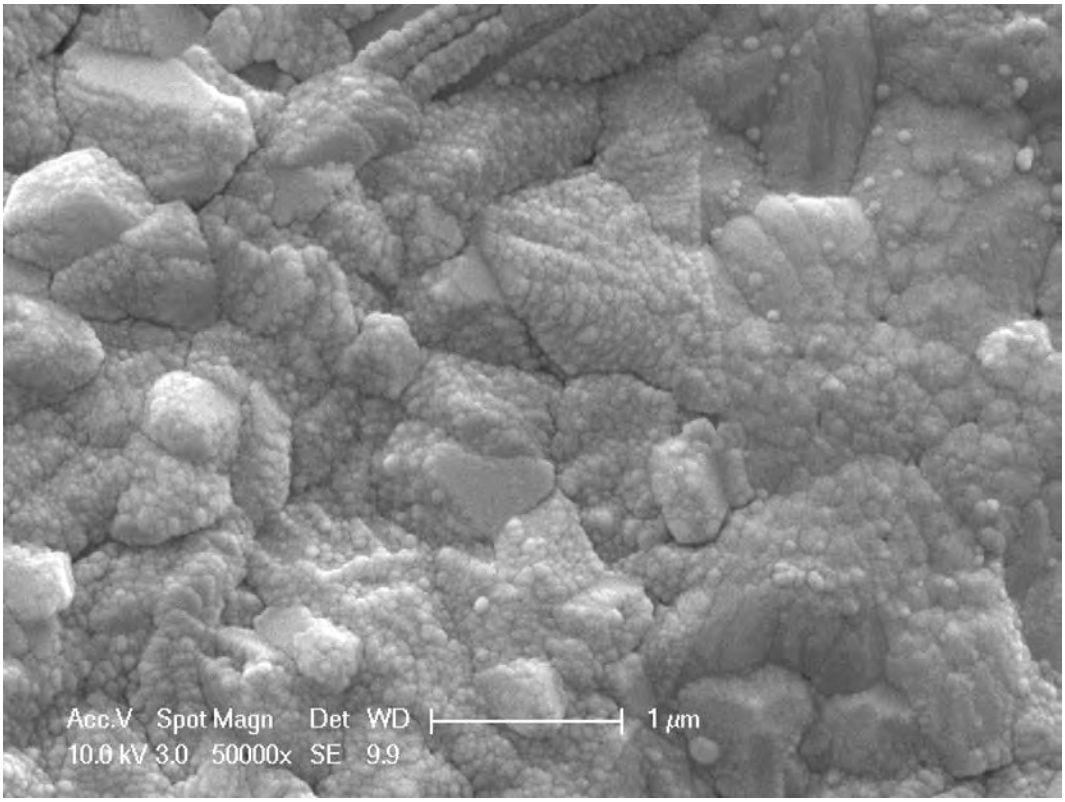

Figure F-8: A hardened hydrated Calcium Chloride 50,000x

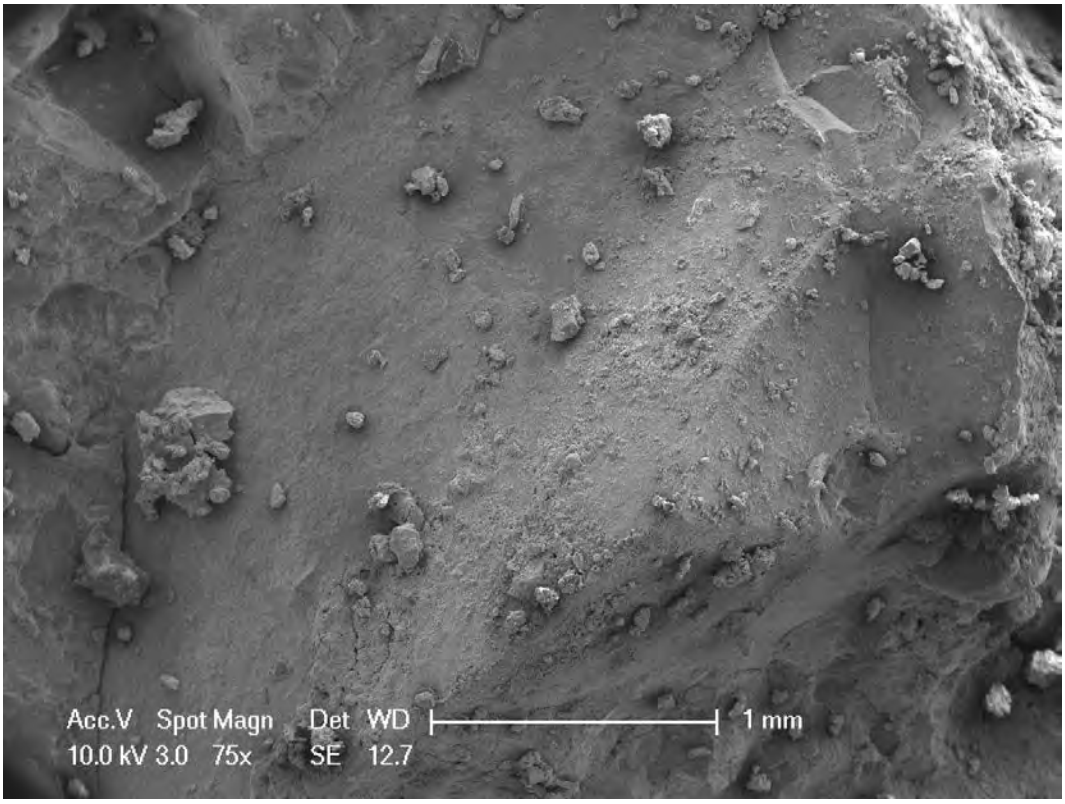

Figure F-9: Site trials raked concrete footing 75x.

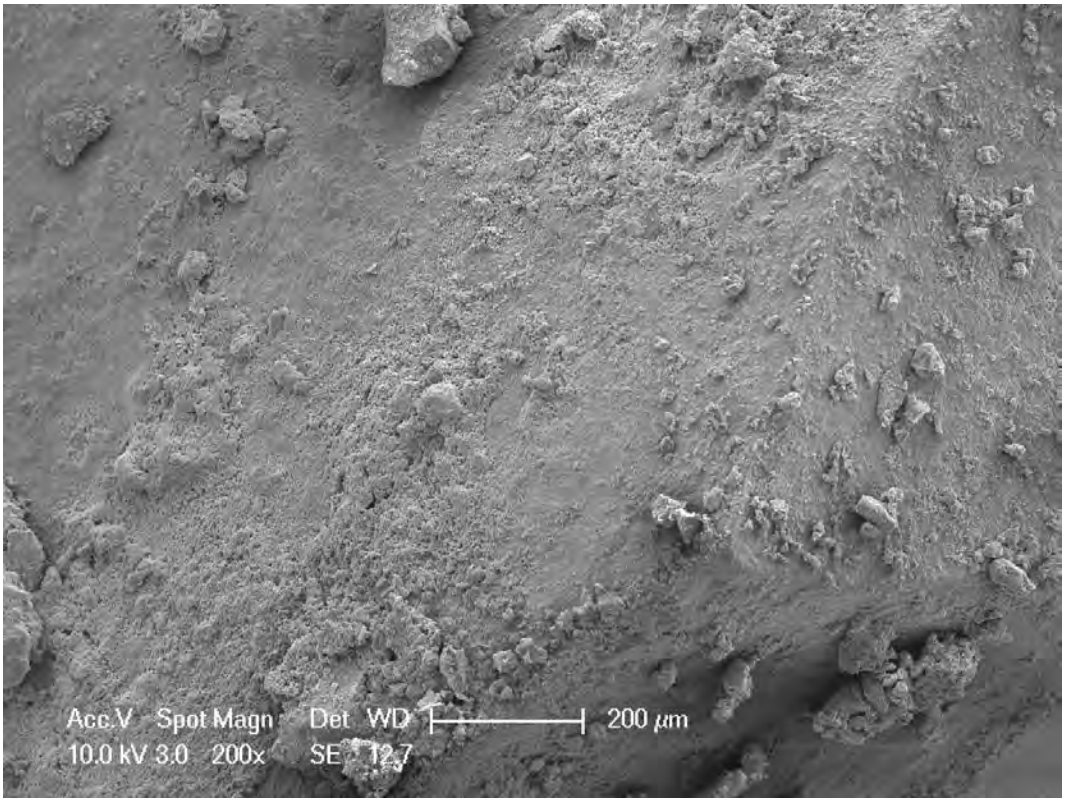

Figure F-10: Site trials raked concrete footing 200x

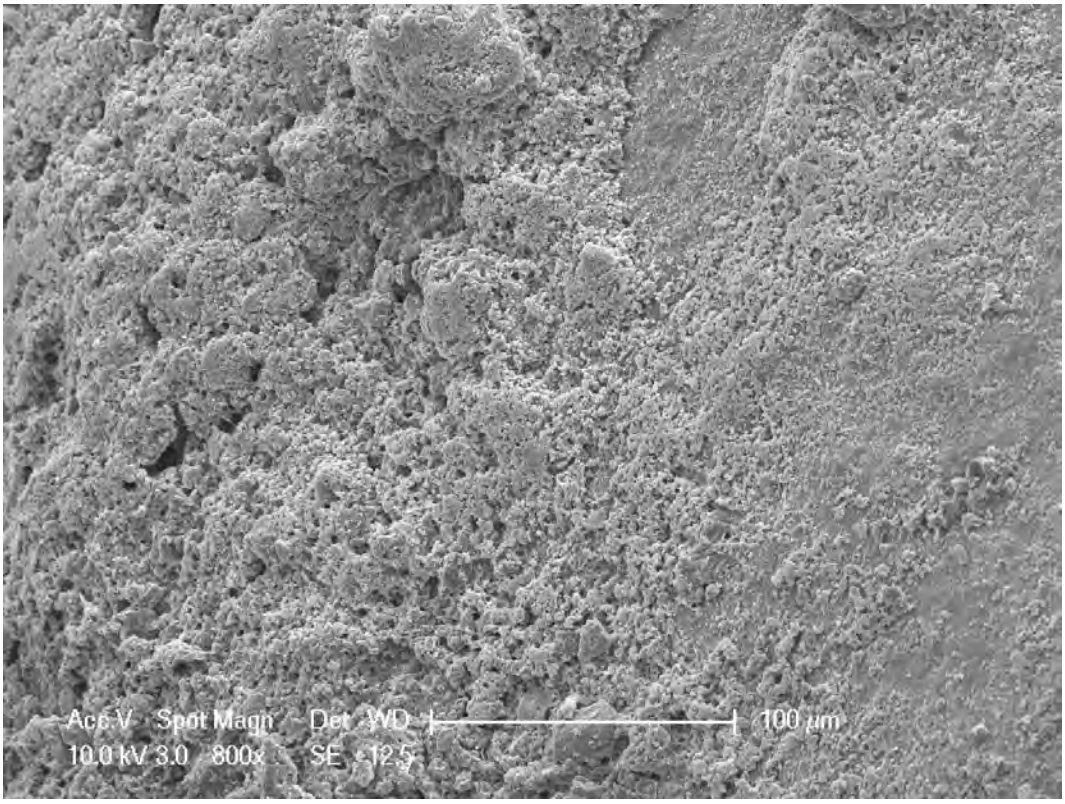

Figure F-11: Site trials raked concrete footing 800x

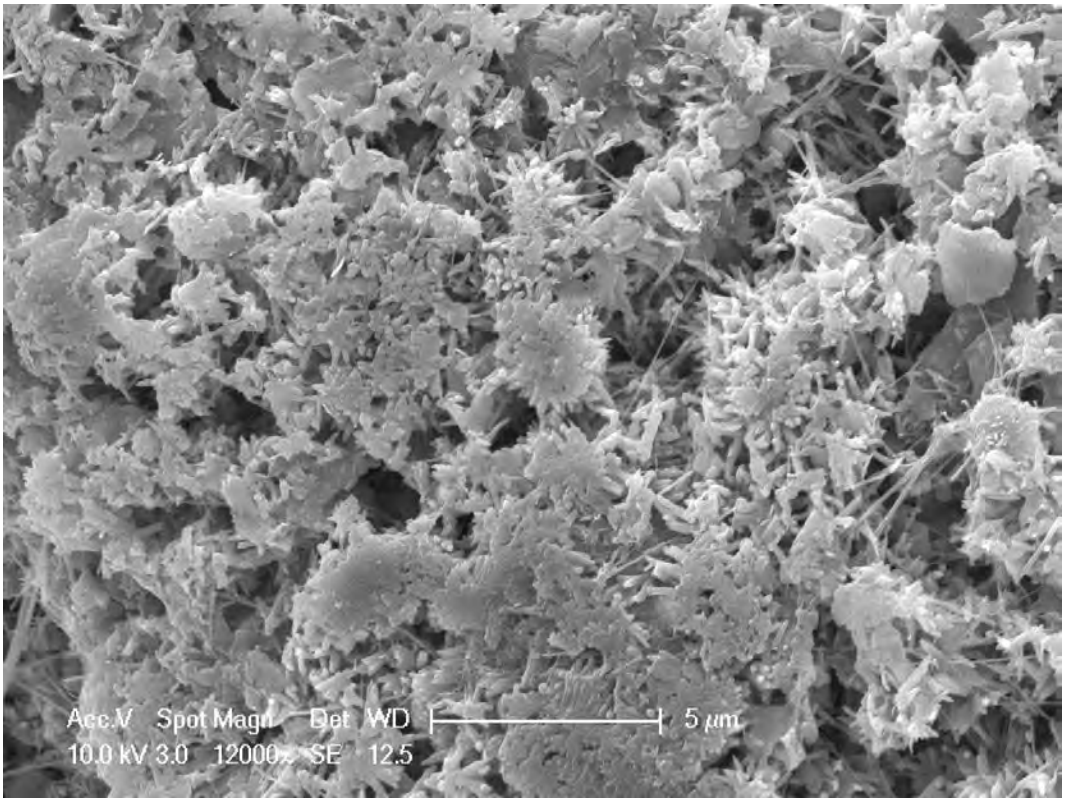

Figure F-12: Site trials raked concrete footing 12,000x

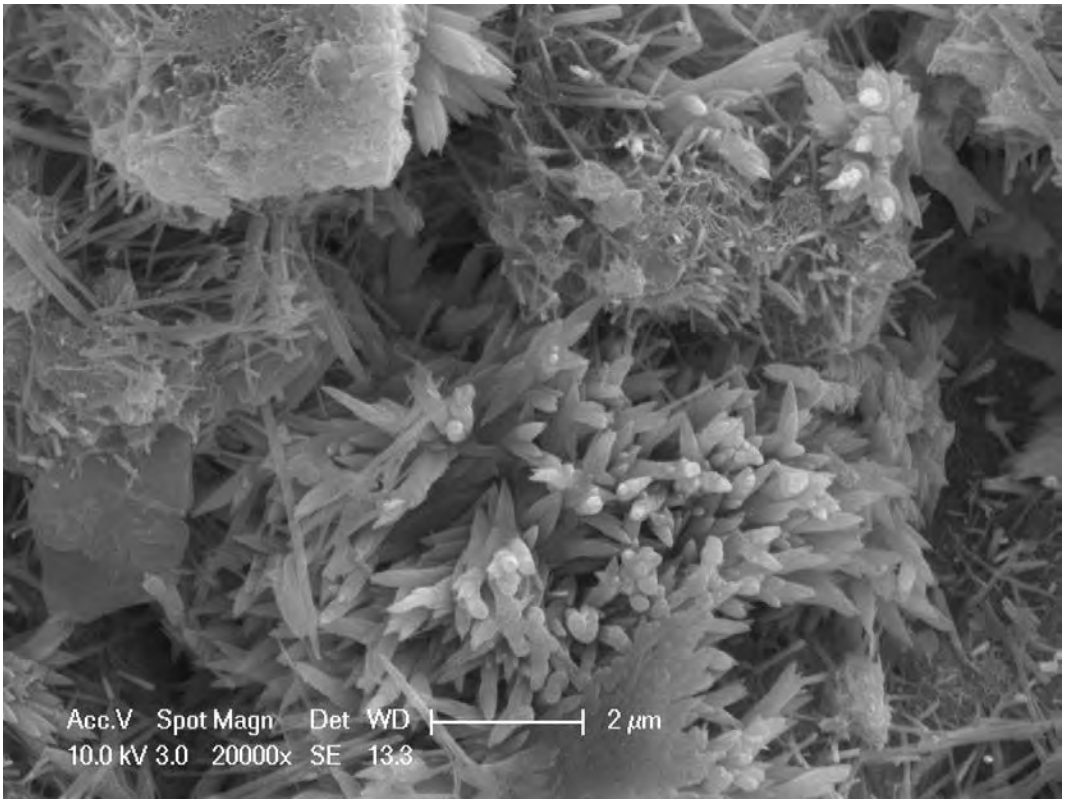

Figure F-13: Site trials raked concrete footing 20,000x

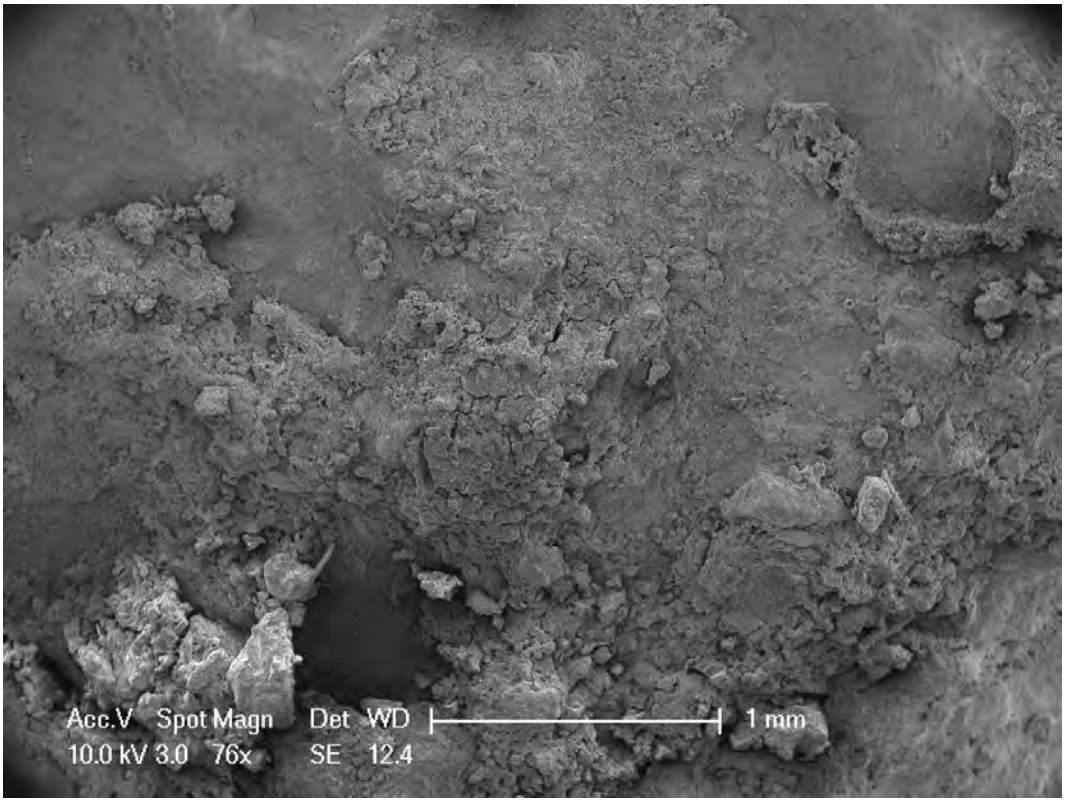

Figure F-14: Site trials vertical concrete footing 76x

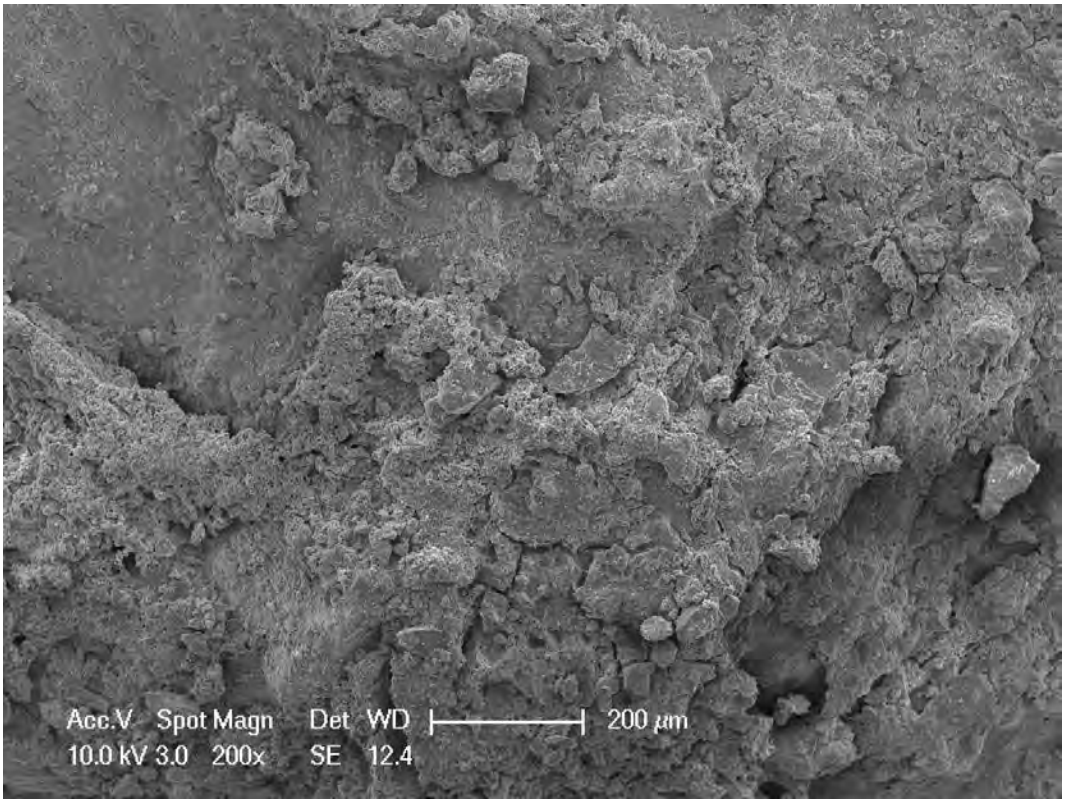

Figure F-15: Site trials vertical concrete footing 200x

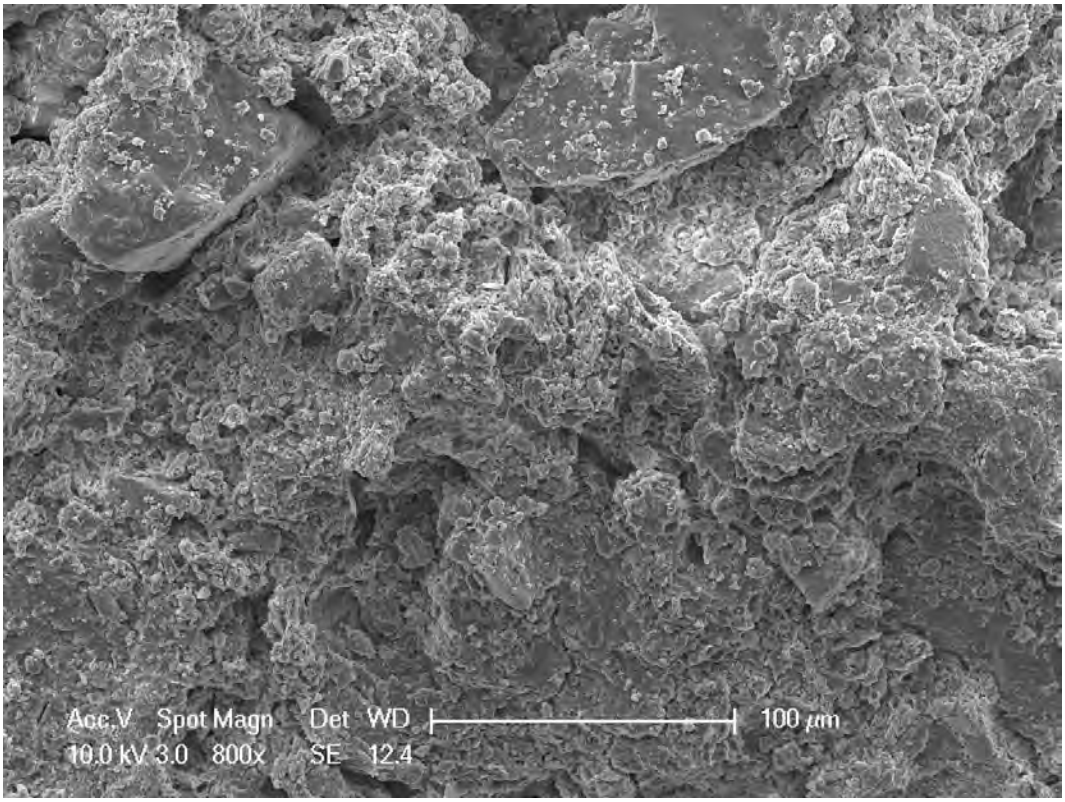

Figure F-15: Site trials vertical concrete footing 800x

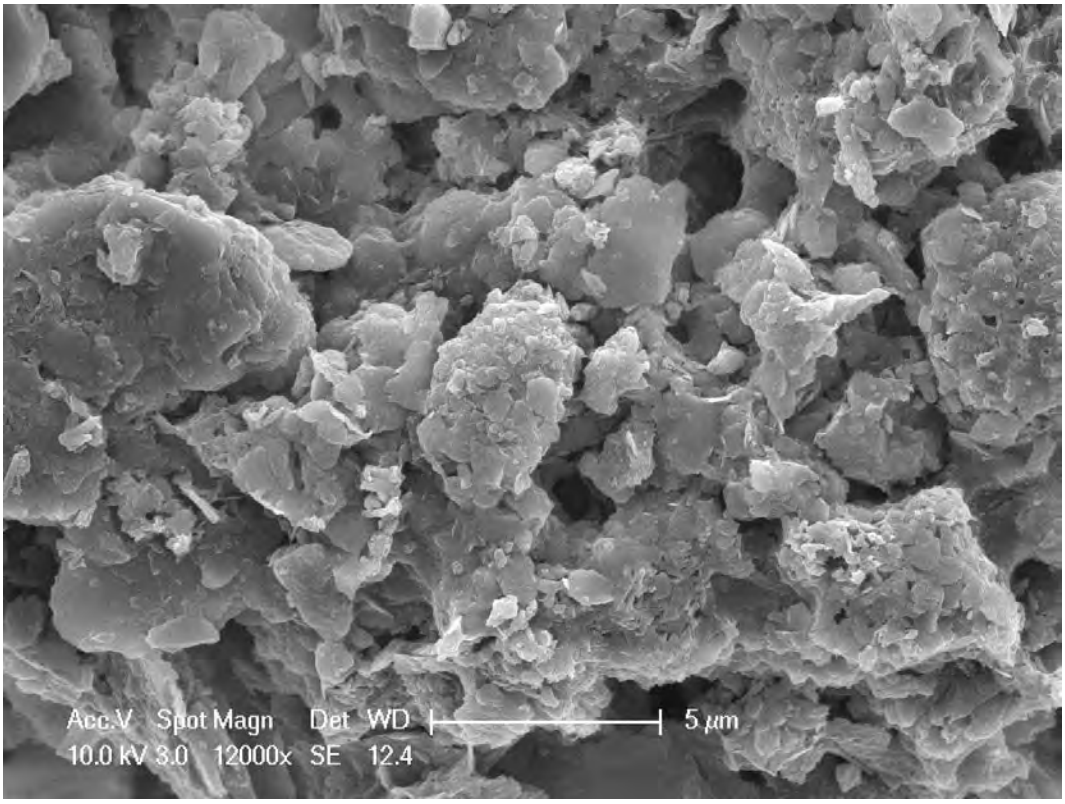

Figure F-16: Site trials vertical concrete footing 12,000x

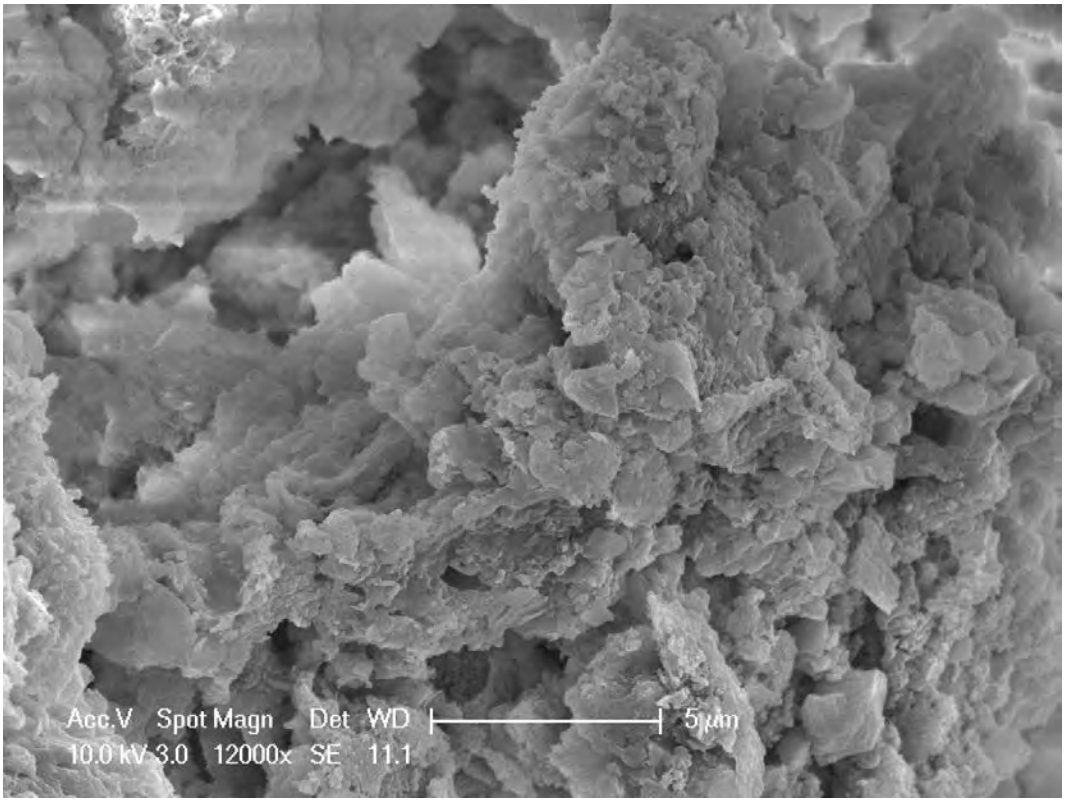

Figure F-17: Site trials vertical concrete footing 12,000x

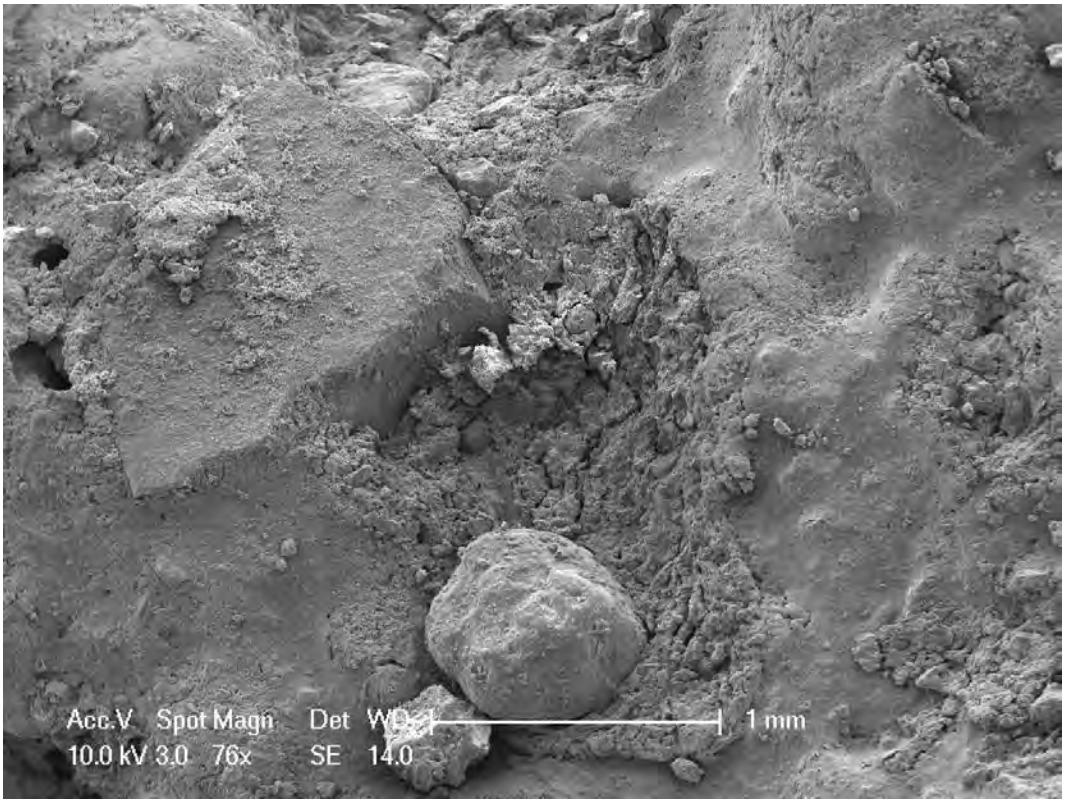

Figure F-18: Site trials control concrete footing 76x

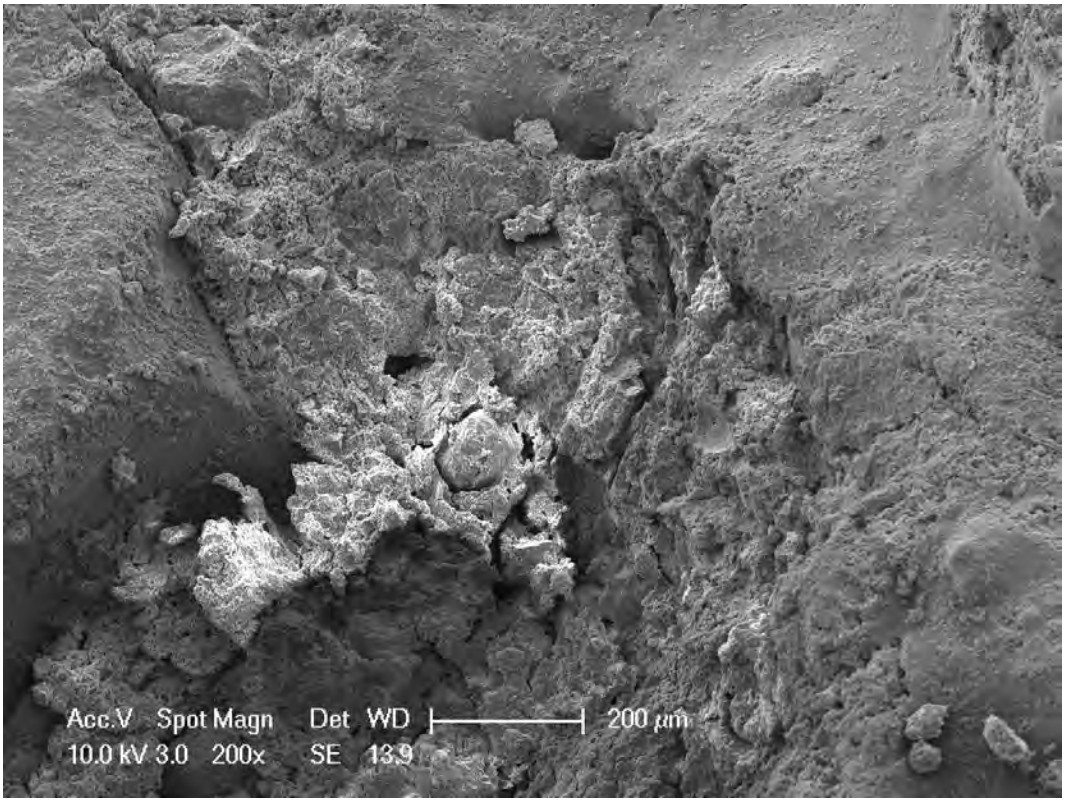

Figure F-19: Site trials control concrete footing 200x

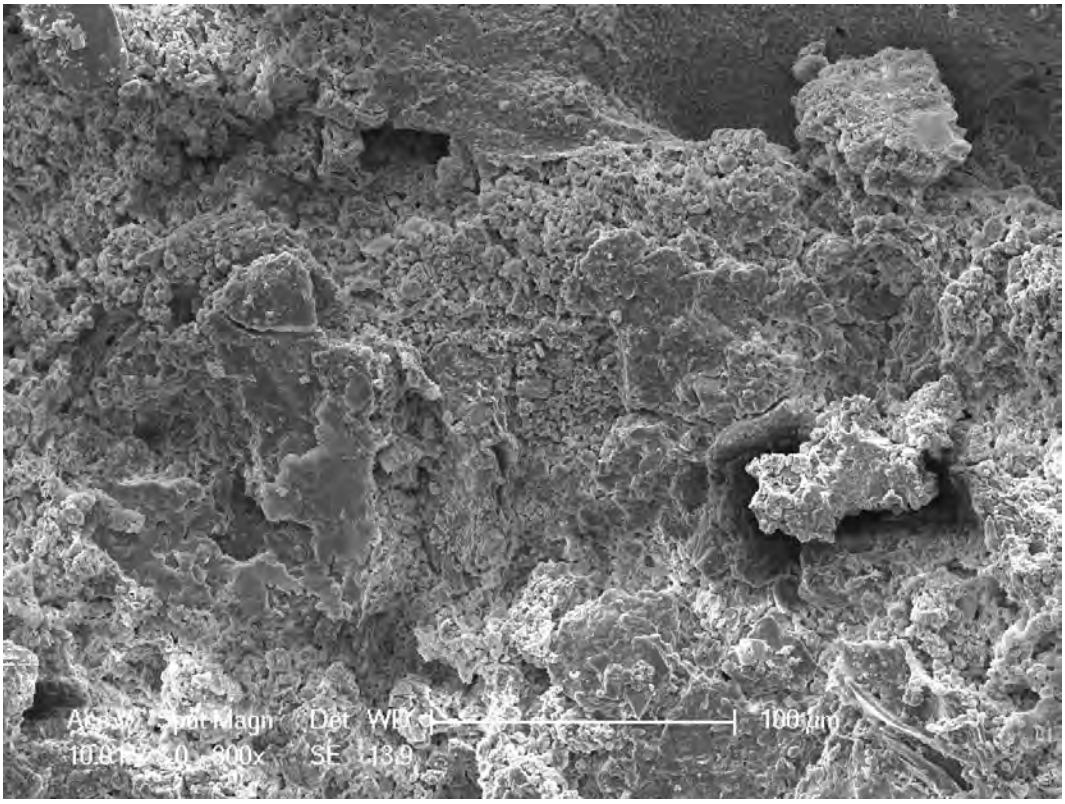

Figure F-20: Site trials control concrete footing 800x

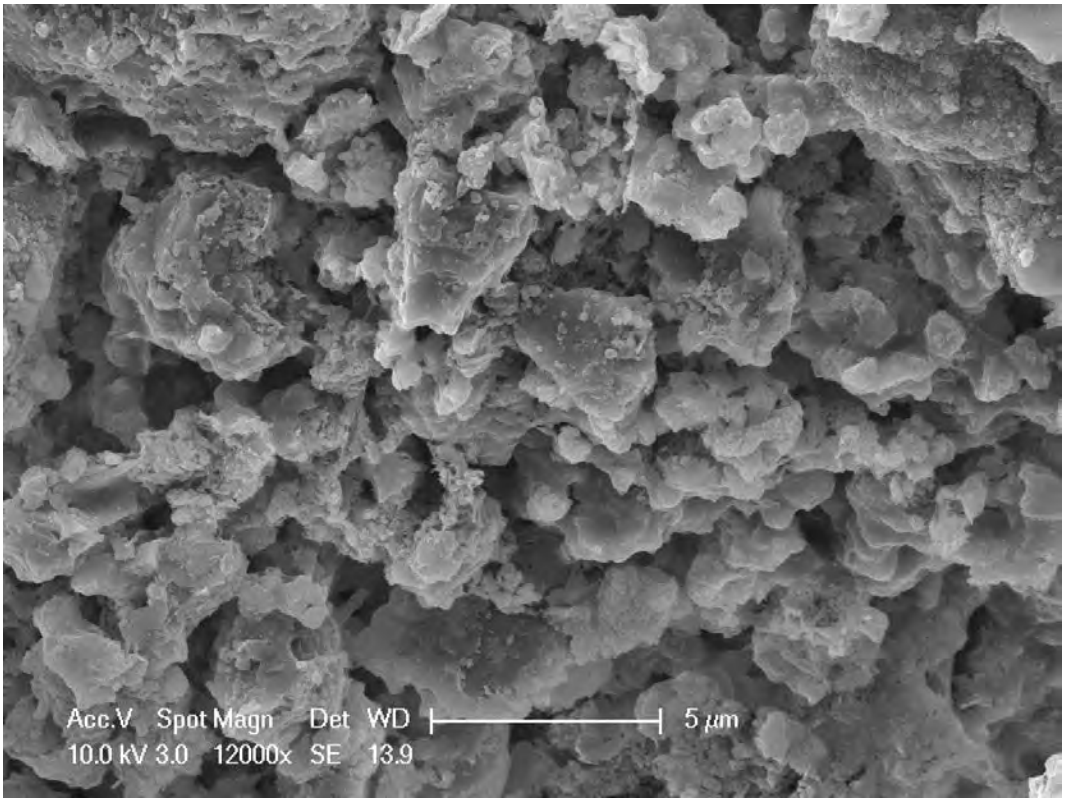

Figure F-21: Site trials control concrete footing 12,000x

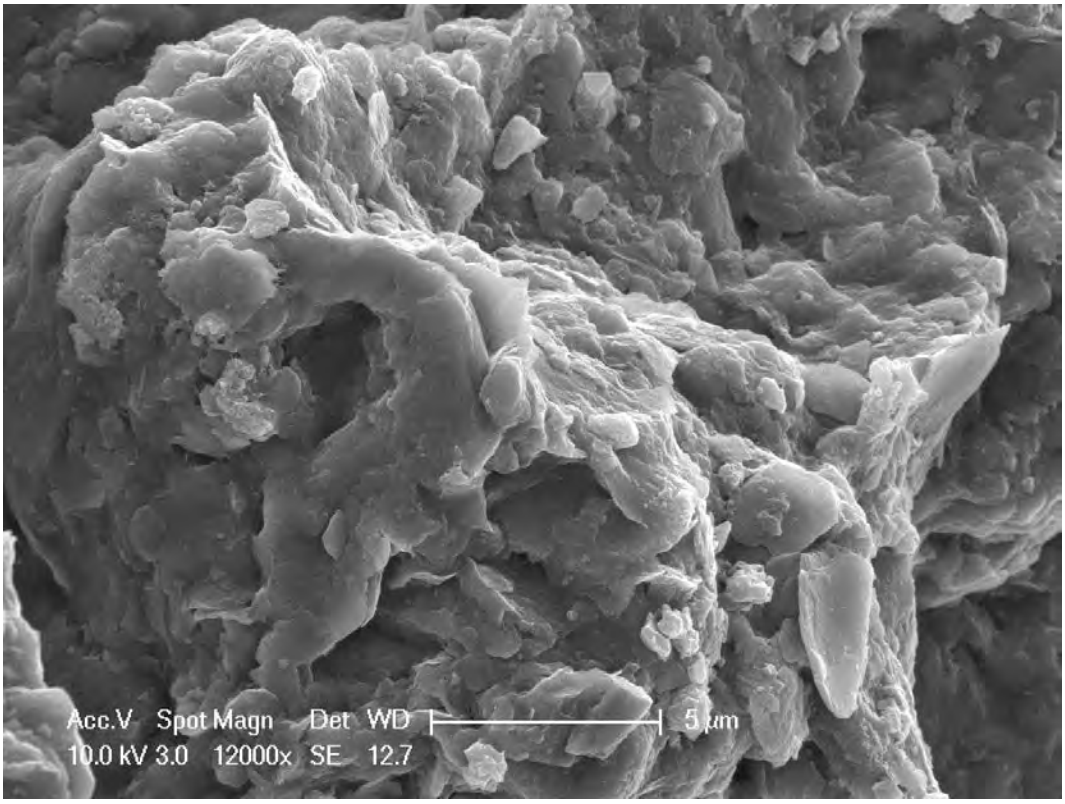

Figure F-22: Site trials control concrete footing 12,000x

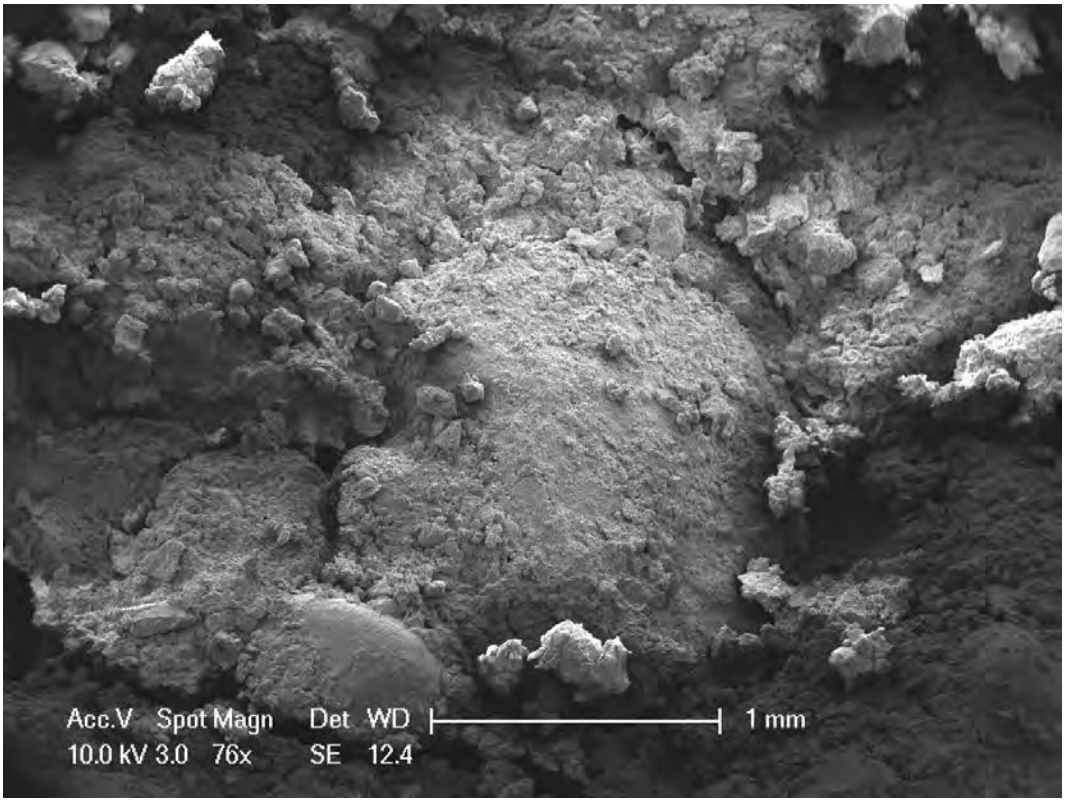

Figure F-23: Site trials current intermittence concrete footing 76x

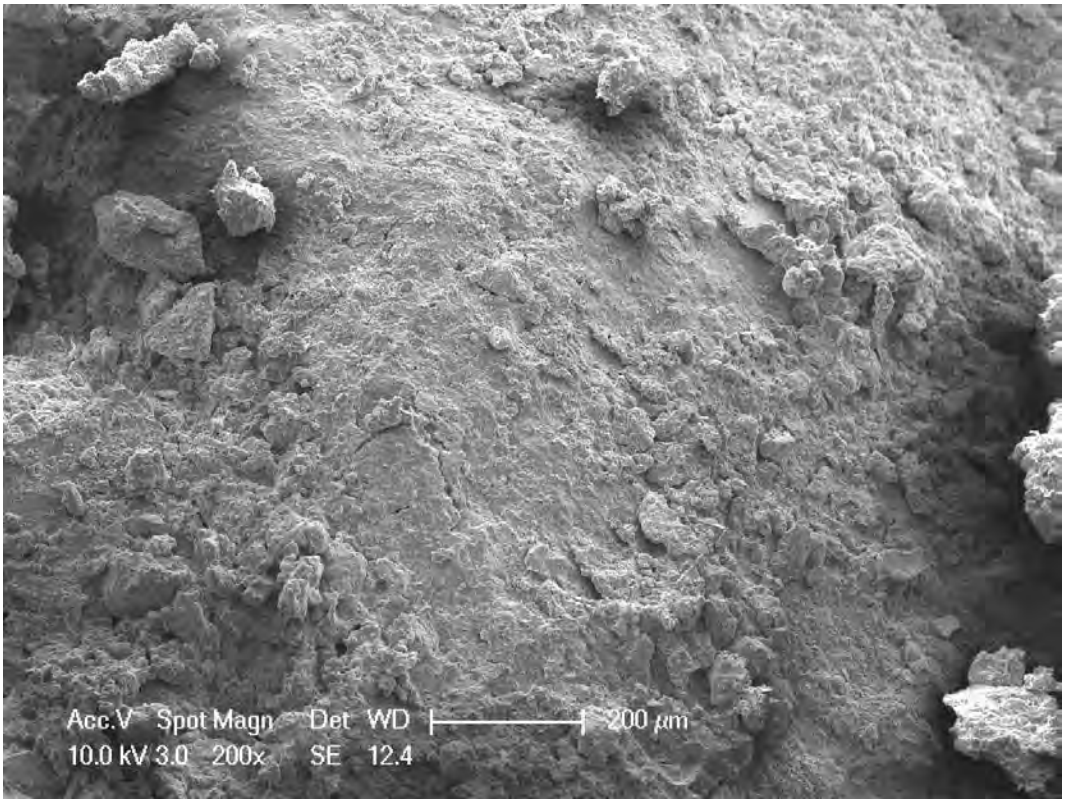

Figure F-24: Site trials current intermittence concrete footing 200x

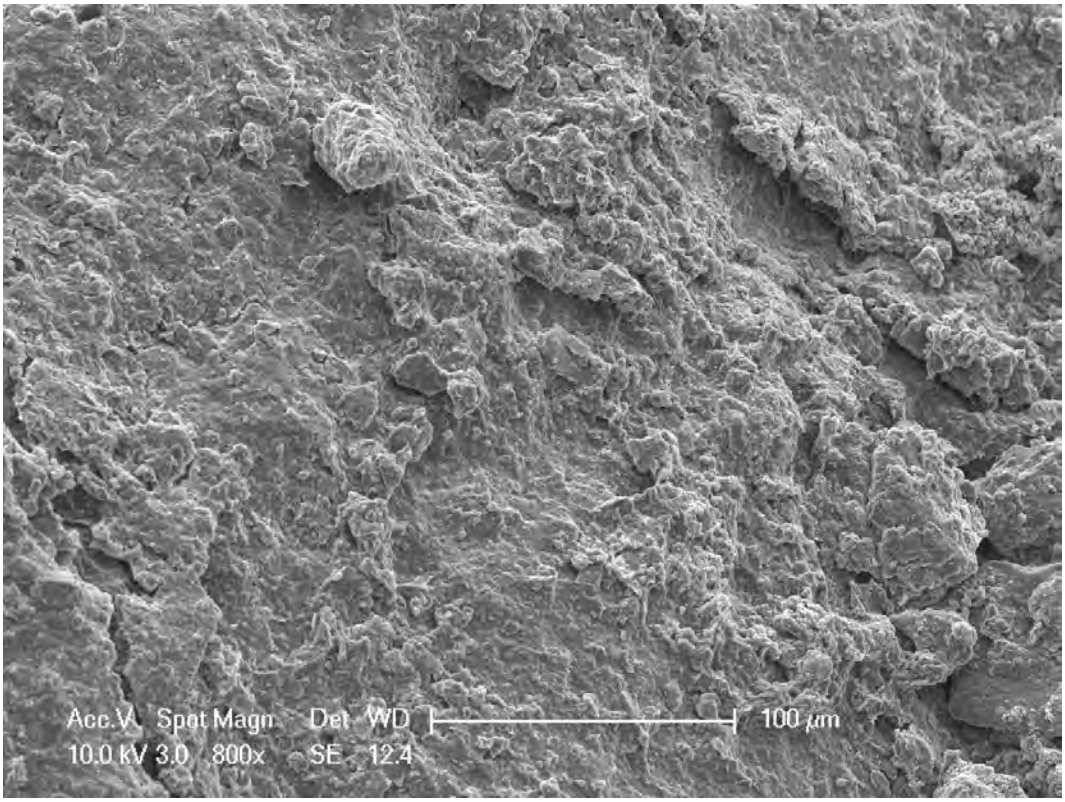

Figure F-25: Site trials current intermittence concrete footing 800x

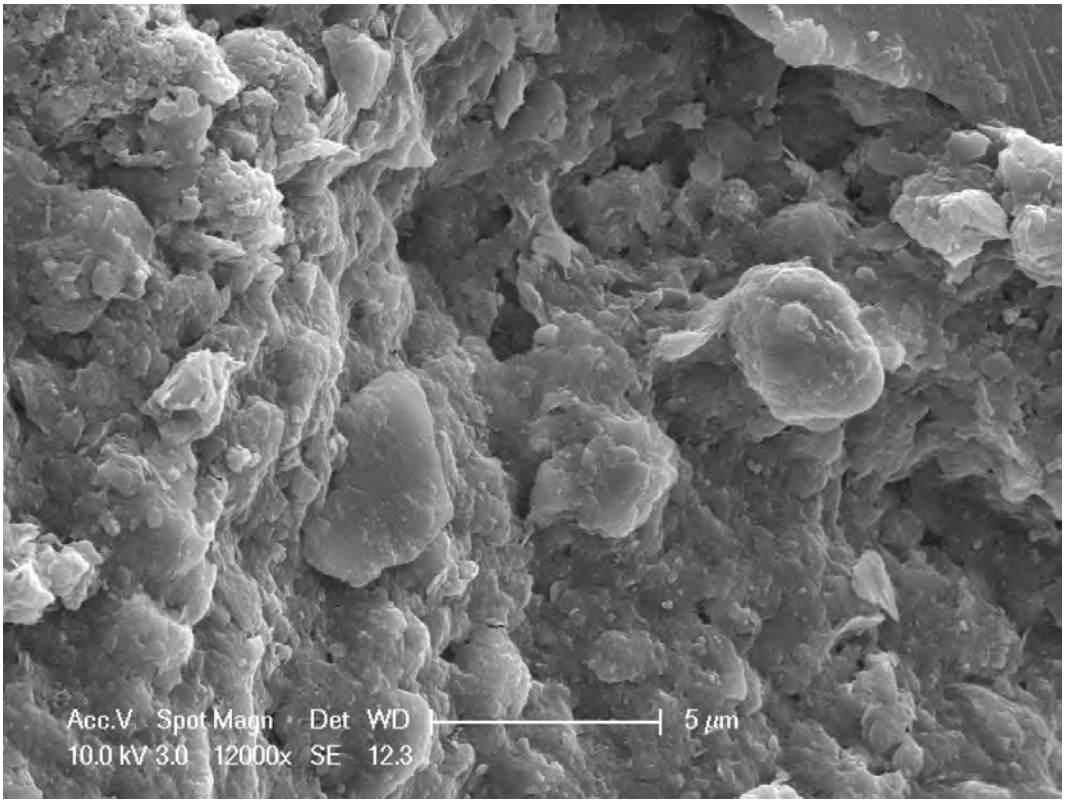

Figure F-26: Site trials current intermittence concrete footing 12,000x

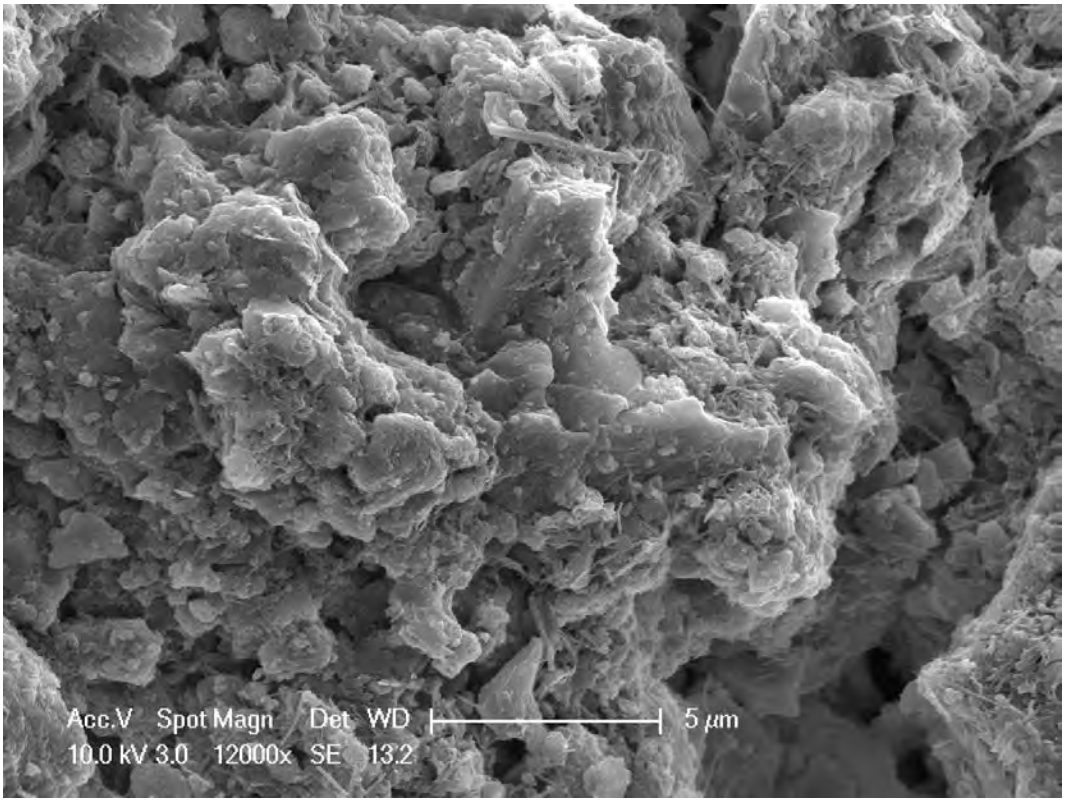

Figure F-27: Site trials current intermittence concrete footing 12,000x

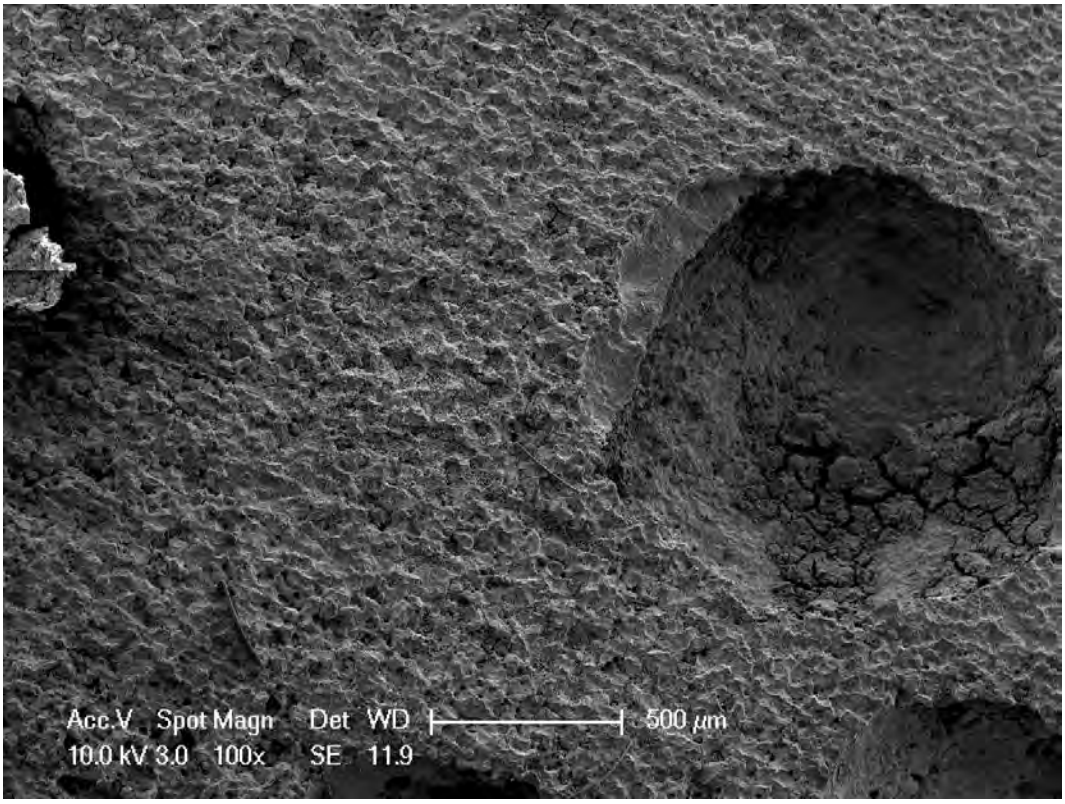

Figure F-28: Site trials vertical anode 100x

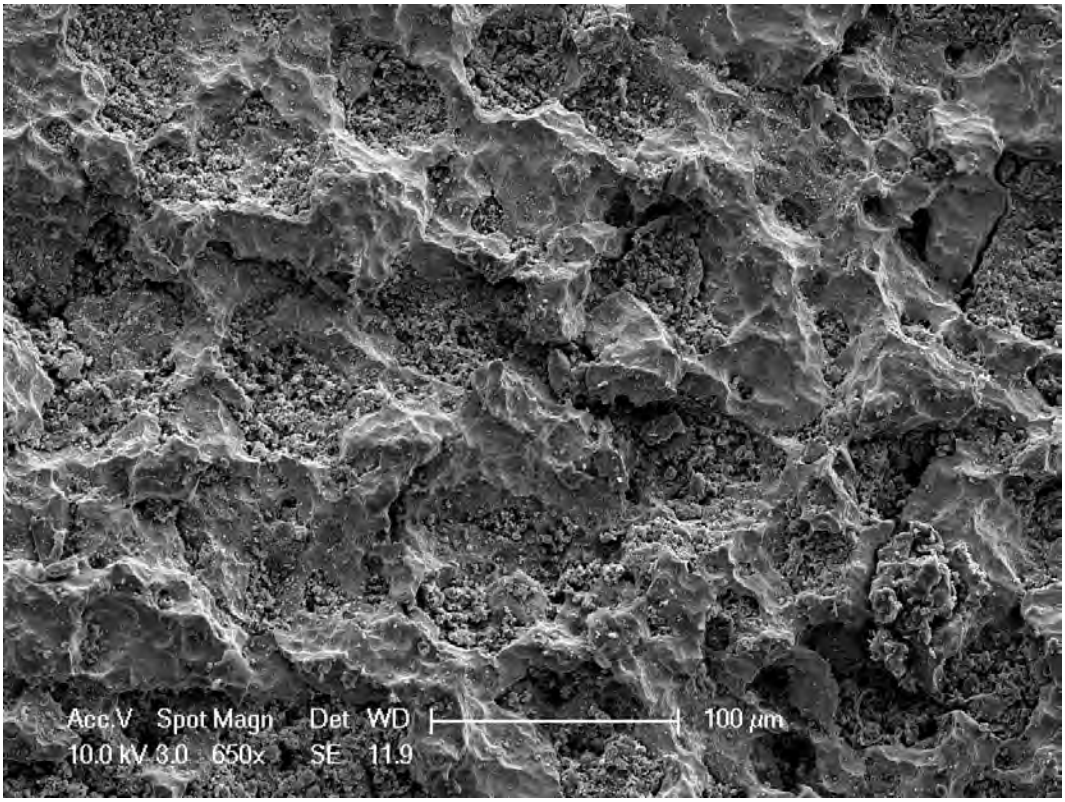

Figure F-29: Site trials vertical anode 650x

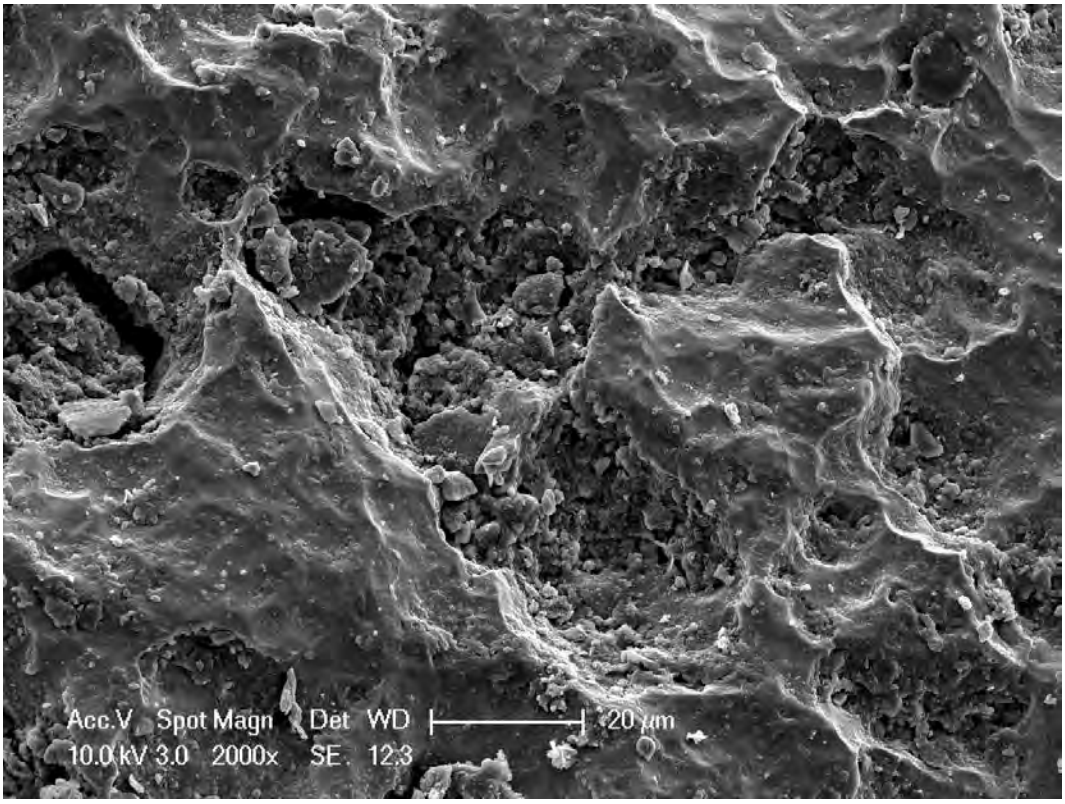

Figure F-30: Site trials vertical anode 2000x

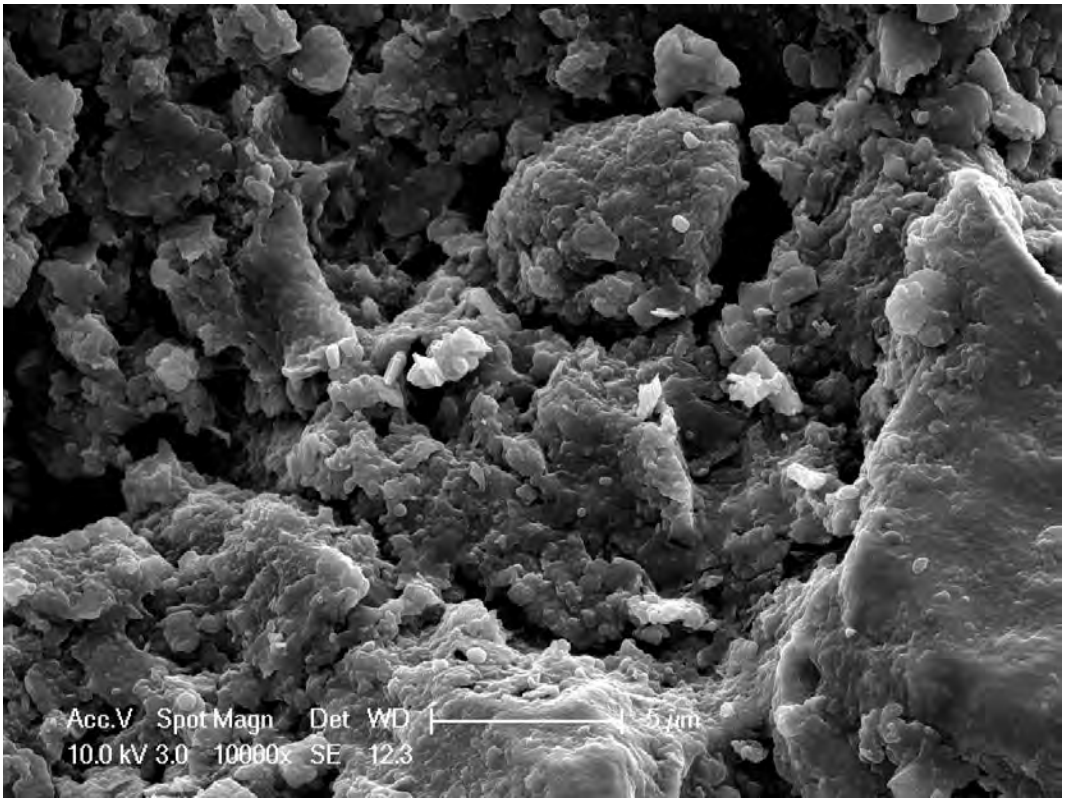

Figure F-31: Site trials vertical anode 10,000x

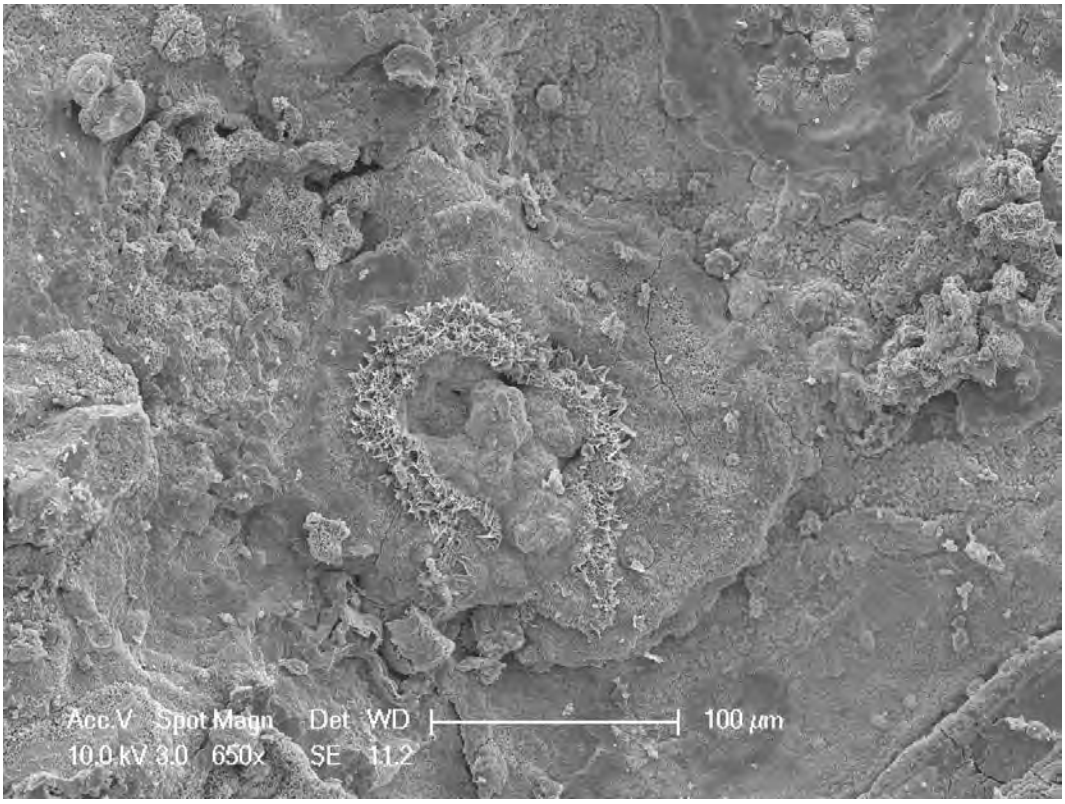

Figure F-32: Caclium Chloride growth on laboratory Stainless Steel anode 650x.

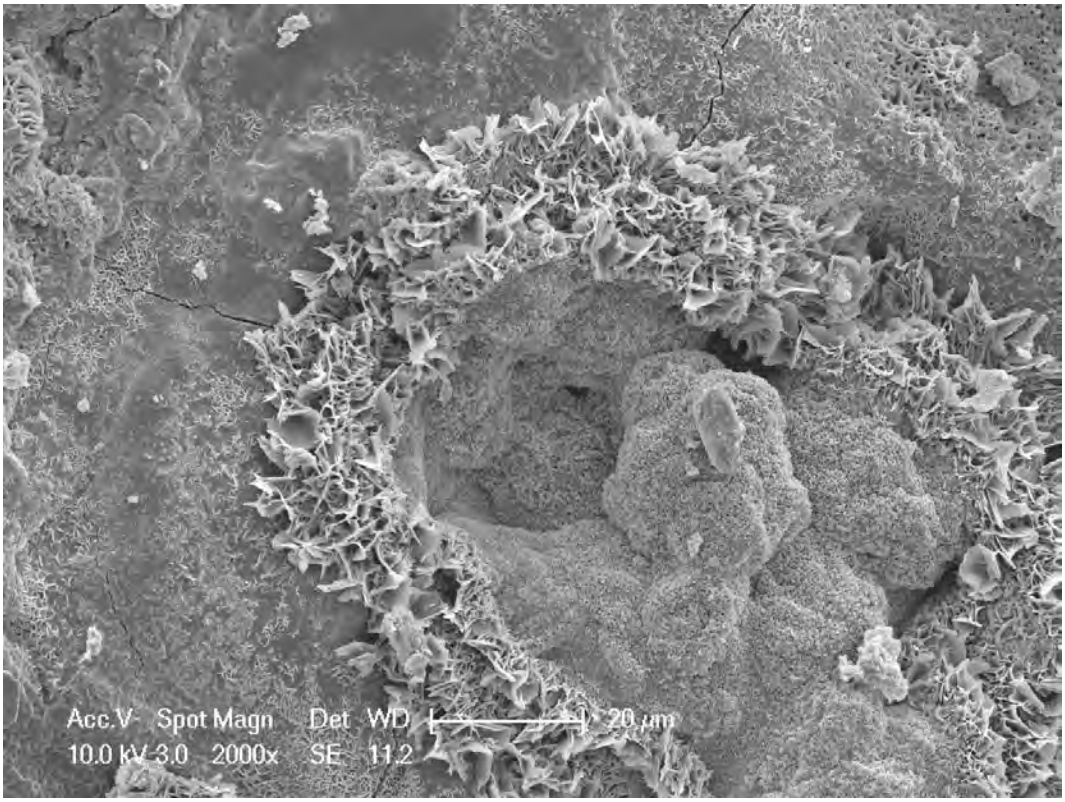

Figure F-33: Caclium Chloride growth on laboratory Stainless Steel anode 2,000x.

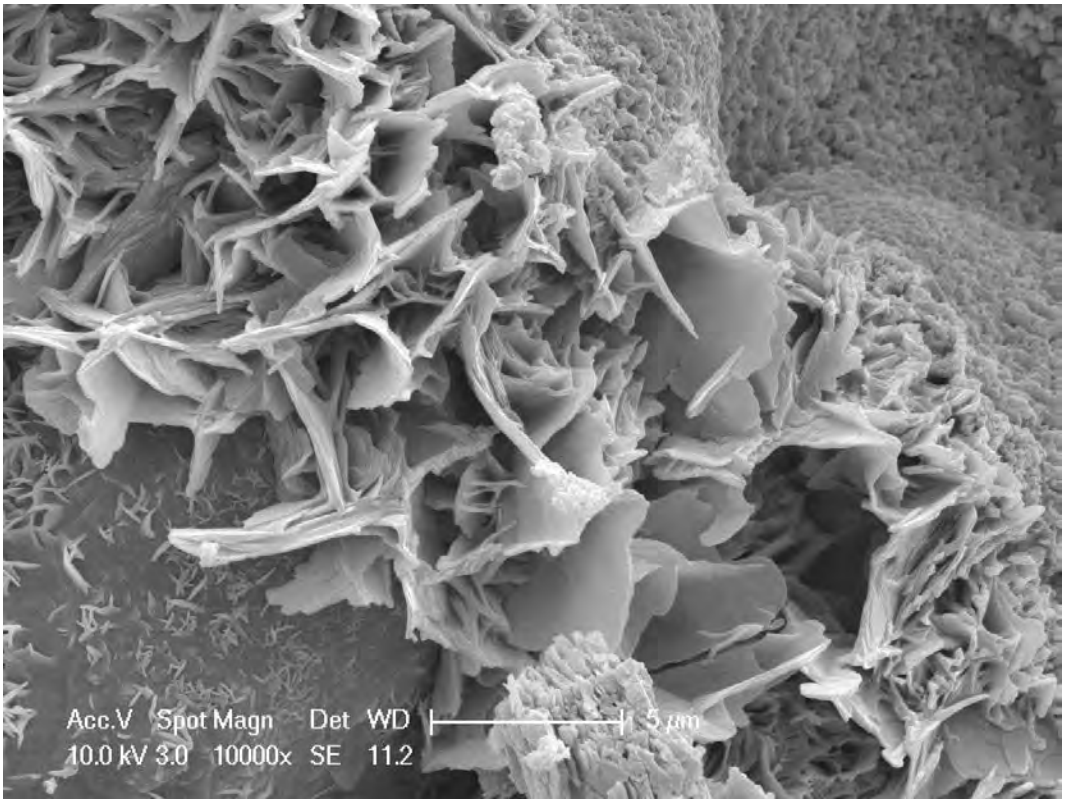

Figure F-34: Caclium Chloride growth on laboratory Stainless Steel anode 10,000x

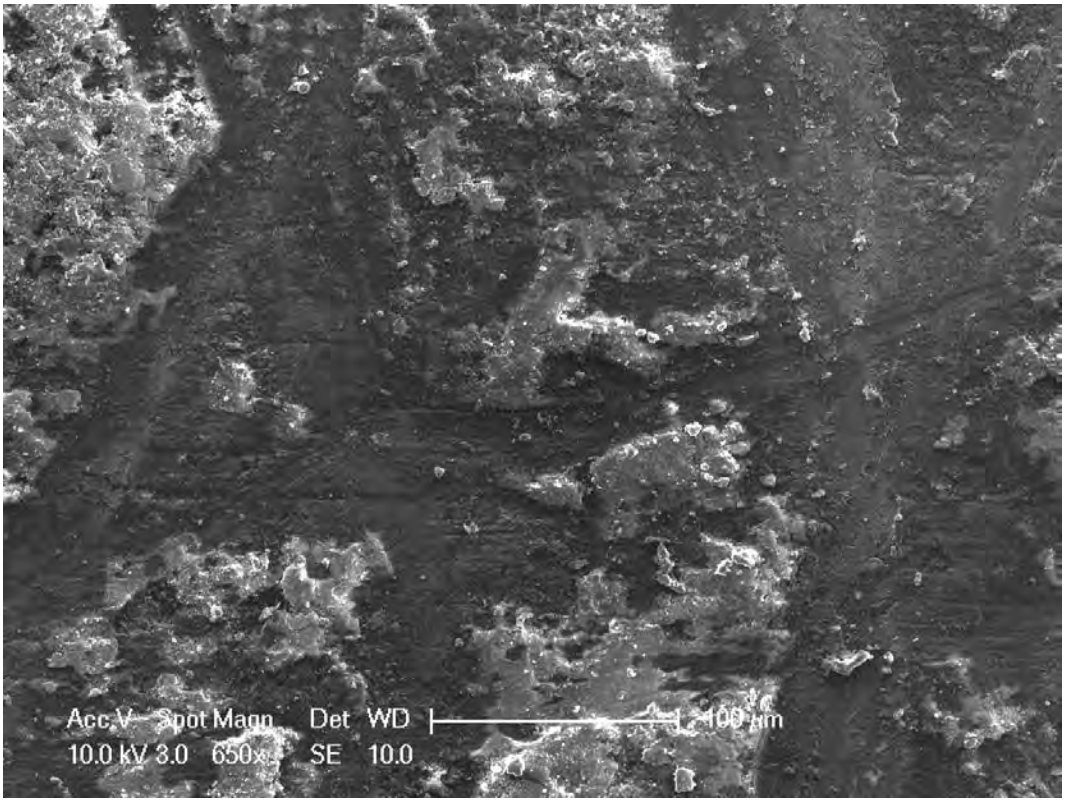

Figure F-35: Laboratory Stainless Steel cathode 650x

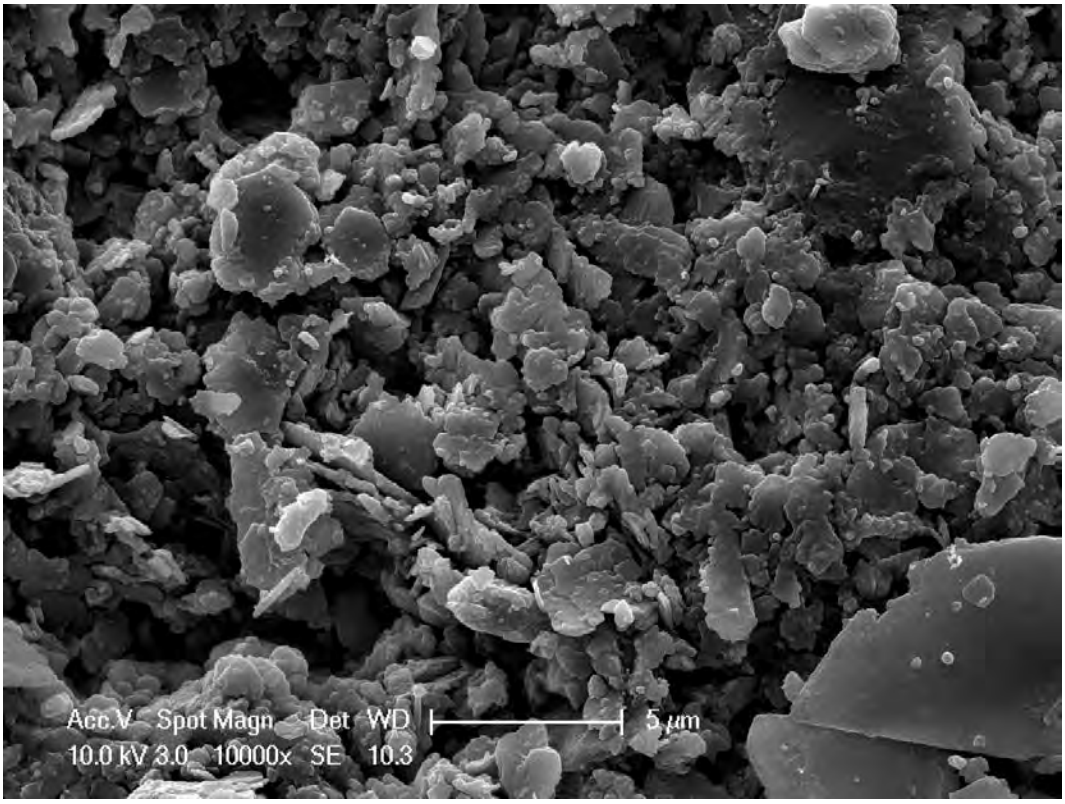

Figure F-36: Laboratory Stainless Steel cathode 10,000x

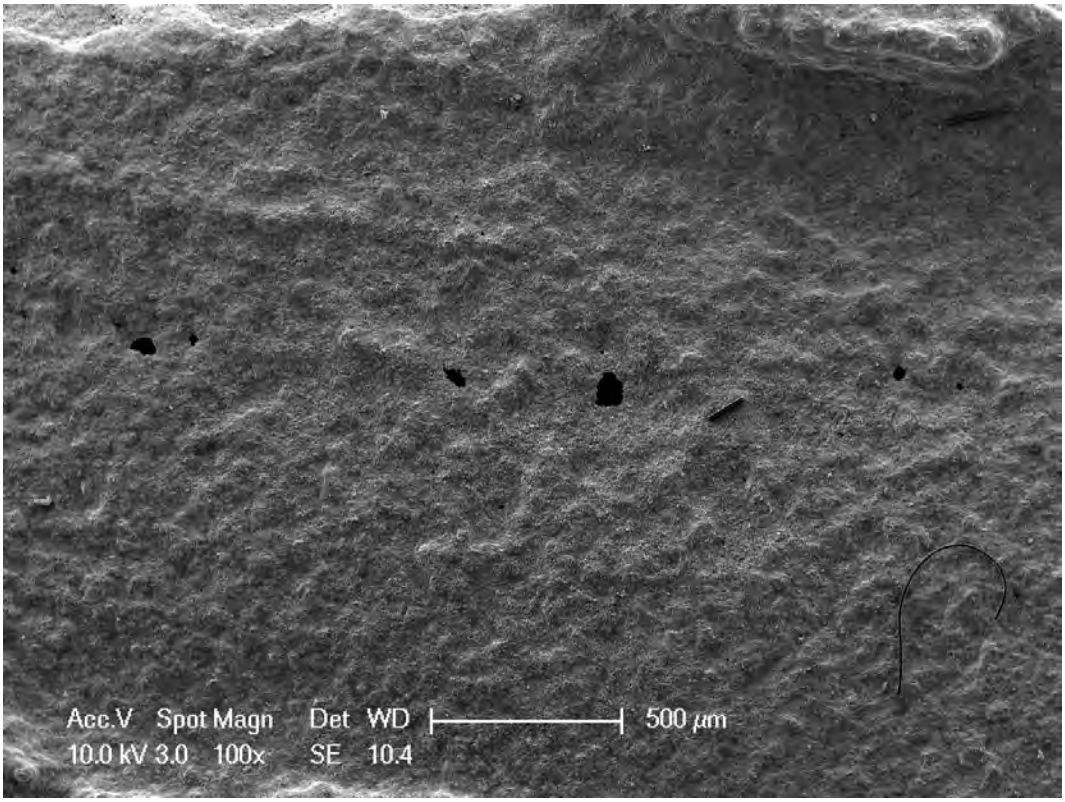

Figure F-37: Laboratory PEG anode 100x

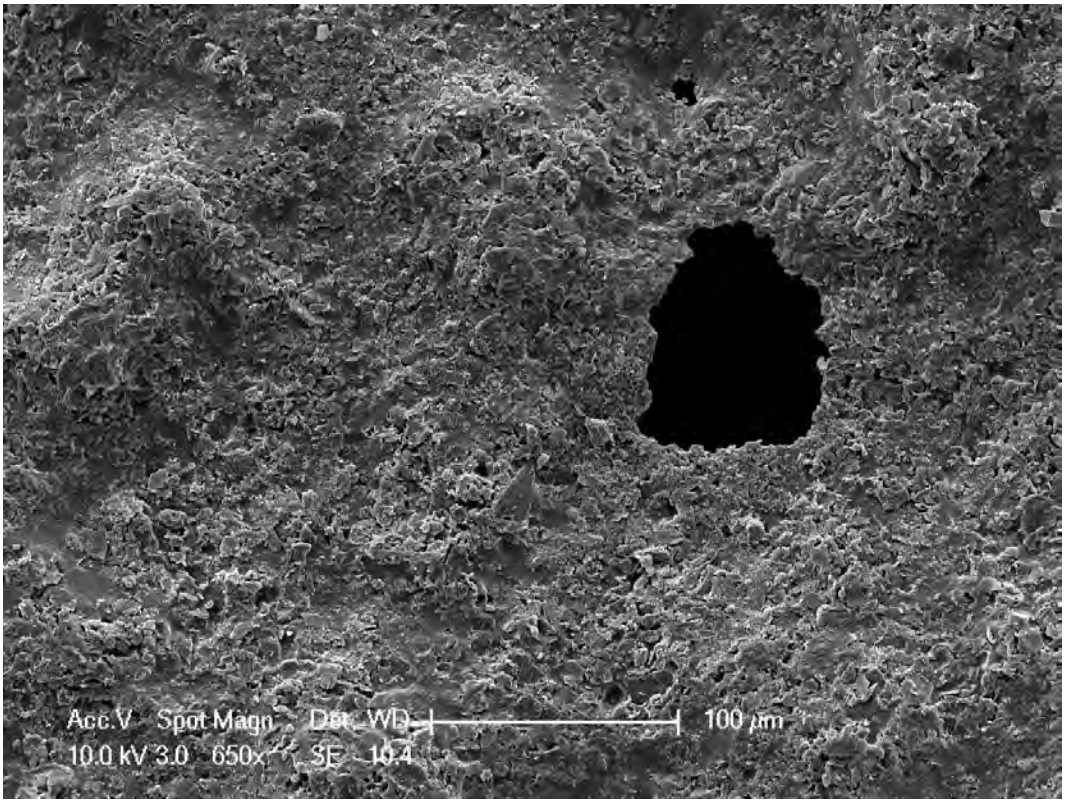

Figure F-38: Laboratory PEG anode 650x

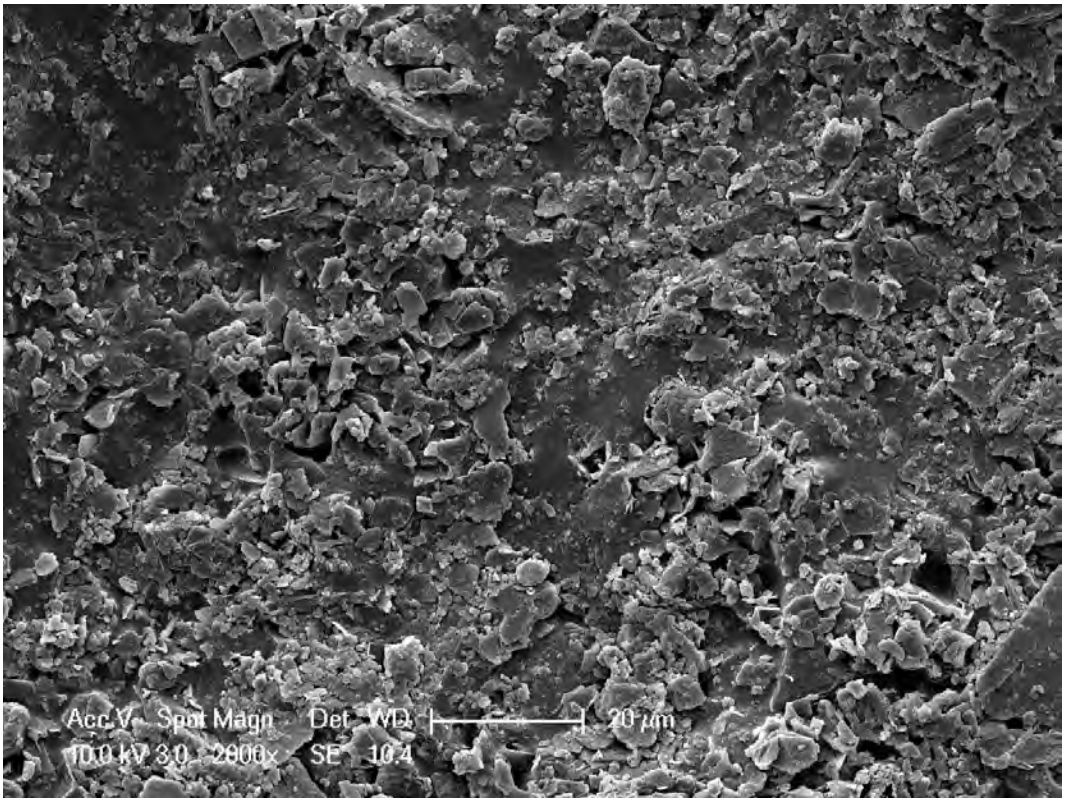

Figure F-39: Laboratory PEG anode 2000x

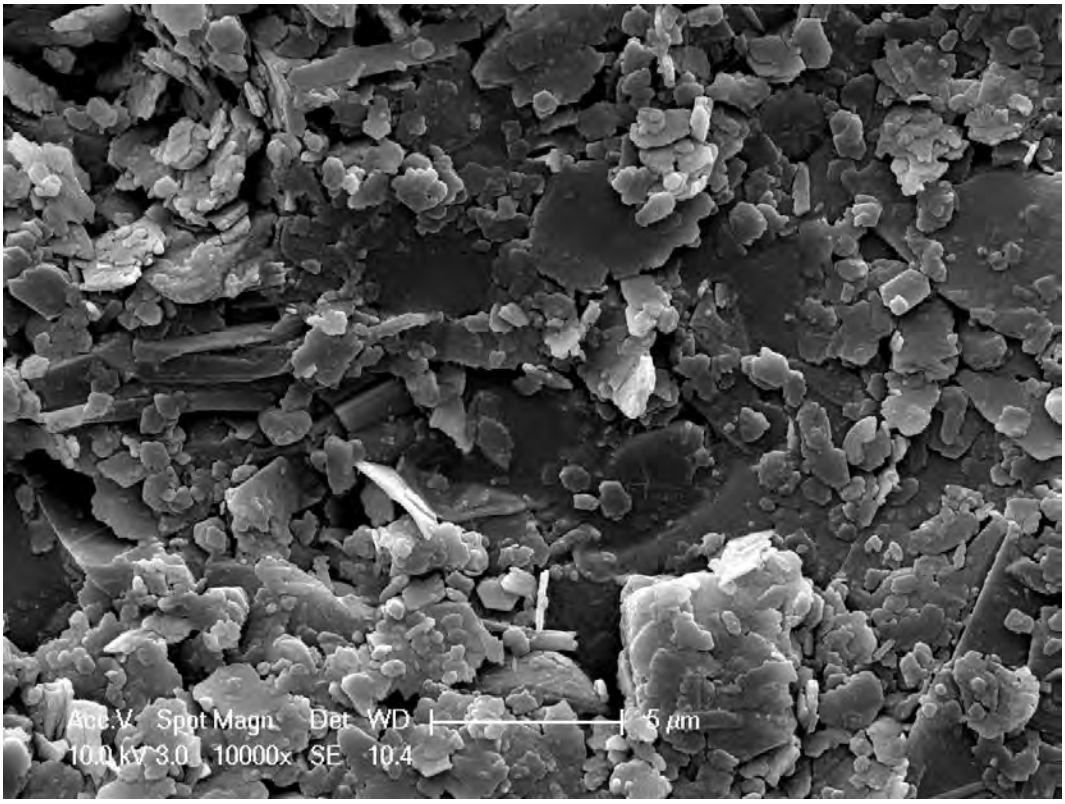

Figure F-40: Laboratory PEG anode 10,000x

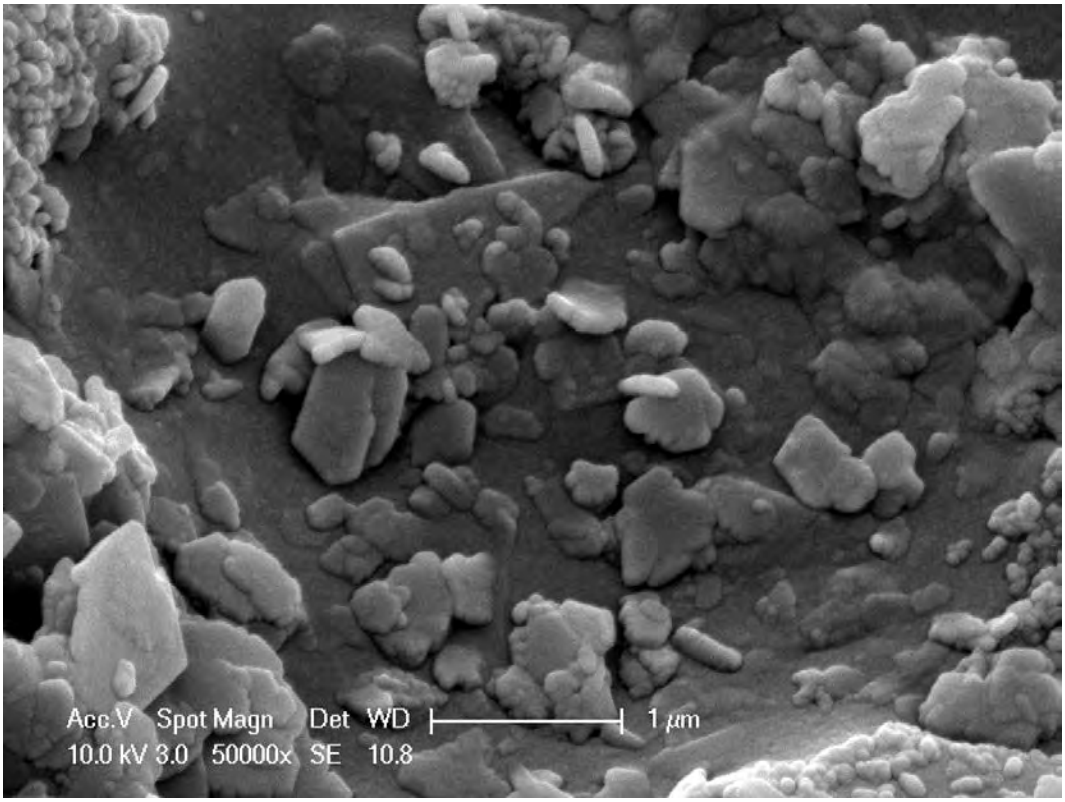

Figure F-41: Laboratory PEG anode 50,000x

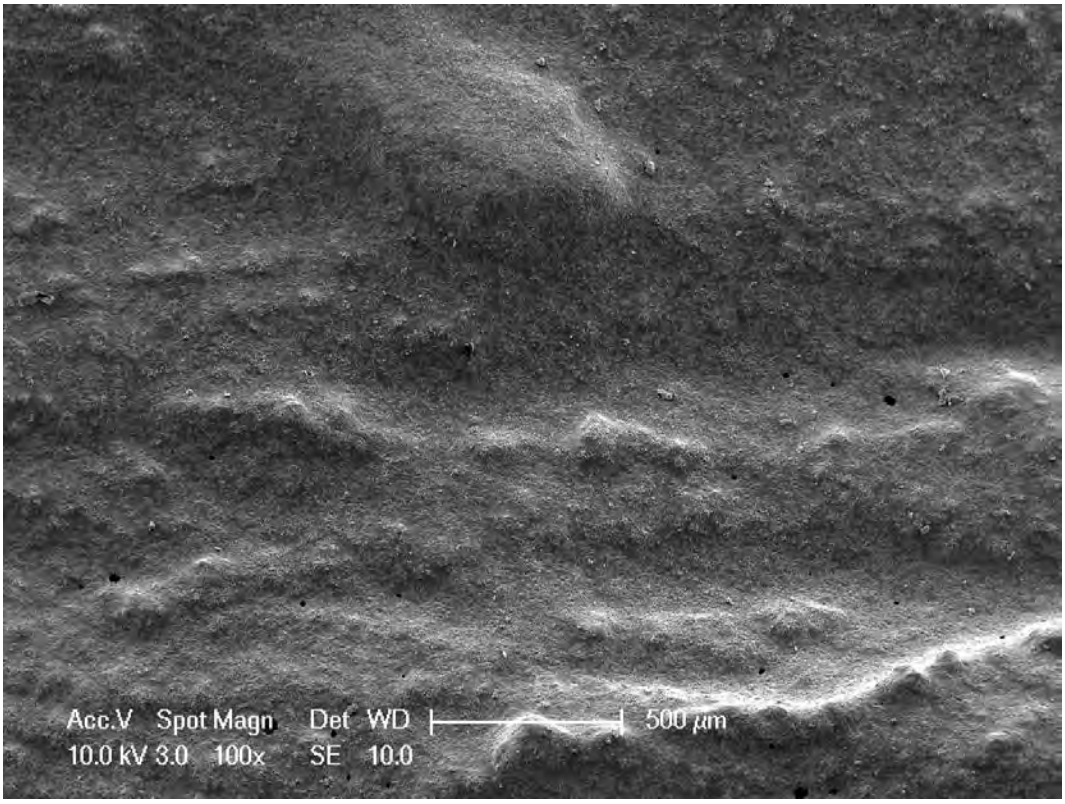

Figure F-42: Laboratory PEG cathode 100x

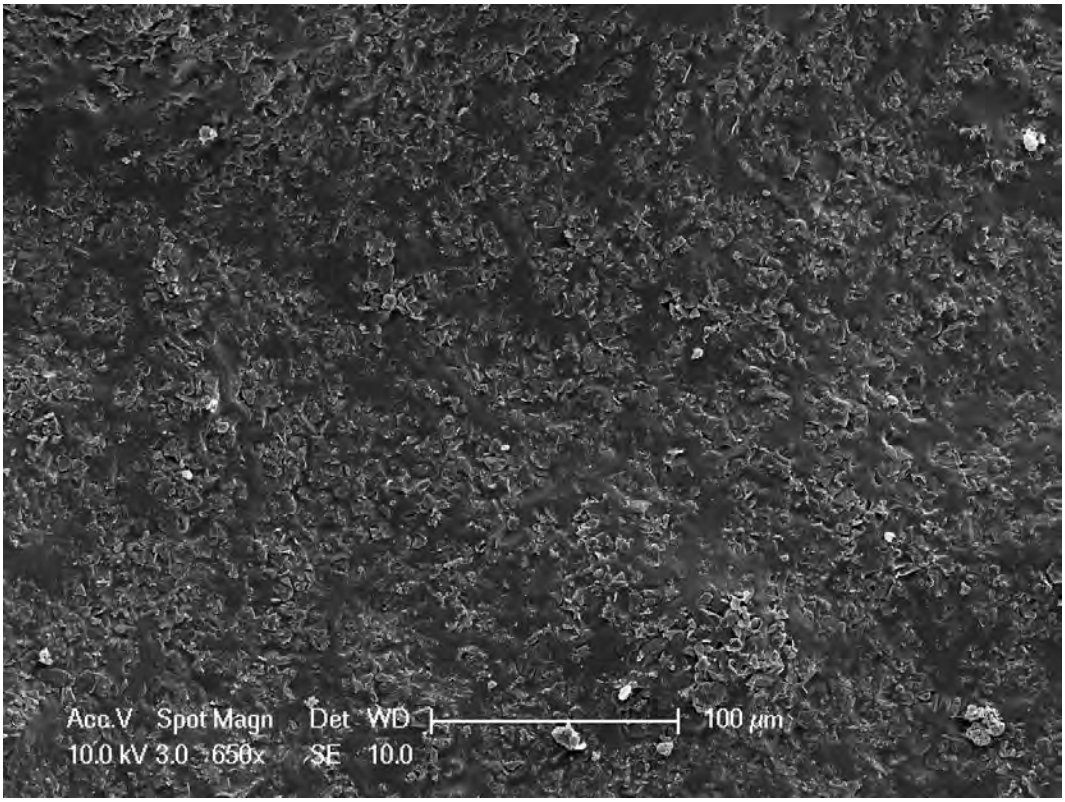

Figure F-43: Laboratory PEG cathode 650x

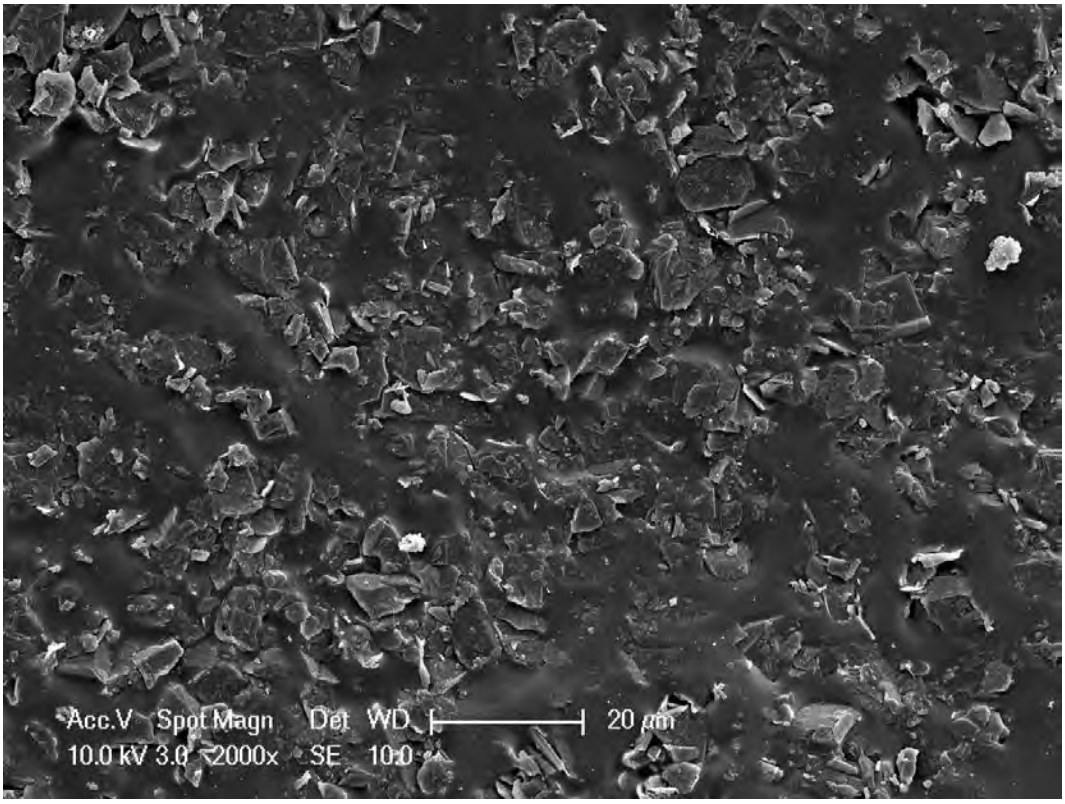

Figure F-44: Laboratory PEG cathode 2000x

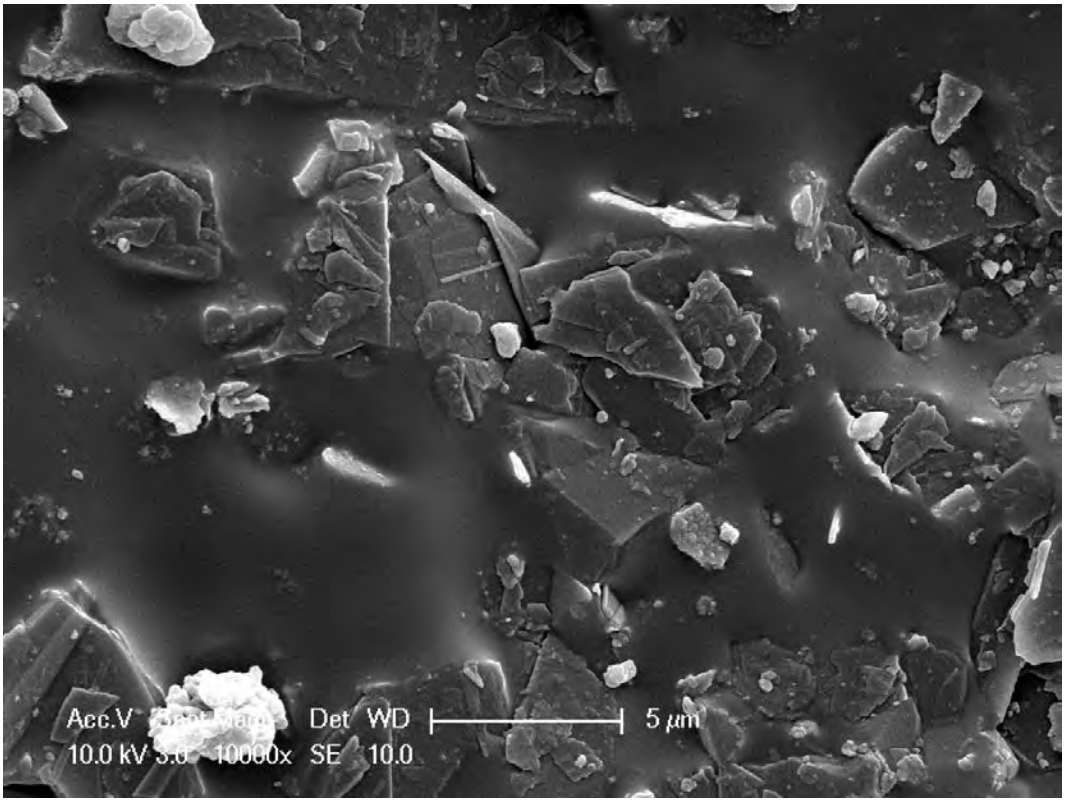

Figure F-45: Laboratory PEG cathode 10,000x

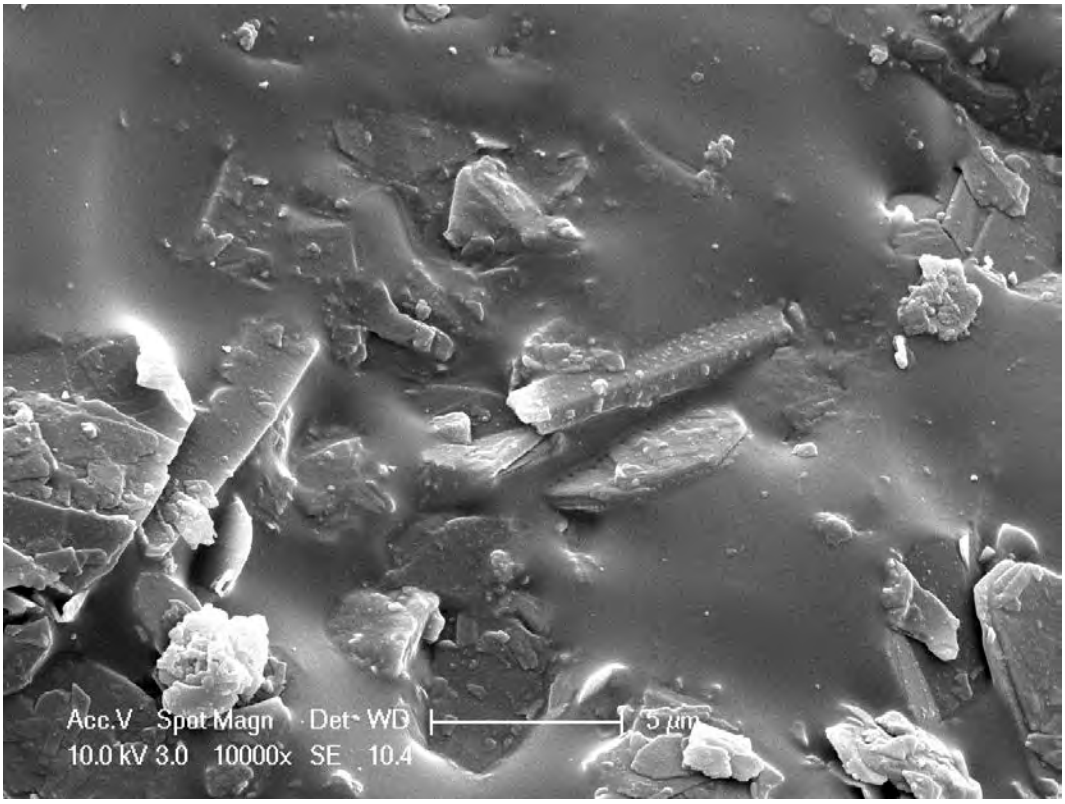

Figure F-46: Laboratory PEG cathode 10,000x

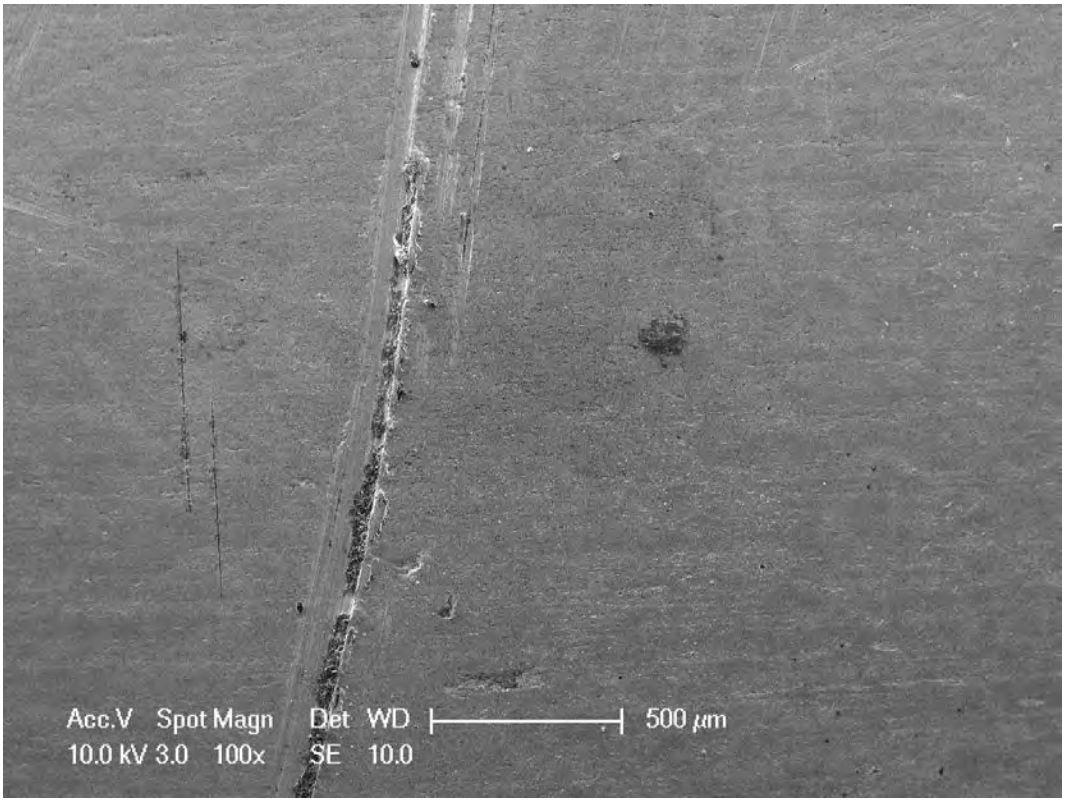

Figure F-47: Unused Stainless Steel 100x

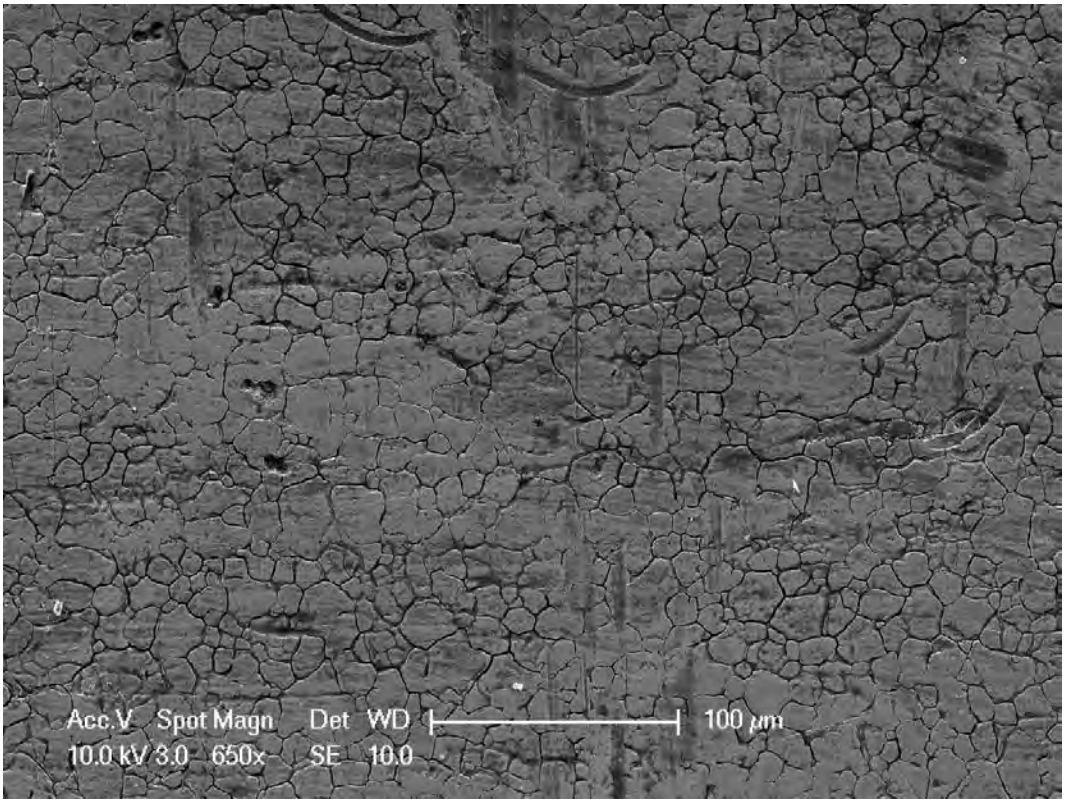

Figure F-48: Unused Stainless Steel 650x

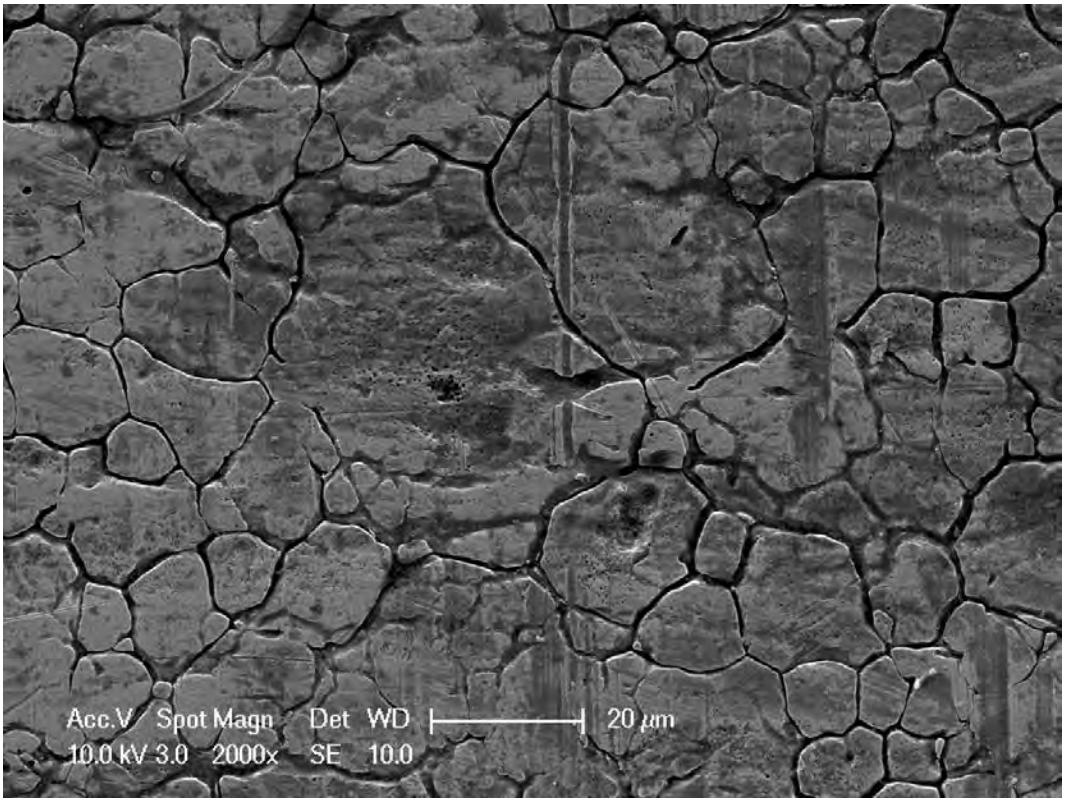

Figure F-49: Unused Stainless Steel 2000x

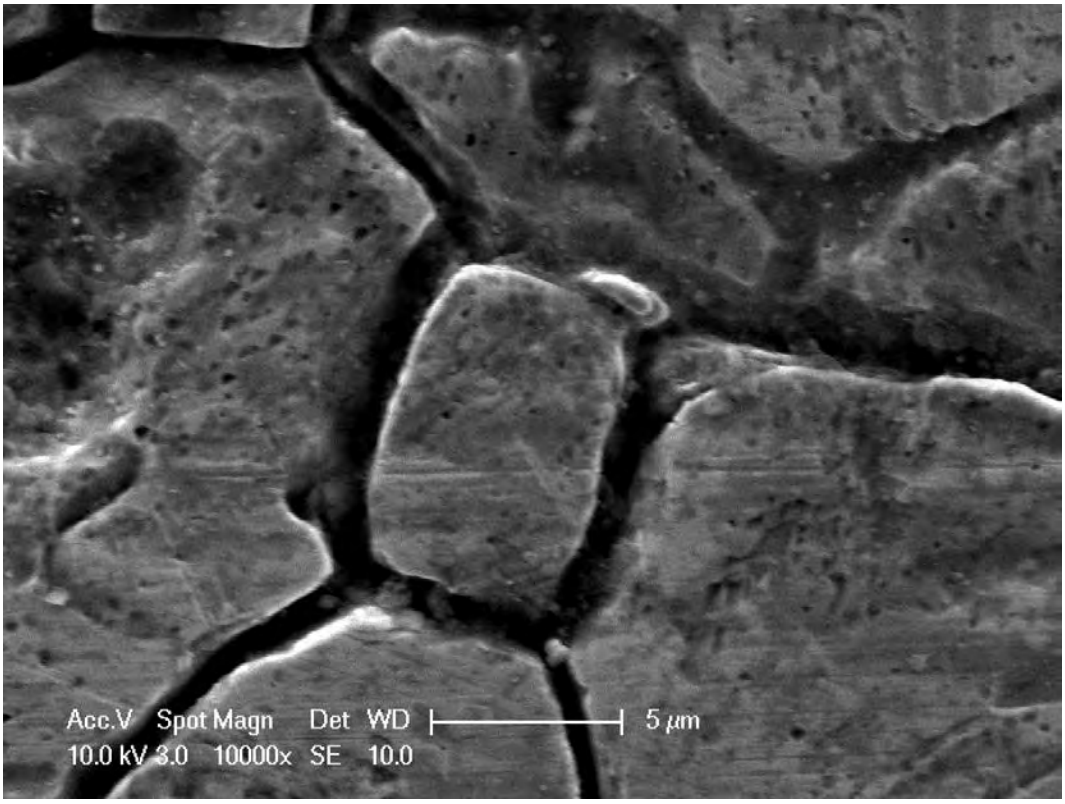

Figure F-50: Unused Stainless Steel 10,000x

APPENDIX G – Site Trial Photographs

Figure G-1: Site trial location

Figure G-2: Site trial location

Figure G-3: Completed thermocouple

Figure G-4: Footing excavations

Figure G-5: Rebar cage in excavation

Figure G-6: Rebar cage


Figure G-7: Excavations and cages


Figure G-8: Rebar cage with spacers

Figure G-9: Concrete footing in place

Figure G-10: Piling

Figure G-11: Concrete wagon


Figure G-12: Completed piles

Figure G-13: Completed pile with scaffold reinforcement

Figure G-14: Completed reference frame setup

Figure G-15: Level gauge

Figure G-16: Picket fence

Figure G-17: Warning sign

Figure G-18: Warning signs

Figure G-19:Completed setup with resistivity array

Figure G-20: Completed setup with resistivity array

Figure G-21: Current Intermittence setup with fluid tanks

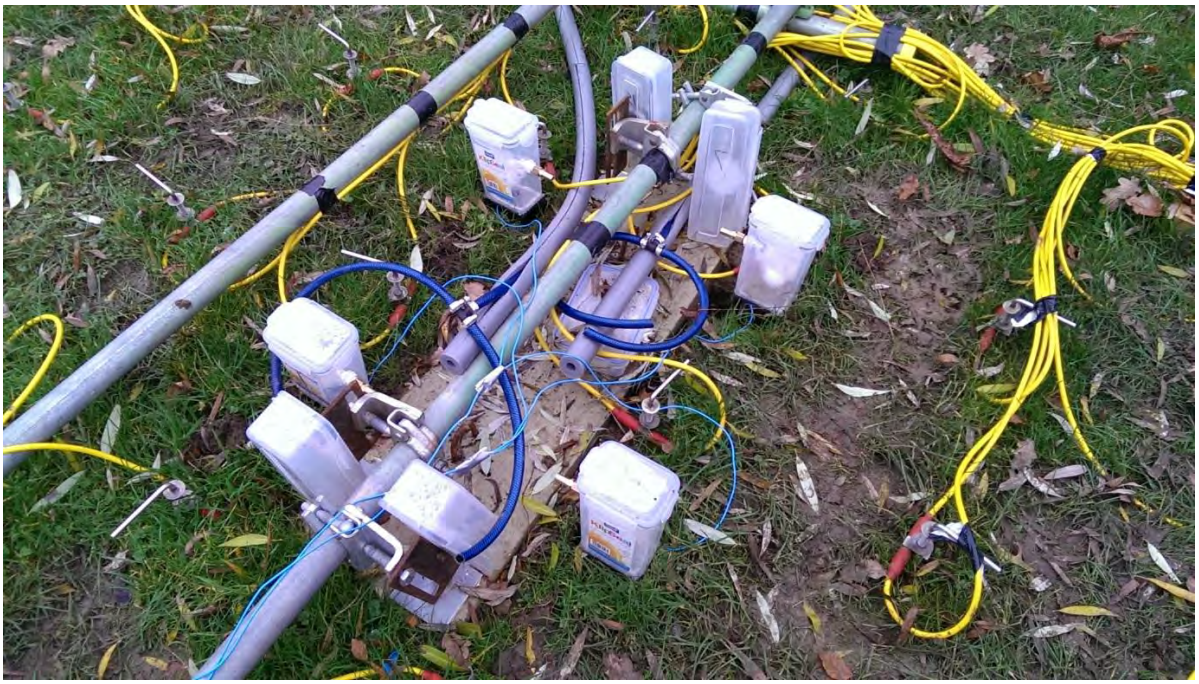

Figure G-22: Vertical electrode setup

Figure G-23: Completed setup

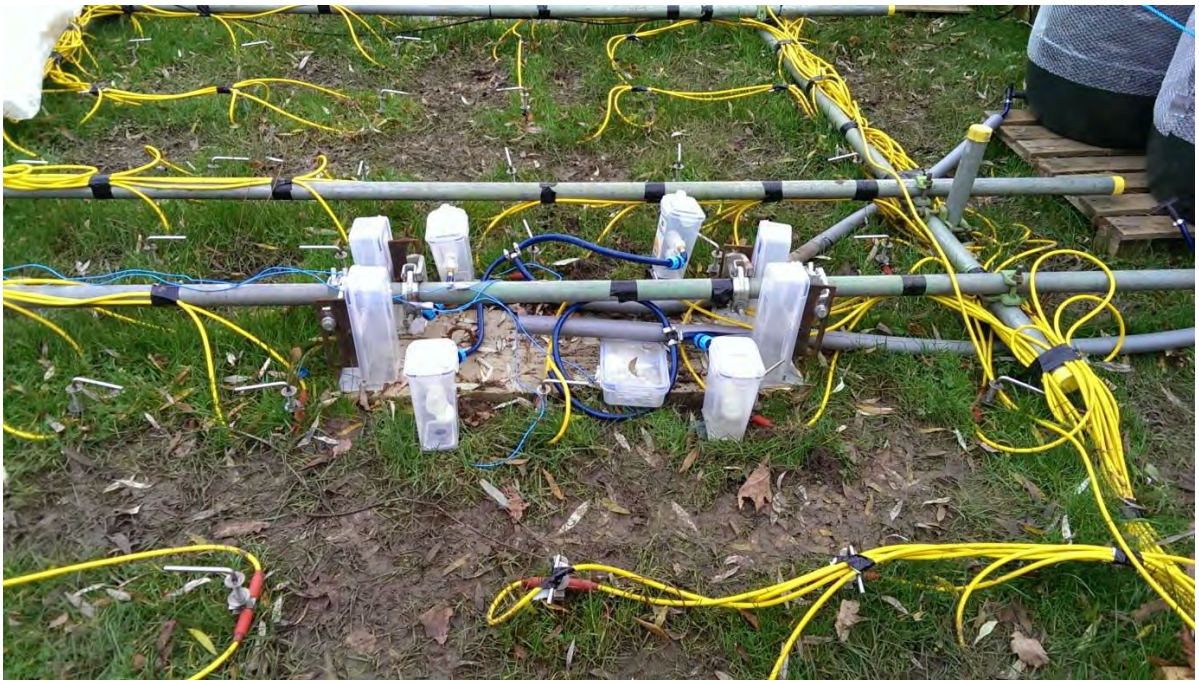

Figure G-24: Vertical electrode setup